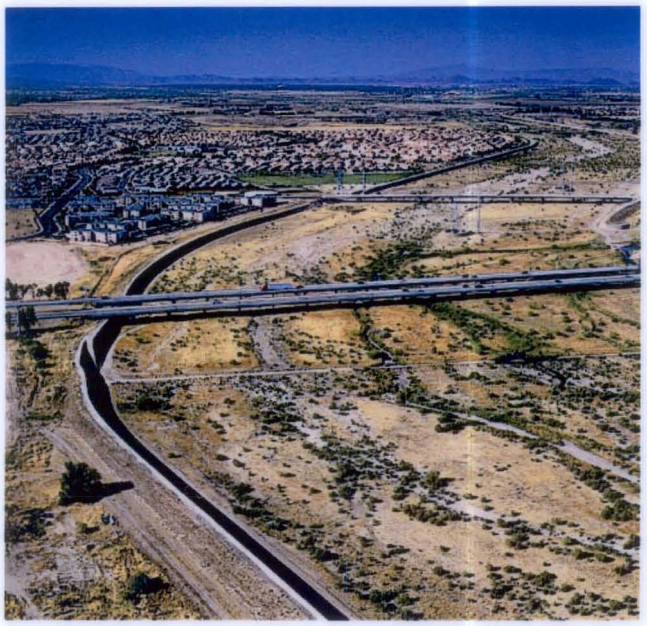

AGUA FRIA
WATERCOURSE MASTER PLAN

Lateral Migration Report

Prepared for

Flood Control District of Maricopa County

June 2001

JE FULLER HYDROLOGY & GEOMORPHOLOGY, INC

Kimley-Horn and Associates, Inc.

Property of
Flood Control District of MC Library
Please Return to
2801 W. Durango
Phoenix, AZ 85009

Acknowledgements

This watercourse master plan was prepared by a group of Maricopa County and Consulting professionals dedicated to improving the way we protect people and property from flood damages while meeting the multiple use needs of a growing population. The commitment to this ideal was demonstrated throughout this project by the Maricopa County Board of Supervisors and by leaders of the Flood Control District of Maricopa County. Finally, the plan for the West Valley Recreation Corridor captures the vision of John F. Long — a man who has spent his entire life trying to improve and promote quality of life for families in the West Valley.

Maricopa County Board of Supervisors

Supervisor, District 1, Fulton Brock
Supervisor, District 2, Don Stapley
Supervisor, District 3, Andrew Kunasek
Supervisor, District 4, Janice K. Brewer, Chair
Supervisor, District 5, Mary Rose Wilcox

Flood Control District of Maricopa County

Mike Ellegood
Doug Williams, Project Manager
Kris Baxter
Theresa Hoff
Dennis Holcomb
Joe Tram
Amir Motamedi
Dave Degerness

Consultant Team

Doug Plasencia, Project Manager, Kimley-Horn and Associates, Inc.
Alan Humphrey, Assistant Project Manager, Kimley-Horn and Associates, Inc.
Bob Eichinger, Sediment Transport, Kimley-Horn and Associates, Inc.
Lisa Burgess, Newsletter, Kimley-Horn and Associates, Inc.
Bruce Wilcox, Environmental Sciences, Kimley-Horn and Associates, Inc.
Jay Hicks, Landscape and Vegetation, EDAW, Inc.
Leslie Dornfeld, Recreation Master Planning, Cornoyer-Hedrick
Jon Fuller, Fluvial Geomorphology, JE Fuller Hydrology and Geomorphology, Inc.
Laurie Miller, Hydraulic Analysis, LTM Engineering, Inc.
Mike Lacey, Groundwater Recharge, Fluid Solutions
Michelle Olson, Public Involvement and Outreach, Lavidge & Baumayr
Nancy Dallett, Historian, Projects in the Public Interest
Barbara Macnider, Archaeology, Archaeological Consulting Services, Ltd.

AGUA FRIA RIVER WATERCOURSE MASTER PLAN

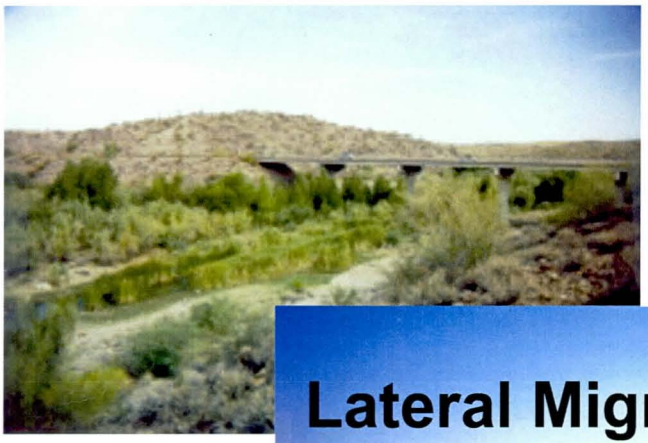

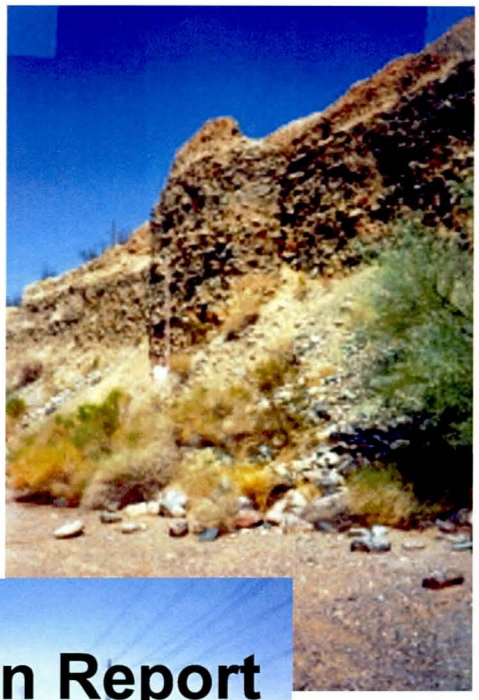

Lateral Migration Report

June 2001

JE FULLER
HYDROLOGY & GEOMORPHOLOGY, INC.

TABLE OF CONTENTS

EXECUTIVE SUMMARY xvi

1. INTRODUCTION 1-1
1.1 Study location 1-1
1.2 Objectives 1-1
1.2.1 Stability Concepts 1-1
1.2.2 Lateral stability 1-1
1.2.3 Vertical stability 1-3
1.3 Data Sources 1-3
1.4 Limitations and Assumptions 1-4
1.5 Report Overview 1-5

2. STUDY AREA 2-1
2.1 Overview 2-1
2.1.1 Watershed Description 2-1
2.1.2 Geologic setting 2-7
2.1.3 Hydrology 2-17
2.1.4 Stream classification 2-41
2.2 Reach descriptions 2-47
2.2.1 Upper 2-50
2.2.2 Middle 2-73
2.2.3 Lower 2-84
2.3 Summary 2-99

3. FIELD DATA 3-1
3.1 Field methods 3-1
3.2 Types of data collected 3-1
3.2.1 Cutbanks 3-2
3.2.2 Location of bedrock outcrops 3-3
3.2.3 Location of caliche and degree of development 3-4
3.2.4 Particle sizes of bed and bank materials 3-5
3.2.5 Armoring 3-6
3.2.6 Vegetation 3-6
3.2.7 Evidence of previous large floods 3-7
3.2.8 Channel form and location 3-8
3.2.9 Location of sand and gravel mining 3-10
3.2.10 Location of structures – bridges, levees, grade control, bank protection measures Nature and geometry of structures 3-11
3.2.11 Location of major tributaries 3-15
3.2.12 Headcuts, slope breaks, and evidence of scour 3-17
3.2.13 Photographs 3-18
3.3 Summary 3-18
3.4 Field forms 3-18

4. GEOGRAPHIC/SPATIAL DATA 4-1
4.1 Distribution of Field Characteristics 4-1
4.2 Longitudinal Profile 4-6

4.3 Sinuosity 4-8
4.4 Geology – "geomorphic mapping" 4-9
4.5 Soils 4-9
4.6 Summary 4-12

5. HISTORIC/TEMPORAL DATA 5-1
5.1 Geologic data 5-1
5.1.1 Quaternary Period 5-1
5.1.2 Limits on Erosion 5-2
5.1.3 Subsidence 5-3
5.1.4 Summary 5-3
5.2 Archeological Data 5-3
5.2.1 Paleo-Indian and Archaic Period 5-4
5.2.2 Hohokam Settlements 5-4
5.2.3 Post-Hohokam Evidence 5-5
5.2.4 Conclusion 5-5
5.3 Historical evidence 5-5
5.3.1 Mining Activity 5-8
5.3.2 Transportation Corridor 5-8
5.3.3 Dam Construction 5-13
5.3.4 Agricultural Activities 5-16
5.3.5 Sand and Gravel Mining 5-18
5.3.6 Summary 5-19
5.3.7 Conclusion 5-19
5.4 Historical Aerial Photographs 5-19
5.4.1 Reach One – Lower Lake Dam to Siphon 5-20
5.4.2 Reach Two – Siphon to CAP Siphon 5-20
5.4.3 Reach Three – CAP Siphon to Beardsley Canal Flume 5-20
5.4.4 Reach Four – Beardsley Canal Flume to Dynamite Boulevard alignment 5-20
5.4.5 Reach Five – Dynamite Boulevard alignment to Hatfield Road 5-21
5.4.6 Reach Six – Hatfield Road to Beardsley Road alignment 5-21
5.4.7 Reach Seven – Beardsley Road alignment to Bell Road 5-22
5.4.8 Reach Eight – Bell Road to Cactus Road alignment 5-22
5.4.9 Reach Nine – Cactus Road alignment to Olive Avenue 5-22
5.4.10 Reach Ten – Olive Avenue to New River confluence 5-22
5.4.11 Reach Eleven – New River confluence to Indian School Road 5-23
5.4.12 Reach Twelve – Indian School Road to Interstate 10 5-23
5.4.13 Reach Thirteen – Interstate 10 to Buckeye Road 5-24
5.4.14 Reach Fourteen – Buckeye Road to Broadway Road 5-24
5.4.15 Reach Fifteen – Broadway Road to Gila River 5-24
5.4.16 Summary 5-24
5.5 Historical Lateral Movement 5-25
5.5.1 Long-term Changes 5-25
5.5.2 Single event Changes 5-33
5.5.3 Summary 5-35
5.6 Historical Vertical Movement 5-35
5.6.1 Long-term Changes 5-35
5.6.2 Comparison of Cross Sections 5-49
5.7 Sinuosity 5-56
5.8 Summary 5-59

6. MATHEMATICAL DATA 6-1
6.1 Introduction 6-1
6.2 Hydraulic data 6-1
6.2.1 HEC-RAS Modifications 6-1
6.2.2 Application to the Agua Fria River Watercourse Master Plan Study Area 6-8
6.3 Sediment data 6-22
6.4 Geomorphic methods 6-24
6.4.1 Bankfull Discharge 6-24
6.4.2 Hydraulic Geometry/Regime Equations 6-31
6.5 Engineering methods 6-64
6.5.1 Allowable velocity 6-64
6.5.2 Equilibrium slope 6-80
6.5.3 Armoring 6-87
6.5.4 Scour 6-91
6.5.5 Comparison of Armoring, Scour, and Equilibrium Slope Predictions. 6-98
6.5.6 HEC-6 Modeling 6-100
6.5.7 Lane relation 6-106
6.6 Summary 6-107

7. TREND ANALYSIS 7-1
7.1 Pre Waddell Dam (before 1927) 7-1
7.2 Post Waddell Dam (1927-1992) 7-3
7.3 Post New Waddell Dam (1992-present) 7-3
7.4 Results 7-3
7.4.1 Comparison of Reach Average Velocities 7-3
7.4.2 Comparison of Reach Average Top Widths 7-8
7.4.3 Comparison of Reach Average Maximum Channel Depth 7-10
7.4.4 Comparison of Equilibrium Slope Estimates 7-12
7.4.5 Regime Channel Characteristics 7-14
7.4.6 Channel Pattern 7-20
7.5 Summary 7-22

8. EROSION HAZARD ZONES 8-1
8.1 Introduction 8-1
8.2 Methodology 8-1
8.2.1 Field Data 8-1
8.2.2 Historical Channel Movement 8-2
8.2.3 Historical Aerial Photographs 8-2
8.2.4 Historical Long-Term Scour 8-2
8.2.5 Archaeological Data 8-3
8.2.6 Mapping of Geomorphic Surfaces 8-3
8.2.7 Longitudinal Profile Analysis 8-3
8.2.8 Hydraulic Geometry/Regime Equations 8-3
8.2.9 Expected Channel Pattern 8-4
8.2.10 Allowable Velocity 8-4
8.2.11 Equilibrium Channel Slope 8-4
8.2.12 Armoring Potential 8-4
8.2.13 Stable Bank Slope 8-5
8.2.14 HEC-6 Modeling Results 8-5
8.2.15 Expected Lateral Erosion Mechanism 8-5
8.2.16 Impacts of Mining-Induced Entrenchment 8-6

8.2.17 Measurements 8-6
8.3 Definition of Erosion Hazard Zones 8-6
8.3.1 Uncertainty 8-7
8.3.2 Floodplain Management 8-7
8.4 Summary 8-22

9. COMPARISON WITH OTHER STUDIES 9-1
9.1 ASU Sedimentation Study 9-1
9.2 Simons, Li & Associates Work for COE and FCD 9-2
9.2.1 SLA, 1983 9-2
9.2.2 SLA, 1984 9-4
9.3 Various Bridge Reports 9-6
9.4 Other Reports 9-6
9.4 Summary 9-7

10. CONCLUSIONS 10-1
10.1 Summary 10-1
10.2 Recommendations 10-3

11. REFERENCES 11-1

12. GLOSSARY 12-1

APPENDIX
CD-ROM of Semi-rectified Historical Aerial Photography
CD-ROM of docs, RAS, shapefiles, dwgs, dxf, etc. of files which make up this report
CD-ROM of field photography and location maps in html format

EXHIBIT MAPS BOOK – See table of contents of Exhibits Map Book

LIST OF TABLES

Table 2-1 Watershed Characteristics: Drainage Area and Peak Discharge 2-1
Table 2-2 Summary of Bridge Locations, Widths, and Approximate Dates of Completion 2-6
Table 2-3 The Geologic Time Scale 2-8
Table 2-4 Regional Long-Term Precipitation Stations 2-18
Table 2-5 USGS Stream Gage Stations in Study Area Vicinity 2-21
Table 2-6 Historical Floods on the Agua Fria River 2-27
Table 2-7 Historical Flood Discharges on the Agua Fria River near Lake Pleasant 2-29
Table 2-8 Distribution of Annual Peak Discharge for Selected Gages, in cfs 2-32
Table 2-9 Comparison of Flood Frequency Estimates 2-33
Table 2-10 Pre-(old) Waddell Dam Discharges 2-35
Table 2-11 Post- (old) Waddell Discharges 2-36
Table 2-12 Post-New Waddell Discharges 2-37
Table 2-13 Brice Classification System 2-42
Table 2-14 Rosgen Classification Data 2-45
Table 2-15 Summary of Reach Characteristics 2-49
Table 4-1 Subreach slopes from examination of longitudinal profile 4-8
Table 4-2 Sinuosity of the Agua Fria River from New Waddell Dam to the Gila River, 1999 4-8
Table 4-3 Soil Unit Landform Classification 4-9
Table 5-1 Towns and Settlements in the Agua Fria Basin (after Lacey and others, n.d.) 5-9
Table 5-2 Single-Event Channel Widening: Agua Fria River, 1980 Flood 5-34
Table 5-3 Maximum Aggradation & Scour as Shown By Comparison of Longitudinal Profiles 5-36
Table 5-4 Agua Fria Aerial Photography Used In Sinuosity Analysis 5-57
Table 5-5 Historical Sinuosity Along the Agua Fria River 5-58
Table 5-6 Historical Sinuosity By Reach 5-58
Table 6-1 - Summary of Sediment Data Sizes Used in the Erosion Hazard Analysis 6-22
Table 6-2 Reach Average Bankfull Discharges 6-28
Table 6-3 Reach Average Top Width at Bankfull Discharge 6-28
Table 6-4 Reach Average Depth at Bankfull Discharge 6-29
Table 6-5 Reach Average Channel Velocity at Bankfull Discharge 6-29
Table 6-6 Reach Average Width/Depth Ratio at Bankfull Discharge 6-30
Table 6-7 Channel Pattern Relationships: Threshold Slope for Braided Channels 6-34
Table 6-8 Observed and Expected Channel Characteristics 6-40
Table 6-9 Approximate Recurrence Interval of Bankfull Discharge Geometry Estimated from Channel Geometry Equations (in years) 6-49
Table 6-10 Hydraulic Geometry Equations – Agua Fria River 6-52
Table 6-11 Average Hydraulic Geometry Exponents for the Agua Fria River Study Reach and Other Regional Stream Systems 6-55
Table 6-12 Agua Fria m/f Ratio Values 6-58
Table 6-13 Comparison of Reach Averages for the Agua Fria River Hydraulic Geometry with Semiarid U.S. Averages 6-59
Table 6-14 Fortier & Scobey Table of Permissible Canal Velocities (ft/s) 6-65
Table 6-15 Suggested Maximum Permissible Mean Channel Velocities (USACOE, 1995) 6-66

Table 6-16 Corps of Engineers Erosive Velocity Data 6-66
Table 6-17 100-year Flood Velocities, All Cross Sections..... 6-67
Table 6-18 100-year Flood Velocities, Without Bridges and Channelized Cross Sections 6-67
Table 6-19 100-year Flood Velocities, Bridges and Channelized Cross Sections Only 6-68
Table 6-20 10-year Flood Velocities, All Cross Sections 6-71
Table 6-21 10-year Flood Velocities, Without Bridges and Channized Cross Sections 6-71
Table 6-22 10-year Flood Velocities, Bridges and Channelized Cross Sections Only 6-72
Table 6-23 2-year Flood Velocities, All Cross Sections 6-75
Table 6-24 2-year Flood Velocities, Without Bridge and Channelized Cross Sections 6-75
Table 6-25 2-year Flood Velocities, Bridge and Channelized Cross Sections Only 6-76
Table 6-26 Allowable Velocity Results..... 6-79
Table 6-27 Equilibrium Slope Analysis Results (Slope in ft/ft)..... 6-86
Table 6-28 Armoring Analysis Results..... 6-90
Table 6-29 Scour Estimates (ft)..... 6-95
Table 6-30 Summary of Long-Term Degradation/Aggradation Data Sources 6-97
Table 6-31 Comparison of Armoring, Scour, and Equilibrium Slope Estimates..... 6-99
Table 6-32 HEC-6 Modeling Assumptions and Limitations 6-101
Table 6-33 HEC-6 Sediment Deficit Translation to Bank Erosion Distance Estimates (ft)..... 6-103
Table 7-1 Revised Pre-Waddell Discharges..... 7-2
Table 7-2 Comparison of slope for braided or meandering channel pattern 7-21
Table 8-1 Some Variables Affecting River Behavior and River Characteristics That Can Change With Time 8-8
Table 8-2 Location and Nature of Areas of Concern..... 8-15

LIST OF FIGURES

Figure 1-1 Study area location map 1-2
Figure 2-1 Physiographic Provinces of Arizona 2-3
Figure 2-2 Lake Pleasant, 12-5-77 2-5
Figure 2-3 Terraces in the Baldy Mountain and Calderwood Butte Quadrangles (adapted from Huckleberry, 1995) 2-13
Figure 2-4 Example of Terrace Formation by Degradation or Aggradation 2-14
Figure 2-5 Land subsidence in the west Phoenix Basin, 1957 – 1991 (from Schumann and O'Day, 1995) 2-16
Figure 2-6 Location of Regional and Statewide Precipitation Stations 2-19
Figure 2-7 Historical Precipitation Data and Average for All Stations in the Agua Fria Watershed, 1893-2000 2-20
Figure 2-8 Long-term Monthly Average Precipitation 2-20
Figure 2-9 Annual Flow Volumes for USGS Gages in the Agua Fria Watershed 2-22
Figure 2-10 Monthly Average Discharges Rates for USGS Gages in the Agua Fria Watershed 2-23
Figure 2-11 Flow Duration Data for USGS Gages in the Agua Fria Watershed 2-24
Figure 2-12 Runoff as a Percentage of Regional Average Precipitation, 1940-1999 2-25
Figure 2-13 Annual Peak Discharges at USGS Gaging Stations 2-30
Figure 2-14 Annual Peak Discharges for USGS Gages in the Agua Fria River Watershed 2-31
Figure 2-15 Seasonal Distribution of Annual Flood Peaks 2-31
Figure 2-16 Simulated 100-year Flood Routing, New Waddell Dam (USACOE, 1995) 2-38
Figure 2-17 Comparison of Flood Flow Frequency Just Downstream of Waddell Dam 2-39
Figure 2-18 Comparison of Flood Flow Frequency at Bell Road 2-39
Figure 2-19 Comparison of Flood Flow Frequency Just Upstream of New River Confluence 2-40
Figure 2-20 Comparison of Flood Flow Frequency Just Downstream of New River Confluence 2-40
Figure 2-21 Comparison of Flood Flow Frequency at Gila River Confluence 2-41
Figure 2-22 - Map of Reaches Defined for Erosion Hazard Analysis 2-48
Figure 2-23 - Photo 64-24 2-50
Figure 2-24 - Photo 65-1 2-50
Figure 2-25 - Map of Reach 1, New Waddell Dam to Dolores Road alignment 2-51
Figure 2-26 - Photo 65-2 2-52
Figure 2-27 - Photo 64-20 2-52
Figure 2-28 - Photo 65-13 2-52
Figure 2-29 - Photo 4-7 2-53
Figure 2-30 - Photo 64-21 2-53
Figure 2-31 - Reach 2, Dolores Road alignment to CAP Canal Siphon 2-54
Figure 2-32 - Photo 66-7 2-55
Figure 2-33 - Photo 65-22 2-55
Figure 2-34 - Photo 65-23 2-55
Figure 2-35 - Photo 66-10 2-56
Figure 2-36 - Reach 3, CAP Crossing to Beardsley Canal 2-57
Figure 2-37 - Photo 5-10 2-58

Figure 2-38 - Photo 5-8 2-58
Figure 2-39 - Photo 5-12 2-58
Figure 2-40 - Photo 7-2 2-59
Figure 2-41 - Photo 6-11 2-59
Figure 2-42 - Reach 4, Beardsley Canal to Calderwood Butte 2-60
Figure 2-43 - Map of Overflow Channel Not Mapped in 1996 Floodplain Delineation Study 2-61
Figure 2-44 - Photo 15-20 2-62
Figure 2-45 - Photo 12-10 2-62
Figure 2-46 - Reach 5, Calderwood Butte to Twin Buttes Wash 2-63
Figure 2-47 - Photo 17-4 2-64
Figure 2-48 - Photo 17-13 2-64
Figure 2-49 - Photo 12-23 2-65
Figure 2-50 - Photo 17-8 2-65
Figure 2-51 - Photo 19-2 2-65
Figure 2-52 - Photo 17-21 2-65
Figure 2-53 - Photo 22-8 2-66
Figure 2-54 - Photo 22-14 2-66
Figure 2-55 - Reach 6, Twin Buttes Wash to Beardsley Road alignment 2-67
Figure 2-56 - Photo 19-4 2-68
Figure 2-57 - Photo 22-4 2-68
Figure 2-58 - Photo 31-22 2-68
Figure 2-59 - Photo 19-18 2-69
Figure 2-60 - Photo 26-2 2-69
Figure 2-61 - Photo 26-3 2-69
Figure 2-62 - Photo 11-8 2-70
Figure 2-63 - Photo 25-8 2-70
Figure 2-64 - Photo 27-11 2-70
Figure 2-65 - Reach 7, Beardsley Road alignment to Bell Road 2-71
Figure 2-66 - Photo 29-24 2-72
Figure 2-67 - Photo 29-13 2-72
Figure 2-68 - Photo 31-7 2-72
Figure 2-69 - Photo 28-4 2-72
Figure 2-70 - Photo 32-5 2-73
Figure 2-71 - Photo 33-19 2-73
Figure 2-72 - Reach 8, Bell Road to Cactus Road alignment 2-74
Figure 2-73 - Photo 38-24 2-75
Figure 2-74 - Photo 35-15 - West terrace 2-75
Figure 2-75 - Photo 32-4 - East terrace 2-75
Figure 2-76 - Photo 36-20 2-76
Figure 2-77 - Photo 39-10 2-76
Figure 2-78 - Photo 33-13 2-77
Figure 2-79 - Photo 23-17 2-77
Figure 2-80 - Reach 9, Cactus Road alignment to Olive Avenue 2-78
Figure 2-81 - Photo 46-11 2-79
Figure 2-82 - Photo 42-8 2-79
Figure 2-83 - Photo 42-6 2-79
Figure 2-84 - Photo 43-17 2-79
Figure 2-85 - Photo 45-21 2-80
Figure 2-86 - Reach 10, Olive Avenue to New River confluence 2-81
Figure 2-87 - Photo 47-2 2-82

Figure 2-88 - Photo 47-5 2-82
Figure 2-89 - Photo 48-20 2-82
Figure 2-90 - Photo 48-17 2-82
Figure 2-91 - Photo 48-11 2-82
Figure 2-92 - Photo 48-1 2-83
Figure 2-93 - Photo 48-24 2-83
Figure 2-94 - 1999 Aerial Photograph of Delta in Gravel Pit Downstream of Northern Avenue 2-84
Figure 2-95 - 1999 Aerial Photograph of Delta in Gravel Pit Downstream of Olive Avenue 2-84
Figure 2-96 - Reach 11, New River confluence to Indian School Road 2-85
Figure 2-97 - Photo 56-11 2-86
Figure 2-98 - Photo 58-11 2-86
Figure 2-99 - Photo 34-24 2-86
Figure 2-100 - Photo 56-1 2-87
Figure 2-101 - Photo 58-3 2-87
Figure 2-102 - Photo 34-22 2-87
Figure 2-103 - Photo 1-5 2-87
Figure 2-104 - Photo 58-18 - View SW from top of upstream wing dike 2-88
Figure 2-105 - Photo 59-6 2-88
Figure 2-106 - Photo 38-4 2-88
Figure 2-107 - Photo 41-18 2-88
Figure 2-108 - Reach 12, Indian School Road to Interstate 10 2-89
Figure 2-109 - Photo 38-5 2-90
Figure 2-110 - Photo 41-9 2-90
Figure 2-111 - Photo 50-15 2-90
Figure 2-112 - Reach 13, Interstate 10 to MC 85 (Buckeye Road) 2-91
Figure 2-113 - Photo 57-5 2-92
Figure 2-114 - Photo 56-23 2-92
Figure 2-115 - Photo 54-15 2-92
Figure 2-116 - Reach 14, MC 85 (Buckeye Road) to Broadway Road alignment 2-94
Figure 2-117 - Photo 60-9 2-95
Figure 2-118 - Photo 62-11 2-95
Figure 2-119 - Photo 62-14 2-95
Figure 2-120 - Photo 60-8 2-96
Figure 2-121 - Photo 54-11 2-96
Figure 2-122 - Photo 54-9 2-96
Figure 2-123 - Photo 0-19 2-96
Figure 2-124 - Photo 62-2 2-97
Figure 2-125 - Photo 64-6 2-97
Figure 2-126 - Reach 15, Broadway Road alignment to Gila River 2-98
Figure 2-127 - Photo 63-15 2-99
Figure 3-1 Cutbank along pleistocene terrace (Photo 31-22) 3-3
Figure 3-2 View of cutbank in fine-grained sediments (Photo 12-10) 3-3
Figure 3-3 View downstream along coarser-grained cutbank (Photo 15-20) 3-3
Figure 3-4 Exposed roots of tree along terrace cutbank (Photo 18-6) 3-3
Figure 3-5 Bedrock in channel bottom just upstream of Morgan City Wash (Photo 65-1) 3-4
Figure 3-6 View of Tertiary conglomerate along right bank in Reach 2 (Photo 66-7) 3-4

Figure 3-7 View of very well developed caliche layer in Early Pleistocene terrace cutbank (Photo 43-7) 3-4
Figure 3-8 Nearly vertical bank along well-developed caliche in Youngtown, note vehicle and building near terrace edge above (Photo 43-8) 3-4
Figure 3-9 View of coarser bed material in upper reach (Photo 66-1) 3-5
Figure 3-10 View of bed material in middle reach (Photo 44-16) 3-5
Figure 3-11 View of finer-grained bed material near Gila River confluence (Photo 63-18) 3-5
Figure 3-12 Fine-grained floodplain sediments over coarser sands below (Photo 22-7) 3-5
Figure 3-13 Example of armoring of bed material in Agua Fria River just downstream of the New River confluence (Photo 56-8) 3-6
Figure 3-14 Vegetation variations by surface (Photo 7-7) 3-7
Figure 3-15 View of historic flotsam in right overbank near Bethany Home Road alignment (Photo 53-17) 3-8
Figure 3-16 View downstream in channel avulsion from 1980 flood (Photo 53-16) 3-8
Figure 3-17 Stand of cholla surrounded by sands deposited during a large flood (probably Feb. 1980)(Photo 9-16) 3-8
Figure 3-18 Pre-avulsion photo, 1977 3-9
Figure 3-19 Example of avulsion, 1980 3-9
Figure 3-20 View on floodplain island in Reach 6 (Photo 22-8) 3-9
Figure 3-21 View downstream in left overbank channel near Olive Ave. (Photo 45-12) 3-9
Figure 3-22 View of exposure in gravel pit near Camelback Road (Photo 56-2) 3-10
Figure 3-23 Gravel pit downstream of Hatfield Road (Photo 19-18 to 21) 3-11
Figure 3-24 Van Buren Street bridge (Photo 52-2) 3-11
Figure 3-25 Culvert on gravel mine access road near Greenway Road alignment (Photo 36-19) 3-11
Figure 3-26 Powerline tower in river (Photo 38-20) 3-12
Figure 3-27 Example of soil cement grade control structure in levee reach (Photo 56-19) 3-12
Figure 3-28 Northern Ave. at-grade crossing (Photo 31-25) 3-12
Figure 3-29 View along south along right soil cement levee (Photo 57-9) 3-12
Figure 3-30 Large angular bank protection downstream of Olive Ave. (Photo 47-6) 3-12
Figure 3-31 Riprap under Buckeye Road bridge (Photo 54-11) 3-13
Figure 3-32 Buried Honda downstream of Bell Road (Photo 32-10) 3-13
Figure 3-33 Shot up trash and shell casings upstream of Jomax Road (Photo 13-18) 3-14
Figure 3-34 Debris dumped over bank (Photo 39-9) 3-14
Figure 3-35 Road in river downstream of Northern Ave. (Photo 48-20) 3-14
Figure 3-36 "Riprap" along Cholla landfill downstream of Grand Ave. (Photo 38-24) 3-14
Figure 3-37 New Waddell and Old Waddell Dams 3-14
Figure 3-38 Confluence of Unnamed Washes 1 & 2 with the Agua Fria River, 2000 3-16
Figure 3-39 Confluence of Twin Buttes Wash with the Agua Fria River, 2000 3-16
Figure 3-40 View Upstream in Agua Fria River Just Upstream of McMicken Outlet Wash Confluence 3-16
Figure 3-41 AT&SF Railroad bridge (Photo 23-17) 3-17

Figure 3-42 Looking downstream into 3 foot deep headcut near Greenway Road alignment (Photo 33-16) 3-17
Figure 3-43 Scour downstream of grade control structure (Photo 41-18) 3-17
Figure 3-44 (Photo 1-7) 3-17
Figure 3-45 (Photo 63-3)) 3-18
Figure 3-46 Photo 61-21 3-18
Figure 4-1 Location of bedrock outcrops in study area 4-2
Figure 4-2 Location of caliche in study area 4-3
Figure 4-3 Location of cutbanks observed in study area 4-4
Figure 4-4 Location of gravel pits observed in study area 4-5
Figure 4-5 Longitudinal Profile of the Agua Fria River from HECRAS model modified by JEF 4-6
Figure 4-6 Large scour hole along bedrock island in Reach 1 (Photo 65-10) 4-7
Figure 4-7 Schematic of meander migration 4-8
Figure 5-1Agua Fria River Chronology 5-7
Figure 5-2 Historical Site Location Map (Source: Lacey and others, n.d.) 5-10
Figure 5-3 Present Site Location Map (Source: MCDOT, 1998) 5-12
Figure 5-4 William Beardsley on Dyer Diversion Dam (Schuyler, 1903) 5-14
Figure 5-5 Carl Pleasant Dam (Source: USBR) 5-15
Figure 5-6 New Waddell Dam (Source: USBR) 5-16
Figure 5-7 Comparison of Longitudinal Profiles Over Time 5-37
Figure 5-8 Reach 1 Historical Longitudinal Profiles 5-38
Figure 5-9 Reach 2 Historical Longitudinal Profiles 5-39
Figure 5-10 Reach 3, 4, 5, & 6 Historical Longitudinal Profiles 5-40
Figure 5-11 Reach 7 Historical Longitudinal Profiles 5-41
Figure 5-12 Reach 8 Historical Longitudinal Profiles 5-42
Figure 5-13 Reach 8, 1964 5-43
Figure 5-14 Reach 8, 1997 5-43
Figure 5-15 Reach 9 Historical Longitudinal Profiles 5-43
Figure 5-16 Reach 10 Historical Longitudinal Profiles 5-44
Figure 5-17 Reach 11 Historical Longitudinal Profiles 5-45
Figure 5-18 Reach 12 & 13 Historical Longitudinal Profiles 5-46
Figure 5-19 Reach 13, 1964 5-47
Figure 5-20 Reach 13, 1992 5-47
Figure 5-21 View of Large Angular Riprap Beneath Buckeye Road Bridge 5-47
Figure 5-22 Reach 14 Historical Longitudinal Profiles 5-48
Figure 5-23 Reach 15 Historical Longitudinal Profiles 5-49
Figure 5-24 Reach 1, RM 33.25 5-50
Figure 5-25 Reach 2, RM 31.29 5-50
Figure 5-26 Reach 4, RM 27.77 5-51
Figure 5-27 Reach 5, RM 25.79 5-51
Figure 5-28 Reach 6, RM 23.219 5-52
Figure 5-29 Reach 7, RM 20.579 5-52
Figure 5-30 Reach 7, RM 19.827 5-53
Figure 5-31 Reach 8, RM 16.385 5-53
Figure 5-32 Reach 8, RM 17.548 5-54
Figure 5-33 Reach 8, RM 15.658 5-54
Figure 5-34 Reach 9, RM 13.663 5-55
Figure 5-35 Reach 10, RM 12.913 5-55
Figure 6-1. Recommended bank stationing for single channel cross sections. 6-5

Figure 6-2. Recommended bank stationing for multiple channels with shallow islands 6-6

Figure 6-3. Recommended bank stationing for multiple channels with shallow, insignificant or small islands. 6-6
Figure 6-4. Recommended bank stationing for multiple channels with exposed islands of significant size 6-7
Figure 6-5. Recommended bank stationing for perched overbank channels 6-7
Figure 6-6. Recommended bank stationing for channels with poorly defined banks. 6-8
Figure 6-7. Agua Fria River Channel Discharge (QCH) vs. Distance. 6-13
Figure 6-8. Agua Fria River Left Overbank Discharge vs. Distance 6-13
Figure 6-9. Agua Fria River Right Overbank Discharge vs. Distance. 6-14
Figure 6-10. Agua Fria River Right and Left Overbank Discharge 100-Year Event 6-14
Figure 6-11. Agua Fria River Maximum Channel Depth vs. Channel Distance 6-15
Figure 6-12. Agua Fria River Hydraulic Channel Depth vs. Channel Distance. 6-15
Figure 6-13. Agua Fria River Channel Flow Area vs. Channel Distance. 6-16
Figure 6-14. Agua Fria River Channel Wetted Perimeter vs. Channel Distance 6-16
Figure 6-15. Agua Fria River Total Wetted Perimeter vs. Channel Distance. 6-17
Figure 6-16. Agua Fria River Channel Topwidth vs. Channel Distance. 6-17
Figure 6-17. Agua Fria River Total Topwidth vs. Channel Distance. 6-18
Figure 6-18. Agua Fria River Channel Velocity vs. Channel Distance. 6-18
Figure 6-19. Agua Fria River Energy Grade Slope vs. Channel Distance 6-19
Figure 6-20. Agua Fria River Distance Between HEC-RAS Cross Sections. 6-19
Figure 6-21. Agua Fria River Weighted Channel and Overbank Manning's n Values. 6-20
Figure 6-22. Agua Fria River Froude Number vs. Channel Distance. 6-20
Figure 6-23. Agua Fria River Head Loss vs. Channel Distance 6-21
Figure 6-24 - Sediment Data for Lower Reach (New River Confluence to Gila River) 6-23
Figure 6-25 - Sediment Data for Middle Reach (Bell Road to New River Confluence) 6-23
Figure 6-26 - Sediment Data for Upper Reach (Bell Road to New Waddell) 6-24
Figure 6-27 Variation in Bankfull Discharge Along the Agua Fria River Downstream of New Waddell Dam 6-25
Figure 6-28 Top width at Bankfull Discharge Along the Agua Fria River Downstream of New Waddell Dam 6-25
Figure 6-29 Depth at Bankfull Discharge Along the Agua Fria River Downstream of New Waddell Dam 6-26
Figure 6-30 Velocity at Bankfull Discharge Along the Agua Fria River Downstream of New Waddell Dam 6-27
Figure 6-31 Width/Depth Ratio Along the Agua Fria River Downstream of New Waddell Dam 6-27
Figure 6-32 Flood hydrographs for Dec. 1978, Jan. 1979, and Feb. 1980 floods on the Agua Fria River 6-31
Figure 6-33 Variation in rate of change of width (b) for post New Waddell hydraulic geometry 6-51
Figure 6-34 Variation in rate of change of depth (f) for post New Waddell hydraulic geometry 6-51

Figure 6-35 Variation in rate of change of velocity (m) for post New Waddell hydraulic geometry 6-52
Figure 6-36 Reach by reach relation of width to discharge for post New Waddell hydraulic geometry 6-53
Figure 6-37 Reach by reach relation of depth to discharge for post New Waddell hydraulic geometry 6-54
Figure 6-38 Reach by reach relation of velocity to discharge for post New Waddell hydraulic geometry 6-54
Figure 6-39 Comparison of width to discharge relationships for Agua Fria and central Arizona streams 6-56
Figure 6-40 Comparison of depth to discharge relationships for Agua Fria and central Arizona streams 6-57
Figure 6-41 Comparison of velocity to discharge relationships for Agua Fria and central Arizona streams 6-57
Figure 6-42 Variation in m/f ratio for post New Waddell hydraulic geometry 6-58
Figure 6-43 100-year Flood Channel Velocities Along the Agua Fria River Downstream of New Waddell Dam 6-69
Figure 6-44 100-year Flood Left Overbank Velocities Along the Agua Fria River Downstream of New Waddell Dam 6-69
Figure 6-45 100-year Flood Right Overbank Velocities Along the Agua Fria River Downstream of New Waddell Dam 6-70
Figure 6-46 10-year Flood Channel Velocities Along the Agua Fria River Downstream of New Waddell Dam 6-73
Figure 6-47 10-year Flood Left Overbank Velocities Along the Agua Fria River Downstream of New Waddell Dam 6-73
Figure 6-48 10-year Flood Right Overbank Velocities Along the Agua Fria River Downstream of New Waddell Dam 6-74
Figure 6-49 2-year Flood Channel Velocities Along the Agua Fria River Downstream of New Waddell Dam 6-77
Figure 6-50 2-year Flood Left Overbank Velocities Along the Agua Fria River Downstream of New Waddell Dam 6-77
Figure 6-51 2-year Flood Right Overbank Velocities Along the Agua Fria River Downstream of New Waddell Dam 6-78
Figure 6-52 Cumulative Bed Elevation Change by Time Period in KHA Existing Conditions HEC6 Model 6-105
Figure 7-1 Comparison of reach average channel velocities, 100-year flood 7-4
Figure 7-2 Comparison of reach average channel velocities, 10-year flood 7-4
Figure 7-3 Comparison of reach average channel velocities, 2-year flood 7-5
Figure 7-4 Comparison of reach average left overbank velocities, 100-year flood 7-5
Figure 7-5 Comparison of reach average left overbank velocities, 10-year flood 7-6
Figure 7-6 Comparison of reach average left overbank velocities, 2-year flood 7-6
Figure 7-7 Comparison of reach average right overbank velocities, 100-year flood 7-7
Figure 7-8 Comparison of reach average right overbank velocities, 10-year flood 7-7
Figure 7-9 Comparison of reach average right overbank velocities, 2-year flood 7-8
Figure 7-10 Comparison of reach average top width for the 100-year flood 7-9
Figure 7-11 Comparison of reach average top width for the 10-year flood 7-9
Figure 7-12 Comparison of reach average top width for the 2-year flood 7-10
Figure 7-13 Comparison of reach average maximum channel depth for the 100-year flood 7-11
Figure 7-14 Comparison of reach average maximum channel depth for the 10-year flood 7-11

Figure 7-15 Comparison of reach average maximum channel depth for the 2-year flood 7-12
Figure 7-16 Comparison of equilibrium slope estimates and bed slope for the 100-year flood 7-13
Figure 7-17 Comparison of equilibrium slope estimates and bed slope for the 10-year flood 7-13
Figure 7-18 Comparison of equilibrium slope estimates and bed slope for the 2-year flood 7-14
Figure 7-19 Average regime width for the 100-year flood 7-15
Figure 7-20 Average regime width for the 10-year flood 7-15
Figure 7-21 Average regime width for the 2-year flood 7-16
Figure 7-22 Average regime depth for the 100-year flood 7-17
Figure 7-23 Average regime depth for the 10-year flood 7-17
Figure 7-24 Average regime depth for the 2-year flood 7-18
Figure 7-25 Average regime velocity for the 100-year flood 7-19
Figure 7-26 Average regime velocity for the 10-year flood 7-19
Figure 7-27 Average regime velocity for the 2-year flood 7-20

EXECUTIVE SUMMARY

Project Background

Lateral Migration Analysis Report

A variety of analyses were performed to assess the potential for future lateral migration of the Agua Fria River from New Waddell Dam to the Gila River.

Base data on the watershed, hydrology, geology, and geomorphology of the study reach establish the context for the lateral stability assessment (Chapter 2). These data were also used to define fifteen stream reaches with relatively uniform geomorphic and geographic characteristics. The stream reaches defined for the lateral stability assessment vary from natural-appearing reaches that are significantly impacted by upstream dams to highly disturbed reaches with active in-stream sand and gravel mining, channelization and floodplain encroachments. The physical and visual characteristics, landscape character, and geomorphic characteristics vary significantly over the length of the study reach.

Despite minimal historical changes in most of the Agua Fria River watershed upstream of New Waddell Dam, the hydrology of the study reach has been significantly modified over the past century due to the following:

- New Waddell Dam. New Waddell Dam was closed in 1992. Together with its historical predecessor, Carl Pleasant Dam, a.k.a. Waddell Dam, these dams have impounded most of the natural low flow runoff from the upper watershed since 1927. Therefore, the natural low flow hydrology has little impact on the existing channel morphology. Currently, floods up to the 10-year event are completely impounded behind the dam. Depending on the pre-flood storage capacity, even less frequent floods could be totally retained in Lake Pleasant.
- Other Dams. Other dams in the Agua Fria watershed include the New River Dam (New River), Adobe Dam (Skunk Creek), Cave Creek and Cave Buttes Dams (Cave Creek), McMicken Dam (Trilby Wash), and White Tanks Flood Retarding Structure (FRS) #3. These flood control dams further reduce the low flows, peak flood discharges, and sediment supply delivered to the study reach. Only 17 percent of the 2,700 square mile watershed is not controlled by dams.
- Diversions. The Arizona Canal Diversion Channel (ACDC), McMicken Dam, and the Interstate 10 channel expand the watershed area that ultimately drains to the study reach, potentially increasing the volume of water delivered to the study reach during large floods.
- Urbanization. Urbanization of the west valley downstream of New Waddell Dam has changed the natural hydrology in the study reach in conflicting ways. Urbanization typically results in more frequent runoff, higher peaks, higher flow volumes, reduced sediment supply, and "flashier" floods relative to non-urbanized watersheds, due to less infiltration and other losses. However, enforcement of storm water retention requirements in areas that were developed in the past 15 years may have reduced flood volumes and peak discharges in some watersheds. Of the 460 square miles of watershed not

controlled by dams, more than half is highly urbanized or will be within ten years.

- Return Flows. Irrigation return flows, discharge from water and wastewater treatment plants, and other point sources of manmade runoff supply water to the study reach at different rates, locations, durations and seasons than the natural water supply.

These changes in the natural hydrology of the Agua Fria River complicate the assessment of lateral stability. Clearly, historical (pre-dam & urbanization) stream behavior in response to periods of low flows is not directly applicable to future channel behavior. However, lateral channel movement during floods may be similar to historical flood responses, but will be complicated by changes in peak discharge, flow duration, and sediment supply. It is likely that floods will be the dominant cause of significant lateral channel movement in the study area.

The geologic record indicates that the Agua Fria River has experienced net degradation at about 0.02 to 0.06 mm/year over the past two million years. Given that shorter cycles of aggradation undoubtedly occurred within this time period, higher rates of degradation are implied over shorter time periods. Net degradation of the Agua Fria River created a series of older, stable terraces that effectively define the limits of long-term lateral channel movement. These geologic estimates of long-term degradation and lateral movement may be used as boundary conditions for predictions of channel response within engineering time scales. Other geologic impacts on the study reach include base level adjustments to the Gila River and land subsidence due to ground water withdrawal. Geomorphic stream classification data indicate that the Agua Fria River is subject to rapid bank erosion rates, except where the banks are stabilized by carbonate-cemented soils, bedrock, or engineered stabilization measures.

Field observations and spatial data were collected that describe the existing conditions of the Agua Fria River study reach (Chapters 3 and 4). Extensive field visits to the study area, conducted over a period of several months, consisted of walking the entire 36-mile study reach, photographing and mapping key features, and recording descriptions of existing channel conditions. Specifically, stream reaches with evidence of recent or historical lateral erosion, degradation or aggradation, human impacts or structures, and points of natural grade control were identified. These data included the following:

- Evidence of active erosion - locations of cut banks, headcuts, slope breaks, unstable bank heights.
- Evidence of lateral erosion limits – locations of bedrock and caliche outcrops, terrace boundaries, armor layers, natural grade control, permanent bank vegetation, and manmade structures.
- Evidence of channel and floodplain processes – bank heights, channel and floodplain particle sizes, bank material composition and stratigraphy, and tributary confluences.
- Evidence of human activities – active and abandoned sand and gravel mines, multi-span bridges and over-narrowed bridge sections, at-grade road crossings, levees, grade controls, bank protection, overhead and underground utility

crossings, irrigation and water supply flume and siphon crossings, residential or commercial development, illegal dumping, and a sanitary landfill.

Field sections, photograph locations, and other spatially-oriented field data were digitized into a GIS for the study reach. The field data indicate that the Agua Fria River study reach has been significantly impacted by development and in-stream mining, and that, despite historical decreases in peak discharges, it is subject to high rates of lateral channel movement during floods. The direct impacts by humans on the channel and floodplain have the potential of completely overshadowing the potential changes due to natural processes.

Historical information was synthesized to illustrate the types of channel changes that have occurred in the past (Chapter 5). Archaeological records imply that channel erosion has affected the Agua Fria River for at least 2,000 years. That is, lateral erosion is not caused solely by human impacts on the channel and watershed. Natural cycles of stream degradation, local aggradation, lateral migration, and climate change must be accounted for in development of the erosion hazard zones and the watercourse management plan. Climatic changes have been significant factors in long-term lateral erosion and channel development.

An inventory of changes to the Agua Fria River based on historical maps and aerial photographs indicates that human impacts have been substantial in the past 100 years. These impacts include construction of eleven major bridges, three dedicated at-grade road crossings, the Beardsley Canal flume, the CAP and RID siphons, numerous in-stream and floodplain sand and gravel mines, overhead and buried utility crossings, floodplain encroachments, a major sanitary landfill, residential and commercial subdivisions, recreational facilities, illegal dumping, off-road vehicle use, water treatment facilities, groundwater recharge facilities, an airport, and several major flood control dams. Additional bridges, at-grade crossings, and utility corridors are proposed for the future. The existing river bears little resemblance to its prehistoric ancestor. Except for the decrease in low flows and reduction of flood peaks due to construction of New Waddell and other dams, human impacts tend to destabilize stream channels and lead to increased rates of lateral erosion due to reduced sediment supply, increased flood flow durations, and direct excavation of the channel for mining.

Although historical changes in watershed hydrology imply that use of pre-New Waddell Dam channel change data may lead to conservative estimates of future channel movement due to decreased peak flow rates, historical data do provide the most reliable physical basis for such predictions. That is, while the future lateral movement of the Agua Fria River may be somewhat muted compared to past lateral movement, the historical data changes, at minimum, represent the upper boundary of predictions of future changes. Furthermore, given the uncertainty in flood storage conditions in Lake Pleasant, the potential for large, sustained, erosive outflows from New Waddell Dam still exists. The scale of lateral erosion during such a large flood would be analogous to the scale of erosion during historical, pre-New Waddell Dam floods. Therefore, measurements of long-term and single event lateral and vertical erosion were made for the Agua Fria River from historical maps and aerial photographs to establish a baseline of potential channel movement.

Historical aerial photographs for the entire study reach were available as early as 1949[1] and extended through 1999. Thirteen individual years of coverage for various extents of the river were evaluated, digitized and catalogued. Historical topographic maps dating to 1903 were available for most of the study reach, although 1957/1962 was the earliest topographic coverage of the entire reach. Six individual years of topographic coverage were used to estimate historical vertical changes along the river. GLO survey data extended the record of channel position back to the late 1800's. The types of channel changes documented by the historical maps and aerial photographs included channel avulsions, bank collapse, channelization, scour, headcutting, channel width changes, formation of multiple channels, braiding, and sediment deposition.

Historical channel width and channel position have changed significantly during the past 100 years. Overall, the average channel width decreased from 1,696 feet in 1953 to about 968 feet in 1999, except in the levee reach where the channel was artificially widened during levee construction. Despite this historical narrowing trend, significant lateral movement was observed. The maximum recorded channel movement during the period of record was more than 2,200 feet. During the 1980 flood alone, the channel near Indian School Road widened by more than 1,100 feet. Avulsions were the primary mechanism for the largest long-term channel movements in the study reach. Bed elevations fluctuated throughout the study reach, with an overall decrease (degradation) during the period of record. The maximum measured degradation between 1903 and 1995 was 17 feet, with most of the degradation occurring after 1957. No reaches experienced net aggradation during the period of record, including the reaches nearest the Gila River confluence. The scale of lateral channel change observed on historical maps and aerial photographs is not significantly different than the scale of the changes estimated by interpreting the age and characteristics of geomorphic surfaces along the river corridor. The rate of lateral movement has been fastest on the youngest, less indurated surfaces and slowest along the margins of the older, more well indurated surfaces. Therefore, the older terrace margins serve as a practical limit for predicted future rapid channel change, although the older terraces are also subject to (slower) lateral erosion where abutted by the main channel.

Mathematics-based engineering and geomorphic analyses were used to predict future channel behavior and to assess the potential for lateral channel migration (Chapter 6). Hydraulic data used in the mathematical analyses were obtained from the HEC-RAS model prepared by Kimley-Horn & Associates (KHA). Modifications were made to the KHA HEC-RAS model to better depict the full range of discharges considered, to focus on bankfull discharge conditions, and to modify the input data for use in the geomorphic assessment. Sediment sampling data for the study reach were provided by KHA from which representative sediment distributions were selected for each of the reaches defined for the lateral stability assessment.

Bankfull discharge varies significantly within the study reach, but averages about 14,000 cfs, which has a post-New Waddell recurrence interval of about the 15-year event in the Upper Reach, a 20-year event in the Middle Reach, and a 10-year event in the Lower Reach. The average bankfull characteristics for the main (low flow) channel are 700 feet wide and 7 feet deep, with a velocity of about 5 feet per second. The main channel appears to be adjusted to the geometry left by the 1980 flood, the most recent large discharge to be conveyed through the study reach. The expected

[1] 1934 coverage was available for the reach downstream of Grand Avenue.

channel pattern is braided, given the existing slope, sediment characteristics and dominant discharge. The actual channel pattern was a compound form, with a braided high flow channel and a slightly sinuous to sinuous low flow channel. Post-New Waddell Dam discharges from the urbanizing watershed downstream of the dam may have caused the formation of the more sinuous low flow channel.

Regime geometry equations indicate that the Agua Fria River is over-widened and under-deepened, and will continue to narrow and deepen in the future. Concentration of floods within a narrower, deeper channel will result in higher flow velocities, erosion of the main channel banks, and continued long-term degradation, but decreased potential for avulsions, except during the largest floods. Flood velocities in the main channel generally exceed allowable velocity limits for non-cohesive sediments, even for the 2-year flood. However, where the channel abuts more cohesive, older surfaces the channel velocities generally are less than the allowable velocity thresholds. Overbank velocities are generally considered erosive, especially for overbank areas dominated by finer-grained sediments and areas of local flow concentrations.

The longitudinal profile and equilibrium slope analyses indicate that the Agua Fria River will continue to degrade during large floods. During smaller floods, the middle reaches (Reach 4-10) will be stable or will aggrade slightly, according to the equilibrium slope equations. These predictions do not account for the effects of in-stream sand and gravel mining, which tends to accelerate long-term degradation and induce headcutting. In general, the bed material of the Agua Fria River is not large enough to form an armor layer that would prevent long-term degradation. Predicted single-event scour depths are moderate, ranging from about one foot for the 2-year event, to about five feet for the 100-year event. The mathematical analyses indicate that lateral erosion and degradation will occur during large floods, but that minimal erosion will occur during small floods, except where the channel has been disturbed by human activity. A large flood is one that has a large peak or a large volume. Therefore, it is possible to have a flood with a smaller peak and large volume cause more lateral erosion than a flood with a large peak and a small volume. For example, extended releases from New Waddell Dam are likely to have a long duration, but have a recurrence interval of about a 10-year (post-dam) event. A 10-year event without prolonged releases from New Waddell Dam is less than the bankfull discharge and would probably result in minimal lateral channel change.

The following erosion hazard zones were defined based on the methodologies and results summarized in the Lateral Migration Report (Chapter 8):

- Severe Erosion Hazard Zone
- Lateral Migration Erosion Hazard Zone
- Long-Term Erosion Hazard Zone

The severe erosion hazard zone is comprised of the active stream channels and the channel margin areas likely to be eroded during a single 100-year flood, or the area likely to be removed if the bank angle were to be reduced to the natural angle of repose. Areas within the limits of existing sand and gravel mining operations were considered to be in the severe erosion hazard zone, since no engineered erosion protection was observed near the mines during field visits.

The lateral migration erosion hazard zone consists of the channel margin area likely to be eroded by a "typical" series of floods over a sixty year period, plus the erosion that

would be caused by a 100-year flood. The lateral migration erosion hazard zone also includes the natural channel movement due to geomorphic processes such as meander migration or channel avulsion. The lateral migration erosion hazard zone includes portions of the floodplain that had been occupied by the main channel during the period of historical record, unless clear and convincing evidence of future stability was available. In general, the lateral migration erosion hazard zone included areas outside the regulatory floodway of the Agua Fria River. The lateral migration erosion hazard zone is recommended for adoption as the regulatory erosion zone for the watercourse master plan.

The long-term erosion hazard zone consists of the channel margin area defined by geologic evidence of channel movement over the past 100 to 1,000 years, and represents expected or potential channel movement over the next 60 to 1,000 years in the future. The boundary of the expected long-term erosion hazard zone envelopes the results of all the predictive methods used to assess channel stability, in addition to application of engineering judgment and interpretation of the site geomorphology. Portions of areas mapped as older geomorphic surfaces, but adjacent to active channels and floodplains, were generally included in the long-term erosion hazard zone. Areas protected by engineered levees or other bank protection were considered the outside limit for the long-term erosion hazard zone.

The following management practices were recommended to minimize future lateral erosion and promote safe development of lands adjacent to the Agua Fria River corridor:

- Adopt the recommended lateral migration erosion hazard zone for floodplain management purposes.
- Amend the regional master plan to avoid structural improvements such as bank stabilization within the erosion hazard boundary limits, except to protect existing structures needed for public safety such as bridges or utility crossings, or where the channel threatens to move outside of the established erosion corridor.
- Regulate all new development within the severe and lateral migration erosion hazard zones by requiring a special use permit. To obtain a special use permit, reach-specific studies and regulatory requirements must be completed by the developer or agency. The studies include analyses of impacts on adjacent parcels, holding the District harmless for future flood-related problems, and consideration of environmental impacts.
- Vegetation Management. Within any of the erosion hazard zones, disturbance of bank and floodplain vegetation is discouraged. Where disturbed, specific mitigation and erosion prevention measures are required.
- Regulation of In-Stream Sand and Gravel Mining. Sand and gravel mining is likely to result in channel degradation and increase bank erosion if it is not properly engineered and managed. Standards for extraction, processing, transport, and reclamation proposed in the Watercourse Master Plan should be followed.
- Future Monitoring. Channel stability should be monitored periodically to assess impacts of floods, to determine whether erosion hazard zones should be

updated, and to document continued channel change for application to other stream systems in Maricopa County.

The results of the lateral migration analysis were compared to previously completed channel stability assessments of the Agua Fria River (Chapter 9). Like the previously completed studies, this analysis concluded that human impacts, especially in-stream sand and gravel mining and impoundment of natural runoff in upstream reservoirs, have been the dominant cause of channel change along the Agua Fria River. High rates of single-event and long-term erosion should be expected, except where structural flood control measures are provided.

1. INTRODUCTION

The Flood Control District of Maricopa County (FCDMC) is preparing a watercourse master plan for the Agua Fria River. The watercourse master plan was prepared by a team of consultants led by Kimley-Horn & Associates, Inc. (KHA), who identified and evaluated structural and non-structural flood control alternatives to protect properties within and adjacent to the regulatory floodplain from flood damage. JE Fuller/Hydrology & Geomorphology, Inc. (JEF) prepared this lateral stability assessment of the Agua Fria River to support the watercourse master planning process.

1.1 Study location

The Agua Fria River Watercourse Master Plan study area is located within the corporate limits of the Cities[1] of Peoria, Surprise, El Mirage, Phoenix, Avondale, Goodyear, Litchfield Park, the Town of Youngtown and portions of unincorporated Maricopa County (Figure 1-1). The study reach extends from New Waddell Dam (Lake Pleasant) to the confluence with the Gila River, a distance of approximately 34 river miles.

1.2 Objectives

Rivers are dynamic features, constantly adjusting their banks, beds, and floodplains in response to floods or human activities along the river corridor. The primary objective of this report was to evaluate the horizontal and vertical stability of the Agua Fria River. The stability assessment summarized in this report provides part of the technical support for the project team's evaluation of the benefits of and opportunities for non-structural flood control and/or the need for structural flood control.

1.2.1 Stability Concepts

The concept of stability can have several meanings. For a natural river, the definition of stability must include an allowance for the river's natural tendency to erode its banks during floods, meander, and adjust its geometry in response to changes in climate and watershed characteristics. For an urban river, the definition of stability must include the interface of the river's natural tendencies with human perception of those tendencies. For example, most people perceive a river to be unstable when some structure, such as a bridge or home site, is threatened by erosion, regardless of whether that erosion is a natural process or whether the erosion has been caused by some non-natural disturbance of the river or watershed. This report evaluates the Agua Fria River's historical (i.e., natural) erosion history relative to human impacts on the stream system and watershed so that the project team can develop a watercourse master plan that tempers human expectations for river stability with the physical realities of a dynamic river system.

1.2.2 Lateral Stability

Lateral stability exists when the river channel moves within expected limits. The primary objectives of the lateral stability assessment were to define the areas within the river corridor that are likely to become part of an active channel of the Agua Fria River in the future, and to identify the causes of lateral movement of the river.

[1] Sun City is not incorporated.

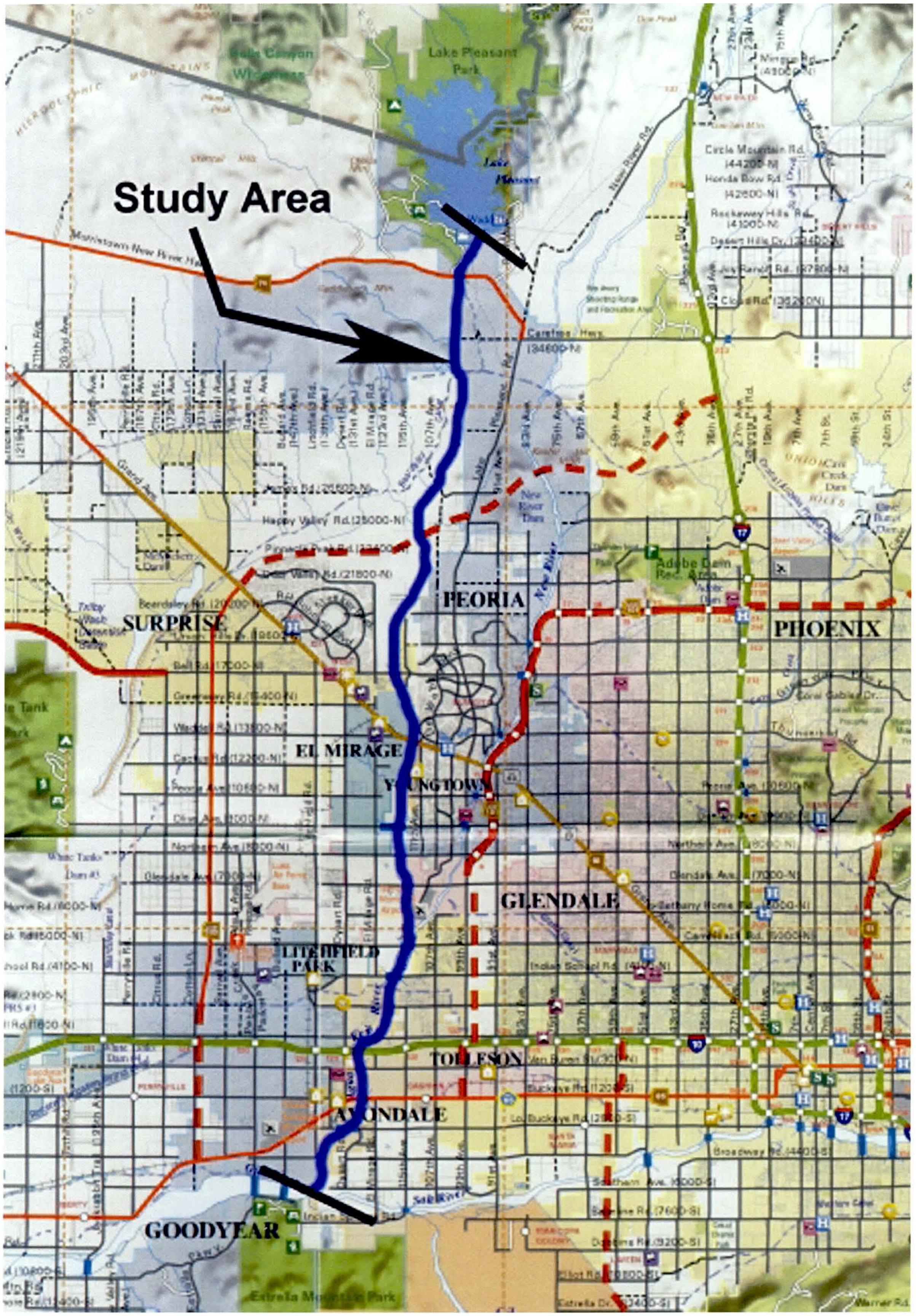

Figure 1-1 Study area location map

1.2.3 Vertical Stability

Vertical stability exists when the river has no net change in the stream bed elevation over the design life of the watercourse master plan or the design life of structures built near the river corridor. The primary objective of the vertical stability assessment was to identify historical trends in stream bed elevation, as well as the causes of those trends. A secondary objective of the vertical stability assessment was to determine the scale of potential vertical changes so that appropriate planning measures could be incorporated in the watercourse master plan.

The Watercourse Master Plan identified and evaluated traditional structural and non-structural flood control alternatives based in part upon the results of the lateral migration assessment. This report summarizes the methods used to evaluate the potential for lateral and vertical channel instability within the study area.

1.3 Data Sources

The methods used to assess the potential for lateral channel migration in the study area relied on a variety of existing information, field data, and new analyses. Existing information was collected from the following key sources:

- Arizona Geological Survey (AZGS)
- Arizona State Land Department (ASLD)
- Arizona State University – Geology Department (ASU)
- Federal Emergency Management Agency (FEMA)
- Flood Control District of Maricopa County (District)
- U.S. Army Corps of Engineers – Los Angeles District (USACOE)
- U.S.D.A – Soil Conservation Service (SCS or NRCS)
- U.S.D.A – Agricultural Stabilization Conservation Service (ASCS)
- U.S. Geological Survey – Water Resources Division (USGS Water Resources)
- U.S. Geological Survey – EROS Data Center (USGS - EROS)
- U.S. Bureau of Land Management (BLM)
- U.S. Bureau of Reclamation (BUREC)
- Kimley Horn & Associates (KHA)

Existing information collected for the study included the following:

- Historical and recent aerial photographs
- Historical and recent topographic maps
- Historical survey records and channel descriptions
- Published and unpublished engineering reports
- Published detailed soils mapping
- Published and unpublished mapping of surficial geology
- Bridge and roadway as-built construction plans
- Regional and local streamflow gaging records
- Regional and local precipitation records

Field data collected for the streams included the following:

- Descriptions of channel bed and bank conditions
- Ground photographs of significant channel features
- Surface sediment samples (sieve analyses)
- Descriptions of watershed conditions
- Descriptions of significant tributaries

A list of references used for the lateral stability assessment is provided in Chapter 11. A glossary of key terms is provided in Chapter 12.

1.4 Limitations and Assumptions

Any technical analysis is limited by the data available, the contracted scope of services, and the assumptions of the methodologies used. For the Agua Fria River Watercourse Master Plan, the following general limitations apply:

- Period of Record. Streamflow data are available for only a portion of the period of interest for the study area (Chapter 2). Collection of additional streamflow data in the future could improve the accuracy of the hydrologic and geomorphic analyses, particularly so that changes in hydrology caused by construction of New Waddell Dam and urbanization of the lower watershed could be better quantified.
- Hydrologic Data. Few streamflow gaging data were available for the post-New Waddell Dam period. Estimates of the 2-, 10-, and 100-year discharges were obtained from hydrologic modeling performed by the U.S. Army Corps of Engineers, as described in Chapter 2. Actual flow rates and frequencies may be significantly different than modeled predictions.
- Hydraulic Modeling. HEC-RAS base models prepared by the project team were originally created to depict the 100-year flood characteristics. As described in Chapter 6, some modifications of the model input were required prior to using the models to assess lateral channel stability, particularly for flow rates other than the 100-year peak discharge. Other modifications of the model input could not be made without additional survey and mapping, which were not part of the scope of services. Field calibration of the HEC-RAS model for the high frequency flow events could improve the accuracy of the hydraulic data used in the lateral stability assessment.
- Topographic Mapping. Detailed topographic mapping for the study reach was taken from previous projects completed by others. Given the degree of encroachment, excavation, and flood-caused channel changes, new topographic mapping could improve the accuracy of the technical analyses described in this report. The topographic data used in this study date to 1988 for the reach from Jomax Road to Waddell Dam and from Indian School Road to the Gila River, and to 1995 for the reach between Jomax and Indian School Roads.
- Sediment Continuity Modeling. Sediment modeling was performed for the study reach by others using HEC-6, a one-dimensional hydraulic model. The applicability of the results of the HEC-6 modeling to the study area is discussed in Chapter 6.
- Geotechnical Data. No geotechnical data were available for the study area, except for limited details of boring logs provided on as-built construction plans for some of the structures located along the river corridor, and shallow surface sieve samples taken for the HEC-6 modeling. Extensive geotechnical investigations of the banks, floodplains and channels could improve the understanding of bank erosion processes and expected future lateral channel movement.
- Gila River Floodplain. The downstream end of the Agua Fria River study reach lies within the geologic and FEMA floodplain of the Gila River. For this study only those flood and erosion hazards associated with the Agua Fria River were evaluated. It is likely that significant erosion hazards from the Gila River impact this reach, and should be included in future flood control master plans.
- Future River Conditions. Continued in-stream mining of the Agua Fria River, construction of additional bridges, and continued urbanization will continue to change the geomorphic processes along the river relative to the conditions at the time of this study, and may necessitate periodic update of the conclusions of this report. In general, continued destruction of the natural river corridor will accelerate erosion and instability.

- Scale of Analysis. This study considered approximately 34 miles of river corridor. It is possible that more detailed evaluation of specific sites could improve the accuracy of the predictions of future channel behavior at those specific sites.

1.5 Report Overview

This report summarizes the methods used to evaluate the potential for lateral and vertical channel migration within the study area. Specific chapters in this report cover the following topics:

- Chapter 1 – Introduction: Project overview and introductory information.
- Chapter 2 – Study Area Description: description of the study area watershed, geologic setting, hydrology, stream classification, and definition of stream reaches used for the study.
- Chapter 3 – Field Data: Description of field data, conditions observed along the stream corridor, examples of evidence of stability and erosion, and photographs of key features.
- Chapter 4 – Geographic Data: Geographic descriptions of the study reach, spatially located features, and descriptive characteristics of the river.
- Chapter 5 – Historical/Temporal Data: Chronology of channel change, including description of historical and prehistoric changes in channel conditions, lateral and vertical channel changes, and changes in channel shape or pattern.
- Chapter 6 – Mathematical Data: Discussion of geomorphic methods of lateral stability assessment, including field data, visual assessment techniques, geomorphic mapping, longitudinal profile, engineering approaches to assessing lateral stability such as allowable velocity, equilibrium slope, armoring, scour, sediment continuity modeling (HEC-6), Lane's Relation, regime equations, and hydraulic geometry.
- Chapter 7 – Trend Analysis: Discussion of expected channel processes and erosion during Pre-Waddell Dam, Pre-New Waddell Dam, and Post-New Waddell Dam, as well as evaluation of expected future responses to likely future changes in watershed conditions relating to water and sediment supply.
- Chapter 8 – Erosion Hazard Zones: Discussion of the development and application of erosion hazard management zones.
- Chapter 9 – Comparison With Other Studies: Discussion of previously completed erosion hazard analyses, sediment transport studies, and mining impact studies relative to the results of this study.
- Chapter 10 – Summary and Recommendations
- Chapter 11 – References
- Chapter 12 –Glossary of technical terms used in this report.

2. STUDY AREA

2.1 Overview

This chapter provides basic information about the following characteristics of the Agua Fria River Watercourse Master Plan study area that affect the lateral stability assessment:

- Watershed Description
- Geologic Setting
- Hydrologic Data
- Stream Classification

The interrelated watershed, geologic, and hydrologic characteristics of a stream combine to determine its unique geomorphology. These types of data for the Agua Fria River were used to define specific stream reaches for more detailed analyses, as described in the second part of this chapter.

2.1.1 Watershed Description

The lateral stability of the Agua Fria River is directly impacted by the watershed drainage area, human activities, and other physiographic characteristics such as the vegetative cover, elevation, the type of development and land use. Watershed characteristics for the Agua Fria River study area are described below.

2.1.1.1 Drainage Area

The Agua Fria River drains a large portion of central Arizona. The Watershed Map (Exhibit Book) shows the drainage basin boundaries identified in the U.S. Army Corps of Engineers' *Hydrologic Evaluation of Impacts of New Waddell Dam on Downstream Peak Discharges in the Agua Fria River* (USACOE, 1995). The drainage areas and 2- and 100-year discharges from this report at several key locations are summarized in Table 2-1.

Table 2-1 Watershed Characteristics: Drainage Area and Peak Discharge (Post-New Waddell Dam)

Concentration Point	Drainage Area* (mi^2)	2-Year Peak Q (cfs)	100-Year Peak Q (cfs)
Upstream of New Waddell Dam	1459	0	135,000
Downstream of New Waddell Dam	0	0	9,000
@ Bell Road	171	1,200	37,500
@ Grand Avenue	183	780	34,500
Upstream of the New River	231	820	30,000
Downstream of the New River	392	5,500	54,400
@ Interstate 10	474	5,400	52,000
@ Buckeye Road	485	5,300	50,900
@ Confluence with the Gila River	485	5,000	48,200

Notes:
* Effective drainage area. Does not include area controlled by dams.
Discharges decrease in the downstream direction due to attenuation from overbank storage.
Source: Table 1, USACOE, 1995.

The effect of dams and diversions within the Agua Fria River watershed complicates the otherwise simple concept of drainage area. Besides the New Waddell Dam, dams within the drainage area include New River Dam on the New River, Adobe Dam on Skunk Creek, Cave Buttes Dam (and Cave Creek Dam) on Cave Creek, Dreamy Draw Dam on Dreamy Draw, McMicken Dam on Trilby Wash, and the White Tanks Flood Retarding Structure (FRS) No. 3 along the base of the eastern flank of the central White Tank Mountains. Therefore, significant portions of the drainage natural drainage area downstream of New Waddell Dam are regulated and/or effectively cut off during many flood events. Prior to construction of any of these dams, the drainage area of the Agua Fria River downstream of the New River was estimated at about 2,243 square miles (mi^2), and 2,388 mi^2 at the Gila River. Comparison of these numbers to the drainage areas listed in Table 2-1 shows the dramatic decrease in effective drainage area, despite the additional drainage area added by the Arizona Canal Diversion Channel (ACDC) and Interstate 10 (I-10) diversions. The ACDC and I-10 diversions, along with flow from Cave Creek which is diverted to the ACDC, add about 310 mi^2 to the drainage area of the Agua Fria River at its confluence with the Gila River.

2.1.1.2 Physiographic Setting

The Agua Fria River drains a 2,388 mi^2 area extending from the Black Hills above Verde Valley to its confluence with the Gila River at the foot of the Estrella Mountains (Watershed Map in Exhibit Book). The Prescott, Bradshaw, Wickenburg, Hieroglyphic and White Tank Mountains bound the western edge of the drainage basin, while the eastern margin is loosely defined by the Black Hills, New River, and Phoenix Mountains.

The Agua Fria basin above Waddell Dam drains an area of about 1460 mi^2 and is characterized by low relief basalt capped mesas at elevations of 3,000 to 5,000 feet and steep, granite and metamorphic mountains rising to elevations of 7,000 feet, separated by a few large alluvial basins filled by Tertiary-aged sediment. This area lies within the Transition Zone Physiographic Province, also referred to as the Central or Mexican Highlands Province (Figure 2-1). The mountainous topography of this province (3,000 to 7,000 ft.) divides the Colorado Plateau on the north from the Basin and Range province of southwestern Arizona. The Basin and Range Province is characterized by a series of narrow, north- and northwest-trending, linear mountain ranges separated by valleys filled with alluvium eroded from the mountains. The Transition Zone is characterized by "tight-clustered ranges and narrower, shallower and less numerous basins" (Chronic, 1989) than the Basin and Range, but also has some features similar to the Colorado Plateau. Within in the study area, the Agua Fria River flows out of the Transition Zone and cuts through the Phoenix Basin. In this report, the Phoenix Basin refers to the area generally bounded by the Bradshaw Mountains to the north, the Mazatzals and Superstitions to the east, the Estrella Mountains to the south, and the White Tank Mountains to the west.

Downstream of Lake Pleasant and the New Waddell Dam, the Agua Fria River crosses through the Sonoran Desert of the Phoenix Basin which lies within the Basin and Range province. This province is characterized by 2,000- to 4,000-foot high rugged bedrock mountain ranges surrounded by gently sloping aprons of eroded material, called piedmonts. These desert piedmonts consist of series of coalescing alluvial fans typically ranging from 1,000 to 2,000 feet in elevation. The mountain ranges are comprised of metamorphic rocks, granitic intrusions, and volcanic flows. The alluvial surfaces generally slope away from the mountain "roots" and are comprised of coarse alluvium shed from the adjacent bedrock ranges. The gentle topography of western Phoenix Basin is typical of the large alluvial basins of southwestern Arizona.

The major tributaries to the Agua Fria River include the New River, Skunk Creek, and Cave Creek. The New River, which drains an area of about 640 mi^2, generally flows southward for 40 miles from its source in the New River Mountains to its confluence with the Agua Fria River, which is located about 10 miles north of the Gila River. Skunk Creek drains an area of about 112 mi^2 before joining with the New River near Sun City, upstream of the New River-Agua Fria

River confluence. The headwaters of Skunk Creek flow south from basalt capped mesas across alluvial deposits of the central Phoenix Basin. Cave Creek originates in the mountains north of the Town of Cave Creek, flows into the Cave Buttes Dam impoundment area and through urbanized Phoenix where it enters the ACDC. The ACDC diverts Cave Creek from its historical course through central Phoenix to Skunk Creek.

Vegetation in the watershed ranges from Ponderosa Pine forest at the highest elevations of the Bradshaw Mountains to the Sonoran Desert assemblage dominated by cacti, palo verde, and creosote downstream of New Waddell Dam. Specific impacts of vegetation in the study reach on channel stability are discussed in Chapters 3 and 5. As discussed below, much of the downstream watershed has been affected by human activity.

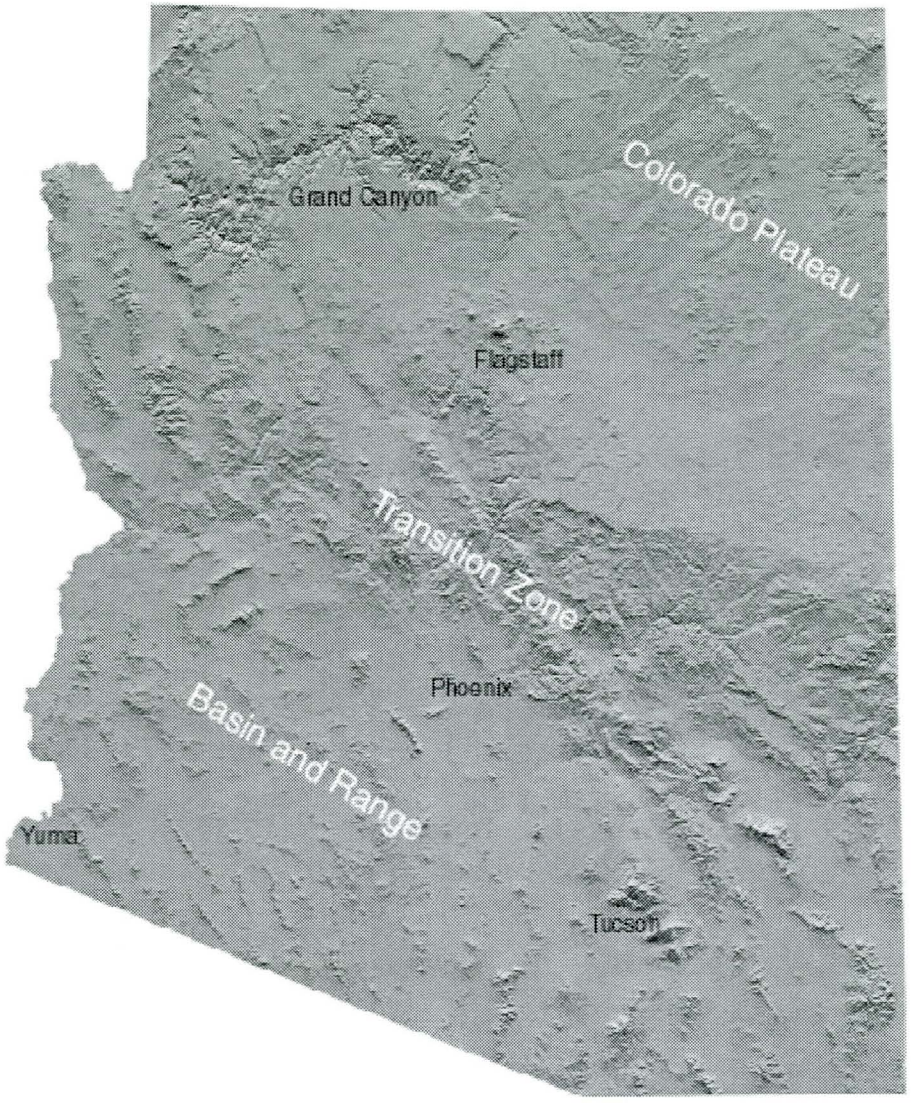

Figure 2-1 Physiographic Provinces of Arizona

2.1.1.3 Human Activities

The Agua Fria River watershed downstream of New Waddell Dam has been significantly impacted by human activity over the past century. A brief description of these impacts follows.

Agriculture. Much of the lower Agua Fria watershed was cultivated by European settlers since well before the beginning of the 20th century. Water for irrigation was supplied both by the Agua Fria River itself as well as from the Salt and Verde Rivers via an elaborate system of canals. These activities withdrew water from the river, depleting the normal low flows and creating a normally dry riverbed. The farm fields also encroached into the river floodplain to take advantage of the fertile floodplain soils deposited by the river, effectively narrowing the natural floodplain and increasing flood stages and velocities in the main channel.

Urbanization. The watershed downstream of the dam has experienced significant urbanization during the last 50 years. Areas historically irrigated for agriculture, as well as large additional undeveloped areas, have been replaced by dense residential and commercial development. The earliest urbanization consisted of small service centers for agriculture, such as the historical towns of Avondale and El Mirage. Following World War II and accelerating ever since, large areas of residential and commercial development spread across the watershed as the cities of Phoenix, Glendale, Peoria, Sun City, and Avondale grew rapidly. Today, most of the watershed downstream of about Beardsley Road is urbanized. Many of the remaining non-urbanized areas are currently planned for urbanization. In the near future the entire lower watershed is likely to be urbanized.

Construction of Dams. In 1927, the Carl Pleasant Dam (later renamed Waddell Dam) was completed. This dam was primarily a water storage facility and as such did not perform dedicated flood control for the lower Agua Fria. However, the dam did effectively prevent most of the low flows and frequent floods from passing the dam. The USACOE indicates that flows less than the 25-year flood were affected by the dam (USACOE, 1988, Plate 4). However, this same report indicates that floods greater than the 25-year event generally passed through the dam with little effect on peak discharges. The dam did, however, have an effect on sediment passing through the reservoir (Figure 2-2). While much of finer-grained suspended sediment load would have passed through the reservoir, larger bed-load sediments were trapped. Aerial photographs from 1977 at very low impoundment levels in the lake show a significant delta formed within the pool area.

In 1992, the Bureau of Reclamation built the 300-foot high earthen New Waddell Dam just downstream of the old Waddell Dam. New Waddell Dam was constructed to store Central Arizona Project (CAP) water from the Colorado River, in addition to the Agua Fria River runoff historically collected by the old Waddell Dam. The new dam can store 1.1 million acre-feet of water, nearly ten times the 157,600 acre-feet capacity of the old dam. The increased storage capacity greatly reduced the likelihood of outflows from the dam to the downstream reaches of the Agua Fria River. Specifically, floods from the upper watershed up to the 25-year event will not pass the dam. Moreover, the maximum release during the 25- to 100-year events is 9,000 cfs, as opposed to 90,000 to 135,000 cfs, respectively, for the old dam (USACOE, 1995). The watersheds downstream of the New Waddell Dam now generate the largest expected peak flow rates in the study reach, although the highest flood volumes are still generated by outflows from the dam.

The lower watershed also contains numerous other dams which regulate discharge on various tributaries. The largest tributary watershed, the New River, has three large dams on each of its primary drainages: New River Dam on New River, Adobe Dam on Skunk Creek, and Cave Buttes Dam on Cave Creek. Two additional earthen dams are located on the western side of the watershed that control runoff from large areas west of the Agua Fria River. McMicken Dam is located on Tribly Wash, and discharges to the Agua Fria River through the McMicken outfall channel. The White Tanks Flood Retarding Structure (FRS) No. 3 flanks the central portion of

the White Tank Mountains, an area which historically drained to the Agua Fria River, but now is completely impounded behind the FRS.

Diversions. The runoff from McMicken Dam enters the Agua Fria upstream of Bell Road via the McMicken Outfall Channel, a long floodway channel which intercepts additional drainage area that historically entered the Agua Fria further downstream. Similarly, the Arizona Canal Diversion Channel (ACDC) diverts runoff from Cave Creek and a few smaller washes draining the North Phoenix Mountains into Skunk Creek, which in turn combines with the New River. In the lower watershed, a channel along the north side of I-10 collects and diverts runoff from portions of west Phoenix that historically joined lower Cave Creek or flowed directly into the Salt River.

Sand and Gravel Mining. Active sand and gravel mining has been taking place within the river channel and its floodplain since at least 1949, according to historical aerial photographs of the study reach. The consequence of in-stream mining is that a significant volume of sediment has been and continues to be extracted from the Agua Fria River. In addition, the completion of the New Waddell Dam significantly decreased the sediment supply (Figure 2-2). These two factors increased the potential for significant degradation, or lowering, of the bed of the Agua Fria River. Degradation of the Agua Fria has been noted in other studies as well (SLA, 1983).

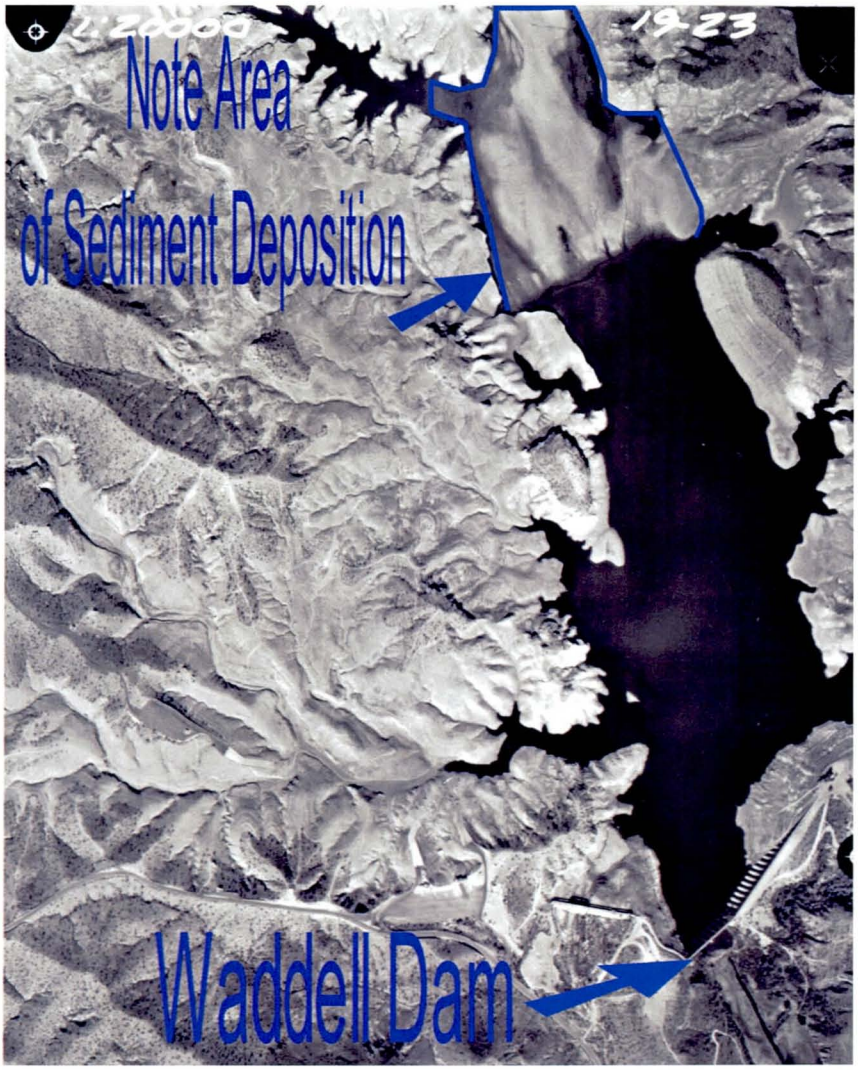

Figure 2-2 Lake Pleasant, 12-5-77

Channelization. In the mid-1980's, a 4.4 mile reach of the Agua Fria River between Indian School Road and Buckeye Road was channelized between fourteen feet high soil cement levees constructed by the U.S. Army Corps of Engineers and the Flood Control District of Maricopa County. Partial (one side) channelization was also constructed for about two miles along the right (west) bank downstream of Buckeye Road and two miles along the left (east) bank upstream to the New River confluence. Soil cement grade control structures were also constructed within the fully channelized reach fixing the horizontal and vertical position of a portion of the lower Agua Fria River. The locations of other channelization features such as bank protection are shown in the Exhibits Maps Book.

Construction of Bridges. There are presently fifteen bridges that cross the Agua Fria River, including 13 road bridges and 2 railroad bridges. Six of the roadway bridges and one railroad bridge completely span the soil cement channelized reach of the river. The Beardsley Canal Flume also completely spans the river. The remaining six bridges constrict the river's historical width to some extent. Table 2-2 lists the Agua Fria River bridges, the bridge widths, and the historical width of the floodplain prior to construction of the bridge. Note that most of the bridges severely constrict the floodplain. At least two more major crossings are planned for the near future, including the Loop 303 crossing near the Lone Mountain Road alignment and the new Estrella Roadway crossing at the Happy Valley Road alignment.

Table 2-2 Summary of Bridge Locations, Widths, and Approximate Dates of Completion

Bridge	River Mile	Historical Floodplain Width (feet)	Bridge Opening Width (feet)	Date of completion (year)	Date Rebuilt (year)	Comments
SR 74	33.0	610	410	1965-77		
Beardsley Flume	29.6	1280	1280	1927?		
Bell Road	19.0	4000	600/1100	1964-67	1982	Old bridge collapsed in 1980
AT&SF RR	16.5	5600	480 + 150	1895		Main bridge + relief bridge
Grand Ave.	16.5	5600	465/520 + 150/24	1919, 1949: Rebuilt 1923: overflow bridge Widened 1946	1992	Main bridge + relief bridge
Olive Ave.	13.5	3445	1500	1985-88		
Glendale	11.4	7950	600	1972-77		
Camelback	9.2	9150	1725	1983-85		
Indian School Rd.	8.0	7660	1623/1460	1970	1983	Old bridge collapsed in 1980; Narrowed by channelization; Total span remains wider
McDowell	5.7	5280	1150*	1985-88		Channel width, bridge at skew
I-10 West	5.3	5300	1150*	1980		1980 - left approach not completed at time of flood. Flow around left end of bridge while under construction
I-10 East	5.3	5300	1150*	1980		1980 - left approach not completed at time of flood. Flow around left end of bridge while under construction
Van Buren	4.8	5210	1150*	1985-88		
SPRR	3.8	7200	1150*	1910		
Buckeye Rd	3.7	7200.	1150*	1967-77		A.k.a. MC 85

Notes:
* = location in channelized reach #/# = old/new bridge widths (Bridge Opening Column)

2.1.1.4 Summary

The Agua Fria River watershed is a moderately large drainage basin draining a large portion of central Arizona. It drains rugged mountainous areas of the Transition Zone before crossing the Phoenix Basin on its way to the Gila River. Construction of the New Waddell Dam and other major dams in the watershed as well as urbanization and diversions have greatly influenced the hydrologic regime of the river in the study reach. Accelerated human activity, such as sand and gravel mining, construction of bridges, utility crossing, channelization, and floodplain development, especially in the last 30 years, has greatly impacted the natural condition of the Agua Fria River downstream of the New Waddell Dam. These factors are likely to influence the nature, magnitude, and location of erosion hazards in the study area.

2.1.2 Geologic Setting

Understanding the overall geology of the study area is fundamental to understanding and predicting the types and magnitude of channel processes such as lateral migration. The geologic history of the area also establishes a context within which more recent channel changes can be examined. The geologic setting of the study area is discussed below.

2.1.2.1 Geologic History

The Agua Fria River Watercourse Master Plan study area is located in the Basin and Range and Transition Zone Physiographic Provinces (Figure 2-1). The headwaters of Agua Fria River are within the Transition Zone, although most of the study reach is within the Basin and Range Province. The Basin and Range Province is characterized by a series of narrow, north- and northwest-trending, linear mountain ranges separated by valleys filled with alluvium eroded from the mountains. The Transition Zone is characterized by "tight-clustered ranges and narrower, shallower and less numerous basins" (Chronic, 1989) than the Basin and Range, but also has some features similar to the Colorado Plateau.

The present configuration of the Agua Fria River drainage basin is a result of long-lived and complex geologic processes, which have exposed rocks from two very different time periods in the modern landscape. Ancient 1.8 to 1.4 billion year old (Ga) granites and metamorphic rocks formed the original landmass of Arizona and comprise the mountains surrounding the study area (See the Watershed Geology Map in Exhibit Maps Book). About 1.4 billion years elapsed between formation of the initial Arizona landmass and formation of the next youngest rocks, the volcanic rocks which crop out east of Lake Pleasant and north of the Union Hills. This 1.4 billion year time gap, called an unconformity, requires that the geologic history of the study area be interpreted using geologic information from other parts of Arizona. The following discussion of the geologic history of the Agua Fria River refers to geologic periods and epochs. Table 2-3 provides the names of these periods of geologic time scale for the reader's reference.

Table 2-3 The Geologic Time Scale

Era	Period	Epoch	Time (Years Before Present)
Cenozoic	Quaternary	Holocene	0-10,000
		Pleistocene	10,000-2 ma[1]
	Tertiary	Pliocene	2-5 ma
		Miocene	5-24 ma
		Oligocene	24-38 ma
		Eocene	38-55 ma
		Paleocene	55-63 ma
Mesozoic	Cretaceous		63-138 ma
	Jurassic		138-205 ma
	Triassic		205-240 ma
Paleozoic	Permian		240-290 ma
	Pennsylvanian		290-330 ma
	Mississippian		330-365 ma
	Devonian		365-410 ma
	Silurian		410-435 ma
	Ordovician		435-500 ma
	Cambrian		500-570 ma
Proterozoic (Precambrian)	Late Proterozoic		570 ma -1.8 Ga
	Early Proterozoic		1.8 – 4.6 Ga
Note: ma = million years			

Proterozoic (1.8 to 1.4 Ga[1]). Proterozoic-aged rocks are evenly distributed throughout the Agua Fria drainage basin and are found in the peaks of the Phoenix, South, White Tank, Hieroglyphic, Bradshaw, and New River Mountains, as well as in the Union Hills (See the Watershed Geology Map in Exhibit Maps Book). These metamorphic rocks formed during Early Proterozoic (~1.8-4.6 Ga) volcanism, sedimentation, and deformation (Livingston and Damon, 1968; Silver, 1978). These processes were driven by subduction of oceanic crust beneath what is now western North America. A modern analogy of this tectonic setting is the volcanic island chain of Japan, which is moving westward on the Pacific Plate. This plate is diving beneath the continental landmass of Russia. Eventually, Japan will "wedge up" against Russia and become part of the continental landmass because it is too buoyant to be dragged underneath. Similarly, continued convergence at the ancestral North American plate margin accreted numerous volcanic arcs and formed the initial continental crust of present day Arizona. Once assembled, sediment shed from these volcanic mountains was deposited in near sea level environments as mudstones and sandstones. Deformation from continued convergence metamorphosed these sedimentary rocks into the schists and phyllites that outcrop in the areas noted above.

Voluminous granitic batholiths then intruded the Proterozoic schists and phyllites during the Mid Proterozoic (~1.45 Ga) (Silver et al., 1977). Evidence of this intrusion is seen in the Bradshaw Mountains where the massive Crazy Basin Quartz Monzonite intruded the Cleator Schist, which now comprises more than half this range (Watershed Geology Map in Exhibit Maps Book). In general, these intrusions occurred well after the deformation that produced the schists and phyllites because the granites are relatively undeformed. These granites outcrop at many locales in the Phoenix Basin, such as in the Union Hills, White Peak, Sunrise Relief Mine, Papago Park, Camelback Mountain and the northern McDowell Mountains.

The next youngest rocks exposed in the study area are Tertiary volcanic units. However, before discussing these units, it is necessary to explain the geologic events that occurred during the

[1] Ga = billion years, ma = million years, ka = thousand years.

1.4 billion year unconformity to understand the more recent geologic history. The following sections summarize the events that shaped Arizona up until eruption of Tertiary volcanics between 38-15 Ma.

Mid Proterozoic (1.4 Ga) to Mid Tertiary (~20 Ma). The following section summarizes the geologic history from the Mid-Proterozoic to Mid-Tertiary Periods in order to provide a framework for understanding the more recent geology, which in turn controls many of the modern channel processes.

After emplacement of the Mid-Proterozoic granitic plutons, a period of erosion followed as Mid-Proterozoic shallow marine and coastal plain sediments were deposited on top of the metamorphic and granitic basement rocks. These oldest rocks are referred to as "basement" rocks because they sit at the deepest stratigraphic level upon which all other rocks have been deposited. During this time, basin development and crustal deformation were occurring, but little is known about the tectonic setting of this period (Wright et al., 1976).

Approximately half a billion years elapsed before deposition of the overlying Paleozoic sediments around 500 Ma. Despite the length of elapsed time, Paleozoic sedimentary rocks were deposited nearly parallel to the underlying Mid Proterozoic rocks. This relation indicates that a very stable continental platform had developed by the Late Proterozoic because tectonic activity would have instead produced an angular unconformity (a situation in which different aged units have significantly different spatial orientations). Near the end of the Proterozoic (~600 Ma), Arizona lay within a large supercontinent. However, deposition of marine limestones during the Mississippian Period (330-365 Ma) indicates that the Proterozoic supercontinent had broken up and subsequent platform subsidence allowed marine waters to flood the area by this time. For example, the Mississippian-aged Redwall Limestone seen in the Grand Canyon must have formed in a shallow marine setting similar to the Great Barrier Reef off the coast of Australia.

During the Late Paleozoic (350-240 Ma) to Early Mesozoic (240-205) Eras, oceanic crust subducted beneath the continental crust of modern day Nevada, causing the Antler and Sonoma Orogenies, or mountain building episodes. During these orogenies wide spread deposition of the Coconino Sandstone and Kaibab Limestone in the north and correlative Scherrer Formation and Concha Limestone in the south indicate stable tectonic conditions throughout Arizona and imply that the orogenies did not affect most of Arizona. However, the Permo-Pennsylvanian (330-240 Ma) Ouachita Orogeny did impinge on the southeastern tip of Arizona, New Mexico and the Mexican state of Chihuahua. This Orogeny is associated with the Ancestral Rockies uplift and formation of basins across what is now the eastern Colorado Plateau.

By the Mid Mesozoic Era (205-138 Ma), oceanic subduction and associated arc magmatism was well developed along the western margin of the Americas. A modern analogy for this tectonic setting is the Cascade Mountains in Oregon and Washington. Extensive Jurassic (205-138 Ma) magmatism covered parts of southern Arizona with 2.5 to 7.5 km of volcanic and volcanoclastic units. The Colorado Plateau was not directly affected by this volcanism or tectonism, but some Mid-Mesozoic formations and volcanic cobbles are found there, suggesting that regional drainage flowed northward during this time (Dodge, 1973; Pierce et al., 1985).

During the late Mesozoic Era (138-63 Ma), a north-south trending volcanic arc was located along the Arizona-California border. Major sedimentary basins developed in both southern and northern Arizona. Three to eight kilometer thick marine and non-marine sedimentary units, called the McCoy Mountains and Bisbee formations, were deposited in basins of southern Arizona. During the late Mesozoic (138-63 Ma) sedimentary units of the Colorado Plateau were tilted gently to the northeast and then beveled to a relatively flat erosion surface. Subsequent inflow of inland sea waters led to deposition of the marine beds of the Dakota Sandstone above this erosional surface.

The high topography of the modern Colorado Plateau (5000-7000 ft.) is a result of uplift and deformation created by the Laramide Orogeny during the late Cretaceous Period (~90-63 Ma) to early Tertiary Period (~63-40). This was the most intense episode of deformation in Arizona since construction of the crust during the Proterozoic (Dickinson, 1989). During this time the magmatic arc migrated eastward from its late Mesozoic (138-63 Ma) position along the California-Arizona border to a NW-SE trending orientation that progressed northeastward across Arizona. This migration is thought to result from shallowing of the subducting oceanic slab that caused the locus of slab-induced melting to move inland beneath central Arizona. This migration resulted in increased stresses, which are thought to have caused crustal thickening and broad uplift of the Basin and Range and Colorado Plateau. Evidence for this migration is shown by folded and thrust faulted Cretaceous-Tertiary aged strata throughout southern and western Arizona and by monoclinal folds on the Colorado Plateau.

The Laramide Orogeny raised much of Arizona above sea level, which signaled the end of marine deposition. Igneous activity was restricted to southern and western Arizona. Crustal thickening across the southern half of the state was apparently sufficient to create an elevated (> 10,000 ft above sea level) low relief erosion surface in southern Arizona that shed sediments northward towards the great Eocene (55-38 Ma) lakes of Utah and Colorado.

Cessation of Laramide deformation signaled the beginning of intense erosion over southwestern Arizona, which continued sometime into the Mid Tertiary. It is likely this erosional event stripped off the entire package of Paleozoic and Mesozoic section along the Transition zone and Basin and Range Province, including the areas within the Agua Fria River study reach. In northern Arizona, this erosion amounted to about a 1 kilometer thick Paleozoic section and a 1.5 kilometer thick Mesozoic section (S. Reynolds, personal communication) That is, erosion denuded all the rock units in the study areas equivalent to those exposed from the Inner Gorge of the Grand Canyon up to the top of the North Rim. Another way to comprehend this amount of erosion is to stand on top of the Proterozoic outcrop in Papago Park and imagine you have X-ray vision and can see the similar granite unit in the bottom of the Grand Canyon. Overlying these granite units were once a mile thick column of Paleozoic and Mesozoic sedimentary rocks, i.e., the same Grand Canyon rocks used to be in Phoenix and have been entirely eroded.

Prior to the Mid Tertiary (40-20 Ma), the major forces that shaped Arizona were compressional and were produced by convergence of the Pacific and North American Plates. The formation of continental crust by accreted arcs during the Mid Proterozoic and the Laramide uplift of Arizona and the Colorado Plateau were both caused by convergence and collision of tectonic plates.

Mid Tertiary (40-20 Ma): Rhyolitic Volcanism and Low Angle Normal Faulting. Following the 1.4 billion years of geologic activity described above, Tertiary volcanic rocks were ultimately deposited on top of Proterozoic-aged granites and metamorphics. In the southern and central portion of the watershed this relation is seen east of Lake Pleasant, north of the Union Hills, and in the Hieroglyphic Mountains and adjacent foothills of the Bradshaws. The Tertiary (rhyolites and dacites) volcanics are not as extensive in the northern portion, but can be seen in the New River Mountains, and the Black Hills.

At the regional scale, the Tertiary-aged volcanic activity was part of extensive magmatism and large-scale extension (as opposed to earlier convergence) of continental crust in southwestern Arizona, which began during the Mid Tertiary (40-20 Ma). An example of this volcanic activity is the Superstition Mountains, which were formed by rhyolitic and tuff eruptions around 20 Ma. At approximately the same time as this volcanism, the over thickened Laramide crust began to relax and southwestern Arizona "collapsed" along low angle normal faults. A normal fault is one in which the rocks above the fault (hanging wall) slide down relative to the rocks below the fault (footwall). These particular normal faults are unique because they have low dips of 10-20°, where typical normal faults dip ~60°. Although examples of this faulting are limited in the Agua

Fria Basin (e.g., the western edge of the White Tank Mountains), it is important to mention this process because it exposed the Proterozoic bedrock seen in the study area today.

In the Phoenix Basin, a good example of the normal faulting process which formed the Basin and Range geology is the detachment fault which cuts through the top of the South Mountains and exposes Tertiary-aged (~20 Ma) South Mountains Granodiorite and Proterozoic Estrella Gneiss. At the Dobbins Lookout, the fault dips 12° to the east and its projection continues under Tempe, beneath Red Mountain, the McDowell Mountains, and the Superstition Mountains. This structure has accommodated ~40 km of top to the east motion and places Proterozoic basement against the Tertiary-aged debris flow deposits of Papago Park. The westward extension of this fault projects skyward and is seen again in the western flank of the White Tank Mountains. Motion on this fault is thought to have occurred before volcanism in this area, according to the evidence presented below. Mid-Tertiary debris flow deposits (or mega-breccia) seen in Papago Park and Camelback are believed to have been triggered by detachment faulting. These deposits primarily contain clasts of Proterozoic granite and no Tertiary volcanic clasts suggesting that volcanism had not initiated at this time (S. Reynolds, personal communication). Continued motion along detachment faults tilted overlying Tertiary strata in the direction of lower plate motion. For example, the mid-Tertiary mega-breccia deposits seen at Camelback and Papago park dip to the west and the footwall (South Mountains) was moving relatively to the west.

Late Tertiary to Quaternary (20-2 MA): Basin and Range Normal Faulting, Pediment and Piedmont Formation. Extension of the crust continued into the late Tertiary Period. However, the style of faulting changed from low angle detachment to high angle "Basin and Range normal faulting." In addition, volcanism changed from silicic-intermediate (rhyolite to dacite) to mafic (basalt and bimodal) compositions around the same time (12-15 Ma; Spencer and Reynolds, 1989). Both of these changes are coeval with the change from subduction to the development of the San Andreas transform system at the plate boundary. Numerous basalt-capped mesas formed by this volcanism are seen in the upper Agua Fria Basin at Williams Mesa, Black Mesa, Joes Hill, west of Cordes Junction and scattered throughout the Bradshaw and New River Mountains (Watershed Geology Map in Exhibit Maps Book). These physiographic features formed about 16-8 Ma from basaltic eruptions and now provide a significant source of modern Agua Fria River sediment.

The normal faulting (tectonism) during this time formed the modern day basin and range topography seen in southwestern Arizona, which accounts for the name of the Basin and Range Province. Examples of Basin and Range tectonism are seen west of Lake Pleasant in the Hieroglyphic Mountains and in the foothills of the Bradshaw Mountains (Watershed Geology Map in Exhibit Maps Book). Here, Tertiary and Proterozoic rocks are cut by many NW-SE trending high angle normal faults. Although these ranges do not have the characteristic shapes associated with the Basin and Range, the White Tank Mountains and Sierra Estrella do form narrow NW-SE trending ranges separated by much wider alluvial filled basins. It seems unusual that normal faults are not mapped at the foot of these large scale Basin and Range landforms. However, subsurface data from well logs and geophysical investigations show buried high angle normal faults a few miles away from the range fronts (Brown and Pool, 1989). These faults, also termed structures, form deep, fault bounded sedimentary basins.

The Luke Basin lies between the White Tank Mountains on the west and approximately I-17 on the east and is presently agricultural fields and infringing suburbia (Watershed Map in Exhibit Maps Book). Well logs show up to 4,000 feet of Quaternary and Tertiary sediments filling a basin bounded by normal faults (Brown and Pool, 1989). Well data also reveal the most prominent structure lies about four miles east of the White Tank range front, dips 62° to the east, and is well located at least 2,500 feet below the ground surface. The opposite (east) side of the Luke Basin also appears to be fault bounded, although the structures are less clearly defined. At the southern margin of the basin near Buckeye and Tolleson, in a cross section

approximately parallel to I-10, the depth to Proterozoic basement rock is estimated at 2,000 feet, based on gravity data. These physical descriptions of the basin containing the Agua Fria River provide a framework for interpreting the geologic events that occurred between about 16 Ma and the present.

Around 13 million years ago, basin and range normal faulting was initiated along the eastern side of the White Tank Mountains and the western side of the Phoenix Mountains and Camelback area. Continued faulting dropped what is now the Luke Basin and elevated the adjacent ranges. Simultaneous (or Syntectonic) erosion of the neighboring range fronts began filling the basin with sediment. Continued range front erosion created gently sloping bedrock surfaces of low relief, called pediments. These pediments probably began to form in the late Miocene (11-5 Ma) or Pliocene (5-2 Ma) Epochs, according to rates of mountain front retreat established elsewhere (Marchand, 1971; Oberlander, 1972). The pediments progressed mountain-ward and resulted in narrower (in cross section) mountain ranges. Following pediment formation, continued degradation of mountain blocks produced thin, coarse grained, alluvial fan deposits overlying the bedrock pediment surfaces. The waning stages of basin and range extension and faulting occurred around 6-4 Ma. The rate of basin deposition probably decreased after termination of faulting, though it continues at slower rates today, and sediment began backing up and migrating mountain-ward, burying pediment surfaces with alluvial fan deposits. The thick deposits of salt, gypsum, and anhydrite found below the ground surface in the Luke and other basins throughout southwestern Arizona indicate that many of the basins were closed (no drainage outlet[2]) during this time (Menges and Pearthree, 1982; Peirce, 1976; Scarborough and Peirce, 1978).

During the late Miocene period (~11-5 Ma), decreased basin subsidence resulting from waning Basin and Range faulting probably allowed for drainage integration by a combination of migrating drainage divides, diversion by stream piracy, and basin infilling overtopping low divides (Hunt, 1983; Menges, 1981). The integration of the Colorado and Gila River systems resulted in large scale incision (up to 300 meters) of former closed basins during the Plio-Quaternary period (~5-1 Ma; Menges and Pearthree, 1989). The timing of the initial incision in the project area (or Phoenix Basin) may be recorded by the oldest fluvial terraces and alluvial fan surfaces; assuming that they represent the geomorphic surface at the time of incision.

Quaternary Period (2 Ma to the present): Incision and Aggradation. Remnants of syn-integration geomorphic surfaces are visible in the landscape we see today. The overall morphology of the present topography has remained virtually unchanged since drainage integration during the Plio-Quaternary transition (~5-1 Ma). However, the modern desert piedmonts surrounding the White Tank, Hieroglyphic, and smaller mountains and channels in the lower Agua Fria drainage basin have also experienced periods of incision and aggradation over the last 2 million years. These events shaped the modern landscape and provide insight into stream behavior that is of concern to land managers. The resulting Quaternary landforms (e.g., terraces, fans) provide a framework for delineating erosion hazard boundaries and estimating rate of incision for the Agua Fria River.

Early studies of terraces along rivers in the Phoenix Basin indicate that the oldest terraces are younger than 2-3 Ma (Pewe, 1976; Lee and Bell, 1975). Pewe identified four ancestral terraces along the Salt River and showed that their profiles, as well as those from the Agua Fria River, New River, and Queen Creek converge downstream. Pewe suggested that gradual uplift of the mountains surrounding the Phoenix Basin tilted these terraces to the southwest, resulting in downstream converging profiles. The cause of this uplift, while speculative, may be a reponse to the unloading of sediments from the Transition Zone. However, Pewe did not preclude the possibility of climatic influencing this geometry. Huckleberry (1995) suggests that the terraces probably result from a combination of these processes.

[2] An example of a closed basin is the Great Salt Lake in Utah.

More recent, surficial geologic mapping of the Baldy Mountain and Calderwood Butte 7.5 minute quadrangles was conducted by the Arizona Geology Survey (AZGS) to determine the physical properties and ages of Quaternary deposits along the lower Agua Fria River. Four alluvial fan and eight fluvial terrace units were identified along this reach, and their ages were estimated based on the relative degree of soil development. Figure 2-3 shows the converging nature of the Agua Fria terraces discussed by Pewe (1976). The colors correspond approximately to the colors shown in the Surficial Geology Map (in Exhibit Maps Book). Huckleberry (1995) estimates the age of the O (Lake Pleasant) terrace to be 1-2 million years old and correlates it with the Sawik terrace along the Salt River. He also estimates an age between 0.5 and 2 million years for the O alluvial fans, which is similar to the greater than 1 million year age of formation for these features reported by Menges and Pearthree (1989). Huckleberry also relates his early Pleistocene, M1, terrace with the Salt River's Mesa Terrace and his M2b terrace (estimated age of 100–200 ka) with the Blue Point Terrace along the Salt River, based on comparisons by Pewe of the Landing Field and Canal Terraces, respectively. A schematic model of terrace formation resulting from aggradation or degradation is shown in Figure 2-4.

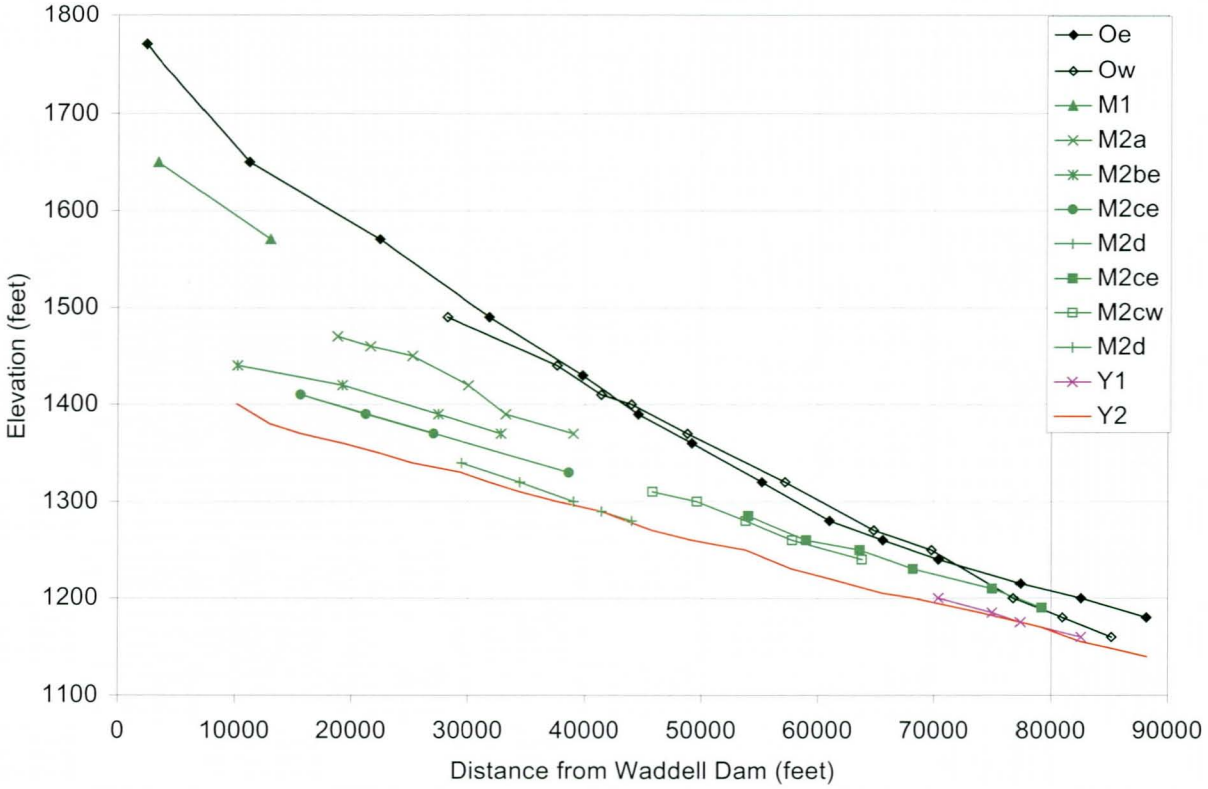

Figure 2-3 Terraces in the Baldy Mountain and Calderwood Butte Quadrangles (adapted from Huckleberry, 1995) Terrace unit names shown on Surficial Geology Map in Exhibits Map Book.

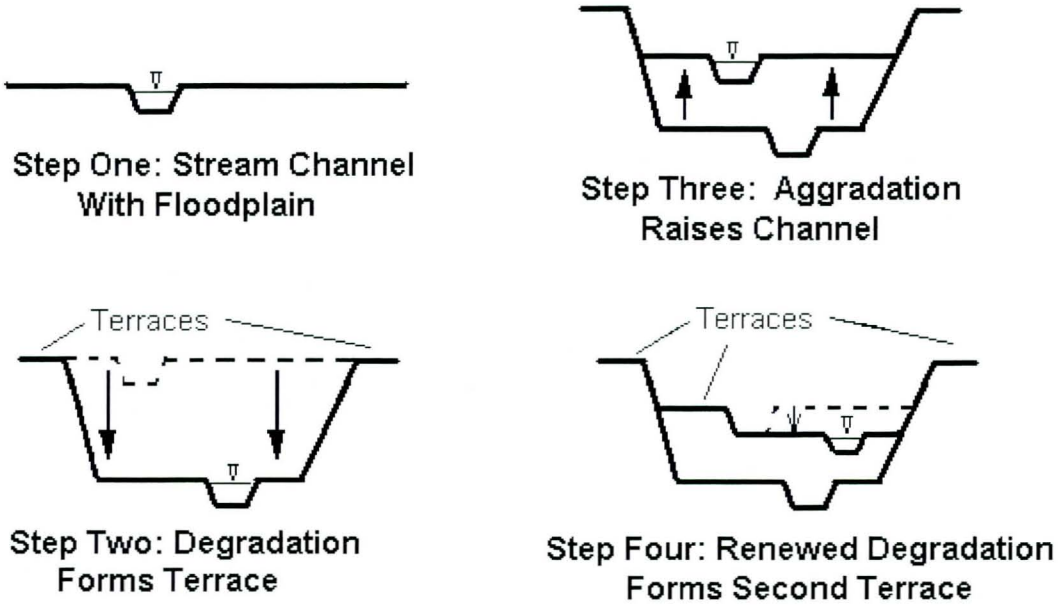

Figure 2-4 Example of Terrace Formation by Degradation or Aggradation

A study from the western slopes of the White Tank Mountains suggests that a major incision event occurred around 2 Ma and was followed by a period of aggradation. These events are inferred from geologic relations between Early Pleistocene (Qo) and Middle Pleistocene (Qm) alluvial fan units, and on preliminary cosmogenic isotope dating of these surfaces (Robinson, personal communication). The first incision event (2 Ma) may correspond with formation of the Sawik Terrace along the Salt River, given the similarity of the cosmogenic age estimates with the ages estimated based on soil development for the O terraces.

2.1.2.2 Implications of Geologic History on Modern Erosion and Lateral Stability

The geologic history summarized above demonstrates that cycles of both aggradation and degradation have formed the modern Agua Fria River drainage basin. This history can be distilled to evaluate long-term degradation rates and to define practical limits of lateral erosion. AZGS mapping of Quaternary (~2 Ma) deposits associated with the Agua Fria River (Surficial Geology Map in Exhibit Maps Book) provide evidence of the geomorphic evolution of the fluvial system over the past several million years. During this period, the study area experienced net degradation, developed a more defined stream corridor, and left a series of stream terraces.

Huckleberry (1995) estimates that the oldest Agua Fria River terrace (O) terrace is about 1-2 million years old, sits over 100 m above the active channel near Waddell Dam and is only 12 m high near Sun City. Similarly, the 5-2 million year old Sawik Terrace is ~130 m above the modern Salt River near Roosevelt Dam. Pewe estimated an uplift rate of 0.064 mm/yr based on this height divided by 2 million years (1978). A number of assumptions are required to estimate incision rates by dividing terrace height by approximate age. The primary assumption of no aggradation is problematic given evidence for periodic aggradation within the net degradation trend that formed the terrace. Therefore, the estimated incision rates can be considered as the net result of the two competing processes (degradation and aggradation). Using Huckleberry's value of 100 m for incision in the upper part of the study area and 12 m for the approximate midpoint and assuming an age of 1.5±0.5 million years for the oldest Agua Fria River terrace yields incision rates of 0.075±0.025 mm/yr and 0.018±0.006 mm/yr for the upper and middle reaches respectively. In comparison, Menges and Pearthree (1989) calculated a minimum

incision rate of 0.03 to 0.1 mm/yr for the Transition Zone. These geologic rates of incision suggest that, without human impacts on channel behavior, the active channel will be about 1 cm lower in 100 years, or 10 cm in 1,000 years. As described elsewhere in this report, human impacts on the Agua Fria River will probably accelerate the rate of incision.

Huckleberry's (1995) M2x surfaces (Late Pleistocene terraces) decrease in elevation above the active Agua Fria River from about 40 feet near Waddell Dam to 10 feet near the confluence with the Gila River. Using a similar process as described in the previous paragraph, these surfaces of lesser age yield net degradation rates of 0.03 to 0.12 mm/year over the past 10,000 years. However, some of the M2x surfaces may be as old as 200,000 years. Over a 200,000 year time period, the net degradation estimates are reduced to between 0.002 to 0.006 mm/year somewhat less than the rate of incision implied by the older terraces.

Similarly, the lateral position of the converging terraces along the study reach provides information on the historical position of the Agua Fria River during recent geologic time. The younger terraces are inset within the margins of the older, higher, and wider terraces, indicating that the river corridor has narrowed as it has incised. These terrace boundaries indicate the limits of channel position within the past 10,000 to 1,000,000 years, and form a practical boundary of likely lateral movement in the immediate future. Regardless of the precise vertical and lateral rates of erosion indicated by the Pleistocene and Holocene terraces, the terraces do provide practical limits on channel change because the river has been stable within these limits for thousands to millions of years. Therefore, it is highly unlikely that any flood would extend beyond the limits defined by these surfaces.

2.1.2.3 Subsidence

Subsidence is a geologic phenomenon in which the ground surface becomes lower over time. Subsidence can happen naturally, or in the case of the Phoenix Basin, as the result of human activity. Surveys of subsidence in the west Phoenix Basin have shown as much as 18 feet of surface subsidence (lowering) to due compaction of basin fill sediments that occurred due to groundwater pumping around Luke Air Force Base. Published reports show that subsidence along the Agua Fria River channel location has been nominal (0-2 feet) (Schumann and O'Day, 1995). Figure 2-5 shows a map of quantities of ground lowering in the west Phoenix Basin. These data show that while land subsidence has been significant near the study area, the effects of subsidence on the Agua Fria River channel have not yet had a great impact on the river. If subsidence extends to the Agua Fria River channel, the channel slope will increase upstream of the subsidence cone, and decrease downstream. Increased slope would lead to increased incision (long-term scour) and lateral erosion. Decreased slope would lead to sediment deposition, loss of channel capacity and widening of the floodplain.

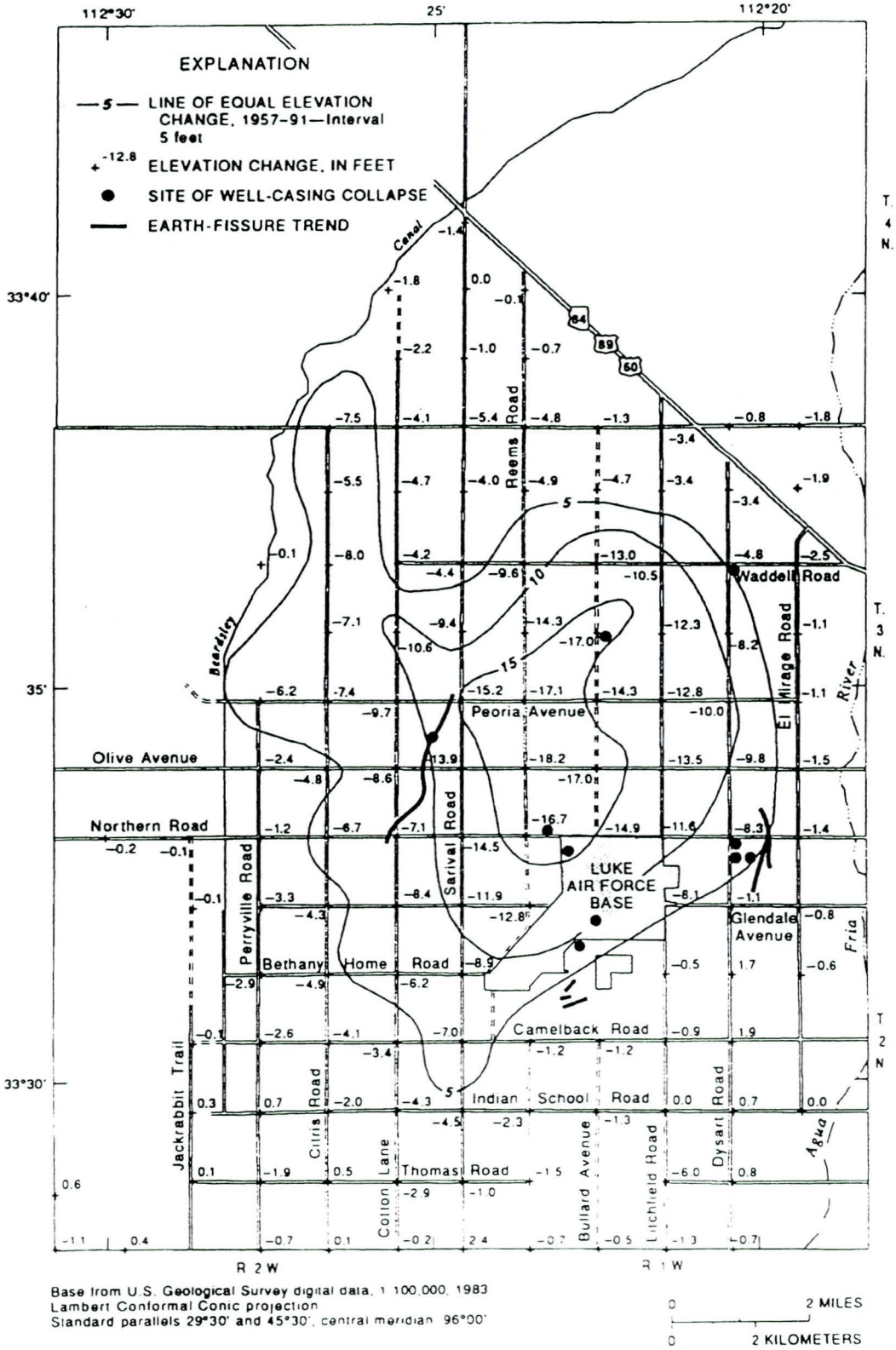

Figure 2-5 Land subsidence in the west Phoenix Basin, 1957 – 1991 (from Schumann and O'Day, 1995)

2.1.2.4 Summary

The presence and characteristics of the fluvial terraces along the Agua Fria River provide the following types of information about the existing and future risk of lateral erosion:

- Erosion limits. Within the past 10,000 years, lateral erosion has been limited to the area of the 600 to 9,000 foot wide stream corridor located between Pleistocene surfaces. Future lateral erosion is most likely within areas composed of the most recent geomorphic surfaces.
- Erosion corridor width. The width of the modern geomorphic surfaces increases and the height of the fluvial terraces generally decreases in the downstream direction, indicating an increased potential for lateral erosion in the downstream direction.
- Net degradation. The height of the fluvial terraces above the existing channel bed suggests that a maximum of about 300 feet of net vertical erosion has occurred since the early Pleistocene, with a maximum of about 40 feet since the late Pleistocene.
- Episodes of aggradation. Episodes of aggradation (e.g., channel filling, floodplain deposition) have occurred at numerous times in the past, and should be expected in the future. During periods of aggradation, the stream corridor tends to occupy a wider portion of the geologic floodplain.
- Rates of degradation. Geologic evidence suggests long-term degradation rates of 0.02 to 0.08 mm/year over the past 2 million years and 0.02 to 0.12 mm/year over the past 10,000 years.
- Land subsidence. Lowering of the ground due to groundwater withdrawal has not likely had a significant impact on the Agua Fria River channel.
- Human impacts. Impacts on degradation rates from the hydrologic impacts of New Waddell Dam and sand and gravel mining may be greater than those experienced over geologic time.

Within the study area, the existing channel of the Agua Fria River has experienced net degradation over the past 2 million years. Therefore, net degradation is expected to continue in the future. Entrenchment during recent geologic time has created a series of older, stable terraces that confine the existing active channels within a relatively well-defined corridor. Likewise, future channel movement is most likely to be confined within the corridor of geologically recent surfaces located near the main channels. Modern rates of degradation may be significantly greater than those experienced over the past 10,000 to 2 million years.

2.1.3 Hydrology

The hydrologic characteristics of a stream have the greatest impact on its morphology and behavior. The hydrologic characteristics of the Agua Fria River have changed significantly from their natural, historical condition. This section presents information on the hydrology of the study area based on data from streamflow and precipitation gages. This discussion is followed by a comparison of the hydrology for the period before Waddell (Carl Pleasant) Dam (<1927), the period after construction of the Waddell Dam (1927-1992), and the post-New Waddell Dam (>1992) conditions.

2.1.3.1 Gage Data

Hydrologic data for the Agua Fria River were collected from regional precipitation gage records, USGS stream gage records, FCDMC ALERT gage records, and hydrologic modeling performed by others (USACOE, 1982, 1988, and 1995). The gage data are presented for context and general understanding of the hydrologic history and response of the basin. The USACOE data (1982, 1988, and 1995) serve as the primary source for discharge-frequency estimates for the study reach that are used elsewhere in this report.

Precipitation Records. For ephemeral streams like the Agua Fria River and its tributaries, runoff is directly related to precipitation. Even the low flow duration and magnitude in nearly perennial reaches such as near the Agua Fria near Rock Springs gage is primarily a function of relatively recent precipitation amounts. Precipitation records also can be used to identify wet/dry cycles, climatic variation, and other trends that may affect stream stability or explain historical channel change. For streams like many of the smaller tributaries in the lower watershed which lack any systematic gage record, precipitation data can be used to identify potential flood years or periods of frequent flow. Also, precipitation records are valuable because they are available dating back to the late 1800's, whereas streamflow records in the watershed cover much shorter periods (see Table 2-5).

Long-term precipitation data were obtained for the Agua Fria River watershed area from the Western Regional Climate Center web site operated by the Desert Research Institute in Nevada.[3] The station names and period of record are listed in Table 2-4. Station locations are shown in Figure 2-6. Long-term average annual and seasonal precipitation data are shown in Figure 2-7 and Figure 2-8. Average annual runoff computed as a percent of the long-term regional average precipitation is shown in Figure 2-12. The data shown in these Figures and Tables are discussed in the following sections.

Table 2-4 Regional Long-Term Precipitation Stations

Station Name	Period of Record	Average Annual Precipitation (in)
Alhambra	1948-1976	7.77
Buckeye	1893-1999	7.74
Carefree	1962-1999	13.37
Castle Hot Springs	1959-2000	15.42
Cordes	1948-2000	15.18
Deer Valley	1950-1985	8.64
Groom Creek	1948-1976	23.44
Litchfield Park	1917-1999	8.13
Marinette	1913-1964	7.90
Mesa	1896-1999	8.33
Phoenix City	1948-1998	7.89
Prescott	1898-2000	19.33
Youngtown	1964-1999	9.17
Wittman	1923-1966	9.42

[3] The internet address for the Western Regional Climate Center precipitation data is http://www.wrcc.dri.edu/index.html.

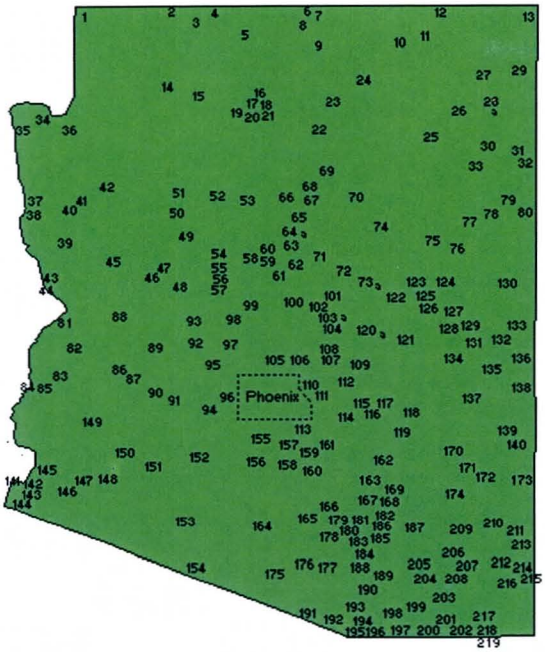

Figure 2-6 Location of Regional and Statewide Precipitation Stations

INSET for Metro Phoenix Area

1 - Marinette
2 - Youngtown
3 - Litchfield Park
4 - Deer Valley
5 - Alhambra
6 - Phoenix City
7 - Paradise Valley
8 - Arizona Falls 1 WNW

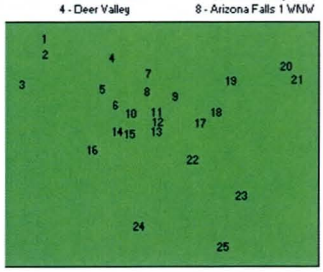

9 - Scottsdale
10 - Phoenix WSFO Airport
11 - Tempe
12 - Tempe ASU
13 - Tempe 3S
14 - South Phoenix
15 - Goulds Ranch
16 - Laveen 3 SSE
17 - Mesa
18 - Falcon Field
19 - Granite Reef Dam
20 - Stewart Mountain
21 - Mormon Flat
22 - Chandler
23 - Chandler Heights
24 - Maricopa 4 N
25 - Sacaton

56 – Prescott
57 – Groom Creek
94 - Buckeye
95 - Wittman
97 – Castle Hot Springs
98 – Crown King
99 - Cordes
105 – Carefree

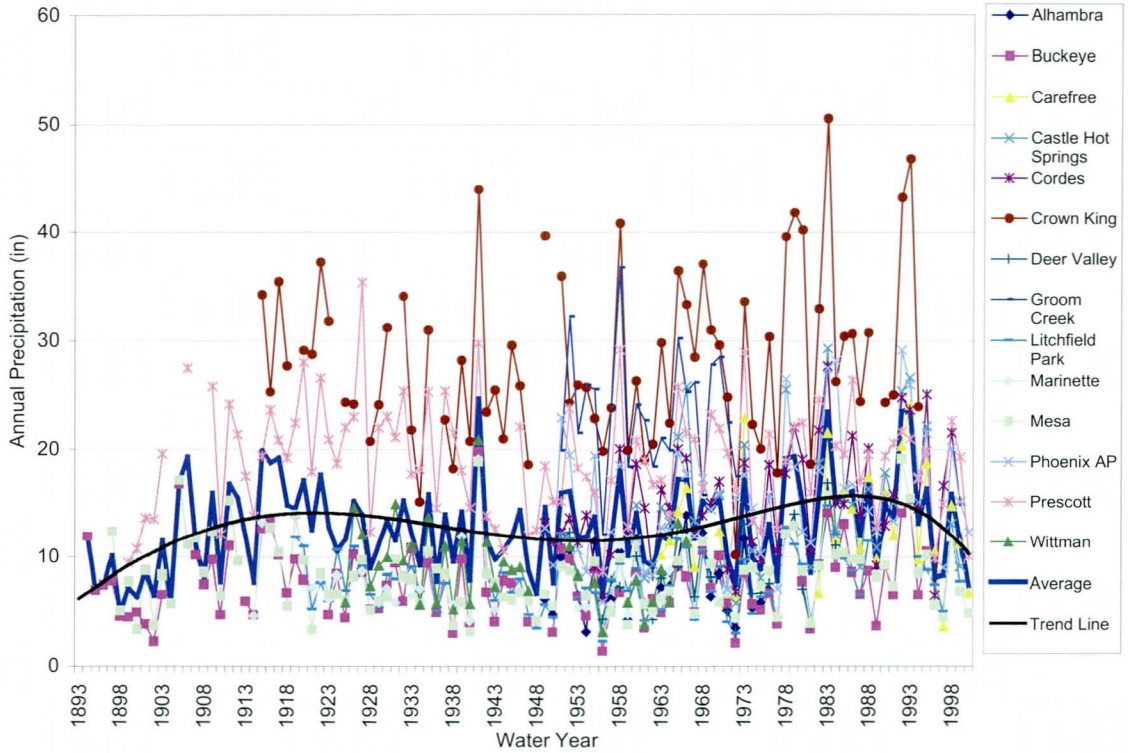

Figure 2-7 Historical Precipitation Data and Average for All Stations in the Agua Fria Watershed, 1893-2000

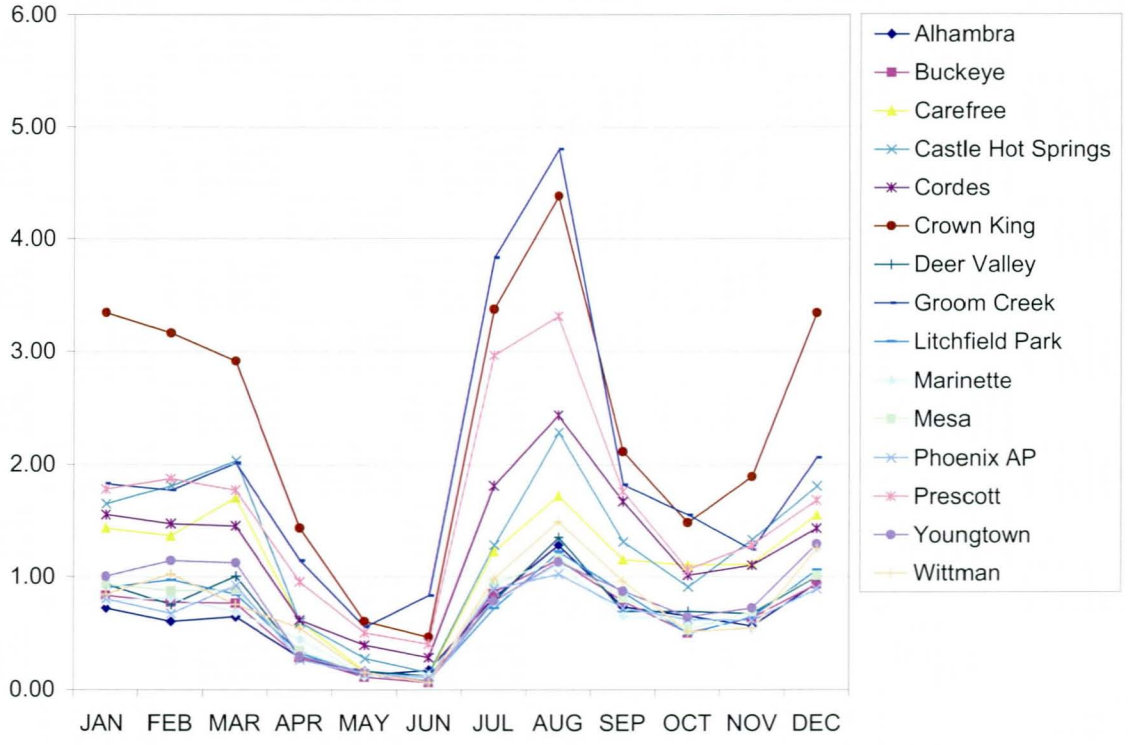

Figure 2-8 Long-term Monthly Average Precipitation

Streamflow Records. USGS stream-gaging stations within the Agua Fria watershed area listed in Table 2-5.

Table 2-5 USGS Stream Gage Stations in Study Area Vicinity

Name	Operator	Station #	Period of Record	Drainage Area* (mi^2)
Agua Fria River				
Agua Fria near Mayer	USGS	9512500	1940-present	585
Agua Fria near Rock Springs	USGS	9512800	1970-present	1111
Agua Fria at Waddell Dam[2]	USGS	9513500	1915-20,28-present	1459
Agua Fria at El Mirage	USGS	9513650	1962-present	1628
Agua Fria near Avondale[1]	USGS	9513970	1960-82	2066
New River				
New River near Rock Springs	USGS	09513780	1966-2000	68.3
New River at Bell Road[1]	USGS	09513835; 5598	1963,65-84, 90-93; 94-2000	185
New River near Glendale[1]	USGS	9513910; 5508	1943,55,60-79,90-98; 98-2000	600
Skunk Creek				
Skunk Creek near New River	FCDMC	5583	1995-2000	4.3
Skunk Creek near Phoenix	USGS	09513860	1960-2000	64.9
Cave Creek				
Cave Creek below Cottonwood Ck.	USGS	09512280	1981-2000	82.7
Cave Creek near Cave Creek[1]	USGS	09512300	1958-2000	121

Notes:
* Drainage area published with USGS gage record data. Differs in some cases from effective area and total area computed for this study.
1. Station is now operated by the Flood Control District of Maricopa County.
2. Station operated by USGS prior to Waddell Dam. Afterward, operated by MCMWCD. Volume data only.

Annual Flow. Lateral channel movement is strongly related to the volume of flow. In addition to the effects saturating the bank materials has on bank stability, long duration periods of high flow have the energy and time to perform significant amounts of geomorphic work. Therefore, years of high annual flow volume are related to likely periods of channel change. Figure 2-9 shows the flow volumes recorded at USGS gages within the Agua Fria River watershed.

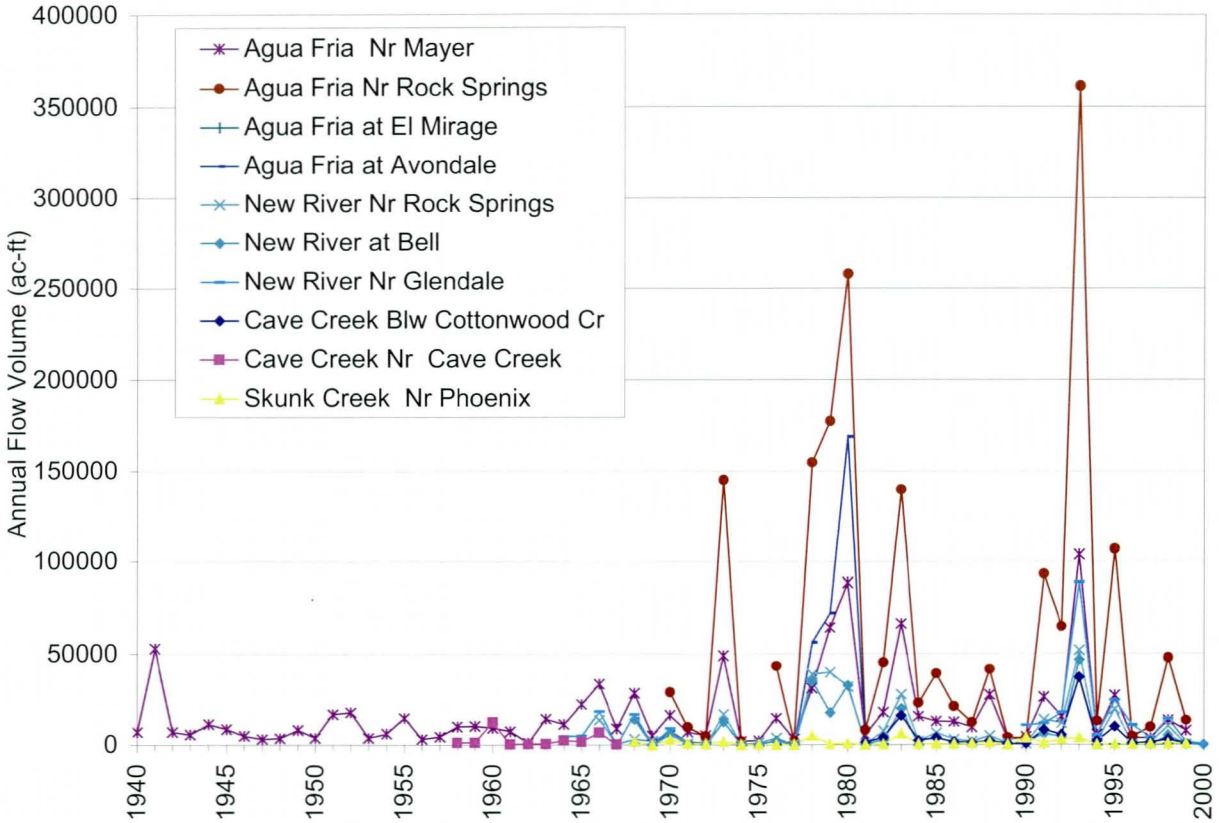

Figure 2-9 Annual Flow Volumes for USGS Gages in the Agua Fria Watershed

The following conclusions may be drawn from the annual flow volume data shown in Figure 2-9:

- Variability. There is a wide range in flow volume between wet years and dry years. There are more than multiple orders of magnitude of difference between the annual volume of the driest years and the wettest years during the period of record for the various gages. Therefore, there will be years of no channel change (dry, low volume years) and years of significant channel change (wet, high volume years). Long-term average rates of channel movement probably will not accurately predict the short-term erosion hazards.
- Cyclical Change. The periods during the later 1970's and early 1980's and again in the early 1990's were wetter compared to drier periods experienced before and between these periods. Also, the period prior to the mid 1970's was drier. High rates and magnitudes of channel change should be expected during wet periods.
- Flow Volume. The quantities of annual runoff for the Agua Fria River near Rock Springs are much larger than near Mayer. A doubling in drainage area results in a tripling or more in volume at the Rock Springs gage in the wettest years. This is likely due to contributions from the higher elevation and steeper subwatersheds draining the Bradshaw Mountains between the two gages. Moreover, a higher percentage of the basin near Rock Springs is from mountainous areas including the Black Hills and New River Mountains. Also, flow volume from the Agua Fria River historically was much greater than that for the New River and its tributaries. For the reaches downstream of the dam, this trend may have been reversed by the completion of the New Waddell Dam.

Seasonal Flow. Flow volume varies seasonally as well as annually. Seasonal trends in flow volume can be used to determine likely periods of high or low flow, and consequently, seasonal

periods of increased susceptibility to lateral erosion and channel change. Monthly average flow rates for the Agua Fria River gages are summarized in Figure 2-10.

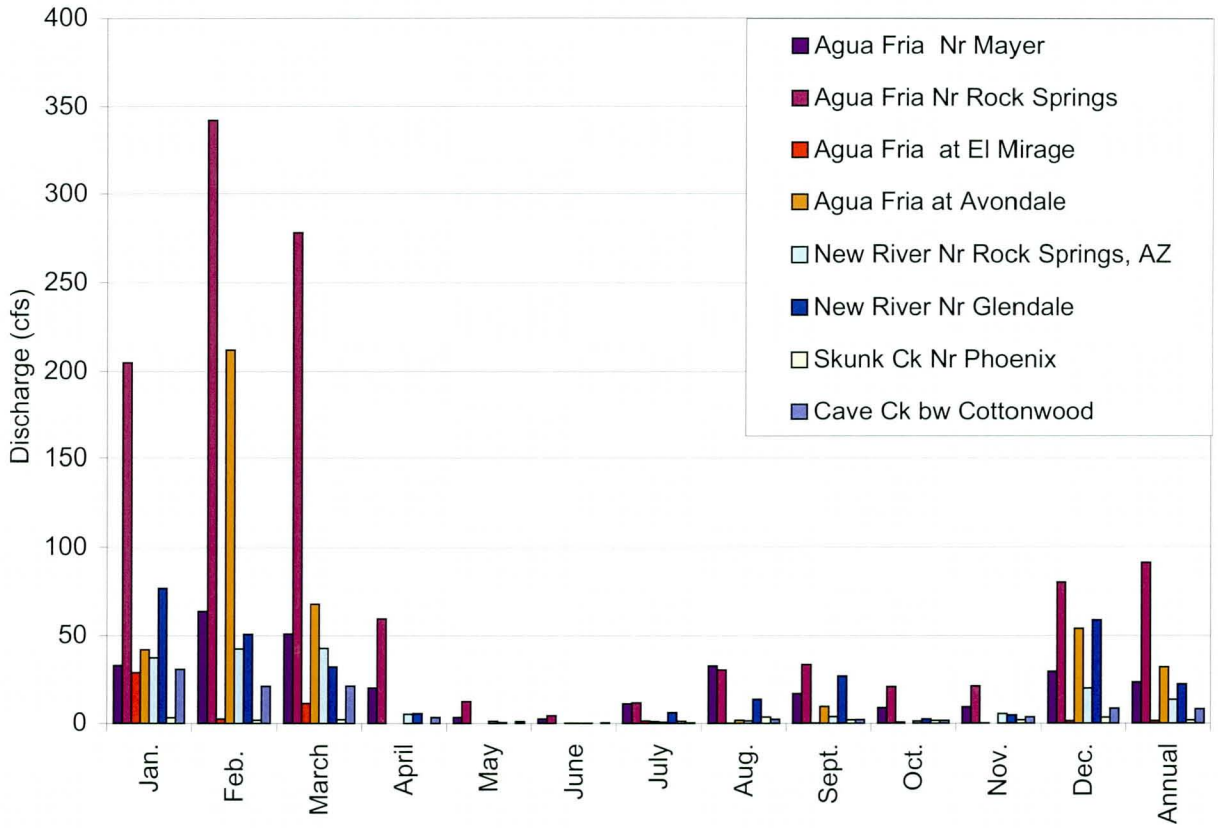

Figure 2-10 Monthly average discharge rates for USGS Gages in the Agua Fria River watershed.

The following conclusions can be drawn from the monthly flow data summarized in Figure 2-10:

- Seasonality. Two seasons of flow occur in the Agua Fria River watershed: (1) winter storm-induced runoff during December through March, and (2) summer monsoon-induced runoff during the months of July through October. The period of seasonal low flow occurs in late spring and early summer from April to June. Moreover, the winter flow period is significantly greater in magnitude than the summer flow period. As monthly discharges, the data also show the large difference in flow volume in the winter floods as compared to the summer floods.
- Effective Precipitation. Comparison of the flow rates in Figure 2-10 with the precipitation totals in Figure 2-8 indicates that despite higher average precipitation during the summer monsoon, more runoff is generated from the upper watershed during winter storms.
- Erosion. Historically, channel change from summer monsoon flooding was not as significant as channel change from winter flooding because the flood magnitudes and volumes of winter floods were much larger. This is no longer necessarily the case for the Agua Fria River downstream of New Waddell Dam. Storage of winter runoff in Lake Pleasant will substantially reduce the ability of winter rains to generate floods that are large enough to cause channel change in the study reach.

Flow Duration. Flow duration statistics depict the percent of time a given flow rate is exceeded at a gaging station. For streams with high flood to low flow ratios (Q_{peak}:$Q_{average}$), flow duration statistics depict typical flow conditions more realistically than average flow statistics, which tend

to be skewed upward by the large volumes which occur during rare floods. Comparison of flow duration and average flow data help identify streams subject to flash floods. Flow duration statistics for gages in the Agua Fria watershed are shown in Figure 2-11.

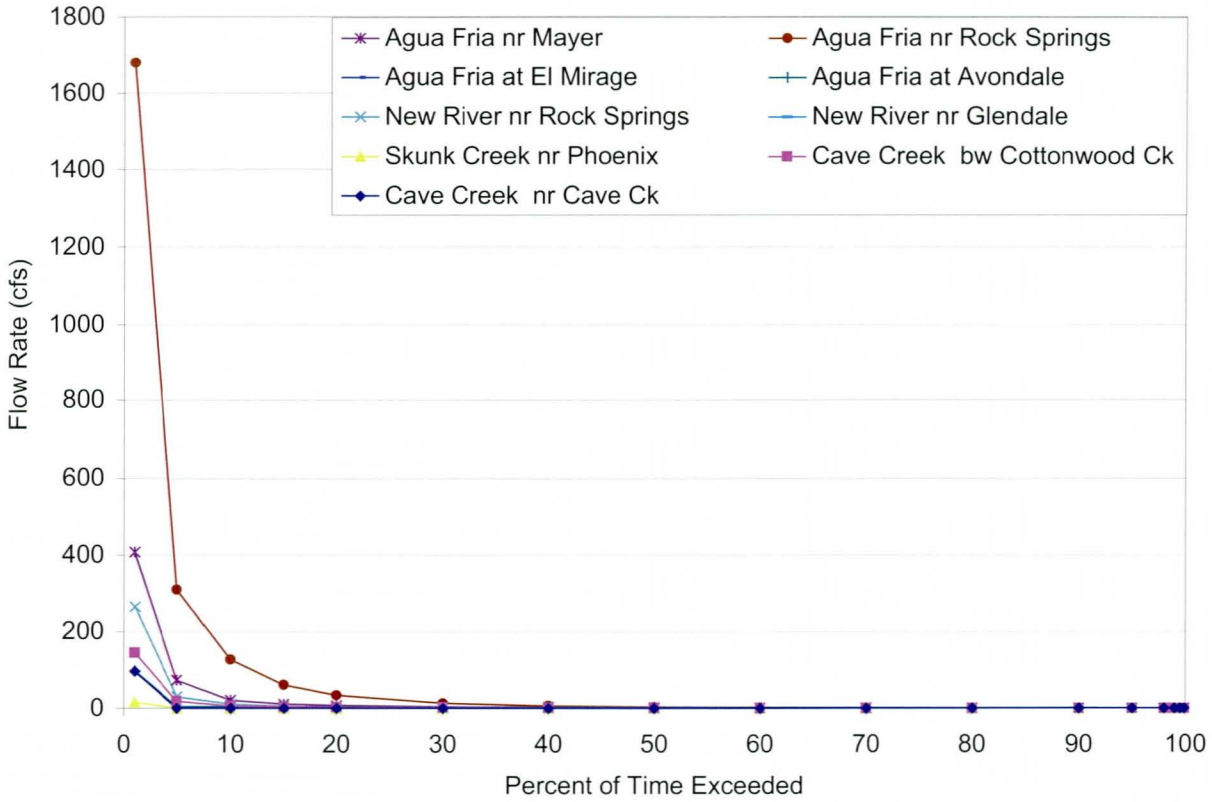

Figure 2-11 Flow Duration Data for USGS Gages in the Agua Fria Watershed

The following conclusions can be drawn from the flow duration data summarized in Figure 2-11:

- Flow Rate. The flow duration and magnitude are greater for the more mountainous portions of the watershed. Longer periods of very low discharges are more common for the gages in the mountainous portions of the watershed. Only rarely are flow rates large enough to accomplish significant geomorphic work anywhere in the watershed.
- Flood Potential. Comparison of average flow data and flow duration data indicate that the Agua Fria River (and its tributaries) are subject to flash floods. Average flow data are skewed by the effects of rare floods. Therefore, infrequent large floods will cause most channel change in the Agua Fria River watershed. Low flows will generally not be effective agents of significant channel change.

Runoff versus Precipitation. Figure 2-12 shows the percentage of the regional average annual precipitation that has become runoff in the Agua Fria River watershed since 1940. The following conclusions can be drawn from examination of Figure 2-12:

- Effective Precipitation. A higher percentage of precipitation becomes runoff during the wettest years.
- Source Areas. The upper New River watershed appears to be the most efficient generator of runoff of the gaged Agua Fria River tributaries.

- Rainfall/Runoff Relationship. Runoff is directly correlated with precipitation. That is, as is the case for other ephemeral streams, the Agua Fria River flows primarily in response to direct precipitation.

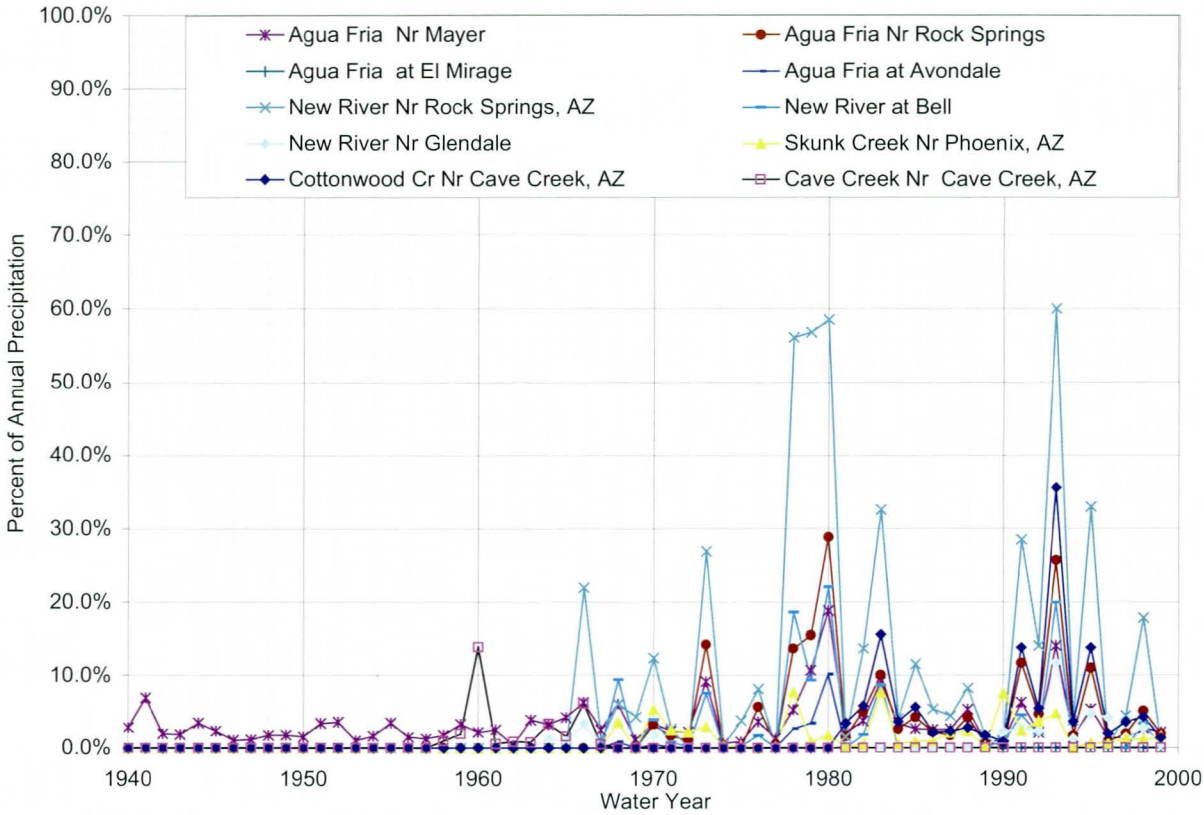

Figure 2-12 Runoff as a percentage of regional average precipitation, 1940-1999

Summary. From the data presented in Figure 2-7 to Figure 2-12, the following conclusions can be drawn:

- Long-Term Trends. Figure 2-7 shows the regional average annual precipitation, as well as a 5-year moving average and a polynomial trend line for the annual values. The trend line indicates that annual precipitation volume was cyclical during the 20th Century with wetter periods at the beginning and end of the century, and a dry period during the mid-century. Although the trend line suggests a decrease in average precipitation during the past few years, this decrease may be over-exaggerated due to the fact that data for a few stations at higher elevations, such as the Crown King station, ended in 1996.
- Wet/Dry Cycles. Channel change should be expected during periods of high runoff resulting from extreme precipitation, particularly when wetter periods immediately follow periods of sustained drought. During dry cycles, little or no channel change may be observed.
- Wet Years. Years of unusually high annual precipitation occurred in 1941, 1983, and 1992-1993. These years correspond to some of the largest state-wide flooding and channel movement.
- Floods. The occurrence of floods during wet years or wet cycles is discussed in the following section of this chapter. A comparison of Figure 2-7 and Figure 2-9 indicates that

years of high annual precipitation correlate moderately well to years of high annual runoff volume.

- Seasonal Variation. Precipitation records support the conclusion of a winter and late summer period of seasonal high flow indicated in Figure 2-8. The seasonal variations in precipitation are expressed more strongly in the precipitation records of the Groom Creek and Crown King stations. These two stations express this difference more strongly because of their generally higher elevation and somewhat more northerly location compared to the other stations. The stations upstream of New Waddell Dam (Castle Hot Springs, Cordes, Crown King, Groom Creek, and Prescott) all show a more pronounced summer monsoon than the other stations. Interestingly, as will be discussed later, most of the largest damaging floods on the Agua Fria River have occurred as the result of winter precipitation events.

More detailed interpretation of the implications of these long-term hydrologic records will be provided in the following section and in later chapters of this report.

Flooding. In arid regions, much of the geomorphic work of channel change occurs during the largest floods (Baker et. al., 1986). Records of large and small floods were obtained primarily from USGS gage records.

Historical Floods. Historical records of floods on the Agua Fria River were obtained from engineering reports and historical documents. A list of large floods that impacted the study area is provided in Table 2-6 and Table 2-7.

The effect of storage behind New Waddell dam is profound. As shown in Table 2-7, depending on antecedent storage conditions in Lake Pleasant, no outflows are expected from New Waddell Dam for inflow events with peak discharges less than about 48,000 cfs. Therefore, of the floods listed in Table 2-7, only 12 events during the past 111 years or so would have resulted in releases into the lower Agua Fria River. Because of the operation of Lake Pleasant, water levels from Central Arizona Project canal water pumped into the lake are typically at a minimum in October and a maximum level in late March. Therefore, large floods in the summer and fall are not as likely to result in releases as floods in February or March. Consequently, about half of these 12 events may not have resulted in releases from the dam because of the time of year that they occurred. It is also noted that at least five of these floods that exceeded 48,000 cfs, and five of the ten largest floods occurred in February and March. That is, while many of the small to moderate floods will be absorbed in the storage pool of Lake Pleasant prior to reaching the study reach, the potential for the largest, erosion causing floods still exists.

Table 2-6 Historical Floods on the Agua Fria River

Date	Details	Source	Location
1891 February	"...swollen by melting snow."	Major Storms and Floods in Arizona 1862-1983	Anthony Brazel, 1984
	"80,000 cfs"	Agua Fria River Study 1981, Draft	FCD (A109.928)
1908	"...produced a large runoff..."	Major Storms and Floods in Arizona 1862-1983	Anthony Brazel, 1984
1915 January	Major flood reference	Phoenix City Stream, Arizona: Agua Fria River	FCD (A109.919)
1916 January	Major flooding	Floods of August 14-22 in Central Arizona	Aldridge, 1968
	Major flooding	Compilation of Flood Data in Arizona, 1862-1953	FCD (803.001)
	Major flooding	Phoenix City Stream, Arizona: Agua Fria River	FCD (A109.919)
1917 7/27/17	Flood reference	Agua Fria River Study 1981, Draft	FCD (A109.928)
1919 November	Major Flooding	Summary of Floods in the United States During 1963: USGS Water Supply Paper 1830-B	Rostvedt, J.O.
	Major Flooding	Compilation of Flood Data in Arizona, 1862-1953	FCD (803.001)
1922 September	Major Flooding	Phoenix City Stream, Arizona: Agua Fria River	FCD (A109.919)
1927 February	Major Flooding	Phoenix City Stream, Arizona: Agua Fria River	FCD (A109.919)
1931 August	"...ran unusually high."	Major Storms and Floods in Arizona 1862-1983	Anthony Brazel, 1984
Date	Details	Source	Location
1951 8/3-4/51	"Agua Fria was running 8 feet at the Grand Ave crossing..."	Phoenix Gazette	FCD (802.053)
	"...force of flash flood in the Agua Fria River smashed out a 200 foot section of Luke Airforce Base main thoroughfare..."	Arizona Republic	FCD (802.053)
	Flooding in Summer	Report of Flood Conditions in Phoenix: Summer of 1951	FCD (802.053)
1951 8/26-30/51	"...flooding..."	Arizona Climate: The First Hundred Years	Sellers, 1984
1965 12/24/65	"High Waters Bring Crossing Woes."	Arizona Republic	FCD (007.114)
1966 1/4/66	Photos	Newspaper Articles and Photos: Flooding Events 1965-1966	FCD (007.102)
1967 12/20-22/67	"...rampaging Agua Fria River..."	Arizona Republic	FCD (007.114)
	Photos	Newspaper Articles and Photos: Flooding Events 1966-1970	FCD (007.105.1)
1970 9/5/70	"...flooding..."	Floods of September 1970 in Arizona, Utah, and Colorado	FCD (802.006)
1977 October	Near Rio Rico	Floods of October 1977 in Southern Arizona...	FCD (802.041)

1978 March	"The peak discharge in Agua Fria Canyon was the highest since 1900."	Floods of October 1977 in Southern Arizona…	FCD (802.041)
	Photos	Flood Photos 1978	FCD (007.107)
1978 11/10-12/78	"…some flooding…"	Arizona Climate: The First Hundred Years	Sellers, 1984
1978 December	"Both bridges on Interstate 17…collapsed."	Major Storms and Floods in Arizona 1862-1983	Anthony Brazel, 1984
	"…extensive damage…from floodwaters…"	Arizona Climate: The First Hundred Years	Sellers, 1984
1979 January	"…farm land and residences were flooded…"	Major Storms and Floods in Arizona 1862-1983	Anthony Brazel, 1984
	"...farm land and residences were flooded…"	Arizona Climate: The First Hundred Years	Sellers, 1984
1980 February	"Severe flooding…raging torrent."	Major Storms and Floods in Arizona 1862-1983	Anthony Brazel, 1984
	"…raging torrent."	Arizona Climate: The First Hundred Years	Sellers, 1984
	Journel Notes	Flood February 1980. FCD Journel	FCD (802.045)
1982 October	"…swollen…"	Major Storms and Floods in Arizona 1862-1983	Anthony Brazel, 1984
1990	Photos	Newspaper Articles and Photos: Flooding Events 1983-1990	FCD (007.108)
NOTES: References listed with FCD (##) codes in this Table are on file at the FCDMC Library.			

Table 2-7 Historical Flood Discharges on the Agua Fria River near Lake Pleasant

Date	Location	Estimated Peak Discharges (cfs)	Source
Mar. 1889		Flood*	USACOE, 1968
Feb. 20-23, 1890		Flood*	USACOE, 1968
Feb. 19, 1891	Near Waddell	80,000	USACOE, 1968
Jan. 1895		Flood*	USACOE, 1968
Mar. 1905		Flood*	USACOE, 1968
Nov. 1905		Flood*	USACOE, 1968
Mar. 1906		Flood*	USACOE, 1968
Mar. 3, 1907		Flood*	USACOE, 1968
Feb. 1911		Flood*	USACOE, 1968
Jan. 29, 1915	Near Waddell	60,000	USACOE, 1968
Jan. 19, 1916	Near Waddell	45,000	USACOE, 1968
Jan. 27, 1916	Near Waddell	105,000	USACOE, 1968
Apr. 18, 1917	Near Waddell	26,000	USACOE, 1968
Jul. 27, 1917	Near Waddell	80,000	USACOE, 1968
Aug. 6, 1918	Near Waddell	39,600	USACOE, 1968
Sept. 8, 1918	Near Waddell	53,500	USACOE, 1968
Nov. 27, 1919	Near Waddell	105,000	USACOE, 1968
Feb. 22, 1920	Near Waddell	30,000	USACOE, 1968
Jan. 3, 1922	Near Waddell	25,000	USACOE, 1968
Sept. 2, 1922	Near Waddell	60,000	USACOE, 1968
Dec. 27, 1923	Near Waddell	39,000	USACOE, 1968
Sept. 19, 1925	Near Waddell	18,600	USACOE, 1982
Feb. 1927	Near Waddell	62,000	USACOE, 1982
Feb. 13, 1931	Near Waddell	43,000	USACOE, 1982
Feb.19, 1932	Near Waddell	26,000	USACOE, 1982
Feb. 8, 1935	Near Waddell	21,000	USACOE, 1982
Mar. 17, 1937	Near Waddell	44,000	USACOE, 1982
Mar. 4, 1938	Near Waddell	38,000	USACOE, 1982
Mar. 2, 1941	Near Waddell	41,000	USACOE, 1982
Aug. 3, 1943	Near Waddell	24,000	USACOE, 1982
Aug. 29, 1951	Near Waddell	66,000	USACOE, 1982
Jan. 19, 1952	Near Waddell	26,000	USACOE, 1982
Sep. 13, 1958	Near Waddell	20,000	USACOE, 1982
Dec. 26, 1959	Near Waddell	27,000	USACOE, 1982
Apr. 4, 1965	Near Waddell	23,000	USACOE, 1982
Dec. 23, 1965	Near Waddell	41,000	USACOE, 1982
Dec. 19, 1967	Near Waddell	46,000	USACOE, 1982
Sep. 6, 1970	Near Waddell	50,100	USACOE, 1982
Oct. 7, 1972	Near Waddell	22,000	USACOE, 1982
Feb. 10, 1976	Near Waddell	30,900	USACOE, 1982
Mar. 2, 1978	Near Waddell	47,000	USACOE, 1982
Dec. 19, 1978	Near Waddell	79,500	USACOE, 1982
Feb. 20, 1980	Near Waddell	73,300	USACOE, 1982
Aug. 29, 1988	Near Rock Springs	19,200	Pope, et al, 1998
Mar. 1, 1991	Near Rock Springs	53,500	Pope, et al, 1998
Jan. 8, 1993	Near Rock Springs	52,500	Pope, et al, 1998
Feb. 15, 1995	Near Rock Springs	35,700	Pope, et al, 1998

Notes: Flood* = peak discharge not determined

Gaged Floods. Gage records have been kept intermittently on the Agua Fria River near the location of Waddell Dam since 1910. Elsewhere, gaging began in 1940 near Mayer, in 1960 at Avondale, and in 1970 near Rock Springs. The data collected at Waddell Dam after its closure are lake level and estimated mean daily discharges only. No authoritative source of peak discharge of inflows exists. The U.S. Army Corps of Engineers has attempted to reconstruct peak inflows (USACOE, 1982).

The annual flood series for several gages are shown in Figure 2-13. A depiction of the distribution of flood occurrence by month is shown in Figure 2-15 and *Table 2-8*. A list of significant gaged floods is provided in Table 2-7.

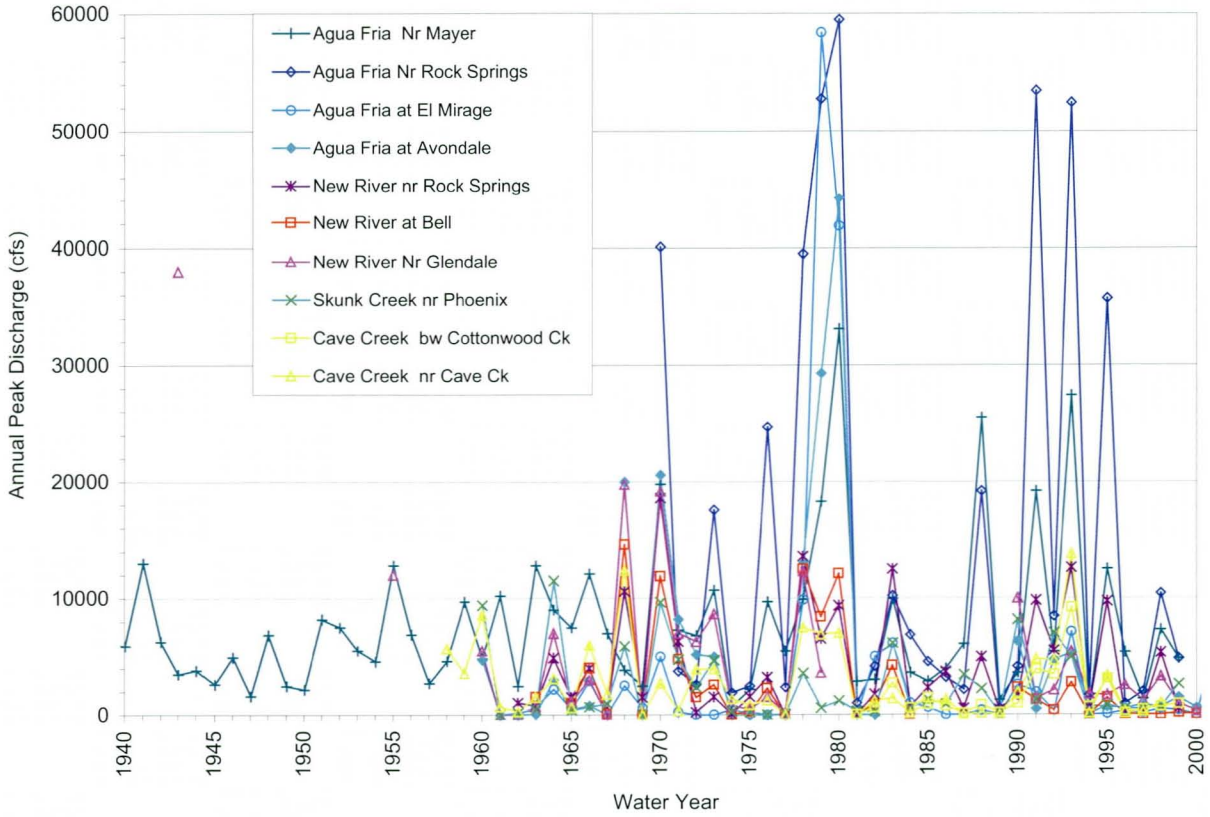

Figure 2-13 Annual Peak Discharges at USGS Gaging Stations

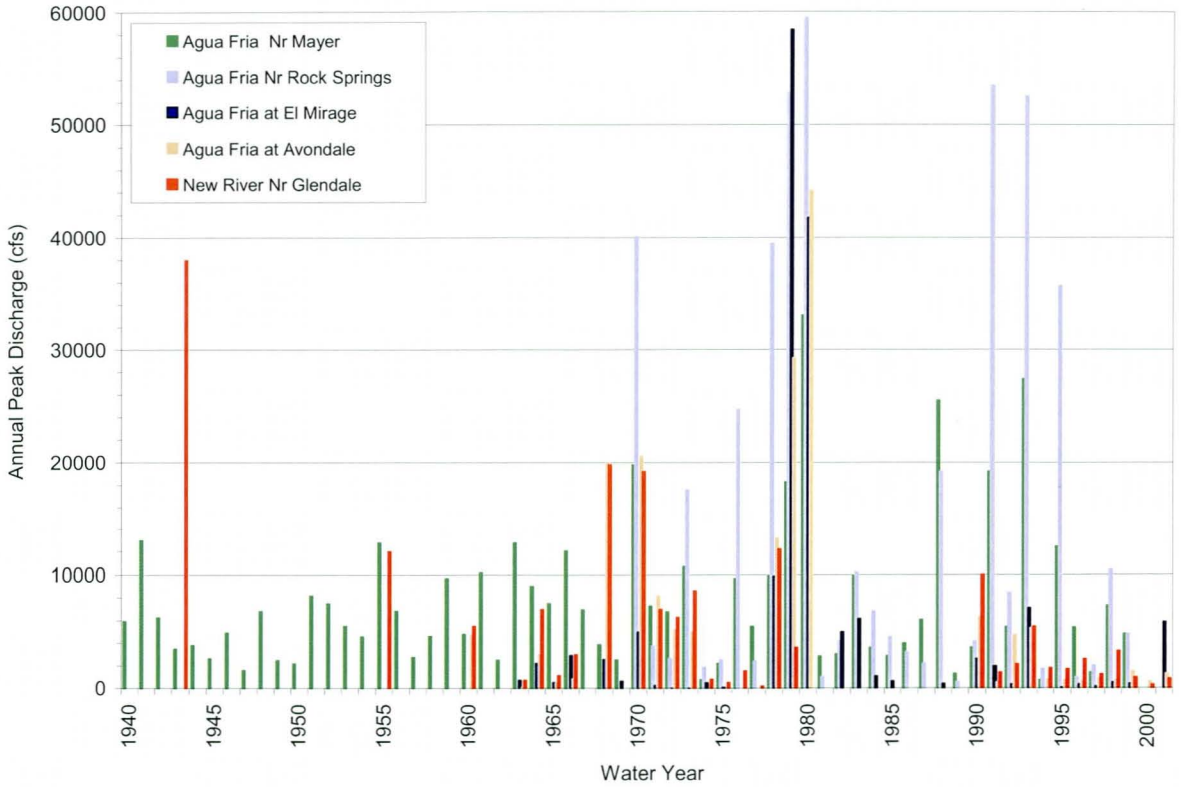

Figure 2-14 Annual Peak Discharges for USGS Gages in the Agua Fria River Watershed

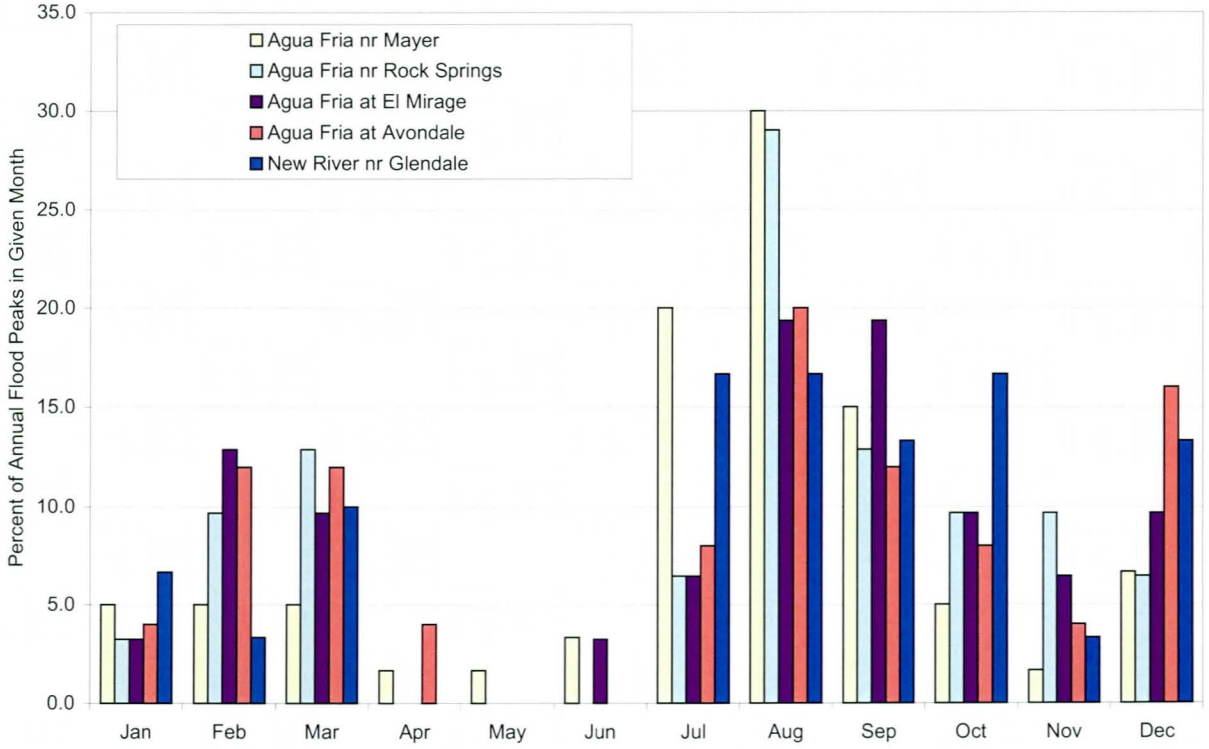

Figure 2-15 Seasonal Distribution of Annual Flood Peaks

Table 2-8 Distribution of Annual Peak Discharge for Selected Gages, in cfs

Jan	Feb	March	April	May	June	July	August	Sept	Oct	Nov	Dec
Agua Fria near Mayer (09512500): 1940-1999											
27400	33100	19200	7470	1380	5920	10200	25500	19800	10700	3970	18300
7500	12500	13000			4620	9000	12800	9940	6070		12100
2460	9700	9900				6880	12800	4570	688		3850
		7280				5510	9700	3810			2880
						5370	8180	3600			
						4930	7280	3500			
						4820	6960	3040			
						2620	6830	2850			
						2190	6800	2470			
						2170	6280				
						740	5480				
							5410				
							4820				
							3620				
							2710				
							2490				
							1610				
							1280				
Agua Fria near Rock Springs (09512800): 1919,1970-1999											
52500	59500	53500				2490	19200	40100	2160	85000	52800
	24700	39500				4150	8460	17600	1700	10200	4560
		35700					6860	4830		3220	
		10400					3750	2030			
		4190					2620	1020			
							2390				
							1900				
							968				
							562				
Agua Fria at El Mirage (09513650): 1963-2000											
77	41800	9870			10	2200	5000	5000	500	50	58400
	7100	6140				380	2900	2580	20	9	2520
	503	1950					460	1050			331
	155						370	700			
							334	621			
							250	600			
Agua Fria at Avondale (09513970): 1960-2000											
5300	44200	13100	460			5180	20600	6300	5000	765	29300
	680	500				4700	8200	856			20000
	680	575					3000	575			4700
							1477				800
							63				
New River near Rock Springs (09513780): 1962-1999											
12600	9710	13600	1510			1670	6320	18600		12500	10600
510	9350	9810				529	4900	1530		4980	4020
428	5510	6530				77	765	1050		3700	2310
	3230	5320					231	245		1570	1550
		1760					68			604	692
		545					4				
		35									
New River near Glendale (09513910): 1960-2000											
5450	1220	12300				12000	38000	19200	8650	2540	19800
1100		1400				6300	7000	10000	1770		5500
		300				3290	7000	1690	490		3620
						2110	775	1550	168		3000
						948	690				

The following conclusions may be drawn from the flood data shown in Figure 2-13 to Figure 2-15 and Table 2-7 and Table 2-8:

- Upper Watershed. The upper watershed experiences a greater number of its maximum annual floods during the summer monsoon. However, many of the largest discharges occur in the winter or early spring likely as the result of rain-on-snow flooding or high intensity rainfall occurring on a watershed saturated from an entire winter of prior precipitation.
- Lower Watershed. The lower watershed (e.g. Avondale) shows a greater percentage of maximum annual floods occurring in the winter. This may be the result of the presence of the Waddell Dam and the fact that larger volume events are required for runoff to flow from the mountains all the way to the Gila River. These types of events are associated with winter storms.
- Largest Floods. Large floods can occur in both the winter and summer seasons. However, with the exception of the New River, the largest gaged floods have occurred during the winter.
- Droughts. Long periods of no significant flooding have occurred and will likely be repeated in the future.

Flood Frequency. Estimates of flood frequency were obtained from the work of others, including the USGS (Pope et. al., 1998) and the USACOE (1995). Note that the frequency estimates reported for the Agua Fria near Rock Springs gage in Pope et. al (1998) differ dramatically from those in the USACOE (Table 2-9). Physical evidence from the study reach examined for the geomorphic analyses performed by JEF imply that the Pope et. al. estimates overestimate the low frequency flood magnitudes.

Table 2-9 Comparison of Flood Frequency Estimates

Source	100-year (cfs)	50-year (cfs)	25-year (cfs)	10-year (cfs)	5-year (cfs)	2-year (cfs)	Location
USACOE, 1995	135000	110000	90000	62000	43000	20000	Inflow to Lake Pleasant
Pope, 1998	211800	140100	88900	44300	23300	7000	Near Rock Springs

The Pope, et. al (1998) estimates are based on statistical analysis of gage records from 1970 to 1996 including one historical estimate from Nov. 1919 flood. The Corps considered additional historical peak discharge estimates. They also reconstructed instantaneous peak discharge estimates for inflows to Lake Pleasant from daily discharge data collected by the Maricopa Water Conservation District (see USACOE, 1982 for discussion). Therefore, the data upon which the two analyses are based differ.

One additional item of interest with respect to the historical flood peak magnitude estimates is provided by Carmody (1980). He reexamined 19 historical large flood estimates in Arizona, one of which was the 1916 flood on the Agua Fria River. The magnitude of the 1916 flood has been widely reported as 105,000 cfs (Table 2-7). Carmody researched the original USGS notes on the flood peak estimate. The notes show a peak of 70,300 cfs based on an area of 3,515 sq. ft, a wetted perimeter of 384, an estimated velocity of 20 ft/sec, and a Bazin m value of 0.53. Carmody converts these data to an equivalent Manning's n-value of 0.016, and concludes that a more realistic estimate of the 1916 flood peak is about 35,000 cfs. In addition, since the November 1919 flood peak was estimated as nearly identical to the 1916 flood based on a similar stage, the 1919 peak estimate may also be too high. Consequently, the estimates of flood frequency by both the USACOE (1995) and the USGS (1998) may be grossly overstated for the Agua Fria River.

During the hydraulic modeling performed for this study (Chapter 6), profiles of 105,000 cfs, 150,000 cfs, and 200,000 cfs were computed using the HEC-2 model prepared by others for the effective Flood Insurance Study for the Agua Fria River. Predicted water surface elevations were compared to surfaces on the ground. In general, discharges larger than 150,000 cfs inundated geologically old surfaces that have not been inundated for at least thousands of years. Therefore, it is believed that the USGS estimates of the 100-year discharge are overestimated, and that there is some uncertainty in the Corps frequency estimates. A more detailed investigation of paleoflood evidence in the watershed would provide greater clarity regarding these issues. Nevertheless, for the purposes of this study, the Corps estimates served as the basis of the hydraulic and mathematical computations for the erosion hazard assessment.

2.1.3.2 Hydrologic Modeling.

The design hydrology considered in this study was taken from the U.S. Army Corps of Engineers, *Hydrologic Evaluation of Impacts of New Waddell Dam on Downstream Peak Discharges in the Agua Fria River*, July 1995. This document follows an earlier report entitled *Hydrology for Evaluation of Flood Reduction by New Waddell Dam Agua Fria River Below New Waddell Dam to the New River Confluence* (USACOE, 1988) and the *Hydrology Part 2, Design Memorandum No.2* (USACOE, 1982). These documents together describe the methods, procedures, and results of the design hydrologic data presented in this report.

Data for the three periods of interest (pre-dams, post-old Waddell, and post-New Waddell) were taken from these documents as well as from the Flood Insurance Study HEC-2 models (Jerry Jones, 1989, and Coe Van Loo, 1996) which were also based on the USACE hydrologic analyses.

Pre-Waddell Dam Conditions. Table 2-10 shows the flood frequency for the Agua Fria River downstream of the Waddell Dam for the condition prior to construction of the (old) Waddell Dam.

Table 2-10 Pre-(old) Waddell Dam Discharges

RM (miles)	100-year (cfs)	50-year (cfs)	25-year (cfs)	10-year (cfs)	5-year (cfs)	2-year (cfs)	Drainage Area (sq. miles)
33.82	135000	110000	90000	62000	43000	20000	1459
33.46	133160	109400	89300	61200	42400	19700	
31.39	131370	105700	85200	60300	41800	19500	
29.47	130000	102400	81400	59700	41400	19300	
27.86	128770	99600	78200	59100	41000	19100	
26.47	127440	97100	75500	58500	40600	18900	
25.192	124990	94900	72900	57400	39800	18500	
24.353	123000	93400	71300	56500	39200	18200	
23.504	121000	91900	69600	55600	38500	17900	
22.558	118940	90300	67700	54600	37900	17600	
20.675	115000	87000	64000	52800	36600	17000	1840
17.548	108120	81800	60200	49700	34400	16000	
16.385	109000	82000	59000	50100	34700	16100	
9.79	90000	66000	45000	41300	28700	13300	1900
9.696	95000	69700	47500	43600	30300	14100	2243
5.305	91000	66800	45500	41800	29000	13500	
3.77	90000	66000	45000	41300	28700	13300	2312
0.16	90000	66000	45000	41300	28700	13300	2388
Sources:							
	COE, 1995, Table 1.						
	Jerry Jones, 1989, Agua Fria FIS.						
	Ratio of QT/Q100 at RM 33.82 and at RM 20.675 for RM 17.548 50- and 25-yr						
	Computed proportional to increases and decreases for Q100 at same RM for 50- and 25-yr						
	From COE, 1988, Plate 4						
Ratios	1.00	0.81	0.67	0.46	0.32	0.15	@ RM 33.82
	1.00	0.76	0.56				@ RM 20.675

Post-Waddell. Table 2-11 shows the flood frequency for the Agua Fria River downstream of the (old) Waddell Dam, after construction of Waddell Dam. Comparison of discharges at RM 33.82 in Table 2-10 with discharges in Table 2-11 show that Lake Pleasant affected discharges less than the 25-year flood. The 5- and 10- year floods were attenuated, while the 2-year flood generally did not result in outflow from the old dam. Releases from the dam are know to have occurred in 1941, 1966, 1968, March 1978, December 1978, and February 1980 (Thomsen, 1980). The data in Table 2-11 reflect the post- (old) Waddell condition following completion of the Arizona Canal Diversion Channel (ACDC) and the New River, Adobe, and Cave Buttes Dams, all of which were completed in the mid-1980's. Therefore, between 1927 and the mid-1980's discharges downstream of the New River would have been different than shown in Table 2-11. The Corps states that the more frequent discharges have increased downstream of the New River due to the ACDC and related flood control construction (USACOE, 1995).

Table 2-11 Post- (old) Waddell Discharges

RM	100-year	50-year	25-year	10-year	5-year	2-year	Drainage Area *	JJ RM
(miles)	(cfs)	(cfs)	(cfs)	(cfs)	(cfs)	(cfs)	(sq. miles)	(miles)
33.82	135000	110000	90000	48000	16000	0	0	33.82
33.46	133160	109400	89300	47300	15700	600	24	33.46
31.39	131370	105700	85200	43400	14000	700	26	31.39
29.47	130000	102400	81400	39700	12400	700	39	29.47
27.86	128770	99600	78200	36700	11100	800	47	27.86
26.47	127440	97100	75500	34000	10000	900	49	26.47
25.192	124990	94900	72900	31600	8900	900	53	25.18
24.353	123000	93400	71300	30000	8200	1000	56	24.26
23.504	121000	91900	69600	28400	7500	1100	64	23.44
22.558	118940	90300	67700	26600	6700	1100	70	22.32
20.675	115000	87000	64000	23000	5200	1200	171	20.55
17.548	108120	81800	60200	21600	4900	1200	182	17.55
16.385	109000	82000	59000	22000	4800	780	183	
9.79	90000	66000	45000	18000	4600	820	231	
9.696	95000	69000	50000	19000	10000	5500	392	
5.305	91000	68200	47600	18200	10000	5400	474	
3.77	90000	68000	47000	18000	10000	5300	485	
0.16	89000	67000	47000	17800	9000	5000	485	

Sources:

	COE, 1995, Table 1.
	Jerry Jones (JJ), 1989, Agua Fria FIS.
	COE, 1982, Table 14
	Ratio of QT/Q100 at RM 33.82 for RM 33.46-22.558, and at RM 20.675 for RM 17.548
	Computed as proportional to increases and decreases for Q100 at same RM

Ratios	1.00	0.81	0.67	0.36	0.12	@ RM 33.82
	1.00	0.76	0.56	0.20	0.05	@ RM 20.675

* Drainage area does not include area controlled by dams.

Post-New Waddell. Table 2-12 shows the discharges for the 2- to 100-year floods for the Post-New Waddell Dam condition used in this study. Note that no flow is released from the dam for less than about the 25-year event. According to the USACOE (1995), the flood frequency for the watershed downstream of the New Waddell Dam is controlled by rainfall on the lower watershed alone. That is, the lower watershed is capable of generating higher discharges more frequently by itself than in combination with outflows from the dam. Therefore, downstream of Morgan City Wash (RM 33.41) outflow from the dam no longer plays a role in the flood frequency estimates for the Agua Fria River.

Table 2-12 Post-New Waddell Discharges

RM	100-year	50-year	25-year	10-year	5-year	2-year	Drainage Area *
(miles)	(cfs)	(cfs)	(cfs)	(cfs)	(cfs)	(cfs)	(sq. miles)
33.82	9000	9000	9000	0	0	0	0
33.41	19000	14700	10400	5600	2600	600	24
31.86	21000	16200	11500	6200	2900	700	26
30.46	23000	17800	12600	6700	3200	700	39
29.04	25000	19300	13700	7300	3500	800	47
27.77	27000	20900	14800	7900	3700	900	49
26.37	29000	22400	15900	8500	4000	900	53
25.098	31000	24000	16900	9100	4300	1000	56
23.692	33000	25500	18000	9700	4600	1100	64
22.273	35000	27100	19100	10300	4900	1100	70
20.675	37500	29000	20500	11000	5200	1200	171
17.548	36000	27800	19700	10600	5000	1200	182
16.385	34500	26500	19000	10000	4800	780	183
9.79	30000	23000	16000	8700	4600	820	231
9.696	54400	39000	26000	16100	10000	5500	392
5.305	52000	38000	25000	15300	10000	5400	474
3.77	50900	37000	25000	15000	10000	5300	485
0.16	48200	35000	23000	14200	9000	5000	485
* Drainage area does not include area controlled by dams.							
Sources:							
	COE, 1995, Table 1.						
	CVL, 1996, Agua Fria FIS.						
	Ratio of QT/Q100 at RM 20.675						
Ratios	1.00	0.77	0.55	0.29	0.14	0.03	

Figure 2-16 below shows the 100-year inflow and outflow hydrographs for the New Waddell Dam. One can see the drastic reduction in peak discharge from 135,000 cfs to 9,000 cfs as well as the significant change in the shape of the hydrograph from a rapidly rising and falling hydrograph lasting about one day, to a flat prolonged hydrograph lasting several days.

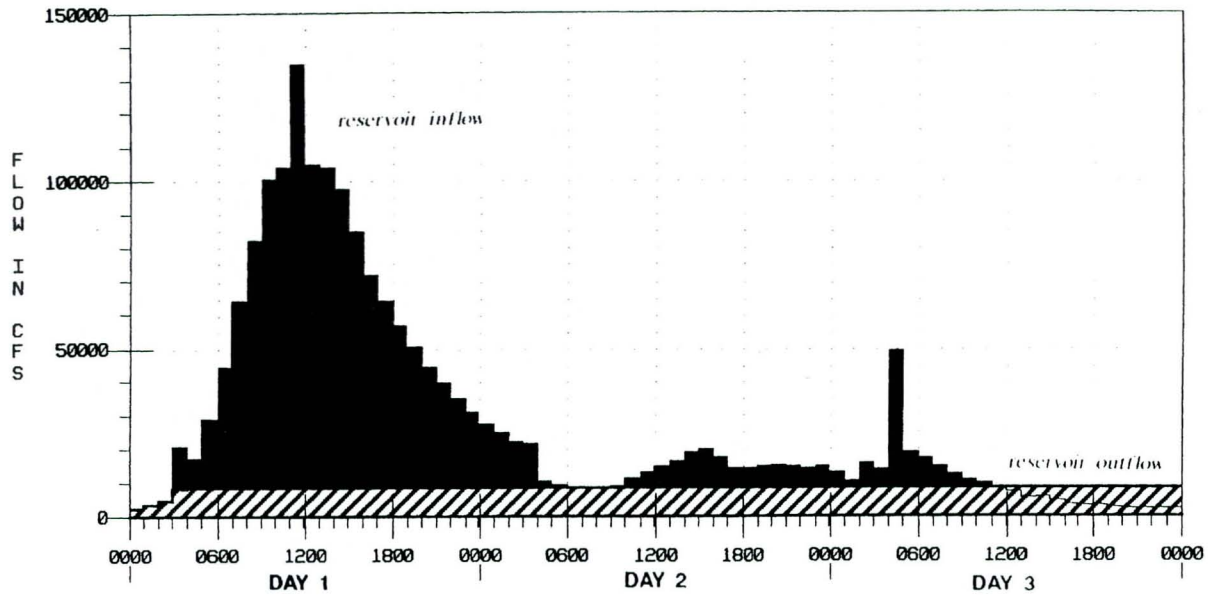

Figure 2-16 Simulated 100-year Flood Routing, New Waddell Dam (USACOE, 1995)

While the peak discharge frequency may no longer be affected as strongly by the outflows from New Waddell Dam, sediment transport modeling (Chapter 6) suggests that erosion in the channel can be strongly affected by prolonged moderate discharges from the dam. This issue is discussed further in Chapter 6.

Comparison of Three Periods. Comparison of Table 2-10 - Table 2-12 and examination of Figure 2-17 - Figure 2-21 illustrate the dramatic alterations to the lower Agua Fria as the result of the construction of the Waddell and New Waddell Dams. Prior to the dams, the lower Agua Fria experienced relatively large discharges on a more frequent basis, which is supported by the historical recording of repeated flooding on the river before 1927. The post-New Waddell 100-year discharge is comparable to the 2- to 5-year flood prior to construction of either dam. Therefore, it should be expected that the river will experience a transformation of its morphology as it adjusts to the processes imposed by the New Waddell Dam. Also, given that the magnitude of peak discharges was substantially reduced by dam construction, and that much of the geomorphic work of channel change occurs during the largest floods, the frequency of significant channel change should decrease relative to the pre-dam conditions. These effects will be examined in the remaining chapters of this report.

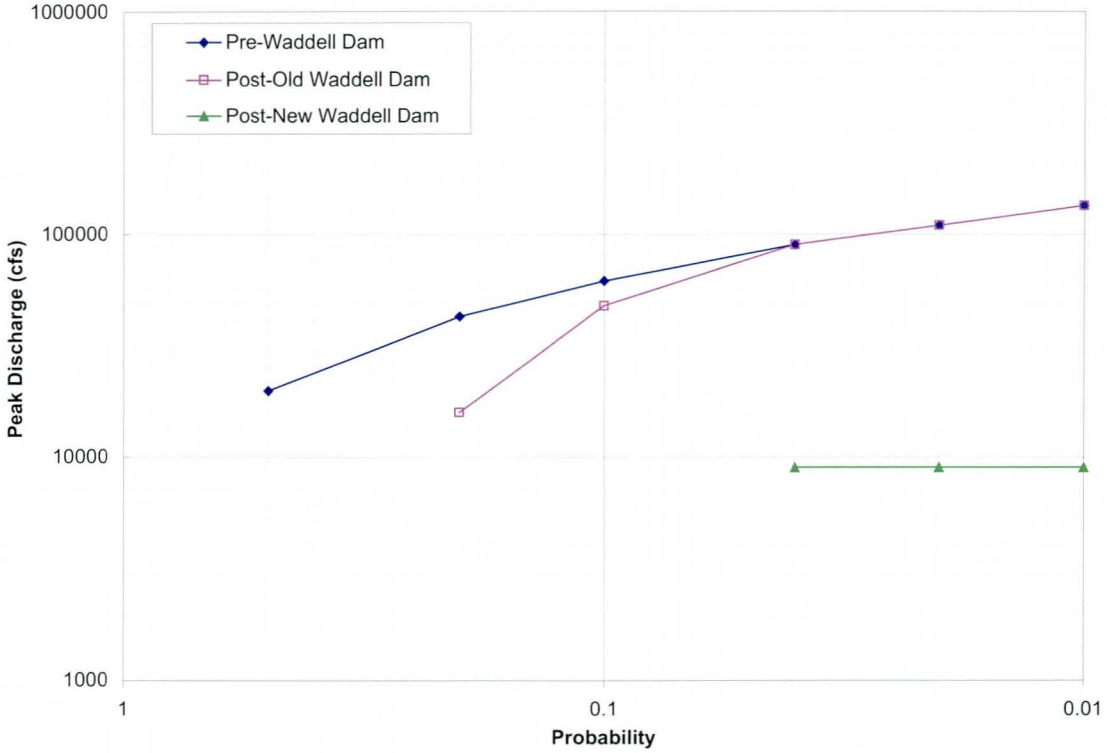

Figure 2-17 Comparison of Flood Flow Frequency Just Downstream of Waddell Dam

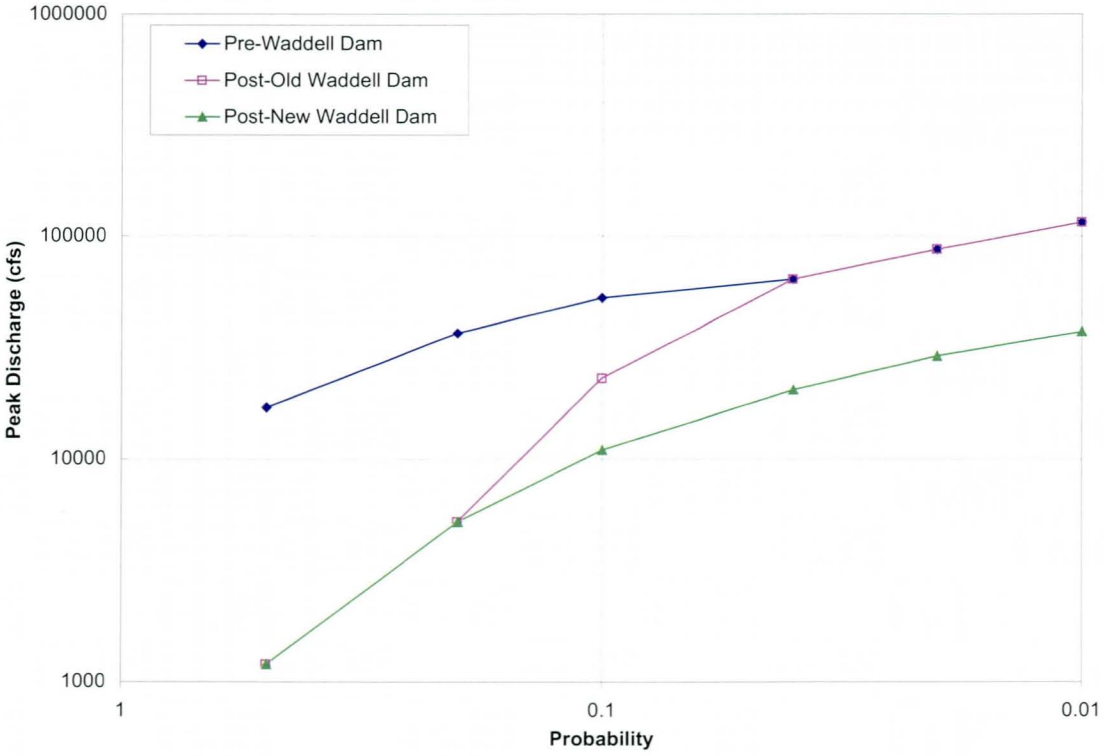

Figure 2-18 Comparison of Flood Flow Frequency at Bell Road

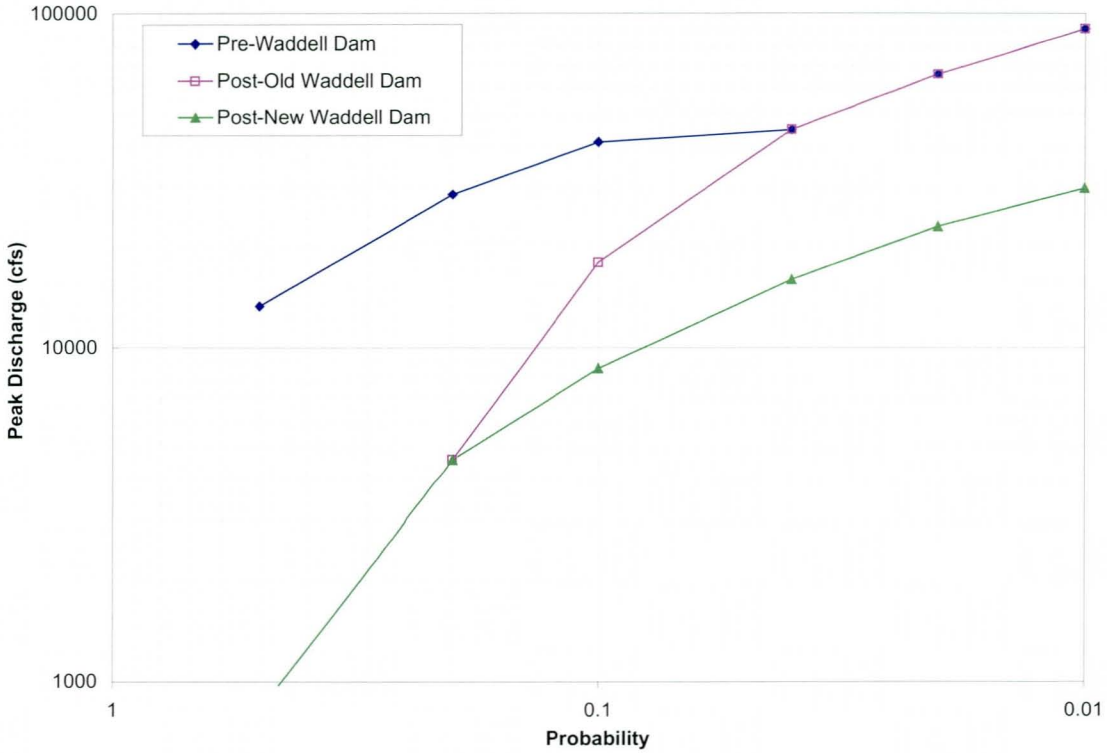

Figure 2-19 Comparison of Flood Flow Frequency Just Upstream of New River Confluence

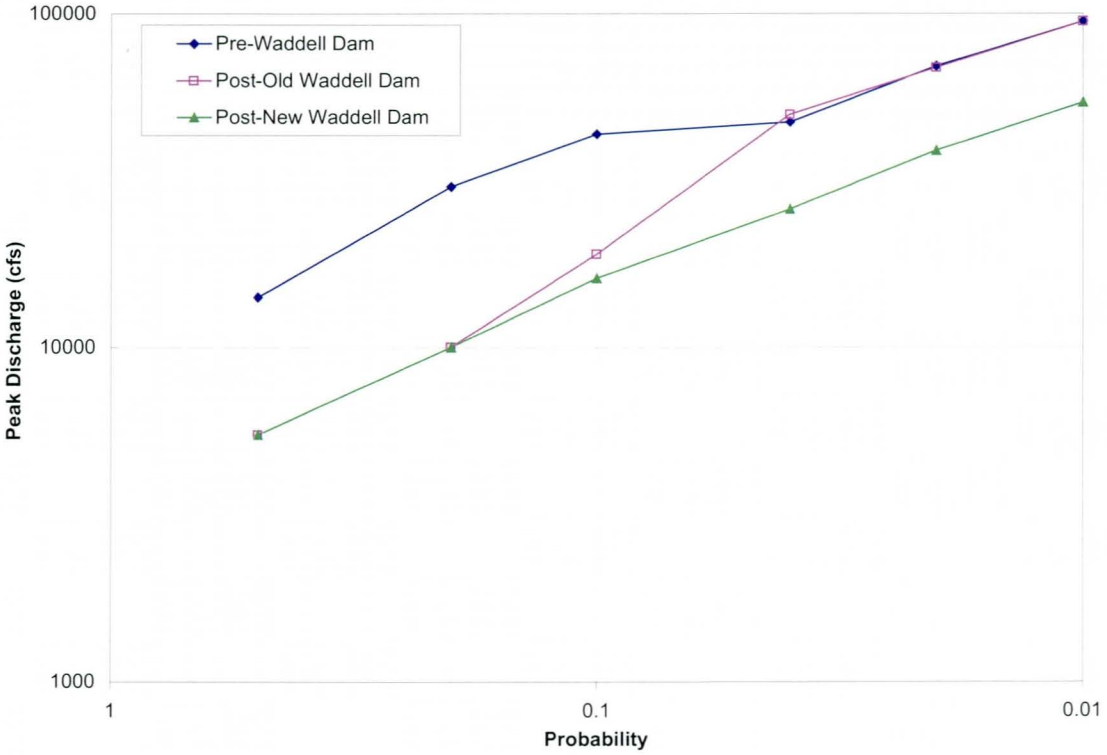

Figure 2-20 Comparison of Flood Flow Frequency Just Downstream of New River Confluence

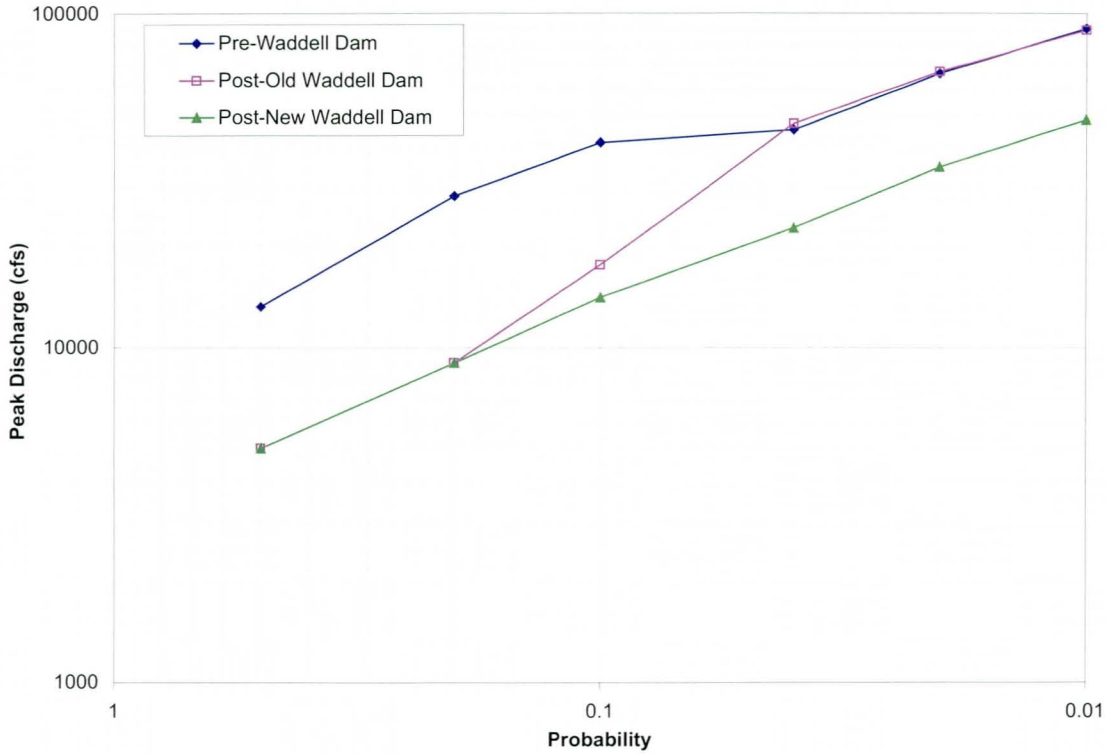

Figure 2-21 Comparison of Flood Flow Frequency at Gila River Confluence

2.1.4 Stream classification

The primary objective of stream classification is to match measurable stream characteristics with expected river responses. The following two classification systems were applied to the stream segments within the study area: (1) a descriptive classification system based on the Brice system, and (2) the Rosgen system. Data for the stream classification were obtained from field surveys of the project site, topographic mapping, aerial photographs, and published reports. Only the channel characteristics required to perform the stream classification are presented here. More detailed discussions of specific channel characteristics and specific reaches are provided later in this Chapter as well as in Chapters 3, 4, 5, and 6 of this report.

2.1.4.1 Brice Classification System

The Brice system was developed primarily for the evaluation of stream stability near roadways or bridge structures, but is not limited to highway design applications. The Brice System uses readily identified stream characteristics to make subjective predictions of lateral stability (FHWA, 1991; Brice and Blogett, 1978). Use of the Brice Classification system is appropriate for the Agua Fria River Watercourse Master Plan since one of its primary objectives is to assess stream stability and the potential for lateral migration. The Brice system assigns relative erosion potential classifications based on the 13 stream characteristics summarized below (Table 2-13). These classifications can be used to prepare a subjective, relative assessment of the potential for lateral migration. Where high or moderate potential for lateral migration is identified, more detailed analysis of lateral erosion potential is warranted.

Table 2-13 Brice Classification System

Stream Characteristic	Agua Fria River
Stream Size	Wide (> 500 ft) Average channel width = 1300 ft.
Flow Habit	Ephemeral, Flashy; downstream of dam
Bed Material	Gravel (sand to small cobbles) Upper: D_{50} = 2.2 mm; D_{90} = 28 mm Middle: D_{50} = 1.1 mm; D_{90} = 23 mm Lower: D_{50} = 0.5 mm; D_{90} = 1.9 mm
Valley Setting	Low relief valley (<100 ft.)
Floodplain	Wide (> 10x channel width) Avg. floodplain width = 5400 ft. (4x)*
Natural Levees	Little or none
Apparent Incision	Slightly incised Average bank height = 5-11 ft.
Channel Boundaries/ Bank Materials	Alluvial Local bedrock in banks upstream of Cowtown in Reaches 1 and 2
Bank Vegetative Cover	< 50 percent Average = 25 %; Range = 0-90 %
Sinuosity	Slightly sinuous (S = 1.0-1.2) Average sinuosity = 1.09
Braiding	Generally braided (> 35 %) (natural sections)
Anabranching	Locally anabranched
Width Variability Bar Development	Random variation Irregular point & lateral bars
Notes: Channel width includes multiple braids. Differentiation of channel and floodplain not often meaningful.	

Each of the Brice classification system categories are discussed briefly below. More detailed descriptions of the geomorphic characteristics of the study area are provided in Chapters 3-6 and in Appendix B. Definitions of key terms are provided in the Glossary (Chapter 10).

1. Stream Size. The potential for, and scale of, lateral erosion generally increases with stream size. The Agua Fria River has a large channel and hence a large potential for lateral channel movement based on its size alone.
2. Flow Habit. Perennial streams tend to experience more frequent erosion than ephemeral streams in equivalent climates. However, in arid regions where flash floods and unstable bank materials can cause significant lateral erosion, ephemeral streams are often highly erosive. The Agua Fria River in the study reach is ephemeral and experiences flash floods, and thus may be subject to rapid rates of lateral movement and long-term fluctuations in bed elevation. It may also experience prolonged clear-water discharges from New Waddell Dam. These releases may be capable of significant local erosion.
3. Bed and Bank Material. The bed sediment distributions range from fine sands to boulders but are predominantly sands and gravels. Bed and bank material size varies along the study reach as well as across a cross section. Sediments generally decrease in size with increasing distance downstream or laterally from the channel. Bed and bank materials are typically stratified with sizes varying widely with depth and distance. Stream banks with stratified sediments may be more vulnerable to scour and bank

erosion than stream banks with comparable uniform sediment material due to the potential for selective erosion of less resistant layers.

4. Valley Setting. Channel reaches with low valley relief (< 100 ft.) typically have more erosion-prone banks than streams in valleys with high relief. The Agua Fria River in the study area exhibits low relief. Its channel is entrenched between Pleistocene-aged alluvial terraces which have little lateral relief beyond the terraces.
5. Floodplains. Channels with wide floodplains (floodplain width > 10 times channel width) typically experience more lateral channel movement than channels with little or no floodplain (< 2 times channel width). The average Agua Fria River 100-year floodplain width is about 4 times the average channel width, which corresponds to an intermediate risk of lateral erosion. However, the average channel width includes multiple braids of braided reaches and the floodplain is often not well differentiated from the floodplain. In general, the river has historically actively occupied the entire corridor between Pleistocene terraces which become more widely spaced in the downstream direction.
6. Natural Levees. Streams with natural levees tend to have low rates of lateral migration. The Agua Fria River does not have natural levees.
7. Apparent Incision. Streams with vertical cut banks are generally unstable. Where a main channel is visible on the Agua Fria River, there are often cutbanks. Some of these cutbanks are along individual braids within the larger braided river pattern. Others are along the Pleistocene terraces. All of these banks are subject to erosion. The rate of erosion will be greater along internal cutbanks than along the Pleistocene terraces. The Pleistocene terraces are subject to erosion by undercutting of the least consolidated of the stratified materials.
8. Channel Boundaries and Bank Materials. Alluvial streams are more susceptible to lateral erosion than non-alluvial streams. Bedrock crops out in numerous places on the banks in the upstream two reaches (see Reach 1 and 2 descriptions later in this Chapter). Downstream of the Central Arizona Project Canal, no bedrock was observed in the bed or banks of the Agua Fria. The channel banks and floodplain in the remainder of the study area are comprised of alluvium. Where the channel intersects geomorphic surfaces of middle to late Pleistocene age, carbonate (caliche) accumulation cements some layers to near bedrock hardness. However as mentioned in item 7 above, the banks containing carbonate layers are generally stratified and subject to failure by undercutting and erosion of the non-carbonate layers.
9. Vegetation. Streams that lack adequate vegetative cover along the banks tend to be more susceptible to erosion. Dense, woody vegetation may also slow flood velocities against the banks, as well as redirect flow away from the banks. Roots can also stabilize the soils in the banks, by providing a structure that tends to hold bank materials together. Deeper and denser root networks provide greater stability than shallow, less dense roots which tend to be undercut. In general, field evidence indicates that the banks of the Agua Fria River are poorly vegetated, and therefore are subject to erosion.
10. Sinuosity. The streams in the study area have sinuosity values of less than 1.2 and are not considered "meandering" streams. Therefore, their patterns cannot be accurately predicted by published meander geometry relationships.[4] The Agua Fria River has an average sinuosity of about 1.1.
11. Degree of Braiding. Braided streams tend to be laterally unstable. The Agua Fria River is generally braided. This pattern may be changing in response to extraction of sediments by mining, channel encroachments, and in response to changes in hydrology caused by upstream dams.
12. Degree of Anabranching. The Agua Fria is locally ananbranched, especially in Reach 6 downstream of Hatfield Road where several floodplain islands lie between divided active

[4] By definition, meandering streams have sinuosity greater than 1.2. Therefore, meander relationships are not applicable to streams with sinuosity less than 1.2.

channels. Two of these islands have creosote bush growing on them. Anabranching in this reach may be the result of avulsions that formed new channels away from the main channel. Anabranching streams are subject to high rates of lateral erosion.

13. Variability of Width and Development of Bars. Streams with relatively uniform width and narrow, regular point bars tend to have slow lateral migration rates. The Agua Fria River has irregular channel widths, irregular point bars, and is subject to rapid lateral migration.

According to the Brice classification scheme, the Agua Fria River exhibits many characteristics that indicate that it is subject to high rates of lateral erosion. These broad stream characteristics indicate potential for frequent bank erosion and rapid lateral channel movement within the study area.

2.1.4.2 Rosgen Classification System

The Rosgen classification system (Rosgen, 1996) is based on measurable channel characteristics observed on streams located primarily in the western mountain region of the United States, although the classification system is now used in many parts of North America. The Rosgen (1996) system was applied to the study area because it has many adherents among State and Federal agencies in the western United States. The field survey techniques used for the study reach incorporated procedures recommended by Rosgen (1996) for obtaining channel sections, pool and riffle spacing, bankfull elevations, entrenchment ratio, slope, meander geometry, bank characteristics, and bed sediment distribution.

The least disturbed reaches in the study area appear to best match Rosgen's D5 category (Table 2-14), although there are a few significant differences from Rosgen's criteria. The reaches generally consist of medium to coarse sand beds, with slopes between 0.0016 and 0.0044 ft./ft. and an average sinuosity of less than 1.2, all of which are criteria that fit within the range of expected stream type D characteristics. The width/depth ratio, however, is generally much greater than 40, the cutoff for Rosgen's D5 category.[5] The reaches are generally not truly braided during flows that impact its banks, but because the Rosgen classification system is strongly weighted to low flow conditions (2-year or less), it was considered braided. Within the study reach, the Agua Fria River has some braided characteristics at very low flow rates and at the highest flow rates. For intermediate discharges, the channel pattern may be more like a straight single channel than a true braided stream. Therefore, the D category was assumed to be the most applicable. The Rosgen entrenchment ratio parameter varies greatly, from well entrenched (1.09) to slightly entrenched (7.92), with an arithmetic average for the reaches of 2.78 (slightly entrenched). It should be noted, however, that some of these values result from the anthropogenic modification of the river corridor and that an arithmetic average of the reaches may not be the best approach to characterizing the channel morphology.

[5] The Rosgen categories with lower width/depth ratios have much higher sinuosity and lower entrenchment ratios, and are therefore, a worse fit than the D5 category selected.

Table 2-14 Rosgen Classification Data

River Reach	1	2	3	4	5	6	7	8	9	10	11	12	13	14	15
Rosgen Classification	DA5	D5	DA4	D5	D5	D4	D4	D5	D5	D5	D5	F5	F5	D5	D5
Entrenchment Ratio	2.96	3.12	2.16	3.61	4.17	3.16	2.91	2.83	7.92	2.17	1.77	1.09	1.34	1.34	1.21
Width/Depth Ratio	30	80	34	128	189	199	120	54	95	63	156	78	68	129	116
Sinuosity	1.021	1.018	1.027	1.099	1.085	1.127	1.135	1.120	1.118	1.077	1.038	1.079	1.019	1.206	0.986
Channel Slope	0.0044	0.0029	0.0043	0.0033	0.0031	0.0026	0.0034	0.0026	0.0026	0.0023	0.0024	0.0022	0.0016	0.0025	0.0022
Channel Materials (D50)	0.6 mm	0.4 mm	3.9 mm	1.7 mm	1.7 mm	2.8 mm	4.5 mm	1.7 mm	0.6 mm	1.3 mm	0.6 mm	0.6 mm	0.5 mm	0.4 mm	0.5 mm
Size Class	MS	MS	FG	VCS	VCS	FG	FG	VCS	CS	VCS	CS	CS	MS	MS	MS
Channel Pattern	S	S	S	B	B	B	B	DIST	B	DIST	DIST	DIST/S	DIST/S	DIST/B	B

Notes:

1. Sinuosity – measured on 1999 aerial photographs
2. Entrenchment ratio – Larger of channel or total flow topwidth ¸ Q2 topwidth (data from HEC-RAS)
3. Width/Depth ratio – Q2 flow width ¸ Q2 flow depth (data from HEC-RAS)
4. Channel slope – reach average of HEC-RAS So values
5. Channel materials – best fit sediment distribution from sieve and boulder count data
6. Channel pattern codes: B = braided; MC = multiple channel; S = single channel; DIST = disturbed
7. Channel materials codes: F = fine; M = medium; C = coarse; S = sand; G = gravel; V = very (SCS gradations)

The Rosgen description of D5 stream types follows:

> *The D5 stream types are multiple channel systems, described as braided streams found within broad alluvial valleys and on alluvial fans consisting of deposited sand-sized materials. The braided system consists of interconnected distributary channels formed in depositional environments. The D5 stream type occurs in gentle gradient , narrow, U-shaped glacial valleys consisting of glacio-lacustrine deposits, sand dunes (eolian); in very low relief alluvial valleys; and in glacial outwash areas and deltas. The D5 stream channels may be found in Valley Types III, V, VIII, IX, X, and XI[6]. Channel bed materials are predominantly sand, with interspersed amounts of silt/clay materials on deltas and in varves of lacustrine depositional areas. The braided channel system is characterized by high bank erosion rates, excessive deposition occurring as both longitudinal and transverse bars, and annual shifts of the bed location. Bed morphology is characterized by a closely spaced series of rapids and scour pools formed by convergence/ divergence processes that are very unstable. The channels generally are of the same gradient as their parent valley. A combination of adverse conditions are responsible for channel braiding, including high sediment supply, high bank erodibility, moderately steep gradients, and very flashy runoff conditions which can vary rapidly from a base flow to an overbank flow on a frequent basis. Characteristic width/depth ratios are very high, exceeding values of 40 to 50 with values of 400 or larger often noted. D5 channel gradients are generally less than 2%, however, D5 types can also develop within alluvial fans which have slopes of 2% to 4% (D5b). Observations have been made of braided streams on alluvial fans with slopes greater than 4% (D5a). The D5 is a very high sediment supply system, and typically produces high bedload sediment yields. (Emphasis added.)*

The primary differences between the river reaches in the Agua Fria River system and Rosgen's D5 category, as described above, include the following:

- Braided channel pattern. Because of human impacts on the river such as encroachment, channelization, and in-stream mining, and reservoir impoundment impacts on the hydrology, the channel pattern is difficult to discern. The observed channel pattern has characteristics of braided, straight and meandering streams.
- Depositional environment. The Agua Fria River has experienced net degradation during the past 50 years, due primarily to human impacts, as opposed to the net aggradation as defined by Rosgen. Evidence of localized deposition of fine-grained sediments was observed at many places within the study area.
- Bed material. Cobbles and boulders material comprise a significant percentage of the bed material in the upper reaches, rather than a small percentage as described by Rosgen. The bed is significantly finer in the downstream reaches.
- Instability. The bed features and channel characteristics, while certainly not stable, are probably not as unstable as implied in the Rosgen definition primarily because of the impoundment of the frequent floods in reservoirs upstream of the study reach, and the low frequency of runoff events.
- Overbank flow. The streams in the study area do not experience frequent overbank flow, as defined by the Rosgen classification system, primarily due to upstream impoundment of flood flows.

[6] These valley types encompass the range of valley types found in the study area.

- Highly active bank erosion. The streams in the study area have been subject to extreme rates of bank movement and shifts of bed locations, but only during the largest floods. More channel movement occurs during floods than during moderate flows.

The reasons for these discrepancies may include the following:

- Entrenched of the low flow channel due to in-stream mining, floodplain encroachment, flow depletion, upstream reservoirs and dams, and reduced sediment supply.
- Inadequacy of the Rosgen system for disturbed, incised, ephemeral, coarse-bed streams in central Arizona.

Regardless of these differences, if the Rosgen classification is applicable to streams in central Arizona, then the expected channel processes on the Agua Fria River system include high rates of sedimentation, susceptibility to bank erosion, and potential shifts in low flow channel characteristics.

2.1.4.3 Summary

Stream classification data presented above indicate that the Agua Fria River has many characteristics typical of braided, ephemeral streams, although the channel pattern itself is not truly braided along its entire length. More detailed discussion of specific channel characteristics will be provided elsewhere in Chapters 2 and 6 of this report. The classification systems indicate that high rates of lateral channel movement should be expected for the study area and that more detailed evaluation of lateral stability is warranted.

2.2 Reach descriptions

The Agua Fria River Watercourse Master Plan Report prepared by KHA and other team members divides the study area into three reaches, the "Upper Reach," the "Middle Reach," and the "Lower Reach." Because of the greater level of technical analysis required for the geomorphic/erosion hazard assessment, fifteen (15) reaches were differentiated by JEF, as shown in Figure 2-22. Reaches 1 through 7 are located within the "Upper Reach" defined in the main report prepared by KHA. Reaches 8 through 10 are located within the "Middle Reach," and Reaches 11-15 correspond to the "Lower Reach." The fifteen reaches were defined to provide for reasonable assessment of erosion hazards along the study reach. Reach divisions were made based on similarity of channel and sediment characteristics, locations of tributaries, impacts of man, and convenience of presentation at an understandable scale. Table 2-15 summarizes some of the key characteristics of each of the fifteen study reaches.

Descriptions of the each of fifteen reaches are provided in the remainder of this chapter. The reach descriptions include information about:

- Reach Length and Limits
- Channel Slope
- Active Channel Width
- Channel Pattern
- Geomorphic Setting – terraces, bedrock, geographic features
- Channel Bed Material
- Channel Bank Characteristics
- Floodplain Limits – geologic, pre-Waddell, post-Waddell, post-New Waddell
- Sand and Gravel Mining – location, extent, dates

- Floodplain and Channel Encroachments
- Structures – bridges, utilities, canals, bank stabilization, grade control
- Channel and Floodplain Vegetation

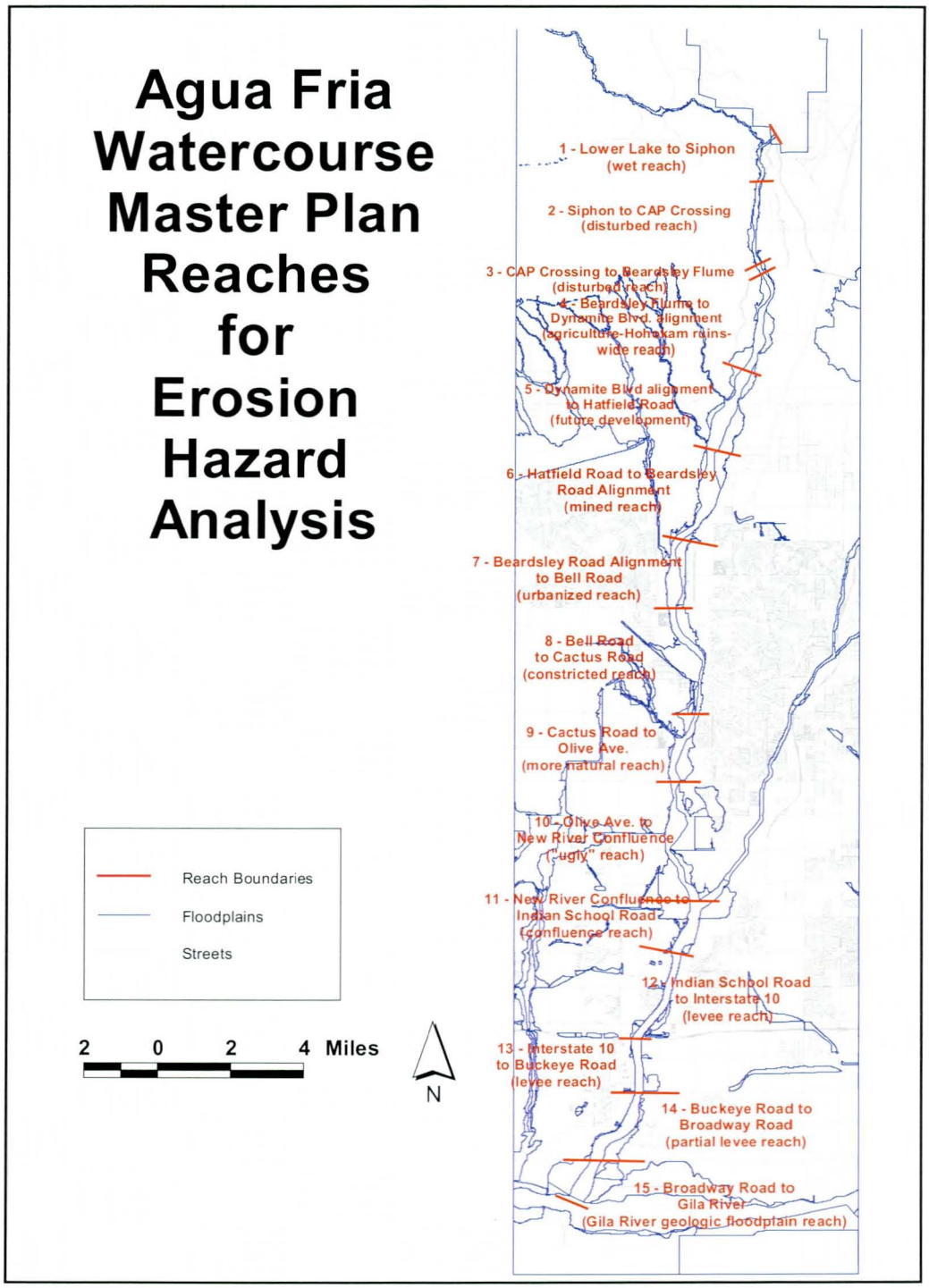

Figure 2-22 - Map of Reaches Defined for Erosion Hazard Analysis

Table 2-15 Summary of Reach Characteristics

Longer Reach Names	JEF Reach No.	Description of Reach Limits	RAS Cross Sections		High Elev. (feet)	Low Elev. (feet)	Length (feet)	Length (miles)	Slope (ft/ft)	RAS Slope (ft/ft)	Sinuosity	Q100 (cfs)	Q50 (cfs)	Q25 (cfs)	Q10 (cfs)	Q5 (cfs)	Q2 (cfs)
			Start RM	End RM													
Upper	1	Lower Dam to Dolores	33.82	32.34	1410	1373	8391	1.59	0.0044	0.0019	1.02	19000	14700	10400	5600	2600	600
	2	Dolores to CAP	32.24	29.89	1373	1335	13219	2.50	0.0029	0.0033	1.02	23000	17800	12600	6700	3200	700
	3	CAP to Beardsley Flume	29.8	29.54	1335	1328	1639	0.31	0.0043	0.0006	1.03	23000	17800	12600	6700	3200	700
	4	Beardsley Flume to Dynamite	29.47	26.55	1328	1274	16449	3.12	0.0033	0.0030	1.10	27000	20900	14800	7900	3700	900
	5	Dynamite to Hatfield	26.47	24.165	1274	1231	14022	2.66	0.0031	0.0033	1.09	31000	24000	16900	9100	4300	1000
	6	Hatfield to Beardsley	24.067	21.157	1231	1188	16571	3.14	0.0026	0.0030	1.13	35000	27100	19100	10300	4900	1100
	7	Beardsley to Bell	21.061	18.97	1188	1150	11308	2.14	0.0034	0.0030	1.14	37500	29000	20500	11000	5200	1200
Middle	8	Bell to Cactus	18.962	15.658	1150	1103	18137	3.44	0.0026	0.0028	1.12	37500	29000	20500	11000	5200	1200
	9	Cactus to Olive	15.564	13.4585	1103	1073	11661	2.21	0.0026	0.0029	1.12	34500	26500	19000	10000	4800	780
	10	Olive to New River	13.45	9.79	1073	1032	17933	3.40	0.0023	0.0022	1.08	30000	23000	16000	8700	4600	820
Lower	11	New River to Indian School	9.69	8.005	1032	1000	10871	2.06	0.0029	0.0022	1.04	54400	39000	26000	16100	10000	5500
	12	Indian School to I-10	8.00	5.29	1000	971	14720	2.79	0.0020	0.0019	1.08	54400	39000	26000	16100	10000	5500
	13	I-10 to Buckeye	5.27	3.7405	971	954	8498	1.61	0.0020	0.0023	1.02	52000	38000	25000	15300	10000	5400
	14	Buckeye to Broadway	3.734	1.4	954	925	13747	2.60	0.0021	0.0018	1.21	50900	37000	25000	15000	10000	5300
	15	Broadway to Gila	1.33	0.16	925	910	6922	1.31	0.0022	0.0025	0.99	48200	35000	23000	14200	9000	5000

Notes:
1. Elevations estimated from USGS 7.5 minute topographic quadrangles except from Indian School to Buckeye Road which were taken from the 1988 FIS topography.
2. Lengths measured along primary flow channel as observed in 1999 aerial photographs.
3. First slope column based on elevations from USGS data and 1999 lengths.
4. RAS slope calculated as channel minimum elevation at upstream reach limit cross section minus channel minimum elevation at downstream reach limit cross section divided by total reach channel length from the model.
5. Sinuosity based on lengths measured along primary flow channel as observed in 1999 aerial photographs.
6. QT discharges from Table 1, USACOE July 1995.

2.2.1 Upper Reach

Reaches 1 through 7 correspond to the "Upper Reach" defined in the Watercourse Master Plan report. The Upper Reach extends from the New Waddell Dam to Bell Road. The Upper Reach begins in a relatively narrow corridor, with a single primary channel confined between two high Pleistocene terraces and emerges into a much wider, braided area downstream of the Beardsley Canal flume. The Upper Reach also has a short section of perennial flow with lush riparian vegetation near Morgan City Wash. Bedrock and caliche outcrops are much more common in the Upper Reach than elsewhere in the study area. Impacts from gravel mining and urbanization begin in the lower sections of the Upper Reach.

2.2.1.1 Reach 1 - New Waddell Dam to Dolores Road Alignment

Reach 1 is a 1.59 mile long reach from the Lower Lake dam to a point across from the second siphon on the Beardsley Canal near the Dolores Road alignment (Figure 2-25). The reach has a slope of 0.0044 as measured from the USGS 7.5 minute topographic quadrangles. The active channel width varies from about 350 feet in the upper portion of the reach to about 580 feet near the reach's downstream limit. The low flow channel within the reach varies from about 100 feet at the upstream end of the reach to about 200 feet at the downstream end. An older high flow channel (pre-Waddell) varies from an average of about 600 feet wide to about 900 feet wide at several locations within the reach.

The low flow channel is perennial from just upstream of Morgan City Wash to near the Carefree Highway (SR 74). The extent of the perennial section varies throughout the year and from year to year. During wet parts of the year, the wetted area extends to very near the downstream limit of the reach ending in a series of deep pools. The source of flow is apparently from seepage from Lake Pleasant along bedrock contacts or other geologic conduits.

Vegetation within the perennial portions of the reach is quite dense due to the abundant water supply (Figure 2-23). Large cottonwood and willow trees line portions of the low flow channel. Additionally, numerous large tamarisk and stands of cottontail reeds exist within the perennial section. Higher bars and the ephemeral sections are characterized by an unidentified green bush (GUB[7]) and various low shrubs. The highest floodplain areas are covered with stands of mesquite.

Figure 2-23 - Photo 64-24

Figure 2-24 - Photo 65-1

[7] Project staff were unable to positively identify the species, and is therefore referred to as GUB (green ubiquitous bush) per the notes of the field crew. GUB may be snakeweed, a "useless plant" that "provides no erosion protection or soil stablization" (Mielke, 1993; Bowers, 1993).

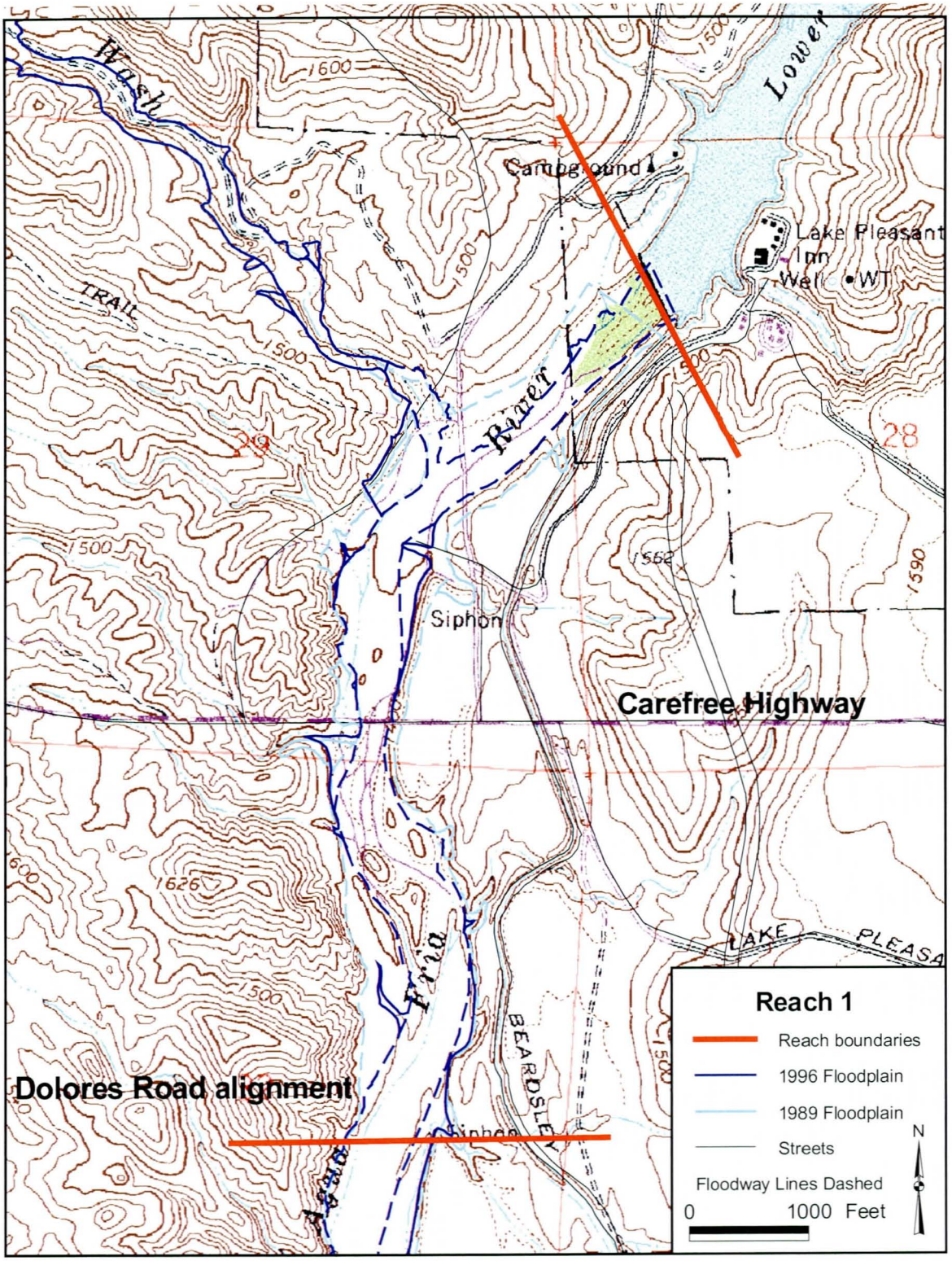

Figure 2-25 - Map of Reach 1, New Waddell Dam to Dolores Road alignment

The channel pattern in Reach 1 is generally straight and characterized by a single channel between bedrock throughout the reach. One exception is a short reach downstream of Carefree Highway where several large bedrock island outcrops divide the stream into multiple channels.

Bedrock is a dominant feature within the channel and banks throughout Reach 1 (Figure 2-24). Lateral and vertical erosion is limited by the resistant bedrock. The bedrock itself is predominantly mid-Tertiary sandstones and conglomerates. The left bank terrace is composed of bedrock at its base overlain by Pleistocene-aged alluvial gravels. The age of the left bank terrace is reported as between 10,000 and 200,000 years old (Huckleberry, 1995).

The floodplain is generally confined between the Pleistocene terrace on the left bank and the Tertiary bedrock on the right bank. At a few locations historical deposits of sands and finer sediments are found along the right bank (Figure 2-26). These deposits represent portions of the floodplain of the Agua Fria River prior to the construction of the New Waddell Dam and maybe even the old Waddell Dam. The alluvial sediments within low flow channel and mid channel bars in the reach are generally coarse gravels and sands.

Figure 2-26 - Photo 65-2

Figure 2-28 - Photo 65-13

Figure 2-27 - Photo 64-20

The channel banks within the reach are either bedrock exposures along the far east and west margins of the corridor (Figure 2-27), exposures of the sandy deposits on the higher old floodplain surfaces (Figure 2-28), or sandy gravel deposits on banks along the low flow channel. The alluvial deposits are all easily eroded while the bedrock exposures are resistant to erosion.

The only significant manmade structure within the reach is the Carefree Highway Bridge (Figure 2-29). The bridge approaches are located well above the active floodplain. The bridge piers appear to be founded on bedrock. A small concrete weir is also located within the reach

upstream from Carefree Highway (Figure 2-30). While a four foot deep scour hole is located on the downstream side of this weir, the structure is only about 20 feet wide, does not span the entire channel, and therefore probably does not have a significant impact on larger discharges.

Figure 2-29 - Photo 4-7

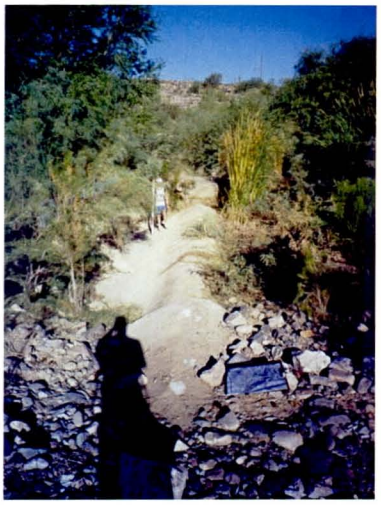

Figure 2-30 - Photo 64-21

The only significant tributary entering Reach 1 is Morgan City Wash. In addition to contributing perennial low flow to the reach, Morgan City Wash can generate significant flood discharges in excess of those possible from a controlled release from New Waddell Dam. The 100-year peak discharge estimated for Morgan City Wash in the North Peoria Area Drainage Master Plan (ADMP) is 11,800 cfs from a drainage area of 22.9 square miles. The maximum controlled release from the dam is about 9,500 cfs. The estimated 2-year peak discharge from Morgan City Wash is 250 cfs. Several smaller local tributaries enter within the reach, but none of their drainage areas are larger than one square mile in area.

2.2.1.2 Reach 2 - Dolores Road Alignment to CAP Canal

Reach 2 is a 2.50 mile long reach which extends from the Dolores Road alignment to the Central Arizona Project (CAP) Canal siphon crossing (Figure 2-31). The reach has a slope of 0.0029, as measured from the USGS 7.5 minute topographic quadrangles. The active channel width varies from about 600 feet to 900 feet. The low flow channel within the reach is about 200 feet wide, and includes three smaller multiple channels just upstream of the CAP siphon. Near the at-grade road crossing to Cowtown, a separate high overbank channel flows parallel to the 200 foot wide low flow channel for about 0.7 miles before it rejoins the main low flow channel.

The channel pattern in Reach 2 is generally a straight channel. Some braided channel characteristics occur at moderate flood stages in the wider reach downstream of Cowtown. Just upstream of the CAP crossing, the river has 3 distinct channels which become joined at higher discharges. Bed material in the reach is predominantly gravels and sands, with some large cobbles. The right half to two-thirds of the channel downstream of Cowtown is composed of finer sediments, predominantly sands.

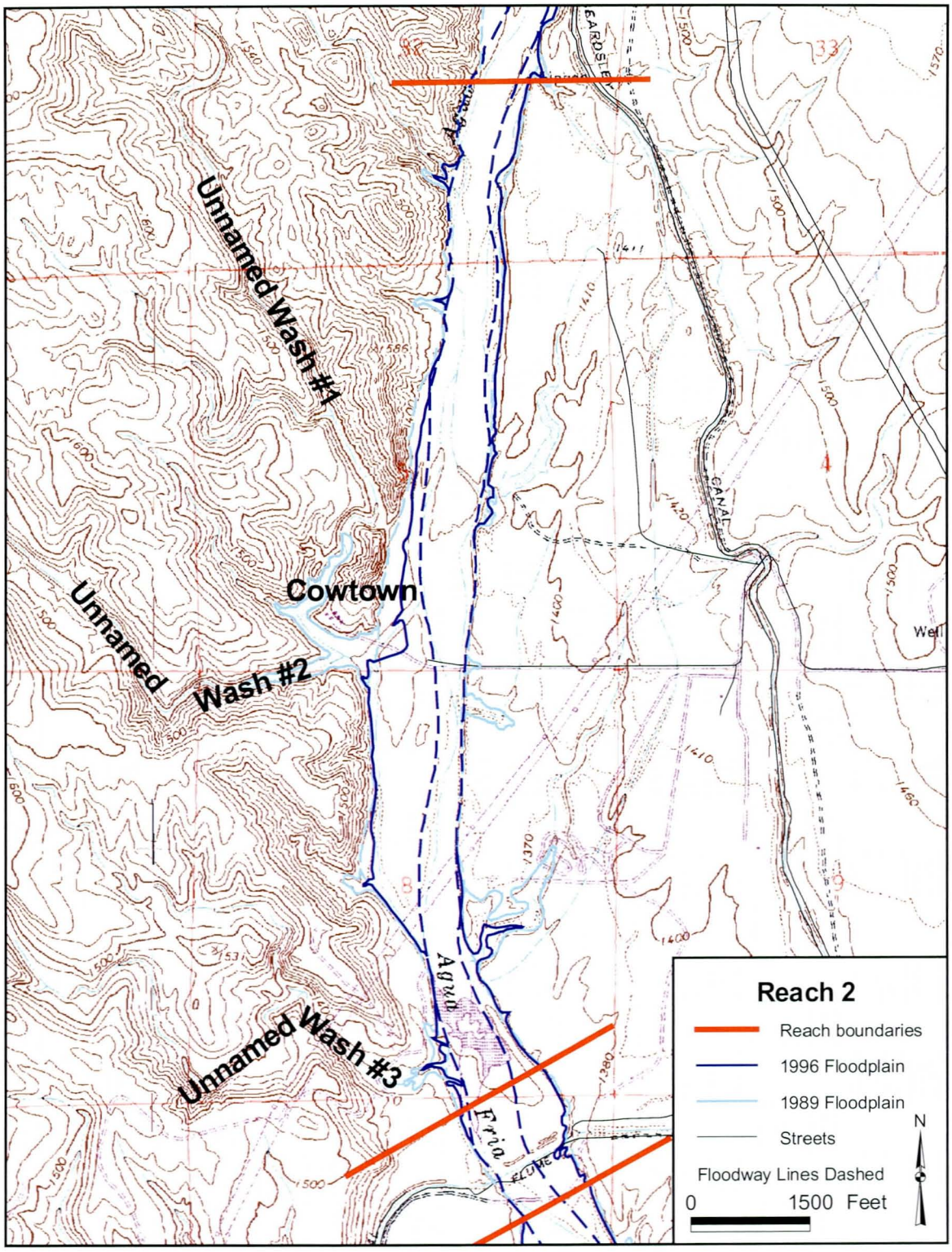

Figure 2-31 - Reach 2, Dolores Road alignment to CAP Canal Siphon

The channel corridor is confined between bedrock outcrops on the west (right bank) and Pleistocene-aged alluvial terraces underlain by bedrock on the east (left bank). Lateral movement of the river channel outside this confined corridor is therefore restricted by these bedrock features. The channel banks within Reach 2 are composed of bedrock along the outer margins on the far right and left banks (Figure 2-32). Internal banks are composed either of sandy coarse gravels or predominantly sand deposits (Figure 2-33). The banks of finer material are located primarily in the right half to two-thirds of the channel in the portion of the reach downstream of Cowtown.

Figure 2-32 - Photo 66-7

Figure 2-33 - Photo 65-22

The floodplain is generally confined between the bedrock hills of the west bank and the Pleistocene terrace on the east bank. The post-New Waddell Dam floodplain shows a narrow strip along the right bank upstream of Cowtown as lying out of the new 100-year floodplain. This area was shown as lying within the floodplain prior to the construction of New Waddell Dam. The alluvial portions of this strip, while outside of the Post-New Waddell floodplain, are still subject to lateral erosion hazards that extend to the Pre-Waddell floodplain limits.

Vegetation within the reach is generally limited to small low shrubs within the channel (Figure 2-34). The right portion of the channel downstream of Cowtown does have larger trees, such as mesquite and palo verde, and some large cholla growing in areas with fine-grained deposits. The outer banks also have some palo verde trees and shrubs growing along them where bedrock does not prevent their growth.

Figure 2-34 - Photo 65-23

About 2,000 feet downstream of the upstream end of Reach 2, there is an area that was formerly part of a sand and gravel mine (Figure 2-35). Within this area, the bed of the channel has been lowered about 6 to 8 feet across most of the width of the channel. The low flow channel extending upstream from the mined area has cut down to meet the lowered local base

level for about 800 feet upstream. Sedimentation within the mined area observed at the surface is limited to a delta-like sand deposit near the upstream portion of the mined area and extensive silty deposits in the downstream portion of the mined area. Historical aerial photographs show that the mining began between 1985 and 1992. Conditions observed during August 2000 field visits suggest that mining has been discontinued.

Figure 2-35 - Photo 66-10

Two major tributaries enter the Agua Fria River within Reach 2. The first tributary enters the river near Cowtown, and drains the rugged mountainous area of unnamed washes #1 and #2 of the North Peoria Area Drainage Master Plan (ADMP) study area (Figure 2-31). The first tributary has a combined drainage area of 12.8 square miles, and a 100-year peak discharge of 7,300 cfs (Stantec, 2001). The 2-year peak discharge is estimated as 140 cfs. The second tributary enters Reach 2 near the downstream end of the reach, and is called unnamed wash #3 in the North Peoria ADMP (Figure 2-31). Unnamed wash #3 has a drainage area of 3.6 square miles, a 100-year peak discharge of 2,600 cfs, and an estimated 2-year peak discharge of 50 cfs.

There are no major structures or encroachments within Reach 2.

2.2.1.3 Reach 3 - CAP Canal to Beardsley Canal

Reach 3 is a 0.31 mile long reach that consists primarily of area around the CAP Canal siphon crossing and the Beardsley Canal flume bridge crossing (Figure 2-36). The reach has a slope of 0.0043 as measured from the USGS 7.5 minute topographic quadrangles. The disturbance of Reach 3 due to the construction and maintenance of the CAP crossing is still very evident in the field. Examination of historical aerial photographs indicates that additional grading in the right-of-way was done sometime between 1992 and 1997, and has altered the visible effects on the channel caused by the 1993 flooding. CAP personnel reported that the original concrete siphon was replaced by a steel pipe during that period.

The most notable feature within the reach with respect to lateral erosion hazards is the dominant cutbank along the right side of the river. Jacks (large steel structures that resemble toy jacks) have been placed along the toe of the bank to mitigate the erosion of the bank (Figure 2-37), and to induce sediment deposition. Field examination of the jacks indicates that they have not yet prevented erosion or induced any significant sediment deposition. The cutbank has a nearly vertical slope cut into a Pleistocene terrace surface with an estimated age of 10,000 to 200,000 years in age. This terrace is also the lowest of the multiple terraces along the river downstream of Waddell Dam to Sun City (Huckleberry, 1995).

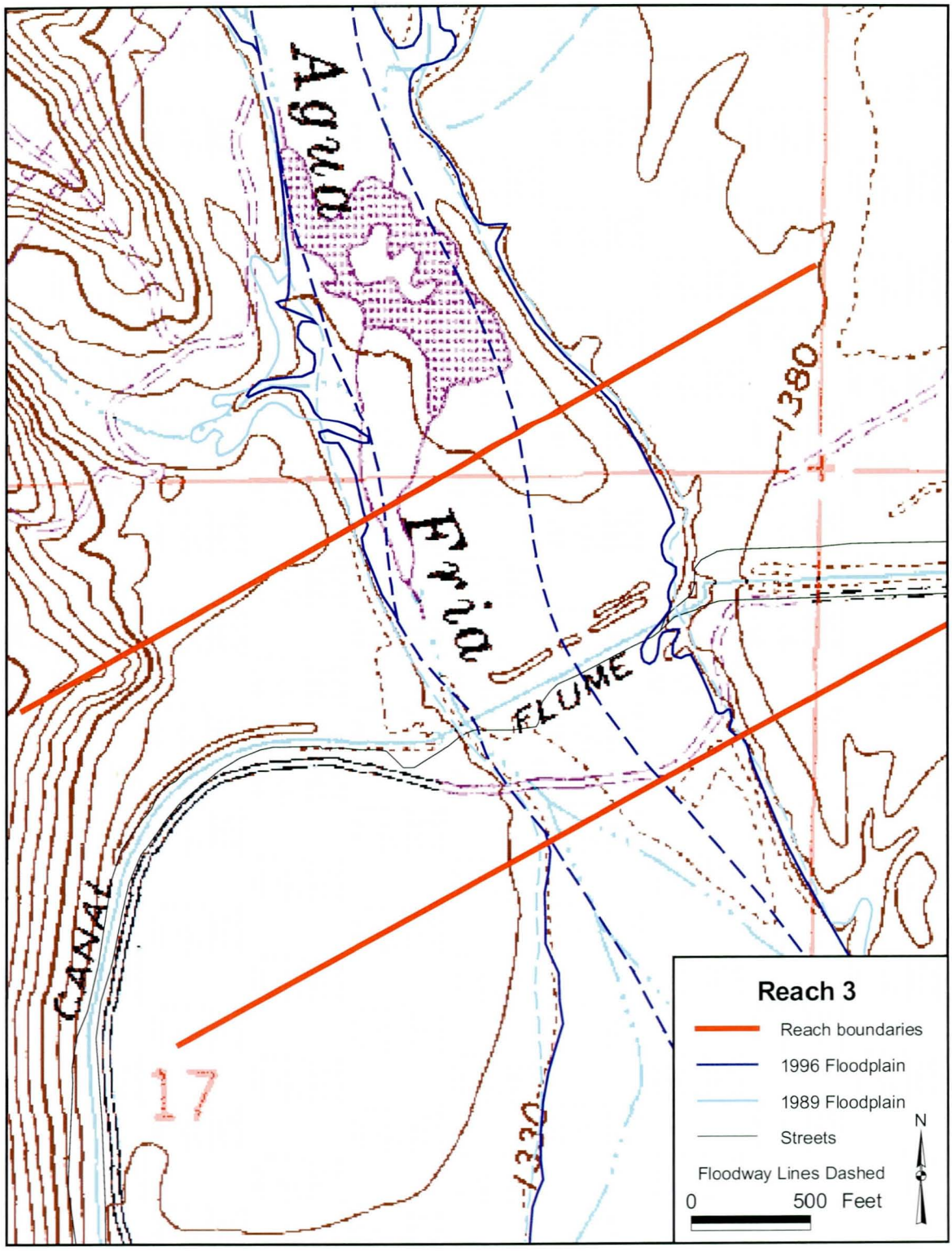

Figure 2-36 - Reach 3, CAP Crossing to Beardsley Canal

Figure 2-37 - Photo 5-10

Figure 2-38 - Photo 5-8

The CAP siphon and Beardsley Canal flume do not appreciably constrict the channel from its historical width. Both structures span the river corridor between the Pleistocene terraces on either side of the geologic floodplain. A large concrete structure on the west side of the CAP siphon where an outflow pipe is located to allow for direct discharges from the CAP into the Agua Fria River (Figure 2-38), and which will serve as the water source for the CAP Recharge Project currently under construction in Reach 5. This structure and a riprap protected earthen dike extend east into the river beyond the west terrace about 400 feet. Discharges from the outflow pipe have resulted in a large scour hole immediately downstream of the outlet. Historical aerial photographs also show that an earthen dike was constructed into the river from the right bank upstream of the CAP. This dike appears to have been built to deflect flood water from the Agua Fria River and from unnamed wash #3 which enters just upstream, perhaps to prevent damage during the construction of the outlet pipe tower structure. Two small fences cross Reach 2, but do not cause any significant impact on the river. An at-grade dirt road which provides access to the CAP and the Beardsley Canal also crosses the channel in the reach. Neither the road nor its approaches have any significant impact on the river morphology.

Beneath the Beardsley Canal flume, the low flow channel flows along the vertical cutbank described above (Figure 2-39). Lateral erosion of low flow channel at this cutbank may eventually undermine the right abutment of the flume.

Figure 2-39 - Photo 5-12

Vegetation within the reach consists predominantly of low shrubs with a few scattered mesquite and palo verde trees. Much of the low vegetation has grown up in the disturbed area of the CAP siphon since the siphon replacement between 1992 and 1997.

2.2.1.4 Reach 4 - Beardsley Canal to Calderwood Butte

Reach 4 is a 3.12 mile long reach which extends from the Beardsley Canal flume bridge crossing to the Dynamite Road alignment (Figure 2-42). The reach has a slope of 0.0033 as measured on the USGS 7.5 minute topographic quadrangles. In Reach 4, the active channel area becomes much wider than in the upstream reaches. The limits of the active channel(s) vary throughout the reach from about 800 feet to over 2,000 feet, although the low flow channel itself is only about 300 feet wide where it is confined to a single channel. In one portion of the reach near the Dixileta Drive alignment, the low flow channel becomes very braided, dividing into several narrower channels. The channel pattern of the entire reach is best characterized as braided. In addition to the braided low flow channel area near the Dixileta Drive alignment, the channel also has multiple higher flow channels just downstream of the Beardsley flume. Large overbank areas of fine-grained sediments also exist along Reach 4. Two of these areas on the right overbank are currently under cultivation as citrus orchards.

Bed and bank materials within the active portions of the channel are predominantly gravels and sands. The banks along the large floodplain overbank areas are composed primarily of sands and silty fine sands (Figure 2-40). All of these fine-grained banks are not resistant to lateral erosion. Beyond the overbank floodplain areas and at some locations immediately adjacent to the active channel, the banks are formed by the Pleistocene-aged river terraces. These terraces are composed of old river gravels and sands (Figure 2-41). The upper portions of these terraces contain significant accumulation of calcium carbonate, reflecting their geologic age, and are more resistant to erosion. However, the most resistant calcium carbonate layers are generally located well above the level at which the banks are attacked by flood water discharges. Hence, these terrace banks are subject to undercutting and bank failure, albeit at a slower rate than the internal, fine-grained, unconsolidated channel banks.

Figure 2-40 - Photo 7-2

Figure 2-41 - Photo 6-11

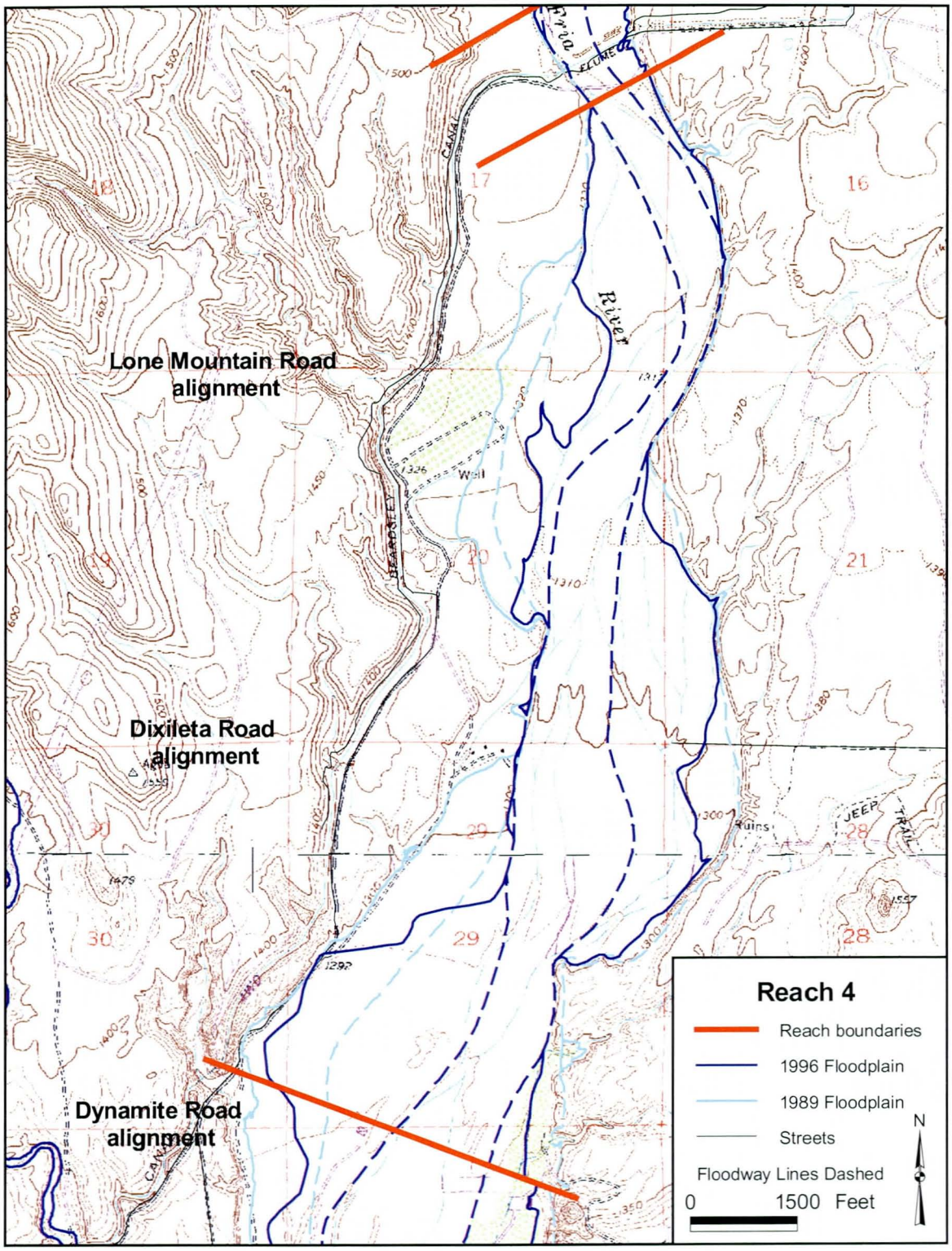

Figure 2-42 - Reach 4, Beardsley Canal to Calderwood Butte

The pre-New Waddell Dam floodplain covers most of the areas between the lowest Pleistocene terraces within the reach. The post-New Waddell floodplain maps show some of the historical overbank areas as now outside the 100-year inundation limits. Moreover, the new floodplain maps also show one area of the active channel as outside the floodplain limits. This area, located about 4,000 feet south of the Beardsley Canal flume, is connected to the floodplain upstream via a high flow channel (Figure 2-43). Field examinations of the area indicate that if flood water does enter the high flow channel as shown on the floodplain map, it will continue to flow through this area, and therefore should be included as within the current 100-year floodplain.

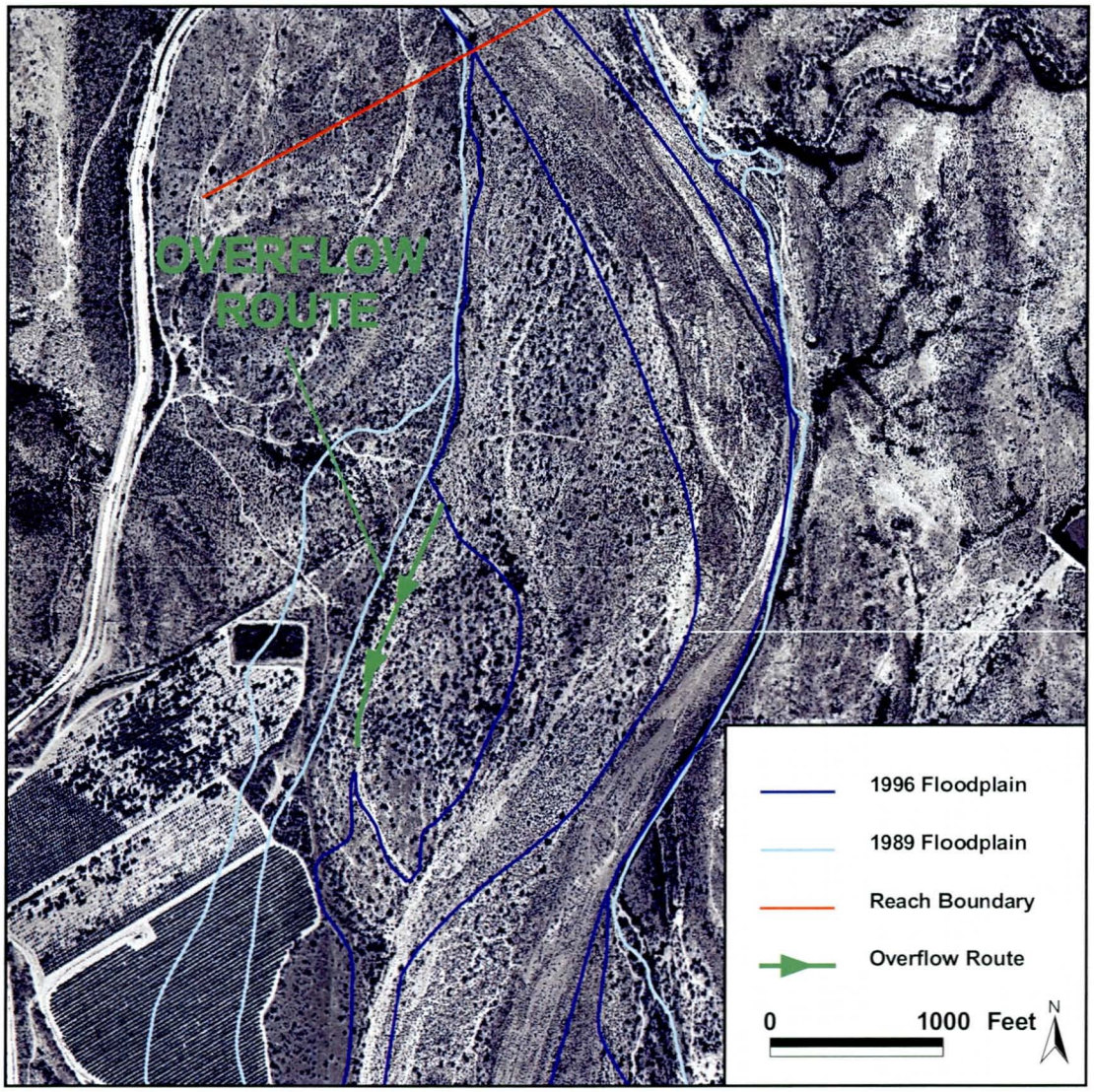

Figure 2-43 - Map of overflow channel not mapped in 1996 Floodplain Delineation Study

Aside from small irrigation features within the citrus orchards in the right overbank, there are no structures within Reach 4. However, the Central Arizona Project has plans to release water from the CAP canal through this reach to recharge basins located in Reach 5. This project is scheduled to begin construction in the next year.

There are no major tributaries entering the Agua Fria River within Reach 4. Several small tributaries enter the reach from both sides of the river. The two largest of these watersheds are about 1.2 square miles in area each and enter the Agua Fria River from the east.

2.2.1.5 Reach 5 - Calderwood Butte to Twin Buttes Wash

Reach 5 is a 2.66 mile long reach that extends from the Dynamite Road alignment to just downstream of Hatfield Road (Figure 2-46). The reach has a slope of 0.0031 as measured on the USGS 7.5 minute topographic quadrangles. The active channel in Reach 5 is quite wide. Near the upstream limit of the reach, the active channel is about 1,200 feet wide and is composed of multiple smaller channels with wide active bars between them. Downstream, at Jomax Road, a single prominent low flow channel about 200 feet wide crosses the at-grade road crossing before widening again downstream. The channel widens rapidly to about 1,300 feet and then widens further to about 1,700 feet before narrowing slightly back to about 1,400 feet at Hatfield Road. Downstream of Jomax Road, the wide channel is comprised of several smaller braided channels separated by wide gravel bars.

As indicated above, the channel pattern within Reach 5 is highly braided with multiple smaller channels separated by gravel bars and islands of finer materials. The overbank floodplain areas are also subject to formation of new channels or avulsions. Examination of historical aerial photographs shows that channel avulsions into the overbanks have occurred in the past and are therefore likely to occur in the future. Except for at the Jomax Road crossing, the reach has wide overbank floodplain areas on both the left and right sides of the channel. These areas are topographically below the high Pleistocene-aged terraces and are within the geologic and pre-Waddell Dam floodplain. Even the post-old Waddell Dam floodplain was shown as inundating the entire overbank area. The post-New Waddell Dam floodplain shows small portions of both the right and left overbank upstream of Jomax Road as free from 100-year inundation under the new conditions (Figure 2-46).

The bed and bank materials within the active channel are primarily composed of gravel and sand (Figure 2-44). The outer banks along the overbank floodplains are composed of sand and silty fine sand (Figure 2-45). None of the banks are resistant to lateral erosion, as indicated by field evidence of extensive gravel cutbanks.

Figure 2-44 - Photo 15-20

Figure 2-45 - Photo 12-10

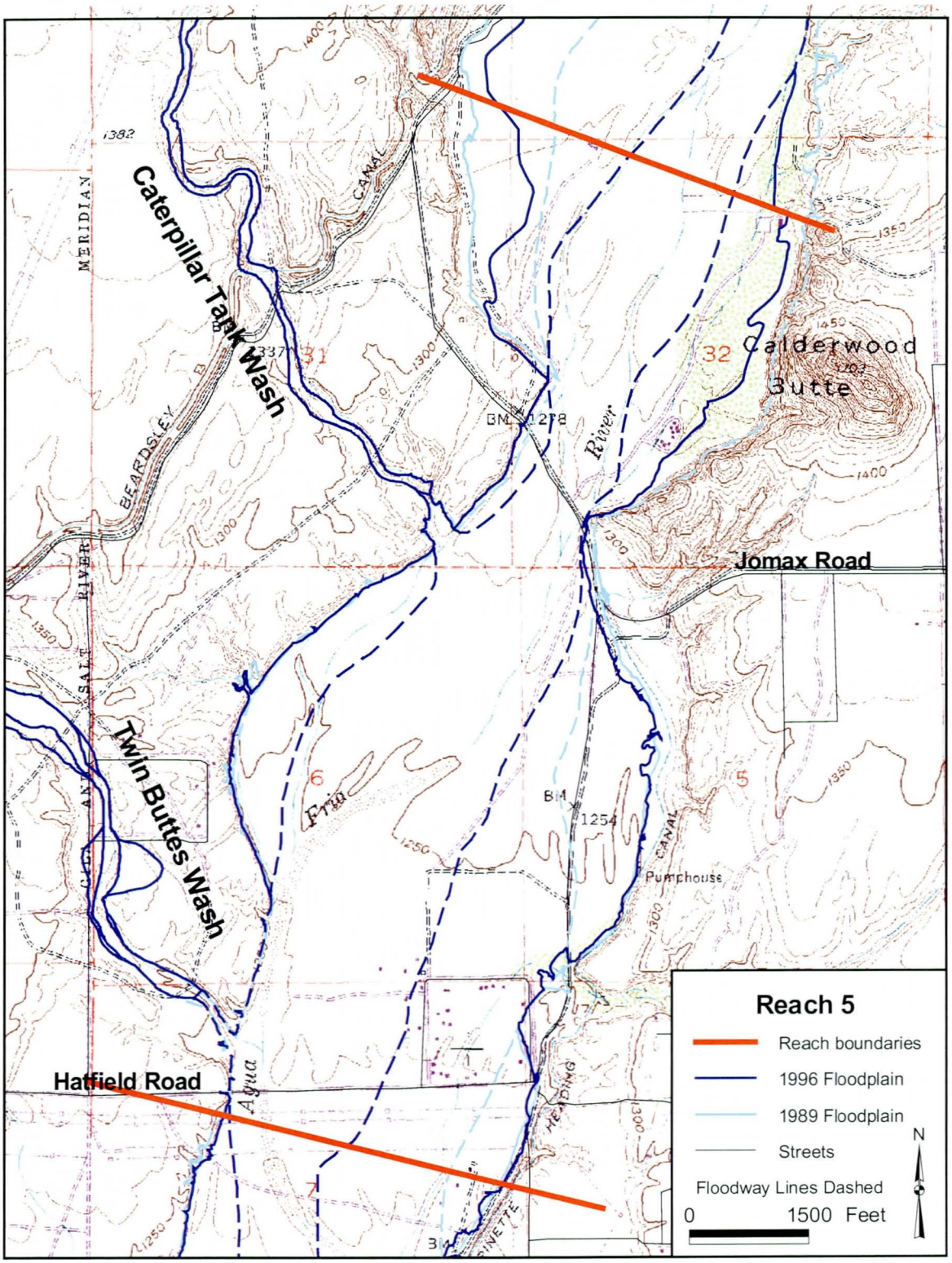

Figure 2-46 - Reach 5, Calderwood Butte to Twin Buttes Wash

The outer terraces that confine the floodplain are composed of Pleistocene-aged alluvial sand and gravel, with significant calcium carbonate accumulations in their upper portions. While these carbonate layers are relatively resistant to erosion, they do not extend downward to an elevation that would be attacked by flood water. Instead, flood waters only reach the lower layers which are less resistant and subject to erosion, which will lead to undercutting of the overlying resistant calcium carbonate layers (Figure 2-47). Within Reach 5, however, finer overbank floodplain deposits are found abutting the Pleistocene terraces. The fine-grained overbank deposits indicate that relatively slow flood velocities occur in the overbanks, and that erosion and undermining of the terraces is not likely to occur except where the main channel abuts the older terraces. An example occurs along the right bank terrace, downstream of Jomax Road, where local tributary flows and high flood discharges from the Agua Fria River form a small channel along the base of the right bank terrace (Figure 2-48). Velocities within this overbank channel may be expected to be higher, and thus capable of more erosive work. Near Jomax Road, bedrock crops out at the edge of the active channel, and effectively limits lateral erosion.

Figure 2-47 - Photo 17-4

Figure 2-48 - Photo 17-13

Two named tributaries enter the Agua Fria River within Reach 5. Caterpillar Tank Wash enters the river from the west about 1,500 feet downstream of Jomax Road (Figure 2-46). Caterpillar Tank Wash has a drainage area of 3.26 square miles, a 100-year peak discharge of 1,560 cfs, and an estimated 2-year peak discharge of 30 cfs. Twin Buttes Wash enters the river near the downstream limit of Reach 5 immediately upstream from Hatfield Road (Figure 2-46). Twin Buttes Wash has a drainage area of 8.61 square miles, a 100-year peak discharge of 3,800 cfs, and an estimated 2-year peak discharge of 70 cfs. The CAP recharge project basins, currently under construction, will be located in the bed of the Agua Fria River between the Caterpillar Tank Wash and Twin Buttes Wash confluences. Another unstudied tributary enters the river from the east about 2,600 feet upstream of the lower limit of the reach. This tributary has a drainage area of about 2.6 square miles.

Vegetation within the reach varies depending on channel position. Within the most active low flow channels, the dominant plant is the GUB. On higher channel bars, the dominant shrub is the YUB[8] (Figure 2-49). Some larger riparian trees, such as palo verde, may also be found on the channel bars. The finer deposits of the overbank areas are also home to denser riparian communities that include palo verde and willow, and larger shrubs such as desert broom and creosote (Figure 2-50). Occasionally, various cactus species, such as cholla and saguaro, were observed in the overbank areas.

[8] Project staff were unable to positively identify the species of this plant. Therefore, the name applied by the field crews, YUB (yellow ubiquitous bush) is used in this report. YUB may actually be burrobush or cheesebush.

Figure 2-49 - Photo 12-23

Figure 2-50 - Photo 17-8

Currently, there are two at-grade road crossings within the reach. Jomax Road is paved for about one half of the width of the river with the remaining portion having a gravel surface. Hatfield Road is unpaved. Additional structures within the reach include a small storage yard at the southwest corner of Hatfield Road and 107th Avenue and a high tension powerline crossing at the downstream limit of the reach. The powerline towers are founded on small islands of alluvial sands and gravels (Figure 2-51). Neither the roads, storage yard, or powerline islands appear to exhibit significant impacts on flood water or sediment discharges within the reach. Another notable structural feature within Reach 5 is the abandoned Marietta Canal. The canal heads at Calderwood Butte on the left bank just upstream of Jomax Road. The canal follows along the base of the Pleistocene terrace along the east edge of the left overbank floodplain. Finally, CAP recharge basins and their water supply canal will be constructed in the near future in Reach 5.

Figure 2-51 - Photo 19-2

Figure 2-52 - Photo 17-21

One 10-acre sand and gravel pit is located within Reach 5 about ¼ mile upstream of Hatfield Road (Figure 2-52). Examination of historical aerial photographs indicates that the mining activity began between 1997 and 1999. Another, larger active mine is located in the right overbank area near the upstream limits of the reach. This mining activity began after the 1999 aerial photographs were taken.

Finally, portions of the left overbank floodplain upstream of Hatfield Road were once occupied by several residential structures. The area around these residences is within a portion of the floodplain formerly occupied by the main channel, and is now an area of potential avulsive channel change. The homes were removed after they were damaged by flooding in 1978 and 1980. Concrete foundations and some landscaped plants can still be found within the old subdivision area.

2.2.1.6 Reach 6 - Twin Buttes Wash to Beardsley Road

Reach 6 is a 3.14 mile long reach that extends from just downstream of Hatfield Road to the Beardsley Road alignment (Figure 2-55). The reach has a slope of 0.0026 as measured on the USGS 7.5 minute topographic quadrangles. The active channel in Reach 6 is strongly braided in the upper 1.5 miles of the reach. Downstream of the Deer Valley Road alignment the river remains braided, but the braiding is limited to a 1,000 feet wide corridor. In the upstream portion of the reach, the historical main low flow channel has been truncated by berms constructed adjacent to a sand and gravel mine, which is located along the east half of the river bottom below the Pleistocene terraces. The encroachment by the berms has pushed the low flow channel further west and caused different braids of the river to become the dominant low flow channels.

Within the middle portion of the reach, two distinctive floodplain islands have formed. These islands are composed of a two- to four-feet thick layer of sand and silty fine sand lying over large river cobbles and gravel. The vegetation on these islands is dominated by creosote bush (Figure 2-53), as opposed to the rest of the reach, where the vegetation is similar to the adjacent reaches. The lowest, most active channels are either completely devoid of vegetation or contain scattered GUB. Higher channel bars are occupied by shrubs such as YUB and desert broom (Figure 2-54). The higher surfaces also have some riparian trees such as palo verde, willow, and ironwood.

Figure 2-53 - Photo 22-8

Figure 2-54 - Photo 22-14

The bed and banks of the inner braided channels are predominantly composed of gravel and sand (Figure 2-56). The floodplain island banks are composed of sand and silty fine sand overlying coarser river gravels (Figure 2-57). An extensive, very tall, nearly vertical cutbank makes up much of the left bank of the reach (Figure 2-58). This prominent feature of the reach towers about 40 feet above the channel, and extends from just downstream of the Pinnacle Peak Road alignment to just upstream of Rose Garden Lane. The soil column exposed in the cut bank is capped by a thick layer of erosion resistant calcium carbonate, although the lower layers that crop out at the flood water levels are less resistant and more likely to erode. Removal of the more erodible material near the base of the cutbank has undercut the carbonate layers, creating the vertical cliff seen today. The surface above the cutbank is a Pleistocene-aged terrace identified by Huckleberry (1995) as unit M2c (see Surficial Geology Map in the Exhibits Map Book), with an estimated age of 10,000 to 200,000 years old.

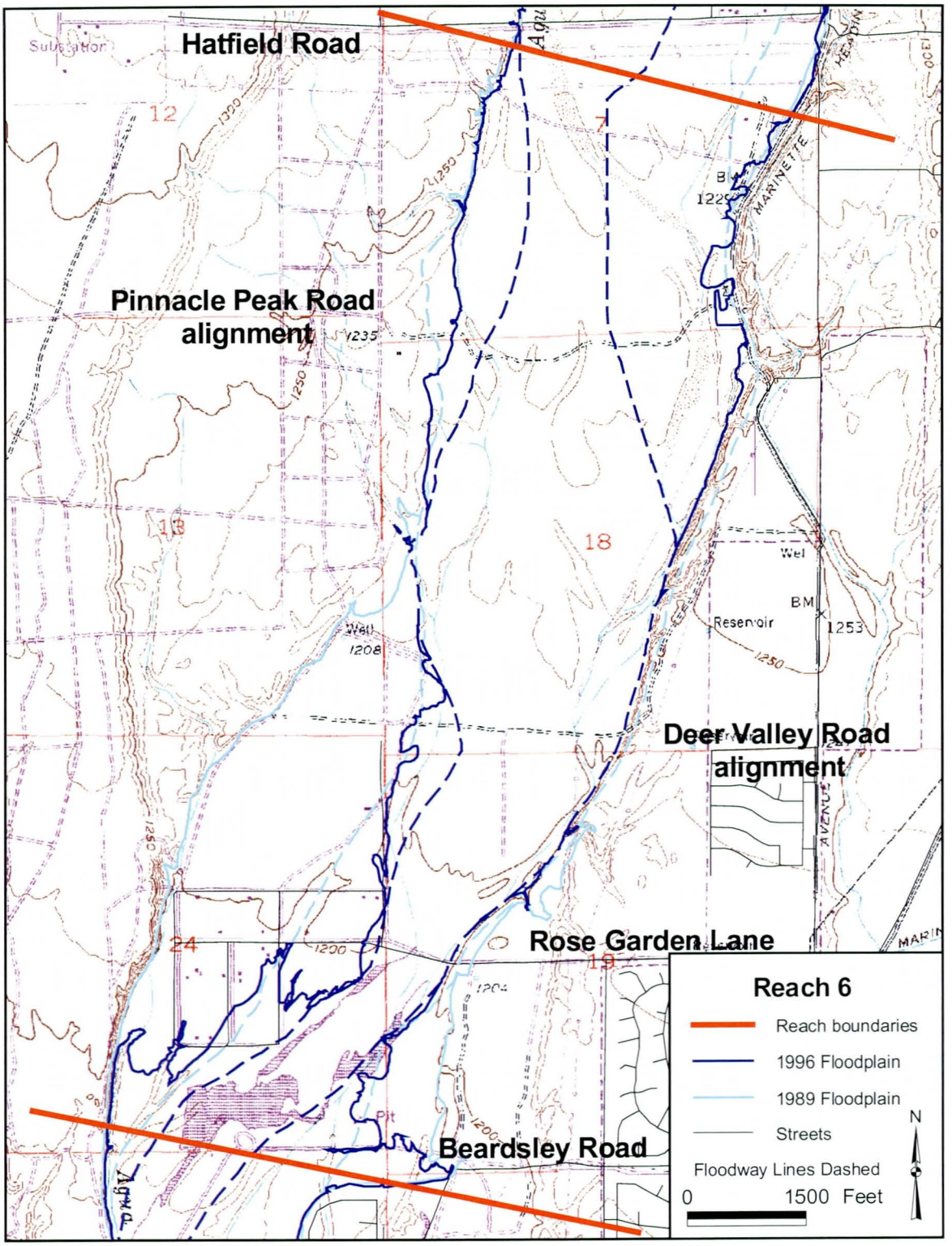

Figure 2-55 - Reach 6, Twin Buttes Wash to Beardsley Road alignment

Figure 2-56 - Photo 19-4

Figure 2-57 - Photo 22-4

Figure 2-58 - Photo 31-22

Along the west edge of the active channel, Huckleberry (1995) identifies two areas of a unit designated as Y1, Holocene alluvium. This surface is described as being located outside the modern Agua Fria River channel and subject to inundation by large floods prior to the construction of the old Waddell Dam.

Three significant active sand and gravel mining operations are located in Reach 6. The first is located within the left half of the channel immediately downstream of Hatfield Road (Figure 2-59; see also the Historical Photo Comparisons and Erosion Hazard Maps in the Exhibit Maps Book). The upstream and west edges of the mine area are surrounded by large earthen berms which appear to be composed of gravel and sand. The southern portion of the west berm is blanketed by large rounded river cobbles that presumably provide erosion protection from the impinging low flow channel. To the extent that the berms have prevented flow from entering the mining area, the mine has cut off the historical primary low flow channel from the river. Low flows are now diverted to the west around the mine.

Figure 2-59 - Photo 19-18

The second sand and gravel mine in Reach 6 is located in the right portion of the channel and floodplain upstream from Rose Garden Lane (Figure 2-60). The largest pit areas are located outside of the current (Post-New Waddell) floodplain. Although Huckleberry (1995) states that geologic evidence indicates that this area is outside the modern channel, this area was mapped as within the pre-New Waddell Dam floodplain in the 1989 FIS. Two smaller pits were observed in the current rightmost active low flow channel. Field observations indicate that the upstream area of these two pits has been expanded since the 1999 aerial photographs were taken.

Figure 2-60 - Photo 26-2

Figure 2-61 - Photo 26-3

The third sand and gravel mine in Reach 6 extends from Rose Garden Lane to the downstream reach limit (Figure 2-61). The excavations for this mine span the main channel and extend into the east and west floodplains. The pit for this operation is located within the floodway from the downstream reach limit upstream for about ½ mile. Smaller additional pit areas are located outside the floodway both east and west of the floodway pit.

A residential subdivision is located along Rose Garden Lane within the right overbank pre-New Waddell floodplain (Figure 2-62). The buildings within this subdivision are currently shown as outside the post-New Waddell Dam floodplain (Figure 2-55), although the deposits upon which these lots sit are clearly fluvial in origin, indicating that the area was part of the active floodplain in the recent past.

Another man-made structure within the reach is the at-grade crossing of Rose Garden Lane. This paved road shows evidence of significant degradation. About 440 feet west of the east floodplain limit, there lies about 300 feet of concrete along the downstream side of the road. This concrete appears to have been an apron poured to help protect the roadway from scour, although the apron now sits about five feet above the invert of the current low flow channel (Figure 2-63). Apparently, scour during a flood lowered the main low flow channel five feet at some time in the recent past. Examination of historical aerial photographs suggests that about 150 feet of this apron disappeared between 1992 and 1997, presumably as a result of the 1993 flooding.

Figure 2-62 - Photo 11-8

Figure 2-63 - Photo 25-8

Powerlines also traverse the reach a few hundred feet west of the prominent left terrace cutbank. No significant tributaries enter the Agua Fria River in Reach 6.

2.2.1.7 Reach 7 - Beardsley Road to Bell Road

Reach 7 is a 2.14 mile long reach that extends from the Beardsley Road alignment to Bell Road (Figure 2-65). The reach has a slope of 0.0034 as measured on the USGS 7.5 minute topographic quadrangles. The channel pattern within Reach 7 is braided. The width of the active braided corridor is about 2,000 feet. The most active channels within the overall braided corridor are about 650 feet wide.

The active low flow channel flows against the edge of the Pleistocene-aged terrace on the right (west) side of the floodplain from about ¼ mile south of the upstream limit of the reach to the confluence of the McMicken Outlet Wash (Figure 2-64). The terrace bank is actively being cut by the low flow channel in this area. However, field evidence of bank erosion is limited to the lower six to eight feet of the terrace slope. As in Reach 6, the river is attacking the less erosive lower layers of the terrace slope, effectively undermining the more resistant overlying calcium carbonate layers, and leaving an impressive tall cutbank cliff.

Figure 2-64 - Photo 27-11

Downstream of the McMicken Outlet Wash confluence the main low flow channel is deflected east around a delta-like feature that has formed at the confluence of the McMicken Outlet Wash with the Agua Fria River. Field observations indicate that a portion of the low flows from McMicken Outlet Wash actually flow north in the Agua Fria for a short distance in order to flow around this delta. Further downstream, the most active low flow channel flows near the center of the floodplain and has a width of about 230 feet. A second, slightly narrower overflow channel flows along right bank terrace before joining with the main low flow channel as it approaches Bell Road.

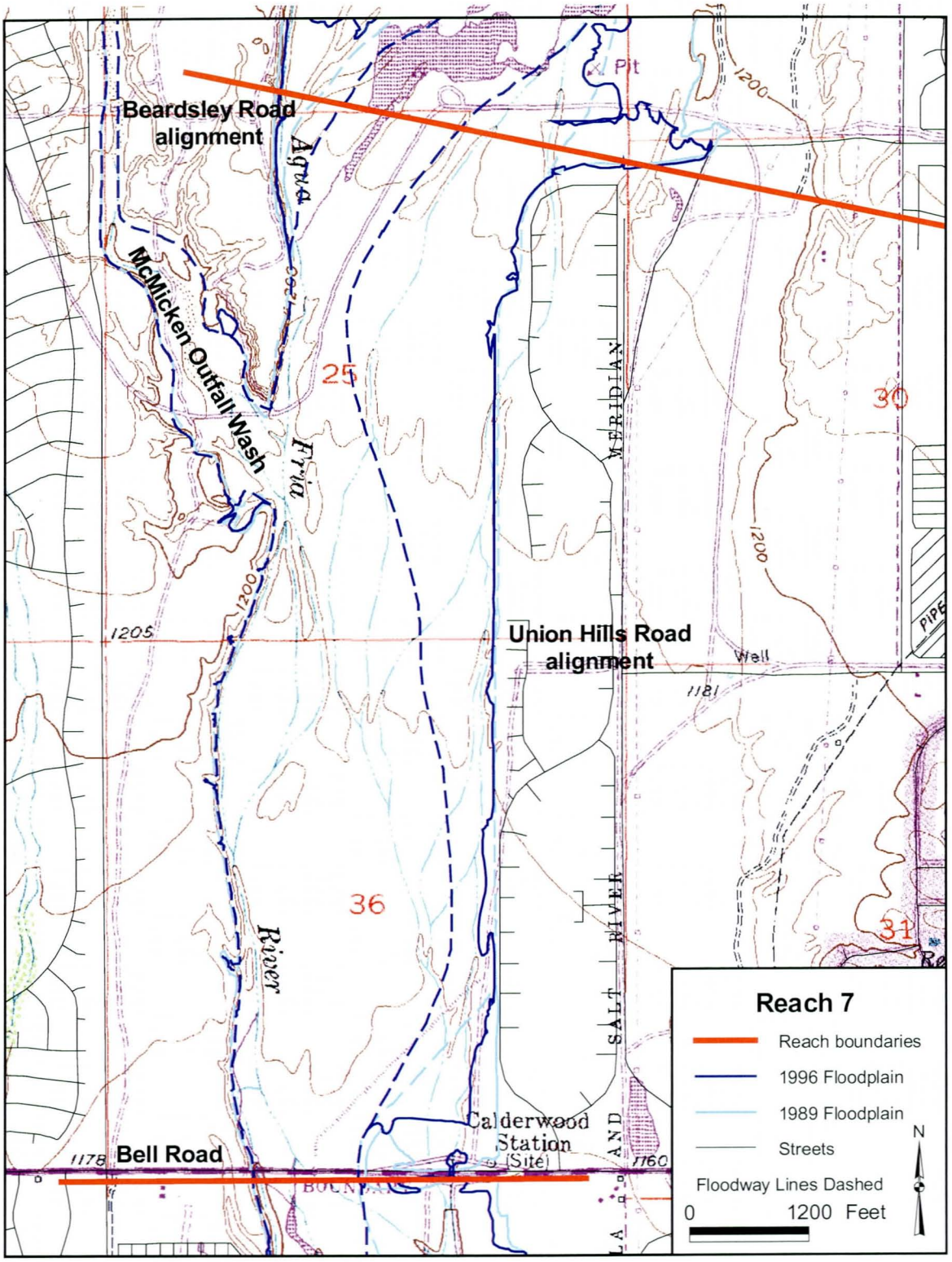

Figure 2-65 - Reach 7, Beardsley Road alignment to Bell Road

Internal (low flow channel) banks within Reach 6 range from three to six feet in height and are composed of sand and gravel (Figure 2-66). The banks along the islands located between the low flow channels are composed predominantly of sand. The right bank of the main channel

upstream of Bell Road is formed by the Pleistocene-aged terrace (Figure 2-67). While somewhat lower in height and relatively younger than the taller terrace upstream of McMicken Outlet Wash, the terrace exhibits similar characteristics. Specifically, the upper third to half of the bank is composed of calcium carbonate while the lower layers are relatively erosive sand and gravel.

Figure 2-66 - Photo 29-24

Figure 2-67 - Photo 29-13

Vegetation within the reach is similar to adjacent reaches where the dominant vegetation varies depending on relative channel position. Within the most active low flow channels, vegetation is sparse and generally limited to GUB and YUB. On higher channel bars YUB dominates with desert broom and some riparian trees including palo verde and willow trees. On the low islands located between the low flow channels lie broad areas of fine sands covered with palo verde, YUB, and creosote bush.

The single major tributary enters the Agua Fria River in Reach 6 (Figure 2-65). McMicken Outlet Wash collects runoff from a 323 square mile drainage area which includes the McMicken Floodway. The drainage area of the natural wash into which the McMicken Floodway enters is only about 19 square miles, with the remaining 304 square miles of drainage area from the McMicken Floodway. The 100-year peak discharge of the McMicken Outlet Wash at the Agua Fria River is 6,500 cfs, and the 10-year discharge is about 2,900 cfs. A second, smaller gunite-lined channel enters the river from the west just upstream of Bell Road. This channel drains much of the urbanized area of Sun City West. No discharge estimate was determined for this wash.

Figure 2-68 - Photo 31-7

Figure 2-69 - Photo 28-4

Several structures exist in Reach 6. The first major structure within Reach 6 is the riprap-protected embankment located along the Coyote Lakes development. Coyote Lakes is located along the east side of the Agua Fria River and extends the entire length of the reach. The

embankment ranges in height from about 6 to 9 feet. The bank protection consists of large, angular riprap from Bell Road to a point about 2,300 feet north of Bell Road where the angular riprap (Figure 2-68) changes to rounded river cobbles with a median diameter of about one foot (Figure 2-69). The second major structure, located at the downstream limit of the reach, is the Bell Road Bridge. The bridge reduces the width of the channel and floodplain from about 2,400 feet immediately upstream to about 1,000 feet at the bridge opening.

2.2.2 Middle Reach

Reaches 8 through 10 correspond to the "Middle Reach" defined in the Watercourse Master Plan Report. The Middle Reach is a transitional reach between the less impacted Upper Reach and the nearly completely channelized Lower Reach. Urbanization impacts, encroachments, and sand and gravel mining are significant characteristics of the Middle Reach.

2.2.2.1 Reach 8 - Bell Road to Cactus Road alignment

Reach 8 is a 3.44 mile long reach that extends from Bell Road to the Cactus Road alignment (Figure 2-72). The reach has a slope of 0.0026 as measured on the USGS 7.5 minute topographic quadrangles. The constriction of the channel created by the Bell Road bridge continues downstream through Reach 8 with the constriction increasing as the channel enters an area of historical and active sand and gravel mining. The channel constriction continues as the channel passes under the ATSF railroad and US 60 (Grand Avenue) bridges and passes the Cholla landfill on the west bank to the Cactus Road alignment.

The active channel begins near Bell Road with a width of about 1,000 feet narrowing rapidly to about 800 feet (Figure 2-70). Near the Greenway Road alignment, about one mile downstream of Bell Road, the channel narrows further as it enters an active area of sand and gravel mining. Near the Greenway Road alignment the active channel width is reduced to about 350 feet, and is located between tall earthen berms presumably constructed by the mines (Figure 2-71).

Figure 2-70 - Photo 32-5

Figure 2-71 - Photo 33-19

The channel widens somewhat about ¼ mile downstream of the Greenway Road alignment before narrowing again to about 300 feet as it flows along a tall Pleistocene terrace on the left bank through the US 60 Bridge. After passing under the Atchison Topeka and Santa Fe (ATSF) railroad and US 60 bridges, the channel corridor widens to about 750 feet with the Pleistocene terrace, locally covered with emplaced fill material, on the left bank and the riprap protected landfill on the right bank. The low flow channel in this lower portion of the reach has entrenched five to eight feet within the wider corridor (Figure 2-73). The low flow channel progressively narrows a short distance downstream of the bridges from about 300 feet wide to 100 feet wide near the downstream limit of the reach. As it narrows, depth of the low flow channel entrenchment increases.

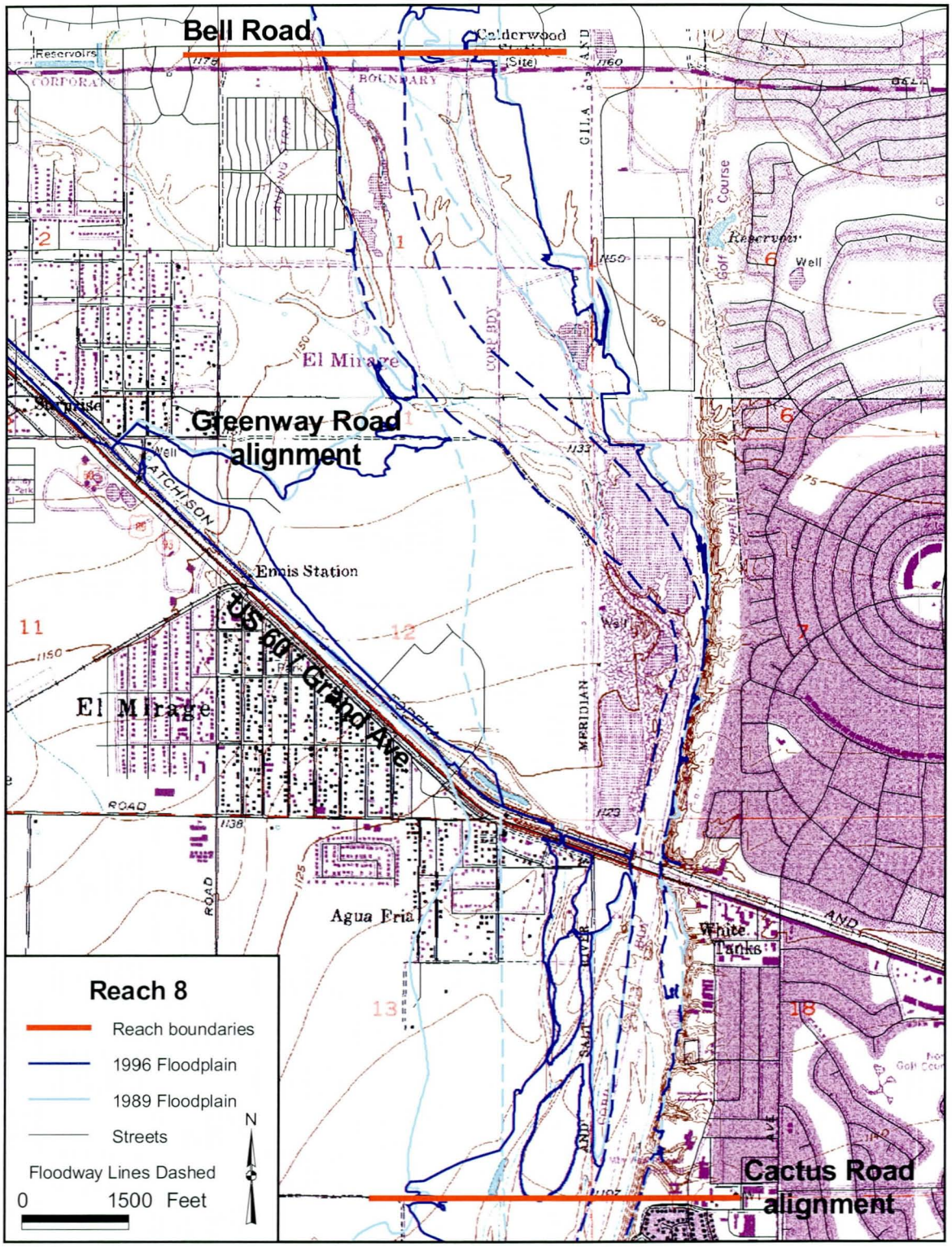

Figure 2-72 - Reach 8, Bell Road to Cactus Road alignment

Figure 2-73 - Photo 38-24

The channel pattern, which is mostly a function of historical human impacts, is generally straight with a single predominant channel throughout most of the reach. However, downstream of the ATSF railroad and US 60 bridges, overflows of the entrenched low flow channel have created several small channels which collect into a second low flow channel along the left bank.

As is the case for the upstream reaches, the channel generally lies within high Pleistocene-aged terraces on either side. The channel moves from flowing against the west terrace near Bell Road to the east terrace upstream of US 60. The east terrace is much higher than the west terrace in this reach (Figure 2-75 vs. Figure 2-74). The margin of the west terrace turns west away from the active channel and floodplain about ½ mile south of Bell Road. On the east, between the high Pleistocene-aged terrace and the active part of the channel lies an area identified by Huckleberry (1995) as unit Y1 (See Surficial Geology Map in Exhibits Map Book). This unit is described as "Holocene alluvium located outside the modern Agua Fria channel…(consisting) of both moderately sorted and bedded gravelly and cobbly channel deposits and sandy overbank deposits" (Huckleberry, 1995).

Figure 2-74 - Photo 35-15 - West terrace

Figure 2-75 - Photo 32-4 - East terrace

The bed and bank materials within the reach consist predominantly of sand and somewhat finer gravel than in the upstream reaches. However, impacts from human activities have also left some low areas within the channel where extensive deposits of very fine material are found in the active channel. Again, the Pleistocene terraces, while capped with resistant calcium carbonate layers, are underlain by less resistant alluvial sands and gravels that crop out at the flood water level.

Similar to adjacent reaches, the vegetation within the reach varies with channel position. Disturbance of large stretches of the reach have little to no vegetation whatsoever. YUB is the dominant vegetation on the channel bars. Tamarisk and desert broom are common in

undisturbed areas. Sparse riparian trees along banks and higher surfaces include willow, palo verde, ironwood, and a few struggling cottonwood trees that were observed near the Acoma Road alignment.

Significant structures and encroachments as well as extensive sand and gravel mining exist within Reach 8. These structures have also had a significant impact on the shape and location of the channel and the floodplain within the reach. The most significant structural features within the reach are the ATSF railroad and US 60. The railroad embankment prevents flood water in the right overbank from continuing southward, and directs overbank flow east along the embankment to one of two openings under the railroad - the 450-foot wide bridge crossing, or a relief bridge about 1,000 feet west of the main bridge. The relief bridge is a set of 3-4'x8' box culverts. The discharge through the relief bridge for the 100-year flood is 500 cfs, according to the most recent FIS.

Along the right bank between Bell Road and the Greenway Road alignment, development has encroached into the pre-Waddell Dam floodplain. A trailer park just downstream of Bell Road and the Sun City recreational vehicle parking area sit on the Y1 surface (Huckleberry, 1995) in the right overbank below the high Pleistocene terrace, but outside the current 100-year floodplain. A north-south road along the 115th Avenue alignment provides access to the gravel mining operation site. This dirt road crossing is elevated above the channel about 10 feet. Passage for very low discharges is provided by three 4 foot diameter reinforced concrete pipes (Figure 2-76).

Figure 2-76 - Photo 36-20

Figure 2-77 - Photo 39-10

Downstream of the ATSF railroad and US 60, the Cholla Landfill, a large capped landfill, has filled the former channel bed and portions of the right floodplain. The landfill lies between the existing channel, which flows through the main bridges and the relief bridge to the west. The east side of the landfill is protected by a hodgepodge of concrete rubble acting as riprap (see Figure 2-73 shown previously). No detailed engineering drawings were available for the landfill "bank protection" or for design of the landfill itself.

The left bank of the river downstream of the ATSF railroad and US 60 consists of numerous developed parcels where fill has been placed in irregularities in the natural bank of the Pleistocene-aged terrace. On some of these parcels the fill extends beyond the historical limits of the terrace a short distance into the historical floodplain (Figure 2-77).

A large sand and gravel mine operation is located within Reach 6. The operation, including the pits and processing plant, occupies portions of the main channel and right overbank upstream of US 60. The largest pit is located to the left of the main channel downstream of Bell Road (Figure 2-78). Other pits are also located within the right overbank and within the channel. The operation has also constricted the channel by constructing large sand and gravel berms along the channel. The combination of removal of sediment from the channel, lowering of the channel bed elevation, and constriction of the channel by the berms has caused the channel to degrade.

Currently, the bridge crossing at the railroad is 21 feet above the channel invert. A painted sign on the bridge says "CLEARANCE 12 FT" (Figure 2-79), implying that about nine feet of degradation has occurred since the sign was painted on the bridge. Upstream of the bermed portion of the reach, two headcut channels about three feet in depth are migrating upstream toward Bell Road.

Figure 2-78 - Photo 33-13

Figure 2-79 - Photo 23-17

No significant tributaries enter the Agua Fria River in Reach 8, although an urban drainage channel does enter the river from the east, and appears to drain a portion of Sun City north of Grand Avenue. Data from the USGS gaging station and FCDMC ALERT network suggest that this drainage channel is the most frequent contributor of runoff to the reach. However, the magnitude and volume of these flows are very small compared to the size of the channel downstream of the railroad/highway bridges.

2.2.2.2 Reach 9 - Cactus Road alignment to Olive Avenue

Reach 9 is a 2.21 mile long reach that extends from the Cactus Road alignment to Olive Avenue (Figure 2-80). The reach has a slope of 0.0026 as measured on the USGS 7.5 minute topographic quadrangles. Reach 9 is more natural relative to the upstream and downstream reaches. The active channel increases in width downstream through the reach. Near the upstream limit the most active part of the channel is about 400 feet wide. Near the Peoria Avenue alignment the most active part of the channel has increased to about 900 feet wide. Downstream, the active channel widens to about 1,200 feet, narrows briefly and then widens again before it passes under the Olive Avenue bridge, which has a 1,450 foot wide opening. Within the most active channel areas of Reach 9, the channel has a straight or braided pattern. The braided pattern is more strongly pronounced in the wider sections, where large gravel bars are present, with multiple smaller low flow channels around the bars. These low flow channel braids are about 100 to 200 feet in width.

Beyond the most active part of the channel, the river also exhibits a wider braided pattern of channels that are utilized by the river at higher discharges. These overbank braided channels provide opportunities for the overbank flows to concentrate and do more erosive work. Many of the intermediate surfaces between these overbank channels, especially downstream of the Peoria Avenue alignment in the left overbank are composed of fine-grained sediments. Further left and above this area lies a floodplain surface of predominantly fine-grained sediments. This floodplain area was shown as within the pre-New Waddell Dam floodplain, but is mapped as outside the post-New Waddell Dam 100-year floodplain.

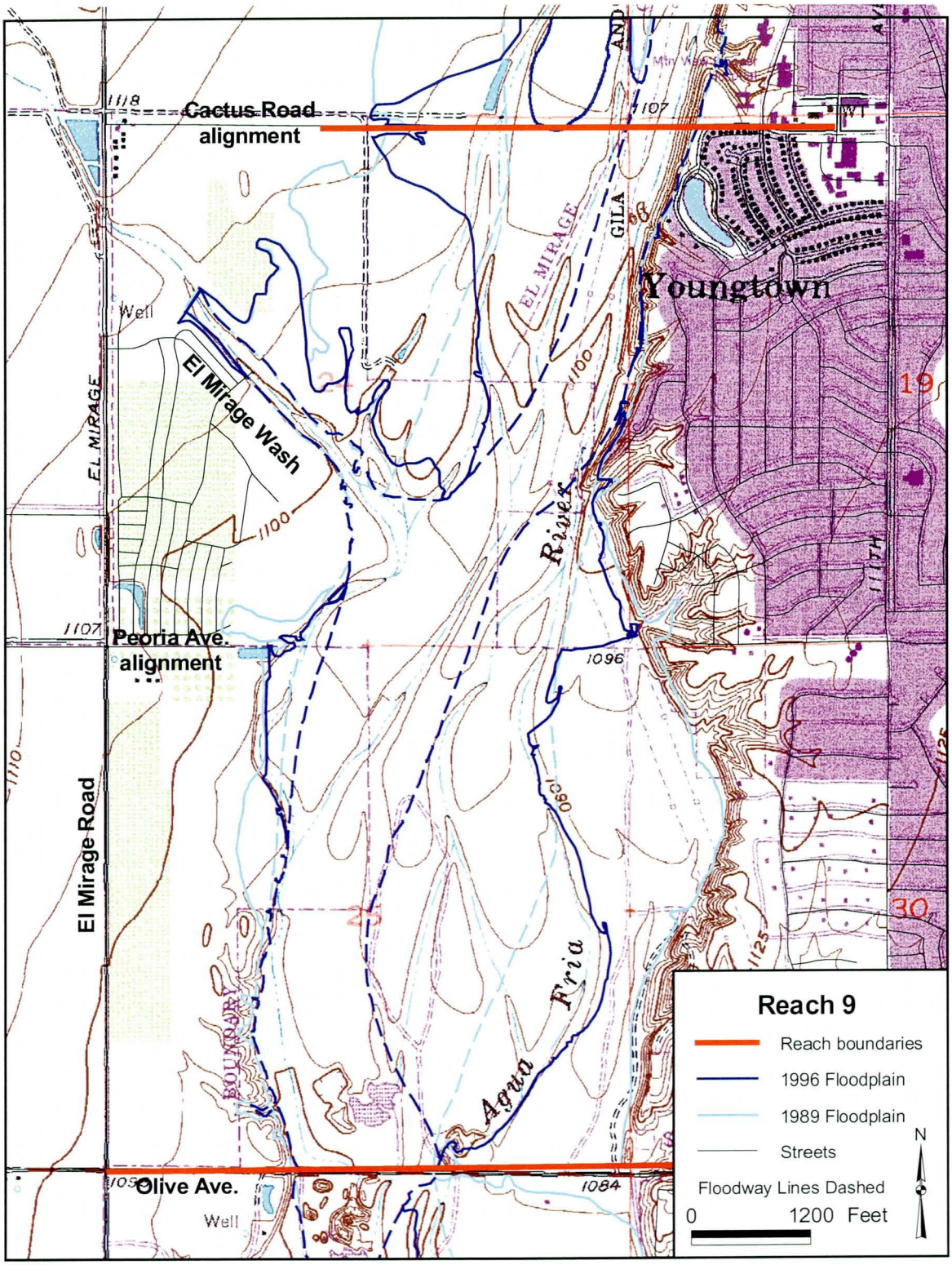

Figure 2-80 - Reach 9, Cactus Road alignment to Olive Avenue

Bed and bank materials within the most active portions of the channel are composed of gravel and sand (Figure 2-81). The banks and bars along the sides of the most active area are dominated by sandy sediments overlying coarser gravel (Figure 2-82). The higher islands between overbank channels are predominantly comprised of fine sand and silty fine sand (Figure 2-83).

Figure 2-81 - Photo 46-11

Figure 2-82 - Photo 42-8

Vegetation within the reach varies with channel position. The most active low flow channels are generally devoid of vegetation except for scattered GUB, YUB, desert broom, and tamarisk. The higher mid-channel bars are dominated by YUB, with some desert broom, willow, and smaller palo verde. The overbank areas and highest islands as well as some of the sand dominated side bars have larger riparian trees growing on them along with many "horsetail bush" shrubs (Figure 2-84).

Figure 2-83 - Photo 42-6

Figure 2-84 - Photo 43-17

The modern and geologic floodplain in Reach 9 are contained below a high Pleistocene-aged terrace along the left bank of the reach. The right bank limits are less well defined. About ¼ mile downstream of the Peoria Avenue alignment, the right bank is also a Pleistocene-aged terrace, although it is topographically lower and younger than the high left bank terrace. Upstream, however, the Pleistocene terrace is bisected by a tributary which enters the river through a golf course on the west. The Arizona Geological Survey (AZGS) 1:100,000 scale geology map (Reynolds, et al., 1997) shows that this Pleistocene terrace reemerges north of the tributary under the town of El Mirage. However, a wide area of younger Holocene alluvium between the terrace and the active portion of the channel is cut off from the river by the railroad and highway upstream (see Surficial Geology Map in Exhibits Map Book).

Low flow channels flow directly against the Pleistocene terrace along the left bank from about the Cactus Road alignment to about ¾ mile downstream, as well as along the right bank for about ¼ mile upstream of Olive Avenue. In these locations the terraces are being undercut

leaving a nearly vertical bank as the less resistant underlying alluvium is removed by flood waters (Figure 2-85).

Figure 2-85 - Photo 45-21

Examination of historical aerial photographs dating to 1954 revealed only one location where sand and gravel mining occurred within the reach. The 1964 photographs show a small area of mining just upstream of Olive Avenue in the left half of the active portion of the channel. This mining operation is also present in the 1977 photographs. During the 1980 flood, however, the mined area was filled in by sediment and no further mining is seen in subsequent photographs.

There are no significant encroachments into the river within the reach. On the left bank, minor amounts of fill have been placed to fill in deep local tributary canyons, but the fill does not extend very far into the river. Along the right bank, a golf course and a wastewater treatment plant are located near the edge of, or slightly into, the historical river channel. However, these encroachments are not significant, especially given the level of encroachment that occurred at the ATSF/US 60 bridges and Cholla Landfill upstream. The most significant encroachment in Reach 9 is the roadway embankment of Olive Avenue, which consists of a 4 to 5 feet high embankment that extends from the base of the left terrace to the bridge opening. This embankment forces the 100-year discharge west under the Olive Avenue bridge.

2.2.2.3 Reach 10 - Olive Avenue to the New River confluence

Reach 10 is a 3.40 mile long reach that extends from Olive Avenue to the New River confluence (Figure 2-86). The reach has a slope of 0.0023 as measured on the USGS 7.5 minute topographic quadrangles. Reach 10 is one of the more heavily impacted reaches in the river. Several historical and active sand and gravel operations are located within this reach. Additionally, a landfill, groundwater recharge facility, and the Glendale airport lie within the geologic floodplain. The most active portion of the channel in this reach varies in width from about 400 feet wide downstream of Olive Ave. to 150 feet wide between Northern and Glendale Avenues to about 1,200 feet wide near the New River confluence. The variation in width reflects the level of disturbance of the natural channel.

The channel pattern, while historically strongly braided, due to human impacts is now generally straight throughout most of the reach. Near the downstream limit of the reach the channel begins to become more braided again. Bed and bank materials within the reach consist of gravel and sand. Between Olive and Northern Avenues, the left bank of the active channel is predominantly composed of sand and gravel (Figure 2-87), while the right bank is comprised of large angular stone riprap (Figure 2-88).

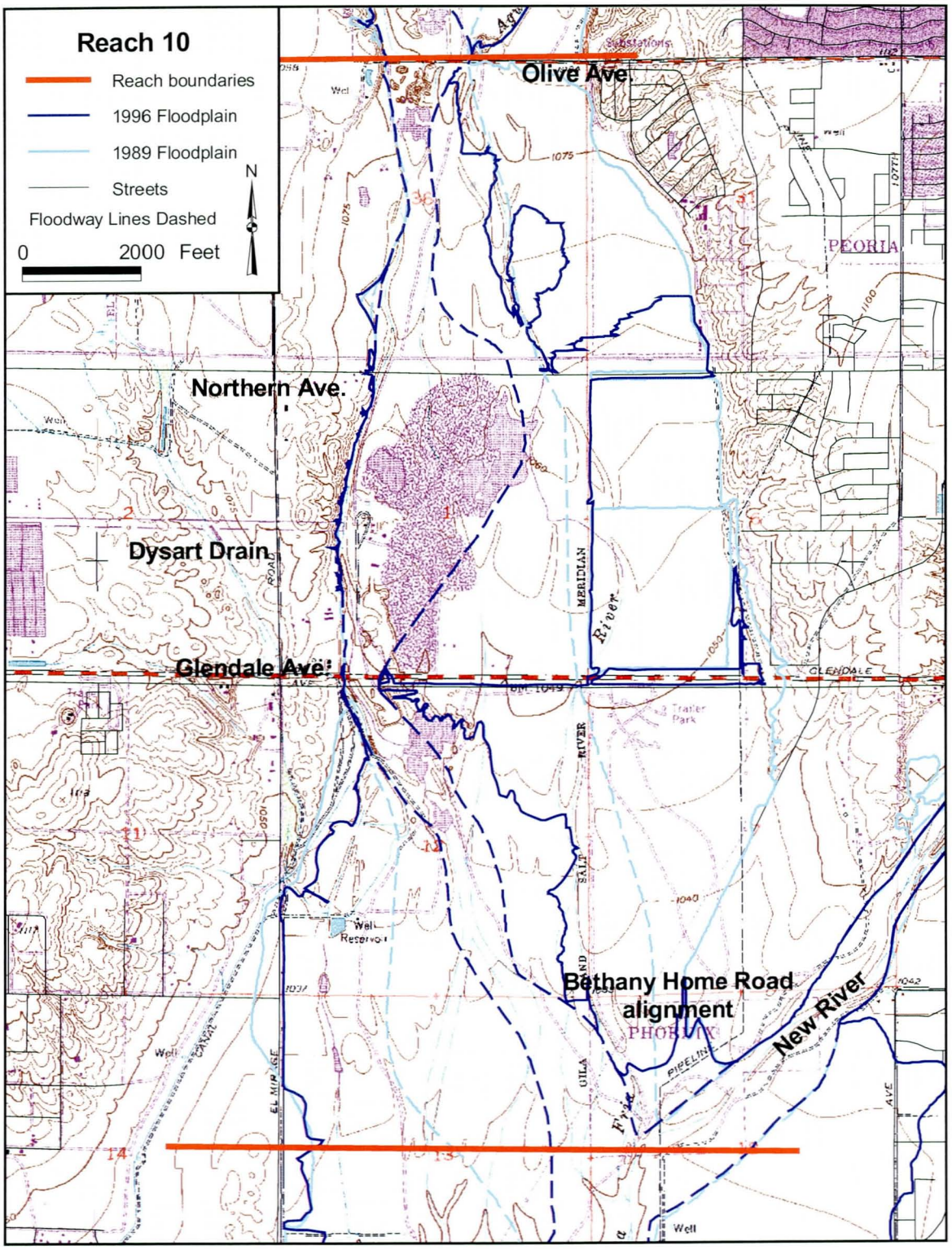

Figure 2-86 - Reach 10, Olive Avenue to New River confluence

Figure 2-87 - Photo 47-2

Figure 2-88 - Photo 47-5

Downstream between Northern and Glendale Avenues, an extensive sand and gravel mining operation has directed floodwaters (or attempted to direct floodwaters) into a narrow, 150 feet wide channel along the right bank (Figure 2-89). The left bank in this portion of the reach consists of a gravel road embankment protected by "free poured" concrete (Figure 2-90).

Figure 2-89 - Photo 48-20

Figure 2-90 - Photo 48-17

The right bank of Reach 10 is a Pleistocene-aged terrace capped with a relatively thin layer of more resistant calcium carbonate. The lower layers, however, are less resistant and have been actively cut by floodwaters directed into this narrow channel (Figure 2-91).

Figure 2-91 - Photo 48-11

Figure 2-92 - Photo 48-1

Figure 2-93 - Photo 48-24

The Dysart Drain enters the reach from the west about ½ mile upstream of Glendale Avenue (Figure 2-86). The 100-year discharge in the Dysart Drain at El Mirage Road is estimated at about 4,000 cfs. This concrete-lined channel directs frequent storm water and agricultural tailwater into the river (Figure 2-92). The result is a dense stand of riparian vegetation which extends downstream of Glendale Avenue about 1,200 feet. These thick stands of willow, cottonwood, tamarisk, and reeds create significant roughness to flood waters in this portion of the low flow channel (Figure 2-93). Downstream of the Glendale Avenue and the dense riparian area the channel banks are predominantly composed of sand and fine sand. Other than the Dysart Drain, there are no significant tributaries entering the Agua Fria River within Reach 10.

Aside from the dense riparian area downstream of the Dysart Drain, vegetation in the reach is generally similar to that of adjacent reaches. However, disturbance in much of the active channel has prevented much vegetation from establishing itself. The finer grained deposits above the active channel are home to riparian species such as palo verde and willow, as well as widespread "horsetail shrubs" (joint-fir or Morman tea).

The geologic floodplain of the Agua Fria River in Reach 10 is confined between Pleistocene-aged terraces, although the width of the geologic floodplain expands significantly beginning at about the Northern Avenue alignment. Historically, the active channel corridor also widened in this reach. The Pleistocene terraces are separated by as much as a mile and a half in this reach, and the pre-New Waddell Dam floodplain was mapped as spanning the entire area between the terraces. The current (post-New Waddell) 100-year floodplain is mapped as well within these limits, except along the right bank from just upstream of Northern Avenue to Glendale Avenue where the floodplain directly impinges on the terrace. The left edge of the current floodplain is generally ¼ mile or more west of the left bank terrace. This narrowing of the floodplain is partially the result of construction of levees and other structures, such as the Glendale landfill, and partially due to the reduced peak discharges in the river.

Sand and gravel mining has been occurring in the reach since at least 1954. Examination of historical aerial photographs reveals that the 1978 flooding inundated the large gravel pit downstream of Northern Avenue and deposited significant deltas of sand and gravel (Figure 2-94). Additionally, the deep, narrow pit downstream of Olive Avenue had smaller deltas of gravels deposited at its upstream end during the 1993 flooding (Figure 2-95).

Figure 2-94 - 1999 Aerial Photograph of Delta in Gravel Pit Downstream of Northern Avenue

Figure 2-95 - 1999 Aerial Photograph of Delta in Gravel Pit Downstream of Olive Avenue

The gravel pits located between Northern and Glendale Avenues, along with the construction of the Glendale Avenue bridge and roadway embankment have also changed the historical channel pattern and position. Prior to these activities, the main braids of the Agua Fria River flowed in the more eastern half of the river corridor. Since at least 1977, the river has been forced under the relatively narrow (450 foot wide) Glendale Avenue bridge located on the west side of the river.

2.2.3 Lower Reach

Reaches 11 through 15 correspond to the "Lower Reach" defined in the Watercourse Master Plan Report. The Lower Reach is channelized at least partially along almost its entire length. The New River enters the Agua Fria at the upstream end of the Lower Reach. It delivers relatively frequent and prolonged discharges from the New River, Adobe, and Cave Buttes Dams. Also, the watershed of the New River and its tributaries downstream of these dams is almost completely urbanized. These urbanized areas include numerous storm drains and flood control channels. These efficient conveyance systems contribute to additional frequent discharges numerous times during all but the driest years.

2.2.3.1 Reach 11 - New River confluence to Indian School Road

Reach 11 is a 2.06 mile long reach that extends from the New River confluence to Indian School Road (Figure 2-96). The reach has a slope of 0.0029 as measured on the USGS 7.5 minute topographic quadrangles. The most active portion of the channel near the upstream limit of the reach is about 1,200 feet wide. Where the New River enters, there is also an additional distinctive low flow channel that is about 250 feet wide. Downstream from Camelback Road the low flow channel enters a broad area of a gravel pit. The pit, about 8 feet in depth, continues downstream about ½ mile. A narrow channel about 200 feet wide exits the pit area. This narrow channel becomes more diffuse as it widens near the Indian School Road bridge.

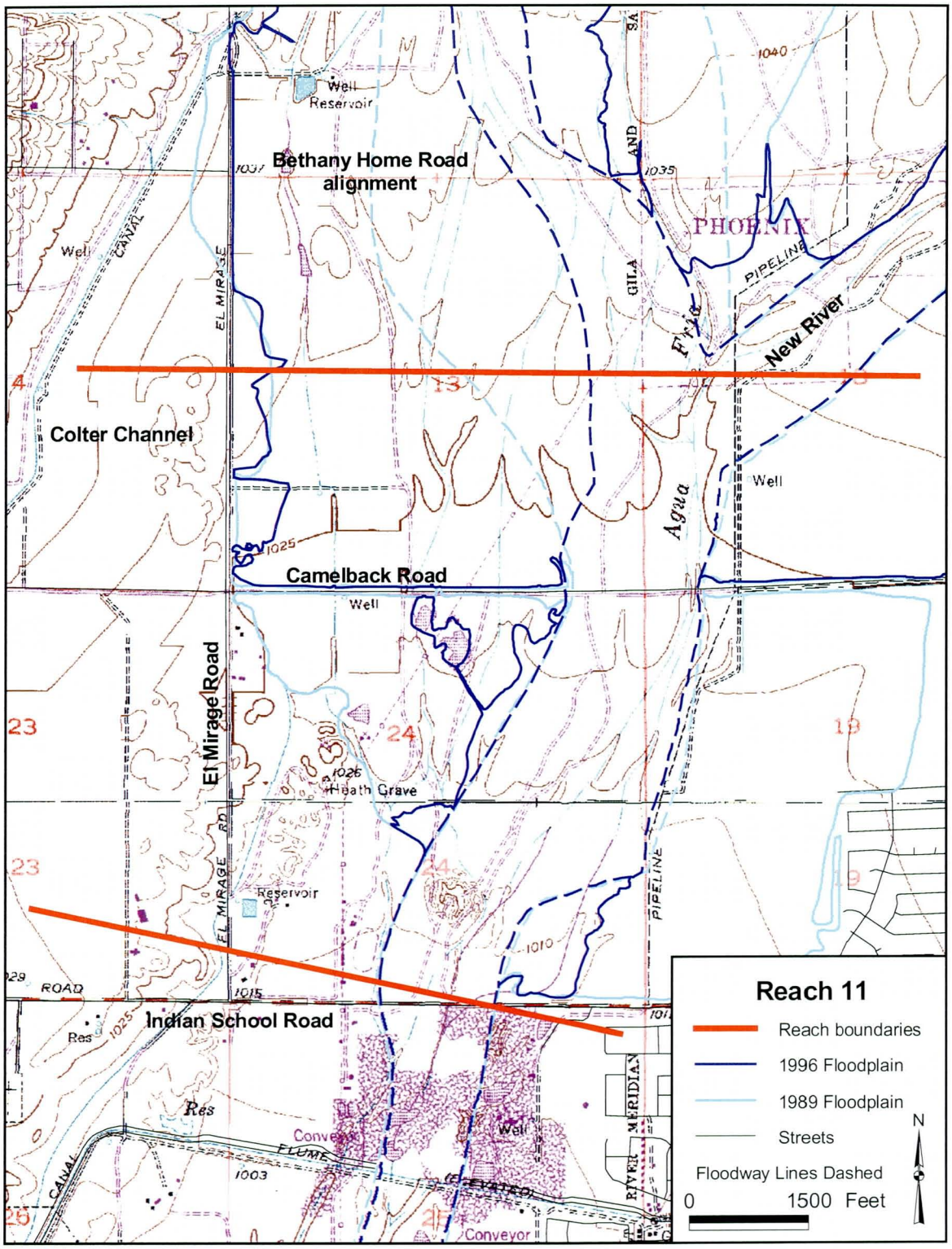

Figure 2-96 - Reach 11, New River confluence to Indian School Road

The channel pattern is highly disrupted by the levees, bridges, and gravel mining within the reach. Historically, Reach 11 was strongly braided. Today, the portion of Reach 11 upstream of Camelback Road retains some of this braided character. Urbanization, construction of dams, and channelization within the New River watershed may be responsible for formation of a more dominant single low flow channel downstream of the New River.

Bed and bank materials within the river generally consist of sand and gravel (Figure 2-97). The outer east bank is composed of soil cement (Figure 2-98), while the west bank is made up of predominantly sandy material downstream to another soil cement levee which begins about 2,000 feet upstream of Indian School Road.

Figure 2-97 - Photo 56-11

Figure 2-98 - Photo 58-11

Figure 2-99 - Photo 34-24

Lowering of the channel bed by a gravel mine downstream of Camelback Road has exposed reddish, clay-rich sands and gravels below about three to four feet of grayish sands (Photo 34-24). The contact between the two distinctive units probably represents the historical limit of scour of the pre-mining Agua Fria River. Vegetation within the reach is scarce downstream of Camelback Road. Upstream of Camelback Road, the typical setting of channel position-dependent vegetation suites described for the upstream reaches exists.

Two tributaries enter the Agua Fria River within Reach 11. On the west, a flood control channel called the Colter Channel enters the river just upstream of Camelback Road (Figure 2-96). The 100-year discharge from the Colter Channel is 1,040 cfs at El Mirage Road. The largest tributary for the entire study area, the New River, enters the Agua Fria River in Reach 11. The New River enters the Agua Fria River from the east just upstream of Camelback Road (Figure 2-96). The drainage area of the New River at the Agua Fria River is 605 square miles. Of that area, 445 square miles are regulated by the New River, Adobe, and Cave Buttes Dams. Downstream of the dams, the watershed is generally unregulated with the exception of some

smaller dams around the Phoenix Mountains, such as Dreamy Draw Dam and numerous small detention dams owned by the City of Phoenix. Most of the lower New River watershed is highly urbanized. The 100-year discharge from the New River is 39,000 cfs (USACOE, 1982), and the 2-year discharge is 5,500 cfs (USACOE, 1995). The New River is the most significant contributor of flood water to the lower Agua Fria River in terms of flood magnitude, frequency, and duration.

Three relatively large sand and gravel pits are located in the right overbank upstream of Colter Channel (Figure 2-100). Additionally, downstream of Camelback Road is an extensively mined area covering most of the width of the river bottom (Figure 2-101). In this area sediment has been removed to an average depth of about 8 feet.

Figure 2-100 - Photo 56-1

Figure 2-101 - Photo 58-3

Degradation of the channel bed in Reach 11 has led to significant scour along the east side of the channel and the east soil cement levee between the mining pit and Camelback Road (Figure 2-102). Another large, very deep pit exists between the two wing dikes upstream of Indian School Road on the east side of the river (Figure 2-103). This pit could conceivably collect flood water and experience some significant bank failure.

Figure 2-102 - Photo 34-22

Figure 2-103 - Photo 1-5

Significant structures within the reach include the Camelback Road Bridge, the north and south Camelback Levee along the east bank of the river, and two large wing dikes which direct flood water into the Indian School bridge crossing (Figure 2-104). The levees and wing dikes are composed of soil cement. Another soil cement levee is located along the west bank of the river for about 2,000 feet upstream of Indian School Road (Figure 2-105).

Figure 2-104 - Photo 58-18 - View SW from top of upstream wing dike

Figure 2-105 - Photo 59-6

The Glendale Airport and the water treatment facility on the east bank of the Agua Fria River and north bank of the New River also confine flood water. The nose of this embankment around the Glendale facilities is protected by soil cement which continues upstream into the New River. Beyond the embankment nose to the north, the airport embankment is not protected. However, the current floodplain does not show flood water flowing along this portion of the embankment.

2.2.3.2 Reach 12 - Indian School Road to Interstate 10

Reach 12 is a 2.79 mile long reach that extends from Indian School Road to Interstate 10 (Figure 2-108). The reach has a slope of 0.0020 as measured from on the 1989 Flood Insurance Study topography. At Indian School Road, the Agua Fria River is completely channelized between 14-foot high, parallel soil cement levees that are about 1,100 feet apart (Figure 2-106). The channel gradient is controlled by soil cement grade control structures which span the entire channel between the levees. In Reach 12, there are three such grade control structures. The first is located just downstream of Indian School Road, the second is located just downstream of the Thomas Road alignment, and the third is located about ½ mile upstream of Interstate 10. While the upstream grade control is mostly buried and easy to miss, the downstream two structures have 2 to 4 feet of local scour immediately downstream of them (Figure 2-107).

Figure 2-106 - Photo 38-4

Figure 2-107 - Photo 41-18

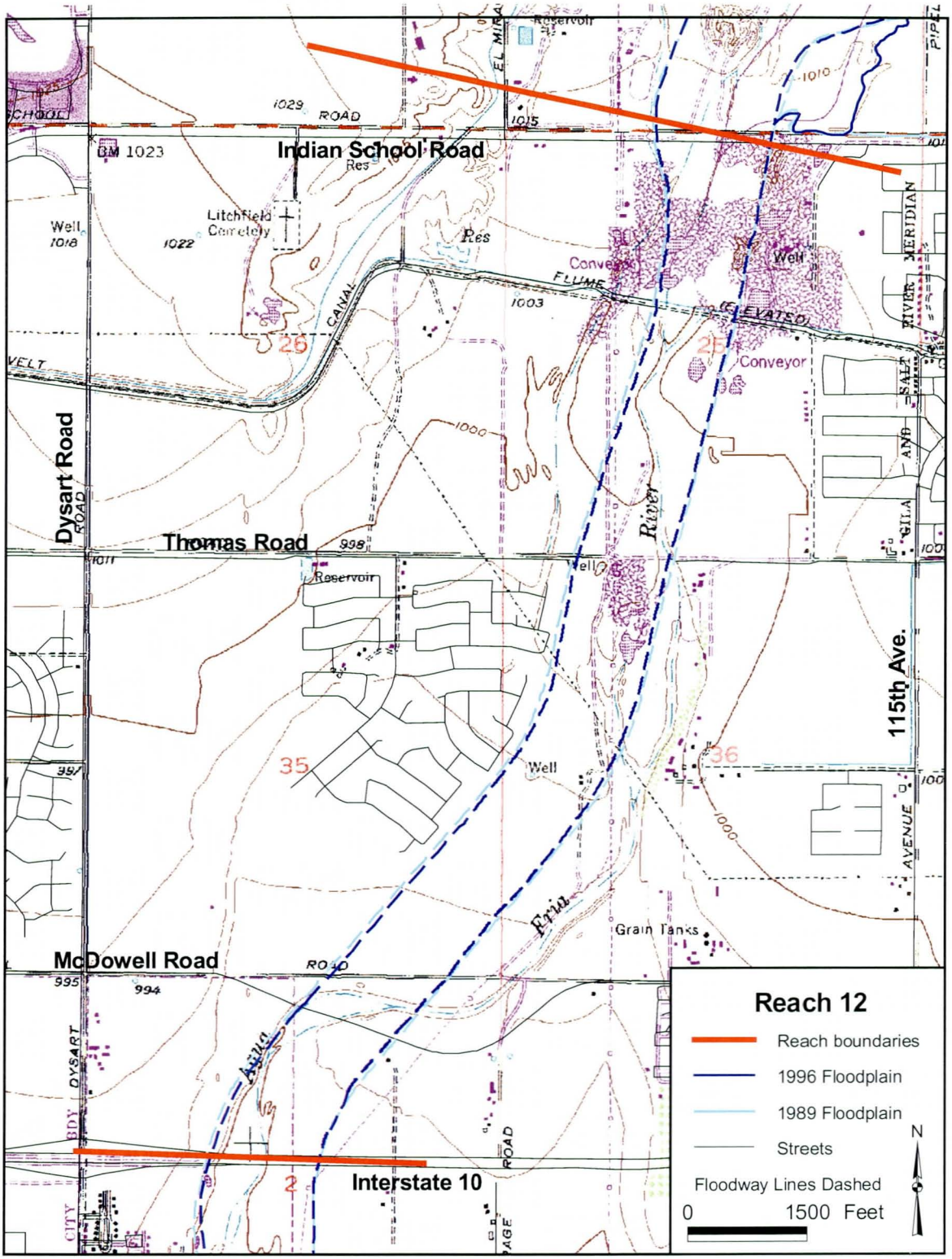

Figure 2-108 - Reach 12, Indian School Road to Interstate 10

Additional structures in Reach 12 include the powerline islands (Figure 2-109), and the McDowell Road and Interstate 10 Bridges. A cluster of seven islands is located near the Thomas Road alignment, and two more islands are located near McDowell Road. Also, the Roosevelt Irrigation District canal passes under the river in a siphon between Indian School and Thomas Roads. None of these structures appear to have had an adverse effect on the river as yet.

Figure 2-109 - Photo 38-5

Figure 2-110 - Photo 41-9

Reach 12 has a distinct low flow channel running near the center of the channelized floodplain. This low flow channel is about 220 feet wide and one to two feet deep (Figure 2-110). The sediments within the low flow channel are predominantly sand. At the two downstream grade control structures, the low flow channel widens as it approaches the structure and then reconcentrates just downstream of the grade control, forming a pattern looking like a leaf rake (upstream braided section) and handle (downstream single channel).

Vegetation within the reach is limited. The low flow channel has almost no vegetation while the "overbank" areas have scattered shrubs, such as desert broom and tamarisk, and other low plants. The exception to this vegetation pattern occurs at the confluence with the Interstate 10 drainage channel, the single significant tributary to Reach 12. This channel enters from the east just upstream of Interstate 10 (Figure 2-111), and contributes frequent low flows to the river. The result is a dense stand of tall grasses and some extensive deposits of very fine sediments and frequent standing or very slow moving water.

Figure 2-111 - Photo 50-15

No sand and gravel mining is presently occurring within the channel in Reach 12.

2.2.3.3 *Reach 13 - Interstate 10 to MC 85 (Buckeye Road)*

Reach 13 is a 1.61 mile long reach that extends from Interstate 10 to Buckeye Road (Figure 2-112). The reach has a slope of 0.0020 as per the 1989 Flood Insurance Study topography.

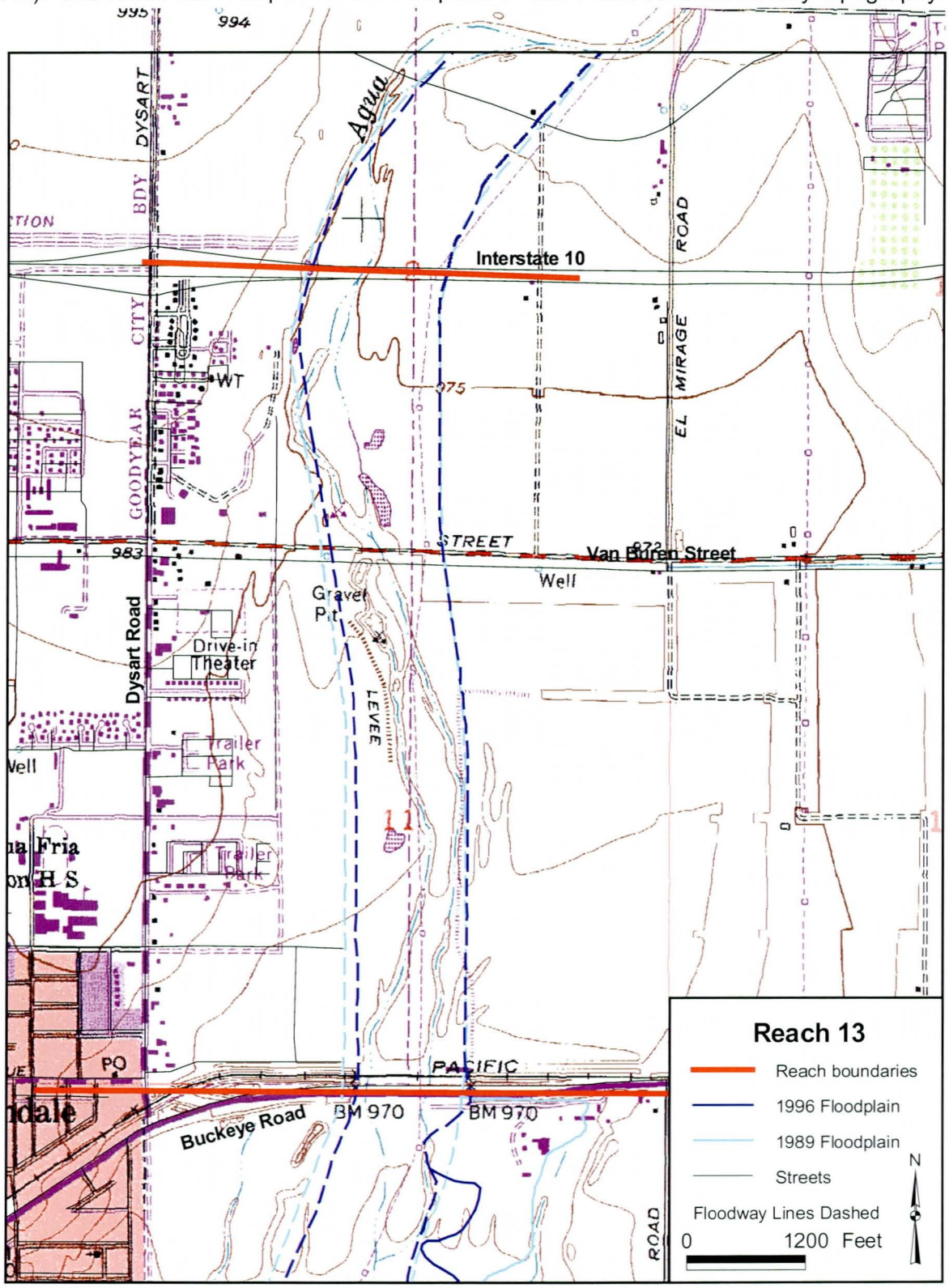

Figure 2-112 - Reach 13, Interstate 10 to MC 85 (Buckeye Road)

Reach 13 is very similar to Reach 12. The entire length of the reach is confined between soil cement levees. There are two soil cement grade control structures within the reach. The first is located just downstream of Interstate 10, and the second is located about 1,900 feet upstream of Buckeye Road. The significant difference between Reach 12 and 13 is the disappearance of the low flow channel in Reach 13. Several smaller, braided channels are present downstream of the upstream grade control structure, but they become smaller and less distinct as they pass under Van Buren Street. Most of the width of the channel between the soil cement levees is covered in thick tall grass (Figure 2-113). The grass is likely the result of the more frequent wetting from discharges from the Interstate 10 channel.

Figure 2-113 - Photo 57-5

Figure 2-114 - Photo 56-23

Scour was observed on the downstream side of both grade control structures in Reach 13, with deeper scour at the downstream structure. Locally, the scour holes on the downstream side of the downstream structure exceed 5 feet in depth (Figure 2-114). Other structures in Reach 13 are the Van Buren Street Bridge, the Southern Pacific Railroad Bridge (Figure 2-115), and a line of powerline tower islands in the east half of the channel. None of these structures appear to have had any adverse effects on the channel as yet.

Figure 2-115 - Photo 54-15

2.2.3.4 Reach 14 - MC 85 (Buckeye Road) to Broadway Road

Reach 14 is a 2.60 mile long reach that extends from Buckeye Road to the Broadway Road alignment (Figure 2-116). The reach has a slope of 0.0025 as measured on the USGS 7.5 minute topographic quadrangles.

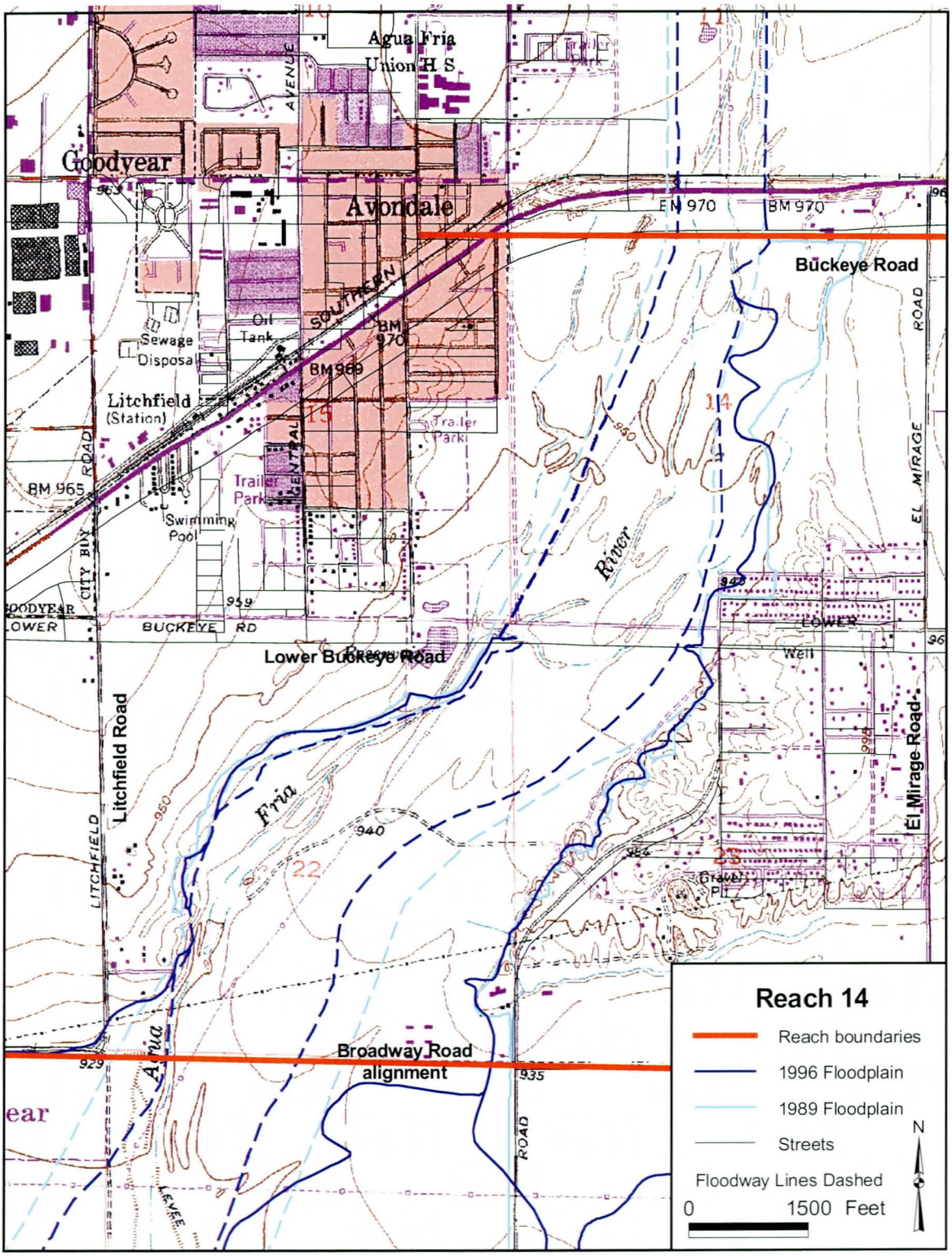

Figure 2-116 - Reach 14, MC 85 (Buckeye Road) to Broadway Road alignment

Two entrenched low flow channels extend downstream from Buckeye Road. These channels join about 1,000 feet downstream of the road. Another 700 feet downstream the channels again

diverge around a powerline tower. The left channel becomes wider and more diffuse for about ½ mile before reconcentrating about 1,200 feet upstream of Lower Buckeye Road. The area where the flows begin to reconcentrate has a network of shallow headcuts which converge into a single channel just upstream of the road (Figure 2-117). The right channel continues south, paralleling the right bank levee before turning east and crossing Lower Buckeye Road. The right channel is about 100 feet wide and 2 to 3 feet deep. South of Lower Buckeye Road, a single low flow channel continues downstream. The channel widens as it progresses further downstream. A distinctive cutbank about 4 feet high lines the channel along its left bank. The channel in this area is about 400 feet in width.

Figure 2-117 - Photo 60-9

The channel bed sediments consist primarily of sand throughout most of the reach, but especially so downstream of Lower Buckeye Road. Between Buckeye and Lower Buckeye Roads, smaller gravels are also present. The internal banks within the reach are composed of predominantly of sand (Figure 2-118), but the outer cutbanks along the left bank downstream of Lower Buckeye Road are sandy with a higher percentage of finer sand and silt (Figure 2-119).

Figure 2-118 - Photo 62-11

Figure 2-119 - Photo 62-14

Downstream of Buckeye Road, the soil cement levee continues only on the west bank. The levee ends about 4,000 feet downstream of Lower Buckeye Road. Another short soil cement levee protects a small subdivision on the east bank just upstream of Lower Buckeye Road (Figure 2-120). The levee begins on the northeast side of the subdivision and wraps around the subdivision, continuing south across Lower Buckeye Road until it meets the Pleistocene terrace.

Figure 2-120 - Photo 60-8

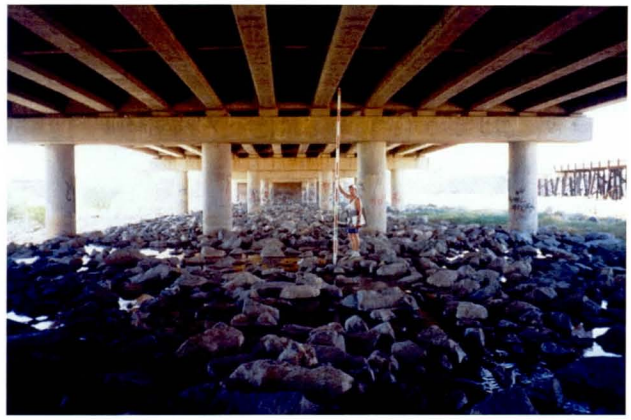

Figure 2-121 - Photo 54-11

Underneath and immediately downstream of Buckeye Road, large angular riprap has been placed to protect the bridge (Figure 2-121). However, for some unknown reason, this riprap does not span the entire width of the bridge. During the field visits, only riprap in the western 2/3 of the section on the downstream face of the bridge was observed. On the upstream side of the bridge on the east, a small agricultural tailwater ditch enters the river. This ditch supplies frequent low flows into the area beneath and just downstream of the bridge, and helps supply water to a thriving riparian thicket downstream of Buckeye Road (Figure 2-122).

Elsewhere in the reach, vegetation within the low flow channel is generally limited to a few scattered low shrubs and a handful of large tamarisk. The overbank areas contain a greater density of shrubs including desert broom, mesquite, and tamarisk. However, the density of vegetation is not high relative to other portions of the study area.

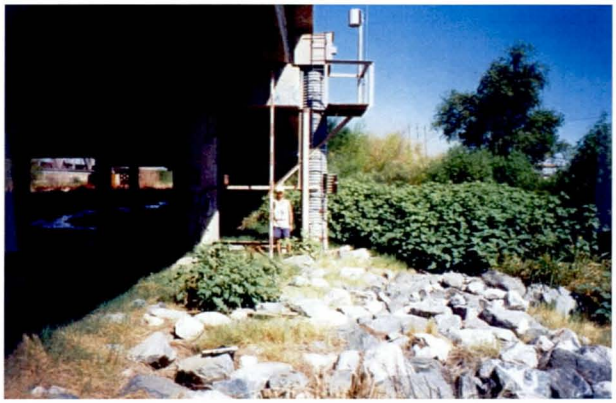

Figure 2-122 - Photo 54-9

Figure 2-123 - Photo 0-19

Lower Buckeye Road is an at-grade crossing (Figure 2-123). Two 4'x5.6' elliptical culverts pass very low discharges under the road. Low flows are directed into the culverts with the help of two five foot high "sugar" dikes across the two separate low flow channels immediately upstream of the road crossing. At higher stages these dikes wash out and allow floodwater to pass over the roadway. Additionally, the roadway drops down from the levees on either bank down to the channel. These ramps are about 600 feet in length each. As such they constrict the channel as it crosses Lower Buckeye Road. The banks of the ramps are covered with concrete to protect them from flood waters.

An agricultural hay storage area is located in the far left overbank. The storage area is surrounded by a six-foot high sand and gravel dike. The floodplain within the reach is limited by the soil cement levee on the right bank and an area of higher ground downstream of the levee on the right bank. Along the left bank between Buckeye and Lower Buckeye Roads, the floodplain extends along the edge of some farm fields, a dairy, and the short levee around the

subdivision at Lower Buckeye Road. Downstream of Lower Buckeye Road the floodplain is confined by a higher, dissected Pleistocene surface which extends downstream almost to the Broadway Road alignment.

2.2.3.5 Reach 15 - Broadway Road to the Gila River

Reach 15 is a 1.31 mile long reach that extends from the Broadway Road alignment to the Gila River (Figure 2-126). The reach has a slope of 0.0022 as measured on the USGS 7.5 minute topographic quadrangles. The active low flow channel within Reach 15 is a relatively narrow single channel varying in width from about 150 feet to 400 feet through the reach (Figure 2-124 and Figure 2-125). Channel and bank sediments within the reach are composed primarily of sands.

Figure 2-124 - Photo 62-2

Figure 2-125 - Photo 64-6

At two locations the channel divides around stands of larger vegetation. The left overbank area is about 1,000 feet wide. It is confined to the left by agricultural fields with little increase in relief from the overbank to the fields. Along the right bank is a sand and gravel dike which extends downstream along the entire reach into the Gila River floodway (Figure 2-127). This dike protects a sand and gravel mining operation immediately west of the dike.

Reach 15 lies within the geologic floodplain of the Gila River, which begins in the general vicinity of the Broadway Road alignment. As such, the entire reach is within the long term erosion area of the Gila River. Near the Gila River the left overbank area contains stands of dense riparian trees. Some of these have been planted by the Flood Control District of Maricopa County as part of the environmental mitigation requirements associated with their channelization of the Agua Fria River upstream. Other than the earthen dike along the right bank, there are no significant structures within the reach. An irrigation canal is also present in the far left overbank near Southern Avenue. This canal may confine moderate to high discharges to the west. However, this area is all within the 100-year floodplain of both the Gila and Agua Fria Rivers.

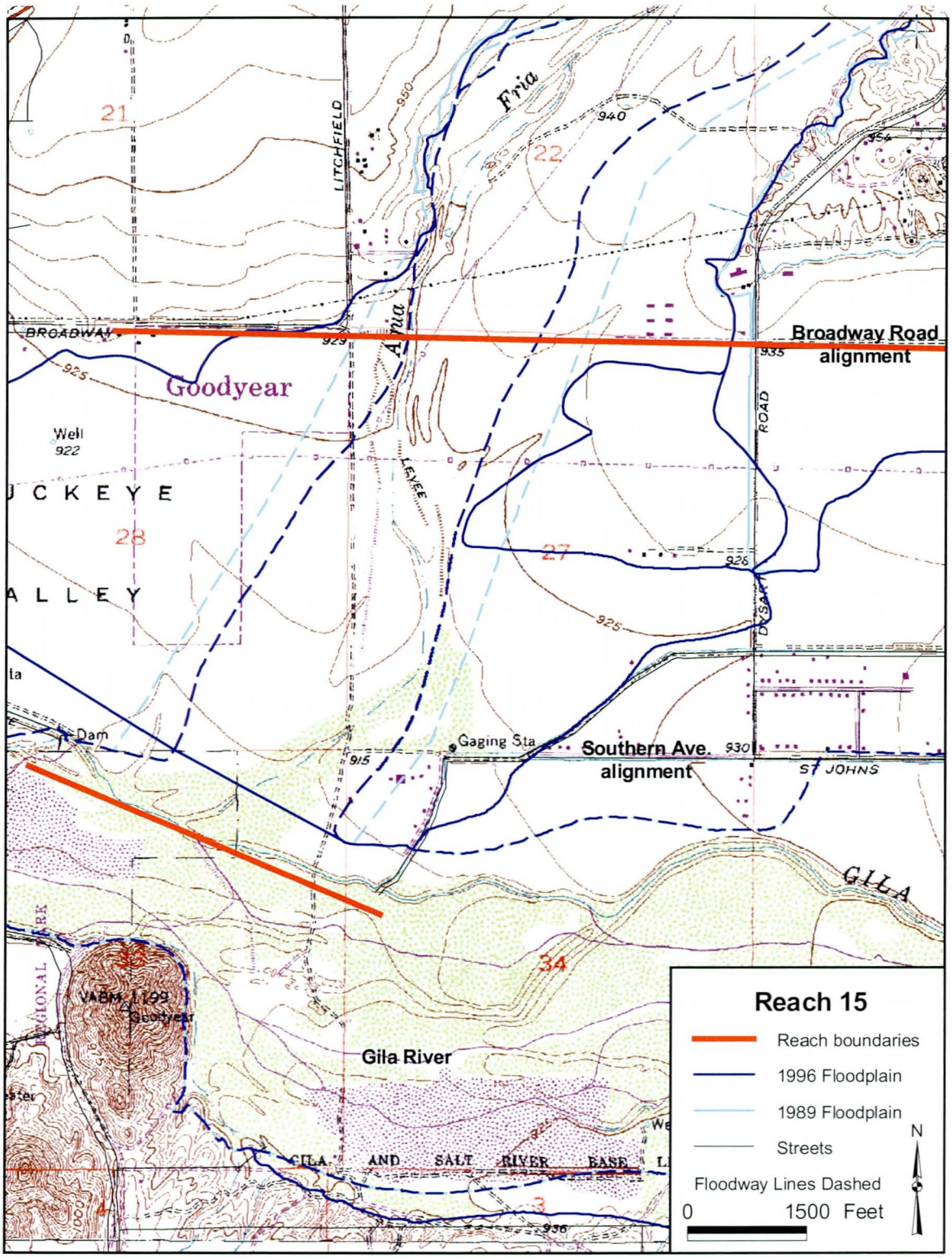

Figure 2-126 - Reach 15, Broadway Road alignment to Gila River

Figure 2-127 - Photo 63-15

2.3 Summary

The Agua Fria River is a wide, braided stream that has been heavily impacted by the activities of humans. Sand and gravel mining, constrictions by bridges, channelization and construction of dams on the Agua Fria and its primary tributaries have significantly impacted its form and behavior. Moreover, these impacts are likely to continue to influence its future as the river continues to respond to these impacts. Large floods in the past have caused significant movement of the stream channel both vertically and horizontally. Future large floods are expected to cause significant horizontal and vertical changes in the river channel and its floodplain. The existing characteristics of the river described in this chapter provide information vital to understanding the nature and geographic location of erosion hazards along the river and its floodplain. An understanding of these characteristics along with its geologic and historical history will greatly facilitate definition of the extent and magnitude of future erosion hazards. This history and its relevance to future erosion hazards will be detailed in the remaining chapters of this report.

3. FIELD DATA

3.1 Field methods

Field Observations. Field visits to the study area were conducted over a period of about 12 weeks during the summer of 2000. Field crews walked the entire study reach, photographing and mapping key features, and recording descriptions of existing channel conditions. The mapping efforts, while extensive, were not comprehensive. That is, not every inch of every braid of the Agua Fria River was mapped. However, an effort was made to examine and map all outer banks of the primary braids and areas of interest identified in aerial photographs and from overlooks in the field. More detailed observations were recorded at typical cross sections defined every mile throughout the study area. Additionally, all road crossings and other significant structures located in or adjacent to the river were visited and documented.

The objectives of the field visits included the following:

- Document stream conditions
- Identify stream reaches with evidence of recent or historical lateral erosion
- Identify reaches with evidence of recent or historical degradation or aggradation
- Identify evidence of lateral erosion within recent geologic time
- Identify stream responses to human impacts or structures
- Identify points of natural grade control

The most relevant data collected during the field visits were synthesized and are shown on the Field Data Maps in the Exhibit Maps Book. Field data collected and shown on the Field Data Maps included the following:

- Locations of cut banks (active erosion)
- Locations of bedrock outcrops in the bed and channel banks
- Location of headcuts and slope breaks
- Location and extent of stream terraces and natural floodplains[1]
- Location of human impacts, structures, and road crossings
- Channel characteristics at representative cross sections

3.2 Types of data collected

The following types of characteristics that have bearing on both horizontal and vertical erosion were observed and recorded in the field.

- Cutbanks – location, heights, characteristics
- Bedrock – location, outcrops
- Caliche – location, degree of development

[1] Natural floodplains, which have physical expression in the landscape, are distinguished from the FEMA (100-year) floodplain, which is a regulatory concept and may not coincide with natural features observed in the field.

- Particle sizes – channel bed, bank materials, floodplains
- Armoring
- Vegetation – channel, banks, floodplain
- Evidence of previous large floods – high water marks, avulsions
- Channel form and location – pattern, avulsions, floodplain characteristics
- Location of sand and gravel mining
- Location of structures – bridges, levees, grade control, bank protection measures
- Location of major tributaries
- Headcuts/slope breaks – long-term scour, local scour
- Field photographs

Examples and photographic documentation of each of these characteristics are presented in the following sections of this chapter. The examples are supplemented with a discussion of the relevance of each characteristic to the assessment of lateral and vertical erosion in the Agua Fria River. The spatial extent and distribution of the recorded characteristics are shown on the Field Data Maps and in Chapter 4, which includes discussion of their spatial distribution and how their distribution affects the lateral erosion hazards in the study area.

3.2.1 Cutbanks

A cutbank is a stream bank that has been eroded (cut) to a steep, vertical or overhanging slope. The location and dimensions of cutbanks observed in the Agua Fria River were recorded in the field. Actively eroding cut banks were observed throughout the river. Cut banks were observed on channels cut into both young and old geomorphic surfaces (Figure 3-1 vs. Figure 3-2), regardless of the calcium carbonate content (caliche) or grain size of the bank material. Bank vegetation appeared to increase the stability of the bank soils, but did not prevent lateral erosion or the formation of cut banks. Undercut trees and brush with exposed roots were observed in several places (Figure 3-4). Piles of alluvium which accumulate at the base of vertical cut banks provide basal control to the bank slopes. The absence of piles of collapsed soil material indicates that the stream is actively eroding and transporting the bank materials (Compare Figure 3-1 and Figure 3-4). The presence of cut banks indicates that active lateral erosion can occur within the stream systems in the study area, regardless of bank vegetation, soil lithology, and soil composition. Cut banks observed in the field are plotted on the Field Data Maps in the Exhibit Maps Book.

Figure 3-1 Cutbank along pleistocene terrace (Photo 31-22)

Figure 3-2 View of cutbank in fine-grained sediments (Photo 12-10)

Figure 3-3 View downstream along coarser-grained cutbank (Photo 15-20)

Figure 3-4 Exposed roots of tree along terrace cutbank (Photo 18-6)

3.2.2 Location of Bedrock Outcrops

Bedrock crops out in the channel bed and banks of in Reaches 1 and 2 of the study area (Figure 3-5 and Figure 3-6). Elsewhere bedrock protrudes into the channel at prominent points such as at Calderwood Butte upstream of Jomax Road. Outside of Reaches 1 and 2, bedrock is unusual within the channel or any of its banks or terrace slopes. In Reaches 1 and 2, lateral and vertical erosion is generally prevented by the presence of bedrock at or near the surface.

The location of bedrock outcrops observed in the field are plotted on the Field Data Maps in the Exhibit Maps Book.

Figure 3-5 Bedrock in channel bottom just upstream of Morgan City Wash (Photo 65-1)

Figure 3-6 View of Tertiary conglomerate along right bank in Reach 2 (Photo 66-7)

3.2.3 Location of Caliche and Degree of Development

Outcrops of calcium carbonate-rich soil layers (a.k.a. "caliche") were observed in cutbanks formed in the Pleistocene-aged terrace margin. Where caliche layers were observed in the channel banks, the caliche appeared to do little to protect the overlying surfaces from lateral erosion of the main channel (Figure 3-7 and Figure 3-8). While the caliche layers themselves are more resistant to erosion than the non-carbonate-cemented soil layers, field data suggests the carbonate layers erode primarily by undercutting the non-cemented or poorly-consolidated underlying soil layers, resulting in cantilever failures of the overlying material. Generally, the degree of caliche development (i.e. its thickness and degree of cementation) increases with time. Therefore, the more well-developed caliche is found in the oldest, most stable terraces.

Figure 3-7 View of very well developed caliche layer in Early Pleistocene terrace cutbank (Photo 43-7)

Figure 3-8 Nearly vertical bank along well-developed caliche in Youngtown; note vehicle and building near terrace edge above (Photo 43-8)

3.2.4 Particle Size of Bed and Bank Materials

The bed of the main channel in the study area is composed primarily of sand and gravel (Figure 3-9 through Figure 3-11), becoming finer in the downstream direction (see also Chapter 6). The floodplains typically consist of finer sand and silty fine sand deposits often overlying coarser material (Figure 3-12). The difference in composition between the floodplain and channel materials indicates that fine-grained sediments are transported through the main channels without being deposited. The decrease in particle size along the stream also indicates that flow velocities are generally greater in the upper reaches compared to the lower reaches, due in part to the increasing width of the Agua Fria River in the downstream direction.

Figure 3-9 View of coarser bed material in upper reach (Photo 66-1)

Figure 3-11 View of finer-grained bed material near Gila River confluence (Photo 63-18)

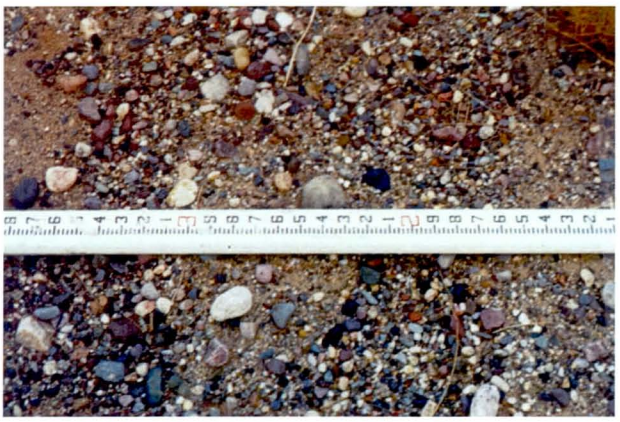

Figure 3-10 View of bed material in middle reach (Photo 44-16)

Figure 3-12 Fine-grained floodplain sediments over coarser sands below (Photo 22-7)

3.2.5 Armoring

Armoring occurs when a layer of sufficiently sized particles covers the channel bottom and prevents bed scour. The armor layer forms by selective transport of smaller particles leaving behind the larger particles because they are too big to be transported. In general, armor layers were not observed in the Agua Fria River study area, except in isolated portions of certain braids. Figure 3-13 shows an example of armoring observed in the study area. More frequent, relatively clear-water discharges from the New River have formed an armor layer of large pebbles.

Figure 3-13 Example of armoring of bed material in Agua Fria River just downstream of the New River confluence (Photo 56-8)

3.2.6 Vegetation

Bank vegetation. In most locations, the banks of the main channel are poorly vegetated. Palo verde, mesquite, ironwood, willow, and desert broom occupy portions of the bank, but well-vegetated banks are not a dominant characteristic of the Agua Fria River in the study area (see Historical Aerial Photo Comparisons and Erosion Hazard Maps in the Exhibit Maps Book). Therefore, the aspects of the bank vegetation that enhance bank stability, such as root material increasing cohesion of soil material, do not play a major role in reducing potential lateral erosion.

Variations by surface. A more noteworthy aspect of vegetation in the study area is the variation of vegetation with surface type and relative topographic position within the geologic floodplain, as discussed in the reach descriptions portion of Chapter 2. Vegetation also appears to vary longitudinally along the river. That is, different species occur in some reaches along the river and not in others. For example, willow trees first appear along the river downstream of Jomax Road. Joint-fir (a.k.a. Mormon-tea) first appear in fine-grained overbank areas in Reach 9.

Figure 3-14 Vegetation variations by surface (Photo 7-7)

3.2.7 Evidence of Previous Large Floods

Flood High Water Marks. Flotsam from a very large flood was observed in overbank channels, across the tops of high bars, and within portions of the floodplain (Figure 3-15). This debris was most likely deposited by the flood of February 1980, since that event was the last large flood to occur on the Agua Fria River. Another type of flood evidence is deposited sediment. Figure 3-17 shows a stand of cholla cacti around which a flood deposited a sheet of sand. The sand was probably deposited by the February 1980 flood. Even twenty years later the effects of this flood are evident throughout the study area.

Avulsions. An avulsion is the formation of a channel in a portion of the floodplain not previously occupied by a channel. Avulsions are responsible for some of the most significant lateral channel movement on the large stream systems in central Arizona. Figure 3-16 shows a view downstream in a bifurcation (flow split). This channel carried significant flow in the February 1980 flood. Large sand dunes formed by the flow are visible in the channel shown in Figure 3-16. Large future floods which are capable of exceeding the elevation of the main channel banks nearby could direct flood water down this overbank channel into areas more than 1,000 feet from the existing main channel, resulting in formation of an avulsive channel.

Figure 3-15 View of historic flotsam in right overbank near Bethany Home Road alignment (Photo 53-17)

Figure 3-17 Stand of cholla surrounded by sands deposited during a large flood (probably Feb. 1980)(Photo 9-16)

Figure 3-16 View downstream in channel avulsion from 1980 flood (Photo 53-16)

3.2.8 Channel Form and Location

Channel Pattern. The dominant channel pattern of the Agua Fria River in the study reach is a slightly sinuous, multiple channel braided stream. In some reaches, a more defined single main channel cuts through the larger system of bars and braids. The primary channels were observed and documented throughout the study area.

Avulsions. Where the floodplain elevation is low relative to the main channel, avulsive channel change can occur. With time, new avulsive channels formed on the floodplain can capture the main channel and cause an avulsive shift of the main channel from one side of the floodplain to the other. Remnants of past avulsions or incipient avulsive channels were observed in several places on the Agua Fria River. An example of an avulsion which occurred in the left overbank as a result of the February 1980 flood is shown in Figure 3-18 and Figure 3-19 for the area between Jomax and Hatfield Roads. Avulsive channel changes have likely been a significant mechanism of channel adjustment between the Pleistocene terraces over the geologic history of the river. Channel avulsions are likely continue to occur in the future.

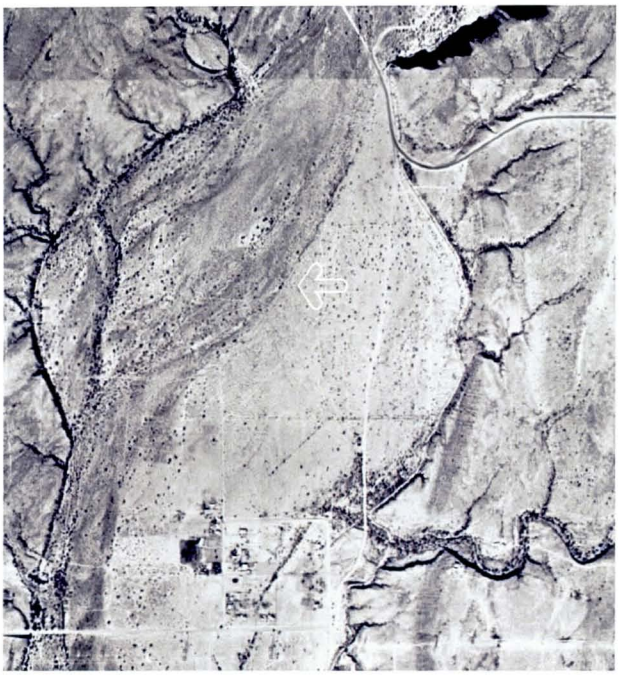

Figure 3-18 Pre-avulsion photo, 1977

Figure 3-19 Example of avulsion, 1980.

Floodplain Characteristics. The floodplain of the Agua Fria River generally increases in width in the downstream direction from New Waddell Dam. Exceptions are the engineered and disturbed reaches, and a few spots such as near Jomax Road where bedrock confines the floodplain. Differentiation of the floodplain from the braided channel is somewhat subjective for some parts of the Agua Fria River because of the presence of low floodplain islands between braids. While distinctive channels do exists, areas above and beyond these primary channels are characterized by large gravel or sand bars, or broad areas of fine-grained sediments dissected locally by smaller overbank channels. In Reach 6 there are even locations of floodplain islands in the middle of the larger corridor between the Pleistocene terraces.

Figure 3-20 View on floodplain island in Reach 6 (Photo 22-8)

Figure 3-21 View downstream in left overbank channel near Olive Ave. (Photo 45-12)

3.2.9 Location of Sand and Gravel Mining

Locations of sand and gravel mining operations were identified in the field and are plotted on the field data maps provided in the Exhibits Map Book. Exposures in gravel pits provide additional information about the subsurface and practical vertical limits of erosion during recent geologic time. Figure 3-22 shows a good example of an exposure in a pit near Camelback Road. Note how the color and angle of the wall change about eight feet below the surface. The lower materials are redder and stiffer than the lighter colored, loose sediments above. This color and compositional change probably reflect the vertical limit of scour by the Agua Fria River over the past several thousand years. Note also the alternating lenses of sands and gravels in the lower portion of the exposure. These strata indicate that the Agua Fria River has been a braided river for a very long time.

Figure 3-22 View of exposure in gravel pit near Camelback Road (Photo 56-2)

The gravel pits observed in the Agua Fria River study area are very large features, and occur throughout the study reach. The scale of these operations is difficult to portray even in a single photograph (Figure 3-23). These operations play an important role in the future economics, politics, and geomorphology of the Agua Fria River. They also greatly impact the horizontal and vertical distribution of flood and erosion hazards on the river.

Figure 3-23 Gravel pit downstream of Hatfield Road (Photo 19-18 to 21)

3.2.10 Location of Structures

In general, the potential for lateral erosion increases near structures due to flow acceleration through constrictions or over concrete surfaces, disruption of sediment continuity, and/or removal of bank vegetation and placement of fill material. The location, dimensions, and impacts from structures observed in the field were documented in structure impacts forms developed specifically for the Agua Fria River field work. An example of one of these forms is shown in Section 3.4. Some examples of the types of constructed features in the study reach are shown below.

- Bridges
- Culverts
- At-grade roadways
- Grade control
- Levees

Figure 3-24 Van Buren Street bridge (Photo 52-2)

Figure 3-25 Culvert on gravel mine access road near Greenway Road alignment (Photo 36-19)

Figure 3-26 Powerline tower in river (Photo 38-20)

Figure 3-27 Example of soil cement grade control structure in levee reach (Photo 56-19)

Figure 3-28 Northern Ave. at-grade crossing (Photo 31-25)

Figure 3-29 View along south along right soil cement levee (Photo 57-9)

Figure 3-30 Large, angular bank protection downstream of Olive Ave. (Photo 47-6)

Figure 3-31 Riprap under Buckeye Road bridge (Photo 54-11)

- Trash and Modern Human Artifacts

Figure 3-32 Buried Honda downstream of Bell Road (Photo 32-10)

Figure 3-33 Shot up trash and shell casings upstream of Jomax Road (Photo 13-18)

- Human activities – gravel mining, ATV use, access roads, target shooting

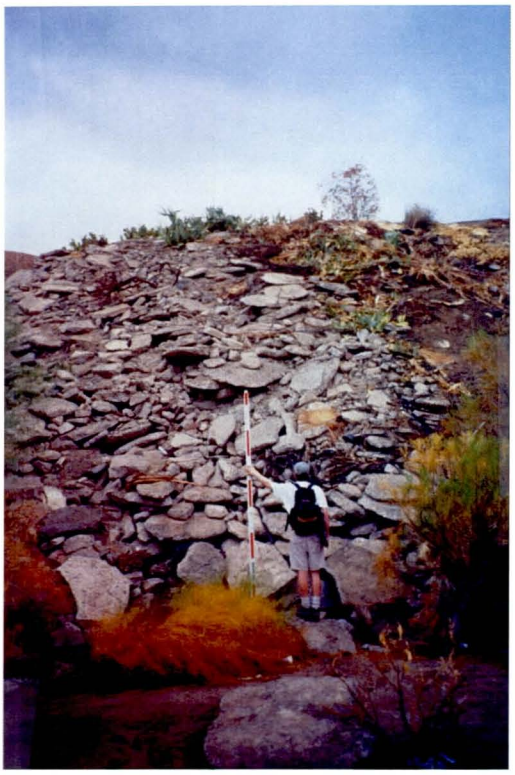

Figure 3-34 Debris dumped over bank (Photo 39-9)

Figure 3-35 Road in river downstream of Northern Ave. (Photo 48-20)

Figure 3-36 "Riprap" along Cholla landfill downstream of Grand Ave. (Photo 38-24)

- Dams – diversions, canals, flumes, siphons

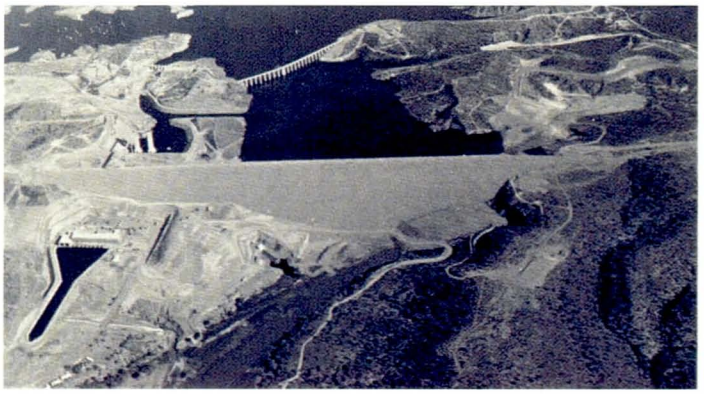

Figure 3-37 New Waddell and Old Waddell Dams

3.2.11 Location of major tributaries

Major tributaries entering the Agua Fria River were located and observed, and are described in Chapter 2. Items of interest to the erosion hazard assessment were the elevation of the tributary channel invert relative to the Agua Fria channel elevation. "Hanging" tributaries, that is, tributaries with channel inverts above the main channel, indicate rapid or recent incision on the main channel. Conversely, significant deposition or delta formation near the confluence may suggest that the tributary is delivering sediment to the main channel more frequently or in greater quantities than the main channel can carry away or redistribute. In the case of wide, shallow channels like the Agua Fria River, the main channel may be pushed away from the tributary confluence if the tributary has been delivering large quantities of sediment to the river. One might expect this scenario of excess tributary sediment supply to be the case for the Agua Fria River for two reasons. First, the channel of the Agua Fria River is generally shallow and wide, and will tend to absorb or decrease the transport capacity of tributary floods, leaving a deltaic sediment deposit. Second, decreases in the frequency and magnitude of large floods caused by the Waddell and New Waddell Dams have reduced the ability of the Agua Fria River to transport tributary sediments away from their confluences. Prior to construction of the Waddell dams, large floods on the Agua Fria River would transport sediment accumulated at the tributary mouths during years of no flooding on the Agua Fria River. Many of the larger tributaries upstream of the New River confluence appear to be depositing deltas near their confluences. Also, the tributaries' main channels are beginning to extend themselves into the Agua Fria River more as an extension of the tributary rather than an integration with the Agua Fria channel. For example, at the Unnamed Wash 1 & 2 confluence and the Twin Buttes Wash confluence the main channels of the tributaries parallel the main channel of the Agua Fria River for some distance before the two become indistinguishable (Figure 3-38 and Figure 3-39). In another case, at the confluence of the McMicken Outlet Wash, recent tributary flow was observed to have flowed "upstream" in the main Agua Fria River channel (Figure 3-40).

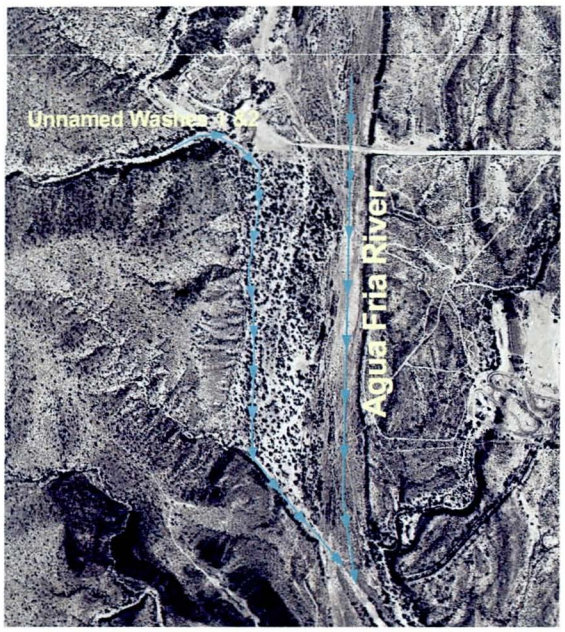

Figure 3-38 Confluence of Unnamed Washes 1 & 2 with the Agua Fria River, 2000

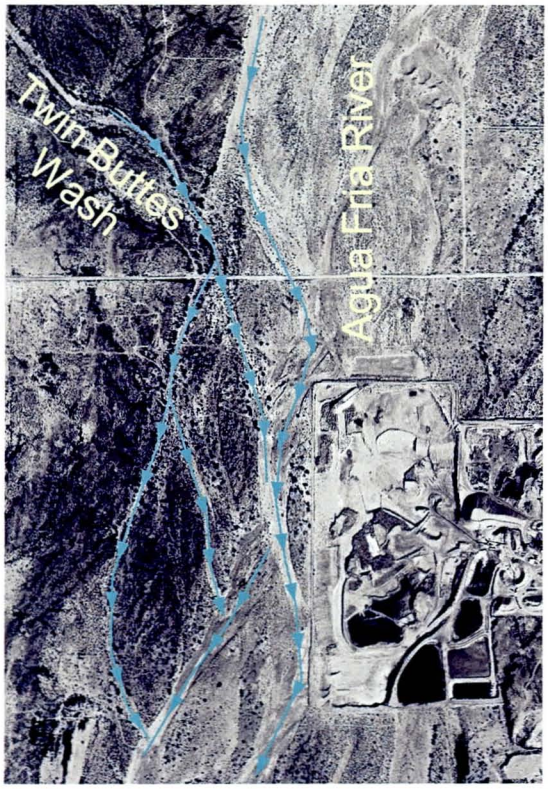

Figure 3-39 Confluence of Twin Buttes Wash with the Agua Fria River, 2000

Figure 3-40 View upstream in Agua Fria River just upstream of McMicken Outlet Wash confluence. Note flotsam in right center of photo and fine-grained sediments deposited along toe of left bank.

3.2.12 Headcuts, Slope breaks, and Evidence of scour

Long-term scour. Evidence of significant historical long-term degradation was observed in the field in numerous places along the Agua Fria River. At Grand Avenue, a low clearance warning on the AT & SF railroad bridge reads "Clearance 12 FT" where the height to the low cord of the bridge is now 21 feet (Figure 3-41). Headcuts or broader reaches of locally increased slope were observed upstream of almost every gravel pit (Figure 3-42).

Figure 3-41 AT&SF Railroad bridge (Photo 23-17)

Figure 3-42 Looking downstream into 3 foot deep headcut near Greenway Road alignment (Photo 33-16)

Local scour. Scour holes several feet deep were observed locally in the study area as well as downstream of grade control structures (Figure 3-43) and along fixed bank protection (Figure 3-44). Power poles at several locations in the Lower Reach (Figure 3-45 and Figure 3-46) showed evidence of scour as well. Examination of historic aerial photographs indicated that the erosion near the power poles probably resulted from lateral movement of the channel bank.

Figure 3-43 Scour downstream of grade control structure (Photo 41-18)

Figure 3-44 (Photo 1-7)

Figure 3-45 (Photo 63-3))

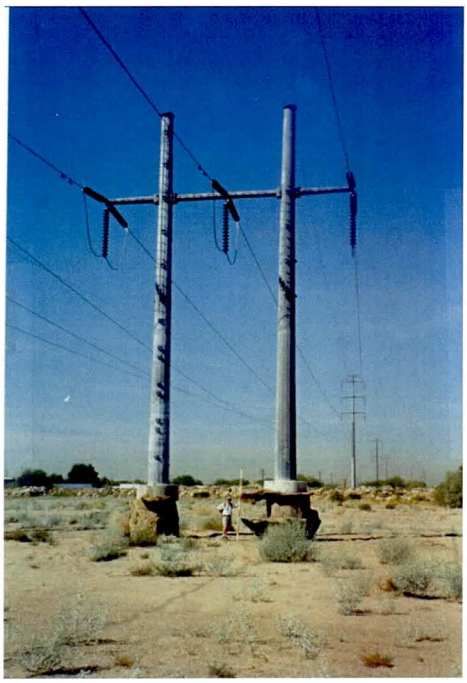

Figure 3-46 Photo 61-21

3.2.13 Photographs

Over 1,500 photographs were taken as support documentation of the field conditions in the Agua Fria River in the summer of 2000. Many of these are provided throughout various portions of this report. The photo numbers referred to in each photo caption is the identifier used by JEF to cross-reference their exact locations. All of these photographs are available through an html interface provided on a CD-ROM in the back of this report.

3.3 Summary

The examples shown above demonstrate the types of characteristics observed and recorded in the field and their relevance to the assessment of lateral and vertical erosion in the Agua Fria River. The spatial extent and distribution of the recorded characteristics are shown on the Field Data Maps and in Chapter 4. Chapter 4 also includes a discussion of the spatial distribution of these characteristics and how their distribution affects the distribution of lateral erosion hazards in the study area.

3.4 Field forms

Examples of the forms used to collect information in the field are provided below. The first form is for recording channel characteristics at each channel cross section for which data was collected. Representative cross sections were described at about one mile increments throughout the study reach using this form. The second form is a structure impacts evaluation form. All bridges, at-grade crossings, and grade control structures were inventoried, collecting the information shown in the fields of this form. The last form is a photography log form. Throughout the 34 mile study reach over 1500 photographs were taken. This large number includes all the photos taken at the inventoried cross sections, the structures, as well as hundreds of photographs of other features observed in the study area that have a bearing on the stream characteristics which affect the erosion hazards of the Agua Fria River.

FIELD CHECK LIST – CHANNEL CHARACTERISTICS

STREAM NAME:	DATE:	FIELD CREW:
DESCRIPTION OF SECTION LOCATION:		☐ GPS LOCATION

1. PHOTO-DOCUMENTATION (RECORD PHOTO # & TIME)

NOTES: 1. INCLUDE SCALE IN PHOTOGRAPHS 2. PLOT PHOTO LOCATION & ASPECT ON AERIAL

PHOTO #	DESCRIPTION	PHOTO #	DESCRIPTION

2. INFORMATION TO PLOT ON AERIALS

☐ POOL/RIFFLE BOUNDARY	☐ MISC. CHANNEL CHARACTERISTICS
☐ CUTBANKS	☐ HEADCUTS/ SLOPE BREAKS
☐ BEDROCK OUTCROP	☐ CALICHE/ CARBONATE OUTCROP
☐ HUMAN IMPACTS	☐ STRUCTURES
☐ ACTIVE FLOODPLAIN LIMIT	☐ TERRACE BOUNDARIES
☐ TRIBUTARIES	☐ OVERBANK CHANNELS

3. CHANNEL STABILITY INFORMATION

PRIMARY Banks	LEFT	RIGHT
☐ BANK HEIGHT		
☐ BANK MATERIAL		
☐ BANK VEGETATION		
☐ BANKS ERODIBLE?		
☐ RECENT EROSION ?		
☐ FAILURE MECHANISM		
☐ SCOUR OR DEPOSITION?		
ADDITIONAL BANKS (NOTE RELATIVE LOCATION)		
☐ BANK HEIGHT		
☐ BANK MATERIAL		
☐ BANK VEGETATION		
☐ BANKS ERODIBLE?		
☐ RECENT EROSION ?		
☐ FAILURE MECHANISM		
☐ SCOUR OR DEPOSITION?		
ADDITIONAL BANKS (NOTE RELATIVE LOCATION)		
☐ BANK HEIGHT		
☐ BANK MATERIAL		
☐ BANK VEGETATION		
☐ BANKS ERODIBLE?		
☐ RECENT EROSION ?		
☐ FAILURE MECHANISM		
☐ SCOUR OR DEPOSITION?		
☐ BED MATERIAL	D10_____ D50_____ D90_____ (BY EYE)	
	UPSTREAM LAMINATION _____ ARMORING? _____ VEGETATION _____	

#: _____ DATE: _____ INITIALS: _____

☐ SKETCH CHANNEL CROSS SECTION (SEE FIELD MAP AERIALS FOR PLANIMETRIC FORM)

FIELD CHECK LIST – STRUCTURE IMPACT REPORT

STREAM NAME:	DATE:	FIELD CREW:	STRUCTURE TYPE:
DESCRIPTION OF STRUCTURE LOCATION:			☐ GPS LOCATION

1. PHOTO-DOCUMENTATION (RECORD PHOTO # & TIME)

NOTES: 1. INCLUDE SCALE IN PHOTOGRAPHS 2. PLOT PHOTO LOCATION & ASPECT ON AERIAL

PHOTO #	DESCRIPTION	PHOTO #	DESCRIPTION

2. INFORMATION TO PLOT ON AERIALS

☐ STRUCTURE FEATURES & EXTENT	☐ STRUCTURE IMPACTS
☐ AREAS OF ACTIVE EROSION	☐ LIMITS OF ACTIVE DEPOSITION
☐ AREAS OF EXPECTED EROSION	☐ LIMITS OF EXPECTED DEPOSITION

3. STRUCTURE STABILITY INFORMATION

☐ UPSTREAM IMPACTS	
☐ DOWNSTREAM IMPACTS	
☐ DIFFERENCES FROM ADJACENT REACHES	
☐ ROADWAY APPROACH CONDITION	
☐ VEGETATIVE CHARACTERISTICS	

7. DESCRIPTION OF UNIQUE CHANNEL & REACH CHARACTERISTICS

☐ STRUCTURE PLAN VIEW

STRUCTURE CROSS SECTION

PHOTO RECORD FIELD FORM

STREAM NAME:	DATE:	FIELD CREW:

UPSTREAM CROSS SECTION/STRUCTURE:

DOWNSTREAM CROSS SECTION/STRUCTURE:

1. PHOTO-DOCUMENTATION (RECORD PHOTO # & TIME)

NOTES: 1. INCLUDE SCALE IN PHOTOGRAPHS 2. PLOT PHOTO LOCATION & ASPECT ON AERIAL

PHOTO #	DESCRIPTION	PHOTO #	DESCRIPTION
	☐ GPS		☐ GPS
	☐ GSP		☐ GPS
	☐ GPS		☐ GPS
	☐ GPS		☐ GPS
	☐ GPS		☐ GPS
	☐ GPS		☐ GPS
	☐ GPS		☐ GPS
	☐ GPS		☐ GPS
	☐ GPS		☐ GPS
	☐ GPS		☐ GPS
	☐ GPS		☐ GPS
	☐ GPS		☐ GPS

2. OTHER NOTES & OBSERVATIONS

4. GEOGRAPHIC/SPATIAL DATA

In Chapter 4, the geographic or spatial distribution of data relevant to vertical and horizontal erosion hazards in the Agua Fria River is presented. The distribution of field characteristics between various reaches will be discussed. Also, data that are geographic in nature (e.g. surficial geology, soils, topography) will be described and their influence on the distribution of erosion hazards will be discussed.

4.1 Distribution of Field Characteristics

Four of the important characteristics observed in the field which have a significant influence on the distribution of erosion hazards include bedrock outcrops (Figure 4-1), caliche outcrops (Figure 4-2), active cut banks (Figure 4-3), and gravel pits (Figure 4-4).

- Bedrock Outcrops. The locations of bedrock outcrops observed during field work are plotted on Figure 4-1. Bedrock crops out in the channel banks or at the margins of the floodplain in Reaches 1, 2, and to a lesser degree in Reaches 4 and 5. Bedrock is an effective barrier to riverine erosion and scour. In Reach 3 and Reaches 6 to 15 no bedrock outcrops were observed during the field work, nor was any shallow bedrock mapped on any of the geologic maps used in this study. Therefore, it may be assumed that downstream of Reach 5, lateral erosion will not be limited by bedrock.
- Caliche Outcrops. Caliche, or calcium carbonate, crops out in soil profiles exposed in the main channel banks or floodplain margins upstream of Reach 10. The locations of caliche outcrops observed during the field work are plotted in Figure 4-2. The caliche outcrops were typically observed in the soils that comprise the highest, most stable terraces. While field evidence indicates that soils with caliche development are susceptible to erosion, historical evidence suggests that the rate of erosion of caliche-cemented soils is significantly less than the rate of erosion for soils with no caliche development. The younger floodplain surfaces typically had no significant caliche accumulation, and consequently are more vulnerable to lateral erosion.
- Cut Banks. Cut banks are steep, vertical, or overhanging channel banks that have been recently eroded, and are evidence of active lateral channel movement. The locations of cut banks observed during the field work are shown in Figure 4-3. Cut banks of various heights, lengths and extent were observed throughout the entire study reach, from New Waddell Dam to the Gila River. Cut banks were observed in poorly consolidated channel deposits, highly indurated soils with thick caliche layers, and in intermediate surfaces with highly variable soils. Field photographs of typical cut banks were provided in Chapter 3 of this report.
- Gravel Pits. In-stream sand and gravel mining has occurred within the Agua Fria River floodplain corridor since the 1950's. The locations of more than 20 active and historical gravel pits are plotted in Figure 4-4. To date, these pits have been unevenly distributed in Reaches 2 and 5 to 12 and 15, although proposals for additional pits in Reaches 2, 4, 14, and 15 have been reported by the Flood Control District of Maricopa County. In-stream pits lower the bed elevation by direct excavation or indirectly through headcutting or depletion of the sediment supply. The pits also widen the channel when they are breached during floods, but may also narrow the active channel if diversion dikes are constructed to control flooding around the excavation.

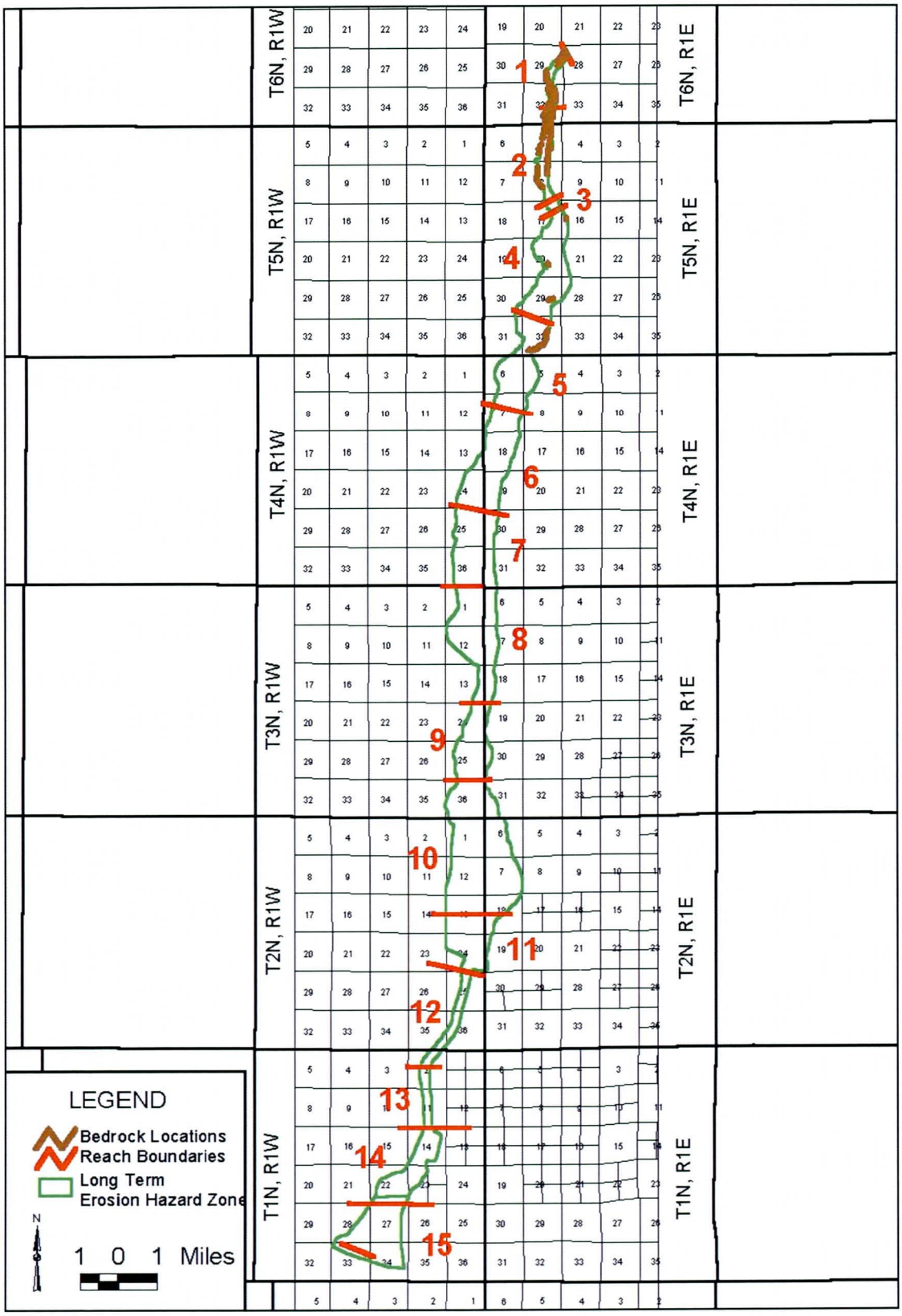

Figure 4-1 Location of bedrock outcrops in study area

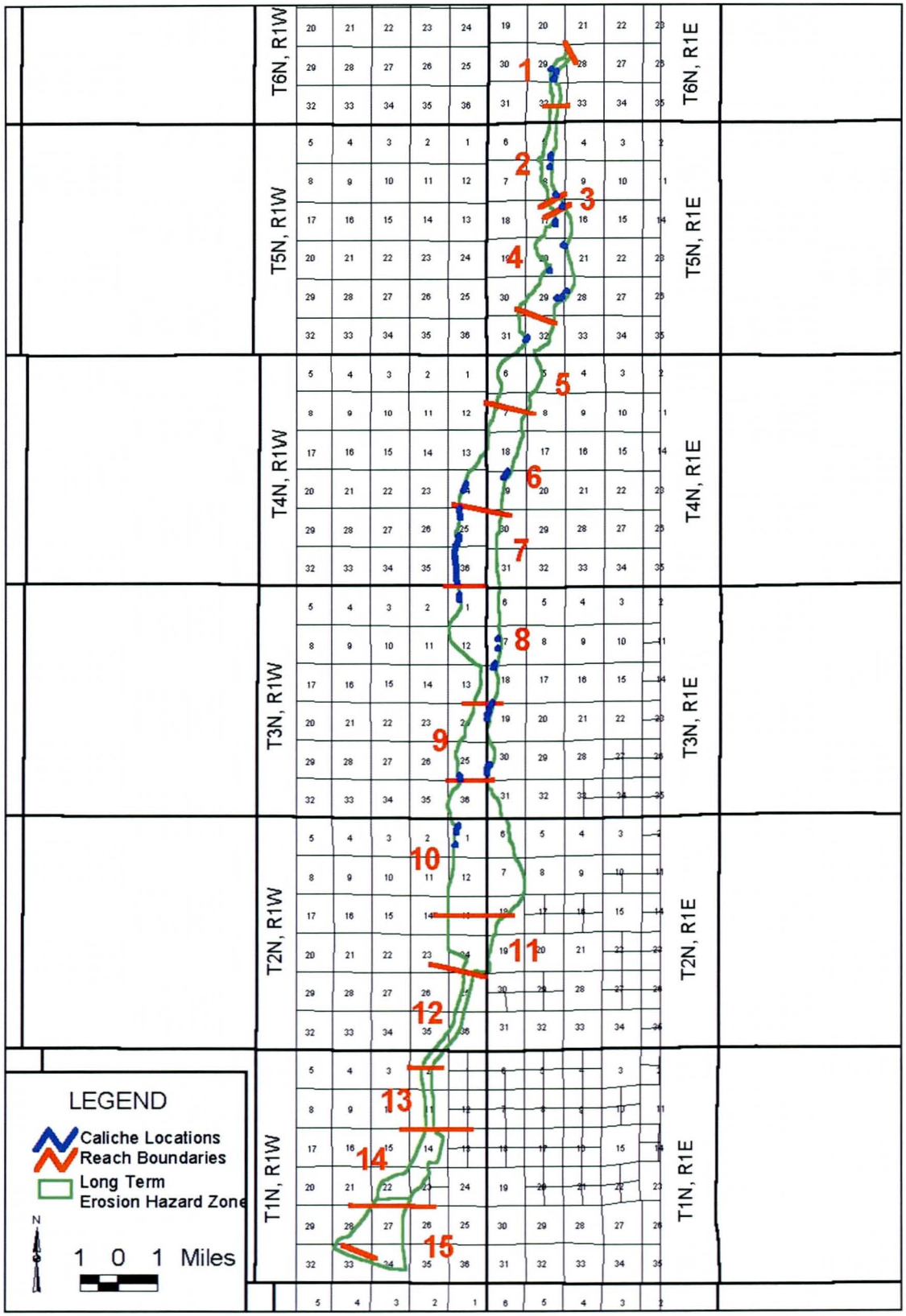

Figure 4-2 Location of caliche in study area

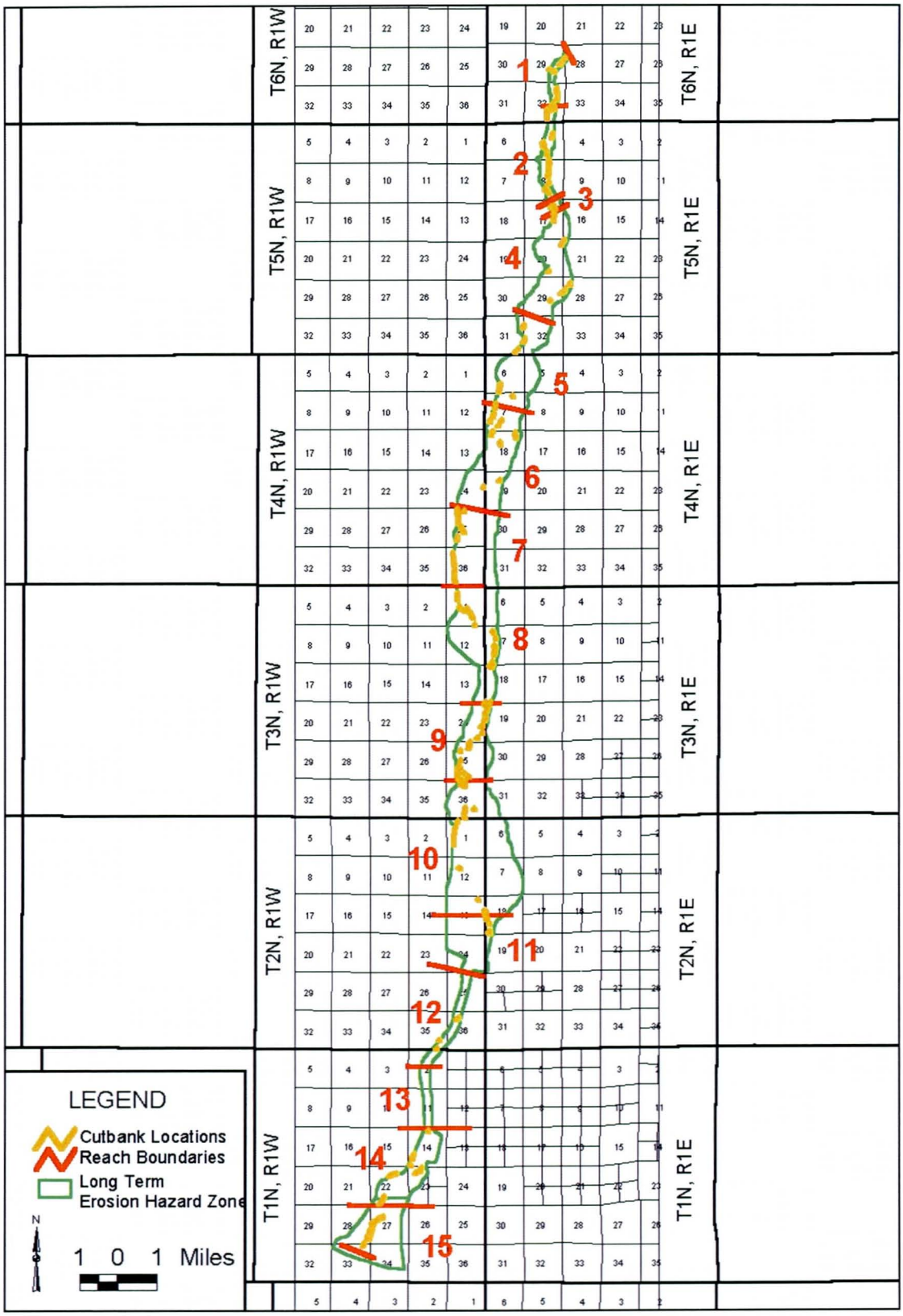

Figure 4-3 Location of cutbanks observed in study area

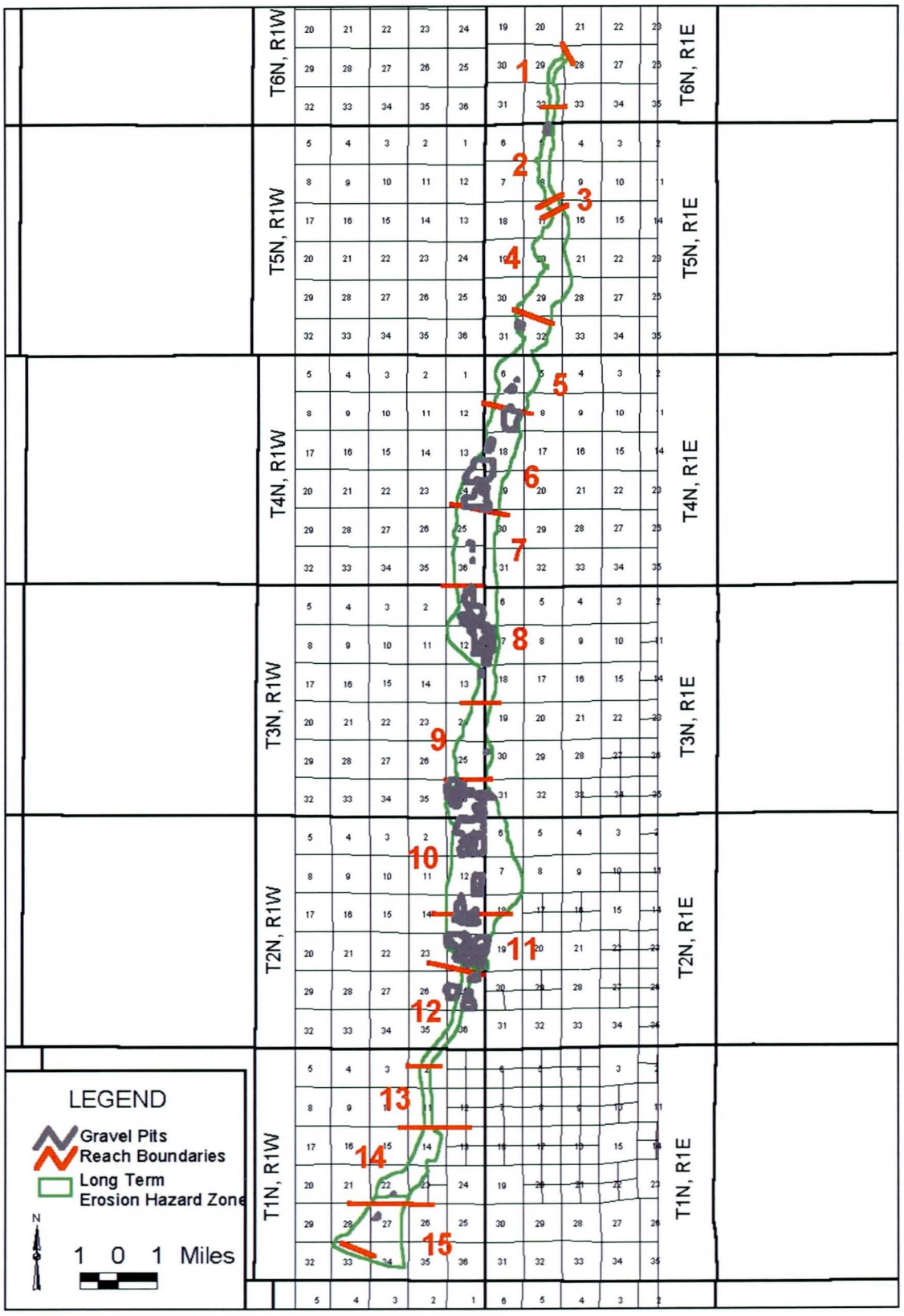

Figure 4-4 Location of gravel pits observed in study area

4.2 Longitudinal Profile

The longitudinal profile is a plot or picture of the variation in the elevation of the channel along the stream. Figure 4-5 shows the longitudinal profile of the Agua Fria River over the study reach from the Lower Lake dam to the Gila River confluence. The data reflect the minimum elevation in the channel as defined in the HECRAS model modified by JEF for the purposes of the erosion hazard assessment for the Watercourse Master Plan.

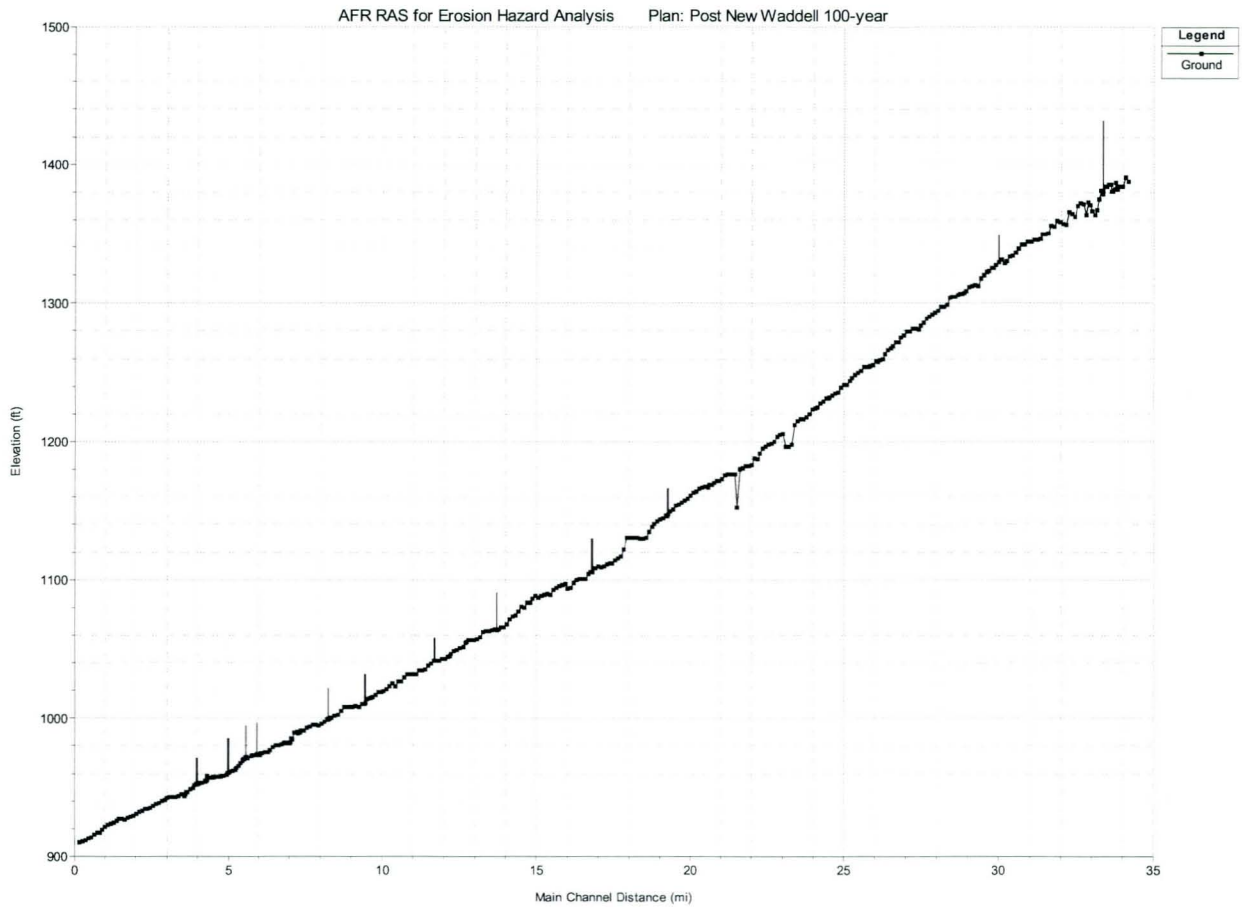

Figure 4-5 Longitudinal Profile of the Agua Fria River from HECRAS model modified by JEF

Graded streams, that is, streams that have adjusted themselves to the prevailing conditions of sediment and water discharges over a long period of time, tend to exhibit smooth concave up longitudinal profiles. The Agua Fria River profile in the study reach is slightly concave up. This shape is more noticeable if one turns the page and looks 'up' the profile from the downstream end. This concave pattern for the Agua Fria suggests that perhaps the Agua Fria River has been a reasonably graded braided river over a long period of time. Although often associated with 'over-loaded' aggrading streams, a braided channel pattern can be considered an equilibrium condition for many streams in central Arizona. This is likely the case for the pre-historic Agua Fria River as indicated by its longitudinal profile.

Figure 4-5 also shows the following other noteworthy characteristics with respect to the longitudinal profile of the river:

- The long vertical black bars protruding above the ground points are locations of bridges along the river.

- In the upper three miles or so of the channel, the profile exhibits a flatter slope and an irregular or jagged profile. This pattern is most likely the result of scour caused by clear-water discharges from the dam upstream. In an attempt to pick up sediment, the clear-water outflows degrade the bed and decrease the channel slope for some distance downstream until the flood water is able to entrain sufficient sediment to satisfy its sediment transport capacity. The reach with the slightly flattened profile downstream of New Waddell Dam has large areas of bedrock outcrops within the channel (see also Chapter 2 and 3 for photographic examples) that probably have prevented some of the scour that would otherwise have occurred. Numerous large scour holes were also observed in this area in the field (Figure 4-6).

Figure 4-6 Large scour hole along bedrock island in Reach 1 (Photo 65-10)

- Obvious gravel pits in the main channel are also shown near mile 23 and 21.5 as abrupt drops, or "holes," in the profile. These drops are the result of direct excavation of the channel, and are not necessarily headcuts or degradation upstream of the pits.
- Another area around mile 17 shows a very flat, then very steep reach caused by intensive and prolonged gravel mining in the stream bed. Some of the degradation in this area is located outside of the area of direct channel excavation.
- The channelized reach from about mile 8 to 4 shows a somewhat stair-stepped look which reflects the flatter channel slope between the grade control structures located in this reach.

The profile may also be subdivided into sections of similar slopes. Table 4-1 divides the profile based on subreaches with similar slope. One can visualize these by placing a straight-edge on Figure 4-5 between the indicated mile marks shown in the table. Breaking up the profile into these shorter subreaches emphasizes the slightly convex 'bumps' between mile 21 and mile 14. Also, the profile suggests that slope adjustments downstream may have future adverse impacts on the bridge near mile 19 (Bell Road).

Table 4-1 Subreach slopes from examination of longitudinal profile

Reach (mile to mile)	Slope	Comments
0 to 14	0.0023	Flatter than rest of area; stair-stepped in channelized reach
14-22	0.0028	Irregular; locally convex; gravel mining influences
22-32	0.0033	Fairly uniform; gravel pit downstream
32-end	0.0027	Degraded due to dam outflows; jagged = scour holes

4.3 Sinuosity

Table 4-2 shows the sinuosity of the Agua Fria River by reach and overall in the study area. Sinuosity is a measure of the ratio of the channel's length compared to the length of the valley it flows through. Typically sinuosity is used to describe the degree of meandering of a river or to distinguish straight or braided rivers from meandering streams. The wiggly pattern of meandering streams tends to migrate down valley (Figure 4-7). Therefore, the general meandering pattern remains similar over time, while the precise location of the channel moves over time. Meander migration can be a significant cause of bank erosion. The Agua Fria River (in 1999) is a straight to slightly sinuous stream that is braided in its wider reaches. Therefore, meander migration is not likely to be a significant cause of erosion in the study area.

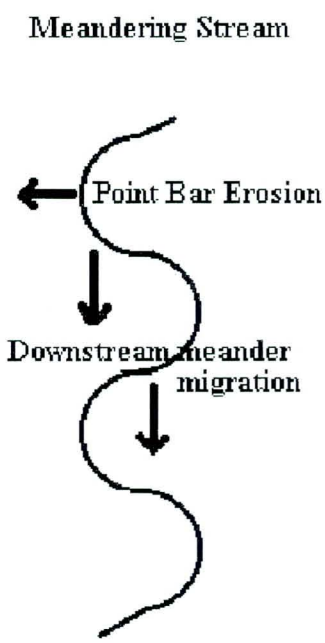

Figure 4-7 Schematic of meander migration

Table 4-2 Sinuosity of the Agua Fria River from New Waddell Dam to the Gila River, 1999

Reach	Sinuosity
1	1.02
2	1.02
3	1.03
4	1.10
5	1.09
6	1.13
7	1.14
8	1.12
9	1.12
10	1.08
11	1.04
12	1.08
13	1.02
14	1.21
15	0.99
Overall	1.09

Sinuosity reported for Reach 15 is less than 1.0 (i.e. valley length longer than channel length) due to straightening of the channel by humans following the 1980 flooding. Comparisons of changes in measured sinuosity over time will be presented in Chapter 5.

4.4 Geology – "Geomorphic Mapping"

The AZGS Surficial Geology Map shown in the Exhibit Maps Book shows the spatial distribution of Quaternary surfaces located within the Agua Fria River corridor. A descriptive summary of the geology of the study area and the geologic history relative to stream stability was provided in Chapter 2. The geomorphic surfaces mapped along the river corridor generally parallel the floodplain, primarily because these surfaces represent former floodplains during previous geologic epochs. The surfaces form a descending series of inset, converging terraces that record the net degradational history of the Agua Fria River, and a gradual narrowing of the floodplain with reduced flow rates through time. The descending terraces may serve as an appropriate analog for possible future river response to the reduced water supply caused by construction of upstream reservoirs.

4.5 Soils

The NRCS Soils Map in the Exhibit Maps Book shows the spatial distribution of soils classified by predominant landform type as described in the (formerly) Soil Conservation Service (SCS now NRCS) soil survey reports for the study area (Hartman, 1977; Camp, 1986). The primary division noteworthy on the map is the differentiation between "Terrace" and "Floodplain" soils. The "Terrace" category includes those soil units described as 'stream terraces' or 'fan terraces' in the map unit descriptions. The "Floodplain" category includes soils described as being found on 'floodplains' and 'drainageways'. Table 4-3 lists the NRCS map units that were assigned to each landform class depicted on the NRCS Soils Map in the Exhibit Maps Book.

Table 4-3 Soil Unit Landform Classification

Soil Survey Predominant Landform	Landform Classification for AFWMP	NRCS Map Unit	NRCS Map Unit Name
Alluvial Fans	Alluvial Fan	55	Gilman loams
		AbB	Antho sandy loam, 1 to 3 percent slopes
		AdB	Antho gravelly sandy loam, 1 to 3 percent slopes
		AGB	Antho-Carrizo complex, 0 to 3 percent slopes
		AGB	Antho-Carrizo complex, 0 to 3 percent slopes
		CV	Coolidge-Laveen association
		Gf	Gilman fine sandy loam, saline-alkali
		GgB	Gilman loam, 1 to 3 percent slopes
Floodplains	Floodplain	10	Brios-Carrizo complex, 1 to 5 percent slopes
		3	Antho-Carrizo-Maripo complex
		Aa	Agualt loam
		Br	Brios loamy sand
		Cb	Carrizo gravelly sandy loam
		CF	Carrizo and Brios soils
		Cn	Cashion clay, saline-alkali
		Gb	Gadsden clay loam
		Gc	Gadsden clay
		Gd	Gadsden clay, saline-alkali
		Ge	Gilman fine sandy loam
		GgA	Gilman loan, 0 to 1 percent slopes
		Gh	Gilman loam, saline-alkali
		Gu	Glenbar clay loam, saline-alkali
		Ma	Maripo sandy loam

Soil Survey Predominant Landform	Landform Classification for AFWMP	NRCS Map Unit	NRCS Map Unit Name
		TD	Torripsamments and Torrifluvents, frequently flooded
		Vg	Vint loamy fine sand
		Vh	Vint fine sandy loam
		Vk	Vint loam
Gravel Pit	Gravel Pit	GPI	Gravel pit
Mountain Slopes	Mountain Slopes	18	Cheriono-Rock outcrop complex, 5 to 60 percent slopes
		51	Gachado-Lomitas complex, 8 to 25 percent slopes
		52	Gachado-Lomitas-Rock outcrop complex, 7 to 55 percent slopes
		CO	Cheriono-Rock outcrop complex
		RS	Rock outcrop-Cherioni complex
Pediments	Pediment	63	Gran-Wickenburg-Rock outcrop complex, 1 to 7 percent slopes
Fan Terraces	Terrace	110	Suncity-Cipriano complex, 1 to 7 percent slopes
		112	Tremant gravelly sandy loams
		113	Tremant gravelly loams
		118	Tremant-Rillito complex
		12	Carefree cobbly clay loam, 1 to 8 percent slopes
		13	Carefree-Beardsley complex
		22	Contine clay loam
		45	Ebon very gravelly loam, 8 to 20 percent slopes
		47	Ebon-Gunsight-Cipriano association, 3 to 25 percent slopes
		48	Ebon-Pinamt complex, 3 to 20 percent slopes
		49	Ebon-Pinamt complex, 20 to 40 percent slopes
		68	Gunsight-Cipriano complex, 1 to 7 percent slopes
		70	Gunsight-Rillito complex, 1 to 25 percent slopes
		77	Mohall clay loam
		98	Pinamt-Tremant complex, 1 to 10 percent slopes
		EPD	Ebon-Pinamt complex, 0 to 10 percent slopes
		GWD	Gunsight-Pinal complex, 1 to 10 percent slopes
		GxA	Gunsight-Rillito complex, 0 to 1 percent slopes
		GxB	Gunsight-Rillito complex, 1 to 3 percent slopes
		GYD	Gunsight-Rillito complex, 0 to 10 percent slopes
		La	La Palma very fine sandy loam
		Lb	Laveen sandy loam
		LcA	Laveen loam, 0 to 1 percent slopes
		LcB	Laveen loam, 1 to 3 percent slopes
		Ld	Laveen loam, saline-alkali
		Mp	Mohall loam
		Mr	Mohall clay loam
		Pa	Perryville sandy loam
		PeA	Perryville gravelly loam, 0 to 1 percent slopes
		PeB	Perryville gravelly loam, 1 to 3 percent slopes
		PRB	Perryville-Rillito complex, 0 to 3 percent slopes

Soil Survey Predominant Landform	Landform Classification for AFWMP	NRCS Map Unit	NRCS Map Unit Name
		PsB	Pinal loam, 1 to 3 percent slopes
		PT	Pinal gravelly loam
		PYD	Pinamt-Tremant complex, 1 to 10 percent slopes
		RaA	Rillito sandy loam, 0 to 1 percent slopes
		RaB	Rillito sandy loam, 1 to 3 percent slopes
		RbA	Rillito loam, 0 to 1 percent slopes
		RbB	Rillito loam, 1 to 3 percent slopes
		Te	Tremant loam
		TfA	Tremant gravelly loam, 0 to 1 percent slopes
		TfB	Tremant gravelly loam 1 to 3 percent slopes
		Tg	Tremant clay loam
		Th	Tremant gravelly clay loam
		TrB	Tremant-Rillito complex, 1 to 3 percent slopes
		TSC	Tremant-Rillito complex, 0 to 5 percent slopes
		Tu	Tucson loam
		Tw	Tucson clay loam
		Vf	Vecont clay
Stream Terraces		AbA	Anthosandy loam, 0 to 1 percent slopes
		An	Avonda clay loam
		Ao	Avondale clay loam
		Ap	Avondale clay loam, saline-alkali
		BE	Beardsley loam
		Bs	Brios sandy loam
		Bt	Brios loam
		CA2	Calciorthids and Torriorthents, eroded
		Gt	Glenbar clay loam
		Gv	Glenbar clay
		PsA	Pinal loam, 0 to 1 percent slopes
		PvB	Pinal-La Palma loams, 1 to 3 percent slopes
		PWB	Pinal-Suncity complex, 0 to 3 percent slopes
		RpE	Rillito-Perryville complex, 5 to 20 percent slopes
		Ta	Toltec loam
		TPB	Tremant complex, 0 to 3 percent slopes
		Tt	Trix clay loam
Valley Plains	Valley Plain	Ac	Antho sandy loam, saline-alkali
		Ch	Casa Grande loam
		Cp	Coolidge sandy loam
		Es	Estrella loam
		GM	Gilman-Antho association
		Gr	Glenbar loam
		Le	Laveen clay loam
		Mo	Mohall sandy loam
		MTB	Mohall-Tremant complex, 0 to 3 percent slopes
		Va	Valencia sandy loam
Water	Water	W	Lakes, ponds, reservoirs - perennial

Also shown on the Soils Map is the Long-Term Erosion Hazard Zone boundary (see Chapter 8 for a definition and explanation of its delineation). The reader should note that the terrace soils generally fall outside the long-term erosion hazard zone while the floodplain soils fall inside it. This reflects the similarity of landforms, soils, and criteria used by the NRCS and the AZGS in the mapping of geomorphic surfaces. The similarities also demonstrate the reproducibility of geomorphic techniques to differentiate landforms and consequently erosion hazards. Areas with floodplain soils are generally subject to erosion hazards unless protected by engineered bank protection or levees.

4.6 Summary

Patterns of various characteristics of the Agua Fria River vary spatially throughout the study area both longitudinally along the channel as well as horizontally across its valley. The distribution of these features helps explain the spatial distribution of erosion hazards in the study area. These patterns will be complemented with the historical information collected along with geomorphic and engineering computations to map the extent of erosion hazards defined and discussed in Chapter 8.

5. HISTORICAL/TEMPORAL DATA

Historical data describe the behavior of the Agua Fria River over time. These data are an invaluable component of the assessment of the magnitude and extent of erosion hazards in the study area. Chapter 5 presents the following types of information:

- Geologic data
- Archaeological data
- Historical records
- Historical aerial photographs
- Historical lateral movement
- Historical vertical movement
- Sinuosity

Geologic data provide information about the river during the last two million years. Archeological data provides information about the river over the past several hundred to thousand years. Historical records provide information about the river over the past 100 years. In particular, historical aerial photographs and topography provide qualitative and quantitative estimates of lateral and vertical erosion during individual flood events and over the entire period of record.

5.1 Geologic data

The modern desert piedmont surrounding the White Tank, Hieroglyphic, and smaller mountains and channels in the lower Agua Fria drainage basin have experienced periods of incision and aggradation over the last two million years in response to tectonic and climate event. These events not only shaped the modern landscape, but also provide insight into stream behavior that is of concern to land managers. The Quaternary landforms (e.g., terraces, fans) created by these geologic events provide a framework for delineating erosion hazard boundaries and estimating long-term rates of incision for the Agua Fria River. A detailed discussion of the geologic history of the Agua Fria River basin was provided in Chapter 2 of this report.

5.1.1 Quaternary Period: Incision and Aggradation

Early studies of terraces along the major river systems of the Phoenix Basin indicate that the oldest terraces are Quaternary in age (2-3 Ma; Pewe, 1976; Lee and Bell, 1975). Pewe identified four ancestral terraces along the Salt River and showed that their profiles, as well as those from the Agua Fria River, New River, and Queen Creek, converge in the downstream direction. He suggested that gradual uplift of the mountains surrounding the Phoenix Basin tilted these terraces to the southwest resulting in downstream converging profiles. The cause of this uplift, while speculative, may be a isostatic response to the unloading of sediments eroded from mountains of the Transition Zone. However, Pewe did not preclude the possibility of climatic influences affecting the converging terrace profile. Huckleberry (1995) suggests that the terraces probably result from a combination of tectonic, climatic, and isostatic processes.

More detailed surficial geologic mapping of the Baldy Mountain and Calderwood Butte 7.5 minute quadrangles was conducted by the Arizona Geologic Survey (AZGS) to determine the physical properties and ages of Quaternary deposits along the Agua Fria River downstream of Lake Pleasant. Four alluvial fan and eight fluvial terrace units were identified along this reach. The ages of these twelve surfaces were estimated based on the relative degree of soil development, topographic expression, and other surficial features. Figure 2-3 (Chapter 2) shows the converging profile of the Agua Fria terraces discussed by Pewe (1976). The colors

correspond approximately to the colors shown on the Surficial Geology Map (Exhibit Maps Book). A study from the western slopes of the White Tank Mountains suggests that a major incision event occurred around two million years ago and was followed by a period of aggradation. These events are inferred from geologic relations between Early Pleistocene (Qo) and Middle Pleistocene (Qm) alluvial fan units, and on preliminary cosmogenic isotope dating of these surfaces (Robinson, personal communication). Similar patterns of regional incision and aggradation have occurred throughout the Quaternary period, and have left a series of inset, descending terraces along the Agua Fria River in the study reach.

5.1.2 Limits on Erosion

Cycles of aggradation and incision have woven a complex history which has shaped the morphology of the modern Agua Fria River drainage basin. In the following paragraphs, the Quaternary geologic history is distilled to evaluate long-term degradation rates and to define practical limits of lateral erosion. According to Huckleberry (1995), the oldest Agua Fria River terrace (O) terrace is estimated to be 1-2 million years old. The O terrace sits over 100 meters (m) above the active channel near Waddell Dam, but only about 12 m above the active channel near Sun City. Similarly, the 2-5 million year old Sawik Terrace is about 130 m above the modern Salt River near Roosevelt Dam but converges with the modern floodplain upstream of Tempe Butte. Pewe (1978) estimated a maximum uplift rate of 0.064 mm/yr based on the maximum terrace height divided by minimum age of the terrace (2 Ma).

A number of assumptions are required to estimate incision rates by dividing terrace height by approximate age. The primary assumption of no aggradation since formation of the terrace is problematic in light of formation of younger, inset terraces. However, estimated incision rates can be considered as the net result of the two competing processes (degradation and aggradation). Using Huckleberry's value of 100 m for incision in the upper part of the study area and 12 m for the approximate midpoint and assuming an age of 1.5 ±0.5 million years for the oldest Agua Fria River terrace yields incision rates of 0.075 ±0.025 mm/yr and 0.018 ±0.006 mm/yr for the upper and middle reaches; respectively. In comparison, Menges and Pearthree (1989) calculated a minimum incision rate between 0.03 and 0.1 mm/yr for the Transition Zone. These geologic rates of incision suggest that the active channel will be about 1 centimeter (cm) lower in 100 years. It is important to realize that these calculations are based on the last two million years, a time when the Agua Fria River was flowing in a natural system. These rates do not account for influences created by the New Waddell Dam and sand and gravel mining within the channel.

Huckleberry's (1995) M2x surfaces (Late Pleistocene terraces) decrease in elevation above the active Agua Fria River from about 40 feet near Waddell Dam to 10 feet near the confluence. These surfaces of lesser age yield net degradation rates of 0.03 to 0.12 mm/year over the past 10,000 years. However, some of the M2x surfaces may be as old as 200,000 years which reduces the net degradation estimates to between 0.002 to 0.006 mm/year over a 200,000 year time period, somewhat less than the long-term degradation rate implied by the older terraces.

Similarly, the lateral position of the converging terraces along the study reach provides information on the historical position of the Agua Fria River during recent geologic time. The younger terraces are inset within the margins of the older, higher, and wider terraces, indicating that the river corridor has narrowed as it has incised. These terrace boundaries indicate the limits of channel position within the past 10,000 to 1,000,000 years, and form a practical boundary of likely lateral movement in the immediate future. Regardless of the precise vertical and lateral rates of erosion indicated by the Pleistocene and Holocene terraces, they do provide practical limits on channel change because the river has been stable within these limits for thousands to millions of years. Therefore, it is highly unlikely that any flood would extend beyond the limits defined by these surfaces.

5.1.3 Subsidence

Subsidence is a geologic phenomenon in which the ground surface becomes lower over time. Subsidence can happen naturally, or in the case of the Phoenix Basin, as the result of human activity. Surveys of subsidence in the west Phoenix Basin have shown as much as 18 feet of surface subsidence (lowering) due to compaction of basin fill sediments that occurred as the result of groundwater pumping around Luke Air Force Base. Published reports show that subsidence along the Agua Fria River channel location has been nominal (0-2 feet) (Schumann and O'Day, 1995). Figure 2-5 shows a map of quantities of ground lowering in the west Phoenix Basin. These data show that while land subsidence has been significant near the study area, the effects on the Agua Fria River channel have not yet had a great impact on the river. If subsidence extends to the Agua Fria River channel, the effect will be to increase the slope upstream of the subsidence cone, and decrease the slope downstream. Increased slope would lead to increased incision (long-term scour) and lateral erosion. Decreased slope would lead to sediment deposition, loss of channel capacity and widening of the floodplain.

5.1.4 Summary

The presence and characteristics of the fluvial terraces along the Agua Fria River provide the following types of information about the existing and future risk of lateral erosion:

- Erosion limits. Within the past 10,000 years, lateral erosion has been limited to the area of the 600 to 9,000 foot wide stream corridor located between Pleistocene surfaces. Future lateral erosion is most likely within areas composed of the most recent geomorphic surfaces.
- Erosion corridor width. The width of the modern geomorphic surfaces increases and the height of the fluvial terraces generally decreases in the downstream direction, indicating an increased potential for lateral erosion in the downstream direction.
- Net degradation. The height of the fluvial terraces above the existing channel bed suggests that a maximum of about 300 feet of net vertical erosion has occurred since the early Pleistocene, with a maximum of about 40 feet since the late Pleistocene.
- Episodes of aggradation. Episodes of aggradation (e.g., channel filling, floodplain deposition) have occurred at numerous times in the past, and should be expected in the future. During periods of aggradation, the stream corridor tends to occupy a wider portion of the geologic floodplain.
- Rates of degradation. Geologic evidence suggests natural long-term degradation rates of 0.02 to 0.08 mm/year over the past 2 million years and 0.02 to 0.12 mm/year over the past 10,000 years.
- Land subsidence. Lowering of the ground due to groundwater withdrawal has not likely had a significant impact on the Agua Fria River channel.

Within the study area, the existing channel of the Agua Fria River has experienced net degradation over the past 2 million years. Therefore, net degradation is expected to continue in the future. Entrenchment during recent geologic time has created a series of older, stable terraces that confine the existing active channels within a relatively well-defined corridor. Likewise, future channel movement is most likely to be confined within the corridor of geologically recent surfaces located near the main channels.

5.2 Archeological Data

The Agua Fria River, New River, and Skunk Creek played an important role in central Arizona's prehistory. Prehistorical subsistence along the Agua Fria appears to have evolved from hunting and gathering into varying degrees of agricultural dependence (Gladwin, 1937; Haury, 1976).

5.2.1 Paleo-Indian and Archaic Period

Lacey and others (n.d.) report no Paleo-Indian sites and few Archaic period sites are documented for the Agua Fria River Watercourse Master Plan study area, but conclude that the lack of evidence is due to the fact that these early habitations have been buried with post-occupation soil deposition or destroyed by fluvial and erosional processes.

5.2.2 Hohokam Settlements

Hohokam occupation in the Salt and Gila River basins spans the time period from 300 B.C. to A.D. 1450. From tree ring analysis, researchers identified numerous flood years on the Salt River between A.D. 740 and 805, which may have forced many Hohokam populations to leave the Salt River Valley and settle along the Agua Fria, Verde, and New Rivers, and in the Tonto Basin (Sheridan, 1995:13; Dove, 1970). The occupation of the Agua Fria River study area by the Hohokam was restricted to the Colonial and Sedentary periods (A.D. 700 to 1100), and possibly into the early Classic period (Lacey and others, n.d.). The presence of permanent habitation structures along the Agua Fria River, Skunk Creek, and New River indicates that the occupation of this region was permanent (as opposed to seasonal), although the Agua Fria River basin is located in what is referred to as the "Northern Periphery" of the Hohokam sphere of influence (Lacey and others, n.d.). Hohokam may have also moved into the study area due to population pressures in core areas or the may have used the area on a seasonal basis.

Centuries of fluvial action resulted in a series of terraces alongside the Agua Fria River. Section 5.1 of this report describes the geomorphology of these terrace landforms in greater detail. It is on these terraces that virtually all evidence of prehistorical Hohokam habitation is found (Rodgers, 2000; Lacey and others, n.d.; Tellman and others, 1997). Archeological evidence documented in the literature includes small trash mounds, shard scatters, stone compounds and rooms, fieldhouses, and mountain top forts. Land modification and water control features are among the more common Hohokam settlement features found in the Northern Periphery. The Hohokam are considered perhaps the most sophisticated irrigators on our continent north of the civilizations of Mexico (Haury, 1976; Masse 1981; Rogge and others, 1987). Check dams, terraced hill slopes, and gridded and linear stone alignments were used widely by Hohokam farmers in the Agua Fria as well as in the Salt and Gila River basins (Weaver, 1980; Dove, 1970). These methods of runoff diversion and retention are normally associated with "dry" farming techniques. Dry farming utilizes ephemeral water sources, as opposed to "wet" irrigation which relies on perennial or intermittent watercourses. Dry farming features are often reported within the study area (Lacey and others, n.d.:2). Dart (1989) described four prehistorical canals along the Agua Fria River study reach, as follows:

- A canal 27 miles upstream of the Gila River confluence was found to date to circa A.D. 1400.
- Another canal thought to be of Hohokam origin was found about 2 miles east of the Agua Fria River, 23 miles upstream of the Gila River.
- Prior to 1930, there was evidence of an irrigation canal along the Agua Fria River 21 miles north of the Gila River.
- Three miles upstream of the Gila River confluence, a prehistorical canal emanated from the Agua Fria River and conveyed water to fields on the floodplain of the Gila River.

Hohokam settlements are well documented in the Agua Fria River basin. The larger drainage area and alluvial deposits of the Agua Fria River attracted more Hohokam farmers than either New River or Skunk Creek. Lacey and others (n.d.) report a total of five relevant sites along the Agua Fria River study reach described in the literature, including two with documented evidence of irrigation systems and three with evidence suggesting irrigation. These sites are listed in order of downstream flow direction.

- Beardsley Canal Site: Gathering was the principal subsistence activity for this small pit house village, although some evidence suggests agricultural activity (Weed, 1972).
- Calderwood Butte Ruin: Dove (1970) reports at least 80 prehistorical sites within a three-mile length of the river in this general area. Check dams and terrace gardens are recorded in the immediate vicinity of this large village compound.
- Westwing Site: Agriculture at this small pit house village could sustain a sedentary population in this area, suggesting irrigation practices at this location (Weaver, 1974).
- Eastwing Site: This pit house village is located along the east side of the Agua Fria River south of Calderwood Butte. There is evidence of agricultural fields. Prehistorical irrigation canals are suspected, but not found, as only a portion of the site has been excavated. Trade with other Hohokam villages to the south seems to have been the primary activity (Rodgers, 1985).
- Cashion Site: The Cashion archaeological site complex, one of the largest prehistorical Hohokam villages in the Salt/ Gila Basin, sprawled across perhaps as much as three square miles near the confluence of the Agua Fria and Gila Rivers (Rogge and others, 1987; Dittert, 1974; Midvale, 1920-21). A canal system is present, but it appears to have conveyed Gila River water rather than water from the Agua Fria River (Dittert, 1974). What remains of the agricultural complex consists of a canal system that parallels the terrace base and lateral feeder ditches for field irrigation.

5.2.3 Post-Hohokam Evidence

Above normal rainfall in the 11th century led to increased population and expanded irrigation systems (Tellman and others, 1997). It is believed that climate change around A.D. 1130-1159 to a warmer and dryer regime depleted resources (such as wood for fuel) and resulted in a loss of reliable water supply, causing the prehistorical societies to move elsewhere (Lacey and others, n.d.). Other researchers report this drought period to have occurred in the 13th century or later (Tellman and others, 1997; Dove, 1970). Regardless, year-round occupation ended earlier in the Agua Fria River basin than it did further south and the area remained virtually unoccupied for hundreds of years afterwards. No evidence of further occupation by the Hohokam or other groups exists until the period of Anglo occupation.

5.2.4 Conclusion

The archeological data (Rodgers, 2000; Lacey and others, n.d.) show numerous prehistorical sites along the Agua Fria River. However, all of the sites are located on the high Pleistocene terraces well above the river suggesting that: 1) either the Native Americans did not occupy the area below the terraces, possibly due to flooding and erosion hazards; or 2) evidence of their tenure below the terraces has been washed away by flooding and erosion on the river. In either case, the archeological data suggest that the river has had active erosion and flooding within the corridor between the Pleistocene terraces since at least the time of occupation by the Native Americans, which ended around A.D. 1450.

5.3 Historical evidence

The Agua Fria River basin has supported a wide range of human activities since the advent of the modern historical era in the later half of the 19th century. Early settlement of the Agua Fria River basin began around 1870. During the 19th and 20th centuries human activities in the study area included mining, the establishment of transportation depots, water resources development through construction of dams and diversions, and various agricultural activities such as irrigated farming and ranching. More recently, human activities included the encroachment of

urbanization into the floodplain, the construction of bridges and engineered flood control structures in the channel, and the extraction of sand and gravel from the river. These activities comprise very significant disturbances to the natural condition of the Agua Fria River system. Technical data presented in this report indicate the most recent activities constitute the greatest river-altering changes brought about by humans in the Agua Fria River, eclipsing the comparatively minor impacts on the river resulting from the former land use changes in the prehistorical and early historical period. Figure 5-1 presents a chronology of the various human activities along the Agua Fria River and illustrates cause-and-effect relationships between the those activities and the river's response.

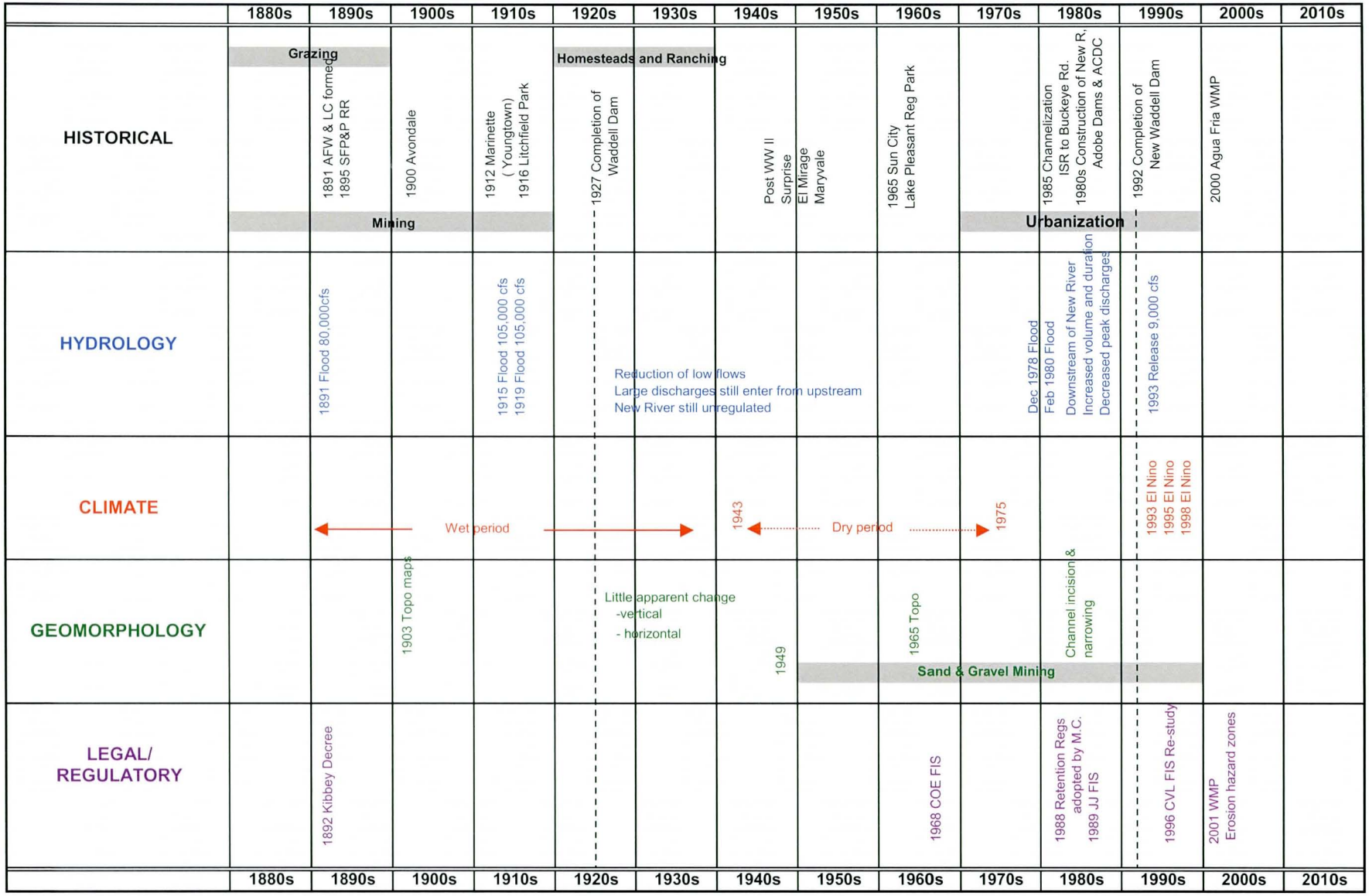

Figure 5-1 Agua Fria River Chronology

5.3.1 Mining Activity

Most mining activity took place outside the study area in the upper Agua Fria River watershed in Yavapai County between 1870 and 1920. The Vulture mine was discovered in 1864 about 30 miles west of the Lake Pleasant region. The boom town of Wickenburg was founded near the mine. From about that time, miners and ranchers began spreading out from this settlement to the present-day Lake Pleasant area. It was not until the 1890s that settlers began to really exploit the study area. For example, historical sources document hydraulic mining on Humbug Creek, a tributary to the Agua Fria River in the Lake Pleasant area (Rogge and others, 1987; Tellman and others, 1997). Rogge and others (1987) report a 35-foot high masonry dam that was built in the 1890's on Humbug Creek as part of the Humbug Hydraulic Works to provide water for a mining operation. Some minor gold deposits were discovered, but the operation failed due to lack of water. Mining activities in the lower reaches of the Agua Fria within the study area were limited. The only working mines in Maricopa County near the river were in the vicinity of the town of Pratt. These mines were insignificant; almost all had closed by 1905 (Lacey and others, n.d.).

5.3.2 Transportation Corridor

The Agua Fria River basin was used extensively in the late 19th and early 20th centuries for transportation purposes (Lacey and others, n.d.). In addition to Wickenburg, the settlements of both Prescott and Phoenix were founded in the 1860s, and travelers between these towns used parts of the Agua Fria River valley as a transportation corridor (Rogge and others, 1987). The Agua Fria River valley was being settled and improved around 1877 as new towns began to appear. Table 5-1 summarizes the towns and the various activities pursued in the area. Figure 5-2 provides a map showing the location of the historical place names.

Table 5-1 Towns and Settlements in the Agua Fria Basin (after Lacey and others, n.d.)

NAME	TYPE	LOCATION/ COUNTY	DATE
Agua Fria/ Calderwood Peak	Stage station/ Ranch	2 mi. N. of where US 60 crosses Agua Fria (T5N R1E)/ Maricopa	1866-1884
Agua Fria Ranch/ Bowers Ranch/ Smetters Ranch	Ranch	Near Calderwood Peak (T5N R1E)/ Maricopa	1870-1921
Avondale	Railroad Station	West bank of Agua Fria near confluence w/ Gila (T1N R1W)/ Maricopa	1900-
Bird Ranch	Ranch	Lake Pleasant State Park	1940-1955
Black Canyon Station	Stage Station	On Agua Fria at old Black Canyon stage crossing (T1N R2E)/ Maricopa	1875-?
Bumble Bee	Mine/ Ranch	Bradshaw Mountains (T10N R2E)/ Yavapai	1874-?
Carl Pleasant Lake	Mine	Current Lake Pleasant (T6N R1E)/ Maricopa	
Camp Dyer	Construction Camp	Near diversion dam/ Maricopa	1891-1893
Castle Hot Springs	Resort/ Ranch	On Castle Creek in Bradshaw Mtns. (T8N R1E)/ Yavapai	1891-1940s
Coldwater	Stage Station	West Bank of Agua Fria, presently Avondale/ Maricopa	1896-1905
Cordes	Stage Station	Approx. 30 mi. east of Prescott (T11N R2E)/ Yavapai	1886-
Crown King	Mine	Bradshaws (T10N R1W)/ Yavapai	1880-?
Dewey	Mine/ Agriculture/ Railroad	18 mi east of Prescott (T13N R1E)/ Yavapai	1872-
El Mirage	Labor Camp	On Agua Fria River (T3N R1W)/ Maricopa	1947-
Foster	Mill	On Agua Fria, exact location unknown	1876-1888
Gibson	Ranch/ Stage Station	On New River, exact location unknown	1890-?
Gillette	Mill/ Stage Station	Left bank of Agua Fria in Bradshaw Mtns, near Yavapai/ Maricopa border	1877-1887
Humbolt	Mine/ Agriculture	18 mi east of Prescott (T13N R1E)/ Yavapai	1899-
Litchfield	Agriculture	On Agua Fria, near Avondale/ Maricopa	1918-
Mayer	Stage Station/ Trading Center	25 mi east of Prescott (T12N R1E)/ Yavapai	1882-
Morgan City Wash	Mine	Near Frog Tanks/ Pratt (T7N R2E)/ Maricopa	1900-1930s
Moore Gulch	Mine	Near Gillette	1877-?
New River	Stage Station	On New River, 32 mi north of Phoenix (T6N R2E)/ Maricopa	1868-1875
Poland	Mine	On Agua Fria, between Mayer/ Humbolt/ Yavapai	1865-
Pratt (Frog Tanks)	Ranches/ Farms/ Mines	Currently Lake Pleasant	1890-1930
Tip Top	Mine	Bradshaw Mtns, near Agua Fria Tributary (T8N R1E)/ Yavapai	1875-1895

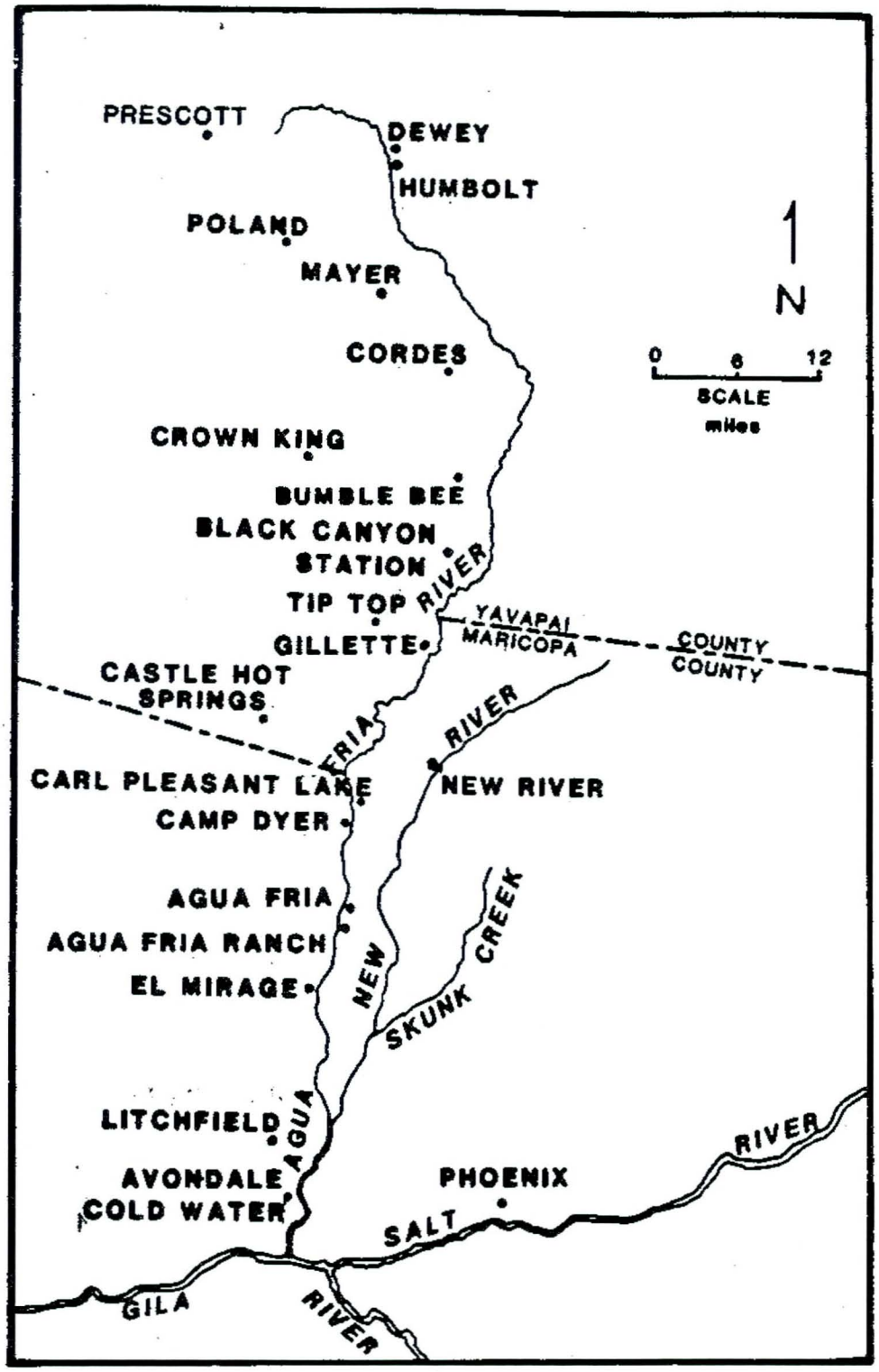

Figure 5-2 Historical Site Location Map (Source: Lacey and others, n.d.)

Lacey and others (n.d.) document the progression of travel within and through the Agua Fria basin as follows:

- Stagecoach and freight wagon routes ran from Phoenix west to Wickenburg, and north to Prescott during the 1880s. These routes roughly paralleled the Agua Fria River. Important stops along the route included Coldwater, Pratt, Agua Fria, Gillette, Black Canyon, Cordes, Mayer, and Humbolt.
- In 1890, the Phoenix and Prescott Toll Road Company constructed a wagon road from the Salt River Valley to the Bradshaw Mountains. The roadway disappeared completely by 1894 due to the insignificant mining operations in the Agua Fria basin (See Section 5.3.1).
- The Santa Fe, Phoenix and Prescott Railroad was built in 1895 along an alignment parallel to the Agua Fria River. After the coming of the railroad, wagon roads were soon abandoned. By 1900, the old wagon routes up the river were being used only by ranchers and settlers in the region. Most of the settlements that were established to serve the wagon roads disappeared.
- Automobile roads were established by 1920, but were hazardous to travel.

Rogge and others (1987) provide a similar description of the evolution of transportation in the Agua Fria River basin. General Land Office (GLO) maps indicate that although there may have been only one toll road, there was actually a network of Phoenix-to-Prescott wagon roads throughout the area. One point common to many of these trails was a place known as Frog Tanks or Pratt. William Pratt mined in the vicinity and established a supply and mail station at a point where subsurface bedrock in the Agua Fria channel caused water to rise to the surface. The resulting pools supported a population of frogs and thus the name Frog Tanks was adopted. Frog Tanks warranted a post office from 1890 to 1896. The demise of Frog Tanks was likely due, in part, to the construction of the Santa Fe, Phoenix and Prescott Railroad, more commonly known as the "Peavine." The Wickenburg-Phoenix link of the line opened in 1891.

One obvious exception to the discussion of the development of transportation in the Agua Fria valley is travel by boat. Historical flood data provide an indication of the velocity of the water, and thus the relative risk of river crossings during floods. Newspaper excerpts demonstrate that some floods were considerably more hazardous than others; i.e., boats were capsized in rescue attempts in one flood, but in others the Agua Fria was forded on horseback. At least one anecdotal account of opportunistic boating during floods exists. According to an interview with one long-time resident, during some high water periods it was possible and even helpful to have a boat to cross the Agua Fria (Lacey and others, n.d.; Rogge and others, 1987). The Arizona Navigable Stream Adjudication Commission (ASNAC, 1997) concluded that there was little or no hydrologic or historical evidence to support a position that the Agua Fria River was navigable for commercial purposes based on criteria contained in Arizona Revised Statues §37-1128.

Ten other towns and communities now exist along the transportation corridor south of the Lake Pleasant area (Rogge and others, 1987). Figure 5-3 provides a map of present-day place names. Some of these were originally railroad sidings, including Morristown, established in 1897, and Wittman, begun in 1920. Other early communities were farming towns, including Beardsley and Peoria, founded in 1888; Glendale in 1891; and Youngtown (originally Marinette) in 1912. More recent towns, including Circle City, Surprise, El Mirage and Sun City, represent post-World War II growth and planned retirement communities. Presently, a total of fifteen bridges span the Agua Fria River to provide transportation to and through these communities. See Table 2-2 for a summary of bridge locations, widths, and approximate dates of completion.

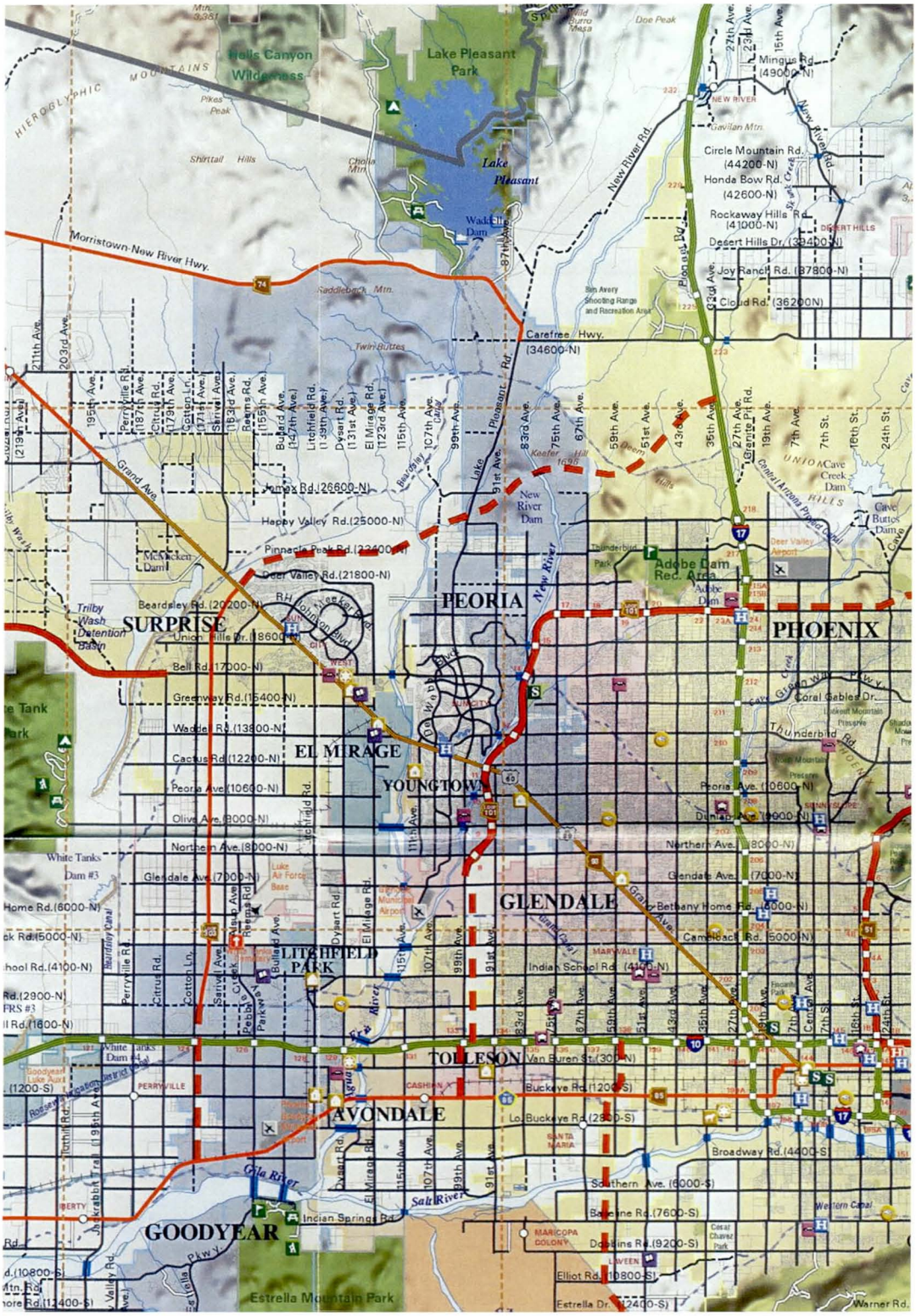

Figure 5-3 Present Site Location Map (Source: MCDOT, 1998)

5.3.3 Dam Construction

The Supreme Court of the Arizona Territory took steps to settle confusion over water rights in 1892, when Judge Joseph H. Kibbey issued the Kibbey Decision. Kibbey reaffirmed in Arizona the established doctrine of prior appropriation (first in time, first in right). Kibbey applied the doctrine to Salt River Valley canal companies to establish the priority of their water rights (Rogge and others, 1995). Setting the basis for establishing order of priority for scarce water resources was important, but legal decisions did nothing to enhance the water supply. It is against this backdrop that efforts were made to build a major irrigation project with large storage dams on the Agua Fria River. These efforts were initiated in the decade prior to the turn of the century, concurrent with the historical settlement of the area.

The first step was taken in 1888 when William A. Hancock, Linville H. Orme and Grant Crow filed for the right to divert water at a location about ten miles upstream of Agua Fria Station and five miles downstream of Frog Tanks, where Waddell Dam was eventually built (Rogge and others, 1987). This location is approximately where the modern Central Arizona Project (CAP) aqueduct and Beardsley Canal cross the river. These plans never materialized, but indicate that flowing water was probably present, at least seasonally, in the upper portions of the Agua Fria River watercourse master plan study reach. Next, settlers and developers joined to form the Agua Fria Water and Land Company (AFW&LC). By 1891, Hancock, who had come to Arizona as a soldier and stayed on to help found the City of Phoenix, was serving as the Secretary and Engineer of the AFW&LC, with J.F. Monihan as President (Rogge and others, 1987). The company proposed building a 300-foot high storage dam and two smaller 150-foot high dams, all above Frog Tanks. This project also did not progress beyond the planning stage until William H. Beardsley and his half-brother George Beardsley arrived from Ohio to pursue the project. William Beardsley, backed by Ohio financiers, obtained control of the AFW&LC. He continued to work with Hancock, who served as chief engineer. Hancock participated in the project as a partner in the company until his death in 1902.

Rogge and others (1987) describe the comparatively modest project designed under Beardsley's direction. It was comprised of a 100-foot high storage dam that was located at Frog Tanks to take advantage of the shallow bedrock that created the tanks (see Section 5.3.2). Beardsley planned to build another dam, approximately 150-feet high, in a canyon about nine miles upstream. The third project component was a 30-foot high diversion dam to be built approximately a mile downstream of Frog Tanks. Fifty miles of main canal and 200 miles of laterals were planned to serve as much as 160,000 acres according to the AFW&LC brochure issued in 1895. This number turned out to be a gross overestimate, by a factor of three to four times, of the acreage that could actually be irrigated by the Agua Fria water supply. The goal was to open the acreage up to crops, including the prized Arizona seedless grapefruit.

Fieldwork for the project was underway by 1892 when dam sites were identified and canal lines surveyed (Tellman and others, 1997). Construction began on the diversion dam in late 1894. Originally known as Beardsley Dam, the dam was later renamed for Edgar Dyer, a surveyor who worked for Beardsley and established the work camp near the dam site (http://dataweb.usbr.gov/dams/az00113.htm). The work stopped suddenly in October 1895 when a flood damaged the unfinished dam and washed away construction equipment. The rubble masonry diversion dam was substantially finished when construction stopped, but was left with an uncompleted notch (see Figure 5-4). Only two to eight miles of the planned 32-mile main Beardsley Canal had been excavated. Financial difficulties prevented renewal of the effort and much of the property of the AFW&LC was soon turned over to creditors. Other property was sold at auction and purchased by a project proponent who immediately quit claimed it back to Beardsley to continue his pursuit of the project.

Figure 5-4 William Beardsley on Dyer Diversion Dam (Schuyler, 1903)

Various researchers (Rogge and others, 1987 and 1995; Gindhart, 1987; Tellman and others, 1997) document the obstacles Beardsley encountered during the years of project implementation, including the following:

- Land Acquisition. Beardsley had difficulty acquiring the lands to be irrigated. The land acquisition problem started with local speculators, but was apparently frustrated by an overlapping federal withdrawal for a reclamation project from 1902 to 1909. A complex land exchange involving the Santa Fe Railroad eventually overcame this problem and Beardsley finally had deeds to sufficient land by about 1915.
- Water Rights. In the mid-1920s, the Southwest Cotton Company and Valley Ranch Company, which had developed large downstream farming operations, sued over losses of water, which they claimed an upstream dam would cause. A lower court found for the plaintiffs, but the State Supreme Court reversed the decision and allowed construction to proceed. The Salt River Valley Water Users Association formed the federal reclamation project made possible by Roosevelt Dam and contested the project as well.
- Financing. The AFW&LC sought funds for private construction of the first large dam in Arizona to be built without government assistance, despite a severe national depression. Financing problems were overcome with the sale of bonds.

The duties of a watchman living at the Camp Dyer construction work camp near the diversion dam site until about 1916 included measuring the Agua Fria flows twice daily. Beardsley made use of these data to support his argument about the feasibility of the project. Maintenance of Camp Dyer also supported his contention that he was continually and diligently pursuing completion of the irrigation project and thus helped preserve his claimed water rights (Rogge and others, 1987). By 1925, Beardsley formed a new company called the Beardsley Land and Investment Company. He also created the Maricopa County Municipal Water Conservation District No. 1 as the legal entity to own and operate the system. Beardsley obtained the services of Carl Pleasant, a prominent engineer based in Tulsa, Oklahoma. Pleasant selected an innovative and controversial design with multiple thin concrete arches supported by hollow buttresses because it was cheaper than designs being built by the federal government (Gindhart, 1987). The dam could be built with substantially less concrete than other designs, but still store a commensurate volume of water. The project almost succumbed to concerns over dam safety.

Construction is variously reported to have begun from May 1925 to March 1926 (Rogge and others, 1987). William Beardsley died in December 1925, just as the project was reinvigorated. His son Robert Beardsley and Carl Pleasant then moved the project forward. When completed, the 170-foot high, multiple-arch dam was the largest in the world (Dallett, 2000) and the largest privately funded dam in Arizona at a time when the federal government was building dams throughout the West (see Figure 5-5). Carl Pleasant Dam was dedicated on November 14, 1927 when actress Gloria Swanson christened the dam with a bottle of (prohibition-era) Arizona grapefruit juice (Tellman and others, 1997:16). Lake Pleasant was impounded by the dam 30 miles northwest of Phoenix, providing water for the Maricopa Water District. Dyer Diversion Dam was completed and put into operation in conjunction with the construction of Carl Pleasant Dam about one mile downstream.

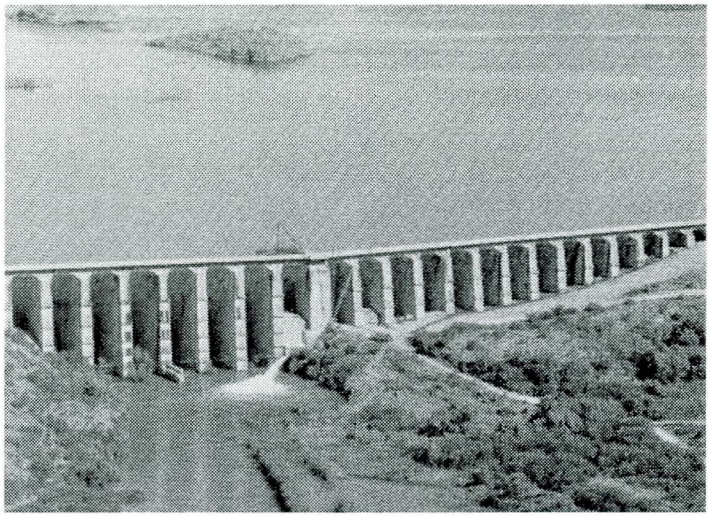

Figure 5-5 Carl Pleasant Dam (Source: USBR)

Gindhart (1987) reports that completion of the dam in 1927 opened up land to southern California land speculators for the first time. More than 39,000 acres were opened up to farming, including 29,000 set aside for grapefruit. The Pacific Development Company of Los Angeles, experts in citrus farm development, purchased land from the Beardsley Land and Investment Company in 1927 and launched a nationwide campaign promoting Arizona's scenery and healthy climate.

Carl Pleasant Dam was later re-named Waddell Dam in 1966 for Donald W. Waddell, who successfully arranged the financing for the project. During the Great Depression of the 1930s, funds provided by the federal Reconstruction Finance Corporation allowed the Maricopa Water District to undertake modifications and salvage the project's technological and economic viability (Introcaso, 1988). The spillway was modified in 1929 and major repairs to the dam were made in 1934. The area surrounding Lake Pleasant was designated a regional county park in the 1960s.

During the 1980's, the U.S. Army Corps of Engineers and the Flood Control District of Maricopa County constructed the New River Dam and Adobe Dam in the Agua Fria River basin. These flood retarding structures serve flood control purposes only and do not permanently store water. During this same period, the U.S. Army Corps of Engineers constructed the Arizona Canal Diversion Channel (ACDC) to intercept and convey runoff from areas north of the Arizona Canal to the New River.

By 1984, there was a unified approach to regional flood control, storage, and delivery called Plan 6 which addressed the water carried by the CAP (Dallett, 2000). One component of Plan 6

was the construction of a new dam on the Agua Fria River. New Waddell Dam provided flexibility to Arizona to import and store Colorado River water. The U.S. Bureau of Reclamation completed the construction of New Waddell Dam in 1992. New Waddell Dam is a 300-foot high earthen structure located between old Waddell Dam and Dyer Diversion Dam, making them obsolete (see Figure 5-6, http://dataweb.usbr.gov/dams/az82929.htm). New Waddell Dam is used for water conservation and regulatory storage, with no dedicated flood storage. Lake Pleasant increased by three to four times the size of the former reservoir as Colorado River water, imported by the CAP, is stored during the winter for release during the summer (Rogge and others, 1987). Dyer Diversion Dam was modified and raised to replace storage at the canal headworks that was lost when New Waddell Dam was built. Old Waddell Dam was breached to the reservoir sediment level and is submerged behind New Waddell Dam (note the partially submerged old dam in the upper center of Figure 5-6).

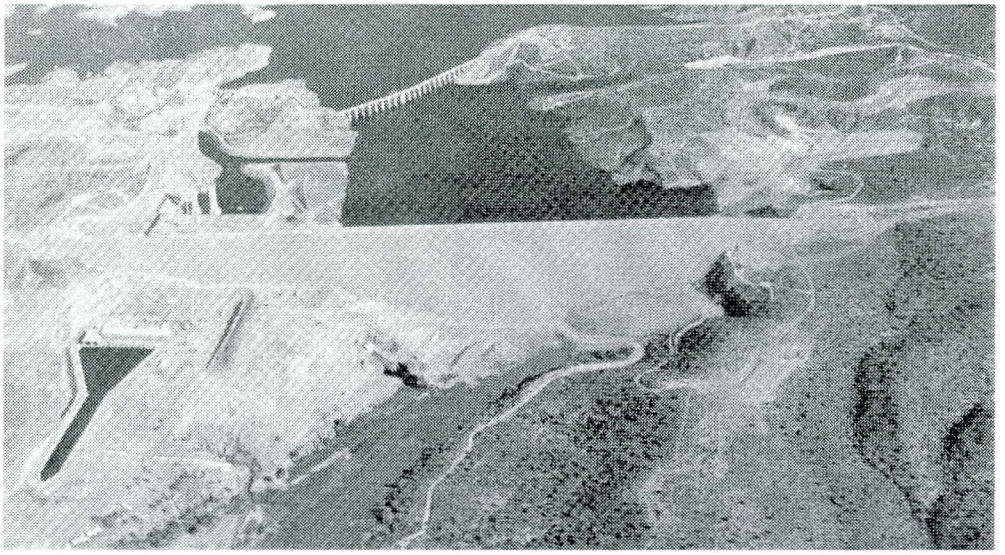

Figure 5-6 New Waddell Dam (Source: USBR)

5.3.4 Agricultural Activities

5.3.4.1 Irrigated Agriculture

The first firm historical evidence of attempts at farming and small-scale irrigation in the study area occurred in the Lake Pleasant vicinity and date to the 1890's (Rogge and others, 1987). GLO surveyors mapped an acequia, or small irrigation ditch, in 1892 approximately six miles downstream of the old Waddell Dam (a.k.a., Carl Pleasant Dam). The acequia was less than a mile long and ran across the Marlowe and Artigo properties (See Exhibit Book Reaches 4 and 5 historical comparison plates for maps of these features). The acequia appears to have served three fields encompassing only about 160 acres. Other irrigated sites in the Lake Pleasant area were also mapped by the GLO and show ditches to irrigate small fields.

Promoters expanded Salt River Valley agriculture to the Agua Fria River study area after its mineral resources were exhausted (Tellman and others, 1997). However, before the construction of Carl Pleasant Dam, the Agua Fria River basin was considered a poor ranching and farming area because the river was not a reliable water source (Lacey and others, n.d.). Much of the land was irrigated by "appropriator's canals" whereby a small group of farmers banded together to build a diversion structure, and construct and maintain a canal system (Seargeant, 1960). These small diversion dams captured seasonal streamflow, but were frequently washed out by floods. When this occurred, the farmers would attempt to re-build the dams quickly before the river dried up once again. Many farms and ranches there started

during wet years, when there was water in the river, only to have the river dry up and farmers lose their crops in succeeding years (Seargeant, 1960).

5.3.4.2 Agricultural Settlements

Many attempts at developing water storage facilities were unsuccessful before the construction of Carl Pleasant Dam in 1927. The upper reaches of the study area were closed to homestead entry from 1902 to 1909 when a federal reclamation project was contemplated (Rogge and others, 1987). The 1920's and 1930's seem to have been the most active time for homesteading and ranching development in the area. Lacey and others (n.d.) describe the following agricultural settlements (Figure 5-2) that grew up along the Agua Fria River:

- The town of Pratt, in what is now Lake Pleasant State Park, was the center of numerous ranches and farms. Farming conditions in the area were favorable because it was a good location for a dam and diversion of water. Many homesteads were established in the late 1880s in this area, the most significant being the Bird Ranch. The success of these farms and ranches depended to a great extent on the water level in the Agua Fria River in a given year (Fireman, 1980).
- Another farming and ranching region was located near the town of Agua Fria on the Maricopa and Yavapai County border. The Agua Fria Ranch, developed in 1870, became an extensive cattle ranch.
- Coldwater Crossing was established on the west bank of the river in 1892. It was one of the earliest stage stations in the region. Coldwater became Avondale when the Atchison, Topeka, & Santa Fe Railroad station in Coldwater was closed. The two towns had originally been a mile apart.
- Avondale, built around 1900, was originally established as a railroad station, but was also the center of a farming and ranching area.
- Litchfield Park was built in 1916 as housing for those growing cotton for the Goodyear Tire and Rubber Company.

In addition to the agricultural settlements listed above, the following agricultural features were also a part of the region's history:

- The Beardsley agricultural region was established between Avondale and Pratt. The Agua Fria River was the water source for irrigation purposes. Beardsley Station was named after William H. Beardsley, who started an irrigation project there in 1888 (See Section 5.3.3).
- The Roosevelt Irrigation District pumps water from water-logged land and delivers it to 38,000 acres of irrigated land in the southern part of the west valley (Dallett, 2000).

5.3.4.3 Ranching

The study area was extensively and consistently used for livestock grazing after the 1880's (Lacey and others, n.d.; Rogge and others, 1987). Cattle were moved from the Mogollon Rim and Colorado Plateau to the Lake Pleasant area to be fattened prior to shipment via the new railroad connections to markets in the East and in California. Several large cattle ranches were formed, but the area was also used for winter sheep pastures from about the turn of the century until the 1940s. A unique aspect of ranching in the study area was the clustering of a number of goat ranches in the vicinity dating from the 1930's. Goats were used to "clean" a range of scrub and thorns before cattle were grazed (Rogge and others, 1987:6). The livestock boom that occurred in Arizona after 1880 and the coming of the railroad lead to overgrazing of many of the watersheds in central Arizona, which in turn is thought to have contributed to regional stream degradation and lateral erosion.

5.3.5 Sand and Gravel Mining

The watershed downstream of Lake Pleasant has experienced significant urbanization within areas historically irrigated for agriculture, as well as in additional areas that never were farmed. The earliest urbanization consisted of the small towns or service centers for agriculture described previously. During World War II, Arizona sent 50,000 people comprising 10 percent of its population to war. At the same time, thousands of service men from the world over were introduced to Arizona by training in installations such as Luke Field, Williams Air Force Base, and Litchfield Park. Between 1948 and 1950, about 100,000 ex-servicemen chose to settle in Arizona (Dallett, 2000). Existing housing built between 1930 and 1945 was insufficient for this new demand. Land developers such as John F. Long built housing in Maryvale at an unprecedented pace to fill the post-war demand. In addition, the concept of planned retirement communities was piloted by Del E. Webb with the construction of Sun City in the mid 1960's. The overwhelming success of this early innovative land development lead to acceleration of pace of urbanization along the Agua Fria River corridor. Large areas of residential and commercial development spread across the watershed as the cities of Phoenix, Glendale, Peoria, Sun City, and Avondale grew rapidly. Today, most of the watershed downstream of about Beardsley Road is completely urbanized. Much of the remaining non-urbanized areas are planned for urbanization in the near future. In the near future the entire watershed downstream of Lake Pleasant is likely to be completely urbanized.

Along with the accelerating pace of residential and commercial development in the area, the need for adequate utilities and transportation infrastructure grew. Major bridge and flood control structures were built throughout the study area. Bridge information was previously provided on Table 2-2. In the mid-1980's, a 4.4-mile reach of the Agua Fria River between Indian School and Buckeye Roads was channelized between 14-foot high soil cement levees designed by the U.S. Army Corps of Engineers and now owned by the Flood Control District of Maricopa County. Partial (one side) channelization was also constructed for about two miles along the right (west) bank downstream of Buckeye Road and another two miles along the left (east) bank upstream of Buckeye Road to the New River confluence. Soil cement grade control structures were also constructed within the fully channelized reach. The consequence has been to fix the horizontal and vertical position of a long reach of the lower Agua Fria River.

In combination, these construction activities drove an ever increasing need for aggregate products for use as raw material for construction. The damming of the Agua Fria River in the 1920's exposed the streambed land and provided some degree of protection from low flows, facilitating the development of a local extractive industry for sand and gravel products located close to the construction activity. Because transportation costs are a major financial component in the cost of sand and gravel products, low-cost West Valley growth was possible because of the proximity to the Agua Fria River aggregate source (Dallett, 2000). Aerial photographic evidence indicates that active sand and gravel mining has been taking place within the river channel and its floodplain since at least 1949. The consequence is that a significant volume of sediment has been and continues to be extracted from the Agua Fria River.

Historical records, described later in this chapter, indicate that degradation (lowering) of the Agua Fria River has been coincident with in-stream sand and gravel mining. Degradation of the Agua Fria River has been noted by other studies as well (SLA, 1983; ADOT, 1989). ADOT (1989) collected data relative to sand and gravel mining in a reach of the Agua Fria River extending from Buckeye Road to Camelback Road to study the impacts of in-stream sand and gravel mining on channel stability. The volume of sand and gravel extraction in this study reach was estimated at 11.8 million tons for the period from 1972 to 1981. Aerial photo interpretation indicated mining activity was concentrated near the Indian School Road bridge. Mining proceeded uniformly, with episodic disruption due to floods and significant impacts from extensive channelization of the river during the 1980's. The change in bed topography in the reach averaged 1.5 feet during this period. Observed changes in the local bed profile at the

bridge sites in the study reach since construction were reported to be four to five feet. In one report, aggradation of about 3 feet at the Buckeye Road bridge site was noted following the 1980 flood.

5.3.6 Summary

Historical data from the past 100 years indicate the following:

- Historical heavy mineral mining activities in the lower reaches of the Agua Fria River within the study area were limited. The only working mines in Maricopa County near the river were in the vicinity of the town of Pratt, upstream of the study reach. These mines were insignificant, and almost all of them had closed by 1905.
- The number of settlements along the Agua Fria River peaked between 1880 and 1900. Mining and stage stations were the major centers of activity. Most of the big mines were shut down by the turn of the century, and the future of the stage stations was sealed with the arrival of the railroad. The agricultural potential of the basin would not be realized until after the construction of Waddell Dam in the 1920's.
- By 1984, there was a unified approach to regional flood control, storage, and delivery called Plan 6, which addressed the water carried by the CAP (Dallett, 2000). One component of Plan 6 was the construction of New Waddell Dam on the Agua Fria River. New Waddell Dam provided flexibility to Arizona to import and store Colorado River water.
- Active sand and gravel mining has been taking place within the river channel and its floodplain since at least 1949, causing a significant volume of sediment to be extracted from the river, and increasing the potential for significant degradation of the bed of the Agua Fria River.
- Historical degradation of the Agua Fria River has been noted by other studies.

5.3.7 Conclusion

The historical evidence demonstrates that human population, structures and infrastructure, social, cultural and political institutions, in conjunction with the natural features existing in an urbanized space, create a complex and varied environment. The interpretation of the temporal chronology (Figure 5-1) of these institutions and their interconnectedness in the Agua Fria basin indicates that human activities in and near the channel in the last 20 years have been more disruptive to the natural system than at any time in the past. Technical data presented above indicate the activities of the past 50 years constitute the greatest river-altering changes brought about by humans in the Agua Fria River, eclipsing the comparatively minor or non-existent impacts on the river resulting from the former land use changes in the prehistorical and early historical period. The encroachment of urbanization into the floodplain, the construction of bridges and engineered flood control structures in the channel, and the extraction of sand and gravel from the river comprise significant disturbances to the natural condition of the Agua Fria River system, and have resulted in an increased potential for significant degradation of the bed of the Agua Fria River.

5.4 Historical aerial photographs

The following discussion of the sequence of historical aerial photographs provides a qualitative overview of the physical changes that have occurred on the Agua Fria River during the period of record. The discussion focuses on the character of the river channel in both planimetric form and relative width, as well as on the encroachment of residential developments and mining operations into the floodplains and main channel of the river. Historical aerial photographs for each of the years of coverage for the study area are provided in the Exhibit Maps Book. Not all

of the years of coverage are available for every part of the study reach. The aerial photographs available for each reach are listed with the discussion of that reach, and are shown in the Exhibits Map Book.

5.4.1 Reach One – Lower Lake Dam to Siphon

Historical Photo Sequence: 1949, 1954, 1960, 1977, 1985, 1992, 1997, 1999

In Reach 1, the Agua Fria River flows between two terraces that have confined the lateral migration of the river over the timeframe covered by aerial photography. The channel bed itself has remained consistent in planimetric form during the 50+ years of aerial photographic record. The most significant encroachment into the riverbed, with the exception of the lower lake Dam, is the Carefree Highway (Highway 74) Bridge, which spans the active channel. Another change is the thick stand of vegetation that has grown along the river banks downstream of the lower lake dam due most likely to standing water, seepage from the lake, and outflows from Morgan City Wash. The vegetation is not prominent on early air photos (1949, 1954) but is noticeable on more contemporary air photos, specifically those later than 1985.

5.4.2 Reach Two – Siphon to CAP Siphon

Historical Photo Sequence: 1949, 1954, 1960, 1977, 1985, 1992, 1997, 1999

In Reach 2, the Agua Fria River can be characterized as either a single-channel or anastomizing channel, depending on time and location. Pleistocene-aged terraces confine the floodplain on both banks, limiting lateral migration of the channel. The most significant change observed in the sequential aerial photographs involves the width reduction of the active channel. In the southern half of Reach 2, a channel occupied the right side of the floodplain from 1949 through sometime before 1977. After 1977, the channel on the right side of the floodplain was no longer as active and vegetation grew up, and the area took on non-active channel appearance. Human encroachment into the reach has been limited to an at-grade road crossing first apparent in 1977, gone in 1979, and then reestablished by 1985. Limited sand and gravel mining, both in extent and duration, occurred in the northern half of the reach between 1985 and 1992.

5.4.3 Reach Three – CAP Siphon to Beardsley Canal Flume

Historical Photo Sequence: 1949, 1954, 1960, 1977, 1985, 1992, 1997, 1999

Reach 3 was significantly modified, especially after 1977, by construction of the Central Arizona Project (CAP) Granite Reef Canal. Prior to 1977, the only obstruction in the floodplain was the Beardsley Canal flume. In Reach 3, the Agua Fria River is a single channel with wide overbank floodplains. The main channel is consistently on the right side of the floodplain. The CAP canal siphon construction greatly disturbed the floodplain in 1977, since the entire siphon alignment was excavated to a depth greater than 20 feet. However, most of the evidence of construction had disappeared by 1985 due to erosion and deposition during the 1980 flood. In 1997, the floodplain was once again disturbed to repair to the CAP siphon. The effects of this repair remain evident in the 1999 aerial photographs. It is noted that the effects of CAP construction appear to be limited to the canal alignment, since the main channel did not shift and flow is not obstructed.

5.4.4 Reach Four – Beardsley Canal Flume to Dynamite Boulevard alignment

Historical Photo Sequence: 1949, 1954, 1960, 1977, 1979, 1985, 1992, 1997, 1999

Reach 4 has apparently remained in a relatively natural condition since at least 1949. The only encroachment of the floodplain is agricultural fields on the right side floodplain. Within Reach 4,

the channel alternates between a single channel and multiple anastomosing pattern. Except for changes in vegetation, the channel has remained fairly consistent in plan view in the south half of the reach over the period of photographic record. A well-defined, single low-flow channel is easily identifiable in the north half of the reach in 1992, and can be traced back to 1979. The new 1979 channel was located to the left of the former main channel. The land between the current main channel and the agricultural fields appears to have become less influenced by flowing water since 1954. The patterns left by flowing water have become indistinct since 1954, and vegetation is more common within the floodplain, obscuring some of the channel features.

5.4.5 Reach Five – Dynamite Boulevard alignment to Hatfield Road

Historical Photo Sequence: 1949, 1954, 1960, 1964, 1977, 1979, 1980, 1985, 1992, 1997, 1999

Reach 5 is similar to Reach 4. In both reaches, the channel pattern alternates between wide multiple channels and constricted, single channels, such as those at Calderwood Butte. Jomax Road crosses at-grade near the base of Calderwood Butte, and is first visible in the 1949 photos. Hatfield Road also crosses the river at-grade, and was constructed sometime between 1964 and 1977. The first historical evidence of floodplain encroachment occurs upstream of Hatfield Road in 1964. By 1977, the group of homes and structures near Hatfield Road was well established. Subsequently, this group of homes was inundated by flooding and subject to a channel avulsion, the evidence of which is visible in the 1980 air photos. The remaining structures were removed by 1992, leaving only the remnants of the access roads.

Upstream of Jomax Road, the channel has consistently split around a low, mid-channel island. The island is especially prominent in the 1980, 1985, and 1992 photos. During the period of record, the river also moved its left bank farther to the east. The change in bank location is especially noticeable when comparing the 1949 and 1980 photos. Downstream of Jomax Road, the active flow area has narrowed, with subsequent avulsive activity. In 1949 and 1954, the photos show a wide, braided or anastomosing channel spreading out to the edge of the right side terrace. The 1964 photos show that outflow from tributaries has incised into the surface. After 1980, the photos suggest that deep flows did not inundate the surface, and the active flow was confined to a narrower channel. Also, at this time an avulsion occurred on the right bank, creating new channels on the former floodplain.

5.4.6 Reach Six – Hatfield Road to Beardsley Road alignment

Historical Photo Sequence: 1949, 1954, 1960, 1964, 1967, 1977, 1979, 1980, 1985, 1992, 1997, 1999

In Reach 6, the river has retained a fairly consistent planimetric form that can be classified as a multi-channel anastomosing channel. Channel positions and mid-channel islands observed on the aerial photographs were remarkably consistent in locations. From 1949 to 1967, no encroachment took place. Two at-grade road crossings were constructed between 1967 and 1977, Hatfield Road to the north and Rose Garden Lane to the south. Between 1967 and 1977 the channel at the Rose Garden Lane at-grade crossing narrowed appreciably. A residential area was developed on the right side of the floodplain between 1967 and 1977. Some of these structures, visible in the 1977 photo, are located where there was an active channel in 1967.

Reach 6 is the furthest upstream reach to be heavily transformed by mining activity. There were three major mining areas established in Reach 6 by 1992, and all three encroach into active flow channels. The first evidence of mining can be found in the channel just upstream of the Beardsley Road alignment in 1985. This pit increases in size and takes up most of the main channel by 1997. Another large mining pit was excavated between 1985 and 1992 on the

parcel of floodplain upstream of the homes near Rose Garden Lane. This pit is significant because it extends into the riverbed and cuts off the right side channel. The river had partially reclaimed the pit by 1997. The main channel of the river is also interrupted by the mining pit located just downstream of Hatfield Road. Like the mining downstream, this pit also appears for the first time in the 1992 photos.

5.4.7 Reach Seven – Beardsley Road alignment to Bell Road

Historical Photo Sequence: 1949, 1954, 1959, 1964, 1967, 1977, 1979, 1980, 1985, 1992, 1997, 1999

The Agua Fria River in Reach 7 is composed of multiple small channels within a larger, high flow area. According to the historical aerial photographs, the location of the smaller channels was consistent between 1949 and 1977. The broad extent of the high flow area is evident in the 1954 photos. In 1954 and 1959 the floodplain located between the left terrace and the main channel was used for agricultural purposes. In 1967 the effective width of the Agua Fria River in Reach 7 was greatly reduced due to the construction of a levee and bridge at Bell Road. Finally, the north end of the Coyote Lakes subdivision is located over a former channel that is visible in the 1980 photos.

5.4.8 Reach Eight – Bell Road to Cactus Road alignment

Historical Photo Sequence: 1949, 1954, 1959, 1964, 1967, 1977, 1979, 1980, 1985, 1992, 1997, 1999

Grand Avenue and the associated constriction of the main channel at the bridge crossings has been in place since at least 1949. Sand and gravel mining began downstream of Grand Avenue in 1959 and continued through 1967. Mining upstream of Grand Avenue began in 1964 and has been expanding through 1999. As a result of encroachment and in-stream mining, the river in Reach 8 has narrowed since 1949, especially in the north part of the reach. The landfill downstream of Grand Avenue cuts off a former active channel that was present on the right side of the floodplain.

5.4.9 Reach Nine – Cactus Road alignment to Olive Avenue

Historical Photo Sequence: 1934, 1949, 1954, 1959, 1964, 1967, 1977, 1979, 1980, 1985, 1992, 1997, 1999

Reach 9 is relatively free of any modern encroachments or mining operations. Nevertheless, the channel has changed during the period of record. The width of the active flow channels prior to 1980 was much greater than after 1980. The main channel apparently incised and narrowed during the 1980 flood, although the braided to anastomosing interior character of the channel remained fairly constant. The only encroachment recorded on the historical aerial photographs is the golf course subdivision, which is located on the right side of the river downstream of the Cactus Road alignment. The bridge that replaced the at-grade crossing at Olive Avenue between 1985 and 1992 stabilized the channel width at the bridge location.

5.4.10 Reach Ten – Olive Avenue to New River confluence

Historical Photo Sequence: 1934, 1949, 1954, 1959, 1964, 1967, 1977, 1979, 1980, 1985, 1992, 1997, 1999

Reach 10 is the most constricted reach within the study limits. A prominent, narrow low-flow channel located along the right bank terrace in 1934 lies within a wider, braided channel. In-

stream mining began in the bed of the river just upstream of Glendale Avenue prior to 1949, but the channel to the east of the pits is still active and has a braided pattern. Mining continues and expands through 1967, by which time the braided channels to the east of the pit have become less defined. The narrow channel between the right terrace and the mining operation is transformed to the main channel by 1977 due to the construction of the narrow section of the Glendale Avenue Bridge. Also, the mining pit is greatly expanded by 1977.

The main channel in Reach 10 continues to be located in the same position, but it became more distinct during the 1980 flood. In the southernmost part of Reach 10, active flow paths on the right side of the floodplain are abandoned by 1985, and currently appear to be part of the overbank floodplain. Sand and gravel mining begins on the new floodplain no later than 1992 and continues through 1999. Additional sand and gravel mines have been excavated adjacent to the left bank of the main channel over the 1992 to 1999 air photo sequence.

A thick stand of vegetation grew up immediately downstream of the Glendale Avenue Bridge in the 1992, 1997, and 1999 photos. This thick vegetation combined with the narrow bridge opening greatly restricts the width of the Agua Fria River.

5.4.11 Reach Eleven – New River confluence to Indian School Road

Historical Photo Sequence: 1934, 1949, 1954, 1959, 1964, 1967, 1977, 1979, 1980, 1985, 1992, 1997, 1999

New River outflow forms the dominant channel in Reach 11. The New River flow created one of two main channels visible in the 1934 photo. The New River channel became especially well-defined in 1959 and has remained well-defined since then. The active channel in Reach 11 widened significantly during the 1980 flood. The resulting width was partially stabilized by construction of the Camelback Road Bridge between 1985 and 1992. During this interval, wing dikes were constructed upstream of Indian School Road to direct the wide flow between the levees downstream of Indian School Road. A continuous levee was constructed along the left bank from Camelback Road to Indian School Road between 1997 and 1999.

5.4.12 Reach Twelve – Indian School Road to Interstate 10

Historical Photo Sequence: 1934, 1949, 1954, 1959, 1964, 1967, 1977, 1979, 1980, 1985, 1992, 1997, 1999

The main channel of the Agua Fria in Reach 12 remained in a fairly consistent position from 1934 to 1980. However, the overbank and floodplain widths were narrowed considerably. Encroachment of the right side of the floodplain began in 1949, and consisted of development of agricultural fields. These fields reworked obvious overflow channel patterns visible in the 1934 photographs. In addition, it appears that the farmers made efforts to stabilize both the right and left bank of the river by planting trees on the banks beginning in 1949.

Mining activity began in the Reach 12 between Indian School Road and Roosevelt Canal sometime between 1967 and 1977. The mining activity created a narrower and less braided main channel, although the flood of 1980 widened the main channel at the bend just downstream of McDowell Road. The active floodplain is confined by continuous soil-cement levees on both the right and left bank. The channel was also straightened considerably when the levees were constructed. The levees have allowed the development of residential subdivisions on former floodplains.

5.4.13 Reach Thirteen – Interstate 10 to Buckeye Road

Historical Photo Sequence: 1934, 1949, 1954, 1959, 1964, 1967, 1977, 1979, 1980, 1985, 1992, 1997, 1999

In 1934, Reach 13 of the Agua Fria River had a wide braided channel with what appear to be extensive overbank and floodplain areas. Buckeye Road and the adjacent railway already spanned the river. An inset low flow channel became more distinct beginning sometime between 1954 and 1959. The inset channel was fairly narrow, but it widened between 1977 and 1979. It was to this channel that the agricultural fields encroached. Mining operations just upstream of the Van Buren road crossing first appear in the 1964 photos, are absent in the 1967 image, and are again present in 1977, 1979, 1980, and 1985. The flood of 1980 widened the channel considerably between Van Buren Street and Buckeye Road, eroding into parts of the agricultural fields. The channel is currently confined by continuous soil cement levees on both the right and left bank. The I-10 drain outflow has created multiple small intertwining channels between the levees.

5.4.14 Reach Fourteen – Buckeye Road to Broadway Road

Historical Photo Sequence: 1934, 1949, 1954, 1959, 1964, 1967, 1977, 1979, 1980, 1985, 1992, 1997, 1999

In the earliest air photos, the main channel of Reach 14 is more sinuous than in the reaches upstream. The main channel is bordered by an overbank and floodplain that reveal evidence of overbank flows visible in the 1934, 1949, and 1954 aerial photographs. The main channel appears more distinct in the 1959 photos than in earlier photographs, and remains so in subsequent years. There appears to be an attempt to artificially straighten the main channel downstream of Buckeye Road beginning in 1964. The straight channel remained in place until about 1977. In 1979 and 1980, the main channel widened, and the river recovered its meandering pattern. A levee was constructed along the right bank for most of the length of the reach between 1985 and 1992. Lower Buckeye Road has remained an at-grade crossing over the historical record, and no additional encroachment onto the floodplain or into the channel was recorded in the photos.

5.4.15 Reach Fifteen – Broadway Road to Gila River

Historical Photo Sequence: 1934, 1949, 1954, 1959, 1964, 1967, 1977, 1979, 1980, 1985, 1992, 1997, 1999

The earliest photos of Reach 15 show the Agua Fria River as a wide, braided stream. The main channel within this braided reach becomes better defined between 1967 and 1977. The most striking change in the river occurred when the main channel was artificially straightened between 1979 and 1980. Although not as prominent, the straightened channel persists as the main channel to through the 1999 photos. Encroachment in Reach 15 consisted of development of agricultural fields in the former floodplains. A brief period of local mining operations was recorded on the 1992 photo.

5.4.16 Summary

The main channel of the Agua Fria River is visible in the earliest (1934) aerial photos. The condition of the main channel has changed greatly during the 65 year period of record. The main channel prior to 1980 typically had a multiple anastomosing channel pattern, or was otherwise located within a wide, braided reach of the river. In general, the active channel width narrowed between 1967 and 1977, and became slightly more prominent. The main channel

became more prominent after the flood of 1980 due to incision relative to the floodplain. Much of the observed channel change occurred during the 1980 flood. Within the incised narrowed channel, braided and anastomosing patterns still occur.

Mining operations in the river began as early as 1949, especially in Reaches 8 to 10. Mining in Reach 6 began in the 1980's, but quickly expanded to rival the older mining operations located further downstream. The mining operations tend to encroach into the channel from the floodplain. The barriers and levees constructed by the mining operation tend to constrain the width of the main channel. In some instances, especially in Reach 6, the mining pit is placed directly in the path of the river, intercepting any discharge before it continues to flow downstream.

The most significant encroachment occurred downstream of Indian School Road (Reaches 12, 13, and 14) where the river has been completely confined by levees on both banks. There are also several instances of residential development in the floodplain. A few have been lasting, such as the one located in Reach 6 at Rose Garden Lane and the Coyote Lakes subdivision in Reach 7. The new communities tend to have associated levees that attempt to restrict the lateral movement of the river. Residential areas developed on the floodplain in Reach 5 were less permanent, and did not survive the 1980 flood.

5.5 Lateral Movement

Measurements of historical lateral channel movement were made from aerial photographs of the study reach. Historical lateral channel movement was measured in three ways. First, changes in channel width were measured at index cross sections defined in each of the fifteen reaches. Width changes occur when the channel position remains essentially unchanged, but the channel becomes wider or narrower. Width changes can occur in response to floods, droughts, encroachment, channelization, or changing watershed conditions. Second, changes in channel position were measured over the entire study reach by comparing the thalweg position shown in aerial photographs. Channel position can change over time due to bank erosion or avulsions during periods of flow, narrowing due to incision or floodplain accretion, or physical relocation of the channel to accommodate human activities. Finally, channel movement during a single large flood, the 1980 event, was measured at the index cross sections defined for each reach. Erosion during a single event includes any type of lateral movement, as well as widening (or narrowing) of the channel.

The historical data support the conclusion of the geologic history analyses that lateral movement of the Agua Fria River is not a modern phenomenon, nor is it trivial in scale. For example, a historical account reported in the Arizona Republic on November 28, 1919 states that "in 1916, ...a great volume of water coming down the Agua Fria River changed the channel of that stream, moving it one-half mile west. This flood occurred while the railroad bridge of the Agua Fria was being built.[1] Since 1916 the state highway department has been gradually moving the river back under the bridge at an estimated cost of $60,000." (cited in USACOE, 1968). This account of more than 2,000 feet of lateral erosion is consistent with the findings of this rest of this study, including the measurements made from historical aerial photographs described below.

5.5.1 Long-Term Changes

Long-term lateral movement was analyzed by measuring changes in channel width and by comparing changes in thalweg position over the period of record of the historical aerial photographs.

[1] The bridge is located in Avondale.

5.5.1.1 Channel Width

Channels widths were measured at index cross sections defined within each of the fifteen reaches between Lake Pleasant and the Gila River. The index cross sections were selected during the field work at points representative of the average reach characteristics and/or at locations with significant geomorphic features. The locations of the index sections are shown on the Index to Field Sections in the Exhibit Maps Book.

Channel width is defined as the distance between the channel banks. For the Agua Fria River, application of this definition of width requires some judgment for several reasons. First, the Agua Fria River is braided, meaning that there is typically more than one channel, and therefore, more than one set of banks. If the width of only one of the braids is measured, then the width is underestimated. If the width between the outermost banks is measured, then areas between braids that are not truly part of the channel are included and the channel width is overestimated. Second, because the Agua Fria River is subject to massive amounts of channel change, avulsions, long-term degradation, and human interference, there may be no temporal continuity between the dates of the aerial photographs. That is, a channel visible in one photograph may no longer exist in the next photograph, or an entirely new channel may be formed in another part of the floodplain. Therefore, direct comparison of widths is difficult. Third, in reaches where low floodplains are present, the visible differences between the channel and floodplain are subtle, which makes identifying the banks difficult. Fourth, if the river becomes incised, the abandoned former channel often remains visible and may have more readily identified bank characteristics than the current, active channel. Finally, the Agua Fria River has a compound channel. That is, the low flow channel(s) exist within a larger flood channel, which may also exist within a higher flow channel, all of which have channel characteristics and banks. Therefore, there are multiple widths to be measured at most cross sections, making comparisons between time periods difficult.

Channel widths were measured on historical aerial photos from 1954, 1977, 1985, 1992, and 1999. These years of coverage were selected because each set provided full coverage of the study reach, and because significant floods occurred between the photo dates. To make the width measurements, the aerial photographs were rectified to a common coordinate system, banks were delineated in ArcView GIS, and channel width was measured digitally at the index sections. The field section locations and reach locations are provided in the Exhibit Maps Book. A discussion of the results for each of the fifteen reaches is provided below.

5.5.1.1.1 Reach 1

In Reach 1, the channel generally narrowed from 1954 to 1999, and did not experience significant lateral movement. Two index sections were defined in Reach 1.

Section B40: In 1954, the width here was 712 feet. The total width remained fairly constant though 1985. The channel had narrowed to 420 feet by 1992. In 1999, the active channel was reduced to 71 feet wide, with a total width of 305 feet including the left overbank. This channel narrowing occurred within the original 1954 channel banks.

Section B41: The channel width varied between 1954 and 1999, although the 1954 and 1999 widths are very similar. In 1954, the channel width was 653 feet. The 1999 width was 657 feet. Between 1954 and 1999 the channel width ranged from a maximum of 675 feet in 1985 to a minimum of 406 feet in 1992, but the channel did not experience any dramatic lateral movement outside the original 1954 banks.

5.5.1.1.2 Reach 2

In Reach 2, the high flow channel width was relatively stable from 1954 to 1999, but the low flow channel narrowed or migrated within the high flow channel. Two index sections were defined for Reach 2.

Section B1: A compound cross section is present at Section B1. In 1954, a high flow channel occupied the entire 862 feet width between the Pleistocene-aged terraces. A distinct 334-feet wide low flow channel was inset within the high flow channel. The high flow channel width varied slightly in the 1977, 1985, and 1992 aerial photos, with the measured high flow width ranging from 844 to 905 feet. The minimal measured widening occurred along the east bank, due to erosion by the low flow channel of the terrace slope. By 1999, the high flow channel narrowed to approximately 436 feet, with its west bank generally congruent with previous bank locations. The low flow channel, therefore, was observed to have moved within the more stable high flow channel.

Section B3: Channel width at Section B3 remained fairly consistent until 1999. The channel section consisted of a low flow main channel and a high flow channel located to the right of the main channel. In 1954, the main channel width was 425 feet. By 1999, the main channel width narrowed to 164 feet. In the process of narrowing, the right bank remained in generally the same position while the left bank moved west. The high flow channel width, including the main channel, was measured at 736 feet, 724 feet, 697 feet, and 714 feet.

5.5.1.1.3 Reach 3

No index sections were defined for Reach 3 due to its short length, and disturbance of the channel and floodplain by construction and repair of the CAP siphon.

5.5.1.1.4 Reach 4

In Reach 4, the river experienced dramatic channel widening, lateral movement, formation of new low flow channels, and abandonment of former high flow channel areas. Three index sections were defined for Reach 4.

Section B5: A compound channel is present at Section B5. Overall, the channel at Section B5 narrowed from 1954 to 1999. The 1954 and 1977 photos show a low flow main channel with a high flow channel area to the right of the main channel. The main channel width was measured at 788 feet in 1954 and 768 feet in 1977. The high flow channel widths were measured at 2021 feet in 1954 and 1903 feet in 1977. By 1985, the channel characteristics had changed. The high flow channel width remained fairly constant at about 2023 feet, but the main channel widened on the right side to 851 feet. Also, an additional inset low flow channel 275 feet wide formed within the main channel. By 1992, the right overbank area appeared perched and outside the active channel area, reducing the high flow channel width to 852 feet, approximately the width of the former main channel. The inset low flow channel width remained constant at about 283 feet. By 1999, the inset low flow channel further narrowed to 160 feet and a new inset low flow channel had formed with a width of 91 feet. The position of the left bank of these channels has remained relatively consistent at the terrace margin since 1954, with the observed narrowing due to changes in the position of the right banks.

Section B6: A compound channel exists at Section B6, which includes a low flow main channel and both left and right side high flow channel areas. The high flow areas appear to have become perched between 1954 and 1999, as indicated by the density and type of vegetative cover. While the 1954 and 1999 overbank and main channel widths are similar, the widths varied significantly in 1977, 1985, and 1992. The sequential widths for the main channel measured from the aerial photographs are as follows: 295 feet (1954), 345 feet (1977), 465 feet (1985), 410 feet (1992), and 264 feet (1999). The sequential widths for the high flow channel

measured from the aerial photographs are as follows: 1632 feet (1954), 1533 feet (1977), 1549 feet (1985), 1543 feet (1992), and 1670 feet (1999). The width increase in 1999 is due to lateral movement at the left bank towards the east.

Section B7: A compound channel exists at Section B7. The main channel at Section B7 changes dramatically from 1954 to 1999. From 1954 to 1977 the main channel maintained the same width (270 feet vs. 262 feet, respectively), and was centered within a larger high flow channel (1143 feet vs. 1123 feet, respectively). In 1985, presumably due to the 1980 flood, the main channel widened to 1120 feet, approximately the width of the former high flow channel. By 1992, the main channel had reestablished itself within a high flow channel, but had shifted its left bank several hundred feet to the east terrace boundary. The 1992 main channel right bank is at the location of the 1977 left bank. By 1999, the high flow channels appear to have become perched and no longer subject to frequent flow.

5.5.1.1.5 Reach 5

In Reach 5, the river experienced channel widening, lateral movement, an avulsion, formation of new high flow channels, and abandonment of former high flow channel areas. Two index sections were defined for Reach 5.

Section B8: A braided compound channel with two inset low flow channels exists at Section B8. The right side inset channel was approximately 105 feet wide in 1954, 408 feet in 1992, and 282 feet in 1999. The left side channel was approximately 188 feet wide in 1954, 421 feet in 1992, and 156 feet in 1999. The inset channels cannot be distinguished from the high flow channel in 1977 and 1985. The high flow channel width varied as well during the period of record, with a width of 2459 feet in 1954, 902 feet in 1977, 2660 feet in 1985, 2455 feet in 1992, and 835 feet in 1999. At section B8, a pattern of widening during large floods and narrowing during periods of low flows occurs.

Section B9: A braided compound channel exists at Section B9. In 1954, the high flow channel was highly braided and was approximately 2558 feet wide. By 1977, the braided pattern was gone and a faint 624-feet wide low flow channel had formed, with its left bank at the same location as the left bank of the braided area in 1954. By 1985, the high flow channel width totaled 3176 feet, and the low flow channel had widened at both the left and right banks to 1400 feet. The 456 feet width increase to the east of the high flow channel was due to an avulsion, with the 1303 feet width increase to the west due to formation of a new high flow overbank channel. In 1992, the high flow channel width was measured at 3277 feet, due to slight changes in the position of the right overbank channel. In 1999, the right overbank channel appeared to be abandoned and the overall width was measured at approximately 1850 feet.

5.5.1.1.6 Reach 6

In Reach 6, measured channel changes included formation of new braids within the high flow channel corridor, significant width changes, and dramatic responses to the 1980 flood. Three index sections were defined for Reach 6.

Section B10: A braided channel pattern exists at Section B10. Changes in the width, location and number of braids during the period of record was documented. Two main low flow channel braids are present from 1954 to 1977. The right channel changed from 1318 feet wide in 1954 to 1269 feet in 1977. The left channel changed from 1360 feet wide in 1954 to 891 feet 1977. The high flow channel widths remained approximately constant from 1954 to 1977. After 1985, and the 1980 flood, three low flow channel braids are present within same high flow corridor.

Section B11: Like Section B10, the position, width and number of braids at Section B11 changed between 1977 and 1985, shifting from two inset low flow channel braids to four inset channel braids. The channel widths were measured as follows:

- Right low flow braid: 993 ft (1954), 984 ft (1977)
- Left low flow braid: 1675 ft (1954), 891 ft (1977)
- High flow channel: 2750 ft (1954), 2540 ft (1977).

After 1985, four low flow channel braids are present with the following widths:

- Right-most low flow braid: 706 ft (1985), 716 ft (1992), 129 ft (1999)
- 2nd-right low flow braid: 403 ft (1985), 367 ft (1992), 153 ft (1999)
- 2nd-left low flow braid: 204 ft (1985), 236 ft (1992), 127 ft (1999)
- Left-most low flow braid: 660 ft (1985), 660 ft (1992), 580 ft (1999)
- High flow channel: 3343 ft (1985), 3374 ft (1992), 3267 ft (1999).

The channel widths were reasonably constant between 1985 and 1992, but had decreased by 1999, with the greatest narrowing in the right-most low flow channel.

Section B12: Section B12 has a compound channel, with single low flow channel within a wider inundation area. The main channel was 952 feet in 1954, 920 feet in 1977, 953 feet in 1985, 1188 feet in 1992, and 1127 feet in 1999. The channel in 1999 was disturbed by mining activity and construction of an access road, and several minor inset channels had begun to form.

5.5.1.1.7 Reach 7

In Reach 7, the high flow channel narrowed or maintained its width, but the low flow channels actively shifted their position, width, and pattern. Two index sections were defined for Reach 7.

Section B13: A compound channel exists at Section B13. Overall, the width of high flow channel narrowed slightly at Section B13 from 1954 to 1999. The high flow channel width was measured as 2584 ft (1954), 2807 ft (1977), 2065 ft (1985), 874 ft (1992), and 2122 ft (1999). Changes in the number and position of the low flow channels occurred throughout the period of record.

Section B14: A compound channel exists at Section B14. The width of the high flow channel at Section B14 did not measurably change from 1954 to 1999. High flow channel widths were measured at 2382 ft (1954), 2365 ft (1977), 2370 ft (1985), 2377 ft (1992), 2380 ft (1999). Section B14 appears to be one of the more stable cross sections in the study reach, based on high flow channel width alone. However, the width, position and number of the low flow channels changed from 1954 to 1999. In 1954, there was one main channel with an inset low flow channel. In 1977, there were no distinct inset channels. In 1985, 1992, and 1999, two inset channels are visible within the main channel.

5.5.1.1.8 Reach 8

In Reach 8, measured channel change included shifts in the pattern, location and width of low flow channels, and narrowing of the high flow channel. Human impacts on the floodplain in Reach 8 probably obscure any natural processes that may have affected natural fluctuations in the natural channel width. Three index sections were defined for Reach 8.

Section B15: A highly active compound channel exists at Section B15, although the channel pattern changed from a braided, multiple channel pattern in 1977 to a wide, single channel in 1985, probably due to erosion during the 1980 flood. In 1954, there were three inset low flow channels. The right low flow channel was 57 feet wide, the center low flow channel was 119 feet wide, and the left low flow channel was 258 feet wide. By 1977, the number of low channels was reduced to two, both on the right side of the river corridor, and each approximately 220 feet

wide. The channel changed to a single 1153 feet wide channel by 1985, and then continued to narrow to 898 feet by 1992, and to 839 feet in 1999.

Section B16: A single high flow channel exists at Section B16, primarily due to human activities in the floodplain. The width of the single channel has varied over time, with the greatest measured width in 1985. The widths measured from the aerial photographs were 145 feet (1954), 250 feet (1977), 315 feet (1985), 296 feet (1992), and 196 feet (1999).

Section B17: The single high flow channel has narrowed since 1954, primarily due to human activities in the floodplain.. The measured channel widths at Section B17 were 2165 feet (1954), 1953 feet (1977), 2092 feet (1985), 687 feet (1999). There was a large reduction in active channel width after 1985.

5.5.1.1.9 Reach 9

In Reach 9, the river narrowed considerably from 1954 to 1999. Two index sections were defined for Reach 9.

Section B18: The width of the river at Section B18 has decreased from 1954 to 1999, from a high flow channel width of 1335 feet and 1328 feet in 1954 and 1977, respectively, to 1177 feet in 1985. The high flow channel width increased to 1285 feet in 1992, but then narrowed to 739 feet by 1999, a decrease of 546 feet. Inset low flow channels could be defined within the high flow channel at some times during the period of record. A single 252 feet wide inset channel was visible in the 1954 photographs, but no such channel was identified in the 1977 or 1985 photographs. In 1992, the inset low flow channel included a right channel (101 feet) and left channel (286 feet). In 1999, the two inset channels remained, but had slightly changed to 104 feet wide (right) and 243 feet wide (left).

Cross Section B19: The width of the river at Section B19, like Section B18, decreased from 194 to 1999. In 1954, the high flow channel was 3362 feet wide, and decreased slightly to 3222 by 1977. By 1985, the channel narrowed considerably to 878 feet. By 1992, the high flow channel widened slightly to 892 feet, but narrowed to 640 feet by 1999, a decrease of 252 feet from 1992 and 2722 feet from 1954. Low flow channels were defined only on the 1954 photograph, one of which was nearly the width of the 1999 high flow channel.

5.5.1.1.10 Reach 10

In Reach 10, the channel width has been heavily impacted by in-stream mining. The low flow and high flow channel have narrowed since 1954, due mostly to human impacts. Four index sections were defined for Reach 10. Section B21a and B21b are located upstream and downstream of the Dysart Drain confluence, respectively.

Section B20: The high flow channel has significantly decreased its width from 1845 feet in 1954 to 383 feet in 1999. The 1954 width remained nearly constant until 1977 (1833 feet), but had decreased to 456 feet by 1985. After an increase to 480 feet in 1992, the channel again narrowed to 383 feet in 1999.

Section B21a: Section B21a is located upstream of the Dysart Drain confluence. A dike built by a sand and gravel mining operation along this reach confines this portion of the river. The low flow channel width has varied from 76 to 150 feet wide, with the widest measurement recorded in 1985. The actual measurements were: 79 feet (1954), 115 feet (1977), 148 feet (1985), 132 feet (1992), 76 feet (1999). The high flow channel width is obscured by the mining operation.

Section B21b: Section B21b is located downstream of the Dysart Drain confluence. A dike built by the channel mining operation along this reach confines this portion of the river. The low flow channel width varied from 88 to 161 feet wide, with the widest measurement recorded in 1992.

The actual measurements were: 105 feet (1954), 88 feet (1977), 136 feet (1985), 161 feet (1992), 90 feet (1999). The high flow channel width is obscured by the mining operation.

Section B22: The high flow channel width at Section B22 consistently decreased since 1954. The channel width for 1954 was measured at 2154 feet, 643 feet in 1977, 544 feet in 1985, 496 feet in 1992, and 317 feet in 1999.

5.5.1.1.11 Reach 11

In Reach 11, the low flow channel width was affected by outflow from the New River. Channel widening occurred during the 1980 flood. Two index sections were defined for Reach 11.

Section B23: In 1954, the high flow channel was 4000 feet wide with multiple braided channels. Since that time, the main channel appears to have adjusted to reduced discharges now dominated by outflows from the New River, rather than by floods from the upper Agua Fria River watershed. By 1977, the high flow channel was 873 feet wide.

Section B24: In 1954, the river was characterized by multiple channels confined in a 3208 feet wide high flow channel. By 1977, the low flow channel had apparently adjusted to the outflows from the New River, like Section B24, and the main channel had narrowed to 177 feet. This low flow channel is not visible in the 1985 aerial photographs, but a high flow channel approximately 2540 feet wide, most likely due to the effects of the 1980 flood, is present. The high flow channel width remains constant until 1992, but by 1999, a 239 feet wide inset low flow channel has formed.

5.5.1.1.12 Reach 12

In Reach 12, levees confine the once wide floodplain of the river to approximately the width of the pre-levee low flow channel. Two index sections were defined for Reach 12.

Section B25: Section B25 is currently bounded by 1100 feet wide levees completed prior to 1992. In 1954, the low flow channel width was 1083 feet. By 1977, the channel had narrowed to 704 feet.

Section B26: Section B26 is currently bounded by 1100 feet wide levees completed prior to 1992. In 1954, the low flow channel width was 540 feet. By 1977, the channel had narrowed to 462 feet.

5.5.1.1.13 Reach 13

In Reach 12, levees confine the once wide floodplain of the river to approximately twice the width of the pre-levee low flow channel. Two index sections were defined for Reach 13.

Section B27: Section B27 is currently bounded by 1250 feet wide levees completed prior to 1992. In 1954, the low flow channel width was 415 feet. By 1977, the channel had widened to 621 feet.

Section B28: Section B28 is currently bounded by 1100 feet wide levees completed prior to 1992. In 1954, the low flow channel width was 707 feet. By 1977, the channel had widened to 847 feet.

5.5.1.1.14 Reach 14

In Reach 14, the river was affected by levee construction, movement of braids, and widening during the 1980 flood. Two index sections were defined for Reach 14.

Section B29: A braided compound channel exists at Section B29. In 1954, the braided high flow channel was 2125 feet wide. By 1977, the width had increased slightly to 2454 feet wide.

By 1985, the braided channel changed to a more compound pattern with distinct 328 feet wide low flow channel within a 1245 feet wide high flow channel. The width changes were equally distributed on both sides of the channel. By 1992, the channel had been confined by a levee on the right bank, built in roughly the same position as the right bank in 1985. The 1992 high flow channel was 1003 feet wide. By 1999, the high flow channel was 1230 feet wide, including the left overbank area.

Section B30: A braided pattern existed at Section B30 in 1954 and 1977. The high flow channel width narrowed from 2800 feet in 1954 to 1107 feet in 1977, with most of the narrowing occurring on the left side of the channel and the right bank remaining in the same location. The high flow channel width expanded by 1985, with a 1605 feet wide main channel, and a high flow channel width of 2823 feet, including the left overbank. The right bank levee built prior to the 1992 photographs terminates just downstream of this cross section. The channel widths increase only slightly between 1992 and 1999. In 1992 the main channel is 410 feet wide with a left overbank that increases the high flow channel width to 1408 feet. In 1999, the main channel is 422 feet wide with a left overbank that increases the channel width to 1430 feet.

5.5.1.1.15 Reach 15

Reach 15 is located within the geologic floodplain of the Gila River. The river has narrowed in Reach 15, after dramatically widening during the 1980 flood. One index section was defined for Reach 15.

Section B31: In 1954, the low flow channel at Section B31 was 362 feet wide. By 1977, the low flow channel was 308 feet wide. After the 1980 flood, the 1985 photographs indicate that the low flow channel was 1053 feet wide. The channel position in 1954 and 1977 was located in the east half of the wider 1985 channel. After 1985, the channel narrowed to 313 feet in 1992 and 245 feet in 1999. The new, narrower channels were located on the right, or west, side of the former 1985 channel.

5.5.1.1.16 Summary

The average width of the high flow channel in the study reach generally decreased from 1954 to 1999, from 1696 feet in 1954 to 968 feet in 1999. However, this decrease does not account for either the movement of the low flow channels within the high flow channel, the movement of the high flow channel itself, or the channel widening that occurred during the 1980 flood. The 1954 to 1999 aerial photographs indicate that the low flow channels shifted over the entire width of the Holocene floodplain in some locations, shifted within the high flow channel, changed their number, width, and pattern, eroded portions of the Pleistocene-aged terraces, and widened by up to an order of magnitude during the 1980 flood. The maximum measured long-term movement and/or widening was over 2,000 feet. The analysis indicates that the most significant channel movement occurs during large floods. Channel erosion measured during the 1980 flood is summarized in the following section of this chapter.

5.5.1.2 Historical Channel and Bank Positions

Channel thalweg and primary bank positions were digitized from each of the 13 individual years of aerial photography coverage, from the GLO surveys, and the 1903 topographic mapping. Plots of thalweg position are shown on the Historical Thalweg and Bank Locations Map in the Exhibits Map Book. The plots of thalweg position shows that the channel has moved back and forth across most of the geologic floodplain during the past 100 years in response to floods and human impacts. The limits of the channel thalweg and banks were generally contained between the lowest Pleistocene terrace boundaries (Section 5.1), indicating that the Agua Fria River has been laterally active within the limits defined by these terraces.

The river has not occupied the entire geologic floodplain in only in two places in the study reach during the period of record. In both cases, human activities have restricted the river's natural erosive potential. One such exception occurs in Section 12, T 3N, R1W just upstream of Grand Avenue. The active channel has remained outside of a portion of the geologically young (Holocene) surface since at least 1903, probably due to the impact of the ATSF Railroad embankment which was built in 1895, and which fixed the river position at the location of the bridge section. The ATSF bridge also greatly constricted the otherwise wide channel, and probably lowered the channel bed. Bed lowering created a condition where higher (and hence less frequent) discharges are required to overtop the banks and cause avulsions, thus reinforcing the channel's planimetric position. The other exception to movement of the channel over the entire geologic floodplain is within the reaches downstream of the New River that are now controlled by the Corps of Engineers levees. Engineering works built in the mid-1980's have confined the river to a much narrower corridor than the river utilized during the past 10,000 years.

The large magnitude and rapid rate of channel movement expressed by the thalweg position plots in the Exhibits Map Book indicate the high potential for future lateral movement of the Agua Fria River within the study reach. Several thousand feet of lateral movement is recorded for most of the study reach during the past 100 years. While construction of upstream reservoirs probably reduced the frequency of lateral channel movement that will occur in the future, the magnitude of future lateral movement probably remains unchanged over any reasonable long-term planning period.

5.5.2 Single event changes

Historical and field evidence suggests that most of the channel change on the Agua Fria River will occur during significant flood events. Each large flood event on the Agua Fria River has the potential to change the morphology, position, and character of the river channel. To understand the potential for channel change during a single flood, channel characteristics were measured on aerial photographs from before and after the 1980 flood, one of the largest known events during the period of record. To complete the single-event analysis, aerial photos from 1979 (pre-flood) and 1980 (post-flood) were rectified using common coordinates and features. Channel banks were delineated on both the 1979 and 1980 photos, and then compared for changes in width, and bank movement at either the right or left bank. The spatial extent of the comparison of channel characteristics was limited to the extent of the 1979 aerial photos, which cover the channel from just upstream of Jomax Road to the confluence with the Gila River.

In general, the channel of the Agua Fria River widened during the 1980 flood. Actual width changes varied greatly within specific reaches. Thus, the average distance of lateral movement has little meaning, and results for individual cross sections are reported for the index sections used for the long-term channel movement analyses (Table 5-2). Analysis of individual sections, however, do indicate some general trends in lateral movement. The main channel rarely moved laterally to the left (east) in Reaches 6 through 8, most likely due to the proximity of the Pleistocene-aged terrace. The largest amount of lateral bank movement occurred along reaches with low banks formed in the geologically youngest material downstream of Reach 8. The maximum amount of channel widening during the 1980 event was approximately 1100 feet, at Section B25 in Reach 11. In Reach 10, levees around sand and gravel mines and the Pleistocene terrace limit the channel width. However, during the 1980 flood, the river bypassed the levees and flowed through the gravel pit, indicating that some of the less well-engineered structures should be considered geologically temporary features.

Table 5-2 Single-Event Channel Widening: Agua Fria River, 1980 Flood

Cross Section	1979 width (feet)	1980 width (feet)	Expansion right (feet)	Expansion left (feet)	Comments
Reach 6: Jomax Road to Beardsley Road alignment					
10	2308	2596	286	0	1979 width includes 2 ROB channels each ~130 ft wide
11	2970	3341	372	0	Alterations in width and prominence of interior channels
12	981	1026	45	0	Avulsion channel on ROB after 1980, 86 ft wide; right bank 1152 ft from right bank main channel
Reach 7: Beardsley Road alignment to Bell Road					
13	unknown	2968	unknown	0	1979 photo incomplete – shows left bank only
14	unknown	2378	unknown	0	1979 photo incomplete – shows left bank only
Reach 8: Bell Road to Cactus Road alignment					
15	969	1166	197	0	Terrace cliffs on left; no change in 2nd channel in ROB ~340 ft wide
16	158	169	11	0	Terrace cliff on left; channel confined by mining operation berm on right bank
17	345	910	345	218	
Reach 9: Cactus Road alignment to Olive Avenue					
18	746	1171	67	358	
18/19	164	1251	507	495	Maximum widening in reach
19	267	929	519	142	
Reach 10: Olive Avenue to New River confluence					
20	227	478	0	251	
21	152	152	0	0	Confined by terrace and mining operation berm; flow into and out of mining pit
22	165	165	0	0	Confined by terrace and mining operation berm; flow into and out of mining pit
23	541	562	0	21	
Reach 11: New River confluence to Indian School Road					
24	712	1485	214	555	
25	1268	2369	1101	0	Maximum widening on river
Reach 12: Indian School Road to Interstate 10					
26	740	824	45	36	
27	382	472	90	0	
27/28	447	1089	0	642	Cutbank erosion upstream of I-10
Reach 13: Interstate 10 to Buckeye Road					
28	634	638	0	4	
29	328	873	339	206	
Reach 14: Buckeye Road to Broadway Road alignment					
30	734	1331	478	119	
31	650	1613	562	402	Maximum widening in reach
Reach 15: Broadway Road alignment to Gila River					
32	633	1743	1082	27	Maximum widening in reach

5.5.3 Summary

In general, the active low flow channel widened during the 1980 flood. The maximum lateral movement measured at the index sections was 1100 feet, which occurred in Reach 11. Lateral movement was precluded by the presence of engineered bank protection, or was partially limited by the resistance of Pleistocene terraces in many locations, reinforcing the conclusion that the older terraces represent a realistic physical barrier to rapid long-term erosion.

While smaller floods are not capable of causing the large lateral variations in channel position shown in Historical Thalweg and Bank Locations plot in the Exhibits Maps Book, larger floods are capable. Although the magnitude and frequency of flood discharges has been greatly reduced by the New Waddell Dam, discharges larger than bankfull discharge (Chapter 6) will still occur in the future. These relatively infrequent, large floods are capable of causing the same types of significant changes in channel thalweg and bank locations as have been experienced in the past.

5.6 Vertical movement

5.6.1 Long-term changes

Long-term changes in the bed elevation of the Agua Fria River were investigated by comparing longitudinal profiles of the river from different time periods, interpreting historical aerial photographs, and comparing cross sections from previous flood insurance study hydraulic models and historical topographic mapping.

5.6.1.1 Longitudinal Profiles

The interpretation and comparison of longitudinal profiles reveals changes in channel slope or stream bed elevation that may have occurred along the river. Changes in the channel slope may indicate adjustments to hydrologic changes or human activity. Degradation or aggradation of the channel bed can also be determined from the comparison of longitudinal profiles.

Data Sources. Four sources for topographic coverage were used in the profile analysis:

1. Davis, A.P., 1904, Salt River Valley Arizona, Topographic and Irrigation Map, surveyed in 1903, contour interval = 5 ft. Map No. 4896, Sheet 2 of 4.
2. United States Geological Survey (USGS) 7.5 minute Topographic Quadrangles. Topography was compiled from varying aerial photographic sources, specified on a given 7.5 minute map. North American Datum (1927). Full coverage is available.
   - Tolleson, AZ: Culture and Drainage compiled from aerial photographs taken 1954. Topography by plane table surveys 1957. Contour interval = 5 Feet.
   - El Mirage, AZ: Culture and Drainage compiled from aerial photographs taken 1954. Topography by plane table surveys 1957. Contour interval = 5 Feet.
   - Calderwood Butte, AZ: Topography by photogrammetric methods from aerial photographs taken 1954 and by plane table surveys 1957. Contour interval = 10 Feet.
   - Baldy Mtn., AZ: Topography by photogrammetric methods from aerial photographs taken 1962. Field checked 1964. Contour interval = 20 Feet.
3. Corps of Engineers, U.S. Army, Los Angeles District, California, 1968: "Flood Plain Information, Agua Fria River." Topography was compiled January 1964 and July 1965.

Contour interval = 5 feet. USC & GS Datum. Partial coverage is available, from Camelback Road upstream to lower Waddell Dam.

4. Jerry Jones & Associates: "Agua Fria River Flood Insurance Study." Topography was compiled 1988. Contour interval = 4 feet. Coverage from Gila River confluence to Indian School Road, and from Jomax Road upstream to lower Waddell Dam.
5. Coe and Van Loo Engineering: "Agua Fria River – Jomax to Indian School." Contour Interval = 2 feet. Coverage from Jomax Road downstream to Indian School Road.

Methodology. The profile analysis described below is a general assessment of the entire Agua Fria River study reach. Elevation data was selected at half-mile increments along the river, so that specific locations could be compared at even intervals. Section lines found on the USGS 7.5 minute Quads were used to locate data points at one mile increments, and half-mile points were interpolated between section lines. The data points are referred to as the "locations" on the x-axis in Figure 5-7.

Sample locations recorded on the USGS maps were then used as a base for locating identical points on the other data sources described above. Where channelization has occurred or where the river is disturbed by in-channel sand and gravel mining, the bed elevation data was taken from the existing "main channel," where the "main channel" is defined as the channel that carries the majority of flow. In some cases, especially in the downstream reaches of the Agua Fria River, roads or bridges obscure the natural topography along the section lines and 'Mile Marker' points. In these situations the data point was read from the channel bottom immediately downstream of the road crossing.

Analysis. Figure 5-7 shows a comparison of the historical longitudinal profiles for the Agua Fria River. Due to the large elevation range over the length of the study area, the presence or magnitude of any changes is difficult to detect in Figure 5-7. Therefore, plots are also included for each individual reach, with a discussion of the vertical changes observed in each reach. However, a few observations from the overall plot in Figure 5-7 can be made:

- The 1995 data indicate that the bed elevations are measurably lower in 1995 than in previous years in the Middle Reach, which extends from the New River to about Bell Road. This reach contains the most active sand and gravel mining, floodplain encroachment, and bridge construction.
- There is an abrupt change in slope near Greenway Road due to in-stream mining.
- The profile has an overall slightly concave up shape that becomes more strongly concave up in the Middle Reach during the period of record.

Table 5-3 shows a summary of the maximum long-term scour and aggradation during any time period for each study reach, as measured from the historical topographic data. The magnitude of long-term scour is greater than the magnitude of aggradation in almost every reach. Note that values less than five feet are generally within the accuracy of the topographic data sets (i.e. +/- 2.5 ft for 5 ft contour interval data).

The most significant scour was measured in Reaches 7 – 13. For reaches 7-11, much of the measured long-term scour is due to direct excavation of the channel for sand and gravel mining. In Reaches 12 and 13, the channel was relocated and straightened somewhat in the mid 1980's, which may be responsible for the lowering of the bed elevation shown by the longitudinal profile comparisons.

Table 5-3 Maximum Aggradation & Scour as Shown By Comparison of Longitudinal Profiles

Reach	1	2	3-6	7	8	9	10	11	12,13	14	15
Maximum Aggradation (ft)	0	1	4	4	0	0	2	2	0	3	2
Maximum Scour (ft)	17	7	3	13	10	7	11	8	8	6	1

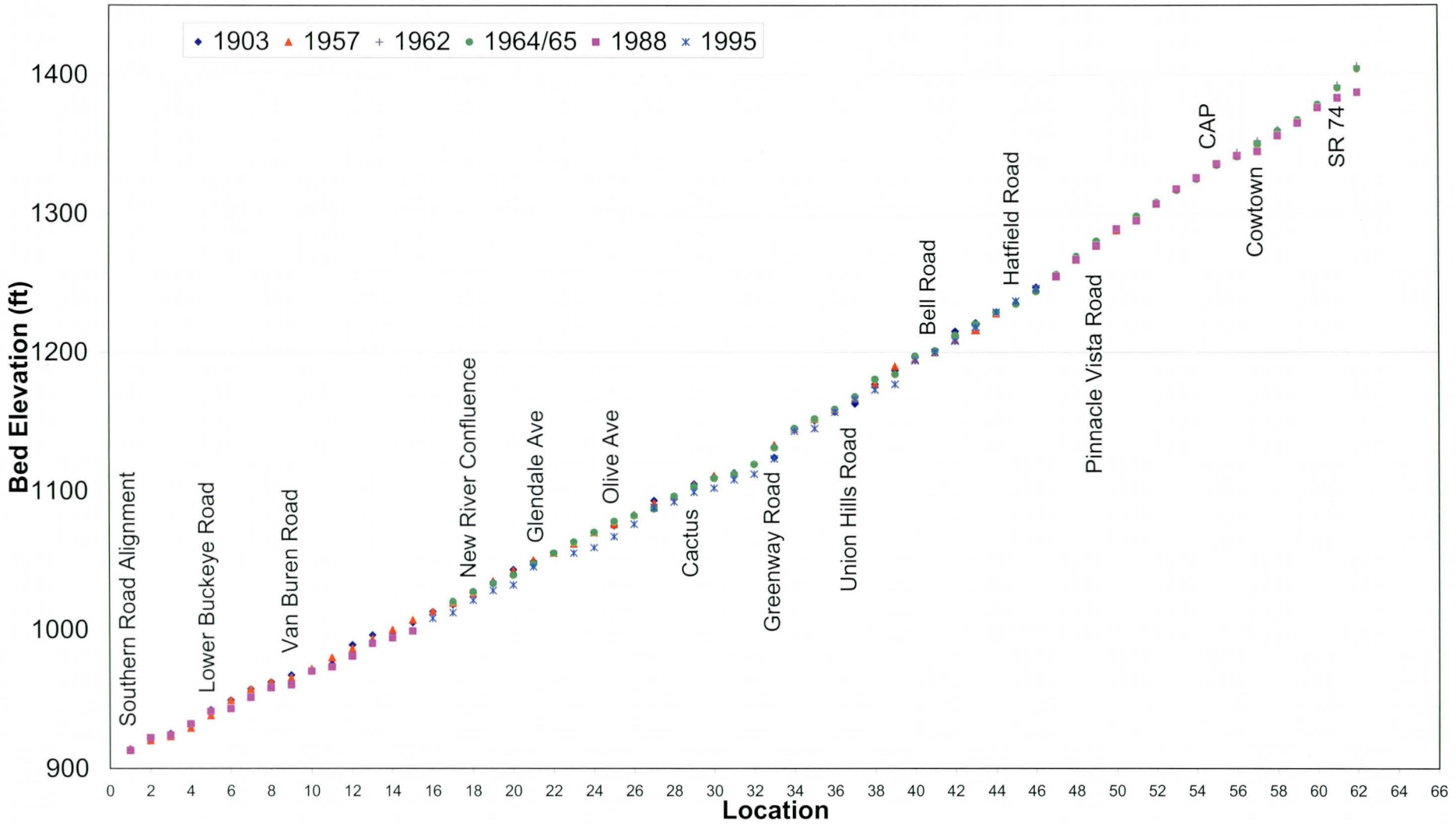

Figure 5-7 Comparison of Longitudinal Profiles Over Time

A discussion of reach-by-reach changes follows. The "locations" referred to on the x-axis of each figure are in half-mile increments from the Gila River confluence.

Reach 1. Figure 5-8 shows a significant decrease in bed elevation between the 1960's and 1988. Because Reach 1 is located immediately downstream of New Waddell Dam, and because two significant floods occurred during this period, channel degradation is expected. Field observations of numerous bedrock outcrops in Reach 1 suggest that further degradation of Reach 1 will be limited by bedrock.

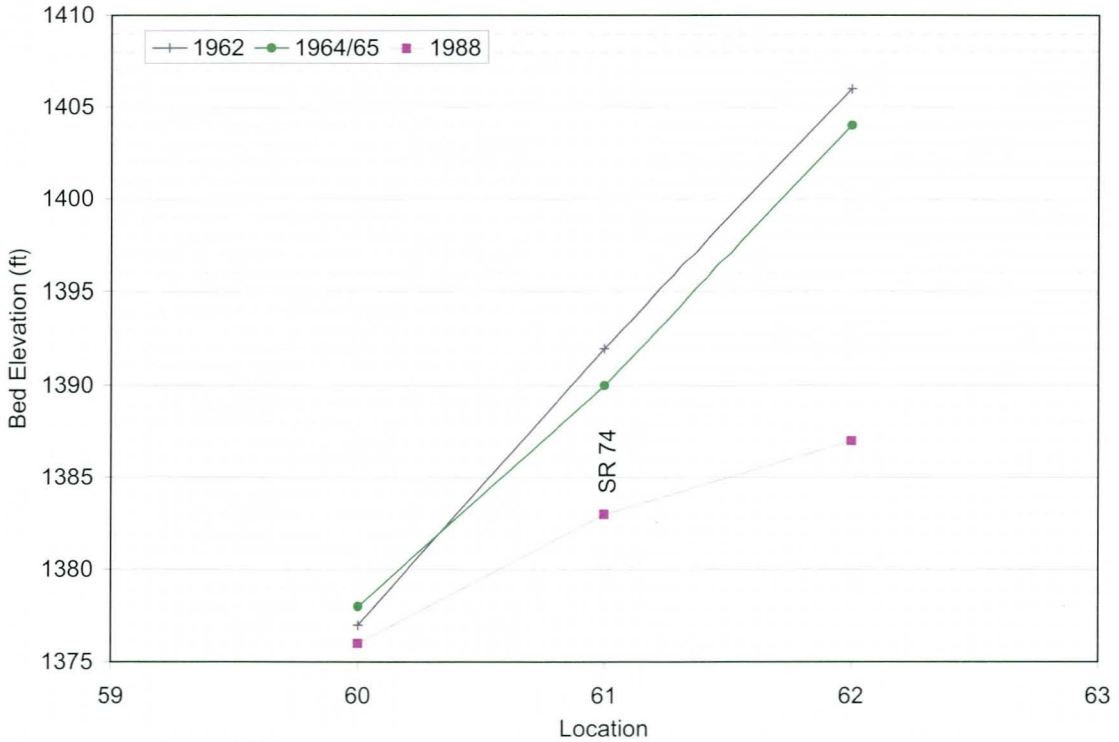

Figure 5-8 Reach 1 Historical Longitudinal Profiles

Reach 2. Figure 5-9 shows bed elevation changes in Reach 2. Many of the overall changes are within the error of the topographic data, although a consistent general trend of degradation is depicted. Near Cowtown, Figure 5-9 shows 7 feet of bed lowering between 1962 and 1988. Historical aerial photography suggests that prior to 1985 the channel divided upstream of the data point, and thus a large amount of flow was being distributed through two different channels. Presumably following the 1978 and 1980 floods the majority of flow was concentrated in the left channel, which may have caused the bed to scour and degrade.

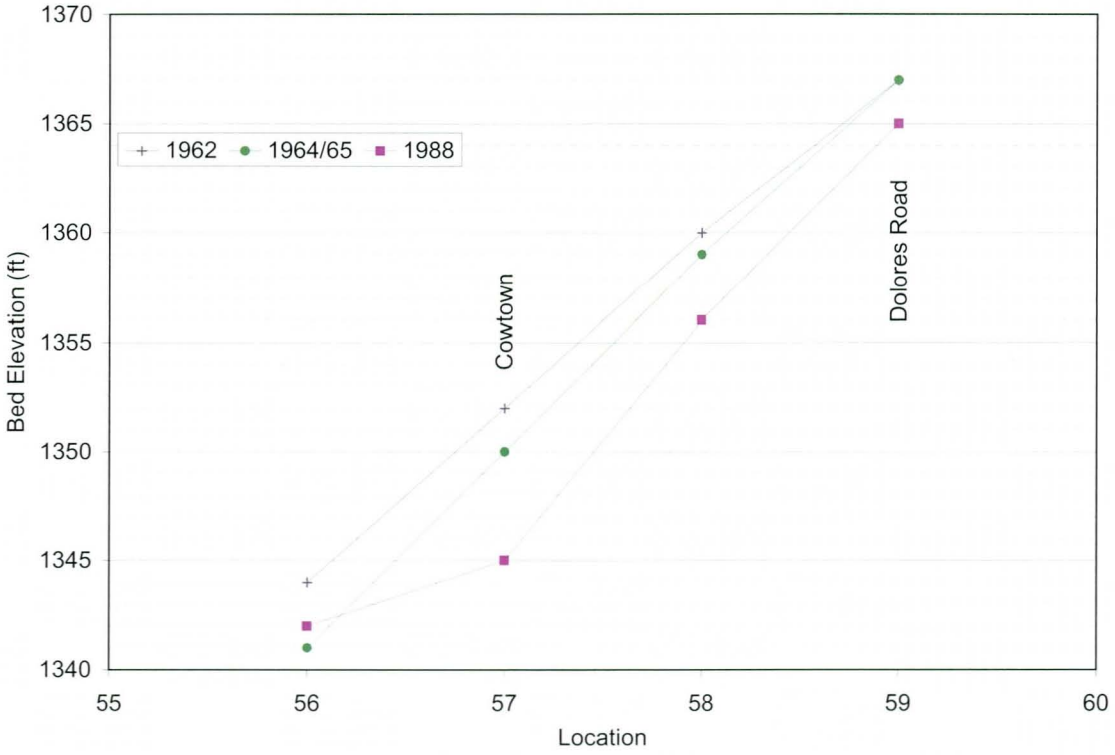

Figure 5-9 Reach 2 Historical Longitudinal Profiles

Reaches 3 to 6. Figure 5-10 shows bed elevation changes in Reaches 3-6. These reaches were considered together because no significant elevation changes were detected during the period of record. The differences in bed elevation between 1957/62,1964/65, 1988, & 1995 shown in Figure 5-10 are all within the error of the topographic data, and therefore, cannot be reliably interpreted as any specific trend in vertical stability. The river is also generally much wider in these reaches than upstream. Therefore, adjustments of the channel morphology may have been expressed horizontally rather than vertically, as suggested by the historical data presented in Section 5-25.5.

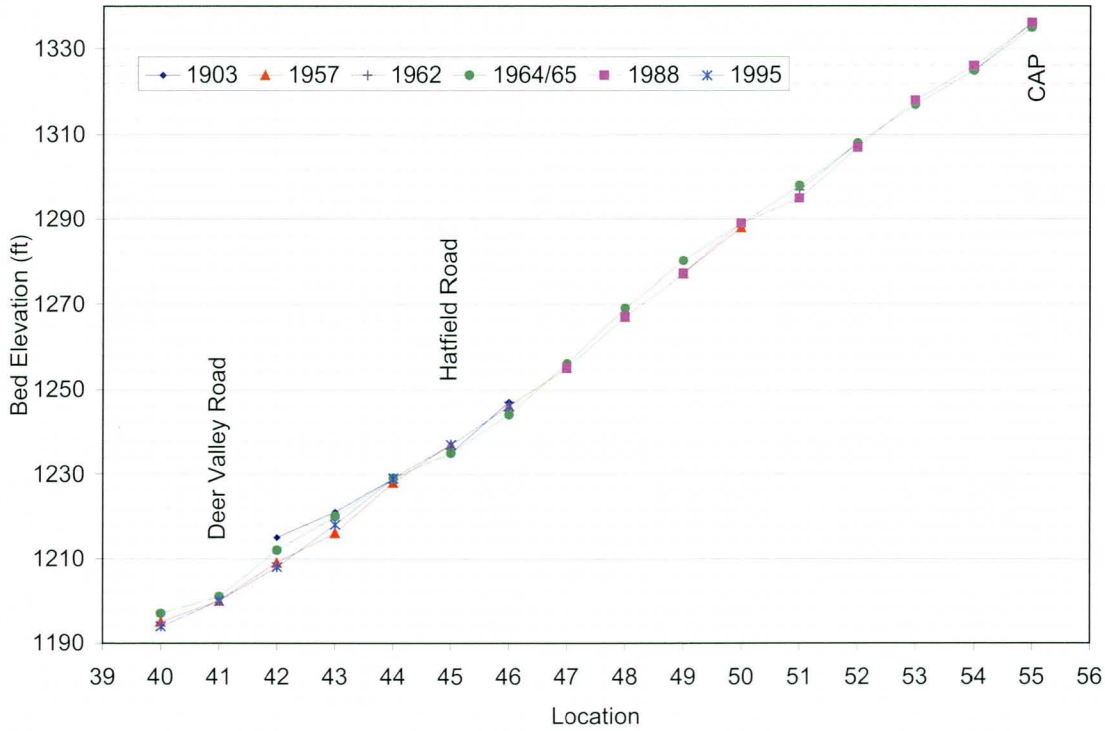

Figure 5-10 Reach 3, 4, 5, & 6 Historical Longitudinal Profiles

Reach 7. Figure 5-11 shows bed elevation changes in Reach 7. Reach 7 has experienced encroachment of the floodplain by development and sand and gravel mining beginning around 1977. Construction of a golf course and residential development on the eastern side of the channel in the mid 1980's narrowed the channel in the upstream direction. The Bell Road bridge was also constructed at the downstream limit of Reach 7 between 1964 and 1967, and then rebuilt following its failure during the 1980 flood. Figure 5-11 shows that the upstream portion of Reach 7 experienced more significant long-term scour than the downstream portion. The greater long-term scour at the upstream end of Reach 7 may be the result of clear-water scour created by the effects of sediment trapping in the gravel pit upstream, or by narrowing of the channel by diversions around the mine. The historical topographic data show 7 to 13 feet of bed lowering in the upper portion of Reach 7.

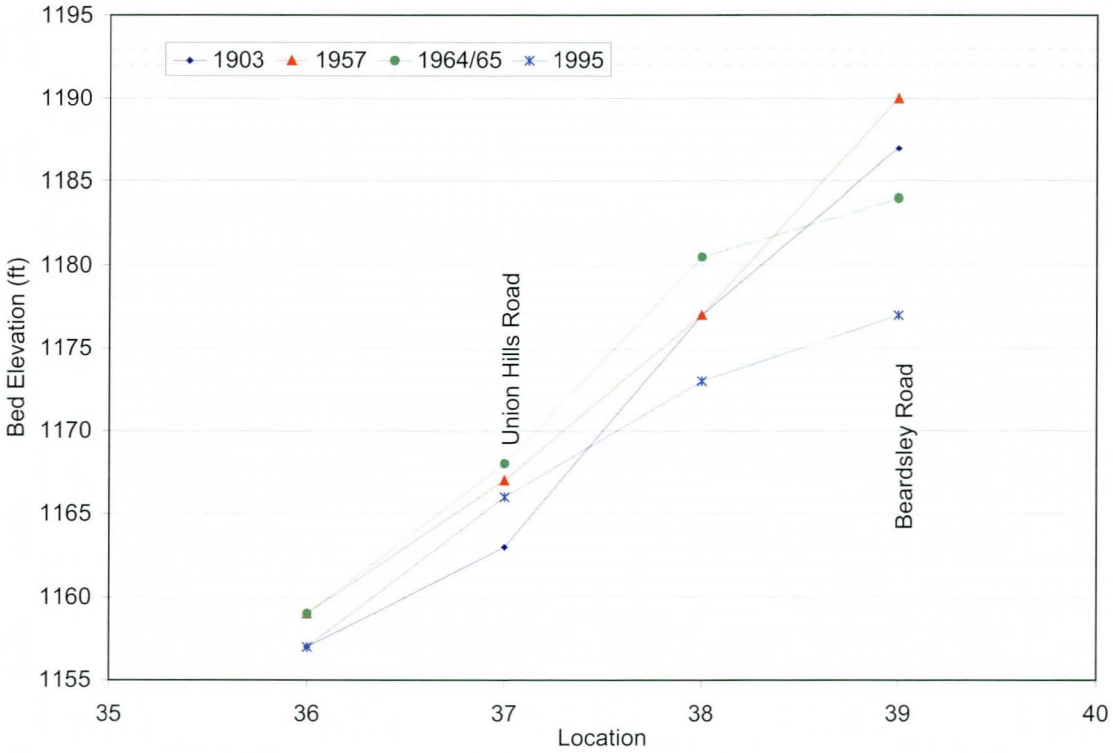

Figure 5-11 Reach 7 Historical Longitudinal Profiles

Reach 8. Reach 8 has been heavily impacted by in-channel sand and gravel mining. Figure 5-12 shows significant lowering in much of the reach. The narrow Grand Avenue/AT&SF railroad bridges are also located in Reach 8 near location 31. In 1964, before gravel mining began on the upstream portions of Reach 8, the channel was wider than it is today, and flow was more evenly distributed between several smaller low flow channels. However, by 1997 the entire eastern side of the high flow channel in the upstream portion of the reach had been excavated for a sand and gravel mine. During construction of the Bell Road Bridge, fill material was added, narrowing the original channel width about 50 percent (Figure 5-13 and Figure 5-14). Similarly, the ATSF railroad bridge, built in 1895, significantly narrowed the channel in Reach 8. The removal of bed material and the narrowing channel at the two bridges contributed to degradation of the bed elevation.

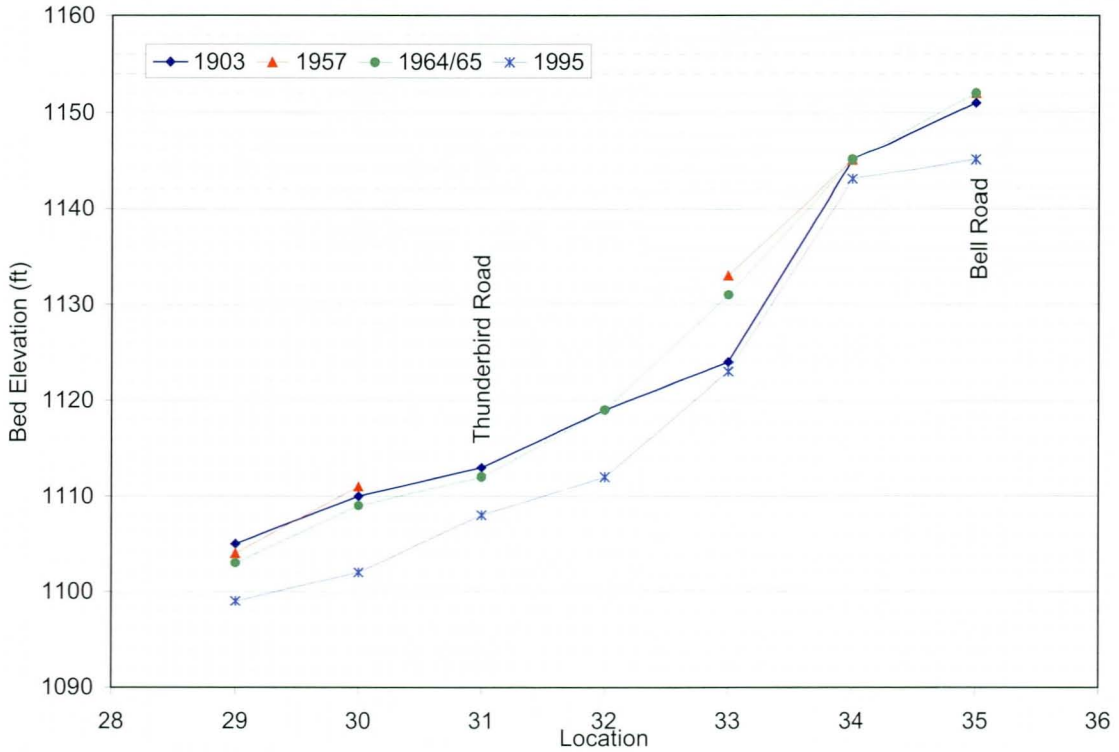

Figure 5-12 Reach 8 Historical Longitudinal Profiles

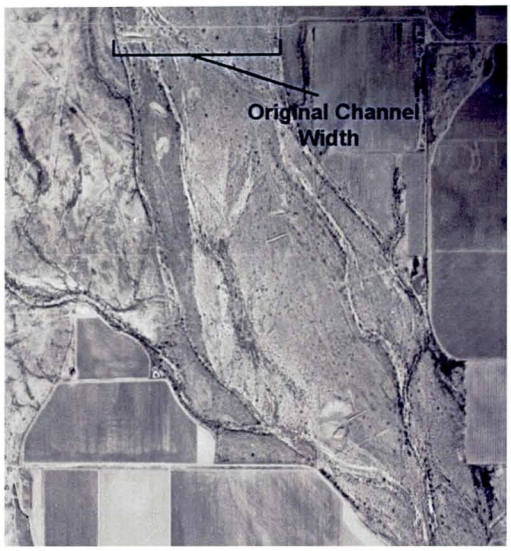

Figure 5-13 Reach 8, 1964

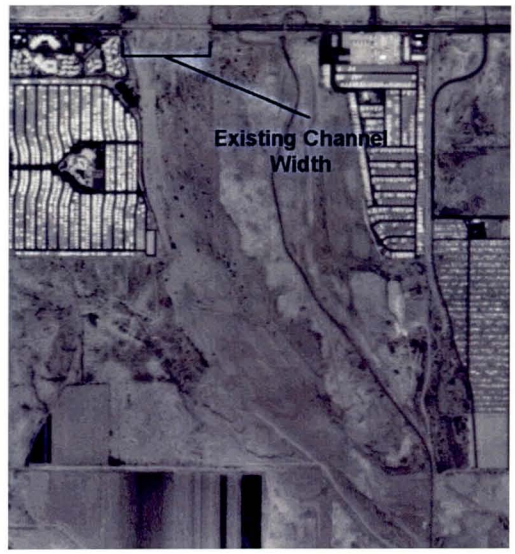

Figure 5-14 Reach 8, 1997

Reach 9. Figure 5-15 shows the bed elevation changes for Reach 9. In-channel sand and gravel mining and bridge encroachment in Reach 8 forced flow to the west side of the floodplain away from the historical flow path. In addition, construction of the Cholla Landfill just upstream of Reach 9 between 1980 and 1985 cut off one of the two low flow channels, leaving just the eastern channel to carry most discharges. This cutoff, together with the effects of the sand and gravel mining and bridge constrictions, may be the cause of the lowering of bed elevations shown in Figure 5-15.

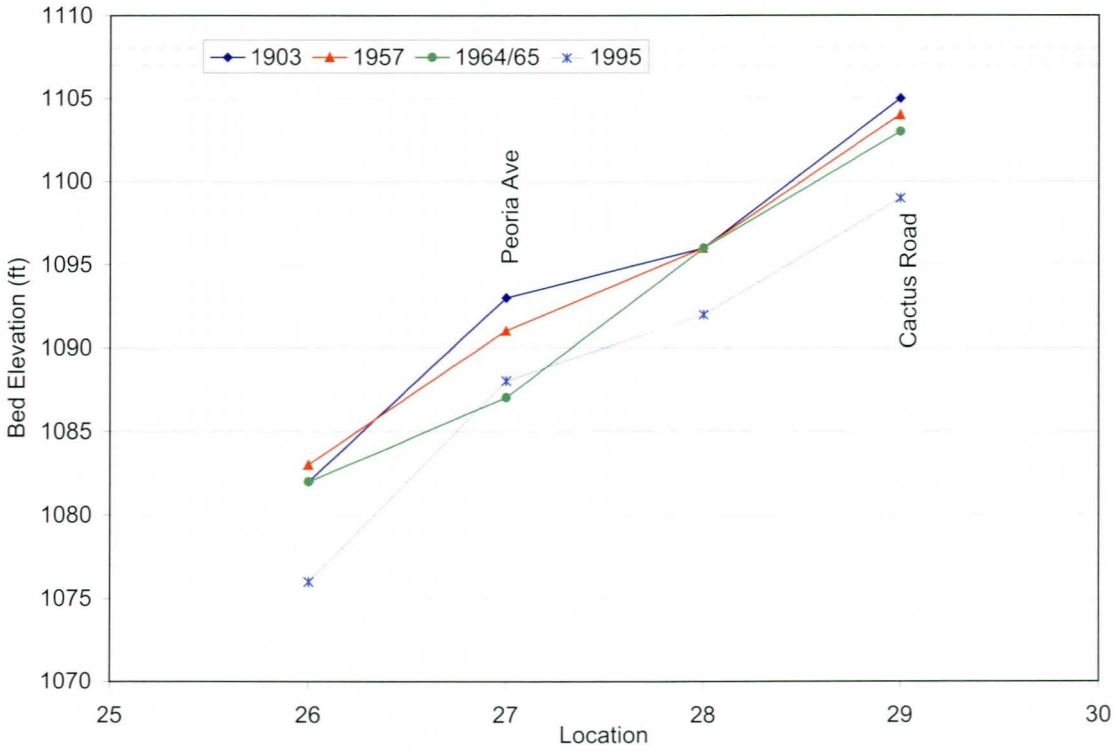

Figure 5-15 Reach 9 Historical Longitudinal Profiles

Reach 10. Figure 5-16 shows bed elevation changes in Reach 10. From 1903 to 1965, the data indicate that bed elevations were essentially unchanged. However, between 1964/65 and 1995, the bed elevation dropped significantly throughout Reach 10. The period of channel degradation is coincident with the period of in-channel sand and gravel mining, urbanization, and floodplain encroachment. Between 1957 and 1995 gravel mining has extended into the main channel, removing a large amount of sediment from the channel bed. The portion of the channel around Glendale Avenue was mined as early as 1949, as indicated on the aerial photographs of the reach. The floodplain was also encroached by bridges at Olive Avenue and Glendale Avenue between 1985 and 1992 and 1967 and 1977, respectively. The floodplain encroachment by these bridges may have also contributed to the lowering the bed elevation in Reach 10. Field evidence supports the five to six feet degradation estimate made by comparing the topographic mapping.

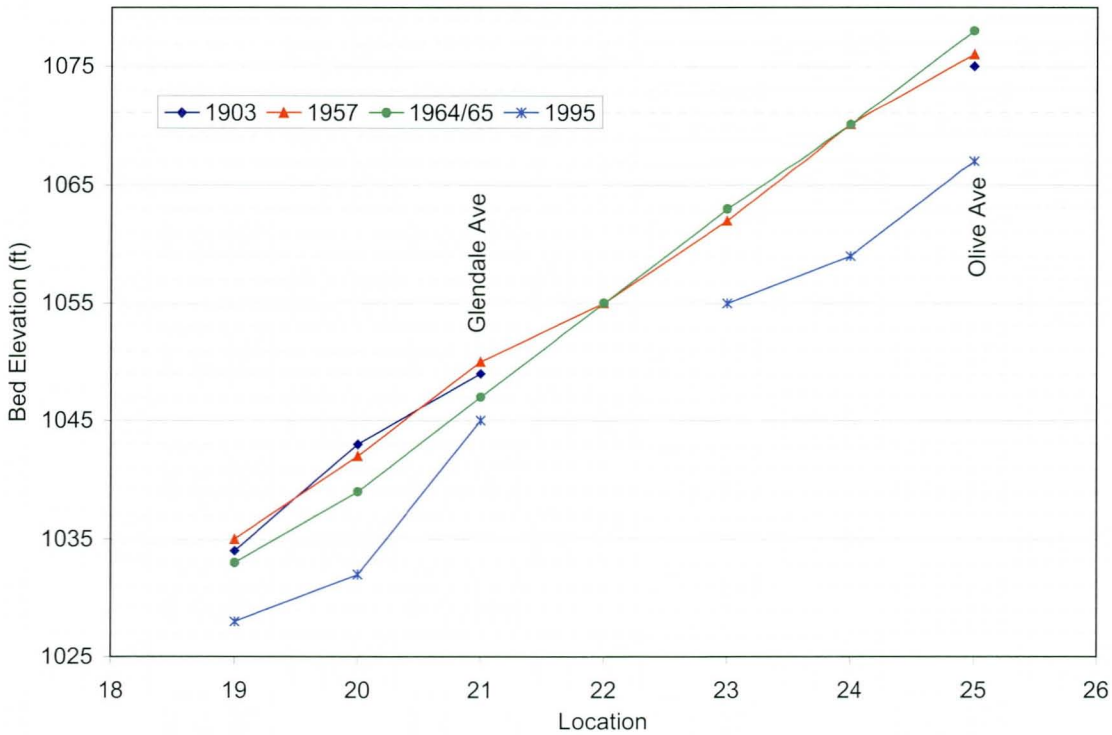

Figure 5-16 Reach 10 Historical Longitudinal Profiles

Reach 11. Figure 5-17 shows bed elevation changes in Reach 11. Significant lowering of the bed is also shown for Reach 11, and is supported by field observations of bed lowering. Significant sand and gravel mining has taken place in the main channel downstream of Camelback Road. Also, construction of upstream dams, diversion of Cave Creek into New River by the ACDC, and urbanization of the New River watershed have increased the duration and frequency of clear-water discharge in Reach 11. The combination in-stream mining and watershed impacts is probably responsible for the degradation of the channel bed in Reach 11.

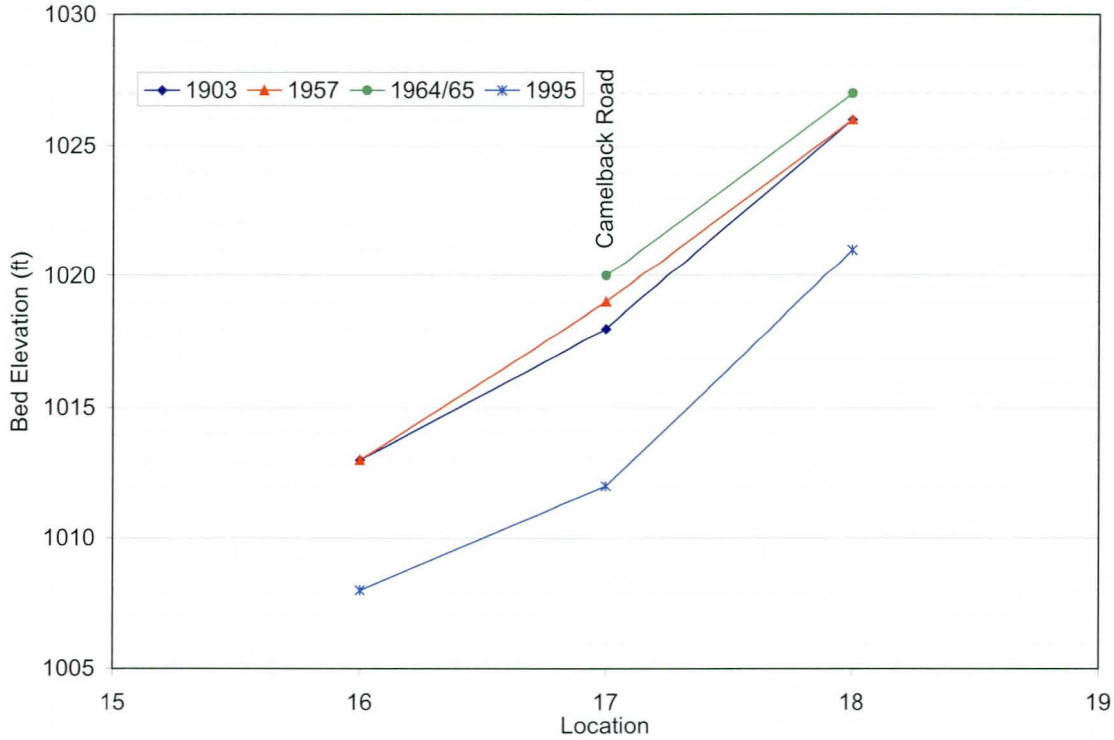

Figure 5-17 Reach 11 Historical Longitudinal Profiles

Reaches 12 &13. Figure 5-18 shows bed elevation changes in Reaches 12 and 13. The channel was shortened about 1,500 feet between Thomas Road and Interstate 10 in the mid 1980's prior to the 1988 topography shown in Figure 5-18. The changes in bed elevation shown are likely due primarily to the channelization of the reach associated with construction of the Corps of Engineers' levees. Figure 5-19 and Figure 5-20 show the changes in channel conditions due to channelization in Reach 13. Degradation of the channel bed due to levee was expected by the Corps, and was addressed by construction of several grade control structures that span the channel between the levees.

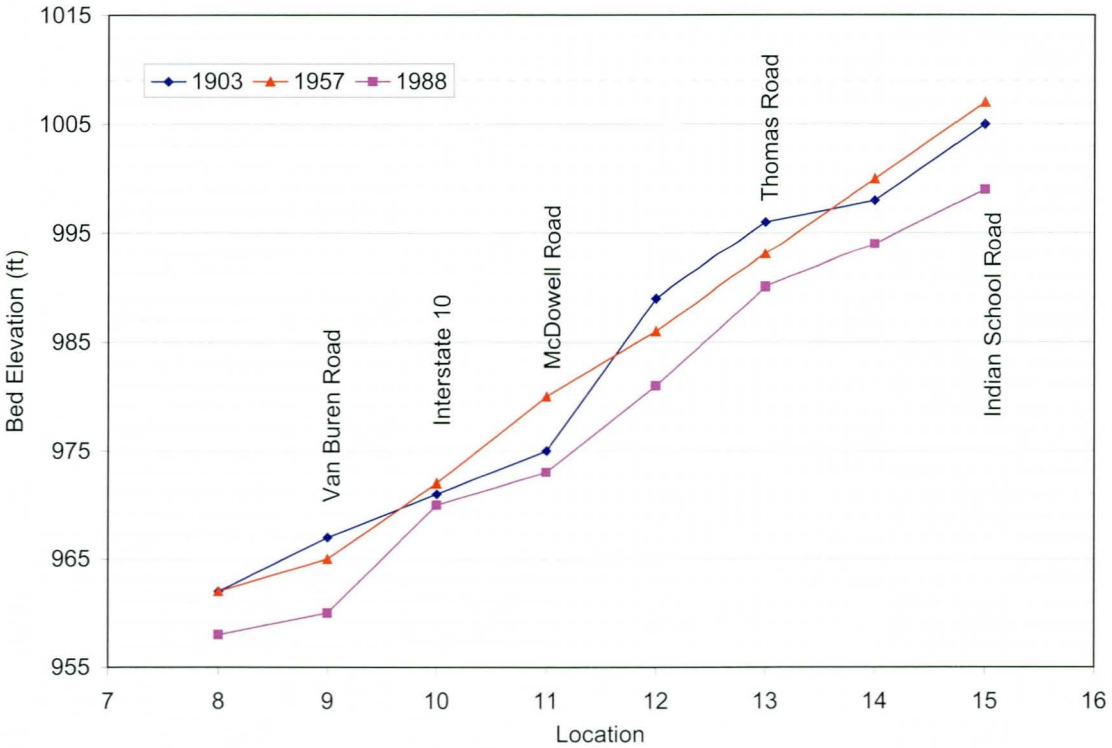

Figure 5-18 Reach 12 & 13 Historical Longitudinal Profiles

Figure 5-19 Reach 13, 1964

Figure 5-20 Reach 13, 1992

Reach 14. Figure 5-22 shows the bed elevation changes in Reach 14. The portion of Reach 14 upstream of Lower Buckeye Road experienced a significant degradation of the bed elevation between 1957 and 1988. The reach upstream of Buckeye Road was channelized and encroached upon prior to 1988 (Figure 5-19 and Figure 5-20). Furthermore, large angular riprap was installed beneath the Buckeye Road bridge at some point in time (Figure 5-21) in an attempt to prevent long-term scour from damaging the at-grade crossing. The aggradation seen downstream of Lower Buckeye Road probably resulted from deposition of the material transported from the channelized reaches upstream. However, it is noted that the data points at locations 4 and 5 are within the accuracy of the topographic data.

Figure 5-21 View of large angular riprap beneath Buckeye Road bridge

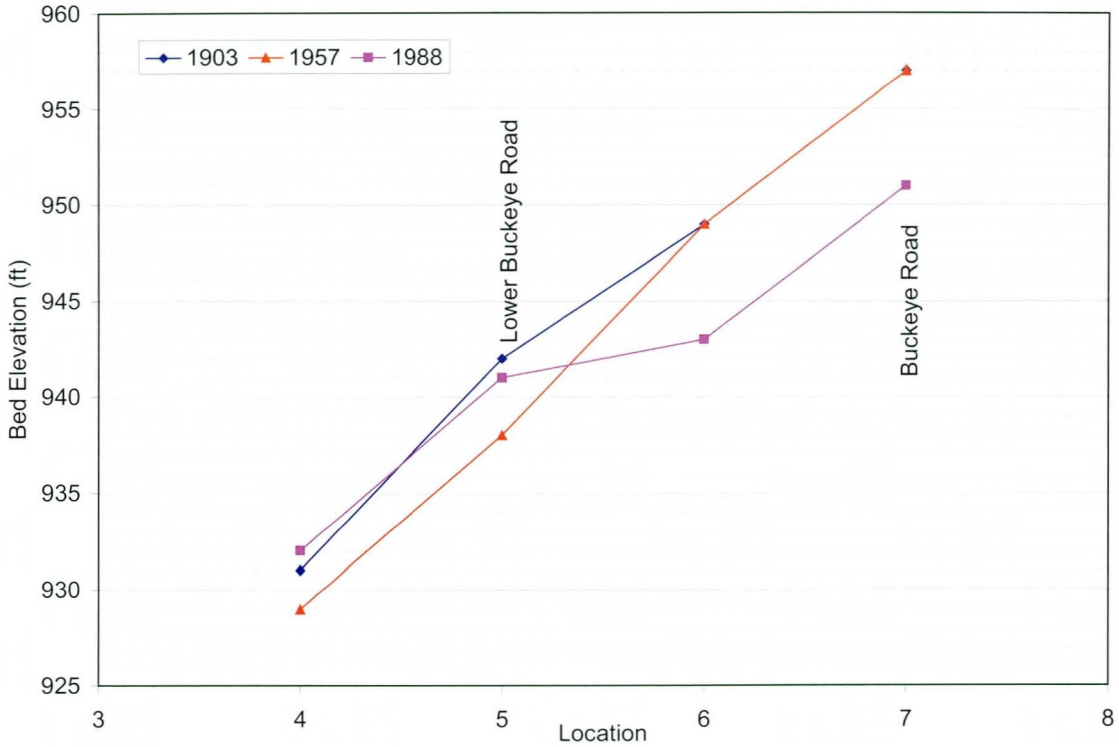

Figure 5-22 Reach 14 Historical Longitudinal Profiles

Reach 15. Figure 5-23 shows the bed elevation changes in Reach 15. The differences shown are all within the error of the topographic data, and no consistent trend is predicted by the data.

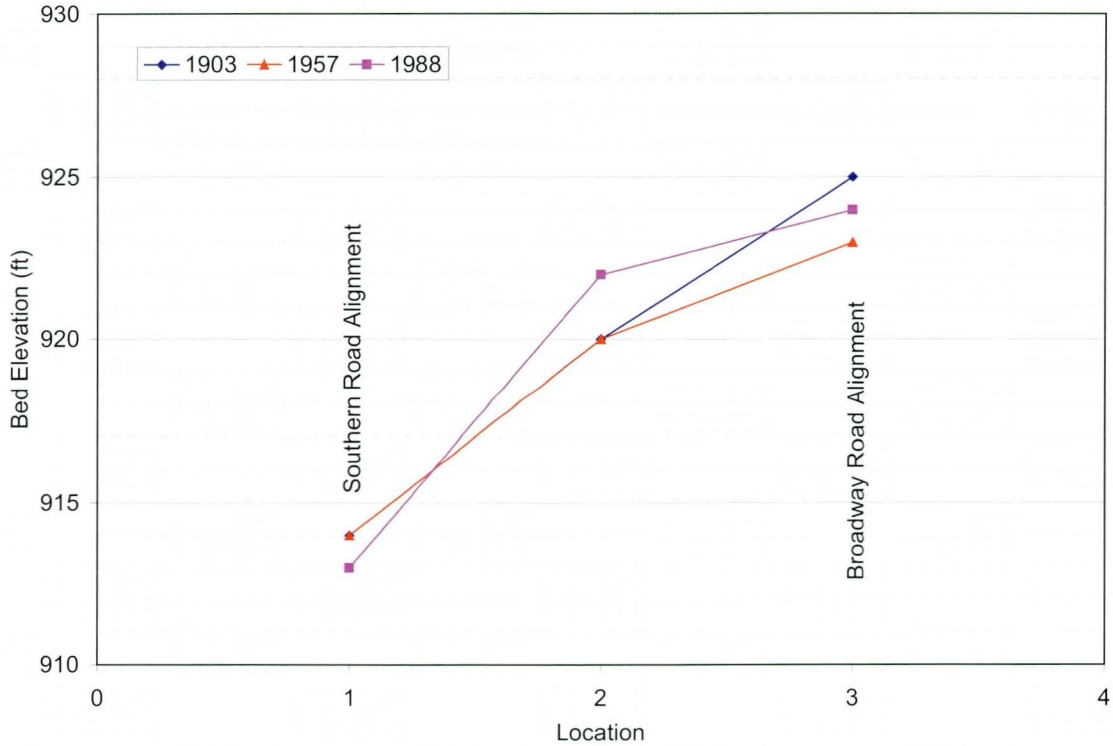

Figure 5-23 Reach 15 Historical Longitudinal Profiles

Summary. The examination of historical longitudinal profiles shows that changes in bed elevation have occurred in the Agua Fria River study reach between 1903 and 1995. In general, the data show either significant degradation of the channel or no measurable change. The reaches that show degradation are primarily in areas impacted by human activity. In particular, clear-water discharge from the dam, encroachments by bridges, channelization, and in-channel sand and gravel mining activity within the channel appear to be the primary causes of channel degradation. Channel bed degradation ranged from 0 to about 17 feet during the period of record, with the greatest measured changes occurring immediately downstream of New Waddell Dam and in Reaches 7 to 10.

5.6.2 Comparison of Cross Sections

The historical longitudinal profiles identified a number of areas with significant long-term degradation during the period of record. In these areas, cross sections from different time periods were compared to identify changes in channel morphology that may have accompanied the long-term degradation. Figure 5-24 through Figure 5-35 show comparisons at key locations along the study reach. The river mile stationing and reach number for each figure are given in the captions. Note that the 1903 data do not always span the entire cross section due to the limits of map coverage.

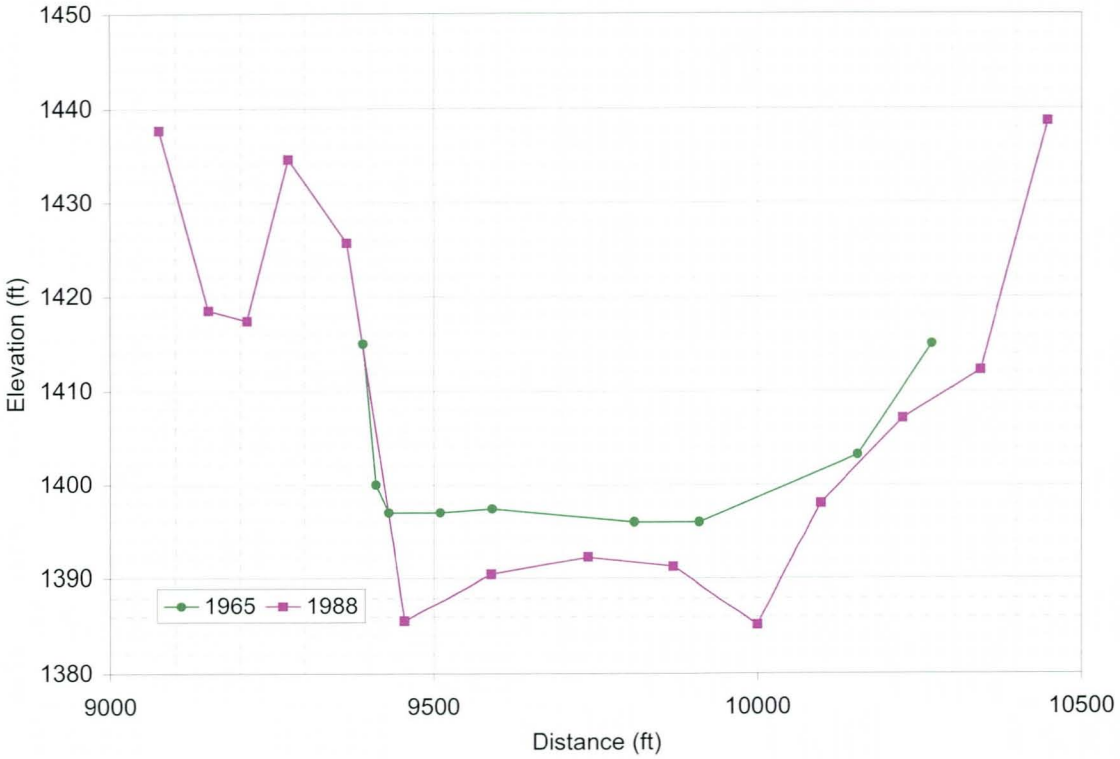

Figure 5-24 Reach 1, RM 33.25

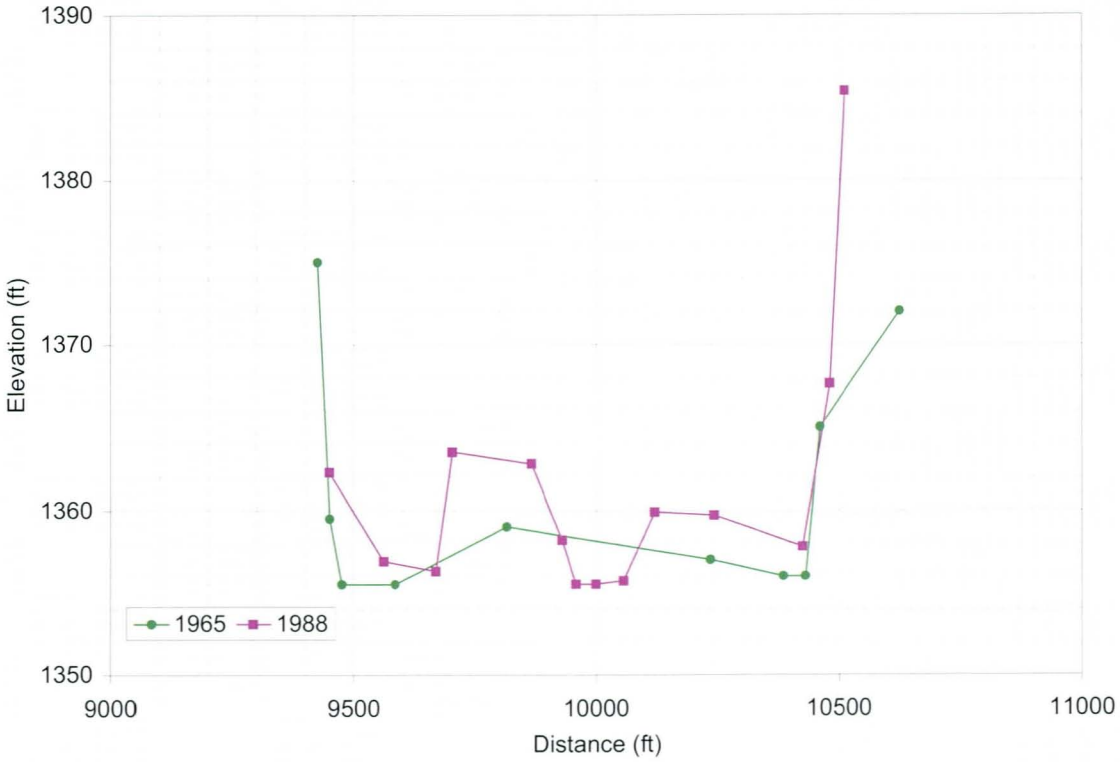

Figure 5-25 Reach 2, RM 31.29

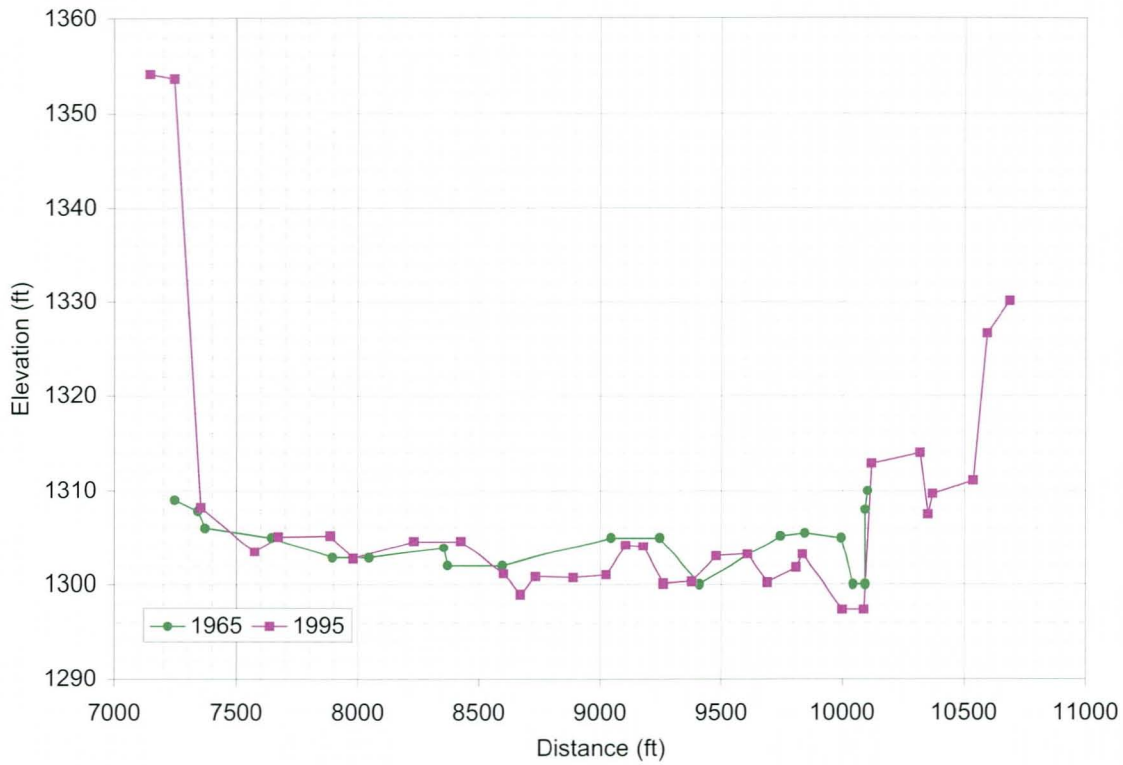

Figure 5-26 Reach 4, RM 27.77

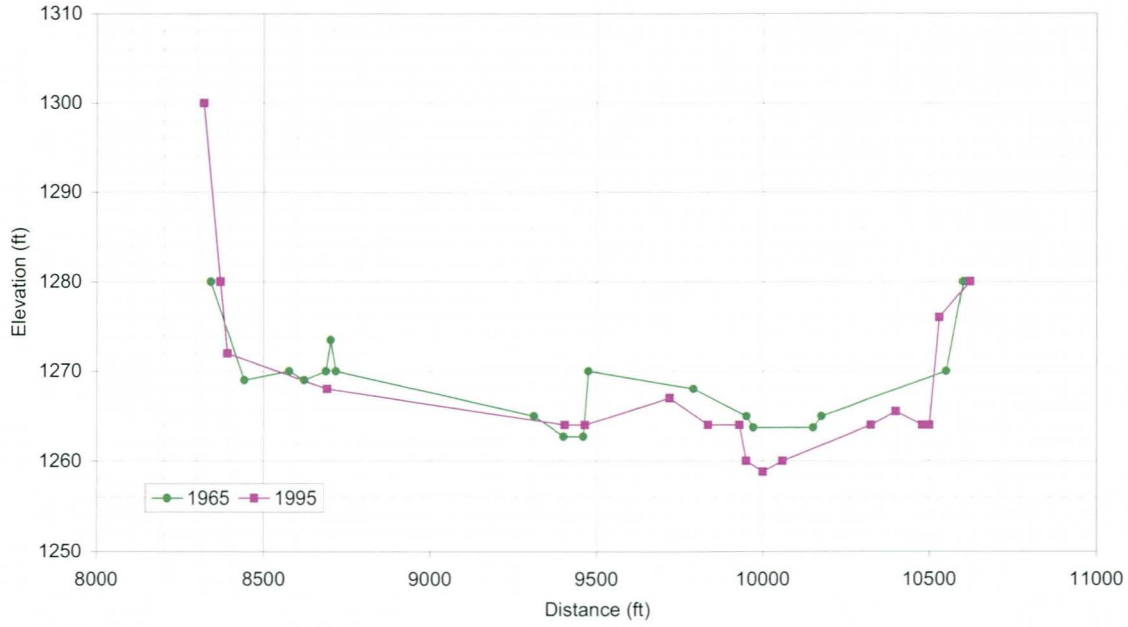

Figure 5-27 Reach 5, RM 25.79

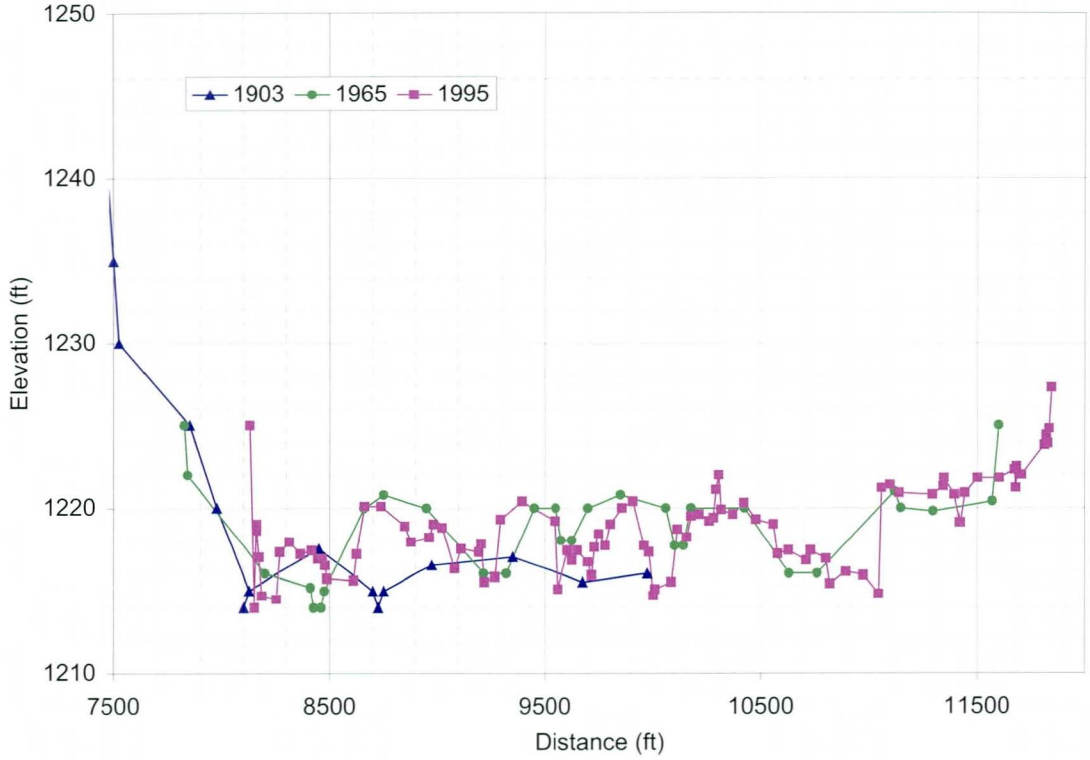

Figure 5-28 Reach 6, RM 23.219

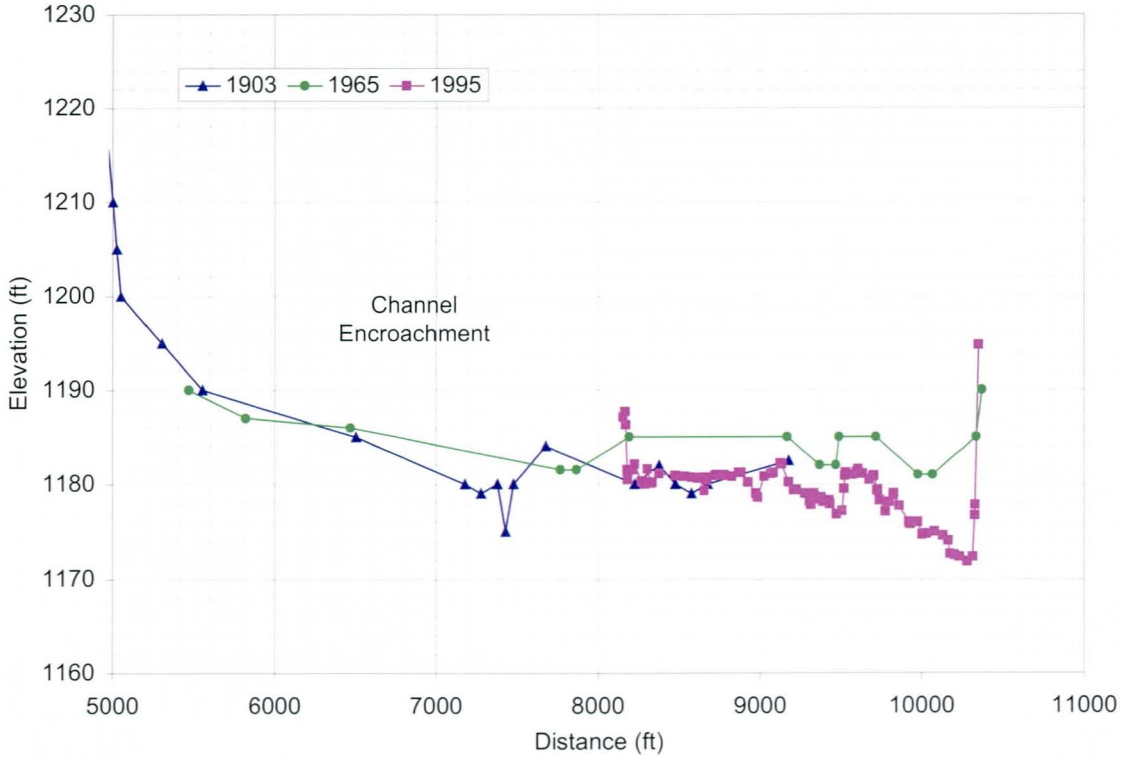

Figure 5-29 Reach 7, RM 20.579

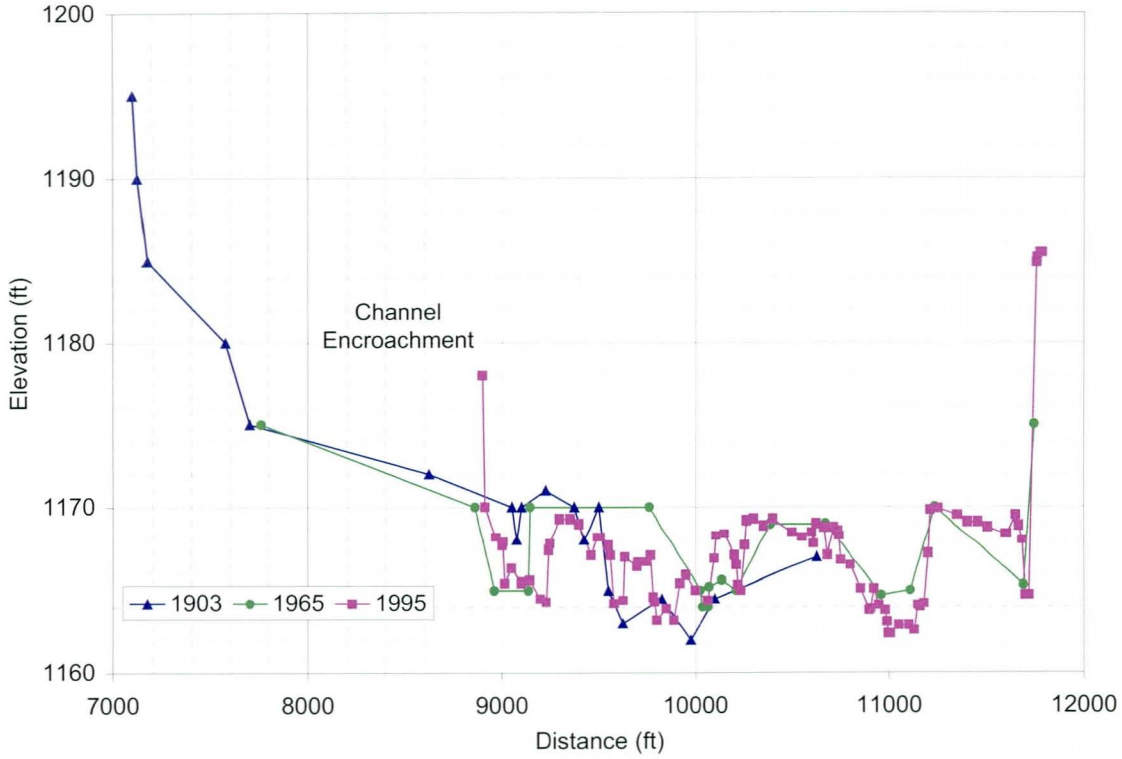

Figure 5-30 Reach 7, RM 19.827

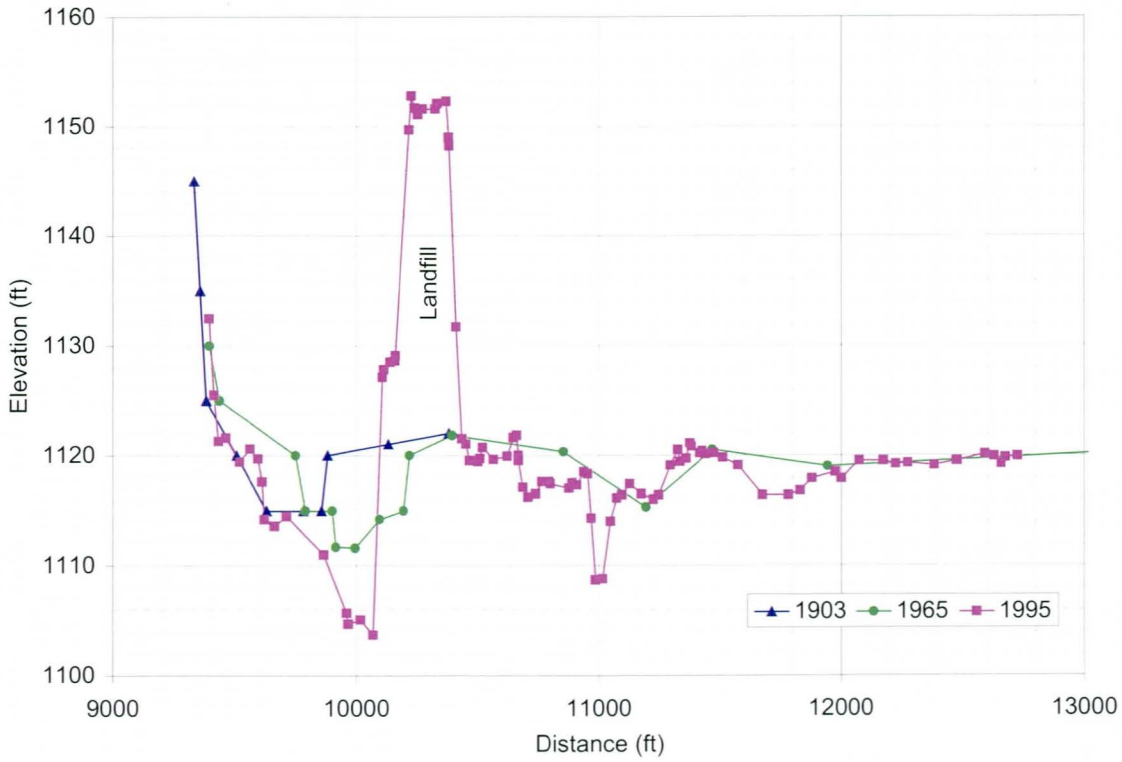

Figure 5-31 Reach 8, RM 16.385

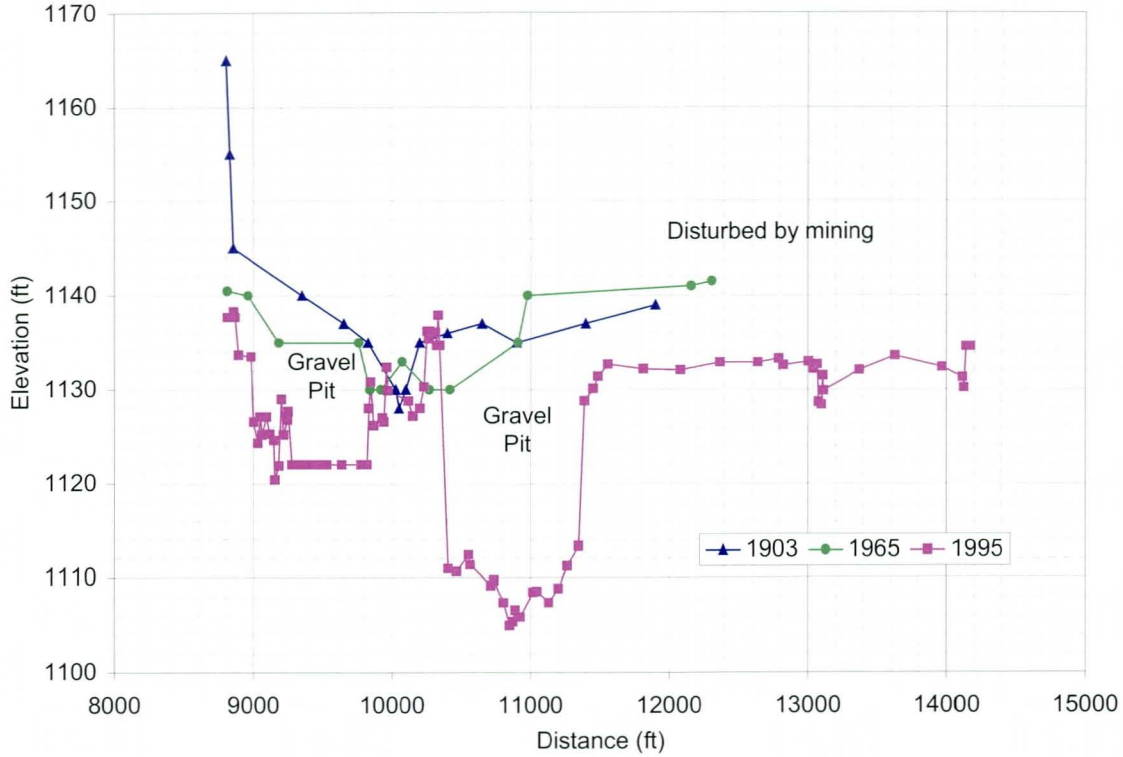

Figure 5-32 Reach 8, RM 17.548

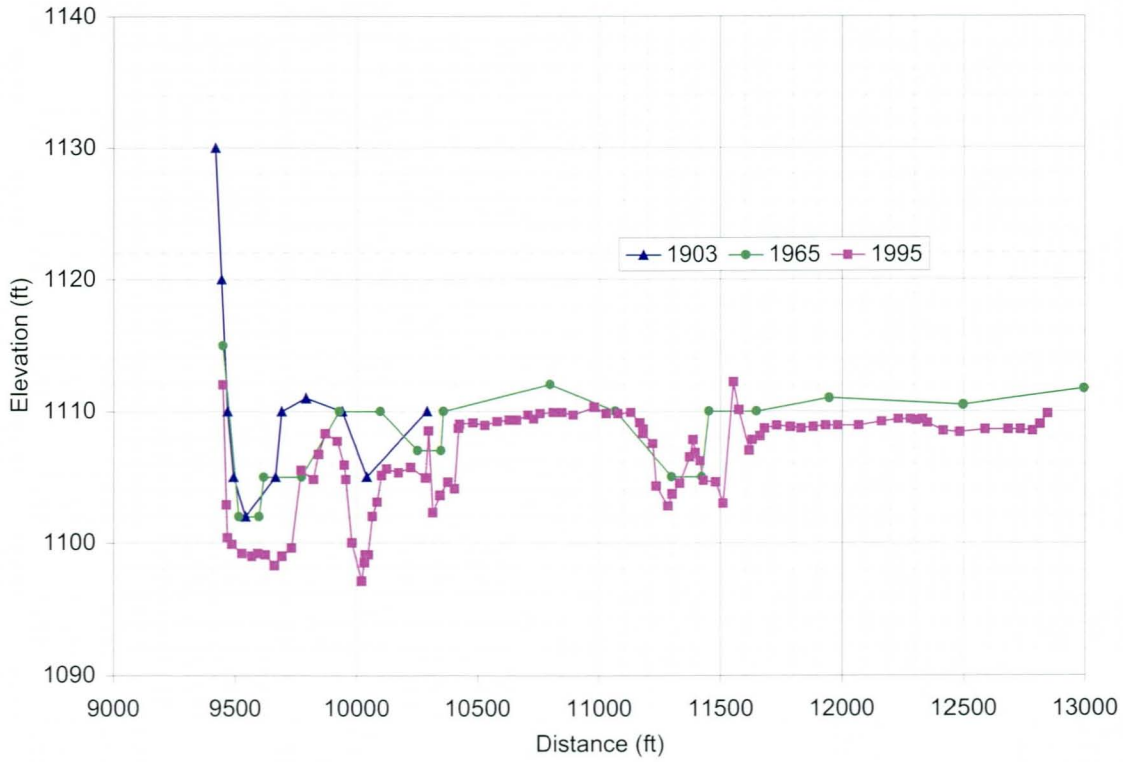

Figure 5-33 Reach 8, RM 15.658

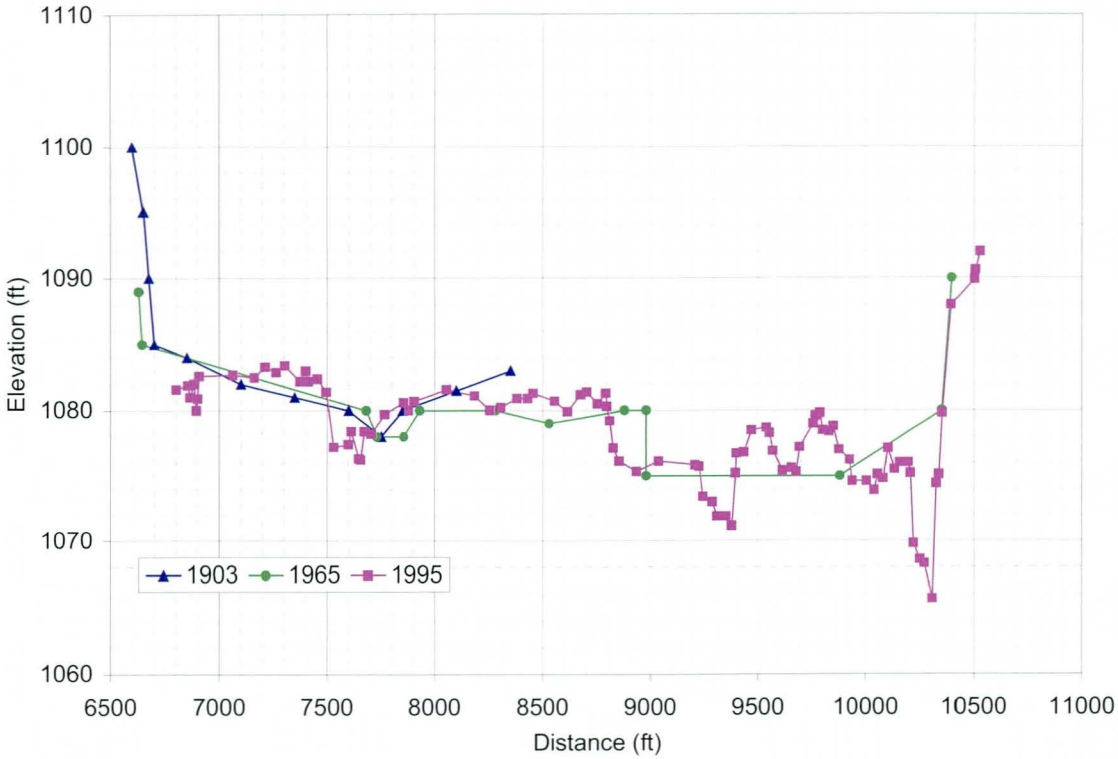

Figure 5-34 Reach 9, RM 13.663

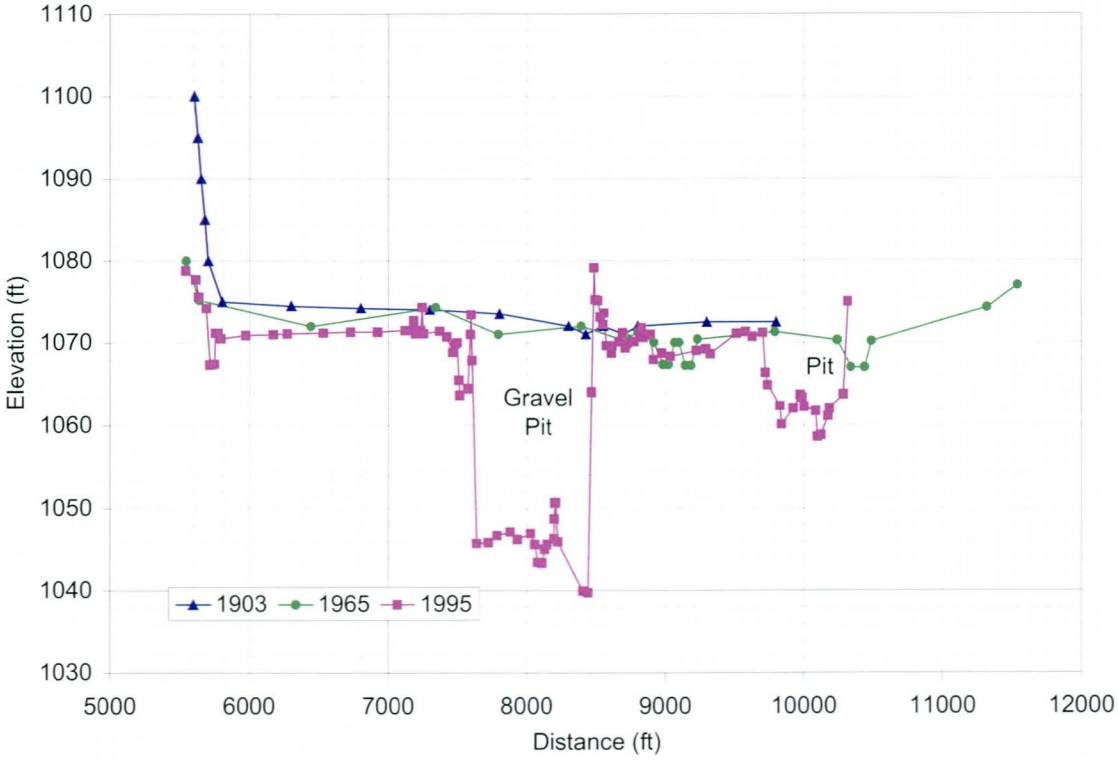

Figure 5-35 Reach 10, RM 12.913

The following conclusions can be drawn from examination of the comparison of historical cross sections shown in Figures 5-24 to 5-35:

- Degradation occurred over the entire floodplain in Reach 1 (Figure 5-24), as opposed to the degradation of the main channel or a portion of the channel section shown in Figures 5-25 to 5-35.
- In Reach 2, the comparison indicates that while no significant long-term degradation is shown, significant changes in the channel cross section occur (Figure 5-25). Two narrower channels scoured the bed while depositing a bar between them. Aerial photos and field observations show a large area of sandy sediments between two narrower channels on either side, confirming the data shown in Figure 5-25.
- Changes in vertical position in Reaches 4, 5 and 6 (Figure 5-26 to Figure 5-28) generally agree with the profile comparisons. The cross sections also show small amounts of vertical change, and realignment of the position and shape of individual braids and bars between the mid 1960's and 1988/1995.
- The cross section comparisons for Reach 7 (Figures 5-29 to 5-30) indicate broad and perhaps more extensive degradation of the channel near Beardsley Road adjacent to the sand and gravel mines, and less significant channel changes both vertically and horizontally adjacent to the Coyote Lakes encroachment near Bell Road. Encroachment by the Coyote Lakes subdivision post-dates the 1978 and 1980 flooding.
- The significant degradation of the channel at Grand Avenue and the Cholla Landfill in Reach 8 observed in the field is confirmed by the cross section comparison shown in Figure 5-31. The data show that the bed has dropped about 10 feet since 1903 (just 8 years after construction of the original railroad bridge). Field observations suggested at least 9 feet of degradation during the historical period.
- Downstream of Grand Avenue, gravel mining complicates comparison of "natural" conditions in the river channel (Figures 5-32 to 5-35). In general, the section comparisons indicate that the bed has been lowered and the low flow channels have narrowed.

5.7 Sinuosity

Sinuosity is a measure of the ratio of the thalweg length to the valley length. Streams may become more or less sinuous as a mechanism to adjust their slope in response to watershed stimuli. Alternatively, channel sinuosity is modified by encroachment of the floodplain, construction of bridges, or channelization. A more sinuous channel travels a further distance for the same elevation drop than a less sinuous channel and hence has a shallower slope. Sinuosity is generally used to describe the degree of meandering in a meandering stream. Since the Agua Fria River is braided, measurements of sinuosity are less diagnostic of expected behavior than if it were a meandering stream. For this study, sinuosity was examined to detect any adjustments to slope that may have occurred on the Agua Fria River in response to the changes to the hydrologic and sediment inputs created by the construction of the Waddell and New Waddell Dams.

Data. Two data sources were used in the sinuosity analysis for the Agua Fria River.

1. Topographic Maps: "Salt River Valley Arizona Topographic and Irrigation Map." A.P. Davis & R.W. Hawley, 1903. Contour interval is 5 feet. Datum is mean sea level. Coverage from Gila River confluence to Jomax Rd.
2. Historical Aerial Photography of the study reach, as described previously and summarized in Table 5-4.

Table 5-4 Agua Fria Aerial Photography Used In Sinuosity Analysis

Date	Source	Media Type
1934	SRP	images scanned from 1:15840 paper prints
02-20-49	National Archives	9 x 9 paper prints, B&W, scale 1:20000
01-14-54	National Archives	9 x 9 paper prints, B&W, scale 1:20000
02-20-59	Maricopa County FCD	.tif images, original prints 1:24000, scanned 1:7200
10-09-67	Landiscor Aerial	9 x 9 paper prints, B&W, scale 1:40000
12-05-77	Cooper Aerial Co.	9 x 9 paper prints, B&W, scale 1:20000
05-13-79	Agricultural Stab. & Cons. Serv.	9 x 9 paper prints, B&W, scale 1:40000
12-15-80	Landiscor Aerial	9 x 9 paper prints, B&W, scale 1:40000
03-02-85	Aerial Mapping Company	9 x 9 paper prints, B&W, scale 1:32000
09-06-92	USGS (NAPP)	9 x 9 paper prints, B&W, scale 1:40000
04-30-97	USGS (NAPP)	9 x 9 paper prints, B&W, scale 1:40000
01-02,05-99	FCDMC	CD-ROM (.tif with .tfw)

Methodology. Thalweg positions for all flow paths and splits were digitized in AutoCAD from the sources described above. However, because measurement of sinuosity requires that a single thalweg line be defined, the apparent low flow channel was used for the given year of aerial photographic coverage. The resulting line lengths were compared with other years of coverage that spanned the same portion of the river. That is, not all years of aerial photography covered all 15 reaches. Valley length was calculated in AutoCAD based on the USGS 7.5 minute topographic maps. A separate valley length was calculated for the limits of each year of aerial photographic coverage. Sinuosity was calculated as follows:

Sinuosity = (Stream Length / Valley Length)

After sinuosity was calculated for each year of coverage, the lines were divided into separate reaches followed by reach-specific sinuosity calculations. Since not all the data sources described above cover the entire study area, some years of coverage are not included in certain reaches.

Results. Table 5-5 and Table 5-6 show changes in sinuosity along the Agua Fria River over time. Table 5-5 shows sinuosity changes for longer reaches of the river based on the limits of the various data sources. Table 5-6 shows sinuosity changes for each study reach.

Table 5-5 Historical Sinuosity Along the Agua Fria River

All Reaches				Downstream of Happy Valley Rd				Downstream of Cactus Rd			
Year	Length (ft)	Length (mi)	Sinuosity	Year	Length (ft)	Length (mi)	Sinuosity	Year	Length (ft)	Length (mi)	Sinuosity
1949	189534	35.9	1.11	1903	135292	25.6	1.12	1903	89033	16.9	1.12
1954	189296	35.9	1.11	1949	138233	26.2	1.14	1934	88843	16.8	1.12
1977	186909	35.4	1.09	1954	138123	26.2	1.14	1949	89497	17.0	1.13
1985	188703	35.7	1.10	1967	136264	25.8	1.13	1954	91291	17.3	1.15
1992	186383	35.3	1.09	1977	135362	25.6	1.12	1959	86565	16.4	1.09
1997	185989	35.2	1.09	1979	135141	25.6	1.12	1967	87598	16.6	1.11
1999	186324	35.3	1.09	1980	136852	25.9	1.13	1977	86405	16.4	1.09
Valley	170835	32.4		1985	137847	26.1	1.14	1979	87113	16.5	1.10
				1992	134084	25.4	1.11	1980	88894	16.8	1.12
				1997	135823	25.7	1.12	1985	90468	17.1	1.14
				1999	134890	25.5	1.12	1992	85936	16.3	1.09
				Valley	120757	22.9		1997	87515	16.6	1.10
								1999	86197	16.3	1.09
								Valley	79200	15.0	

Table 5-6 Historical Sinuosity By Reach

	Reach														
Year	1	2	3	4	5	6	7	8	9	10	11	12	13	14	15
1903						1.08	1.03	1.09	1.12	1.14	1.10	1.23	1.05	1.19	1.05
1934									1.04	1.09	1.02	1.26	1.04	1.37	1.10
1949	1.05	1.01	1.01	1.12	1.06	1.18	1.14	1.09	1.07	1.07	1.07	1.24	1.03	1.25	1.13
1954	1.00	1.02	1.01	1.09	1.09	1.13	1.03	1.09	1.07	1.09	1.10	1.25	1.05	1.28	1.18
1959								1.07	1.10	1.08	1.11	1.18	1.05	1.14	1.23
1967						1.16	1.12	1.12	1.07	1.07	1.09	1.17	1.04	1.16	1.15
1977	0.98	1.02	1.02	1.13	1.07	1.15	1.15	1.13	1.07	1.06	1.09	1.17	1.02	1.14	1.06
1979						1.12	1.05	1.14	1.07	1.08	1.06	1.15	1.01	1.11	1.06
1980						1.12	1.07	1.11	1.16	1.07	1.10	1.16	1.06	1.24	0.96
1985	1.06	1.02	1.01	1.08	1.05	1.10	1.08	1.10	1.14	1.06	1.17	1.19	1.10	1.29	0.97
1992	1.00	1.00	1.00	1.14	1.14	1.12	1.09	1.12	1.13	1.09	1.11	1.07	1.03	1.17	0.97
1997	1.00	1.01	1.01	1.07	1.09	1.12	1.10	1.12	1.13	1.07	1.09	1.08	1.03	1.24	1.08
1999	1.02	1.02	1.03	1.10	1.09	1.13	1.14	1.12	1.12	1.08	1.04	1.08	1.02	1.21	0.99

Summary. The data show that sinuosity has not varied radically over time, indicating that the Agua Fria River has not changed its low flow channel length, or slope, in response to changes in hydrologic or sediment inputs to the system. Note that the earliest data set predates the construction of the Waddell Dam. Reaches 6 to 8 have become slightly more sinuous since 1903, while the remaining reaches downstream have generally become less sinuous. The decrease in sinuosity is due partly to the channelization of the river by the Corps of Engineers in Reaches 12 and 13. However, prior to the levee channelization a slight decrease in sinuosity is shown for the Lower Reach.

In one instance in Reach 1 and four instances in Reach 15 the sinuosity is less than 1.0. That is, the stream length was shorter than the valley length. In the case of Reach 15, this is the

result of straightening of the thalweg by human activity. Following the 1980 flood an earthen dike was raised along the right side of the channel directing the low flow more directly south than the historical valley orientation which bends to the west.

5.8 Summary

The Quaternary geology investigations along the study reach indicate that the terraces are effective lateral limits to erosion. Subsidence near the study reach has had no impacts on the degradation of the river channel. No evidence of Hohokam settlement has been found in the floodplains, and the impact of the few Hohokam canals on the river was limited. Anglo settlements and activity along the river had limited impact prior to World War II. The settlements were established as either stage stops between Phoenix and Prescott, or farming settlements. The major human impacts on the river, namely sand and gravel mining and floodplain encroachment, began with post-World War II population growth and the resulting need for building materials.

The width of the Agua Fria River is highly variable within the study reach. The width is dependent on natural features such as bedrock outcrops or the position of geologically old terrace, as well as on human impacts such as bank protection and mining-related features. In general, average the width of the high flow channel has decreased over time, although the low flow channels remain highly active and tend to occupy the entire geologically recent floodplain.

While smaller floods have not been capable of causing the large lateral variations in channel position, larger floods have caused the channel to move by nearly ½ mile over the period of record. Although the magnitude and frequency of flood discharges has been greatly reduced by the New Waddell Dam, discharges larger than bankfull discharge are still possible on the Agua Fria River. These relatively infrequent, large floods are capable of causing the same types of significant changes in channel thalweg and bank locations as has been experienced in the past. The maximum change in width during a single flood was approximately 1100 feet.

The examination of historical longitudinal profiles shows changes in bed elevation in the Agua Fria River from 1903 to 1995. The data generally show either significant degradation of the channel or no significant changes. No evidence of significant historical aggradation was identified. The reaches that show degradation are primarily in areas impacted by the human activity. In particular, clear-water discharge from the dam, encroachments by bridges, channelization, and sand and gravel mining activity within the channel appear to be the primary causes of channel degradation. Channel bed lowering ranged from 0 to about 17 feet.

The data show that sinuosity has not varied radically over time. The absence of sinuosity changes suggests that the Agua Fria River has not been changing the length of the low flow channel, and hence its slope, significantly in response to changes in hydrologic or sediment inputs to the system.

6. MATHEMATICAL DATA

6.1 Introduction

This chapter describes various types of data analyzed using mathematical means, such as equations or algorithms, to quantify the erosion hazards in the Agua Fria River study reach. The types of mathematical analyses presented include the following:

- Hydraulic modeling – development of hydraulic data from HEC-RAS
- Sediment size estimation – sieve analyses and field estimates
- Geomorphic methods - bankfull discharge and hydraulic geometry relationships
- Engineering methods - allowable velocity, equilibrium slope, armoring, scour, Lane's relation, and HEC-6 modeling

The data and analyses are described relative to the information they yield on the degree and extent of erosion hazards along the Agua Fria River.

6.2 Hydraulic Data

6.2.1 HEC-RAS Modifications

The HEC-RAS model developed from the Flood Insurance Study HEC-2 can be used to generate hydraulic data for use in geomorphic assessments and channel stability studies. The primary objective of a Flood Insurance Study is to estimate the 100-year water surface elevation for a stream reach. Therefore, the other hydraulic data developed by a HEC-RAS model for a detailed floodplain delineation study generally are not as thoroughly evaluated as the 100-year water surface elevation estimates. Furthermore, the cross section division into channel and overbank sections is performed to optimize the water surface elevation estimates, and may not accurately reflect other hydraulic characteristics of the channel and floodplain, particularly for more frequent floods. Therefore, prior to using a HEC-RAS model developed for a floodplain delineation study for a geomorphic analysis, the HEC-RAS model must be evaluated and modified. The following types of modifications are addressed:

- Discharge
- Starting Water Surface Elevation
- Selection of N Values
- Section Limits
- Cross Section Alignment
- Bank Station Definition
- Ineffective Flow Areas

6.2.1.1 Discharge

For most geomorphic studies, a number of recurrence intervals are evaluated over the entire hydrograph. Therefore, the parameterization of the HEC-RAS model must be applicable for the entire range of discharges that may occur in the study reach, not just the peak of the 100-year flood. Where the model cannot be realistically modified for the full range of flows, the model should be optimized for flows approximating the bankfull discharge.

6.2.1.2 Starting Water Surface Elevation

To achieve conservative estimates of velocity at the downstream limit of the model, the starting water surface should be based on normal depth. Where significant backwater conditions are present at the outfall, the potential for backwater-induced sedimentation should be analyzed separately. In addition, use of the normal depth method allows the full range of discharges to have the most appropriate starting elevations.

6.2.1.3 Selection of N Values

It is important to recognize that geomorphic analyses typically consider existing conditions and long-term future conditions. Over any reasonable planning horizon, channel vegetation changes and the channel itself evolves. Therefore, n values should be selected to reflect the uncertainty of the modeling effort; precision beyond two significant figures is not warranted. If the HEC-RAS model is to be used as the input code for HEC-6 or another sediment continuity computer model, options such as NH (horizontal variation of n values by station) or NV (vertical variation of n values) records should not be used. N values should be selected based on bankfull conditions. Sensitivity analyses can be conducted to evaluate the effect of changing n values on key hydraulic variables such as channel depth and velocity.

6.2.1.4 Section Limits

In order to examine a range of discharges in excess of the post-New Waddell Dam 100-year discharge, additional cross section points needed to be added to a number of cross sections within the model. The 1988 and 1995 FIS topographic data sets were used whenever possible to obtain these additional points. In some cases, the USGS 7.5 minute maps were used when the needed data extended beyond the limits of the FIS topographic mapping.

6.2.1.5 Cross Section Alignment

Sections aligned perpendicular to the primary flow direction of the 100-year flood may be skewed relative to the primary flow direction of more frequent floods that occupy only the main channel. If sections are skewed to the low flow channel, the misalignment will cause the channel dimensions to be too large, resulting in erroneous estimates of channel capacity, topwidth, and area. The flow distribution at a range of discharges should be evaluated, particularly where divided flow occurs. For discharges less than the 100-year event, divided flow may occur. Flow in these divided paths must connect to the main channel both upstream and downstream. If no connection exists, the unused flow areas should be coded out of the model. The most active flow paths can be readily identified in the field or on aerial photographs.

6.2.1.6 Bank Station Definition

Definition of the left and right bank stations is critical to obtaining accurate hydraulic data for the following reasons:

- Bankfull discharge. Some elements of river stability assessments and many geomorphic principles are based on the concept of bankfull discharge. Therefore, it is necessary to accurately define the channel stations to distinguish channel and overbank characteristics and processes.
- Sediment movement. When using hydraulic models, it is necessary to distinguish areas where sediment moves primarily as bed-material load (i.e., channels, subject to both scour and deposition) from areas where sediment moves primarily as wash load or suspended

load (i.e., overbanks, primarily subject to deposition). If portions of the overbank areas are included in the channel, the channel velocity and hydraulic depth will be underestimated, resulting in low estimates of sediment transport capacity and/or erosion potential.

6.2.1.7 Physical Characteristics of Channel Banks

Channel bank stations can be identified using the procedures summarized in the following features or procedures, which are described below:

- Ordinary High-Water Mark
- Flood Frequency
- Cross Section Geometry

6.2.1.7.1 Ordinary High-Water Mark

The U.S. Army Corps of Engineers, in identifying the bank station associated with the ordinary high-water mark, uses the following three characteristics:

- Vegetation. A change from terrestrial to aquatic vegetation, or the onset of terrestrial vegetation often occurs at the ordinary high-water mark.
- Soils. A change in soil characteristics from undifferentiated, poorly developed soils to more well-developed soils with distinct profiles often occurs at the ordinary high-water mark. This change is caused by frequent scour and fill that prevents soil formation.
- Topography. A break in slope often occurs at the ordinary high-water mark.

The ordinary high-water mark, as defined by the Corps of Engineers, is analogous to a geomorphic definition of the top of the channel bank. Therefore, the Corps' definition can be applied to help define the location of the channel stations used for HEC-RAS modeling. However, the following modifications are required to apply these definitions to streams in central Arizona and the arid west:

- Vegetation. On ephemeral and intermittent streams, vegetation in the channels may not be significantly different from vegetation growing in or above the floodplain. However, the following guidelines are suggested:
    1. Areas swept clean of vegetation. The areas of highest velocity occur in the main channel, and will be periodically swept clear of vegetation during high flows. Therefore, the channel will either lack vegetation, or will be populated with very young, fast growing vegetation. An inspection of the stream's flood history, either from gauge records or field evidence, should be made to determine whether high flows have occurred in the recent past. If no large flows have occurred in the recent past, vegetation may have encroached on the main channel and may obscure the banks.
    2. Bank vegetation. A swath of dense vegetation often lines the banks of ephemeral and intermittent channels. In southern and central Arizona, this vegetation generally consists of mesquite, palo verde, ironwood, and brushy plants, but may also include cactus species such as saguaro. This vegetation is usually distinguished by species and/or density from both the vegetation on the channel bottom and the vegetation in the floodplain.
    3. Age of vegetation. The relative age of the bank vegetation can be used to assess the frequency and/or the age of the most recent channel changes. Older bank vegetation indicates infrequent channel movement in the past, and a stable bank. Young,

intermittent vegetation may indicate the bank of an erodible inset terrace, rather than the primary channel bank.

- Avulsions. If the main channel location is subject to avulsive channel changes, the bank stations required for geomorphic assessment may be well outside the area defined by existing bank vegetation. The potential for avulsive channel changes can be assessed by a field inspection and by comparison of historical aerial photographs. The presence of multiple channels often is evidence of historical channel avulsions. Definition of channel bank stations in reaches subject to avulsive changes is complex. In general, the main channel should be defined at the margins of the portion of the floodplain subject to the most frequent flow and bedload sediment transport.

- Soils. Soil characteristics can be used to distinguish the main channel from less frequently inundated areas.

  1. Sediment size. Overbank areas primarily are subject to deposition, and thus generally are composed of accretive layers of fine grained sediment, or have a mantle of more recently deposited fine grained materials. Areas subject to channel processes typically are underlain by coarser sediments.
  2. Imbrication. Coarse channel sediments are often imbricated in the direction of movement. However, caution should be used when examining areas of recent entrenchment where historical active sediment transport occurred, leaving imbricated sediments in areas that are now perched above the main channel.
  3. Profile development. Areas outside the channel generally have remained undisturbed for longer periods of time, and hence have had time to develop soil horizons, surface pavements, and other features of soil development. Surface characteristics that may indicate subsurface soil profile development include desert varnish, desert pavement, and reddening of surface layers.
  4. Bank cuts. Soil profiles can often be observed in cut banks. Features that indicate soil profile development that can be observed in cut banks include carbonate layers (caliche), clay accumulation (soil texture), reddening of soil layers, and soil structure (ped formation).

- Topography. Most large stream systems consist of compound channels with one or more terraces that reflect different levels of flooding and inundation. Inundation of these terraces corresponds to different flow frequencies – larger floods are required to inundate the highest terraces. Therefore, to some degree, definition of the main channel depends on the frequency of the flow event under consideration.

6.2.1.7.2 Flood Frequency

Use of a predetermined recurrence interval for bankfull discharge based on published reports (such as the 1.65-year flood) is not recommended for estimating the bankfull limits. This practice begs the question of how can the channel-forming discharge be determined unless the channel hydraulics are first estimated. To estimate channel hydraulics, one needs to define the bank stations. The following bank definition criteria relating to flood frequency information are noted:

1. Sediment size. If the channel is armored, and the banks are resistant to lateral erosion, it is unlikely the channel forming discharge is a frequent event (Q2 or less). In these cases, the channel geometry probably is the result of the largest flows (Q25 or greater).
2. Bankfull discharge. Definitions of bankfull discharge recommended by some publications (cf., Rosgen, 1996) are practically irrelevant for lateral stability studies in Arizona. Bankfull discharges that refer to a 1.5-year or more frequent discharge may be relevant

for a micro-channel formed within a compound channel, or for fish habitat studies on perennial streams, but have little meaning for river stability assessments on flood-dominated stream systems in central and southern Arizona. Limiting the scope of analysis to this low flow micro-channel ignores the important role of floods on shaping channels and in causing lateral movement and bank erosion. For entrenched river systems, or for erosion hazard assessments, bankfull refers to the well-defined banks subject to erosion during floods. That is, the banks that if eroded, would be of concern to adjacent property owners.

3. Bank Station. The flood frequency should be high enough to reach an erosive velocity (> 3-5 ft/sec) at the bankfull stage, and high enough to flow against the banks at a significant depth.

6.2.1.7.3 Cross Section Geometry vs. Bank Definition

Figures Figure 6-1 to Figure 6-6 illustrate selection of bank stations for a variety of stream types.

Single Channels. Bank stations are most easily identified for single channel reaches.

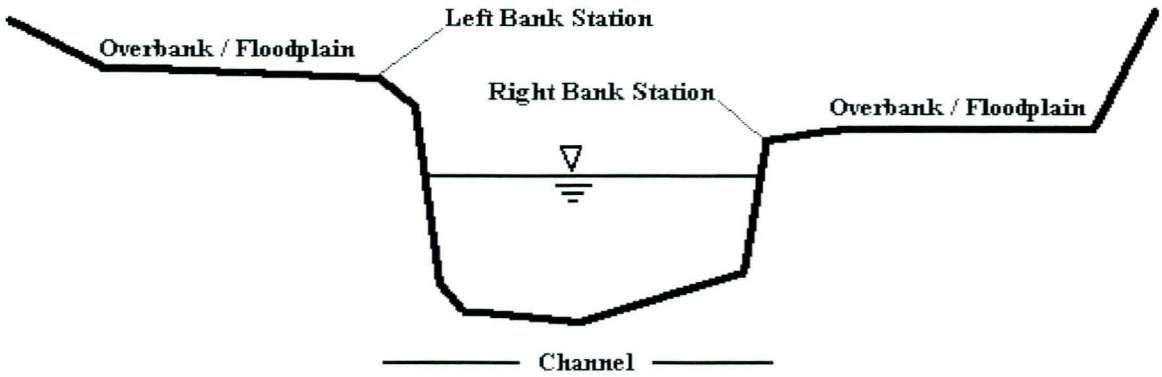

Figure 6-1 - Recommended bank stationing for single channel cross sections.

Multiple Channels. Several types of multiple channel conditions exist. Judgment regarding the study objectives must be used to define the bank stations on multiple channel reaches.

Scenario #1 – Multiple Channel Where Islands Inundated by Flows

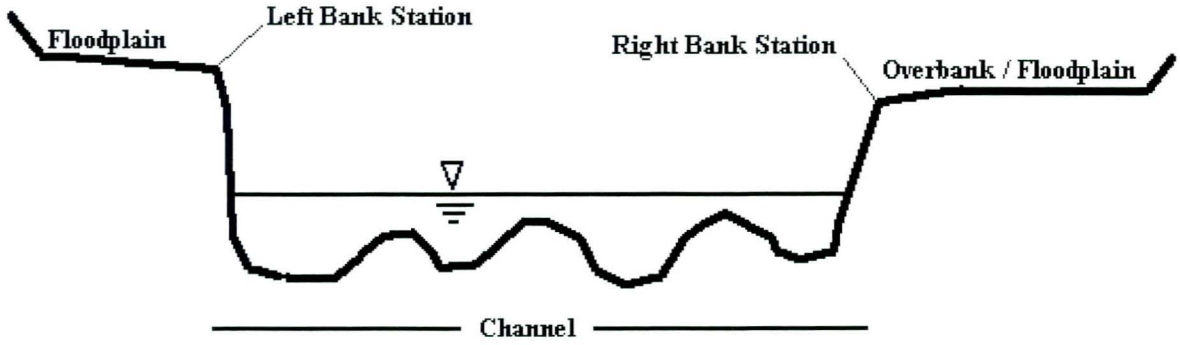

Figure 6-2 - Recommended bank stationing for multiple channels with shallow islands.

Scenario #2a – Multiple Channel Where Islands Not Inundated by Flows: Small Islands

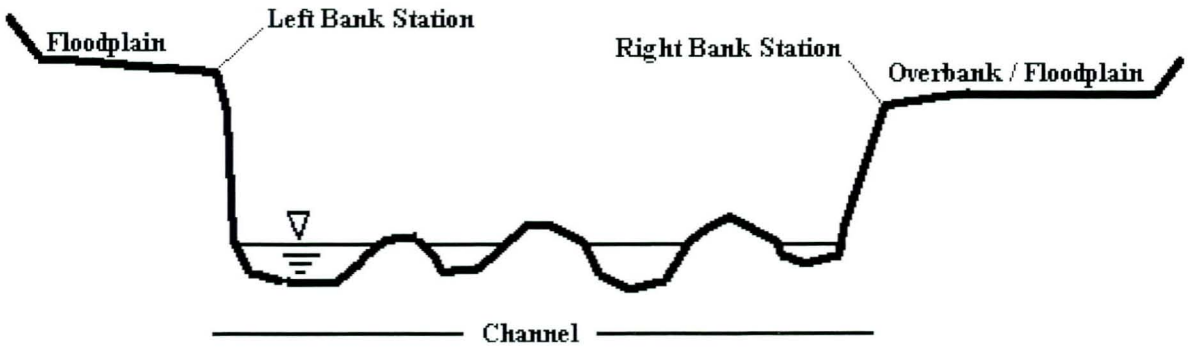

Figure 6-3 - Recommended bank stationing for multiple channels with shallow, insignificant or small islands.

Scenario #2b - Multiple Channel Where Islands Not Inundated by Flows: Large Islands

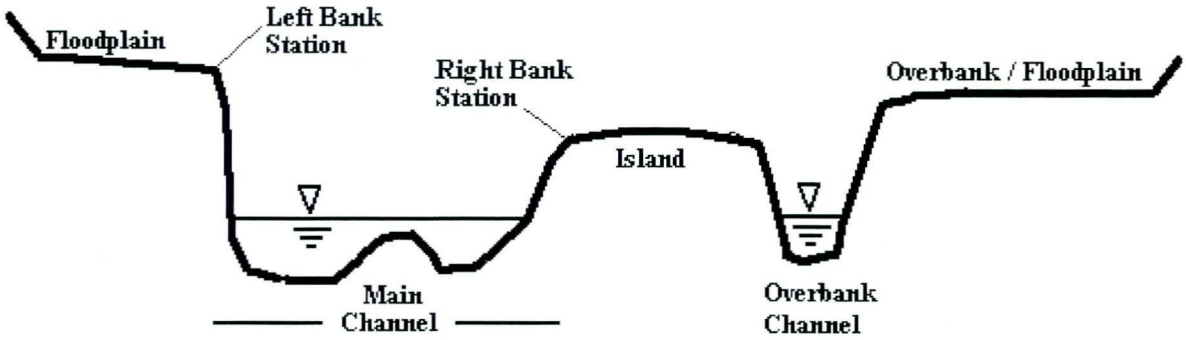

Figure 6-4 - Recommended bank stationing for multiple channels with exposed islands of significant size

Perched Channels. Perched channels are typically overbank conveyance corridors that are hydraulically disconnected from the main channel at a specific section. The bank stations should be selected to reflect the geometry of the main channel.

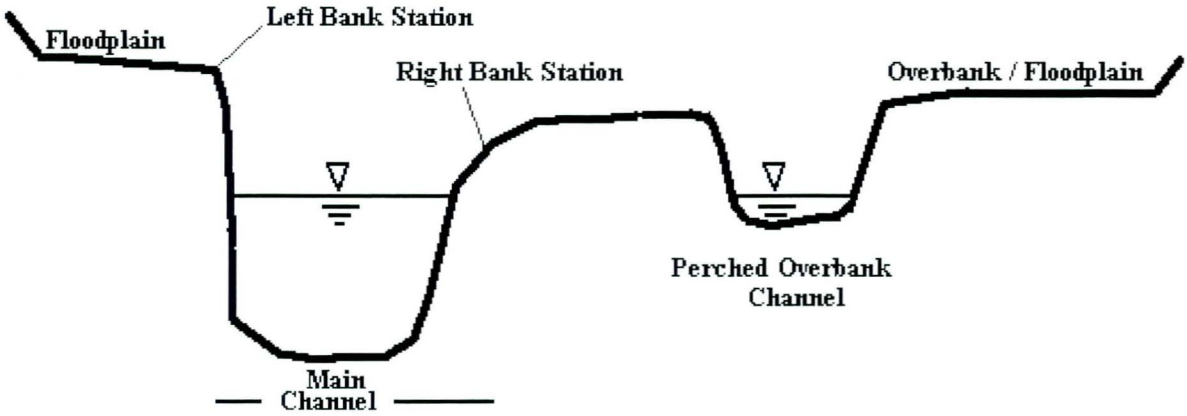

Figure 6-5 - Recommended bank stationing for perched overbank channels

Channels With Poorly Defined Banks. In some cases, a clearly defined bank station cannot be defined solely on geomorphic characteristics. Where the banks are poorly defined, the bank station can be selected using hydraulic criteria (e.g., $d*v^2>18$; where d=flow depth, ft. and v=flow velocity, ft./s.) or by comparison with the channel widths of upstream and downstream sections.

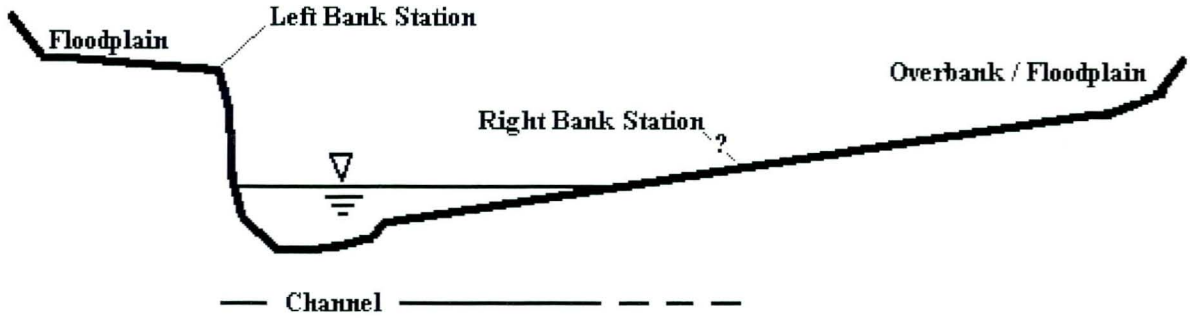

Figure 6-6 - Recommended bank stationing for channels with poorly defined banks.

Ineffective Flow Areas. The ineffective flow areas defined in the model should be appropriate for the full range of discharges. If this is not possible, optimize the ineffective flow areas for bankfull discharge.

Other Guidelines. The following other modeling guidelines are suggested:

- Consistency between cross sections. Large fluctuations in channel width, as defined by the bank stations, should be avoided unless dictated by actual changes in channel width documented in the field. Channel characteristics generally change gradually on stable, natural streams.
- Level of accuracy. HEC-2 is a one-dimensional, gradually varied flow model. It assumes a horizontal water surface, with no waves or no superelevation on bends, and no sediment movement or bank erosion during the passage of the flood. There is uncertainty in the discharge estimate, the channel geometry, and the hydraulic modeling coefficients. The actual accuracy of the predicted water surface probably is not known within one foot. Results should be interpreted accordingly.

6.2.2 Application to the Agua Fria River Watercourse Master Plan Study Area

6.2.2.1 Modifications

The following is a list of the general types of modifications made to the HEC-RAS model provided to JEF by KHA for the erosion hazard assessment. Some specific modifications are also included. The HEC-RAS model input code itself contains a complete list of modifications made at each cross section.

1. The model was imported to RAS 3.0 from a previous version of HEC-RAS.
2. The bridge cross section lengths were modified to satisfy RAS 3.0 guidelines. A length of one foot upstream and downstream was added and the bridge width reduced by two feet.
3. Channel bank stations were moved to provide a depiction of channel compatible with the geomorphic/erosion analyses, as described above. Ground points were inserted into cross sections as necessary to place a bank station at the desired location.
4. Levees and ineffective flow boundaries were added, moved or deleted.
5. Cross sections at river mile (RM) 32.43, 32.34, 32.24, 32.15 had the thalweg on wrong side of channel for low flow. The thalweg station (Sta. 10,000) was not adjusted by JEF, but channel bank stations were moved.

6. The location of Section 32.43 is too near to a peninsula-like point located immediately downstream that protrudes into channel. An ineffective flow area was added to the section account for this point.
7. The left end of the cross section for RM 31.29 appeared to be missing. There was only enough capacity in the section for 21,000 cfs. Additional flow exceeded the topographic capacity. For the purposes of the multiple profile run, the topographic data were extended based on digital contours. Also, a GR point reported at station 9450 was obviously incorrect based on contours and was modified. The stations and elevations beyond GR point 9562 were revised along with the extension of cross section. One additional complication in this area is that the topographic data shows two 1360 contours, but the 1364 contour seems to be missing. Also, the two 1360 contours cross each other at places, indicating some level of error in mapping. Additional GR points were also added to better define the rise to the right bank.
8. The right side of Section 30.92 needed additional GR points to contain higher discharges, which were added from the digital topography. The cross section alignment was bent downstream slightly to meet hillslope on the downstream (south) side of unnamed washes 1 & 2 confluence.
9. The left end of Sections 30.26 and 30.17 lacked enough GR points to contain higher flow rates, and GR points were added from the digital topography.
10. GR points were added to the right ends of Sections 29.99, 29.89, 29.8, 28.21, 28.12 to contain high flows.
11. The imported bridge geometry for the Beardsley Canal Flume is grossly in error. Significant portions of the channel width were shown as blocked out by the bridge, and modified. For the purposes of the geomorphic analysis, it was assumed that the pier was an adequate composite representation of the multiple piers and that the low chord shown was approximately correct and level across the entire channel.
12. Horizontal variation in Manning's n for the orchards in right overbank downstream of the Beardsley Canal Flume was added to obtain a more realistic representation of roughness for higher discharges.
13. A small, newly mined area at Section 24.543 was coded using GR points and blocked out as blocked obstruction.
14. The Cemex sand and gravel mining pit was modeled with blocked obstruction starting at outlet depth sloping upstream at a slope similar to channel bed slope outside pit (0.003 used). While this approach may not be hydraulically accurate over the full ranch of discharges modeled, it is appropriate given the limitations of HEC-RAS which is a one dimensional, fixed bed model applied with a multiple profile run. This approach is conservative with respect to velocity and hence erosion potential. In other words, by making the blocked areas have a slope parallel to the channel bed, flow through the pit probably will be faster than the "true" three dimensional hydraulic condition. A similar approach was used for the pits located downstream near Rose Garden Lane. Sections upstream and downstream affected by pits were handled in a similar fashion, using an assumed effective bed slope of 0.0035 ft./ft. Likewise, at the Walker pit, an outlet elevation of 1180 feet was used to compute blocked obstruction elevations for Sections 21.061 to 21.621.
15. Ineffective flow limits were added at the agricultural area surrounded by earthen dike near the Broadway Road alignment.
16. Comparison of 1999 aerials, field notes, and 1988 topography at Section 1.56 suggests that about 180 feet of lateral erosion has occurred at the left channel bank. The GR points were adjusted to reflect this modified condition. A similar adjustment was made at Section 1.48, using a lateral erosion estimate of about 100 feet, estimated by comparing 1988 GR points, 1999 aerial photos and field observations.

17. The pit in the left overbank (LOB) located between Bell Road and Section 17.73 was modeled similarly to Cemex pit, as described above, with a slope of 0.0037 used to compute blocked obstruction elevations for overbank areas.
18. The weir elevation for high discharge flow over the ATSF railroad near Grand Avenue was modeled at 1130 ft. Therefore, the ineffective flow limits were set at 1130 ft elevation for the upstream cross sections to Section 16.612. Pits in the right overbank (ROB) in this area were modeled as blocked obstruction up to an elevation similar to the general land surface in the vicinity of the section in the ROB.
19. Pits in LOB area between Northern and Glendale Avenues were modeled as blocked obstruction up to an elevation similar to the general land surface in the vicinity of the section in the LOB. Many of these areas were already modeled this way in the 1996 Flood Insurance Study (FIS).
20. The new Glendale Recycling Facility was modeled as a blocked obstruction at stations and elevations provided by LTM Engineering via e-mail on 4/21/01.
21. The north and south Camelback Levees were not modeled in the HEC-RAS model delivered to JEF by KHA. Therefore, these features were added based on the following: North Levee - data was obtained from the CLOMR to LOMR package supplied to JEF by M. Duncan, P.E. of FCDMC on 7-22-00; South Levee – the location shown in 1999 aerial photographs was used, the elevations were inferred from field observations and elevations of Camelback Road (1030 ft) and the upstream wing dike (1020 ft).
22. Manning's n-values were rounded to the nearest hundredth to reflect a more realistic depiction of the true model accuracy.
23. Multiple profiles for a range of flows were run to examine the hydraulics for the range of discharges and to determine the bankfull discharge. Additionally, multiple profiles for the pre- and post-New Waddell Dam were examined.

6.2.2.2 Observations

The following is a list of observations made during the HECRAS modifications regarding various inadequacies of the model which were not corrected by JEF but which affect the accuracy of the model results.

1. The orientation of cross sections 33.820, 33.730, 33.630, 33.540, 33.460, 33.410, 33.360 is not perpendicular to the 100-year flow. Therefore, cross-sectional area is overestimated and water surface elevations are underreported.
2. Floodplain limits plotted at RM 33.630 are higher on the left bank than on the right.
3. The multiple dog-leg alignment of 32.720 is difficult to justify, particularly for a multiple profile run.
4. Flow into far right overbank/split channel around rock islands begins at about 50,000 cfs at RM 32.790, but doesn't occur at lower discharges.
5. The GR points for RM 31.86 don't appear to conform to conditions observed in the field, perhaps due to physical changes since the 1988 topographic mapping was prepared. The topography and current channel conditions are definitely different in the vicinity of RM 31.77-31.59 due to gravel mining.
6. Use of ineffective flow in right overbank of Sections 32.720, 32.64, 32.58, & 32.52 results in top widths wider than inundated areas for discharges less than about 50000 cfs.
7. Bosque in right overbank near RM 32. 52 is shown as inundated by flows above about 90,000 cfs. This finding is consistent with field observations of historic flooding, probably from 1916 and 1919 floods. A discharge of 200,000 cfs is modeled as well within the larger channel entrenched into Pleistocene sediments and Tertiary rocks (conglomerates and volcanics).

8. The floodway fringe along the left bank from Section 32.52 to 31.20 should be considered strongly for a zero-rise floodway since it is already in a relatively entrenched canyon downstream of the dam.
9. Orientation of the left half of 26.63 is skewed relative to the main channel flow direction.
10. The orientation of the right overbank across the lower orchard (approximately RM 27.0 to 26.0) exaggerates the cross sectional area, putting more flow in the ROB than is realistic. The exaggerated area is demonstrated well by the inundation limits of the Feb. 20, 1980 flood (approx. 66,000 cfs) vs. the current FEMA floodplain (delineated at about 29,000 cfs). On the opposite overbank between about Jomax and RM 26.4, the orientation of the sections points too far upstream reducing the area available for flow in the ROB.
11. Cross section orientation is poor near the lower limit of the CAP recharge project area, exaggerating the channel and ROB cross sectional area at Sections 24. 631, 24.721, 24.86.
12. Cross section orientation is poor both upstream and downstream of Hatfield Road, exaggerating the LOB area.
13. The failure level implied by the model at the Cemex pit levees should be reevaluated.
14. The right ends of the cross sections upstream of Lower Buckeye Road are skewed downstream for no obvious reason (e.g. RM 2.60 to 3.270).
15. The cross section orientation at the bend near the end of the right bank soil cement levee under-represents the cross sectional area in the main channel.
16. The higher elevation "banks" about 2000 feet left and right of the FIS Station 10000 in the model match closely with visible edge of the 'active' river bottom visible in 1934 aerial photos.
17. The low flow channel at RM 0.25 appears to have widened about 200 feet along left bank since 1988.
18. In general, it appears that an ET field was used as a levee type option instead of X3. The KHA RAS conversion changed the ET record encroachments to normal ineffective flow, an approach which doesn't effectively model multiple profile runs. Therefore, blocked obstruction or levees were added to the model.

The objectives of the HEC-RAS hydraulic analyses for the study area were to estimate the hydraulic characteristics of the study reach, to identify hydraulically similar subreaches within the study area, and to identify subreaches with limited conveyance capacity. Specific tasks included the following:

- Provide basic data for use in engineering and geomorphic analyses
- Identify hydraulically similar channel reaches
- Estimate existing channel capacity relative to return period

The basic data developed for use in the engineering and geomorphic analyses were described in the previous section of this Chapter. Channel capacity, or bankfull discharge capacity, are discussed in Section 6.4.1 of this report.

Plots of HEC-RAS output are shown in Figures 6-7 to 6-23. The following conclusions can be drawn from the HEC-RAS output:

- Channel Discharge. Although the concept of a bankfull discharge is difficult to apply to the Agua Fria River because of the types and magnitudes of historical disturbance of the river, the HEC-RAS data indicate that the channel, as defined for this study, generally has capacity for more than the 10-year flood (Figure 6-7). The lack of overbank flow (Figure 6-8

and Figure 6-9) in the 2- and 10-year floods confirms the large capacity of the defined main channel. The fluctuations in the computed 100-year channel discharge indicate some degree of poor continuity between adjacent cross sections upstream of River Mile 18. The proportion of flow conveyed in the main channel generally increases in the downstream direction, in part due to channelization and encroachment of the historical floodplain.

- Channel Depth. The fluctuation of the computed maximum (Figure 6-11) and hydraulic depths (Figure 6-12) indicates that gradually varied conditions may not exist between adjacent HEC-RAS cross sections. The fluctuation of computed depths suggests highly irregular bank heights, bed profile, and channel capacity, all of which indicate channel instability. No strong trend in flow depth with distance downstream is apparent in Figure 6-11 and Figure 6-12, despite large increases in flow rate and degree of human disturbance of the floodplain.
- Channel Area. Like the plots of channel depth discussed above, the variation of channel area (Figure 6-13) varies significantly between adjacent cross sections, indicating that gradually varied geometry is not present in the Agua Fria River and that future channel adjustments to a more stable form should be expected.
- Wetted Perimeter/Top width. Plots of channel and total wetted perimeter and top width (Figure 6-14 to Figure 6-17) further substantiate the variation in channel geometry between adjacent cross sections, and potential for large areas of flooded, but ineffective flow within the study reach. These plots also indicate that the 2-year flood generally does not fill the channel bottom of the defined main channel. While the 10-year flood generally flows bank to bank across the main channel, it generally does not reach the top of bank elevation. Finally, the massive increase in channel width caused by construction of the Corps of Engineers levees is apparent in the plots. Narrowing, or formation of an inset low flow channel, should be expected in response to low flows within the levee reaches.
- Velocity. Plots of channel velocity (Figure 6-18) indicate that velocity does not increase significantly with discharge in the downstream direction. Furthermore, 2-year velocities are not substantially lower than 10-year velocities, but are about half of the 100-year velocities. The highest velocities occur in the narrowest channel sections, which are typically located at bridges or in highly encroached reaches.
- Channel Distance. Figure 6-20 indicates that cross sections in the HEC-RAS model are consistently spaced within the study reach.
- Manning's N Value. Figure 6-21indicates that N values were selected in a consistent fashion within the study reach.
- Froude Number. Figure 6-22 indicates that flow in the study reach is strongly subcritical, except at isolated cross sections.
- Head Loss. The consistency of head loss between the 2-, 10-, and 100-year profiles indicates that the computed head loss is driven primarily by elevation difference between adjacent cross sections and that strong backwater conditions probably do not exist, except locally (Figure 6-23).

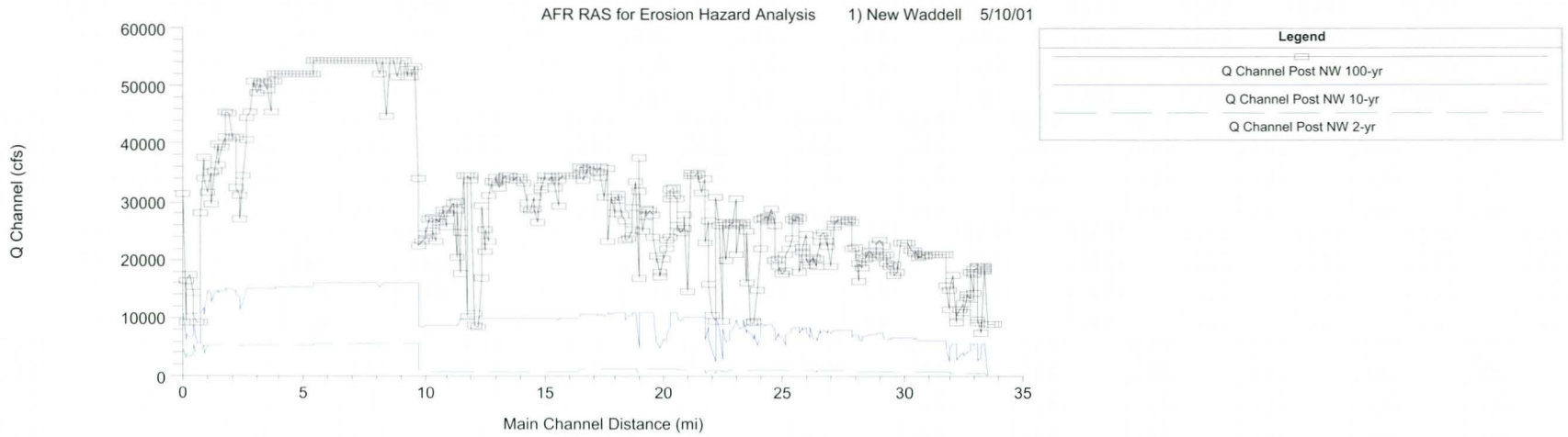

Figure 6-7. Agua Fria River Channel Discharge (QCH) vs. Distance.

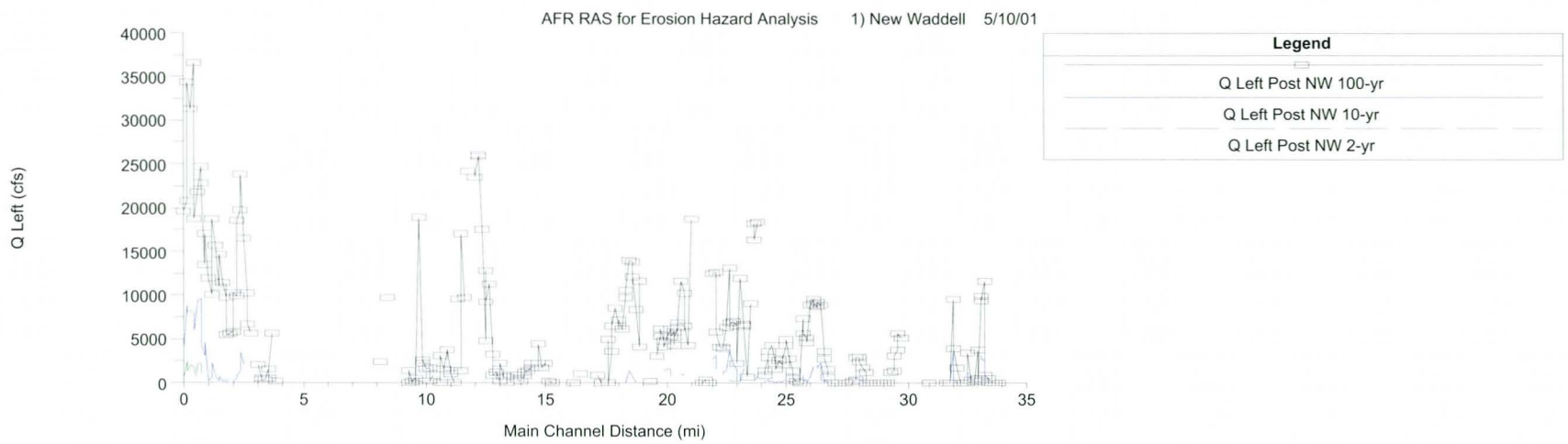

Figure 6-8. Agua Fria River Left Overbank Discharge vs. Distance.

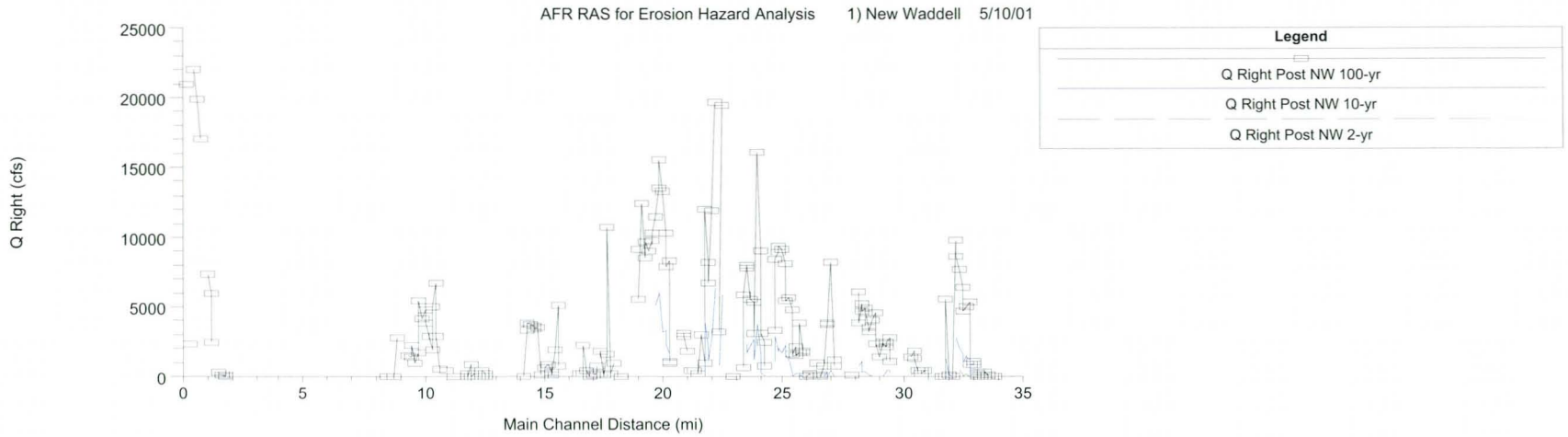

Figure 6-9. Agua Fria River Right Overbank Discharge vs. Distance.

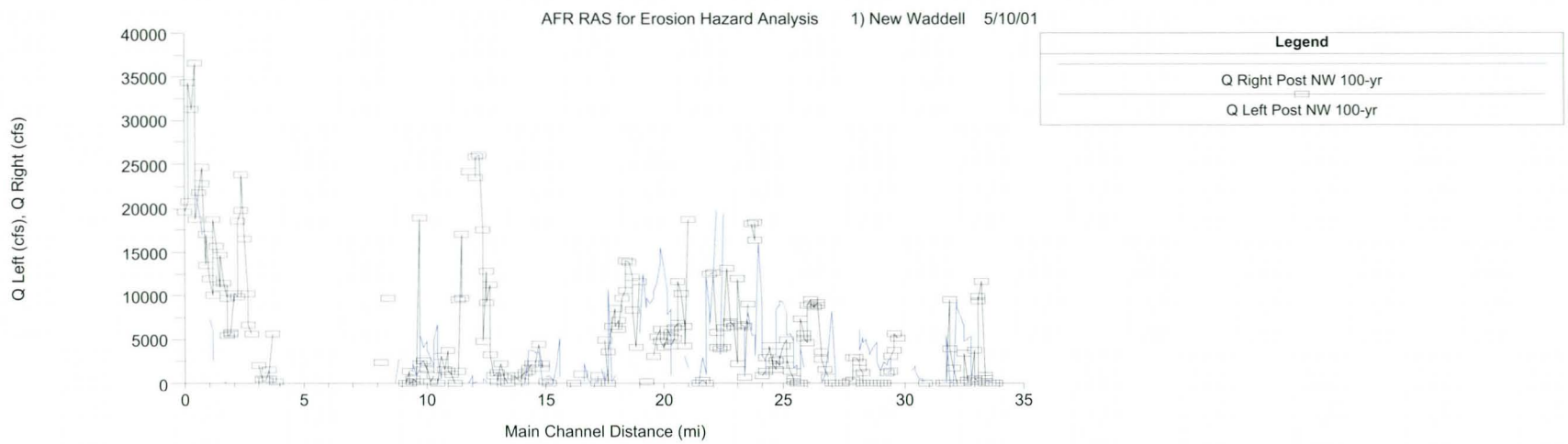

Figure 6-10. Agua Fria River Right and Left Overbank Discharge 100-Year Event.

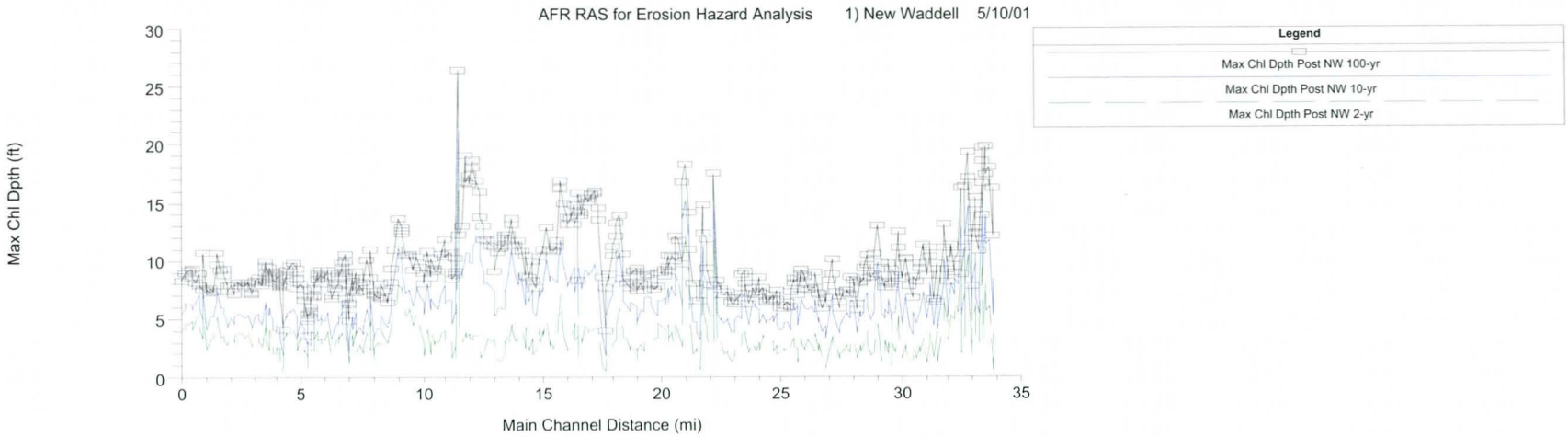

Figure 6-11. Agua Fria River Maximum Channel Depth vs. Channel Distance.

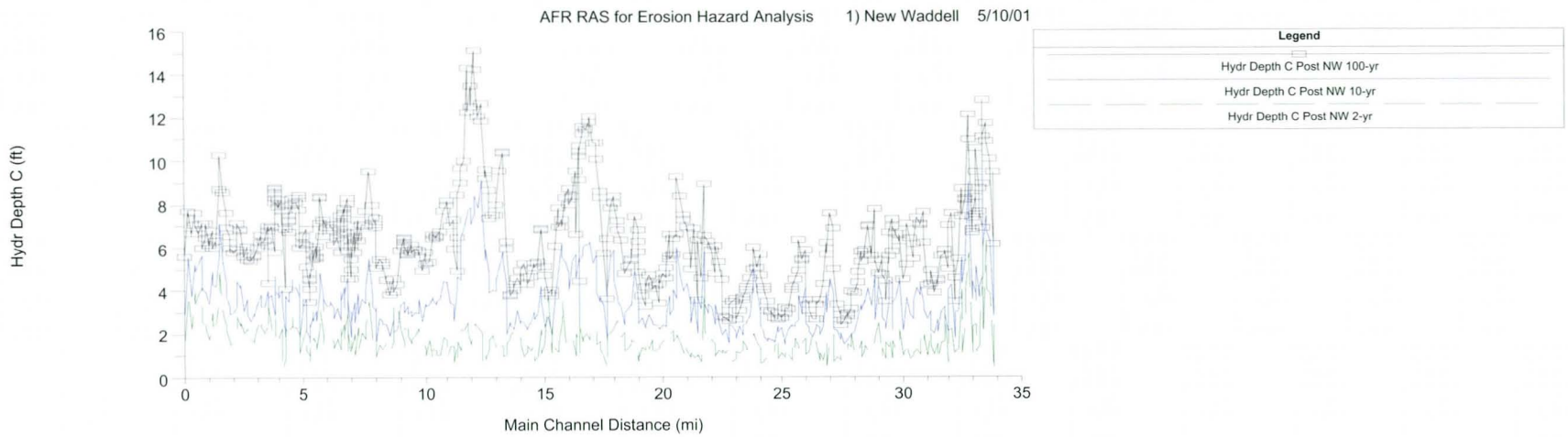

Figure 6-12. Agua Fria River Hydraulic Channel Depth vs. Channel Distance.

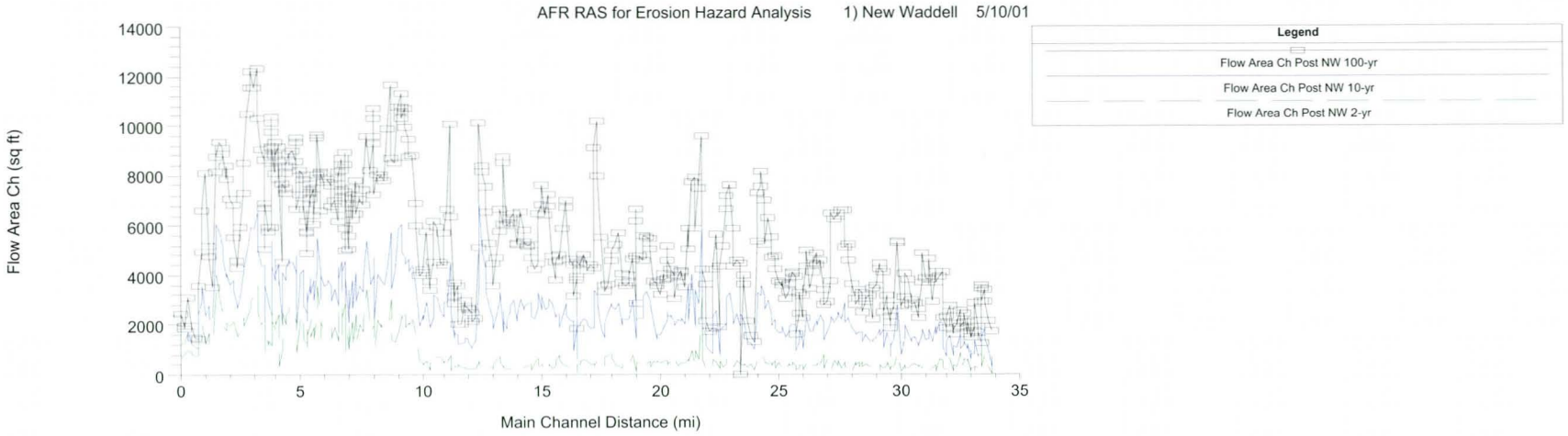

Figure 6-13. Agua Fria River Channel Flow Area vs. Channel Distance.

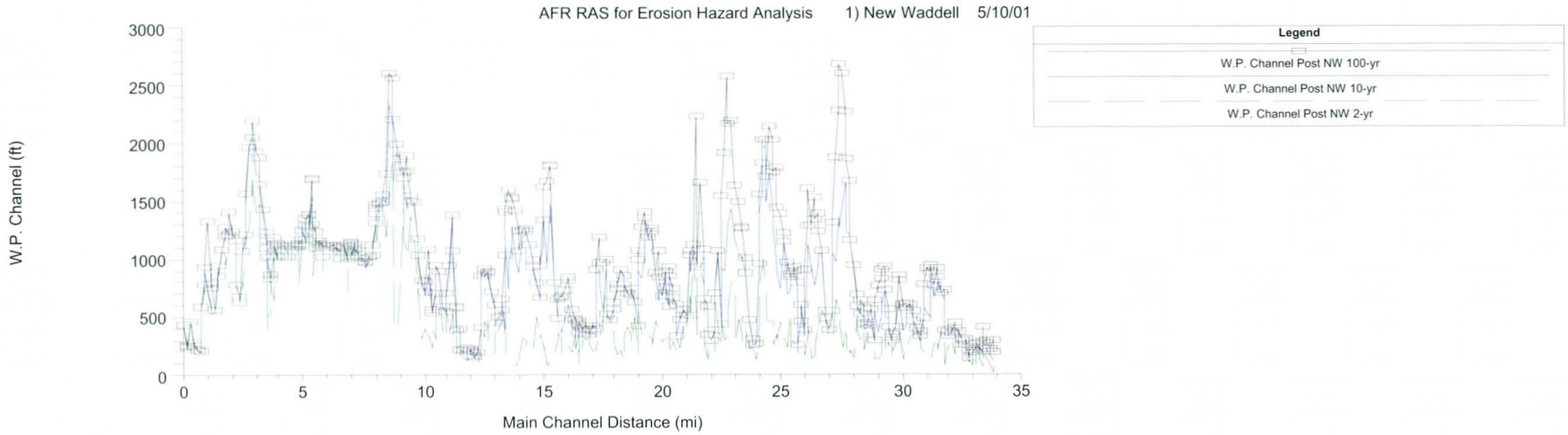

Figure 6-14. Agua Fria River Channel Wetted Perimeter vs. Channel Distance.

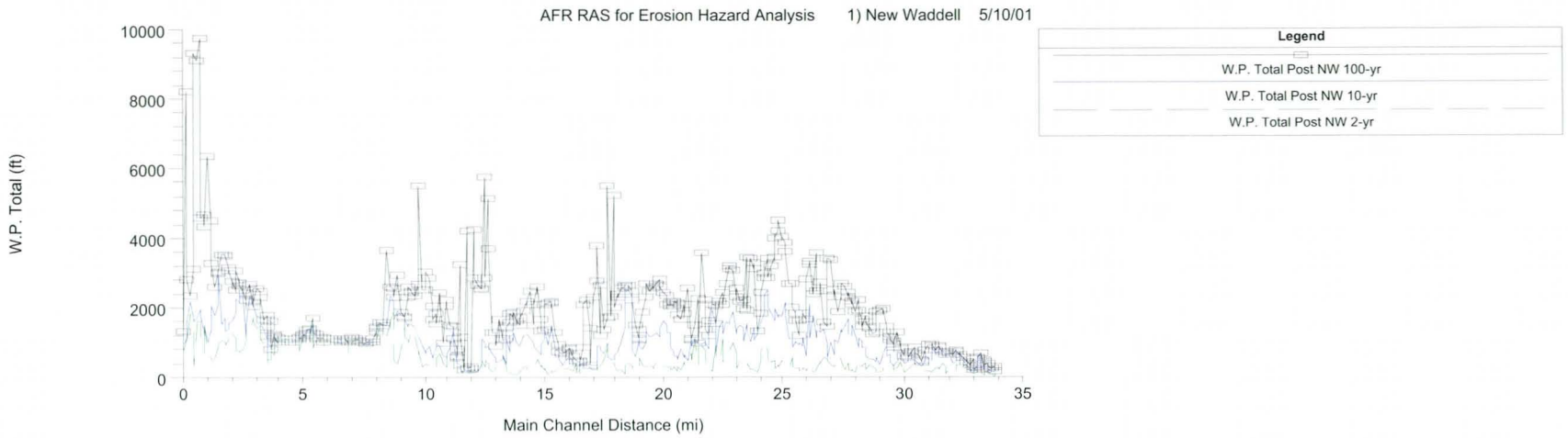

Figure 6-15. Agua Fria River Total Wetted Perimeter vs. Channel Distance.

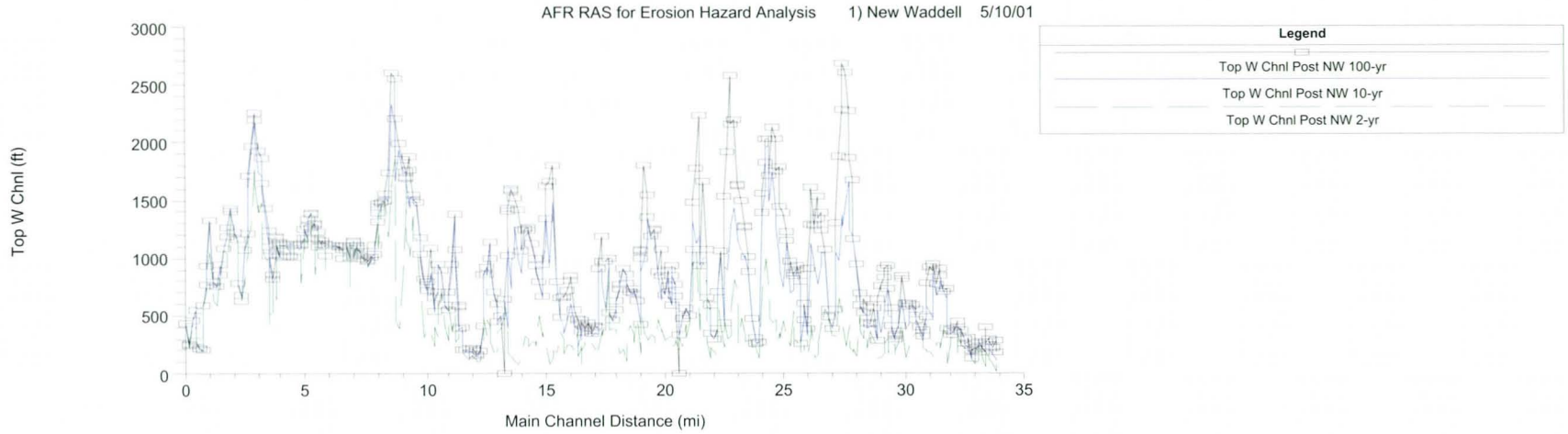

Figure 6-16. Agua Fria River Channel Topwidth vs. Channel Distance.

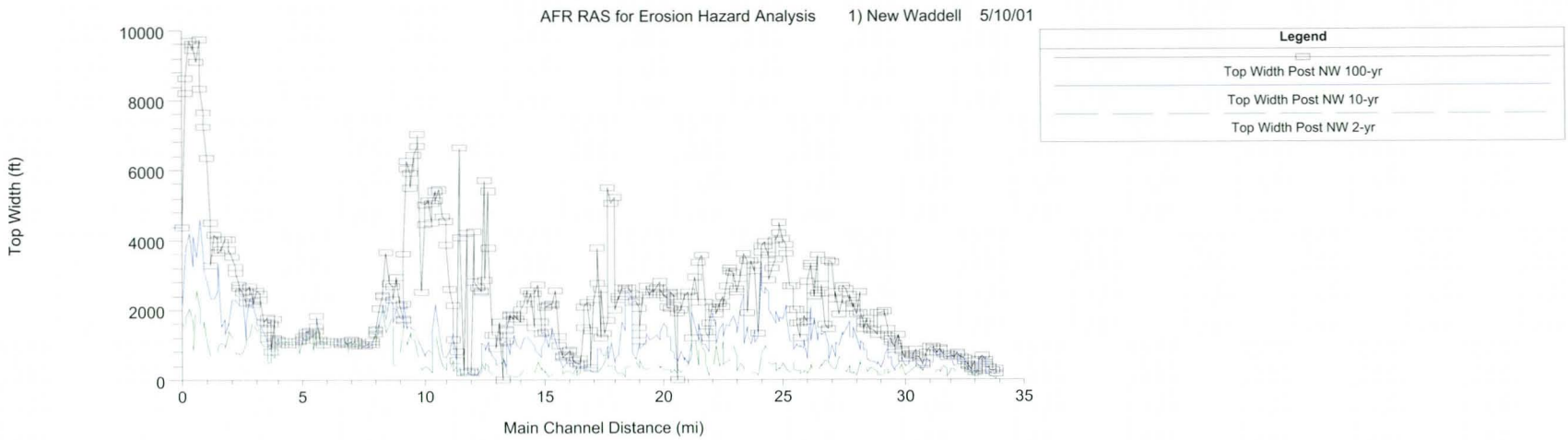

Figure 6-17. Agua Fria River Total Topwidth vs. Channel Distance.

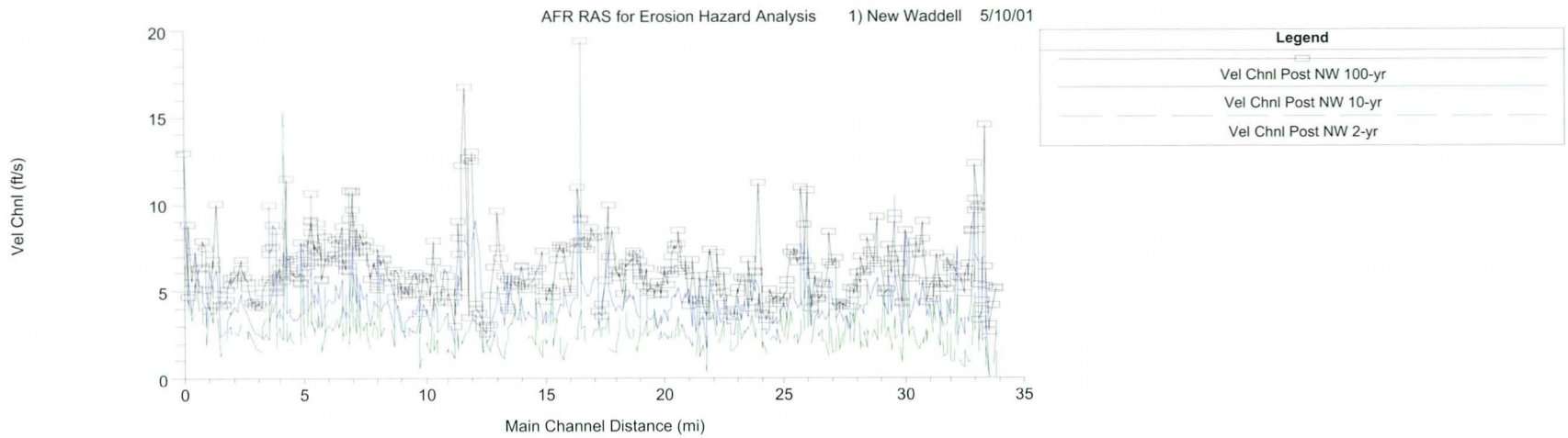

Figure 6-18. Agua Fria River Channel Velocity vs. Channel Distance.

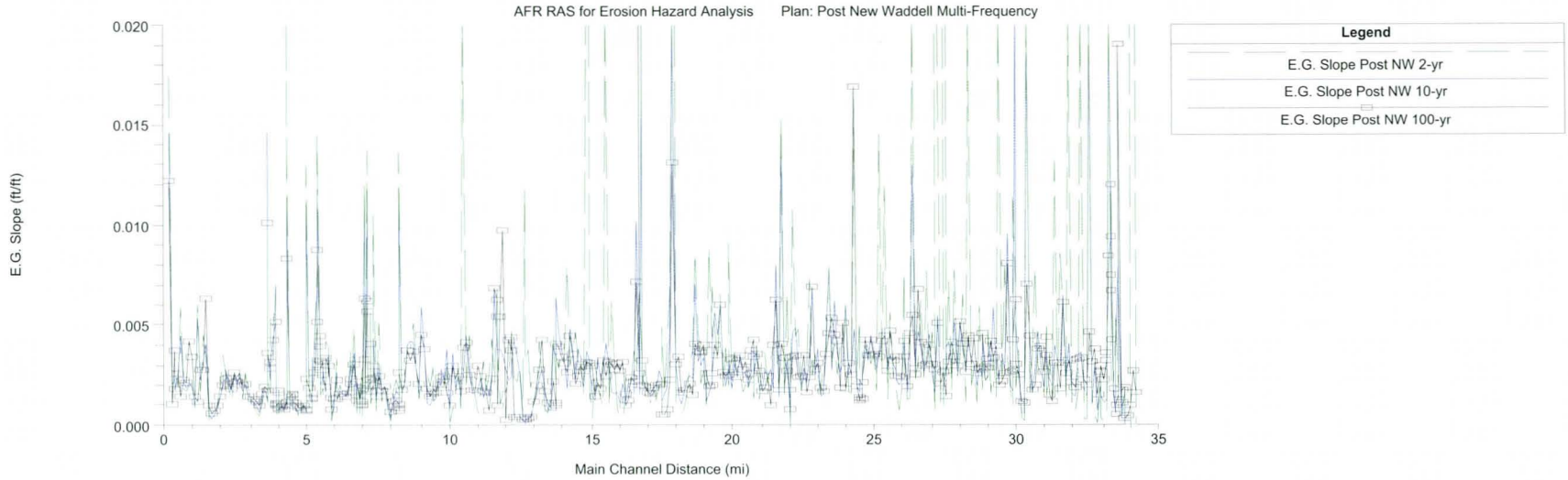

Figure 6-19. Agua Fria River Energy Grade Slope vs. Channel Distance.

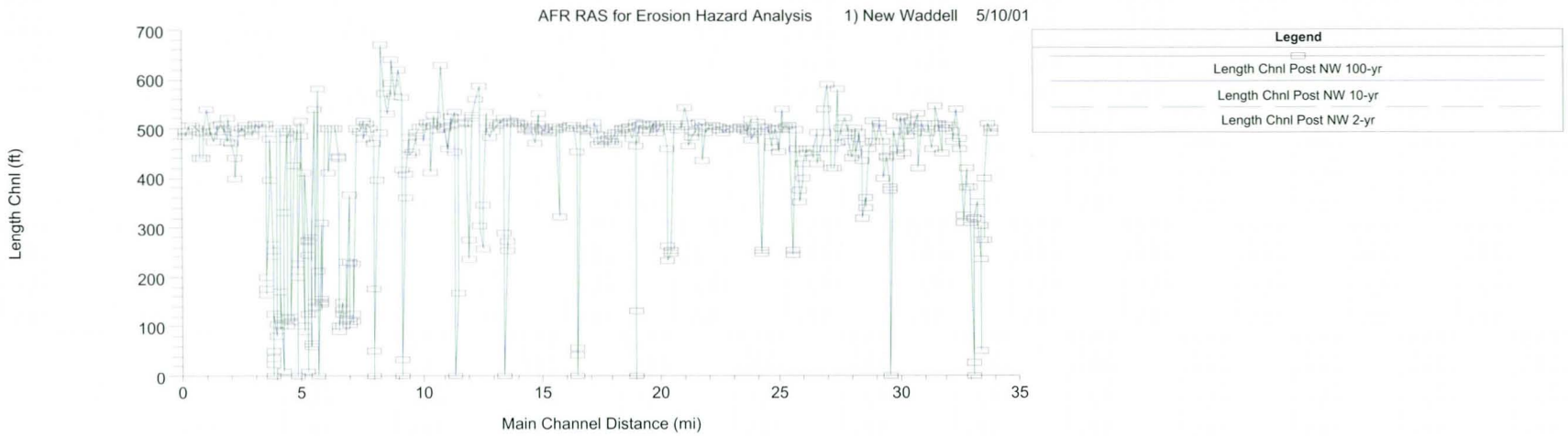

Figure 6-20. Agua Fria River Distance Between HEC-RAS Cross Sections.

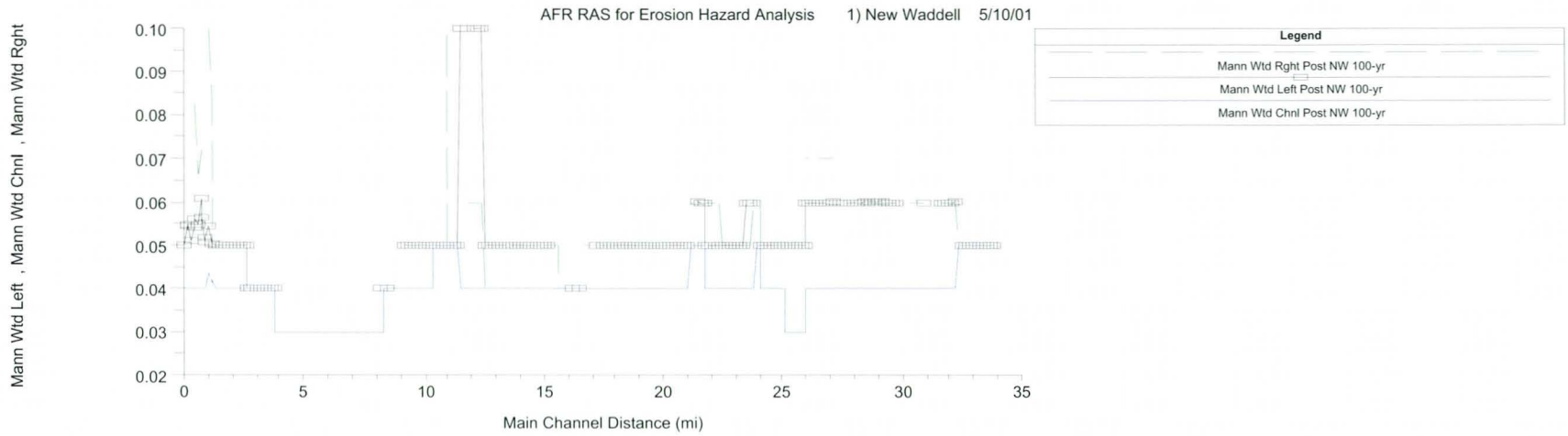

Figure 6-21. Agua Fria River Weighted Channel and Overbank Manning's n Values.

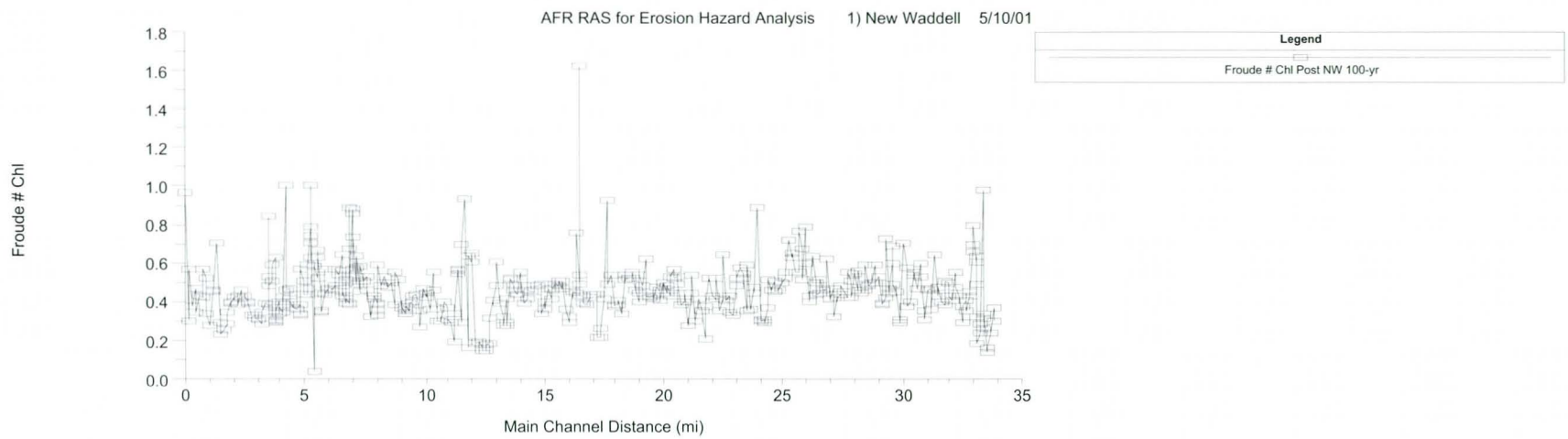

Figure 6-22. Agua Fria River Froude Number vs. Channel Distance.

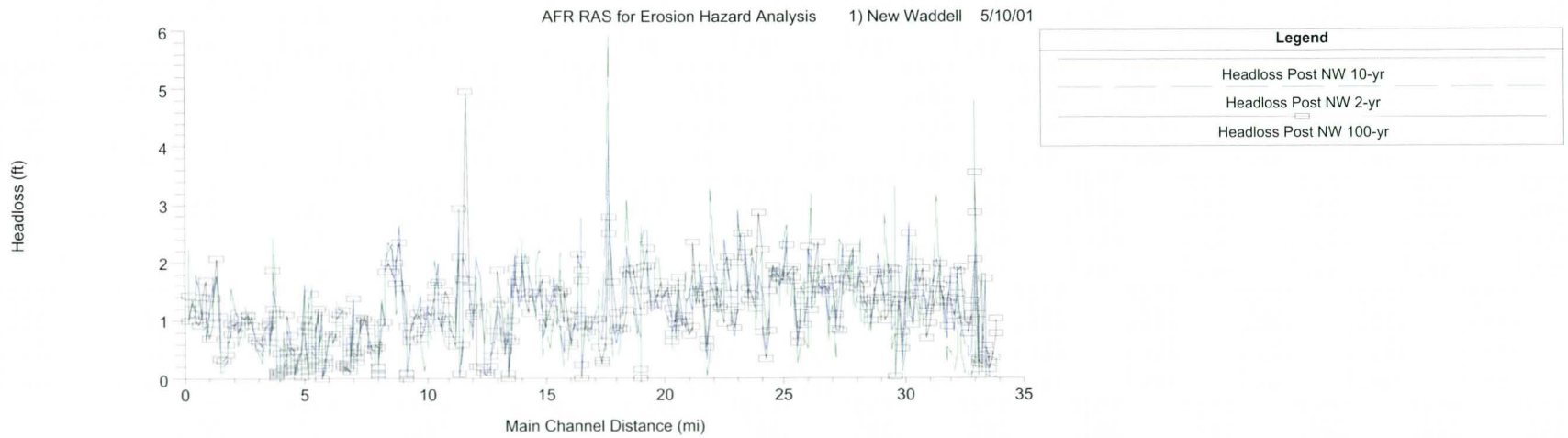

Figure 6-23. Agua Fria River Head Loss vs. Channel Distance.

6.3 Sediment data

The sediment data used in the erosion hazard analyses were provided to JEF by KHA. The sediment sampling and laboratory testing was performed by Hoque & Associates (HA) under contract to KHA. The general procedures as described by HA were as follows (FAX from HA to KHA dated 4/24/01):

> *Representative bulk samples ... were collected from 42 locations designated by KHA.... ... Samples were collected manually by hand utilizing a shovel from the surface to approximately three feet in depth consistent with the procedures described in the Bureau of Reclamation's Computing Degradation and Local Scour, January 1984 or the US Army Corps of Engineers Sedimentation Investigations of Rivers and Reservoirs, October 1995. Particle size analyses were performed on each sample in HA's laboratory in accordance with procedures described in ASTM D422. Samples containing at least ten percent fines (passing a #200 US standard sieve) were tested for grain size-distribution using the hydrometer in accordance with ASTM D422.*

According to the data provided by HA to KHA, samples were generally located within the main channel at each location as identified by KHA.

JEF combined the individual samples into reach representative samples for the Upper, Middle, and Lower Reaches based on similarity of particle size-distributions as shown in plots of percent finer versus sediment size (see Figure 6-24, Figure 6-25, and Figure 6-26). For the Upper Reach, four samples (RM 28.95, 30.92, 31.96, and 32.64) were excluded from the calculation of the reach average sediment size distribution. These samples were excluded based on their deviation from the general distribution for the reach as shown by the remaining fourteen samples (Figure 6-26).

Table 6-1 summaries the numerical particle sizes used in evaluation of the erosion hazards for the study area.

Table 6-1 - Summary of Sediment Data Sizes Used in the Erosion Hazard Analysis

Reach	D10 (mm)	D16 (mm)	D50 (mm)	D84 (mm)	D90 (mm)
Upper	0.4	0.6	2.2	20.0	28.0
Middle	0.2	0.4	1.1	16.0	23.0
Lower	0.2	0.2	0.5	1.3	1.9

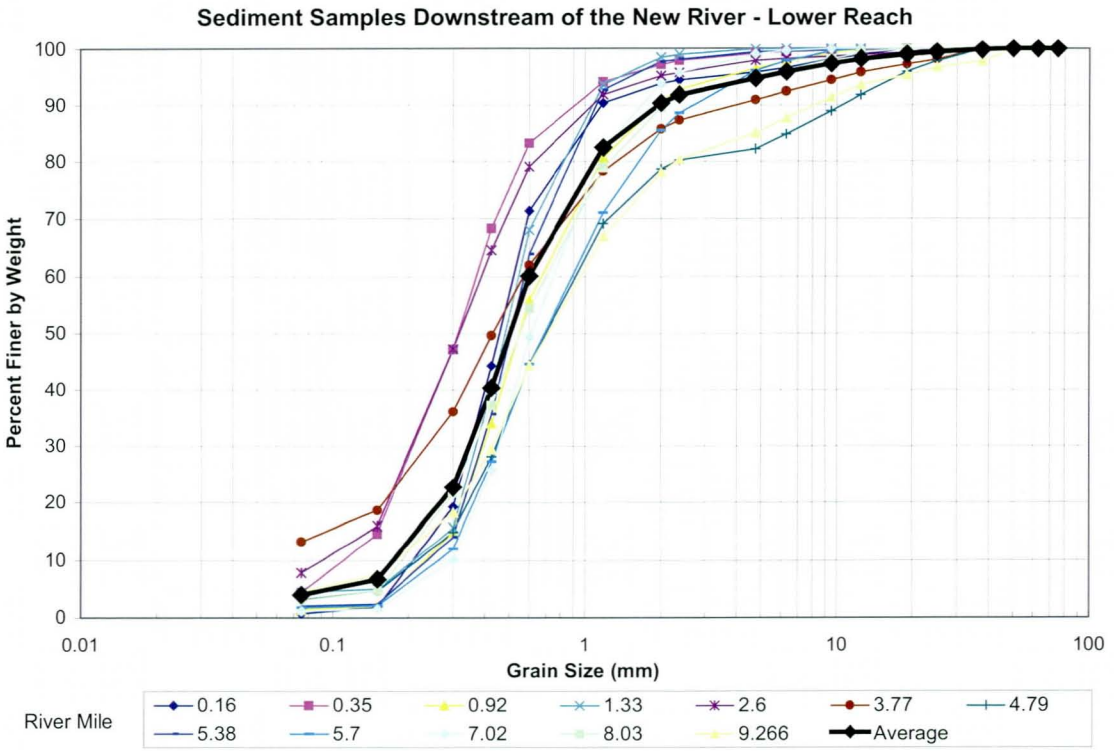

Figure 6-24 - Sediment Data for Lower Reach (New River Confluence to Gila River)

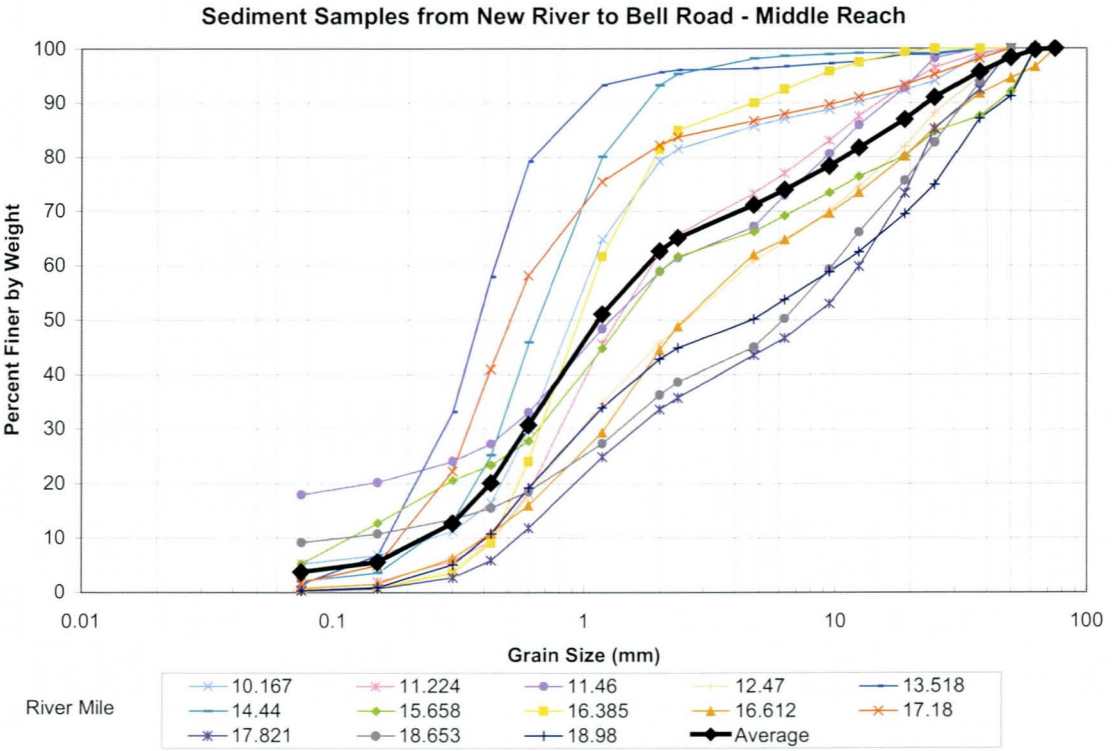

Figure 6-25 - Sediment Data for Middle Reach (Bell Road to New River Confluence)

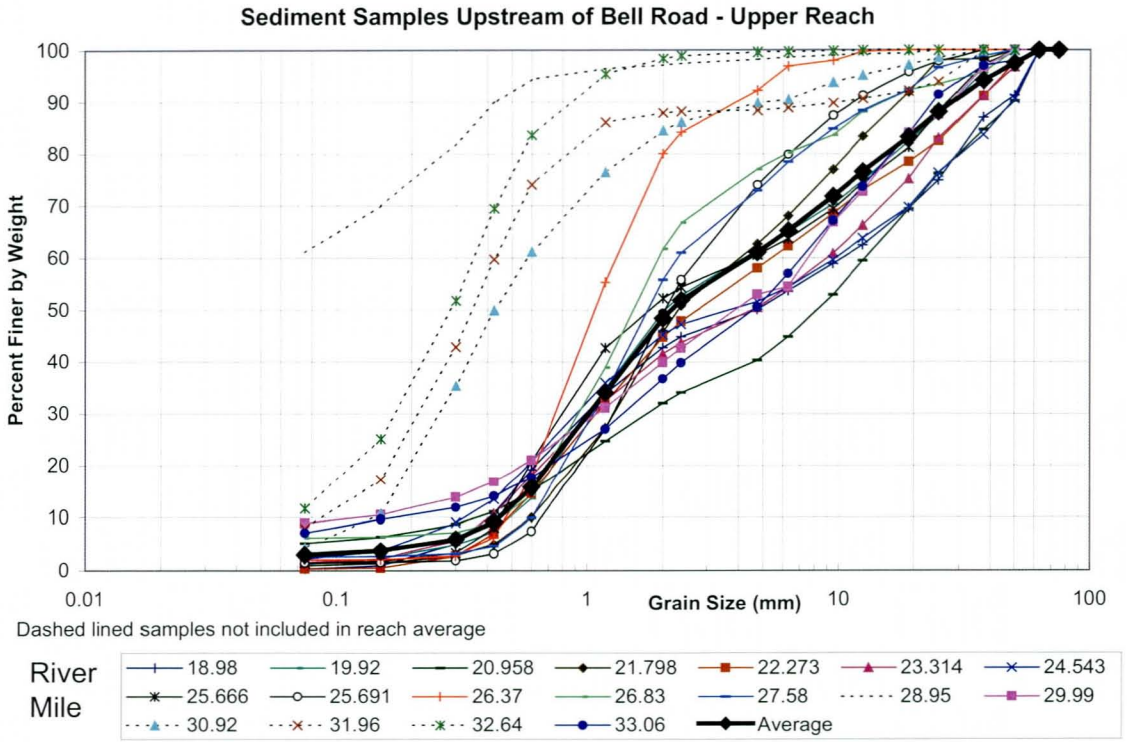

Figure 6-26 - Sediment Data for Upper Reach (Bell Road to New Waddell)

Examination of Table 6-1 and Figure 6-24, Figure 6-25, and Figure 6-26 shows a decrease in sediment particle size from upstream to downstream. This decrease was confirmed by field observations described in Chapter 2. The decrease in sediment size reflects both the overall increase in the channel width between the Pleistocene terraces as well as a decrease in flow rate in the downstream direction, resulting from transmission losses and attenuation in the large overbank areas.

6.4 Geomorphic methods

6.4.1 Bankfull Discharge

Figure 6-27 shows the variation in bankfull discharge along the Agua Fria downstream of New Waddell Dam. The lines and numbers in magenta show the reach divisions used in this report. The heavy black line is a five-station running average computed from the data by the Excel software. Similar figures showing the top width (Figure 6-28), depth (Figure 6-29), velocity (Figure 6-30), and width/depth ratio (Figure 6-31) at bankfull discharge are provided on the following pages. Table 6-2 to Table 6-6 summarize the reach average statistics for each of the variables shown in Figure 6-27 - Figure 6-31.

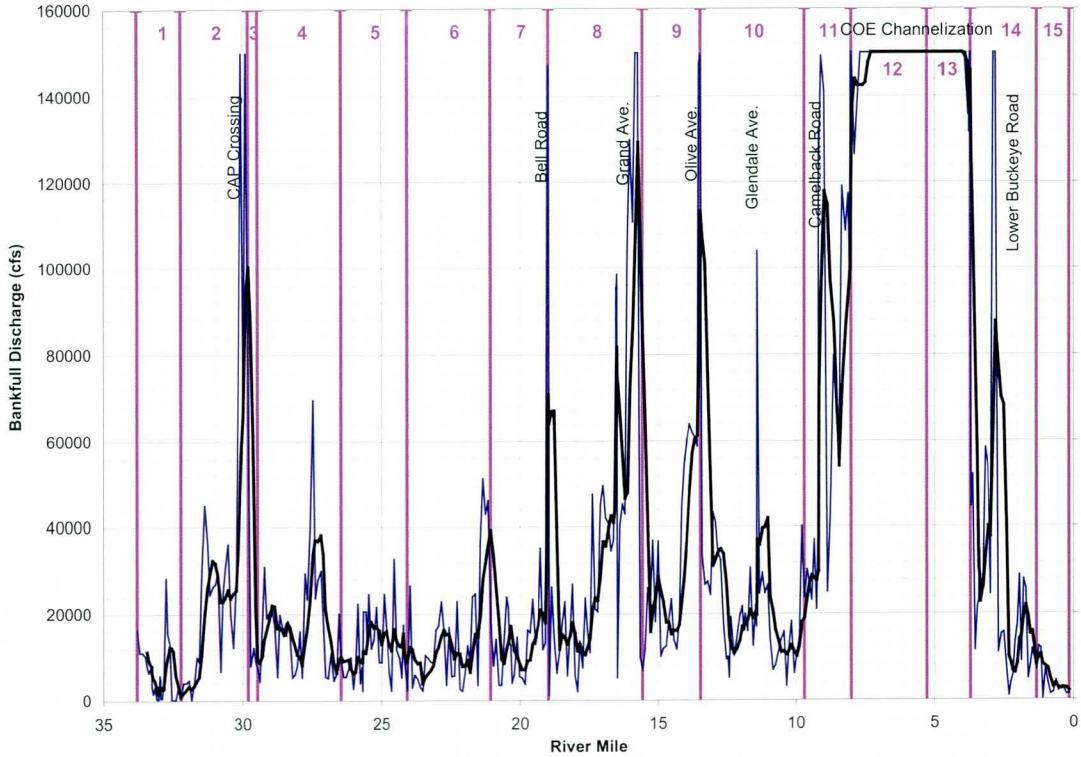

Figure 6-27 Variation in Bankfull Discharge Along the Agua Fria River Downstream of New Waddell Dam

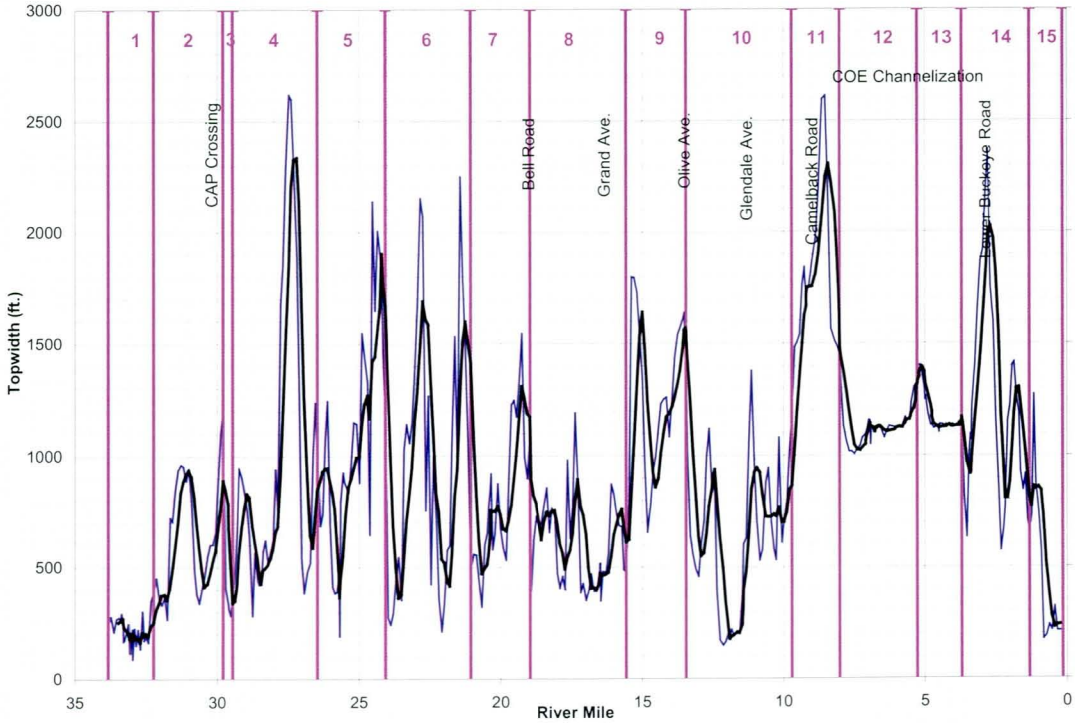

Figure 6-28 Top width at Bankfull Discharge Along the Agua Fria River Downstream of New Waddell Dam

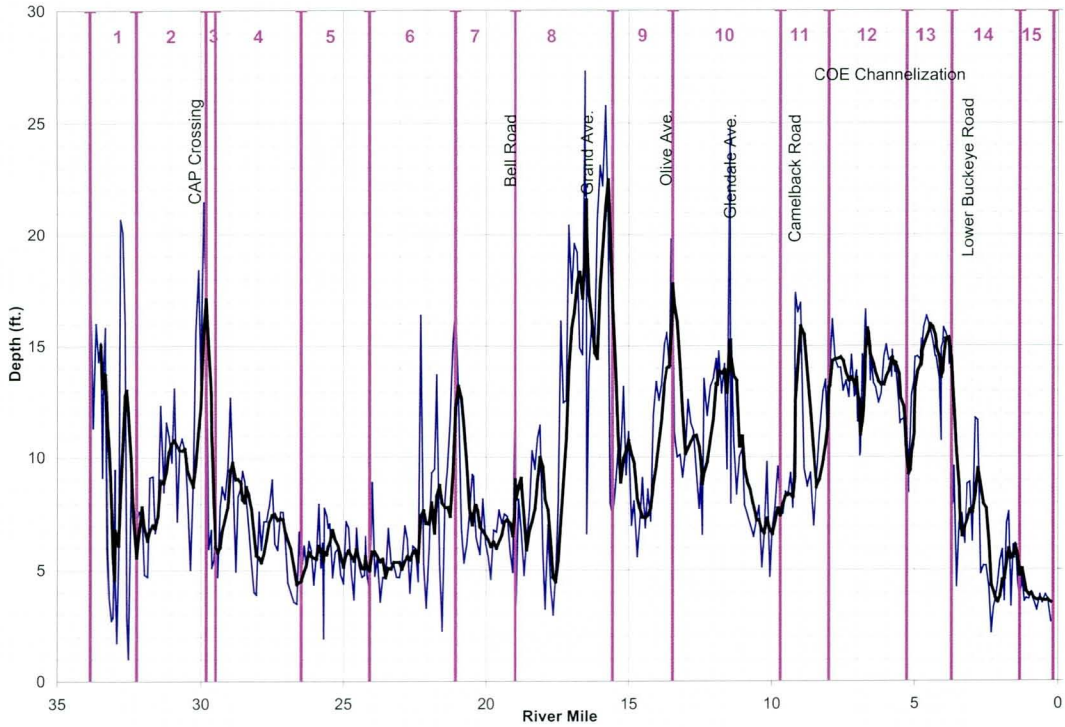

Figure 6-29 Depth at Bankfull Discharge Along the Agua Fria River Downstream of New Waddell Dam

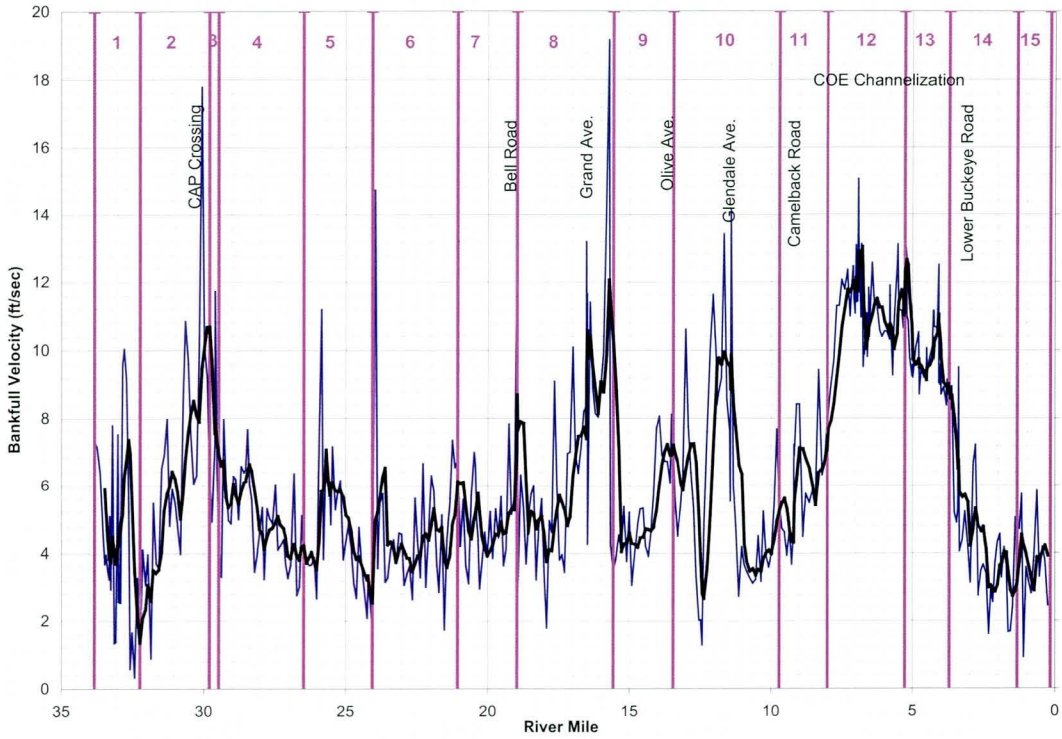

Figure 6-30 Velocity at Bankfull Discharge Along the Agua Fria River Downstream of New Waddell Dam

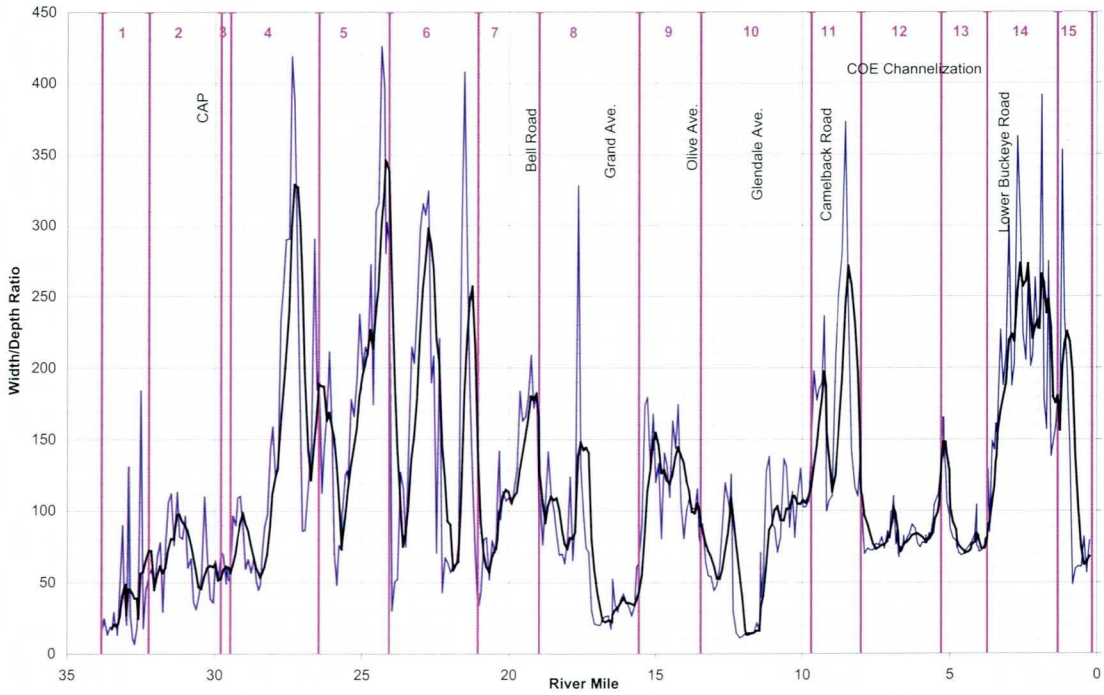

Figure 6-31 Width/Depth Ratio Along the Agua Fria River Downstream of New Waddell Dam

Table 6-2 Reach Average Bankfull Discharges

Reach	Average Qbf (cfs)	Average Qbf (cfs) without Reaches 12-13, and all bridges	Median Qbf (cfs)	Median Qbf (cfs) without Reaches 12-13, and all bridges	Approximate frequency of Median Qbf without Reaches 12-13, and all bridges
1	6400	6900	4500	5300	10-year
2	32800	18800	25500	22200	100-year
3	20700	8500	11300	8500	12-year
4	17800	17800	17600	17600	30-year
5	12200	12200	9800	9800	11-year
6	14900	14900	9400	9400	9-year
7	18600	13300	13500	13400	12-year
8	45700	22900	26900	20500	35-year
9	41100	31300	25200	24000	43-year
10	24600	19700	18300	17800	30-year
11	76700	40800	66500	33800	40-year
12	149300	N/A	150000	N/A	> 100-year
13	147700	N/A	150000	N/A	> 100-year
14	37300	21200	22100	16700	11-year
15	4300	4300	2800	2800	< 2-year
All	52800	18000	22750	14400	
w/o 12-13	27800		16070		

Table 6-3 Reach Average Top Width at Bankfull Discharge

Reach	Average Top Width (feet)	Average Top Width (ft) without Reaches 12-13, and all bridges	Median Top Width (feet)	Median Top Width (ft) without Reaches 12-13, and all bridges
1	220	220	220	220
2	630	600	600	520
3	510	350	330	350
4	970	970	670	670
5	1050	1050	940	940
6	980	980	1010	1010
7	820	810	760	720
8	610	590	560	490
9	1260	1230	1260	1260
10	650	630	610	610
11	1770	1890	1720	1800
12	1150	N/A	1130	N/A
13	1190	N/A	1140	N/A
14	1220	1150	1170	1130
15	490	490	370	370
All	930	840	940	730
W/o 12-13	870		760	

Table 6-4 Reach Average Depth at Bankfull Discharge

Reach	Average. Depth (ft)	Average Depth (ft) without Reaches 12-13, and all bridges	Median Depth (ft)	Median Depth (ft) without Reaches 12-13, and all bridges
1	9.9	10.3	9.4	10.3
2	10.0	8.7	9.1	8.8
3	8.0	5.7	5.9	5.7
4	7.0	7.0	7.2	7.2
5	5.7	5.7	5.8	5.8
6	6.8	6.8	5.5	5.5
7	7.6	7.4	6.9	6.8
8	13.2	10.4	12.6	9.5
9	11.0	10.2	10.2	9.6
10	10.5	10.2	10.0	9.8
11	11.2	8.3	9.5	8.4
12	13.4	N/A	13.8	N/A
13	14.0	N/A	14.5	N/A
14	6.7	5.8	6.2	6.0
15	3.7	3.7	3.7	3.7
All	9.9	8.0	9.1	7.2
w/o 12-13	8.9		7.6	

Table 6-5 Reach Average Channel Velocity at Bankfull Discharge

Reach	Average Velocity (ft/s)	Average Velocity (ft/s) without Reaches 12-13, and all bridges	Median Velocity (ft/s)	Median Velocity (ft/s) without Reaches 12-13, and all bridges
1	4.7	4.6	4.2	3.8
2	6.5	5.5	6.0	5.5
3	7.3	5.7	6.5	5.7
4	5.0	5.0	5.0	5.0
5	4.7	4.7	4.0	4.0
6	4.7	4.7	4.4	4.4
7	5.2	4.9	5.0	4.8
8	7.2	5.8	6.4	5.6
9	5.4	5.2	5.2	5.0
10	6.0	5.8	5.3	5.3
11	6.1	5.0	5.7	5.1
12	11.0	N/A	11.1	N/A
13	9.9	N/A	9.4	N/A
14	4.7	4.2	4.2	3.9
15	3.8	3.8	3.8	3.8
All	6.5	5.0	5.7	4.7
w/o 12-13	5.5		4.9	

Table 6-6 Reach Average Width/Depth Ratio at Bankfull Discharge

Reach	Average W/D	Average W/D without Reaches 12-13, and all bridges	Median W/D	Median W/D without Reaches 12-13, and all bridges
1	38	40	23	22
2	67	70	66	68
3	60	60	61	60
4	146	146	109	109
5	191	191	176	176
6	165	165	138	138
7	116	117	109	111
8	66	77	61	70
9	120	123	112	118
10	72	72	75	81
11	174	228	148	217
12	87	N/A	82	N/A
13	89	N/A	78	N/A
14	201	210	195	203
15	131	131	101	101
All	114	126	88	106
w/o 12-13	120		100	

Flood hydrographs from 1978, 1979, and 1980 events are presented in Figure 6-32. The majority of the water volume occurs at discharges below 15,000 to 18,000 cfs. It is interesting to note that this discharge matches well with the average bankfull discharge estimated for the whole study length (Table 6-2). This correlation between the observed bankfull discharge channel and the flow rates of the three large historical floods indicates that significant channel forming work was done by the three floods of 1978-1980, and especially the sustained dam outflow that occurred in 1980. Floods after the 1980 event were too small or short to significantly alter the channel shaped by the floods of 1978-1980. The coincidence of the geomorphically-identified bankfull channel and the discharge at which most of the flood volume occurred is evidence of the adjustment of the channel to large floods. This finding points to the relative importance of large floods in long-term channel shaping, during which erosion and movement of the channel is a more serious problem. The correlation also supports the conclusions made based on the field and historical analyses that large flood discharges perform much of the geomorphic work in the study reach.

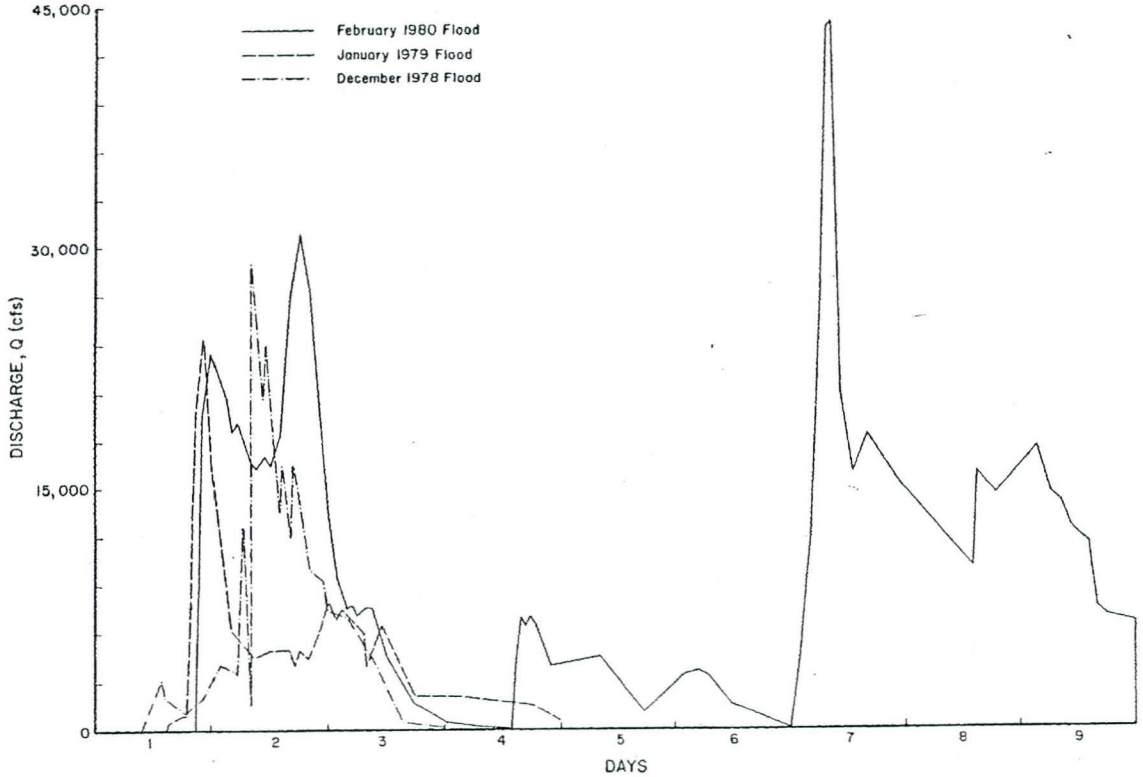

Figure 6-32 Flood hydrographs for Dec. 1978, Jan. 1979, and Feb. 1980 flood on the Agua Fria River

6.4.2 Hydraulic Geometry/Regime Equations

Regime equations and hydraulic geometry analyses attempt to relate measurable stream characteristics, such as sediment size, mean annual discharge or bankfull discharge, to equilibrium channel geometry characteristics such as stream width, channel depth, flow velocity or channel slope. Regime theory originated from studies of non-scouring and non-silting stable alluvial canals (cf. Kennedy, 1895), and has been extended to a wide variety of stream types (cf., Ackers & Charlton, 1971; Blench, 1951). Regime equations are typically based on discharge, sediment characteristics, and channel geometry. Hydraulic geometry analyses are theoretically similar to regime theory, but are based on empirical data gathered from natural streams or flumes and are typically based solely on discharge. Hydraulic geometry expresses the variation of channel characteristics with increasing discharge at a single section or along the length of a stream. The U.S. Geological Survey (cf., Leopold & Maddock, 1953) published the most widely used hydraulic geometry data.

Regime equation and hydraulic geometry analyses were applied to the Agua Fria River study reaches to evaluate the following stream characteristics:

- Channel pattern
- Channel geometry
- Hydraulic geometry

Lateral stability was evaluated by comparing predicted stream characteristics from one or more of these methodologies to the observed characteristics. These analyses assume that over the long-term the alluvial rivers will tend to erode their bed and banks, or adjust their slope or

channel pattern to better match the expected characteristics. In addition, even though regime equations and hydraulic geometry relationships are empirically derived using data sets from very specific stream types (e.g., sand-bed rivers, canals, etc.), the data typically still have a large amount of scatter. The scatter in the original data limits the accuracy of the results. To increase the accuracy of the results, the equations selected for this study were based on data sets from streams which were the most similar to the study area characteristics. It is noted that ephemeral streams in central Arizona are unique, and therefore the results obtained by applying these equations must be interpreted cautiously. In general, the results are best interpreted as order-of-magnitude estimates of the direction of expected change, rather than precise predictions of the magnitude of future channel adjustments.

Data Sources. Stream characteristics and other data used in the analyses described below were obtained from the following sources described elsewhere in this report:

- Recent topographic mapping – Chapters 2 and 3
- USGS gauge records – Chapter 3
- Hydrologic modeling by the COE (1995) – Chapter 3
- Field observations and measurements – Chapter 3
- HEC-RAS modeling – Chapter 6

6.4.2.1 Channel Pattern Relationships

Methodology. The slope of a stream has a strong influence on the channel pattern for a given discharge. Numerous researchers have used empirical data, flume studies, and theoretical relationships to establish a threshold slope that separates braided and meandering stream patterns. Four slope-discharge relationships were selected for evaluation of the streams in the study area.

Lane Equations. Lane (1952) published empirical formulas to define the threshold slope for channel pattern, based on data from alluvial sand bed rivers. His equations leave an intermediate zone between the lines defined by the two slope equations where either pattern occurs. The Lane equations for channel pattern are:

$S_o > 0.010\ Q_m^{-0.25}$ (Braided channels)

$S_o < 0.001\ Q_m^{-0.25}$ (Meandering channels)

Where S_o = channel slope (ft./ft.), and

Q_m = mean annual discharge (cfs)

The mean annual discharge for the Agua Fria River was estimated from USGS gauge records from the Agua Fria at El Mirage station (Q_m = 1.4 cfs), Agua Fria at Avondale station (Q_m = 32 cfs), and New River near Glendale (Q_m = 24.9 cfs). Since the New River and Agua Fria at Avondale stations had similar mean annual discharges and the Avondale period of record was older and shorter, the New River near Glendale data were used to represent the mean annual discharge for the Lower Reach.

Leopold & Wolman Equations. The Leopold and Wolman equations (1957) were developed using data from rivers with coarse bed material (D50 > ¼ inch).

$S_o > 0.06\ Q_{maf}^{-0.44}$ (Braided channels)

$S_o < 0.06\ Q_{maf}^{-0.44}$ (Meandering channels)

Where S_o = channel slope (ft./ft.), and

Q_{maf} = mean annual flood (cfs)

The equations are based on bankfull discharge, which Leopold and Wolman determined to be equal to the mean annual flood. The mean annual flood has a recurrence interval of about 2.33 years (ADWR, 1985). It is noted that the bankfull discharge for the streams in the study area is significantly greater than the 2.3 year flood (Table 6-2). The 2-year discharge was used in this analysis as an approximation of the mean annual flood. Leopold and Wolman found that straight channels could occur on all slopes, and that the occurrence of straight channels had poor correlation to bankfull discharge.

Henderson Equation. Henderson (1961) used Leopold's and Wolman's data, but added a variable describing the mean bed sediment diameter.

$$S_o > 0.64\ D_{50}^{1.14}\ Q_{maf}^{-0.44} \qquad \text{(Braided channels)}$$

Where S_o = channel slope (ft./ft.), and

Q_{maf} = mean annual flood (cfs), and

D_{50} = mean sediment diameter (ft.)

Sediment diameter data were obtained from sieve analyses as described in Section 6.3.

Results. Application of the four channel pattern equations to the study area are shown in Table 6-7. The measured slope for each reach is also shown. Field observations suggest that flow in the Agua Fria River is often straight or slightly sinuous and becomes braided at higher flow rates. The channel pattern equations were applied on a reach-by-reach basis. Table 6-7 compares the predicted channel pattern (braided, intermediate, meandering, single channel, etc.) with the channel pattern observed in the field and on aerial photographs. The predicted channel pattern was indicated by applying the equations described in the previous paragraphs.

As shown in Table 6-7, the channel pattern equations predict all types of patterns. The conclusion that may be drawn from these variable predictions is that the Agua Fria River is in a transitional state with respect to its planimetric form. Therefore, the river pattern may be susceptible to changes in system inputs that affect channel pattern. Also, the pattern for lower flows may tend toward a straight or meandering pattern, while higher discharges will likely result in a more braided channel pattern. The future nature of the Agua Fria River is likely to be a compound channel with a straight to meandering single channel low flow inset into a larger braided river channel, which conveys large flood discharges.

Table 6-7 Channel Pattern Relationships: Threshold Slope for Braided Channels

Reach	Equation	Computed Slope		Observed Slope	Expected Pattern	Observed Pattern
		Meander	Braided			
1	Lane	0.0009	0.0092	0.0019	Intermediate	Straight
	Leopold & Wolman	0.0036			Meander	
	Henderson	0.00014			Braided	
2	Lane	0.0009	0.0092	0.0033	Intermediate	Straight/Braided
	Leopold & Wolman	0.0034			Meander	
	Henderson	0.00013			Braided	
3	Lane	0.0009	0.0092	0.0006	Meander	Straight
	Leopold & Wolman	0.0034			Meander	
	Henderson	0.00013			Braided	
4	Lane	0.0009	0.0092	0.0030	Intermediate	Braided
	Leopold & Wolman	0.0030			Either	
	Henderson	0.00012			Braided	
5	Lane	0.0009	0.0092	0.0033	Intermediate	Braided
	Leopold & Wolman	0.0029			Braided	
	Henderson	0.00011			Braided	
6	Lane	0.0009	0.0092	0.0030	Intermediate	Braided
	Leopold & Wolman	0.0028			Braided	
	Henderson	0.00011			Braided	
7	Lane	0.0009	0.0092	0.0030	Intermediate	Braided
	Leopold & Wolman	0.0027			Braided	
	Henderson	0.0001			Braided	
8	Lane	0.0009	0.0092	0.0028	Intermediate	Straight
	Leopold & Wolman	0.0027			Braided	
	Henderson	0.00005			Braided	
9	Lane	0.0009	0.0092	0.0029	Intermediate	Braided
	Leopold & Wolman	0.0032			Meander	
	Henderson	0.00006			Braided	
10	Lane	0.0009	0.0092	0.0022	Intermediate	Straight
	Leopold & Wolman	0.0031			Meander	
	Henderson	0.00005			Braided	
11	Lane	0.0004	0.0045	0.0022	Intermediate	Straight
	Leopold & Wolman	0.0014			Braided	
	Henderson	0.00001			Braided	
12	Lane	0.0004	0.0045	0.0019	Intermediate	Straight
	Leopold & Wolman	0.0014			Braided	
	Henderson	0.00001			Braided	
13	Lane	0.0004	0.0045	0.0023	Intermediate	Straight
	Leopold & Wolman	0.0014			Braided	
	Henderson	0.00001			Braided	
14	Lane	0.0004	0.0045	0.0018	Intermediate	Straight
	Leopold & Wolman	0.0014			Braided	
	Henderson	0.00001			Braided	
15	Lane	0.0004	0.0045	0.0025	Intermediate	Straight
	Leopold & Wolman	0.0014			Braided	
	Henderson	0.00001			Braided	

6.4.2.2 Channel Geometry Relationships

Methodology. Equations for stable channel geometry have been developed from streams that have been stable for long periods of time. These equations relate bankfull channel width, depth, and velocity to a specific discharge rate, such as the average annual flow or the dominant discharge. Several stable geometry equations were applied to the Agua Fria River to assess the expected direction of future channel change.

Bray Equation #1. Bray (1979) developed equations for the geometry of alluvial gravel-bed rivers based on the 2-year discharge.

$$W = 2.38\ Q_2^{0.527}$$

$$d = 0.266\ Q_2^{0.33}$$

$$V_m = 8.0\ d^{0.6}\ S_o^{\ 0.29}$$

Where W = surface flow width (ft.)

Q_2 = 2-year discharge (cfs.)

d = flow depth (ft.)

V_m = mean channel velocity (ft./sec.)

S_o = channel slope (ft./ft.)

Bray Equation #2. Bray later modified his channel geometry relationships (Hey et. al., 1982) for gravel-bed rivers to include bankfull discharge and the bed material size.

$$W = 2.08\ Q_{bf}^{0.528}\ D_{50}^{-0.07}$$

$$d = 0.256\ Q_{bf}^{0.331}\ D_{50}^{-0.025}$$

$$V_m = 1.87\ Q_{bf}^{0.14}\ D_{50}^{0.095}$$

$$S_o = 0.0965\ Q_{bf}^{-0.334}\ D_{50}^{0.586}$$

Where W = surface flow width (ft.)

Q_{bf} = Bankfull discharge (cfs.)

D_{50} = medium bed sediment diameter (ft.)

d = flow depth (ft.)

V_m = mean channel velocity (ft./sec.)

S_o = channel slope (ft./ft.)

Hey Equation. Hey (1982) developed regime equations for gravel bed rivers in England that relate stable channel geometry to bankfull discharge and bedload transport rate.

$$WP = 2.2\ Q_{bf}^{-0.54}\ D_{50}^{\ -0.05}$$

$$R = 0.161\ Q_{bf}^{0.41}\ D_{50}^{\ -0.15}$$

$$d_{max} = 0.252\ Q_{bf}^{0.38}\ D_{50}^{\ -0.16}$$

$$S_o = 0.679\ Q_{bf}^{-0.53}\ Q_s^{-0.13}\ D_{50}^{\ 0.97}$$

Where WP = Wetted perimeter (m)

Q_{bf} = Bankfull discharge (m)

D50 = Median sediment diameter (m.)

R = Hydraulic radius (m)

d_{max} = Maximum channel depth (m)

S_o = Channel slope (m/m)

Q_s = Bedload sediment discharge (%)

However, because the results of the Hey equation for depth (d_{max}) were so much greater than was computed by the other equations used to compute stable depth, the Hey equation results were not included in the computation of the reach-average statistics shown in Table 6-8.

Parker Equation (Gravel Bed Rivers). Parker (1979) examined gravel bed rivers to obtain his channel geometry equations. He found that, unlike the bed material in sand bed streams, the gravel and cobble bed material in coarse bedded streams is moved only during larger flows. He also noted that the banks of gravel bed streams tended to be more stable and straighter than streams with finer bed materials (MacBroom, 1981). Parker's equations use a dimensionless discharge parameter (Q_*), as described below.

$$W_{bf} = 0.173\ Q_*^{0.5}\ D_{50}$$

$$d = 0.010\ Q_*^{0.415}\ D_{50}$$

$$S_e = 0.223\ Q_*^{-0.410}$$

Where W_{bf} = bankfull width, width at top of bank (ft)

$Q_* = 0.039\ V_m\ d^{-1}\ D_{50} / ((\rho_s-1)/\rho)\ g\ d)^{1/2})$ (dimensionless)

D_{50} = mean sediment diameter (ft.)

d = average channel depth (ft)

S_e = energy slope (ft./ft.)

Ackers & Charlton Equation.[1] The Ackers and Charlton (1971) equations were based on data from flume studies which used sand bed materials.

$$W = K_{ac}\ Q^{0.42}$$

Where W = surface channel width (ft.)

Q = discharge (cfs)

K_{ac} = a coefficient varying from 3.6 for straight channels to 7.2 for meandering channels

Lacey Equation. The Lacey equation (1929) was developed to describe the geometry of silt-laden canals in India. However, Bray reported (1979) that in gravel rivers in Canada, the Lacey equation was as accurate for predicting velocity as the Manning's equation.

$$V = 0.8Q^{0.167}$$

Where V = mean channel velocity (ft./sec.)

Q = discharge (cfs)

[1] The results of the Ackers & Charlton and the Lacey equations are presented on the same line in Tables 4-13 to 4-16 to reduce the length of the tables.

Chang Equation. Chang's (1988) gravel bed equations for channel geometry support the FLUVIAL-12 sediment transport model, which attempts to simulate channel change from sediment continuity data using minimum stream power concepts. Chang provides equations for channel width, depth, and slope.

$$S_o = 0.000442\ D_{50}^{1.15} / Q_{bf}^{0.42}$$

$$W = [1.905 + 0.249(\ln(0.001065\ D_{50}^{1.15} / (S_o\ Q_{bf}^{0.42}))^2]\ Q_{bf}^{0.47}$$

$$d = [0.2077 + 0.0418(\ln(0.000442\ D_{50} / (S_o\ Q_{bf}^{0.42})))^{1.15}]\ Q_{bf}^{0.42}$$

Where S_o = channel slope (ft./ft.)

D50 = median sediment diameter (mm.)

Q_{bf} = bankfull discharge (cfs)

W = channel width (ft)

d = average channel depth (ft)

In general, the Chang equation for slope performed poorly when applied to the study area. Some of the predicted channel geometry values were well outside the range of possibility (e.g., negative flow depths). Therefore, the results of the Chang equation are included in Table 6-8, but the predicted values were not used to obtain the average predicted values that were compared with existing reach characteristics.

Kellerhalls (1967) Equations. Kellerhals developed equations for the equilibrium channel width and depth in gravel bed rivers. The Kellerhals equations use the dominant discharge, which is also referred to as the channel-forming or effective discharge.

$$W = 1.8\ Q_{dd}^{0.5}$$

$$d = 0.166\ Q_{dd}^{0.4}\ K_n^{-0.12}$$

Where W = channel width (ft)

Q_{dd} = dominant discharge (cfs)

d = average channel depth (ft)

K_n = Nikuradse's sand grain roughness coefficient

Schumm Equation. Schumm (1961) preferred to examine the width/depth ratio of semi-arid streams, rather than either parameter separately. Schumm's equation is based on the percentage of fine-grained material in the channel banks.

$$F = 255\ M^{-1.08}$$

Where F = width/depth ratio

M = percentage of silt/clay in the bed.

The percentage of silt and clay in the bed material and banks was extracted from detailed SCS soils mapping of the study area (Camp, 1986). Application of the Schumm equation to streams with stratified bank materials is difficult. The results of the Schumm equation are consistent with the AMAFCA results, and are therefore not reported.

AMAFCA Equations. The AMAFCA (1994) equations for width and equilibrium slope were developed from empirical and theoretical data for application to the arroyo systems of northern New Mexico.

$$W = 0.5\ F^{0.6}\ Fr^{-0.4}\ Q^{0.4}$$

$$S_o = 18.28\ n^2\ F^{0.133}\ Fr^{2.133}\ Q^{-0.133}$$

Where W = width of channel (ft.)

F = width/depth ratio

Fr = main channel Froude number

Q = discharge (cfs.)

S_o = channel slope (ft./ft.)

n = Manning's n value for channel

Moody & Odem Equations. Moody and Odem (1999) recently completed an investigation of bankfull channel geometry relationships on a variety of stream types in Arizona using Rosgen channel classification methods. Channel geometry relationships were defined for a number of regions in Arizona, including a region near the Skunk Creek and Sonoran Wash study area.

$$Q_{bf} = 52.334\ DA^{0.5766}$$

$$A = 11.428\ DA^{0.5291}$$

$$TW = 12.301\ DA^{0.3756}$$

$$d = 0.9455\ DA^{0.1506}$$

Where Q_{bf} = Bankfull discharge (cfs)

DA = Watershed drainage area (mi^2)

A = Section flow area at bankfull discharge (ft.)

TW = Flow width at bankfull discharge (ft.)

d = Average flow depth at bankfull discharge (ft.)

BUREC Equation. The Bureau of Reclamation (Lane and Carlson, 1953) developed relationships that describe stable channel dimensions for canals cut into coarse grained alluvium.

$$d_{max} = (Q_{bf}/2 \tan \phi)^{0.5}$$

$$A = 2\, d_{max}^{2} / \tan \phi$$

$$V_m = 1/n\, (d_{max} \cos \phi / (0.5\, \pi\, (1 - \cos \phi))^{0.667}\ S_e^{0.5}$$

$$TW = d_{max}\, \pi / \tan \phi$$

Where d_{max} = Maximum depth of flow (ft.)

Q_{bf} = Bankfull discharge (cfs)

ϕ = Angle of repose of bank material

V_m = mean flow velocity (ft./sec.)

N = Mannings n value

S_e = Energy slope (ft./ft.)

TW = Top width of flow (ft.)

The results for depth from the BUREC equations were much greater than the results from the other equations and were not considered reasonable to the Agua Fria River. Therefore, these results are presented in Table 6-8 but not included in the calculation of the average statistics for each reach.

Results. The results of applying the channel geometry equations to the Agua Fria River are shown in Table 6-8. The 2-, 10-, and 100-year discharges were substituted for the discharge variable used in the original channel geometry equations to examine the trend of potential adjustments in channel geometry at each flow rate. Predicted values of widths, depths, slopes and velocities from the channel geometry equations were compared to the measured values obtained from field data, topographic mapping and HEC-RAS models. The differences were interpreted as follows:

- Width. Where the predicted channel width is greater than the HEC-RAS modeled channel width, the channel is expected to erode its banks to achieve the greater width during future floods. Where the predicted channel width is less than the HEC-RAS modeled channel width, the channel is assumed to have low potential for lateral movement due to channel widening, and is likely to experience deposition along the banks, at least at the flow rates considered.
- Depth. Where the predicted channel depth is greater than the HEC-RAS modeled channel depth, the channel is expected to erode its bed (degrade) to achieve the equilibrium depth during future floods. Where predicted channel depth is less than the HEC-RAS modeled channel depth, the channel is expected to aggrade (deposit sediment) to reach the equilibrium state.
- Slope. Where the predicted slope is less than the existing slope, the channel is expected to decrease its slope (scour) to achieve a more stable form.
- Velocity. Where the predicted velocity is less than the HEC-RAS modeled velocity, floods will be more erosive than predicted by the channel geometry equations.

Table 6-8 Observed and Expected Channel Characteristics

Equation	Channel Width (ft)			Flow Depth (ft)			Energy Slope (ft/ft)			Channel Velocity (ft/s)		
	Q100	Q10	Q2	Q100	Q10	Q2	Q100	Q10	Q2	Q100	Q10	Q2
Reach 1												
Bray – Equation #1	354	166	54	6.3	3.7	1.8	0.001401	0.004708	0.006498	5.9	4.6	3.5
Bray – Equation #2	441	206	67	6.7	3.9	2.0	0.000229	0.000739	0.001020	4.4	3.4	2.6
Hey				20.9	11.6	5.2	0.000127	0.000579	0.000795			
Ackers & Charlton/Lacey	193	102	42							3.9	2.9	2.1
Parker	648	313	108	6.9	3.7	1.5	0.000067	0.000321	0.000440			
Chang	537	244	65	0.2	0.9	1.4	0.000021	0.000106	0.000145			
Kellerhals	N/A	N/A	N/A	8.9	3.6	0.9	0.000365	0.015534	0.011273	6.3	4.6	3.4
AMAFCA/Schumm	188	153	96				0.003661	0.006075	0.007034			
Moody & Odem	40	40	40	1.5	1.5	1.5						
BUREC	111	70	41	29.6	18.7	11.0	0.000177	0.008180	0.009447			
Average	314	162	64	10.0	5.8	3.1	0.000756	0.004530	0.004581	5.1	3.8	2.9
HEC-RAS Data	248	204	135	8.9	5.4	2.9	0.001899 (Channel Slope)			6.7	3.9	1.7
Bankfull Discharge Data	220			10.3			0.001899 (Channel Slope)			3.8		
Expected Behavior	Erosion	Stable	Stable	Scour	Scour	Scour	Scour	Fill	Fill	Erosion	Stable	Fill
Reach 2												
Bray – Equation #1	431	230	74	7.1	4.8	2.3	0.001223	0.001836	0.003800	6.3	5.3	3.9
Bray – Equation #2	538	287	92	7.6	5.1	2.5	0.000200	0.000298	0.000607	4.7	3.9	2.9
Ackers & Charlton/Lacey				24.1	15.3	6.8	0.000108	0.000174	0.000407			
Hey	227	137	56							4.1	3.4	2.4
Parker	783	432	147	8.1	4.9	2.0	0.000056	0.000092	0.000220			
Chang	653	324	92	-0.3	0.6	0.9	0.000018	0.000029	0.000071			
Kellerhals	264	144	48	9.0	5.0	2.1	0.000395	0.000850	0.002236	6.2	5.3	4.2
AMAFCA/Schumm	432	327	163				0.002409	0.002729	0.004103			
Moody & Odem	49	49	49	1.8	1.8	1.8						
BUREC	115	74	34	30.8	19.7	9.1	0.000244	0.000599	0.002988			
Average	388	232	84	10.7	6.9	3.3	0.000582	0.000826	0.001804	5.3	4.5	3.4
HEC-RAS Data	597	503	245	5.7	3.1	1.4	0.003287 (Channel Slope)			6.2	4.2	2.6
Bankfull Discharge Data	520			8.8			0.003287 (Channel Slope)			5.5		
Expected Behavior	Stable	Stable	Stable	Scour	Scour	Scour	Scour	Scour	Scour	Erosion	Stable	Fill

Equation	Channel Width (ft)			Flow Depth (ft)			Energy Slope (ft/ft)			Channel Velocity (ft/s)		
	Q100	Q10	Q2	Q100	Q10	Q2	Q100	Q10	Q2	Q100	Q10	Q2
Reach 3												
Bray – Equation #1	427	247	75	7.1	5.0	2.4	0.001222	0.001740	0.003767	6.3	5.4	4.0
Bray – Equation #2	532	308	93	7.5	5.3	2.5	0.000200	0.000283	0.000602	4.6	4.0	2.9
Hey				24.0	16.2	6.8	0.000108	0.000163	0.000403			
Ackers & Charlton/Lacey	225	146	56							4.1	3.5	2.4
Parker	776	462	149	8.0	5.2	2.0	0.000056	0.000086	0.000217			
Chang	661	403	93	-0.4	0.0	0.8	0.000018	0.000027	0.000070			
Kellerhals	247	147	48	11.4	7.5	3.0	0.000260	0.000393	0.000971	6.7	6.1	4.8
AMAFCA/Schumm	349	290	178				0.002498	0.003681	0.003676			
Moody & Odem	54	54	54	1.9	1.9	1.9						
BUREC	113	75	34	30.3	20.0	9.1	0.000206	0.000461	0.002511			
Average	376	248	87	11.0	7.5	3.5	0.000571	0.000854	0.001527	5.4	4.7	3.5
HEC-RAS Data	442	390	257	6.6	3.6	1.3	0.000584 (Channel Slope)			7.4	5.8	2.5
Bankfull Discharge Data	350			5.7			0.000584 (Channel Slope)			5.7		
Expected Behavior	Stable	Stable	Stable	Scour	Scour	Scour	Stable	Fill	Fill	Erosion	Erosion	Fill
Reach 4												
Bray – Equation #1	467	258	82	7.5	5.1	2.5	0.001154	0.001695	0.003565	6.4	5.5	4.0
Bray – Equation #2	582	321	102	8.0	5.5	2.7	0.000189	0.000276	0.000570	4.8	4.1	3.0
Hey				25.6	16.6	7.3	0.000101	0.000158	0.000378			
Ackers & Charlton/Lacey	242	151	60							4.3	3.5	2.5
Parker	845	480	162	8.6	5.4	2.2	0.000053	0.000083	0.000204			
Chang	749	374	103	-0.9	0.3	0.8	0.000016	0.000026	0.000065			
Kellerhals	270	153	52	12.2	7.7	3.2	0.000243	0.000382	0.000910	6.8	6.1	4.9
AMAFCA/Schumm	670	469	216				0.002386	0.002520	0.003949			
Moody & Odem	57	57	57	2.1	2.1	2.1						
BUREC	118	78	35	31.6	20.8	9.4	0.000287	0.000680	0.003475			
Average	445	273	97	11.6	7.8	3.7	0.000554	0.000728	0.001639	5.6	4.8	3.6
HEC-RAS Data	995	732	313	4.9	2.9	1.3	0.002992 (Channel Slope)			6.0	4.1	2.5
Bankfull Discharge Data	670			7.2			0.002992 (Channel Slope)			5.0		
Expected Behavior	Stable	Stable	Stable	Scour	Scour	Scour	Scour	Scour	Scour	Erosion	Fill	Fill

Equation	Channel Width (ft)			Flow Depth (ft)			Energy Slope (ft/ft)			Channel Velocity (ft/s)		
	Q100	Q10	Q2	Q100	Q10	Q2	Q100	Q10	Q2	Q100	Q10	Q2
Reach 5												
Bray – Equation #1	471	266	88	7.5	5.2	2.6	0.001148	0.001662	0.003408	6.4	5.5	4.1
Bray – Equation #2	588	332	109	8.0	5.6	2.8	0.000189	0.000270	0.000546	4.8	4.1	3.1
Hey				25.7	17.0	7.7	0.000100	0.000155	0.000358			
Ackers & Charlton/Lacey	243	155	64							4.3	3.6	2.5
Parker	852	496	173	8.6	5.5	2.3	0.000052	0.000082	0.000193			
Chang	747	389	110	-0.8	0.3	0.8	0.000016	0.000026	0.000062			
Kellerhals	272	157	55	11.6	7.2	3.0	0.000266	0.000452	0.001158	6.7	6.0	4.8
AMAFCA/Schumm	823	575	215				0.002321	0.002500	0.003697			
Moody & Odem	60	60	60	2.2	2.2	2.2						
BUREC	116	77	35	30.9	20.5	9.3	0.000366	0.000828	0.003951			
Average	464	294	101	11.5	7.7	3.7	0.000557	0.000747	0.001672	5.5	4.8	3.6
HEC-RAS Data	1280	994	375	3.8	2.3	1.2	0.003321 (Channel Slope)			5.7	4.1	2.7
Bankfull Discharge Data		940			5.8		0.003321 (Channel Slope)				4.0	
Expected Behavior	Stable	Stable	Stable	Scour	Scour	Scour	Scour	Scour	Scour	Stable	Fill	Fill
Reach 6												
Bray – Equation #1	470	266	91	7.5	5.2	2.7	0.001180	0.001688	0.003350	6.4	5.5	4.2
Bray – Equation #2	586	331	113	8.0	5.6	2.8	0.000194	0.000275	0.000537	4.7	4.1	3.1
Hey				25.6	17.0	7.8	0.000104	0.000158	0.000351			
Ackers & Charlton/Lacey	242	154	66							4.2	3.6	2.5
Parker	849	495	179	8.6	5.5	2.4	0.000054	0.000083	0.000189			
Chang	751	390	115	-0.8	0.3	0.8	0.000017	0.000026	0.000061			
Kellerhals	271	158	57	12.2	7.9	3.5	0.000250	0.000380	0.000847	6.8	6.1	5.0
AMAFCA/Schumm	764	538	281				0.002367	0.002524	0.003528			
Moody & Odem	64	64	64	2.3	2.3	2.3						
BUREC	123	83	40	32.9	22.1	10.6	0.000334	0.000764	0.003580			
Average	458	290	112	11.9	8.1	4.0	0.000563	0.000737	0.001555	5.6	4.8	3.7
HEC-RAS Data	1153	856	452	4.8	2.9	1.4	0.002980 (Channel Slope)			5.4	3.9	2.4
Bankfull Discharge Data		1010			5.5		0.002980 (Channel Slope)				4.4	
Expected Behavior	Stable	Stable	Stable	Scour	Scour	Scour	Scour	Scour	Scour	Stable	Fill	Fill

Equation	Channel Width (ft)			Flow Depth (ft)			Energy Slope (ft/ft)			Channel Velocity (ft/s)		
	Q100	Q10	Q2	Q100	Q10	Q2	Q100	Q10	Q2	Q100	Q10	Q2
Reach 7												
Bray – Equation #1	503	295	99	7.8	5.6	2.8	0.001104	0.001566	0.003148	6.5	5.7	4.3
Bray – Equation #2	628	368	123	8.3	6.0	3.0	0.000181	0.000255	0.000505	4.8	4.2	3.2
Hey				26.9	18.3	8.4	0.000096	0.000144	0.000327			
Ackers & Charlton/Lacey	256	168	70							4.4	3.7	2.6
Parker	907	546	194	9.1	6.0	2.5	0.000050	0.000076	0.000175			
Chang	788	431	119	-0.8	0.2	0.9	0.000015	0.000024	0.000056			
Kellerhals	289	174	62	12.9	8.6	3.7	0.000231	0.000348	0.000787	6.9	6.3	5.1
AMAFCA/Schumm	594	479	192				0.002083	0.002236	0.002927			
Moody & Odem	85	85	85	3.0	3.0	3.0						
BUREC	128	87	40	34.1	23.1	10.8	0.000256	0.000555	0.002545			
Average	464	307	109	12.5	8.7	4.3	0.000502	0.000651	0.001309	5.7	5.0	3.8
HEC-RAS Data	870	798	318	5.5	3.1	1.5	0.002955 (Channel Slope)			6.0	4.2	2.6
Bankfull Discharge Data		720			6.8		0.002955 (Channel Slope)				4.8	
Expected Behavior	Stable	Stable	Stable	Scour	Scour	Scour	Scour	Scour	Scour	Erosion	Fill	Fill
Reach 8												
Bray – Equation #1	565	311	94	8.4	5.8	2.7	0.001021	0.001502	0.003290	6.8	5.8	4.2
Bray – Equation #2	740	407	123	9.1	6.3	3.0	0.000112	0.000163	0.000351	4.7	4.0	2.9
Hey				32.8	21.3	9.0	0.000045	0.000070	0.000176			
Ackers & Charlton/Lacey	281	175	67							4.5	3.7	2.6
Parker	1204	683	220	10.2	6.4	2.5	0.000022	0.000035	0.000091			
Chang	1097	574	148	-3.1	-1.1	0.3	0.000006	0.000010	0.000027			
Kellerhals	323	183	59	14.4	9.1	3.7	0.000176	0.000276	0.000692	6.9	6.2	4.9
AMAFCA/Schumm	488	383	200				0.001790	0.002154	0.002985			
Moody & Odem	90	90	90	3.1	3.1	3.1						
BUREC	145	94	40	38.7	25.0	10.8	0.000105	0.000242	0.001360			
Average	548	340	116	14.0	9.3	4.3	0.000410	0.000557	0.001121	5.7	4.9	3.6
HEC-RAS Data	636	544	284	8.0	4.4	1.7	0.002759 (Channel Slope)			7.3	5.1	2.8
Bankfull Discharge Data		490			9.5		0.002759 (Channel Slope)				5.6	
Expected Behavior	Stable	Stable	Stable	Scour	Scour	Scour	Scour	Scour	Scour	Erosion	Stable	Fill

Equation	Channel Width (ft)			Flow Depth (ft)			Energy Slope (ft/ft)			Channel Velocity (ft/s)		
	Q100	Q10	Q2	Q100	Q10	Q2	Q100	Q10	Q2	Q100	Q10	Q2
Reach 9												
Bray – Equation #1	566	305	80	8.4	5.7	2.4	0.001017	0.001518	0.003630	6.8	5.7	4.0
Bray – Equation #2	741	399	104	9.2	6.2	2.7	0.000112	0.000165	0.000387	4.7	4.0	2.8
Hey				32.8	21.0	8.0	0.000044	0.000071	0.000197			
Ackers & Charlton/Lacey	282	172	59							4.5	3.7	2.4
Parker	1206	670	187	10.3	6.3	2.2	0.000022	0.000036	0.000102			
Chang	1139	578	127	-3.6	-1.4	0.3	0.000006	0.000010	0.000030			
Kellerhals	324	180	50	14.4	9.0	3.2	0.000175	0.000280	0.000776	6.9	6.2	4.8
AMAFCA/Schumm	758	520	132				0.001724	0.001864	0.002982			
Moody & Odem	91	91	91	3.2	3.2	3.2						
BUREC	140	89	35	37.4	23.8	9.2	0.000165	0.000400	0.002708			
Average	583	353	96	13.8	9.0	3.8	0.000408	0.000543	0.001351	5.7	4.9	3.5
HEC-RAS Data	1254	1021	214	5.0	2.7	1.6	0.002897 (Channel Slope)			5.6	3.9	2.9
Bankfull Discharge Data	1260			9.6			0.002897 (Channel Slope)			5.0		
Expected Behavior	Stable	Stable	Stable	Scour	Scour	Scour	Scour	Scour	Scour	Stable	Fill	Fill
Reach 10												
Bray – Equation #1	503	295	81	7.8	5.6	2.5	0.001117	0.001551	0.003603	6.5	5.7	4.0
Bray – Equation #2	659	386	105	8.5	6.1	2.7	0.000122	0.000168	0.000384	4.5	3.9	2.8
Hey				30.1	20.5	8.0	0.000050	0.000073	0.000195			
Ackers & Charlton/Lacey	256	168	60							4.3	3.7	2.4
Parker	1077	650	189	9.3	6.1	2.2	0.000025	0.000037	0.000101			
Chang	890	485	116	-1.6	-0.3	0.5	0.000007	0.000011	0.000030			
Kellerhals	289	175	51	13.1	8.8	3.3	0.000196	0.000287	0.000769	6.7	6.1	4.8
AMAFCA/Schumm	504	427	212				0.001633	0.001680	0.002534			
Moody & Odem	95	95	95	3.3	3.3	3.3						
BUREC	146	99	38	39.1	26.5	10.2	0.000118	0.000253	0.001591			
Average	491	326	105	13.5	9.4	4.0	0.000409	0.000507	0.001151	5.5	4.9	3.5
HEC-RAS Data	641	591	325	8.6	5.0	1.5	0.002246 (Channel Slope)			6.2	4.5	2.2
Bankfull Discharge Data	610			9.8			0.002246 (Channel Slope)			5.3		
Expected Behavior	Stable	Stable	Stable	Scour	Scour	Scour	Scour	Scour	Scour	Erosion	Fill	Fill

Equation	Channel Width (ft)			Flow Depth (ft)			Energy Slope (ft/ft)			Channel Velocity (ft/s)		
	Q100	Q10	Q2	Q100	Q10	Q2	Q100	Q10	Q2	Q100	Q10	Q2
Reach 11												
Bray – Equation #1	729	392	222	9.9	6.7	4.7	0.000864	0.001290	0.001863	7.2	6.1	5.3
Bray – Equation #2	1008	542	307	10.9	7.4	5.2	0.000060	0.000089	0.000127	4.7	3.9	3.4
Hey				44.6	28.5	19.0	0.000017	0.000027	0.000042			
Ackers & Charlton/Lacey	345	210	134							4.9	4.0	3.4
Parker	1865	1035	605	12.9	7.9	5.1	0.000008	0.000013	0.000020			
Chang	1829	942	500	-7.9	-3.8	-1.7	0.000002	0.000003	0.000005			
Kellerhals	410	228	133	21.4	13.1	8.4	0.000018	0.000035	0.000063	5.2	4.6	4.1
AMAFCA/Schumm	1242	975	678				0.000890	0.001022	0.001074			
Moody & Odem	118	118	118	4.0	4.0	4.0						
BUREC	172	109	73	45.9	29.2	19.5	0.000082	0.000199	0.000444			
Average	858	540	308	17.5	11.4	7.8	0.000243	0.000335	0.000455	5.5	4.7	4.0
HEC-RAS Data	1741	1615	1219	5.5	2.8	1.8	0.002222 (Channel Slope)			5.7	3.8	2.9
Bankfull Discharge Data	1800			8.4			0.002222 (Channel Slope)			5.1		
Expected Behavior	Stable	Stable	Stable	Scour	Scour	Scour	Scour	Scour	Scour	Stable	Fill	Fill
Reach 12												
Bray – Equation #1	745	392	223	10.0	6.7	4.7	0.000850	0.001290	0.001862	7.3	6.1	5.3
Bray – Equation #2	1030	542	307	11.1	7.4	5.2	0.000059	0.000089	0.000127	4.7	3.9	3.4
Hey				45.4	28.6	19.0	0.000017	0.000027	0.000042			
Ackers & Charlton/Lacey	351	210	134							4.9	4.0	3.4
Parker	1904	1036	606	13.1	7.9	5.1	0.000008	0.000013	0.000020			
Chang	1793	861	452	-7.4	-3.0	-1.1	0.000002	0.000003	0.000005			
Kellerhals	N/A	N/A	N/A	11.0	4.2	1.8	0.000032	0.000083	0.000192	4.4	3.5	2.8
AMAFCA/Schumm	1193	1167	1141				0.000799	0.000841	0.000937			
Moody & Odem	118	118	118	4.0	4.0	4.0						
BUREC	165	106	72	44.1	28.4	19.3	0.000058	0.000145	0.000325			
Average	912	554	382	15.6	9.8	6.7	0.000228	0.000311	0.000439	5.3	4.4	3.7
HEC-RAS Data	1121	1106	1083	6.7	3.3	1.8	0.001910 (Channel Slope)			7.4	4.5	3.0
Bankfull Discharge Data	N/A			N/A			0.001910 (Channel Slope)			N/A		
Expected Behavior	Stable	Stable	Stable	Scour	Scour	Scour	Scour	Scour	Scour	Erosion	Stable	Fill

Equation	Channel Width (ft)			Flow Depth (ft)			Energy Slope (ft/ft)			Channel Velocity (ft/s)		
	Q100	Q10	Q2	Q100	Q10	Q2	Q100	Q10	Q2	Q100	Q10	Q2
Reach 13												
Bray – Equation #1	727	381	220	9.9	6.6	4.7	0.000864	0.001313	0.001874	7.2	6.1	5.3
Bray – Equation #2	1006	527	304	10.9	7.3	5.2	0.000060	0.000090	0.000128	4.6	3.9	3.4
Hey				44.6	28.0	18.9	0.000017	0.000028	0.000042			
Ackers & Charlton/Lacey	344	206	133							4.9	4.0	3.4
Parker	1861	1009	600	12.9	7.7	5.0	0.000008	0.000013	0.000021			
Chang	1647	796	462	-6.3	-2.5	-1.1	0.000002	0.000003	0.000005			
Kellerhals	N/A	N/A	N/A	10.3	3.9	1.7	0.000033	0.000088	0.000199	4.4	3.4	2.8
AMAFCA/Schumm	1082	1021	946				0.000818	0.000913	0.003897			
Moody & Odem	126	126	126	4.3	4.3	4.3						
BUREC	172	110	73	45.9	29.4	19.6	0.000061	0.000154	0.000336			
Average	871	522	358	15.7	9.9	6.7	0.000233	0.000325	0.000813	5.3	4.4	3.7
HEC-RAS Data	1154	1142	1112	7.0	3.5	1.9	0.002308 (Channel Slope)			6.7	4.1	3.1
Bankfull Discharge Data	N/A			N/A			0.002308 (Channel Slope)			N/A		
Expected Behavior	Stable	Stable	Stable	Scour	Scour	Scour	Scour	Scour	Scour	Erosion	Fill	Fill
Reach 14												
Bray – Equation #1	666	373	218	9.3	6.5	4.6	0.000918	0.001332	0.001886	7.1	6.1	5.2
Bray – Equation #2	922	516	301	10.3	7.2	5.1	0.000064	0.000091	0.000128	4.5	3.9	3.4
Hey				41.8	27.6	18.7	0.000018	0.000028	0.000043			
Ackers & Charlton/Lacey	321	202	132							4.8	4.0	3.3
Parker	1713	989	594	12.0	7.6	5.0	0.000009	0.000014	0.000021			
Chang	1612	818	438	-6.6	-2.8	-1.1	0.000002	0.000004	0.000005			
Kellerhals	373	218	131	20.4	12.9	8.5	0.000018	0.000031	0.000054	5.2	4.6	4.1
AMAFCA/Schumm	1074	947	781				0.000920	0.000932	0.000953			
Moody & Odem	127	127	127	4.3	4.3	4.3						
BUREC	169	115	80	45.0	30.7	21.3	0.000072	0.000164	0.000352			
Average	775	511	311	16.9	11.5	8.1	0.000253	0.000324	0.000430	5.4	4.6	4.0
HEC-RAS Data	1258	1193	995	6.7	3.8	2.3	0.001836 (Channel Slope)			5.9	3.8	2.7
Bankfull Discharge Data	1130			6.0			0.001836 (Channel Slope)			3.9		
Expected Behavior	Stable	Stable	Stable	Scour	Scour	Scour	Scour	Scour	Scour	Erosion	Fill	Fill

Equation	Channel Width (ft)			Flow Depth (ft)			Energy Slope (ft/ft)			Channel Velocity (ft/s)		
	Q100	Q10	Q2	Q100	Q10	Q2	Q100	Q10	Q2	Q100	Q10	Q2
Reach 15												
Bray – Equation #1	452	293	193	7.3	5.5	4.3	0.001227	0.001584	0.002059	6.3	5.7	5.1
Bray – Equation #2	625	405	266	8.0	6.2	4.7	0.000084	0.000108	0.000140	4.1	3.6	3.3
Hey				31.4	23.1	17.1	0.000026	0.000035	0.000047			
Ackers & Charlton/Lacey	234	166	119							4.2	3.7	3.2
Parker	1183	785	528	8.8	6.3	4.5	0.000012	0.000017	0.000023			
Chang	1144	715	452	-4.9	-2.9	-1.6	0.000003	0.000004	0.000006			
Kellerhals	261	173	116	16.3	11.7	8.6	0.000022	0.000030	0.000040	4.9	4.5	4.2
AMAFCA/Schumm	477	420	367				0.001128	0.001224	0.001311			
Moody & Odem	127	127	127	4.3	4.3	4.3						
BUREC	121	88	65	32.3	23.4	17.4	0.000068	0.000122	0.000225			
Average	514	375	248	12.8	9.6	7.3	0.000321	0.000391	0.000481	4.9	4.4	3.9
HEC-RAS Data	558	540	490	6.8	4.5	3.0	0.002492 (Channel Slope)			6.8	5.3	4.0
Bankfull Discharge Data	370			3.7			0.002492 (Channel Slope)			3.8		
Expected Behavior	Stable	Stable	Stable	Scour	Scour	Scour	Scour	Scour	Scour	Erosion	Erosion	Stable

Notes:
Blank fields indicate that equation used does not predict that variable.
Codes: Erosion = lateral channel movement Scour = net long-term degradation Fill = net long-term aggradation

In general, the channel geometry analysis indicates that the Agua Fria River will tend to trend toward a narrower, deeper, and flatter (lower slope) channel than the present channel geometry. However, except for the 100-year discharge, channel velocities indicate that most flows may lack the energy to cause channel change. The velocity data generally predict fill rather than the scour predicted by the depth and slope calculations.

It is noted that the stable geometry equations described above reflect the dimensions of channels which have been stable over long periods of time. The Agua Fria River has recently experienced a significant change to its geomorphological inputs; namely, magnitude and frequency of both water and sediment discharges were altered by construction of upstream dams. The current geometry largely reflects the effects of two large floods experienced in 1978 and 1980. Since completion of the New Waddell Dam, the only flood of consequence occurred in 1993, when 9000 cfs was released from the dam. Although changes to the channel geometry occurred as a result of this flood, the channel has not yet experienced enough significant flooding to have readjusted to the new hydrologic and sedimentological regime. The stable geometry equations suggest the nature of future channel adjustments to the Agua Fria River. The following conclusions can be drawn from the channel geometry information summarized in Table 6-8 and their implications for future adjustments to the geometry of the Agua Fria River:

- Natural channel width. The main channel of the Agua Fria River appears to be adjusted to the flow width greater than the present 100-year event. This is not surprising given the significant reduction in discharges due to the construction of the New Waddell Dam. The present condition 100-year discharge is more similar to the 5- to 25-year discharge prior to the construction of New Waddell Dam. Since the river has not experienced any significant flooding since the construction of the new dam, the channel has not had a chance to adjust to the new hydrologic regime.
- Channel depth. The predicted channel depths are generally greater than the flow depths computed by HEC-RAS modeling. Therefore, degradation during most floods should be expected in the future.
- Channel slope. The predicted channel slope is flatter than the existing channel slope in all reaches. Therefore, long-term scour (degradation) should be expected.
- Channel velocity. In general, the predicted velocities are higher than the velocities computed by HEC-RAS modeling for the 100-year event. Therefore, sediment deposition and long-term aggradation is predicted by these equations. However, when compared to the results for width, depth, and slope, the predictions of fill for most reaches for lower discharges suggests the formation of a new channel geometry which has as yet largely not been formed.
- The new channel geometry according to these computations is likely to be narrower, deeper, and flatter, with higher velocities in the channel than under the current conditions.

The predicted channel geometry values were compared to the estimated bankfull geometry values described elsewhere in this chapter (Table 6-3, Table 6-4, and Table 6-5). The approximate recurrence interval of the bankfull discharge channel geometry computed using HEC-RAS modeling was estimated by plotting the average 2-, 10-, and 100-year channel geometry results versus probability and interpolating between data points. The data used from the channel geometry equations excluded consideration of cross sections at or near bridges as well as the channelized reaches (12 and 13). Therefore, no data are shown in Table 6-9 for Reaches 12 and 13. The reach-average data were compared to the median bankfull geometry data, excluding bridges and channelized sections (as shown in Table 6-3, Table 6-4, and Table 6-5).

Table 6-9 shows that the recurrence interval of the bankfull discharge geometry varies greatly along the river, from less than the 2-year flood in Reach 15 to the 50-year flood for all variables in Reach 11. Wider reaches such as Reaches 5 and 6 show greater recurrence intervals than narrower reaches like Reach 8. Deeper reaches include Reaches 10 and 11, which are partially channelized. Velocity is also higher in the deeper reaches.

Table 6-9 Approximate Recurrence Interval of Bankfull Discharge Geometry Estimated from Channel Geometry Equations (in years)

Reach	Width	Depth	Velocity
1	22	14	14
2	15	62	46
3	100	15	17
4	8	42	29
5	22	15	5
6	33	7	21
7	8	8	21
8	6	28	29
9	> 100	37	43
10	45	26	29
11	59	49	59
12	N/A	N/A	N/A
13	N/A	N/A	N/A
14	10	15	9
15	< 2	< 2	< 2

6.4.2.3 Hydraulic Geometry Regression Equations

HEC-RAS and field data for the Agua Fria River were used to develop reach-averaged hydraulic geometry regression equations. No published database of hydraulic geometry regression equations currently exists for the unique types of streams found in central Arizona. Therefore, the data presented in this section were compared to other data sets from the arid west, as well as to data collected for the Upper Cave Creek/Apache Wash and Skunk Creek Watercourse Master Plans geomorphic analyses. Following additional data collection and completion of geomorphic analyses for other watercourse master plans in Maricopa County, enough data may exist to provide important information on the stable (or unstable) geometry of local watercourses.

Methodology. Hydraulic data were obtained from the modified HEC-RAS model. These data were used to develop reach-averaged regression equations using the form and variables of the classic hydraulic geometry equations established in Leopold and Maddock (1953). The following three equations were developed using the Microsoft Excel multiple regression statistical software package:

$$w \propto aQ^b \qquad d \propto cQ^f \qquad v \propto kQ^m$$

Where w = width; channel topwidth (ft.)

Q = discharge; channel discharge (cfs)

d = depth; hydraulic channel depth (ft.)

v = velocity, channel velocity (ft./s.)

a, c, k = coefficients

b, f, m = exponents

The principles of continuity and dimensional analysis dictate that the regression equation coefficients relating change of depth, width, and velocity to change in discharge should equal one when multiplied together (i.e., $a \times c \times k = 1$). Similarly, the regression equation exponents also should have a sum of one ($b + f + m = 1$). The expectation of continuity was met at the majority (96%) of river stations: of 444 stations in this study, only 17 did not meet the continuity criteria. Variations in continuity are likely caused by complicated multiple channel geometries and deficiencies in the HEC-RAS modeling. A tabular summary of the intercept, slopes, and correlation coefficients (R^2), for each river station are provided in an Appendix to this report.

The hydraulic geometry regression equations were used to evaluate expected channel change in several ways. First, exponents for velocity (*m*), depth (*f*), and width (*b*) in the study area were compared with the averages for ephemeral streams in the semiarid United States, as well as with previously studied stream segments in the Upper Cave Creek/Apache Wash and Skunk Creek Watercourse Master Plan study areas. In addition, the hydraulic geometry regression equations for each of the reaches were compared to identify anomalies that might indicate lateral or vertical instability. Second, the *m/f* ratio, an indication of the rate of sediment transport within the streams, was compared with the average for ephemeral streams in the semiarid United States. Leopold, Wolman, and Miller (1964) used the *m/f* ratio (change in velocity to change in depth with change in discharge) as an indicator of the rate of sediment transport. The greater the *m/f* ratio, the larger the amount of sediment transported with changes in discharge. Average at-a-station relationships for ephemeral streams in semiarid U.S. are $m = 0.34$ and $f = 0.36$. The average *m/f* ratio is thus 0.94.

Results. The hydraulic geometry equation exponents for width, depth, and velocity at each river station, less bridge stations, are plotted in three graphs (Figures 6-33, 6-34, and 6-35). Wide variation between the hydraulic relationships of adjacent cross sections is evident. The exponent for hydraulic width varies widely around the average value for ephemeral streams. The width tends to increase more slowly than average downstream of river station 12.8, most likely due to constrictions caused by the encroachment of mining operations. The slowest increases in width are associated with the levee reach. The increase in depth with increased discharge experienced by the Agua Fria River tends to be above the average for ephemeral streams. Not surprisingly, the exponent for depth is consistently above average in the levee reach. Increases in velocity with increased discharge vary just as widely from average as do the increases in width and depth. The velocity increase tends to be slower than average in the more natural reaches and faster than average in the encroached and levee reaches. The hydraulic geometry equations emphasize the variability of the Agua Fria River from station to station.

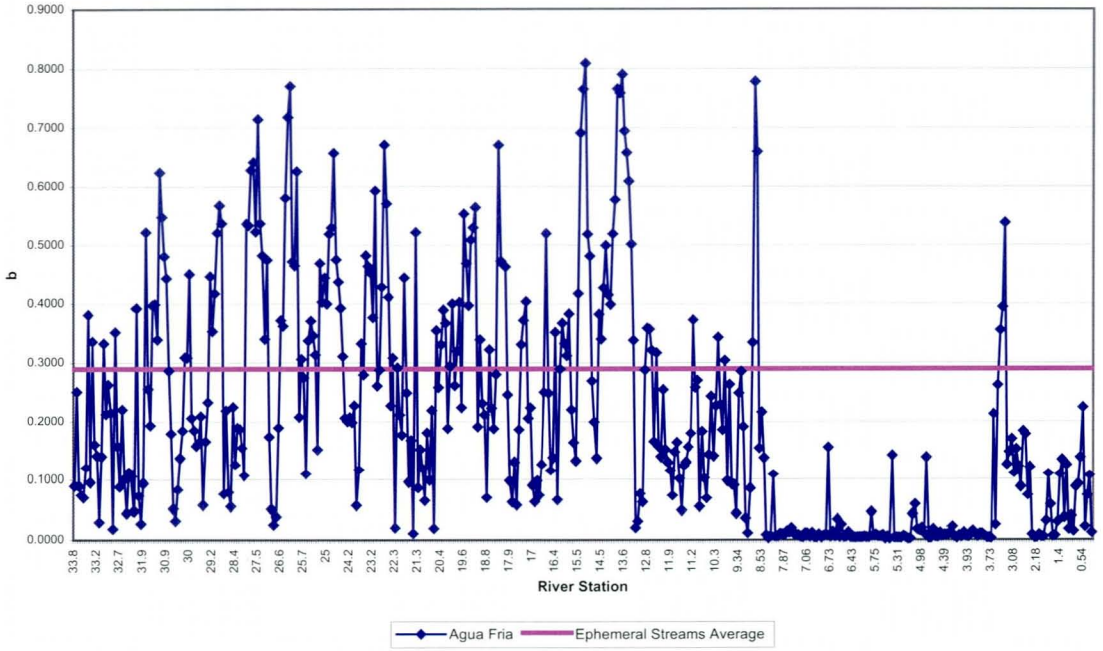

Figure 6-33 Variation in rate of change of width (b) for post New Waddell hydraulic geometry

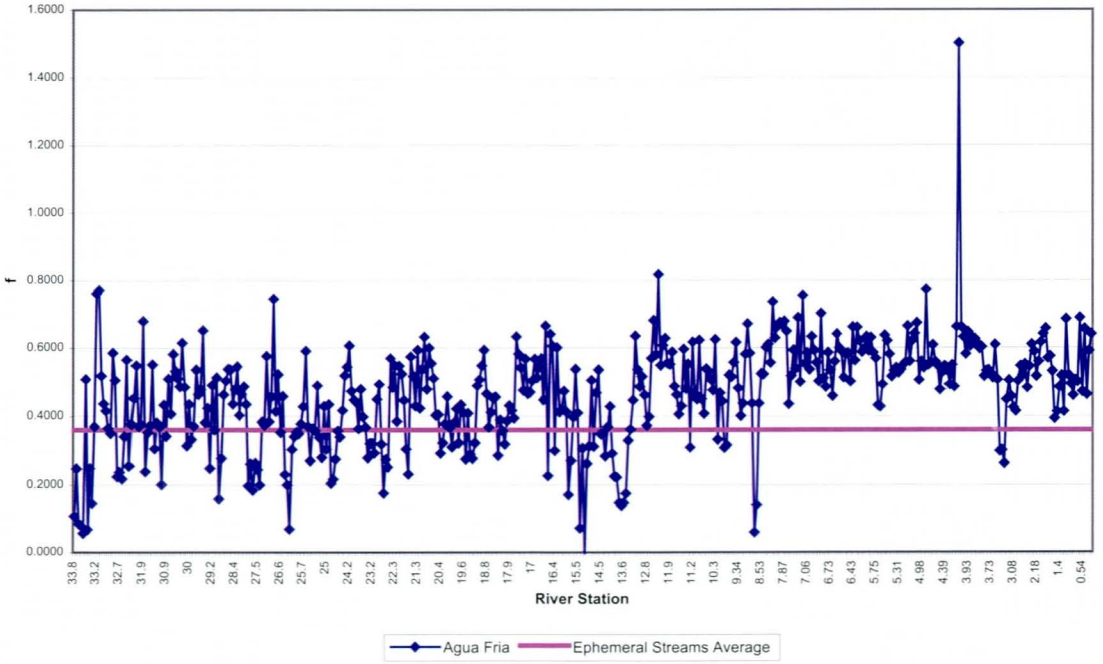

Figure 6-34 Variation in rate of change of depth (f) for post New Waddell hydraulic geometry

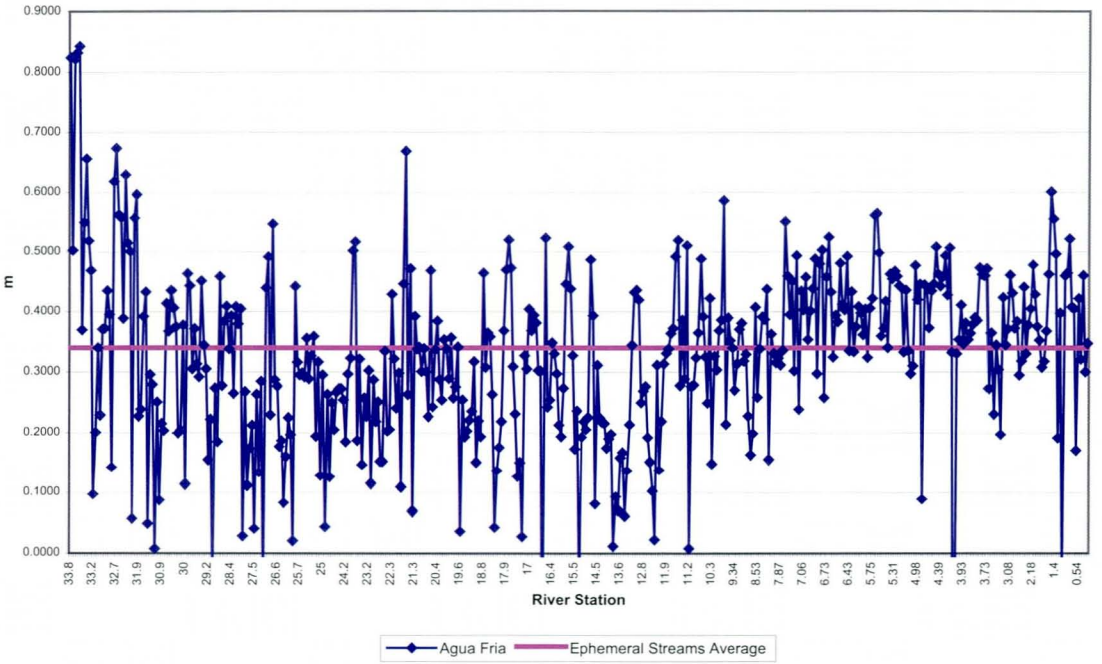

Figure 6-35 Variation in rate of change of velocity (m) for post New Waddell hydraulic geometry

The large variability of the hydraulic geometry exponents makes identification of longitudinal trends difficult. Therefore, hydraulic geometry equations for each reach were calculated using the HEC-RAS model results from the river stations within the reach. Bridge cross sections were removed from the computations in order to reflect more accurately the average (non-constricted) conditions in the reach. Table 6-10 lists the computed hydraulic geometry equation exponents for each of the 15 delineated reaches in the study area based on post-New Waddell hydrology. Reaches 12 and 13 are completely channelized.

Table 6-10 Hydraulic Geometry Equations – Agua Fria River

Stream/ Reach	Width ($w=aQ^b$)		Depth ($d=cQ^f$)		Velocity ($w=kQ^m$)			b + f +
	a	b	c	f	k	m	a x c x k	m
Agua Fria River								
1	79.61	0.12	1.86	0.14	0.01	0.74	1.04	1.00
2	41.32	0.27	0.07	0.43	0.33	0.29	1.00	1.00
3	126.80	0.11	0.02	0.60	0.38	0.30	0.99	1.00
4	27.74	0.35	0.09	0.39	0.40	0.26	1.00	1.00
5	22.22	0.40	0.09	0.36	0.50	0.23	1.00	1.00
6	24.78	0.38	0.10	0.37	0.38	0.26	0.99	1.01
7	38.37	0.31	0.08	0.40	0.31	0.29	0.95	1.01
8	59.40	0.23	0.06	0.47	0.30	0.30	1.00	1.00
9	7.41	0.50	0.20	0.30	0.69	0.20	1.00	1.00
10	73.95	0.20	0.06	0.49	0.24	0.31	0.97	1.00
11	253.01	0.18	0.02	0.50	0.18	0.31	1.00	1.00
12	960.21	0.01	0.01	0.58	0.08	0.41	1.00	1.00
13	976.32	0.02	0.01	0.61	0.11	0.38	1.00	1.00
14	228.95	0.16	0.04	0.48	0.11	0.37	0.98	1.00
15	6.54	0.46	0.40	0.27	0.48	0.26	1.24	0.99
Entire	29.25	0.35	0.22	0.30	0.16	0.36	1.01	1.00

Comparison of Reaches to Arid West Streams. Leopold, Wolman, and Miller (1964) reported the following hydraulic geometry equation exponents for width:discharge (b), depth:discharge (f), and velocity:discharge (m):

b=0.29 f=0.36 m=0.34

The rate of change in the Agua Fria's width as discharge increases varies along the length of the study area. Upstream of the CAP canal (Reach 3) the width increases at a slightly slower rate than average for ephemeral streams. The width increases at a slightly faster rate than that of the average ephemeral wash in Reaches 4, 5, 6, and 7. Reaches 4 and 5 include some of the more undisturbed reaches of the study area. In the levee reaches (Reaches 12 and 13) the width increases at a much slower rate. Between Reach 7 and the levee reaches the rate of change varies between faster and slower than that of the average ephemeral stream. Figure 6-36 illustrates the reach to reach variation in width:discharge.

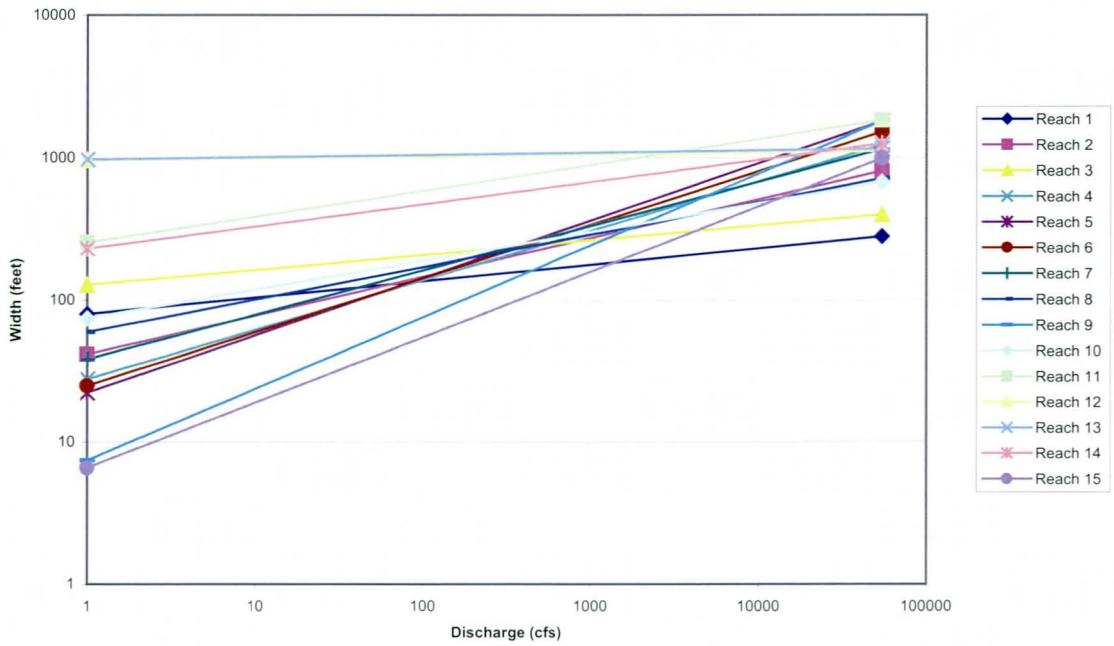

Figure 6-36 Reach by reach relation of width to discharge for post New Waddell hydraulic geometry

According to the hydraulic geometry equations, the depth of the Agua Fria River increases faster as discharge increases than the average for ephemeral washes in semi-arid regions. The depth increases at a rate only slightly faster than average in Reaches 4, 5, 6, and 7. Reaches 4 and 5 include some of the more undisturbed reaches of the study area. The levee reaches downstream of the New River confluence (Reaches 12 and 13) exhibit the fastest rate of increase in depth due to the unnatural confinement of the floodwaters. Figure 6-37 illustrates the reach to reach variation in depth:discharge.

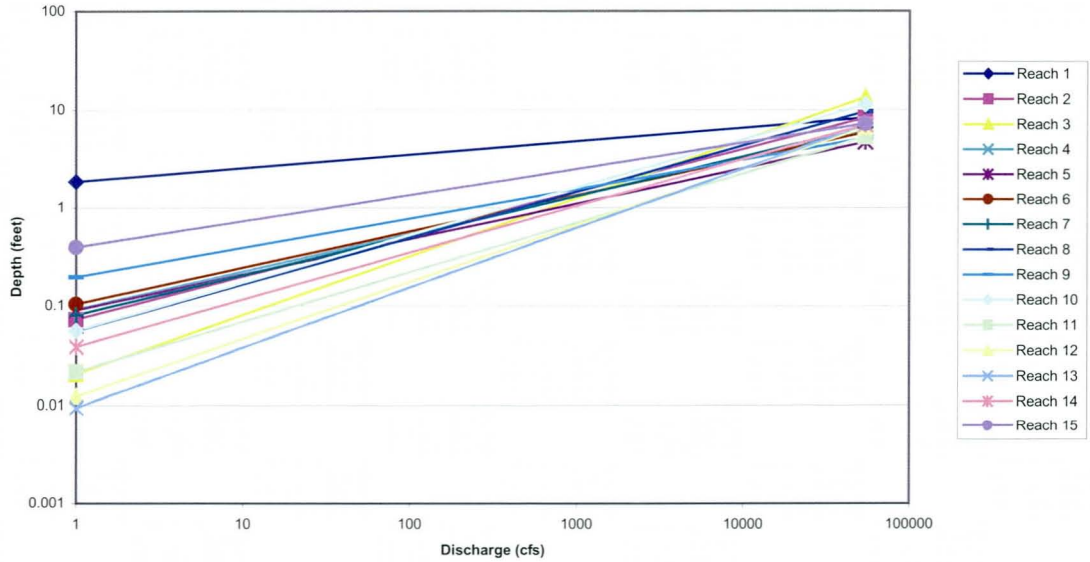

Figure 6-37 Reach by reach relation of depth to discharge for post New Waddell hydraulic geometry

The velocity generally increases at a slightly slower rate than in an average ephemeral wash. The velocity exponents are also fairly constant from one reach to the next. Exceptions include the velocity in Reach 1, where the modeling indicates a much faster than average increase, and the levee reaches (Reaches 12 and 13), where the rate of increase is slightly faster than average. Figure 6-38 illustrates the reach to reach variation in velocity versus discharge.

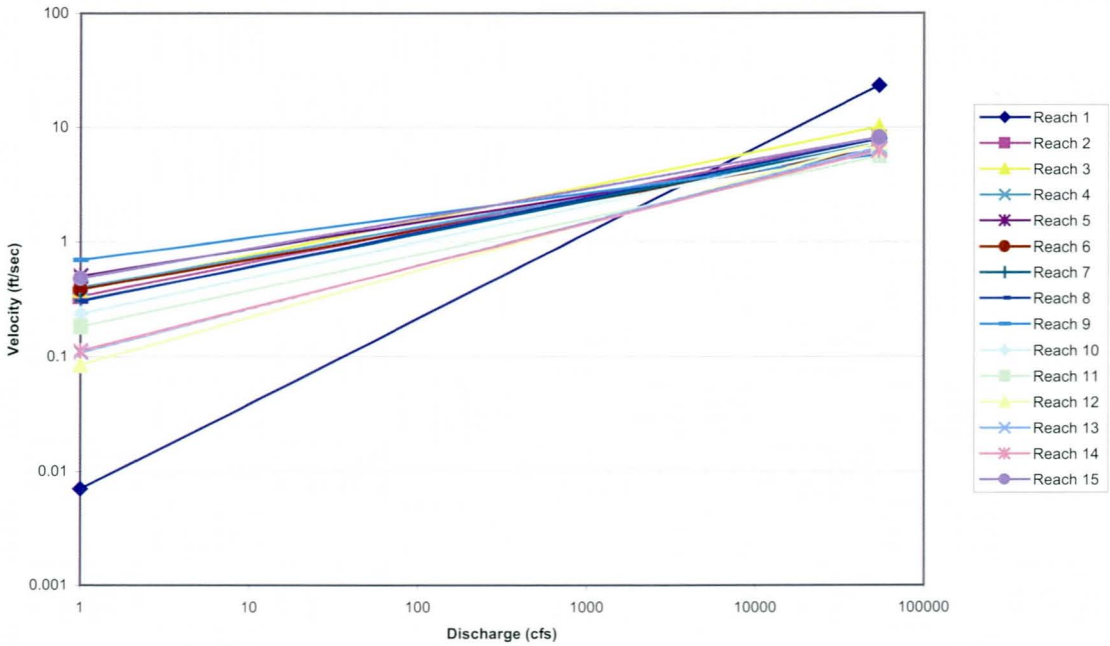

Figure 6-38 Reach by reach relation of velocity to discharge for post New Waddell hydraulic geometry

Table 6-11. Average Hydraulic Geometry Exponents for the Agua Fria River Study Reach and Other Regional Stream Systems.

Stream/ Reach	Width ($w=aQ^b$)		Depth ($d=cQ^f$)		Velocity ($w=kQ^m$)			b + f +
	a	B	c	f	k	M	a x c x k	m
Agua Fria River								
Upper	31.4	0.33	0.43	0.22	0.07	0.45	1.00	1.00
Middle	37.2	0.29	0.08	0.43	0.33	0.28	0.99	1.00
Lower	207.4	0.17	0.03	0.48	0.16	0.34	1.10	0.99
Entire	29.3	0.35	0.22	0.30	0.16	0.36	1.01	1.00
Skunk Creek								
Entire	15.0	0.24	0.099	0.46	0.67	0.30	1.00	1.00
Sonoran Wash								
Entire	12.1	0.23	0.120	0.47	0.69	0.30	1.00	1.00
Cave Creek								
Entire	17.1	0.28	0.095	0.43	0.62	0.29	1.00	1.00
Apache Wash								
Entire	12.6	0.22	0.087	0.49	0.91	0.29	1.00	1.00
Paradise Wash								
Entire	19.5	0.14	0.063	0.54	0.80	0.32	1.00	1.00
Desert Hills Wash								
Entire	13.9	0.12	0.123	0.51	0.58	0.37	1.00	1.00
Leopold, Wolman & Miller (1964) – Average Ephemeral Stream in Semi-Arid United States								
		0.29		0.36		0.34		0.99

Comparison to Central Arizona Streams. The hydraulic geometry equations for the upper, middle, lower reaches of the Agua Fria River are shown in Table 6-11. Hydraulic geometry equation exponents from Skunk Creek, Sonoran Wash, Cave Creek, Apache Wash, Paradise Wash and Desert Hills Wash are provided for comparison. Differences between the hydraulic geometries of the Agua Fria River and nearby streams are most likely the result of physical differences in the stream systems. The Agua Fria River is a larger stream, has a larger watershed area, has a different flood frequency, and is generally more disturbed than the other streams listed. By way of comparison, the hydraulic geometries of Skunk Creek, Sonoran Wash, Cave Creek, Apache Wash, Paradise Wash, and Desert Hills Wash suggest these washes are more incised and narrower than typical ephemeral washes. Paradise Wash and Desert Hills Wash are the most incised of this group.

The upper and middle reaches of the Agua Fria River widen at a faster rate compared to the smaller streams in the area. The width:discharge ratios for the upper and middle reaches are very close to the average for ephemeral streams reported by Leopold, Wolman, and Miller (1964). The lower reach widens at a rate comparable to the incised Paradise and Desert Hills Washes, due to the levees confining the reach. Figure 6-39 illustrates the relationship between the width:discharge ratios. Considered over the entire study length, the Agua Fria River widens at a slightly faster rate with increasing discharge compared to adjacent streams.

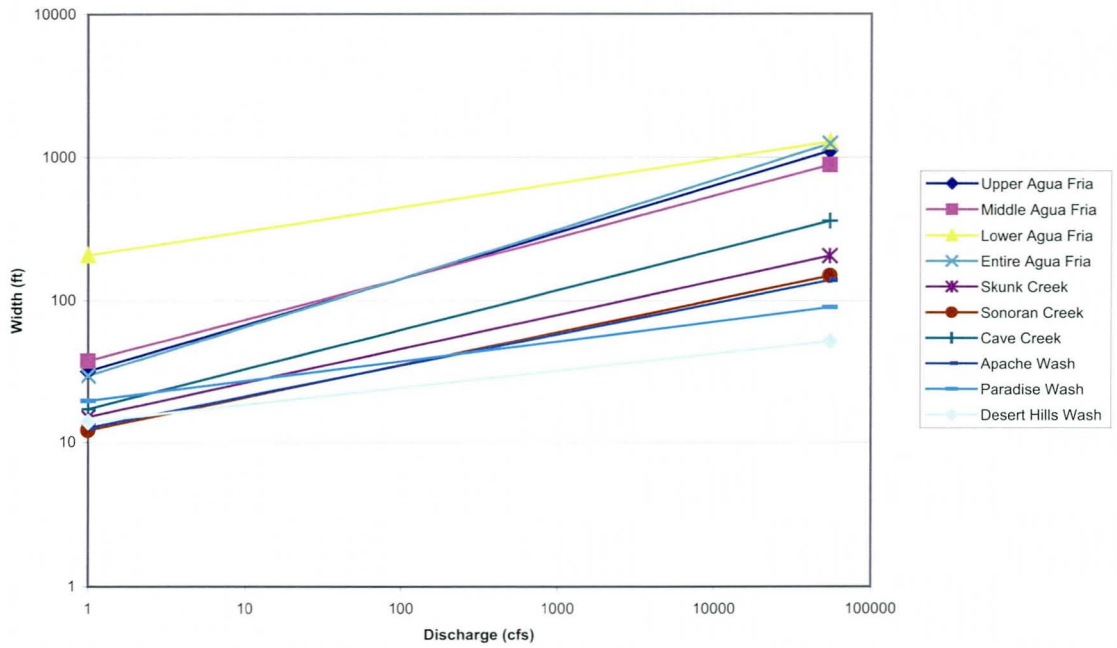

Figure 6-39 Comparison of width to discharge relationships for Agua Fria and central Arizona streams

The middle and lower reaches of the Agua Fria River increase in depth with increasing discharge at rates similar to Skunk Creek, Sonoran Wash, Cave Creek, and Apache Wash. The depth:discharge ratios are larger than the reported average for ephemeral streams. The depth:discharge ratio for upper reach of the Agua Fria River is much lower than the average for ephemeral streams and all the adjacent streams. The upper reach of the Agua Fria River is in a much less disturbed state than the middle and lower reaches. Figure 6-40 illustrates the relationship between the width:discharge ratios. Considered over the entire study length, the Agua Fria River deepens at a slower rate with increasing discharge compared to adjacent streams.

The velocity:discharge ratio for the middle and lower reaches of the Agua Fria River is similar to the ratios for the nearby washes and average ephemeral streams. The hydraulic geometry for the upper reach of the Agua Fria River indicates the velocity increases at a faster rate than that of nearby streams. Figure 6-41 illustrates the relationship between the velocity:discharge ratios. Considered over the entire study length the Agua Fria River's velocity increases at a slightly faster rate with increasing discharge compared to adjacent streams.

The hydraulic geometries for the Agua Fria River reinforce the observational evidence that the Agua Fria River is, overall, a wider and shallower river than other previously studied streams in the central Arizona region. This scenario suggests that the banks of the Agua Fria River may be more susceptible to lateral erosion, especially along banks composed of unconsolidated material. An additional implication of the faster increase in width and slower increase in depth is that the hydraulic radius of the Agua Fria River is larger than other streams, with an especially wide contact on the bed of the river. When combined with slightly faster increases in velocity, the result may be greater amounts of sediment transport than typical streams in the area.

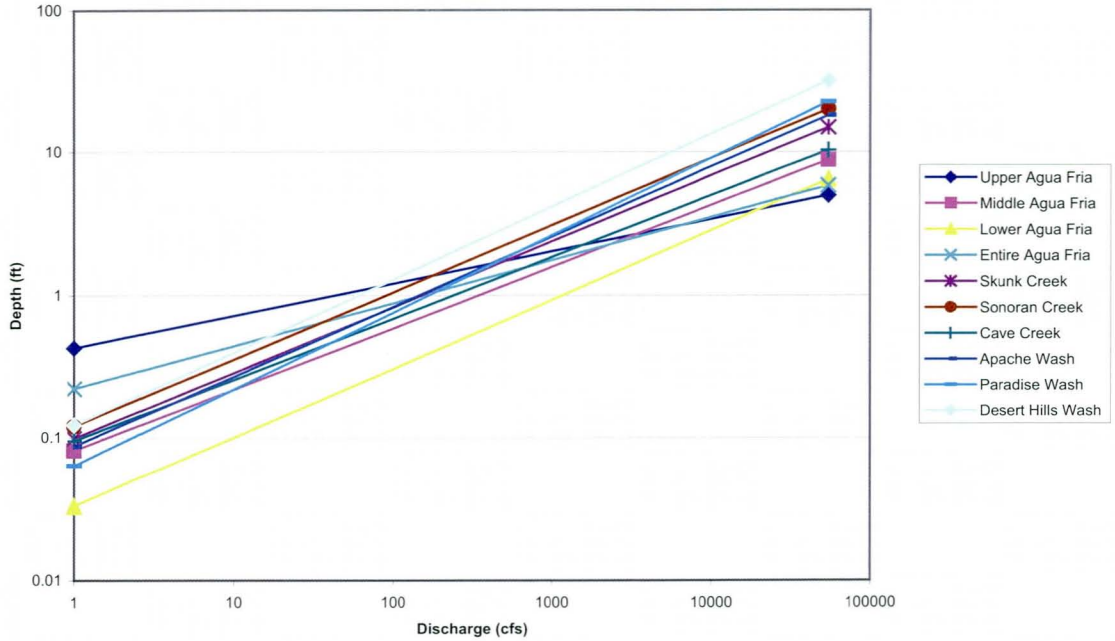

Figure 6-40 Comparison of depth to discharge relationships for Agua Fria and central Arizona streams

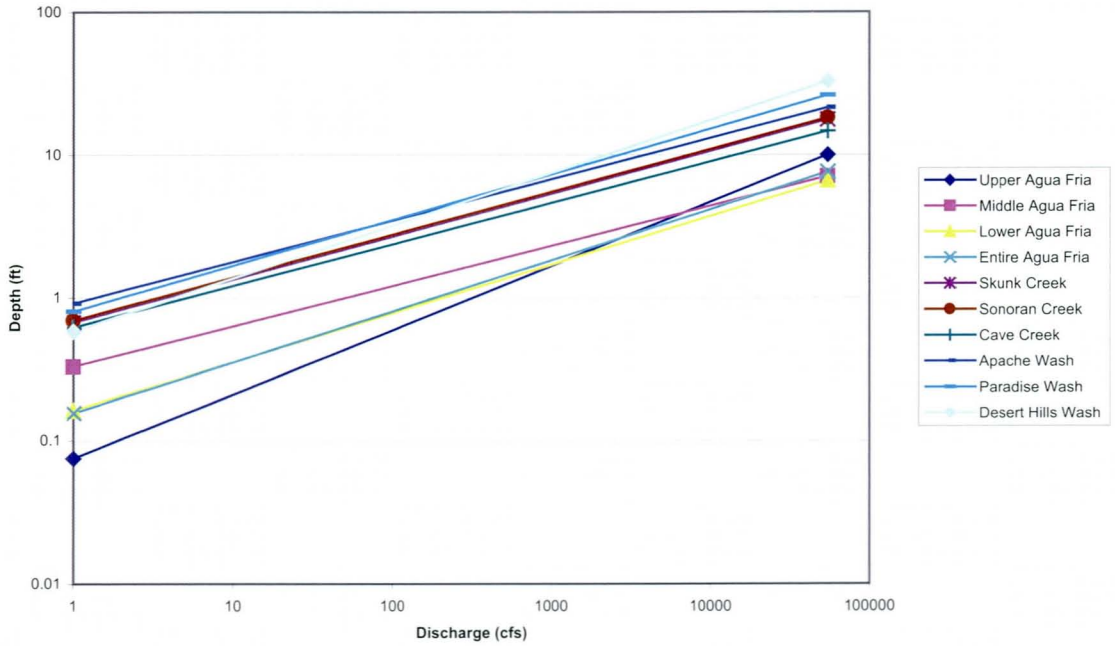

Figure 6-41 Comparison of velocity to discharge relationships for Agua Fria and central Arizona streams

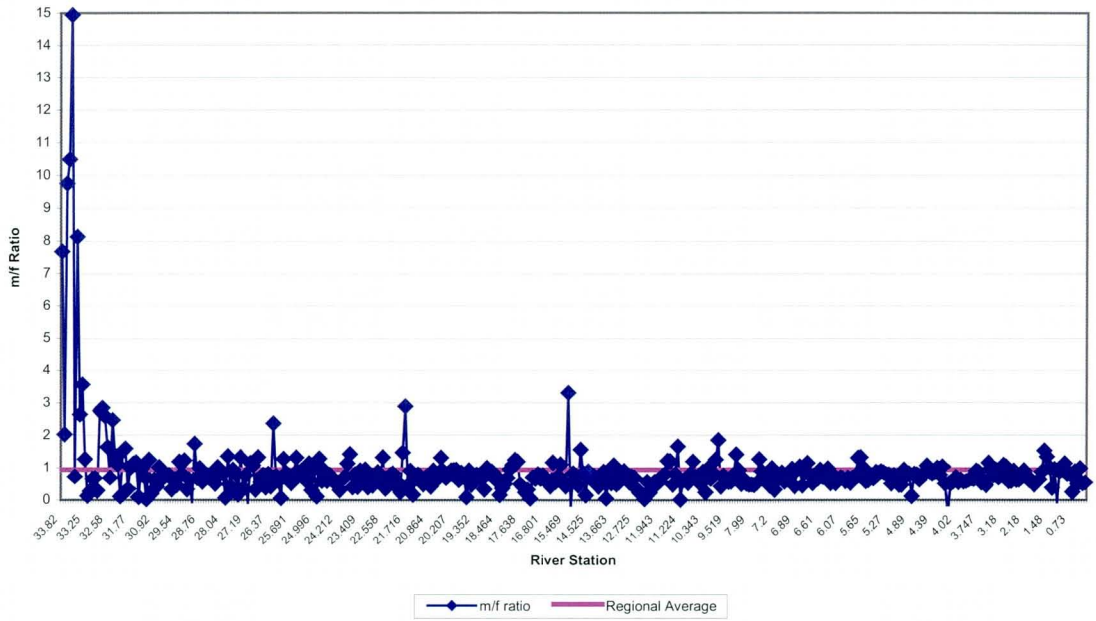

Figure 6-42 Variation in m/f ratio for post New Waddell hydraulic geometry

The *m/f* ratio (change in velocity to change in depth with change in discharge) can be used as an indicator of the rate of sediment transport. The greater the *m/f* ratio, the larger the amount of sediment transported with changes in discharge. The average *m/f* ratio for ephemeral streams in semiarid United States is 0.94. Figure 6-42 illustrates both the variability of the m/f ratio for the Agua Fria River and the general trend for the m/f ratio to be below the average for ephemeral streams. Reach by reach m/f ratio values for post New Waddell hydraulic geometry are presented in Table 6-12.

Table 6-12 Agua Fria m/f Ratio Values

Reach	m/f Ratio	Entire Study Reach	m/f Ratio
1	3.52		
2	0.75		
3	0.51		
4	0.75		
5	0.74		
6	0.77	Maximum	3.52
7	0.73	Minimum	0.51
8	0.67	Mean	0.90
9	0.75	Median	0.74
10	0.69		
11	0.72		
12	0.74		
13	0.68		
14	0.80		
15	0.68		

Table 6-13 Comparison of Reach Averages for the Agua Fria River Hydraulic Geometry with Semiarid U.S. Averages

Reach	Range	Average	Average Semiarid U.S.	Difference Reach Avg – U.S. Avg	Explanation
Reach 1, Agua Fria River					
m (velocity)	0.097-0.843	0.74	0.34	0.40	as Q increases, velocity increases at a faster rate than average
f (depth)	0.056-0.770	0.14	0.36	-0.22	As Q increases, depth increases at a slower rate than average
b (width)	0.019-0.382	0.12	0.29	-0.17	As Q increases, width increases at a slower rate than average
m/f ratio	0.128-14.942	5.42	0.94	4.48	as Q increases, sediment transport increases at much faster rate than average
Reach 2, Agua Fria River					
m (velocity)	0.007-0.596	0.29	0.34	-0.05	as Q increases, velocity increases at a slightly slower rate than average
f (depth)	0.201-0.678	0.43	0.36	0.07	As Q increases, depth increases at a faster rate than average
b (width)	0.0028-0.624	0.27	0.29	-0.02	as Q increases, width increases at a slightly slower rate than average
m/f ratio	0.020-1.588	0.67	0.94	-0.27	as Q increases, sediment transport increases at much slower rate than average
Reach 3, Agua Fria River					
m (velocity)	0.292-0.306	0.30	0.34	-0.04	as Q increases, velocity increases at a slightly slower rate than average
f (depth)	0.536-0.651	0.60	0.36	0.24	As Q increases, depth increases at a faster rate than average
b (width)	0.292-0.306	0.11	0.29	-0.18	As Q increases, width increases at a slower rate than average
m/f ratio	0.449-0.571	0.51	0.94	-0.43	as Q increases, sediment transport increases at much slower rate than average
Reach 4, Agua Fria River					
m (velocity)	-0.052-0.547	0.26	0.34	-0.08	as Q increases, velocity increases at a slower rate than average
f (depth)	0.158-0.744	0.39	0.36	0.03	as Q increases, depth increases at a slightly faster rate than average
b (width)	0.026-0.715	0.35	0.29	0.06	As Q increases, width increases at a faster rate than average
m/f ratio	-0.091-1.729	0.68	0.94	-0.26	as Q increases, sediment transport increases at much slower rate than average
Reach 5, Agua Fria River					
m (velocity)	0.021-0.442	0.23	0.34	-0.11	as Q increases, velocity increases at a slower rate than average
f (depth)	0.068-0.607	0.36	0.36	0.00	as Q increases, depth increases at the average rate
b (width)	0.110-0.771	0.40	0.29	0.11	As Q increases, width increases at a faster rate than average
m/f ratio	0.059-2.356	0.64	0.94	-0.03	as Q increases, sediment transport increases at much slower rate than average

Reach	Range	Average	Average Semiarid U.S.	Difference Reach Avg – U.S. Avg	Explanation
Reach 6, Agua Fria River					
m (velocity)	0.070-0.669	0.26	0.34	-0.08	as Q increases, velocity increases at a slower rate than average
f (depth)	0.175-0.594	0.37	0.36	0.01	as Q increases, depth increases at a slightly faster rate than average
b (width)	0.011-0.671	0.38	0.29	0.09	As Q increases, width increases at a faster rate than average
m/f ratio	0.162-2.886	0.70	0.94	-0.24	as Q increases, sediment transport increases at much slower rate than average
Reach 7, Agua Fria River					
m (velocity)	0.037-0.469	0.29	0.34	-0.05	as Q increases, velocity increases at a slightly slower rate than average
f (depth)	0.275-0.632	0.40	0.36	0.04	as Q increases, depth increases at a slightly faster rate than average
b (width)	0.020-0.564	0.31	0.29	0.02	as Q increases, width increases at a slightly faster rate than average
m/f ratio	0.089-1.314	0.72	0.94	-0.22	as Q increases, sediment transport increases at much slower rate than average
Reach 8, Agua Fria River					
m (velocity)	0.230-0.999	0.30	0.34	-0.04	as Q increases, velocity increases at a slightly slower rate than average
f (depth)	0.286-0.634	0.47	0.36	0.11	As Q increases, depth increases at a faster rate than average
b (width)	0.058-0.671	0.23	0.29	-0.06	As Q increases, width increases at a slower rate than average
m/f ratio	0.049-1.246	0.63	0.94	-0.31	as Q increases, sediment transport increases at much slower rate than average
Reach 9, Agua Fria River					
m (velocity)	-0.072-0.487	0.20	0.34	-0.14	as Q increases, velocity increases at a slower rate than average
f (depth)	-0.002-0.538	0.30	0.36	-0.06	as Q increases, depth increases at a slower rate than average
b (width)	0.134-0.809	0.50	0.29	0.21	as Q increases, width increases at a faster rate than average
m/f ratio	-0.235-3.308	0.65	0.94	-0.29	as Q increases, sediment transport increases at much slower rate than average
Reach 10, Agua Fria River					
m (velocity)	0.008-0.586	0.31	0.34	-0.03	as Q increases, velocity increases at a slightly slower rate than average
f (depth)	0.308-0.817	0.49	0.36	0.13	as Q increases, depth increases at a faster rate than average
b (width)	0.021-0.373	0.20	0.29	-0.09	as Q increases, width increases at a slower rate than average
m/f ratio	0.013-1.855	0.64	0.94	-0.30	as Q increases, sediment transport increases at much slower rate than average

Reach	Range	Average	Average Semiarid U.S.	Difference Reach Avg – U.S. Avg	Explanation
Reach 11, Agua Fria River					
m (velocity)	0.199-0.408	0.31	0.34	-0.03	as Q increases, velocity increases at a slightly slower rate than average
f (depth)	0.141-0.616	0.50	0.36	0.14	as Q increases, depth increases at a faster rate than average
b (width)	0.045-0.659	0.18	0.29	-0.11	as Q increases, width increases at a slower rate than average
m/f ratio	0.411-1.409	0.62	0.94	-0.32	as Q increases, sediment transport increases at much slower rate than average
Reach 12, Agua Fria River					
m (velocity)	0.239-0.565	0.41	0.34	0.07	as Q increases, velocity increases at a faster rate than average
f (depth)	0.428-0.755	0.58	0.36	0.22	as Q increases, depth increases at a faster rate than average
b (width)	0.002-0.156	0.01	0.29	-0.28	as Q increases, width increases at a slower rate than average
m/f ratio	0.317-1.319	0.71	0.94	-0.23	as Q increases, sediment transport increases at much slower rate than average
Reach 13, Agua Fria River					
m (velocity)	-0.507-0.509	0.38	0.34	0.04	as Q increases, velocity increases at a slightly faster rate than average
f (depth)	0.479-1.598	0.61	0.36	0.25	as Q increases, depth increases at a faster rate than average
b (width)	0.002-0.139	0.02	0.29	-0.27	as Q increases, width increases at a slower rate than average
m/f ratio	-0.337-1.063	0.62	0.94	-0.32	as Q increases, sediment transport increases at much slower rate than average
Reach 14, Agua Fria River					
m (velocity)	0.198-0.601	0.37	0.34	0.03	as Q increases, velocity increases at a slightly faster rate than average
f (depth)	0.263-0.658	0.48	0.36	0.12	as Q increases, depth increases at a faster rate than average
b (width)	0.004-0.538	0.04	0.29	-0.25	as Q increases, width increases at a slower rate than average
m/f ratio	0.455-1.526	0.77	0.94	-0.17	as Q increases, sediment transport increases at much slower rate than average
Reach 15, Agua Fria River					
m (velocity)	-0.047-0.522	0.26	0.34	-0.08	as Q increases, velocity increases at a slower rate than average
f (depth)	0.414-0.689	0.27	0.36	-0.09	as Q increases, depth increases at a slower rate than average
b (width)	0.013-0.224	0.46	0.29	0.17	as Q increases, width increases at a faster rate than average
m/f ratio	-0.069-1.133	0.97	0.94	0.03	as Q increases, sediment transport increases at slightly faster rate than average

Reach	Range	Average	Average Semiarid U.S.	Difference Reach Avg – U.S. Avg	Explanation
Skunk Creek					
m (velocity)	0.261-0.319	0.30	0.34	-0.04	as Q increases, velocity increases at a slower rate than average
f (depth)	0.424-0.485	0.46	0.36	0.10	as Q increases, depth increases at a faster rate than average
b (width)	0.216-0.258	0.24	0.29	-0.05	as Q increases, width increases at a slower rate than average
m/f ratio	0.539-0.751	0.65	0.94	-0.29	as Q increases, sediment transport increases at much slower rate than average
Sonoran Wash					
m (velocity)	0.289 -0.337	0.30	0.34	-0.04	as Q increases, velocity increases at a slower rate than average
f (depth)	0.461-0.499	0.47	0.36	0.11	as Q increases, depth increases at a faster rate than average
b (width)	0.164-0.239	0.23	0.29	-0.06	as Q increases, width increases at a slower rate than average
m/f ratio	0.601-0.681	0.65	0.94	-0.29	as Q increases, sediment transport increases at much slower rate than average
Cave Creek					
m (velocity)	0.259-0.323	0.29	0.34	-0.05	as Q increases, velocity increases at a slower rate than average
f (depth)	0.415-0.449	0.43	0.36	0.07	as Q increases, depth increases at a faster rate than average
b (width)	0.250-0.327	0.28	0.29	-0.01	as Q increases, width increases at a rate close to average
m/f ratio	0.610-0.758	0.67	0.94	-0.27	as Q increases, sediment transport increases at much slower rate than average
Paradise Wash					
m (velocity)	0.318-0.322	0.32	0.34	-0.02	as Q increases, velocity increases at a slightly slower rate than average
f (depth)	0.540-0.541	0.54	0.36	0.18	as Q increases, depth increases at a faster rate than average
b (width)	0.137-0.143	0.14	0.29	-0.15	as Q increases, width increases at a slower rate than average
m/f ratio	0.588-0.596	0.59	0.94	-0.35	as Q increases, sediment transport increases at much slower rate than average
Desert Hills Wash					
m (velocity)	0.358-0.391	0.38	0.34	0.04	as Q increases, velocity increases at a faster rate than average
f (depth)	0.499-0.522	0.51	0.36	0.15	as Q increases, depth increases at a faster rate than average
b (width)	0.110-0.121	0.12	0.29	-0.17	as Q increases, width increases at a slower rate than average
m/f ratio	0.686-0.783	0.75	0.94	-0.20	as Q increases, sediment transport increases at much slower rate than average

Reach	Range	Average	Average Semiarid U.S.	Difference Reach Avg – U.S. Avg	Explanation
Apache Wash					
m (velocity)	0.170-0.350	0.29	0.34	-0.05	as Q increases, velocity increases at a slower rate than average
f (depth)	0.419-0.533	0.49	0.36	0.13	as Q increases, depth increases at a faster rate than average
b (width)	0.117-0.375	0.22	0.29	-0.07	as Q increases, width increases at a slower rate than average
m/f ratio	0.374-0.785	0.59	0.94	-0.35	as Q increases, sediment transport increases at much slower rate than average
Note: Data for Skunk Creek does not include m, f, or b values for the disturbed bridge reaches.					

The data in Table 6-12 indicate the following trends for the Agua Fria River:

- The values for *m/f* ratio sediment transport rate for the Agua Fria River are generally below the average for ephemeral streams in the semiarid United States, according to Leopold, et al (1964). Therefore, as discharge increases, the rate of sediment transport will be lower than average. The exception to this trend is Reach 1, where sediment transport is indicated to be much greater.
- The values for *m/f* ratio are variable throughout the length of the Agua Fria River study reaches. Sediment transport will thus be more variable, so the possibility of stability problems is likely.

At the reach scale, all the *m/f* ratios for the study area are below average except for Reach 1, as shown in Table 6-12. The below-average *m/f* ratios seem to contradict the findings of the singular hydraulic geometry equations. Examination of the *m, f,* and *b* values for the Agua Fria River reveals that the velocity increases at a rate similar to average (Table 6-13). At the same time, the depths increase at a slower rate than average, while widths are increasing generally at a faster rate. A faster increase in velocity may indicate that larger bed particles are being entrained at a faster rate. A slower increase in depth combined with a faster increase in width points to more interaction of the volume of water with the bed surface, or a faster increase in the wetted perimeter. These two conditions may explain the lower than average increase in the sediment transport rate.

The hydraulic geometry regression equation results provide some insight into the stability of the stream channels in the study area. A slower increase in depth and a faster increase in width indicate a channel configuration that is shallower than average and wider than average, a conclusion that is supported by the channel geometry equations described above. A faster increase in width as discharge increases might imply that the channel has poorly-consolidated banks, resulting in larger constraining lateral erosion while concentrating erosive work on the bed of the channel, as was hypothesized by Parker (1979). These factors, along with a faster increase in depth, might indicate that the channels are more incised than the average ephemeral wash.

6.5 Engineering methods

6.5.1 Allowable velocity

Allowable velocity criteria have long been used in channel design to estimate the velocity at which channel bed and bank sediments will begin to erode. A variety of allowable velocity data have been published by the US Army Corps of Engineers (1970, 1990, 1995) and the USDA Soil Conservation Service (1977), as well as by many other agencies.

Methodology. The following allowable velocity approaches were applied to the four major streams in the study area:

- Fortier & Scobey Table
- BUREC/Mavis & Laushey Equation
- Neill Equation
- USACOE Permissible Velocity Tables

Fortier & Scobey Table. Fortier and Scobey (1926) published one of the first tables of permissible velocity in 1926. Their data, based on records of seasoned stable canals, was later

republished by a number of federal agencies and other organizations including the FHWA, ASCE, and Chow (MacBroom, 1981). The Fortier and Scobey data (Table 6-14) distinguish erosion hazards for clear water, silt-laden water, and water transporting sand and gravel (bedload). Their data presumably do not account for the stabilizing effect of bank vegetation. Further modifications to this method are described in Chow (1959) from Soviet researchers in 1936. These modifications include an adjustment to the permissible velocity based on depth. An additional modification was proposed by Lane (1955) for sinuous channels. These adjustments are reflected in the reach-average evaluations summarized in Table 6-26.

Table 6-14 Fortier & Scobey Table of Permissible Canal Velocities (ft/s)

Bank Material	Clear Water	Silt-Laden	Sand/Gravel Bedload
Sandy Loam	1.75	2.50	2.00
Firm Loam	2.50	3.50	2.25
Fine Gravel	2.50	5.00	3.75
Stiff Clay	3.75	5.00	3.00
Coarse Gravel	4.00	5.50	6.50
Cobbles	5.00	5.50	6.50

BUREC/Mavis & Laushey Equation. The BUREC (1974) recommends that permissible velocity be estimated using a modification of the Mavis and Laushey equation (Jurnikis, 1971), which was developed by bridge engineers in Great Britain (MacBroom, 1981). The BUREC equation is a function of grain size, and is most applicable to bed material.

$$V_b = 0.64\ D^{(4/9)} \qquad \text{for } D < 6.0 \text{ mm}$$

$$V_b = 0.5\ D^{1/2} \qquad \text{for } D > 6.0 \text{ mm}$$

Where V_b = competent velocity (ft/sec)

D = particle diameter (mm)

Neill Equation. Neill (1975) developed equations that are a function of flow depth and grain size for permissible velocities on gravel and cobble bed streams, with a separate equation for cohesive soils.

$$V_b = 3.15\ d^{(1/3)}\ D^{(2/3)} \qquad \text{(non-cohesive soils)}$$

$$V_b = 7.5\ d^{(1/6)}\ \tau_c^{1/2} \qquad \text{(for cohesive soils)}$$

Where V_b = competent velocity (ft/sec)

d = flow depth (ft)

D = grain size (ft)

τ_c = *critical shear stress* (lb/ft^2)

USACOE Permissible Velocity. The Corps of Engineers (1970; 1995) has established suggested maximum velocities for design of non-scouring flood control channels of various bank materials, as shown in Table 6-15.

Table 6-15 Suggested Maximum Permissible Mean Channel Velocities (USACOE, 1995)

Channel Material	Mean Velocity (ft/sec)
Fine Sand (0.075 – 0.45 mm)	2.0
Coarse Sand (2 – 5 mm)	4.0
Fine Gravel (5 - 20 mm)	6.0
Grass-Lined Banks (< 5% Slope, Sandy Silt, Bermuda Grass)	8.0
Poor Rock (Sedimentary)	10.0
Good Rock (Igneous or Metamorphic)	20.0

The Corps of Engineers (1990) has also developed criteria relating flow depth and velocity to the beginning of movement of granular bed materials and erosion of cohesive bank materials, as summarized in Table 6-16.

Table 6-16 Corps of Engineers Erosive Velocity Data

Grain Size (mm)	Flow Depth (ft)	Velocity (ft/sec)	Cohesiveness	Flow Depth (ft)	Velocity (ft/sec)
1 (sand)	5 10	2.5 4.0	Very Soft	5 10	2.0 2.5
10 (gravel)	5 10	4.5 5.5	Average	5 10	3.5 4.0
100 (cobbles)	5 10	9.5 10.5	Very Stiff	5 10	5.5 6.0

Results. In general, the internal alluvial banks of the Agua Fria River are composed of sand, gravel and cobbles with generally sparse vegetation cover. The outer terrace banks tend to be old Pleistocene surfaces capped with caliche and underlain by less resistant sand, gravel, and cobbles. No significant grass cover was observed in the field.

Table 6-17, Table 6-18, and Table 6-19 show reach-averaged velocities for the channel, left and right overbanks for the 100-year flood. The three tables show three subsets of the cross section averages for each reach. First, Table 6-17 shows the reach average for all cross sections in the HEC-RAS for each reach. Second, Table 6-18 shows the reach averages when cross sections at and near bridges as well as the fully channelized sections have been excluded from the reach-average calculations. Therefore, average values for Reaches 12 and 13 are listed as N/A as all of the cross sections within these two reaches are fully channelized. The third table, Table 6-19 shows the average data for each reach based only on the bridges and/or channelized cross sections in each reach.

The reach-average data show that, aside from the bridges and channelized sections, the Agua Fria River is marginally erosive in the upper reaches and becomes more erosive, according to the permissible velocities shown in Table 6-15, in the finer-grained lower reaches. The most erosive conditions will occur at bridges and within the channelized reaches. Overbank velocities are generally below the erosive limit for gravels, but slightly higher than the erosive limit for sands. Since many of the overbank areas are composed of finer-grained materials, at least at the surface, erosion of the upper layers of the overbank areas is expected during a 100-year flood.

Table 6-17 100-year Flood Velocities, All Cross Sections

Reach	Average Velocity (ft/s)			Maximum Velocity (ft/s)		
	Main Channel	Overbanks		Main Channel	Overbanks	
		Left	Right		Left	Right
1	6.7	3.9	3.2	14.6	10.2	7.3
2	6.2	2.0	2.5	9.0	4.9	5.4
3	7.4	2.9	0.0	9.4	3.8	0.0
4	6.0	1.3	2.0	9.3	3.8	3.5
5	5.7	2.2	2.3	11.0	3.7	4.5
6	5.4	3.0	2.8	11.3	4.9	6.0
7	6.0	2.8	3.5	8.5	3.9	4.7
8	7.3	2.8	1.8	19.4	5.9	5.1
9	5.6	1.9	2.2	7.7	2.7	3.5
10	6.2	1.7	1.4	16.8	7.5	3.4
11	5.7	2.3	1.7	7.5	4.7	3.4
12	7.4	0.0	0.0	10.8	0.0	0.0
13	6.7	0.0	0.0	11.5	0.0	0.0
14	5.9	2.3	1.0	10.1	3.8	1.6
15	6.8	3.3	1.9	12.9	7.7	4.0
Source: HEC-RAS model adapted from the Floodplain Delineation Study HEC-2 model (CVL, 1996) by JEF for this study.						

Table 6-18 100-year Flood Velocities, Without Bridges and Channelized Cross Sections

Reach	Average Velocity (ft/s)			Maximum Velocity (ft/s)		
	Main Channel	Overbanks		Main Channel	Overbanks	
		Left	Right		Left	Right
1	6.1	3.7	3.3	14.6	10.2	7.3
2	6.2	2.0	2.5	9.0	4.9	5.4
3	7.8	2.5	0.0	9.1	2.7	0.0
4	6.0	1.3	2.0	9.3	3.8	3.5
5	5.7	2.2	2.3	11.0	3.7	4.5
6	5.4	3.0	2.8	11.3	4.9	6.0
7	6.0	2.8	3.5	8.5	3.9	4.7
8	7.0	2.8	1.8	11.0	5.9	5.1
9	5.7	1.9	2.2	7.7	2.7	3.5
10	6.2	1.7	1.4	16.8	7.5	3.4
11	5.5	2.2	1.6	6.2	4.0	3.4
12	N/A	N/A	N/A	N/A	N/A	N/A
13	N/A	N/A	N/A	N/A	N/A	N/A
14	6.1	2.3	1.0	10.1	3.8	1.6
15	6.8	3.3	1.9	12.9	7.7	4.0
Source: HEC-RAS model adapted from the Floodplain Delineation Study HEC-2 model (CVL, 1996) by JEF for this study.						

Table 6-19 100-year Flood Velocities, Bridges and Channelized Cross Sections Only

Reach	Average Velocity (ft/s)			Maximum Velocity (ft/s)		
	Main Channel	Overbanks		Main Channel	Overbanks	
		Left	Right		Left	Right
1	10.1	4.8	3.0	12.3	7.3	4.0
2	6.5	0.0	0.0	8.5	0.0	0.0
3	7.0	3.3	0.0	9.4	3.8	0.0
4	N/A	N/A	N/A	N/A	N/A	N/A
5	N/A	N/A	N/A	N/A	N/A	N/A
6	N/A	N/A	N/A	N/A	N/A	N/A
7	6.1	0.0	0.0	6.1	0.0	0.0
8	8.0	0.0	0.0	19.4	0.0	0.0
9	4.9	0.0	0.0	5.7	0.0	0.0
10	6.0	0.0	0.0	8.1	0.0	0.0
11	5.8	2.6	2.6	7.5	4.7	2.6
12	7.4	0.0	0.0	10.8	0.0	0.0
13	6.7	0.0	0.0	11.5	0.0	0.0
14	4.7	0.0	0.0	5.0	0.0	0.0
15	N/A	N/A	N/A	N/A	N/A	N/A
Source: HEC-RAS model adapted from the Floodplain Delineation Study HEC-2 model (CVL, 1996) by JEF for this study.						

Plots of channel and overbank velocities for the 100-year flood are shown in Figure 6-43, Figure 6-44, and Figure 6-45. In general, channel velocities are very near the erosive limit for gravel beds and above the erosive limit for fine sands. Also, the channel velocities oscillate around the erosive limit proscribed by the COE, which means that the channel erosion in the Upper and Middle reaches is likely to be limited to localized areas. Overbank velocities are generally only erosive where fine-grained sediments are present. Therefore, in locations where the overbanks are composed of fine-grained sediments, erosion is expected, while in locations of coarser overbanks sediments, no erosion is expected. Erosion is less likely in the Upper and Middle Reach overbanks than in the Lower Reach areas that have overbanks (i.e. the non-channelized sections).

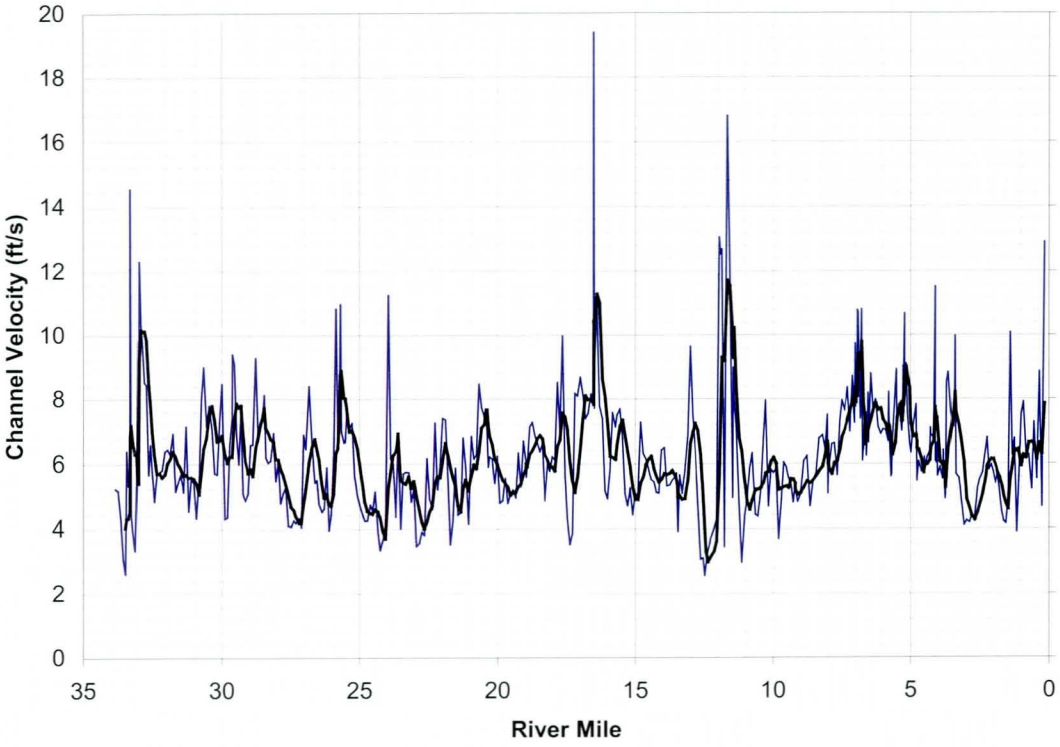

Figure 6-43 100-year Flood Channel Velocities Along the Agua Fria River Downstream of New Waddell Dam

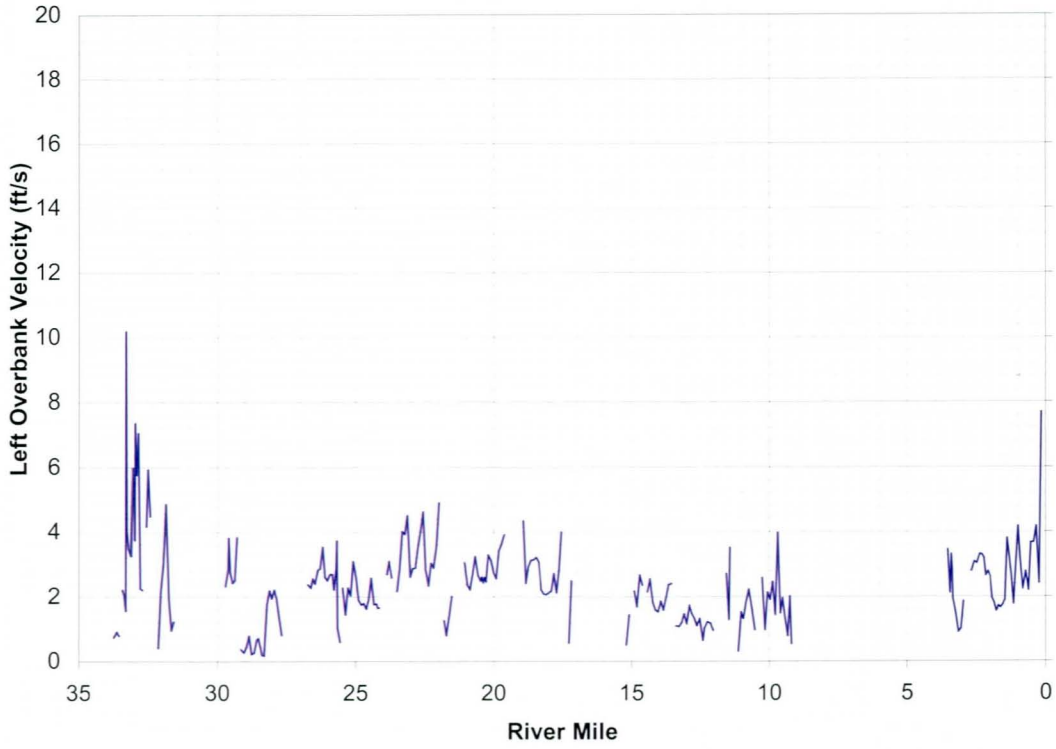

Figure 6-44 100-year Flood Left Overbank Velocities Along the Agua Fria River Downstream of New Waddell Dam

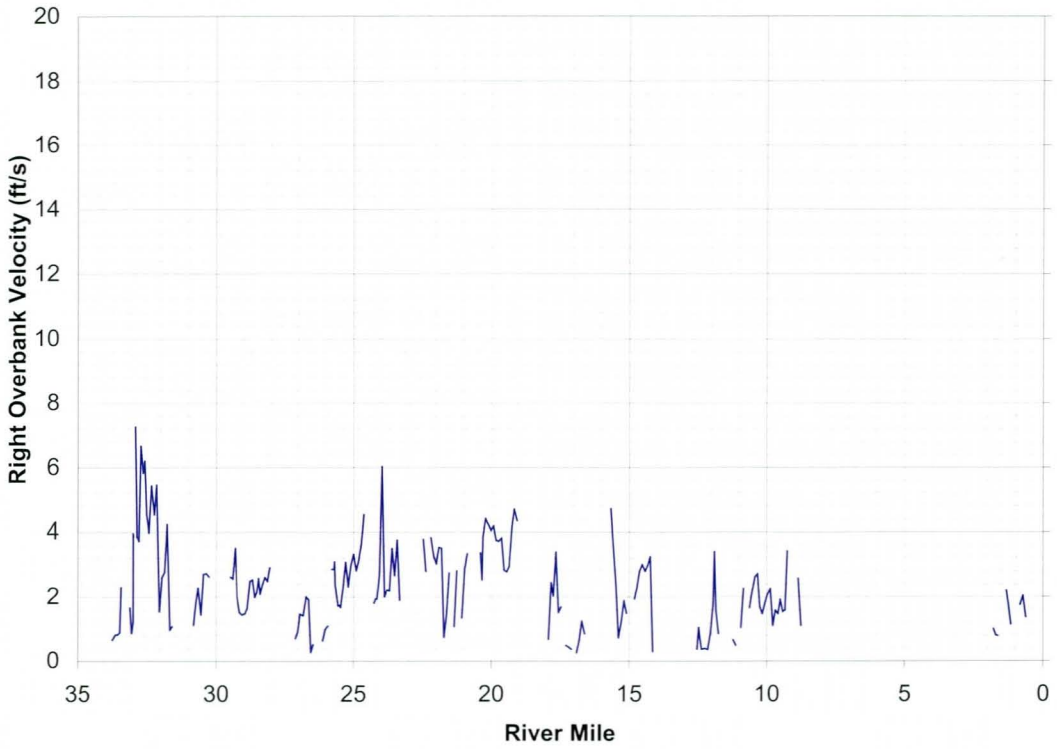

Figure 6-45 100-year Flood Right Overbank Velocities Along the Agua Fria River Downstream of New Waddell Dam

The allowable velocity information summarized above indicates that bank erosion should be expected in localized areas in the Upper and Middle reaches during the 100-year event, and throughout the Lower Reach.

Table 6-20, Table 6-21, and Table 6-22 show reach-averaged 10-year velocities for the channel, left and right overbanks. The three tables show three subsets of the cross section averages for each reach. First, Table 6-20 shows the reach average for all cross sections in the HEC-RAS model for each reach. Second, Table 6-21 shows the reach averages when cross sections at and near bridges as well as the fully channelized sections have been excluded from the reach-average calculations. Therefore, average values for Reaches 12 and 13 are listed as N/A as all of the cross sections within these two reaches are fully channelized. Third, Table 6-22 shows the average data for each reach that contains only the data for bridges and/or channelized cross sections in each reach.

The reach-average data for the 10-year flood show that the Agua Fria River is not erosive for the upper reaches, but is erosive in the finer-grained lower reaches. For the 10-year flood, the most erosion will occur at bridges and within the channelized reaches. Overbank velocities are generally below the erosive limit for gravels, and higher than the erosive limit for sand in localized areas. Since many of the overbank areas are composed of fine-grained materials, at least at the surface, erosion of the upper layers of the overbank areas is expected locally during a 10-year flood.

Table 6-20 10-year Flood Velocities, All Cross Sections

	Average Velocity			Maximum Velocity		
Reach	Channel	LOB	ROB	Channel	LOB	ROB
1	3.9	2.9	2.0	9.6	3.7	3.3
2	4.2	1.3	1.6	8.4	3.4	2.5
3	5.8	0.0	0.0	10.5	0.0	0.0
4	4.1	1.1	1.1	6.0	1.7	2.9
5	4.1	1.4	1.6	7.9	2.8	3.0
6	3.9	2.4	1.9	5.7	3.9	3.2
7	4.2	2.3	2.9	5.2	3.3	3.6
8	5.1	1.4	1.8	17.0	2.4	4.9
9	3.9	0.6	0.6	5.5	0.9	1.1
10	4.5	0.8	0.6	9.1	2.0	1.7
11	3.8	2.9	0.0	7.3	2.9	0.0
12	4.5	0.0	0.0	7.9	0.0	0.0
13	4.1	0.0	0.0	7.7	0.0	0.0
14	3.8	0.9	0.1	9.2	1.5	0.1
15	5.3	2.4	2.0	9.0	4.9	2.0

Table 6-21 10-year Flood Velocities, Without Bridges and Channelized Cross Sections

	Average Velocity			Maximum Velocity		
Reach	Channel	LOB	ROB	Channel	LOB	ROB
1	3.3	2.8	2.3	9.6	3.7	3.3
2	4.2	1.3	1.6	7.6	3.4	2.5
3	5.1	0.0	0.0	5.6	0.0	0.0
4	4.1	1.1	1.1	6.0	1.7	2.9
5	4.6	1.7	1.4	7.9	2.8	2.8
6	3.9	2.4	1.9	5.7	3.9	3.2
7	4.2	2.3	2.9	5.2	3.3	3.6
8	4.8	1.4	1.8	10.2	2.4	4.9
9	3.8	0.6	0.6	4.7	0.9	1.1
10	4.5	0.8	0.6	9.1	2.0	1.7
11	3.8	0.0	0.0	4.7	0.0	0.0
12	N/A	N/A	N/A	N/A	N/A	N/A
13	N/A	N/A	N/A	N/A	N/A	N/A
14	4.0	0.9	0.1	9.2	1.5	0.1
15	5.3	2.4	2.0	9.0	4.9	2.0

Table 6-22 10-year Flood Velocities, Bridges and Channelized Cross Sections Only

	Average Velocity			Maximum Velocity		
Reach	Channel	LOB	ROB	Channel	LOB	ROB
1	6.6	3.7	1.0	7.5	3.7	1.3
2	4.7	0.0	0.0	8.4	0.0	0.0
3	6.3	0.0	0.0	10.5	0.0	0.0
4	N/A	N/A	N/A	N/A	N/A	N/A
5	N/A	N/A	N/A	N/A	N/A	N/A
6	N/A	N/A	N/A	N/A	N/A	N/A
7	4.3	0.0	0.0	4.3	0.0	0.0
8	6.2	0.0	0.0	17.0	0.0	0.0
9	5.0	0.0	0.0	5.5	0.0	0.0
10	4.3	0.0	0.0	4.8	0.0	0.0
11	3.8	2.9	0.0	7.3	2.9	0.0
12	4.5	0.0	0.0	7.9	0.0	0.0
13	4.1	0.0	0.0	7.7	0.0	0.0
14	2.7	0.0	0.0	2.8	0.0	0.0
15	N/A	N/A	N/A	N/A	N/A	N/A

Plots of channel and overbank velocities for the 10-year flood are shown in Figure 6-46, Figure 6-47, and Figure 6-48. In general, channel velocities are very near the erosive limit for gravel beds and above the erosive limit for fine sands. Also, the channel velocities oscillate around the erosive limit proscribed by the Corps of Engineers. Therefore, channel erosion in the Upper and Middle reaches is likely to be limited to localized areas. Overbank velocities are generally only erosive where fine-grained sediments are present. Therefore, in locations where the overbanks are composed of fine-grained sediments, erosion is expected, while in locations of coarser overbank sediments, no erosion is expected. Erosion is less likely in the Upper and Middle Reach overbanks than in the Lower Reach areas that have overbanks (i.e. the non-channelized sections).

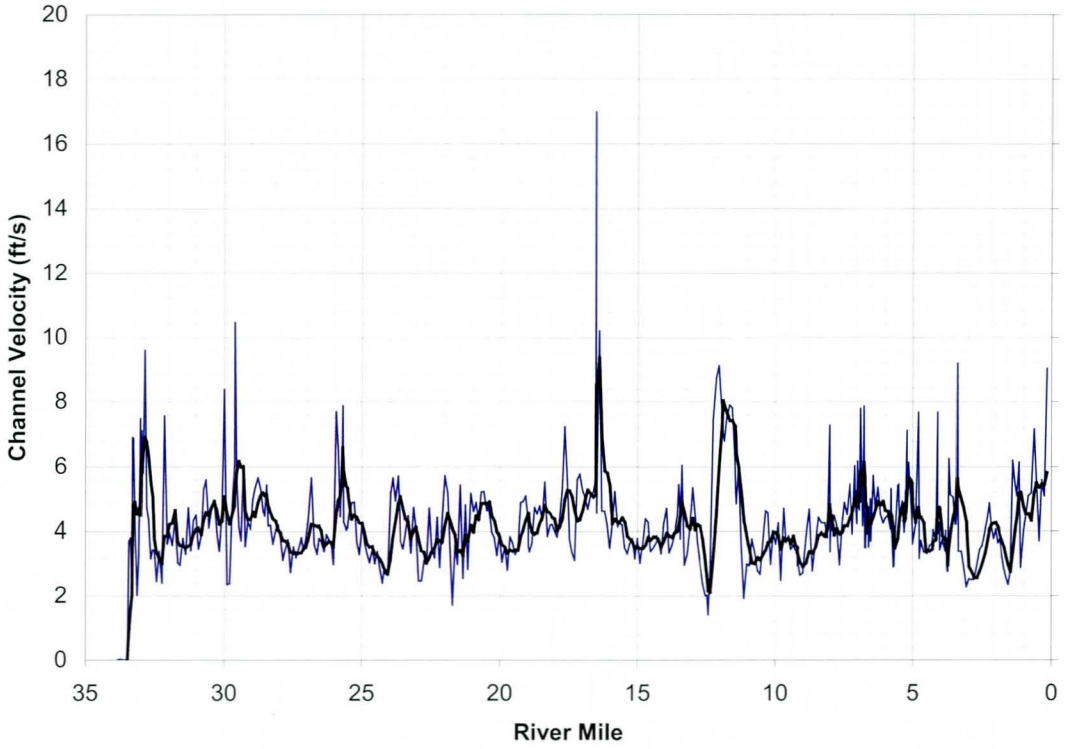

Figure 6-46 10-year Flood Channel Velocities Along the Agua Fria River Downstream of New Waddell Dam

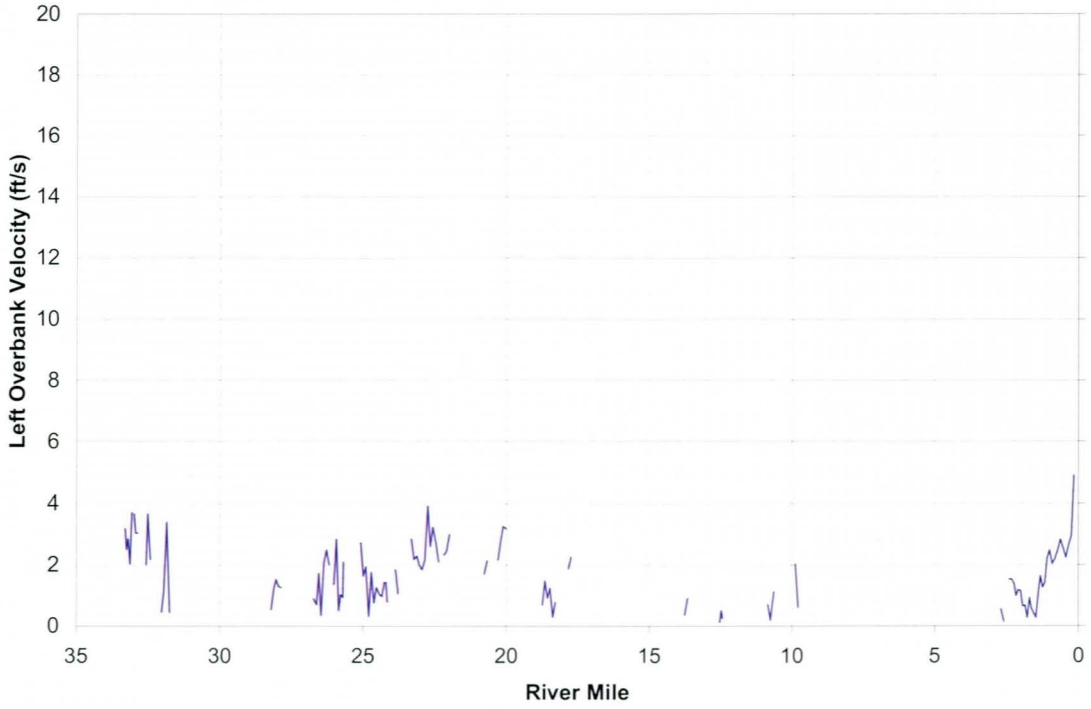

Figure 6-47 10-year Flood Left Overbank Velocities Along the Agua Fria River Downstream of New Waddell Dam

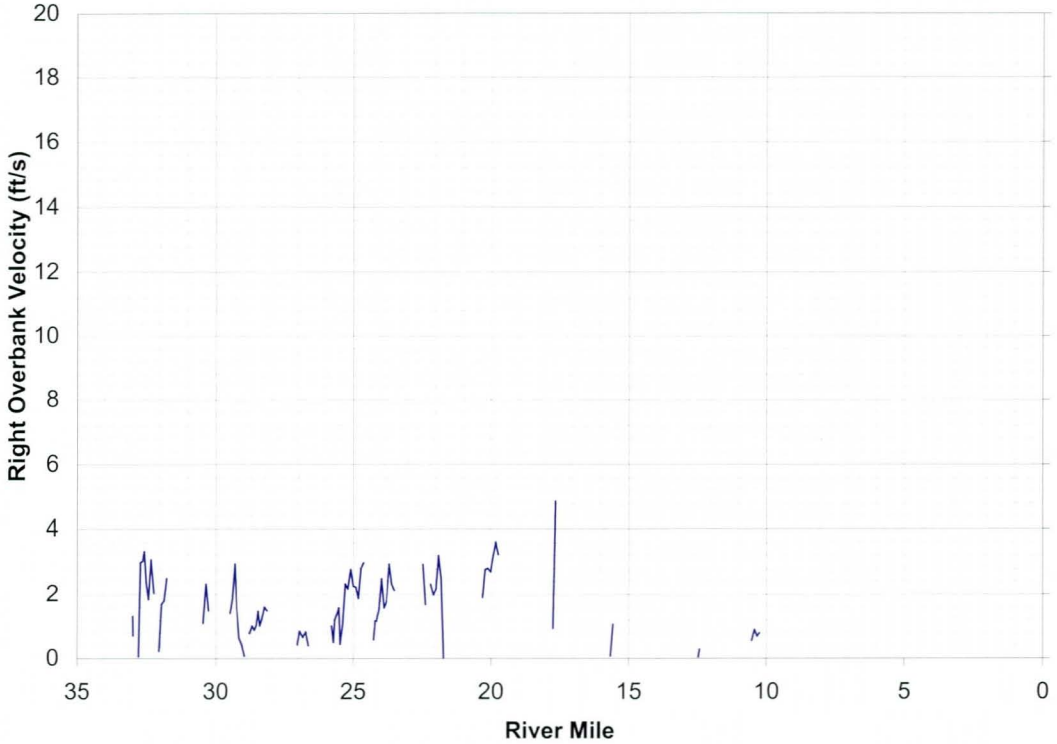

Figure 6-48 10-year Flood Right Overbank Velocities Along the Agua Fria River Downstream of New Waddell Dam

Table 6-23, Table 6-24, and Table 6-25 show reach-averaged velocities for the channel, left and right overbanks for the 2-year flood. The three tables show three subsets of the cross section averages for each reach. Table 6-23 shows the reach average for all cross sections in the HECRAS for each reach. Table 6-24 shows the reach averages when cross sections at and near bridges, as well as the fully channelized sections have been excluded from the reach-average calculations. Table 6-25 shows the average data for only the cross sections in each reach that are located at bridges or are channelized.

The reach-average data for the 2-year flood show that the Agua Fria River is not erosive in the upper reaches and only marginally erosive in the finer-grained lower reaches. For the 2-year flood, the most erosion will occur at the few bridges and channelized reaches where velocities exceed the erosive thresholds. Since the main channel generally contains the 2-year flood at most cross sections, there will be limited flow and hence, erosion, in the overbanks. For those sections where overbank flow does occur, velocities are generally non-erosive.

Table 6-23 2-year Flood Velocities, All Cross Sections

	Average Velocity			Maximum Velocity		
Reach	Channel	LOB	ROB	Channel	LOB	ROB
1	1.7	1.0	0.7	6.6	2.0	1.2
2	2.6	0.0	1.4	5.6	0.0	2.8
3	2.5	0.0	0.0	3.6	0.0	0.0
4	2.5	0.0	0.2	5.7	0.0	0.2
5	2.7	0.6	0.0	5.7	0.9	0.0
6	2.4	1.4	1.0	5.2	1.8	1.2
7	2.6	0.0	0.0	4.0	0.0	0.0
8	2.8	0.2	2.9	13.8	0.2	3.6
9	2.9	0.0	0.0	5.9	0.0	0.0
10	2.2	0.0	0.0	4.9	0.0	0.0
11	2.9	1.8	0.0	5.5	1.8	0.0
12	3.0	0.0	0.0	6.3	0.0	0.0
13	3.1	0.0	0.0	15.3	0.0	0.0
14	2.7	0.6	0.0	6.1	1.3	0.0
15	4.0	1.5	0.7	6.7	3.1	0.7

Table 6-24 2-year Flood Velocities, Without Bridge and Channelized Cross Sections

	Average Velocity			Maximum Velocity		
Reach	Channel	LOB	ROB	Channel	LOB	ROB
1	1.5	1.0	0.7	6.6	2.0	1.2
2	2.6	0.0	1.4	4.9	0.0	2.8
3	3.0	0.0	0.0	3.5	0.0	0.0
4	2.5	0.0	0.2	5.7	0.0	0.2
5	3.0	0.9	0.0	5.7	0.9	0.0
6	2.4	1.4	1.0	5.2	1.8	1.2
7	2.6	0.0	0.0	4.0	0.0	0.0
8	2.6	0.2	2.9	5.6	0.2	3.6
9	2.8	0.0	0.0	5.9	0.0	0.0
10	2.2	0.0	0.0	4.9	0.0	0.0
11	2.8	0.0	0.0	3.8	0.0	0.0
12	N/A	N/A	N/A	N/A	N/A	N/A
13	N/A	N/A	N/A	N/A	N/A	N/A
14	2.8	0.6	0.0	6.1	1.3	0.0
15	4.0	1.5	0.7	6.7	3.1	0.7

Table 6-25 2-year Flood Velocities, Bridge and Channelized Cross Sections Only

	Average Velocity			Maximum Velocity		
Reach	Channel	LOB	ROB	Channel	LOB	ROB
1	3.1	0.0	0.0	4.5	0.0	0.0
2	2.8	0.0	0.0	5.6	0.0	0.0
3	2.2	0.0	0.0	3.6	0.0	0.0
4	N/A	N/A	N/A	N/A	N/A	N/A
5	N/A	N/A	N/A	N/A	N/A	N/A
6	N/A	N/A	N/A	N/A	N/A	N/A
7	3.3	0.0	0.0	3.3	0.0	0.0
8	3.5	0.0	0.0	13.8	0.0	0.0
9	3.0	0.0	0.0	3.2	0.0	0.0
10	2.4	0.0	0.0	2.6	0.0	0.0
11	2.9	1.8	0.0	5.5	1.8	0.0
12	3.0	0.0	0.0	6.3	0.0	0.0
13	3.1	0.0	0.0	15.3	0.0	0.0
14	1.8	0.0	0.0	1.9	0.0	0.0
15	N/A	N/A	N/A	N/A	N/A	N/A

Plots of channel and overbank velocities for the 2-year flood are shown in Figure 6-49, Figure 6-50, and Figure 6-51. Channel velocities are below the erosive limit for gravel beds and slightly above the erosive limit for fine sands. Overbank velocities are generally absent. Again, erosion is not likely in the Upper and Middle Reaches, while even during the 2-year flood the Lower Reach will be erosive within the channel.

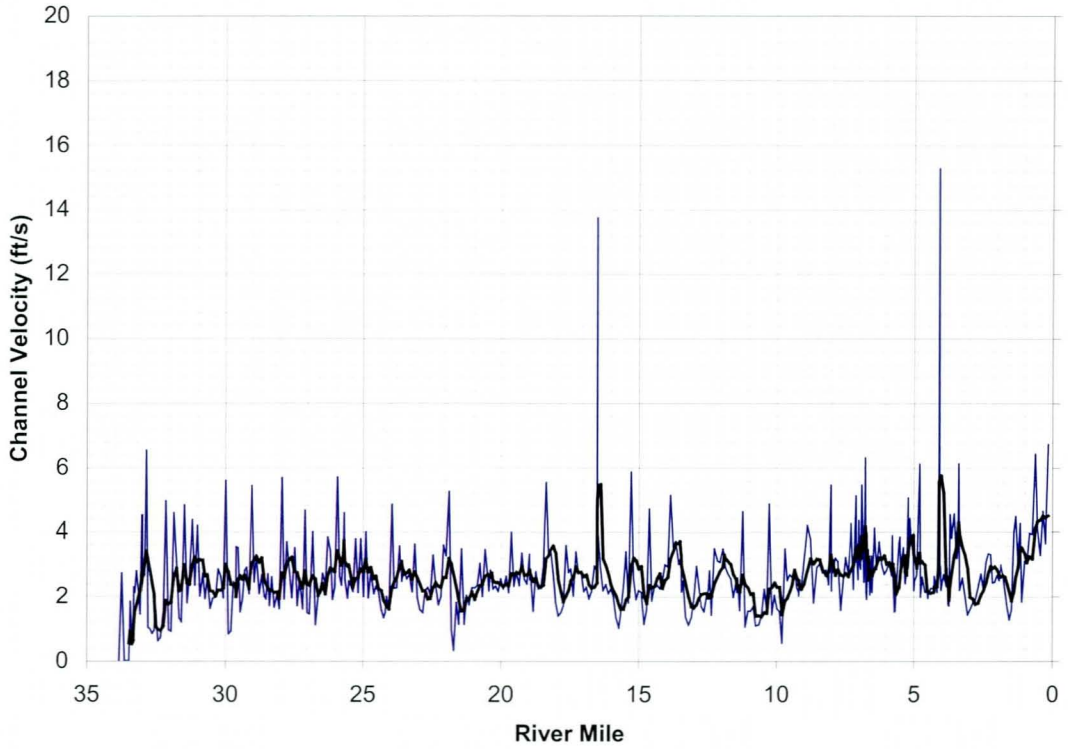

Figure 6-49 2-year Flood Channel Velocities Along the Agua Fria River Downstream of New Waddell Dam

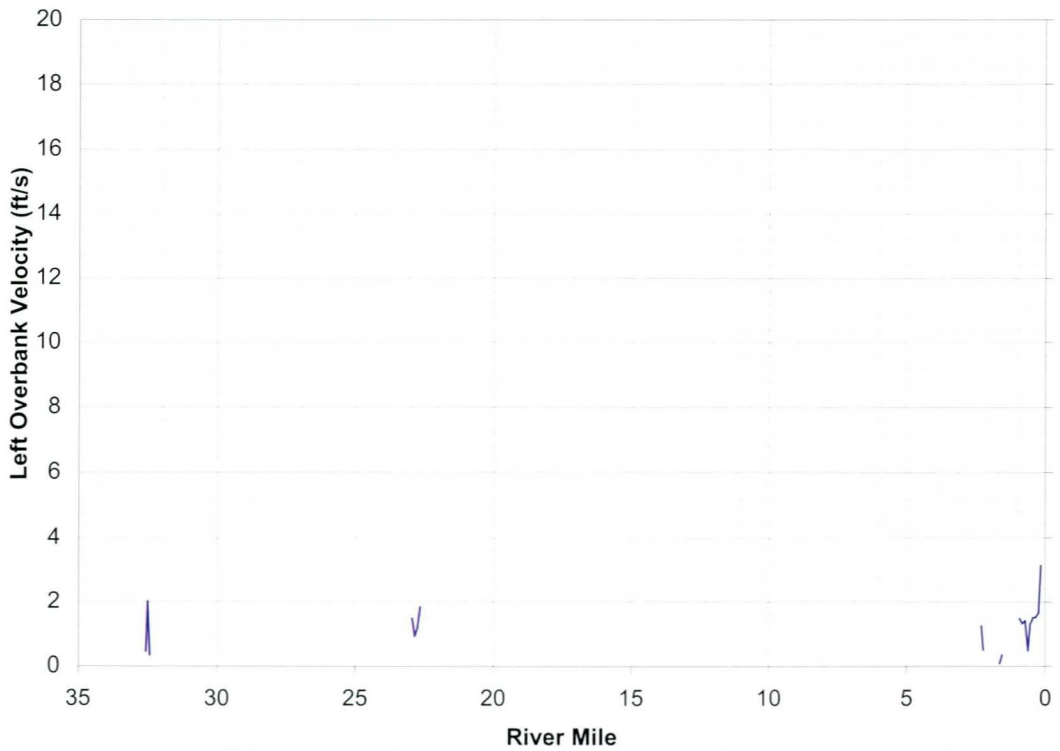

Figure 6-50 2-year Flood Left Overbank Velocities Along the Agua Fria River Downstream of New Waddell Dam

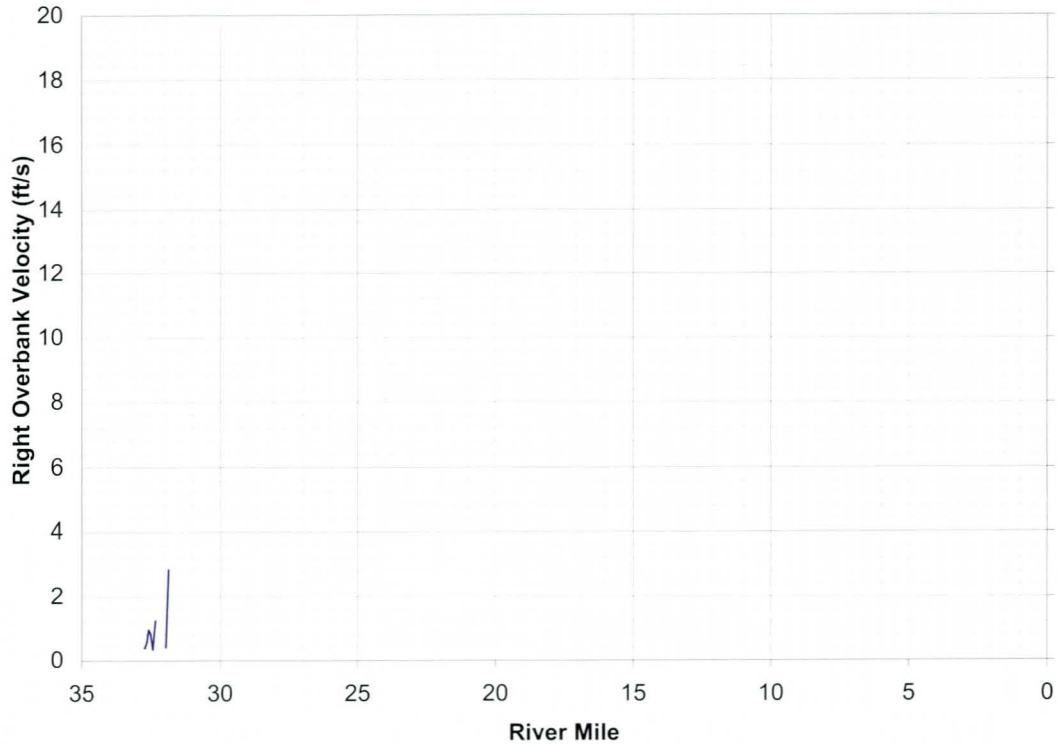

Figure 6-51 2-year Flood Right Overbank Velocities Along the Agua Fria River Downstream of New Waddell Dam

In summary, the allowable velocity criteria and HEC-RAS data show that the Agua Fria River is erosive for the 100-year flood within the channel and the overbanks. For the 10-year flood, the lower reaches, bridges and channelized sections are erosive. Overbanks are locally erosive for the 10-year flood. For the 2-year flood, the channel in the lower reaches is erosive.

Table 6-26 Allowable Velocity Results

Reach	Fortier & Scobey	BUREC	Neill: Non-Cohesive		Neill: Cohesive		USACOE
			Erosive?	Velocity	Erosive?	Velocity	
100-Year							
1	E 96	E 100	E 100	1.1	S 100	13.4	E 100
2	E 100	E 100	E 100	0.9	S 100	9.9	E 100
3	E 100	E 100	E 100	1.0	S 100	11.8	E 100
4	E 100	E 100	E 100	0.9	S 100	9.6	E 100
5	E 100	E 100	E 100	0.8	S 100	8.0	E 100
6	E 100	E 100	E 100	0.9	S 100	9.3	E 100
7	E 100	E 100	E 100	0.9	S 100	9.7	E 100
8	E 100	E 100	E 100	0.7	S 100	11.6	E 100
9	E 100	E 100	E 100	0.6	S 100	9.0	E 100
10	E 100	E 100	E 100	0.7	S 100	10.6	E 100
11	E 100	E 100	E 100	0.3	S 100	8.5	E 100
12	E 100	E 100	E 100	0.4	S 100	8.9	E 100
13	E 100	E 100	E 100	0.4	S 100	8.3	E 100
14	E 100	E 100	E 100	0.4	S 100	9.4	E 100
15	E 100	E 100	E 100	0.4	S 100	10.9	E 100
10-Year							
1	E 73	E 81	E 81	0.9	S 100	7.7	E 81
2	E 100	E 100	E 100	0.8	S 100	6.8	E 100
3	E 100	E 100	E 100	0.8	S 100	9.3	E 100
4	E 100	E 100	E 100	0.8	S 100	6.6	E 100
5	E 100	E 100	E 100	0.7	S 100	5.8	E 100
6	E 97	E 100	E 100	0.7	S 100	6.6	E 97
7	E 100	E 100	E 100	0.8	S 100	6.7	E 100
8	E 100	E 100	E 100	0.5	S 100	8.2	E 100
9	E 100	E 100	E 100	0.5	S 100	6.2	E 100
10	E 98	E 100	E 100	0.6	S 100	7.7	E 98
11	E 100	E 100	E 100	0.3	S 100	5.7	E 100
12	E 100	E 100	E 100	0.3	S 100	5.5	E 100
13	E 100	E 100	E 100	0.3	S 100	5.1	E 100
14	E 100	E 100	E 100	0.3	S 100	6.1	E 100
15	E 100	E 100	E 100	0.3	S 100	8.5	E 100
2-Year							
1	S 62	E 65	E 73	0.7	S 100	3.5	S 58
2	E 69	E 96	E 100	0.6	S 100	4.2	E 54
3	E 80	E 100	E 100	0.6	S 100	4.0	E 80
4	E 71	E 100	E 100	0.6	S 100	4.0	E 62
5	E 90	E 100	E 100	0.6	S 100	3.9	E 80
6	E 81	E 97	E 97	0.6	S 100	4.1	E 66
7	E 100	E 100	E 100	0.6	S 100	4.2	E 100
8	E 88	E 100	E 100	0.4	S 100	4.5	E 83
9	E 96	E 100	E 100	0.4	S 100	4.6	E 92
10	E 81	E 98	E 100	0.4	S 100	3.7	E 56
11	E 100	E 100	E 100	0.2	S 100	4.3	E 100
12	E 100	E 100	E 100	0.2	S 100	3.6	E 100
13	E 100	E 100	E 100	0.2	S 100	3.8	E 100
14	E 97	E 100	E 100	0.3	S 100	4.3	E 97
15	E 100	E 100	E 100	0.3	S 100	6.5	E 100

Notes:
E = allowable velocity exceeded; erosion expected
S = allowable velocity not exceeded; erosion not expected
100 = 100 percent of sections in reach have indicated trend, 87 = 87 percent of sections in reach, etc.

The reach-averaged velocities estimated from the HEC-RAS models for the 2-, 10-, and 100-year events were compared to the allowable velocities determined by the methodologies described above, as shown in Table 6-26. Erosion (E) is expected where the allowable velocities are exceeded by the predicted HEC-RAS reach-averaged velocities. Where the allowable velocities are not exceeded, the channel is expected to be stable (S). The number listed after S or E in Table 6-26 indicates the percent of the cross sections within the reach which exhibit the S or E trend.

Most of the allowable velocity methodologies used indicate that the materials in the bed and banks of the Agua Fria River are erodible. However, Neill's equation for cohesive soils predicts that the banks will be stable up to the 100-year event, even though the 100-year channel velocities approach or exceed the USACOE values of erodibility for igneous bedrock (Table 6-16). Since cohesive soils are generally not present within the study area, the results of Neill's cohesive soil equation are not applicable for most of the reach. Comparison of HEC-RAS channel velocities with the USACOE and Fortier & Scobey erosive velocity thresholds indicate that the channel banks are probably erodible during flows that exceed the 2-year event.

Conclusions. Allowable velocity criteria provide general information on the likelihood of bank and channel erosion. However, accurate predictions of lateral stability based on allowable velocity criteria are difficult to achieve because of the effect of soil cohesiveness, vegetation, carbonate accumulations, and soil physics on erodibility. The range of allowable velocities indicated by the Neill equations illustrates the effect of cohesion on erodibility. Broadly interpreted, the allowable velocity data indicate that all of the channel banks in the study area will erode even in small floods if the banks are not cohesive, but will resist erosion if they are cohesive. Finally, the effects of bank vegetation (increase stability), stratified bank sediments (decrease stability), and other local variations ($CaCO_3$ content, piping, bed scour, etc.) create additional uncertainty for the reliability of allowable velocity predictions.

6.5.2 Equilibrium slope

Equilibrium slope[2] is defined as the slope which causes the channel's sediment transport capacity to equal the incoming sediment supply (ADWR, 1985). If the slope is too steep, channel velocities will be high and net erosion will occur. If the slope is too flat, channel velocities will be low and net deposition will occur. The equilibrium slope is the slope that the undisturbed, natural channel will tend towards over the long term. While there are philosophical and practical problems with applying equilibrium slope concepts to ephemeral streams with variable channel geometry and high flash flood potential, or streams where the natural hydrology has been altered by urbanization or construction of dams, equilibrium slope equations provide a useful order-of-magnitude assessment of the likelihood of vertical channel adjustments.

6.5.2.1 Methodology

Reach-averaged data required for application of equilibrium slope equations to the study area were derived from the following sources:

- Hydraulic data - HEC-RAS modeling (Section 6.2)
- Hydrologic data - HEC-1 modeling and USGS gauge records (Chapter 2)
- Topographic data – Floodplain delineation studies (Chapter 5)

[2] Equilibrium slope is also referred to as stable slope or limiting slope.

Most equilibrium slope equations are based on the mean annual flood, the "channel-forming," or "bankfull" discharge. On many alluvial streams, the mean annual flood and the channel-forming and bankfull discharges are nearly equivalent. However, on ephemeral streams where flow events are rare, the average annual discharge is often difficult to determine. Bankfull discharge estimates were described in Section 6.4.1, and ranged from less than the 2-year event to greater than the 100-year event for the study reach (Table 6-2). To account for the discrepancies in what flow rate is appropriate for equilibrium slope analyses, and to assess the trend of expected slope adjustments during floods, the 2-, 10-, and 100-year peaks were used in the equilibrium slope equations to assess the expected slope adjustment over a range of discharges. The 2-year event approximates the mean annual flood calculated on a weighted probability basis. The 10-year event better approximates bankfull conditions in the study reach. The 100-year event represents possible channel responses during extreme flooding. The following equilibrium slope equations were applied to the study reach:

- Albuquerque Metropolitan Arroyo Flood Control Authority (AMAFCA) Equations
- BUREC Equation
- Bray Equation
- Henderson Equation
- Schoklitsch Equation
- Meyer-Peter Muller Equation
- Shield's Diagram Method
- Lane's Tractive Force Method

AMAFCA Equation. The AMAFCA (1994) equation for the maximum equilibrium slope is based on the sediment transport characteristics of the reach.

$$S_L = \left(\frac{a}{q_s}\right)^{\frac{10}{3(c-b)}} q^{\frac{2(2b+3c)}{3(c-b)}} \left(\frac{n}{1.49}\right)$$

Where S_L = channel slope (ft./ft.)

q_s = unit sediment transport (cfs/ft)

q = water discharge (cfs)

n = Manning's roughness

a, b, c = power function coefficients from sediment transport function

A simplified version of the AMAFCA Equation is written for wide, rectangular channels, similar to the those in the study area, based on the assumptions that steep, wide, rectangular alluvial streams flow at or close to critical depth and that sediment supply is transport limited.[3]

$$S_s = 18.28\ n^2\ F^{0.133}\ F_r^{2.133}\ Q_{dd}^{-0.133}$$

Where S_s = Stable slope (ft/ft)

n = Manning's roughness value for the channel

[3] Transport limited means that the sediment inflow equals or exceeds the reach transport capacity.

F = Width/depth ratio of the channel

F_r = Froude number for the channel

Q_{dd} = Dominant discharge (cfs)

BUREC Equation. The BUREC published an equation for stable slope based on theoretical considerations of sediment transport (MacBroom, 1981).

$$S_L = (0.00021\ D_{50}\ W_{bf} / Q)^{0.75}$$

Where S_L = Stable slope (ft/ft)

D_{50} = Bed sediment diameter (ft)

W_{bf} = Channel width (ft)

Q = Discharge (cfs)

Bray Equation. Bray's (1979) equation for equilibrium slope is based on regime analysis of perennial gravel bed streams in Alberta, Canada.

$$S_L = 0.965\ Q_2^{-0.344}\ D_{50}^{0.58}$$

Where S_L = Equilibrium slope (ft/ft)

D_{50} = Mean bed sediment diameter (ft)

Q_2 = 2-year discharge (cfs)

Henderson Equation. To generate an equation for the slope of stable channels, Henderson (1961) modified the Lane (1952) equations using a threshold theory of shear stress concept.

$$S_L = 0.44\ D_{90}^{1.15}\ Q^{-0.46}$$

Where S_L = Stable slope (ft/ft)

D_{90} = Bed sediment diameter for which 90 percent is smaller (ft)

Q = Discharge (cfs)

The BUREC (Pemberton and Lara, 1984) published a manual for computing scour and channel degradation downstream of dams or other structures that interrupt the natural sediment supply to the downstream channel. The BUREC manual describes the following four approaches for estimating equilibrium slope: (1) Schoklitsch Equation, (2) Meyer-Peter Muller Equation, (3) Shield's Diagram Method, and (4) Lane's Tractive Force Method. The approaches are based on the assumption of zero sediment transport. Therefore, these results represent a minimum probable slope for the study reach, except in the reaches immediately downstream of Lake Pleasant and downstream of the heavily urbanized New River.

Schoklitsch Equation. The Schoklitsch (Shulits, 1935) equation is based on the concept of zero bedload transport.

$$S_L = K_s\ (D\ W_{bf}/Q)^{3/4}$$

Where S_L = Stable slope (ft/ft)

K_s = 0.00174

W_{bf} = Bankfull width (ft)

D = Mean bed sediment diameter (mm)

Q = Dominant discharge (cfs)

Meyer-Peter, Muller Equation. The Meyer-Peter, Muller (1948) equation is based on the incipient motion theory, or the point of initiation of sediment transport.

$$S_L = K_{mpm} (Q/Q_{bf}) (n_s/D_{90}^{1/6})^{3/2} D / d$$

Where S_L = Stable slope (ft/ft)

$K_{mpm} = 0.19$

Q/Q_{bf} = Ratio of total flow to flow over the channel

Q_{bf} = Dominant discharge (cfs)

n_s = Manning's n for the stream bed

D_{90} = Bed sediment diameter for which 90 percent is smaller (mm)

D = Mean sediment diameter (mm)

d = Channel depth (ft)

Shields Diagram Method. The Shields diagram (1936) for determining the boundary condition for no sediment transport can be used to define an equation for stable slope.

$$R_* = U_* D / \upsilon$$

$$U_* = (S_L R g)^{1/2}$$

$$T_* = \tau_c / ((\gamma_s - \gamma_w) D)$$

Where S_L = Stable slope (ft/ft)

R_* = Boundary Reynold's number

U_* = Shear velocity = $(S_L R g)^{\wedge 0.5}$

D = Mean sediment diameter (mm)

υ = Kinematic velocity of water (ft/sec^2)

R = Hydraulic radius for wide channels (ft)

g = Gravitational constant = 32.2 ft/sec^2

T_* = Dimensionless shear stress

τ_c = Critical shear stress (lb/ft^2)

γ_s = Specific weight of sediment (lb/ft^3)

γ_w = Specific weight of water (lb/ft^3)

Lane's Tractive Force Method. Lane's equation for stable slope uses critical tractive force relationships.

$$S_L = (\tau_c/\gamma_w) d$$

Where S_L = Stable slope (ft/ft)

d = Mean flow depth (ft)

τ_c = Critical shear stress (lb/ft^2)

γ_w = Specific weight of water (lb/ft^3)

Results. The results of the equilibrium slope analyses are shown in Table 6-27. The Schoklitsch, Meyer-Peter Muller, Shield's Diagram, and Lane's Tractive Force results represent minimum slopes and are associated with equilibrium slopes expected to form downstream of dams due primarily to the effects of clear-water discharges from the dam. These four equations were applied to Reaches 1 and 2 immediately downstream of the New Waddell Dam. Downstream of Reaches 1 and 2 the results for the AMAFCA, BUREC, Bray, and Henderson equations are considered applicable to expected stable slope estimates due to the availability of sediment sources from tributaries and channel bed and bank materials.

For both sets of equations, long-term degradation (or aggradation) can be predicted by comparing the equilibrium slope and existing channel slopes for a given reach. If the predicted equilibrium slope is less than the existing channel slope, long-term degradation should be expected. Conversely, if the predicted equilibrium slope is greater than the existing channel slope, long-term aggradation should be expected. Where long-term degradation occurs, lateral instability occurs by undercutting the channel banks. Where long-term aggradation occurs, lateral instability occurs due to braiding and avulsions. While the magnitude of long-term degradation or aggradation cannot be reliably predicted using the equilibrium slope equation, the strength of the trend in either direction probably can be gauged. The strongest trends are predicted where the difference between the average equilibrium slope and the existing channel slope is greatest.

In general, the equilibrium slope equations indicate that long-term degradation will occur in the study area in response to large floods, with deposition or no degradation occurring during the smaller floods. This prediction supports the conclusions of the bankfull discharge analysis, the armoring analysis, and scour calculations discussed below. It also is supported by field observations, historical data, and geomorphic interpretations. A greater degree of degradation is predicted when the 10- and 100-year peak discharges are used in the equilibrium slope equations than when the 2-year discharge is used. The difference in expected slope adjustment between large and small floods highlights the sensitivity of the Agua Fria River to the flood series. That is, if a series of small floods occur over time without a significant major flood, less channel change may occur than if a series of very large events occur. Finally, the four equilibrium slope equations that assume no sediment inflow almost always predict long-term scour, which serves as a warning that watershed development guidelines should address sediment supply issues to assure channel stability.

The following trends are indicated by the predicted equilibrium slope values for each reach of the Agua Fria River shown in Table 6-27:

Reaches 1 and 2: The equilibrium slope predicted by the clear-water slope equations indicates that the existing channel bed slope is about 1 to 2 times steeper than the predicted slopes. Therefore, the bed of the Agua Fria River in these reaches is expected to continue to flatten, i.e. degrade. However, as indicated in Chapter 2, much of these upper reaches is confined both vertically and horizontally by the presence of bedrock, especially in Reach 1 where bedrock is already exposed in the bed throughout much of the reach. Therefore, further vertical adjustment to the channel slope will be limited by resistant bed material.

Reach 3: Reach 3 is a very short reach which includes the CAP canal siphon crossing and the Beardsley Canal flume bridge. Although the stable slope equations predict aggradation within Reach 3, it is noted that the channel slope reported in Table 6-27 is anomalously low, probably due to channel modifications associated with recent repair of the CAP canal siphon. Therefore, a more realistic prediction of long-term future slope adjustment would be that made for the adjacent reaches: degradation during large floods and deposition or no change during small floods.

Reaches 4, 5, and 6: The existing bed slope for Reaches 4, 5, and 6 is slightly steeper than the predicted stable slope for the 100-year and 10-year floods. Conversely, the predicted stable slope for the 2-year flood is steeper than the existing bed slope. Therefore, these three reaches are expected to degrade during floods with higher discharges and aggrade or experience no change during smaller floods.

Reach 7, 8, and 9: Reaches 7, 8, and 9 also have existing bed slopes steeper than the predicted stable slope for the 100-year and 10-year floods. Therefore, degradation is also expected in these reaches for higher discharges. However, for the 2-year flood the predicted stable slope is very similar to the existing bed slope. Therefore, it is expected that no vertical adjustment of slope will occur in these reaches for the more frequent discharges.

Reach 10: The stable slope equations predict degradation for higher discharges and moderate degradation for the frequent floods. Therefore, based on the stable slope equations, Reach 10 is expected to degrade during large floods, with no dramatic vertical adjustments in slope during smaller floods.

Reaches 11, 12, 13, 14, and 15: The stable slope equations predict degradation for the entire range of discharges within these five lower reaches. Predicted slopes are about half the existing bed slopes in these reaches. However, at least within the channelized reaches, Reaches 12 and 13, existing grade control structures limit vertical adjustments in slope.

Table 6-27 Equilibrium Slope Analysis Results (Slope in ft/ft)

Reach	Return Period	Bed Slope	Schocklitsch	MPM	Shields	Lane	Average	Bray	Henderson	BUREC	AMAFCA	Average	Predicted Trend
1	100	0.0019	0.0002	0.0003	0.0001	0.0001	0.0002						Degradation
	10		0.0051	0.0005	0.0001	0.0001	0.0015						
	2		0.0039	0.0015	0.0003	0.0003	0.0015						
2	100	0.0033	0.0002	0.0003	0.0001	0.0001	0.0002						Degradation
	10		0.0005	0.0006	0.0002	0.0002	0.0004						
	2		0.0014	0.0012	0.0004	0.0005	0.0009						
3	100	0.0006						0.0062	0.0003	0.0002	0.0033	0.0025	Aggradation
	10							0.0062	0.0005	0.0005	0.0076	0.0037	
	2							0.0062	0.0014	0.0025	0.0046	0.0037	
4	100	0.0030						0.0059	0.0003	0.0003	0.0031	0.0024	High Flow Degradation Low Flow Aggradation
	10							0.0059	0.0005	0.0007	0.0031	0.0025	
	2							0.0059	0.0013	0.0035	0.0052	0.0039	
5	100	0.0033						0.0056	0.0003	0.0004	0.0030	0.0023	High Flow Degradation Low Flow Aggradation
	10							0.0056	0.0005	0.0008	0.0031	0.0025	
	2							0.0056	0.0012	0.0040	0.0040	0.0037	
6	100	0.0030						0.0055	0.0003	0.0003	0.0033	0.0024	High Flow Degradation Low Flow Aggradation
	10							0.0055	0.0005	0.0008	0.0033	0.0025	
	2							0.0055	0.0012	0.0036	0.0038	0.0035	
7	100	0.0030						0.0052	0.0003	0.0003	0.0026	0.0021	High Flow Degradation Stable at Low Flow
	10							0.0052	0.0004	0.0006	0.0028	0.0022	
	2							0.0052	0.0011	0.0025	0.0029	0.0029	
8	100	0.0028						0.0036	0.0002	0.0001	0.0032	0.0018	High Flow Degradation Stable at Low Flow
	10							0.0036	0.0003	0.0002	0.0044	0.0022	
	2							0.0036	0.0009	0.0014	0.0060	0.0030	
9	100	0.0029						0.0040	0.0002	0.0002	0.0025	0.0017	High Flow Degradation Stable at Low Flow
	10							0.0040	0.0003	0.0004	0.0027	0.0019	
	2							0.0040	0.0011	0.0027	0.0042	0.0030	
10	100	0.0022						0.0040	0.0002	0.0001	0.0022	0.0016	High Flow Degradation Low Flow Aggradation
	10							0.0040	0.0003	0.0003	0.0022	0.0017	
	2							0.0040	0.0010	0.0016	0.0035	0.0025	
11	100	0.0022						0.0013	0.00001	0.0001	0.0022	0.0009	Degradation
	10							0.0013	0.00001	0.0002	0.0026	0.0010	
	2							0.0013	0.00002	0.0004	0.0025	0.0011	
12	100	0.0019						0.0013	0.00001	0.0001	0.0018	0.0008	Degradation
	10							0.0013	0.00001	0.0001	0.0019	0.0008	
	2							0.0013	0.00002	0.0003	0.0021	0.0009	
13	100	0.0023						0.0013	0.00001	0.0001	0.0019	0.0008	Degradation
	10							0.0013	0.00002	0.0002	0.0022	0.0009	
	2							0.0013	0.00002	0.0003	0.0030	0.0012	
14	100	0.0018						0.0013	0.00001	0.0001	0.0023	0.0009	Degradation
	10							0.0013	0.00002	0.0002	0.0022	0.0009	
	2							0.0013	0.00002	0.0004	0.0021	0.0010	
15	100	0.0025						0.0015	0.00001	0.0001	0.0030	0.0011	Degradation
	10							0.0015	0.00002	0.0001	0.0033	0.0012	
	2							0.0015	0.00003	0.0002	0.0035	0.0013	

Summary. The scour and deposition caused by the channel's adjustment to its equilibrium slope will be limited to a reach length sufficient for the channel to regain a sediment transport balance. In general, long-term degradation is predicted downstream of New Waddell Dam, although limited by the presence of bedrock. The middle reaches can expect to experience little change in slope or some aggradation for the periods dominated by small floods, with long-term degradation more likely to occur during periods dominated by large floods. The lower reaches are expected to experience long-term degradation, regardless of discharges that occur in the future. However, the extent of vertical adjustment will be limited by existing grade control structures within the channelized reaches. The actual magnitude of the expected bed elevation changes will be based in part on the potential for armoring, sediment supply, and the magnitude and frequency of the flows experienced in the future. The results of the equilibrium slope analysis are consistent with the analyses summarized earlier in this chapter in that they indicate that minimal channel change will occur during the small floods, and that more significant erosion will occur during the large floods.

6.5.3 Armoring

When the channel sediment transport capacity exceeds the upstream sediment supply, the balance of the sediment load may be eroded from the channel bed, causing the channel to degrade. Because fine sediments can be transported at more frequent lower discharges and velocities than coarse sediments, which may require large floods to be moved, fine sediment tends to be preferentially removed from the channel bed. Selective removal of fine sediments causes channel bed material to become progressively coarser over time, as long as the upstream sediment supply is limited. If this process continues over a long period, it ultimately creates a surficial layer of coarse channel sediments, called an armor layer, that the stream is incapable of transporting (Yang, 1996).

Methodology. The BUREC (Pemberton and Lara, 1984) recommends the following methodologies for estimating the minimum sediment size and depth of scour required to form an armor layer for a given flow rate:

- Meyer-Peter, Muller Bedload Transport Function
- Competent Bottom Velocity
- Shields Diagram
- Yang Incipient Motion

Meyer-Peter, Muller Bedload Transport Function. The Meyer-Peter, Muller (1948) bedload sediment transport function for the beginning of transport of individual grain sizes can be used to estimate the non-transportable sediment size.

$$D_c = d\,S \,/\, (K_{mpm}\,(n/D_{90}^{(1/6)})^{3/2})$$

Where D_c = Non-transportable sediment diameter (mm)

d = Average flow depth (ft)

S = Energy slope (ft/ft)

$K_{mpm} = 0.19$

n = Manning's n for the stream bed

D_{90} = Particle size for which 90% of the bed material is finer (mm)

Competent Bottom Velocity. This methodology is based on the work of Mavis and Lushey (1948), who developed an equation for the beginning of sediment movement on a stream bed.

$$D_c = 1.88\ V_m^2$$

Where D_c = Armor size (mm)

V_m = Average channel velocity (ft/s)

Shields Diagram. The Shields (1936) diagram is a standard method used to define the initiation of motion for various channel bed sediment sizes. The method uses an iterative process to compute dimensionless shear stress (T_*) and the armor diagram from the Shields diagram.

$$T_* = \tau_c / ((\gamma_s - \gamma_w)\ D_c)$$

Where T_* = Dimensionless shear stress

D_c = Armor size (mm)

τ_c = Critical shear stress (lb/ft^2)

γ_s = Specific weight of water = 62.4 lb/ft^3

γ_w = Specific weight of sediment = 165 lb/ft^3

Note that for gravel sediment sizes and turbulence levels typical in natural streams:

T_* = 0.05 For sediment sizes greater than 1 mm and Boundary Reynold's Number (R_*) > 500

Yang Incipient Motion. Yang (1973) developed a relationship between dimensionless critical velocity (V_{cr}/w, where w = fall velocity, ft/s) and shear velocity Reynold's number R* at incipient motion. Under natural stream conditions for sediment sizes greater than 2 mm, Yang's equation can be written as follows:

$$D_c = 0.00659\ V_{cr}^2 \qquad \text{(For D > 2 mm)}$$

Where D_c = Armor size (ft)

V_{cr} = Critical average velocity at incipient motion (ft/s)

Depth to Armor Equation. Once the size of material (D_c) that will form an armor layer is estimated from one or more of the equations listed above, the depth of scour required to form a stable armor layer can be estimated from the sediment distribution of the channel bed material. The equation for the depth to armor is the following:

$$Y_d = y_a\ (1/\Delta p - 1)$$

Where Y_d = Depth from original streambed to the bottom of the armor layer (ft)

y_a = Thickness of the armor layer (ft)

Δp = Decimal percentage of the bed material larger than the armor size

Results. The results of the application of the BUREC methodologies to the study area are summarized in Table 6-28. Channel sediment size distribution data for the study reach shown in Figure 6-24 to Figure 6-26 were compared with the critical armoring sediment diameter. The "Armor Layer Likely" column in Table 6-28 was rated using engineering judgment and by comparing field observations in gravel pit exposures with the predicted depth of scour required to form an armor layer. Depth of geologically

recent alluvium within the gravel pits ranges from about 14 feet in the upper reach to about 8 feet in the Middle and Lower Reaches. If the computed depth to armor is excessive, and no evidence of armoring was observed in nearby reaches during the field work, it was assumed that formation of an armor layer was unlikely. Also, the "# N/A / Total #" column in Table 6-28 reflects the number of cross sections for which the critical diameter for formation of an armor layer was greater than 100 percent of the average sediment sizes within the reach. A comparison of the depth of scour required to form an armor layer with the computed general scour depths is presented in another section of this Chapter.

As shown in Table 6-28, the bed of the Agua Fria River will experience general scour during most significant floods. The results of the armoring analysis indicates that the bed material is large enough to form an armor layer in some reaches at the 10- and 2-year peak discharge rates in the Upper and Middle Reaches. However, in the Lower Reach the actual depth of scour and duration of flow during a 2-year flood is insufficient to cause an armor layer to fully develop. Field evidence suggests that the armor layers may form locally in cobble riffles in the Upper Reach. One consequence of the formation of armor locally is an increase of lateral erosion of the banks along these riffles as the flood water searches to satisfy additional sediment load prevented from entrainment by the local armor layer.

Table 6-28 Armoring Analysis Results

Reach	Methodology – Critical Armor Diameter (mm)				Average Critical Diam.	D50 (mm)	Armor Layer Likely?	Depth to Armor	# N/A /Total #
	MPM	CBV	Yang	Shield					
100-Year Flood									
1	34	101	108	104	87	2.2	No	9.0	11/26
2	25	76	81	56	59	2.2	No	17.9	9/26
3	34	108	116	75	83	2.2	No	2.2	4/5
4	24	70	75	53	56	2.2	No	12.6	13/34
5	23	68	73	41	51	2.2	No	18.8	8/30
6	22	60	64	55	50	2.2	No	12.9	8/32
7	23	71	76	52	56	2.2	No	25.8	8/25
8	32	111	119	76	84	1.1	No	25.8	27/41
9	20	61	65	46	48	1.1	No	28.5	5/24
10	25	91	97	65	70	1.1	No	14.6	14/43
11	10	61	65	41	44	0.5	No	N/A	21/21
12	15	107	114	43	70	0.5	No	N/A	55/55
13	13	88	94	37	58	0.5	No	N/A	37/37
14	11	70	75	49	51	0.5	No	34.1	24/32
15	15	94	101	66	69	0.5	No	39.5	12/14
10-Year Flood									
1	16	40	43	51	38	2.2	Yes	1.9	7/26
2	16	37	40	34	32	2.2	Yes	2.8	2/26
3	32	77	82	71	66	2.2	No	17.2	1/5
4	14	33	36	30	28	2.2	Yes	3.7	1/34
5	14	35	37	26	28	2.2	Yes	3.2	3/30
6	13	31	33	32	27	2.2	No	6.0	0/32
7	14	34	37	31	29	2.2	Yes	3.3	0/25
8	22	60	64	51	49	1.1	No	7.2	4/41
9	12	29	31	27	25	1.1	Yes	3.3	0/24
10	15	46	49	38	37	1.1	No	6.0	10/43
11	6	29	31	24	22	0.5	No	14.3	5/21
12	7	41	43	21	28	0.5	No	19.4	22/55
13	7	35	37	19	25	0.5	No	16.1	7/37
14	6	31	33	27	24	0.5	No	13.0	7/32
15	11	57	61	46	44	0.5	No	16.0	11/14
2-Year Flood									
1	6	10	10	18	11	2.2	Yes	0.5	1/26
2	9	16	17	21	16	2.2	Yes	2.0	1/26
3	8	14	15	17	13	2.2	Yes	0.7	0/5
4	8	14	15	18	14	2.2	Yes	2.2	1/34
5	8	15	16	16	14	2.2	Yes	0.6	1/30
6	7	13	14	18	13	2.2	Yes	1.4	0/32
7	7	13	14	15	12	2.2	Yes	0.5	0/25
8	11	22	23	26	21	1.1	Yes	1.8	1/41
9	9	18	19	20	16	1.1	Yes	2.0	1/24
10	6	10	11	14	10	1.1	Yes	2.0	0/43
11	4	17	18	16	13	0.5	No	8.0	1/21
12	4	18	20	12	13	0.5	No	7.9	3/55
13	8	28	30	23	22	0.5	No	4.5	5/37
14	4	16	17	16	13	0.5	No	6.7	3/32
15	7	34	36	31	27	0.5	No	16.2	5/14

MPM = Meyer-Peter, Muller CBV = Competent Bottom Velocity
Yang = Yang's Incipient Motion Shield = Shield's Method
N/A = no sediment is larger than the critical diameter

Conclusions. The following conclusions can be drawn from the armoring analysis results summarized in Table 6-28:

- The channel bed scour depth is probably limited by armoring in some reaches during frequent flows and small floods, but the average bed material is too small to prevent scour during large flood events.
- The channel bed material is mobile, and will be transported during moderate to large flood events. Cobble and boulder transport should be considered in the sediment routing analysis.
- The depth of the inactive layer of alluvium observed in the gravel pits is generally shallower than the depth required to form an armor layer for the 10- and 100-year events. Therefore, scour is probably limited by factors other than formation of an armor layer. One factor that prevents formation of an armor layer is the short duration of most floods.
- Sediments observed in the gravel pits were not significantly more coarse-grained than the material exposed on the surface. That is, effective armor layers were not observed in the field at gravel pits.
- The Agua Fria River historically has adjusted its geometry predominantly by horizontal adjustments of its highly braided channel. Vertical scour has been limited to about 8 to 14 feet based on field observations of exposures of channel alluvium in gravel pits.
- Sand and gravel mining and constrictions by bridges have caused lowering of the channel bed below the limits of scour historically experienced in the Agua Fria River.

6.5.4 Scour

Scour is defined as any lowering of the channel bed elevation that occurs as a result of flowing water. Scour can be caused by changes in the sediment transport capacity of a channel during the passage of a flood wave (general scour), by the formation of bed forms (dune, anti-dune, thalweg scour), by velocity currents around channel bends (bend scour), by local flow obstructions (local scour), or by gradual adjustments to changes in channel morphology (long-term scour). Scour is directly proportional to flow velocity, sediment size, and flow duration.

Methodology. General scour for the Agua Fria River was estimated using procedures outlined in the City of Tucson's *Standards Manual for Drainage Design and Floodplain Management - Chapter VI - Erosion and Sedimentation* (1989; hereafter, "the COT Manual"). Depth of scour in a stream is given in the COT Manual:

$$Z_t = 1.3\ (Z_{gs} + \tfrac{1}{2} Z_a + Z_{ls} + Z_{bs} + Z_{lft})$$

where:

Z_t = Design scour depth, excluding long-term degradation or aggradation (ft)

Z_{gs} = General scour depth (ft)

Z_a = Anti-dune trough depth (ft)

Z_{ls} = Local scour depth (ft)

Z_{bs} = Bend scour depth (ft)

Z_{lft} = Low-flow thalweg depth (ft)

1.3 = Safety factor to account for nonuniform flow distribution

General scour, Z_{gs}, is the component of scour that represents the mobile portion of the bed-material of the channel bottom. General scour was estimated using the following equation:

$$Z_{gs} = Y_{max} [(0.0685 V_m^{0.8})/(Y_h^{0.4} S_e^{0.3})-1]$$

where:

Z_{gs} = General scour depth (ft)

V_m = Average velocity of flow at design discharge (ft/sec)

Y_{max} = Maximum depth of flow at design discharge (ft)

Y_h = Hydraulic depth of flow at design discharge, (ft)

S_e = Energy slope (ft/ft)

Where Z_{gs} was determined to be negative, the general scour component was assumed to be zero.

Anti-dune trough depth, Za, is the component of scour caused by movement of dune shaped bed forms along the bottom of the channel. The anti-dune trough depth was estimated using the following equation:

$$Z_a = 0.0137 V^2_m$$

where:

V_m = Average velocity of flow at design discharge (ft/sec)

The anti-dune trough depth is limited to a maximum of ½ the flow depth. Anti-dunes have been observed on many sand bed streams in Arizona. Therefore, it was assumed that antidunes could form within the study reach.

Low-flow thalweg scour, Z_{lft}, occurs if a small channel forms to convey minor flows within the main channel of a stream. Typically, a low-flow thalweg forms on large streams with a high width to depth ratio and with mobile bed sediments. Differentiation of the low-flow channel thalweg as defined for the COT method from the current main channel of the Agua Fria River is subjective. For this analysis, the main channel was not considered equivalent to the low-flow thalweg. A low-flow thalweg component of scour was assumed to be equal to one foot for this scour analysis. Additional discussion of this point is included in the results to this section.

Bend scour, Z_{bs}, occurs on the outside of bends in a stream channel, and is caused by spiral transverse currents. Bend scour was estimated using the following equation:

$$Z_{bs} = 0.0685 Y_{max} V_m^{0.8} Y_h^{-0.4} S_e^{-0.3} \{2.1 [\sin^2(\alpha/2)/\cos \alpha]^{0.2} - 1\}$$

where:

Z_{bs} = Bend-scour component of total scour depth (ft), and

= 0 when $r_c/T > 10.0$, or $\alpha < 17.8°$

= computed value when $0.5 < r_c/T < 10.0$, or $17.8° < \alpha < 60°$

= computed value when $\alpha = 60°$ when $r_c/T < 0.5$, or $\alpha > 60°$

Y_{max} = Maximum depth of flow immediately upstream of the bend (ft)

V_m = Average velocity of flow immediately upstream of the bend (ft/sec)

Y_h = Hydraulic depth of flow immediately upstream of the bend (ft)

S_e = Energy slope immediately upstream of the bend (ft/ft)

α = Angle formed by the projection of the channel centerline from the point of curvature to a point which meets a line tangent to the outer bank of the channel (degrees)

r_c = radius of curvature along centerline of channel (ft)

T = channel topwidth (ft)

The reach-averaged bend angle was computed from the arccosine of the reciprocal of the sinuosity.

Local scour, Z_{ls}, occurs where there is an abrupt change in the direction of flow caused by obstructions such as bridge piers, abutments, or other structures. Local scour will occur at bridges. However, since local scour at these structures will be limited to the bridge section itself, the local scour component was not included in the estimate of total scour for the entire study reach. Local scour may also occur along the margin of the bank protection or levees where they exist.

Long-term scour, or aggradation and degradation, is best evaluated from historical evidence and field data. Historical evidence of long-term changes in channel bed elevation was discussed in Chapters 3 and 4 of this report. Depending on the time scale considered, long-term scour can be the largest component of scour. For example, if sufficient time is allowed for the channel to achieve its equilibrium slope or to become armored, the long-term scour component could more than double the scour estimate. A practical rule of thumb for determining a reasonable maximum long-term estimate for undisturbed watersheds is to use the height of the floodplain above the channel bottom or the bank height. For disturbed watersheds like that of the Agua Fria River, the long-term scour could exceed the terrace height.

Results. Scour estimates for the Agua Fria River were obtained from the City of Tucson scour equations are summarized in Table 6-29. In general, the largest component of scour other than long-term scour is either the antidune or bend scour. Given that the bend scour is limited to the outside of channel bends, the scour estimates listed in the first columns of Table 6-29 are conservative when applied to an entire reach. However, given the potential for future channel movement within the stream corridor, consideration of bend scour at any point within the reach is prudent for design of any structure with an extended design life. Antidune scour will be limited to areas where the bed sediments are fine enough for antidunes to form. Typically, antidune formation is limited to sand-bed channels. The Upper Reach is composed primarily of cobbles, gravels, and sands. Therefore, antidune formation will generally be limited to local reaches dominated by sands in the Upper Reach. Further downstream in the Middle and Lower Reaches, the channel bed is composed of a much greater proportion of sands. Therefore, antidune scour is most likely to occur in the Middle and Lower Reaches. In almost every reach within the study area, general scour was calculated as a negative value, which the COT Manual dictates should be interpreted as a zero depth of scour. Local scour was estimated as zero for the study, since reach-averaged values for a local condition could not be justified. Thalweg scour was estimated as only one foot because within the main channel a low flow thalweg was not observed during the field work, but may be justified as discussed in the COT Manual. Moreover, consideration of greater "thalweg scour" is also applicable to overbank areas when considering total scour depths. For those

purposes, the thalweg scour depth should be considered as the depth of the main channel adjacent to the overbank in question. Typically, the main channel depth is about 5 to 7 feet.

Scour estimates for the Agua Fria River are shown in Table 6-29. The total scour along the River is one to two feet for the 2-year event, two to four feet for the 10-year event, and three to six feet for the 100-year event. At these relatively small scour depths, formation of an armoring layer is unlikely.

Table 6-29 Scour Estimates (ft)

Reach	Total Zt	General Zgs	Antidune Za	Bend Angle	Bend Zbs	Local Zls	Thalweg Zlft
Q100							
1	3.6	-3.6	3.5	0	0.0	0.0	1.0
2	6.5	-1.3	2.8	34	2.6	0.0	1.0
3	3.4	-1.1	3.2	11	0.0	0.0	1.0
4	3.8	-1.2	2.4	22	0.7	0.0	1.0
5	2.5	-0.7	1.8	16	0.0	0.0	1.0
6	3.6	-1.7	2.3	22	0.6	0.0	1.0
7	5.1	-1.4	2.7	27	1.6	0.0	1.0
8	6.6	-1.5	3.8	28	2.2	0.0	1.0
9	5.4	-1.7	2.4	27	1.9	0.0	1.0
10	5.9	-2.2	3.1	27	1.9	0.0	1.0
11	4.3	-1.3	2.7	23	1.0	0.0	1.0
12	5.6	0.4	3.3	24	1.2	0.0	1.0
13	3.7	0.1	3.5	13	0.0	0.0	1.0
14	3.3	-1.3	3.0	11	0.0	0.0	1.0
15	3.4	-1.1	3.3	11	0.0	0.0	1.0
Q10							
1	2.2	-4.0	1.4	0	0.0	0.0	1.0
2	4.2	-1.3	1.4	34	1.5	0.0	1.0
3	2.3	-1.1	1.5	11	0.0	0.0	1.0
4	2.8	-1.1	1.4	22	0.4	0.0	1.0
5	2.0	-0.8	1.1	16	0.0	0.0	1.0
6	2.7	-1.5	1.2	22	0.4	0.0	1.0
7	3.7	-1.4	1.5	27	1.1	0.0	1.0
8	4.2	-1.4	2.1	28	1.2	0.0	1.0
9	3.8	-1.7	1.3	27	1.3	0.0	1.0
10	4.2	-1.8	1.9	27	1.2	0.0	1.0
11	2.9	-1.4	1.3	23	0.6	0.0	1.0
12	3.1	-0.2	1.6	24	0.6	0.0	1.0
13	2.3	-0.4	1.5	13	0.0	0.0	1.0
14	2.2	-1.2	1.4	11	0.0	0.0	1.0
15	2.7	-1.0	2.2	11	0.0	0.0	1.0
Q2							
1	1.5	-2.6	0.4	0	0.0	0.0	1.0
2	2.4	-0.9	0.5	34	0.6	0.0	1.0
3	1.6	-0.8	0.5	11	0.0	0.0	1.0
4	1.8	-0.7	0.5	22	0.1	0.0	1.0
5	1.7	-0.6	0.6	16	0.0	0.0	1.0
6	1.9	-1.1	0.5	22	0.2	0.0	1.0
7	2.4	-1.1	0.7	27	0.5	0.0	1.0
8	2.3	-1.0	0.6	28	0.4	0.0	1.0
9	2.3	-0.9	0.7	27	0.5	0.0	1.0
10	2.1	-1.1	0.5	27	0.4	0.0	1.0
11	2.4	-1.3	0.8	23	0.4	0.0	1.0
12	2.3	-0.4	0.8	24	0.4	0.0	1.0
13	1.7	-0.4	0.7	13	0.0	0.0	1.0
14	1.8	-0.9	0.8	11	0.0	0.0	1.0
15	2.2	-0.9	1.4	11	0.0	0.0	1.0
Note: Long-term and local scour not included in estimate of total scour.							

Long-Term Scour. The long-term scour component is the progressive scour that occurs over long time periods, rather than in response to a single flow event. Long-term scour was estimated from the following types of data:

- Field estimates of recent scour
- Interpretation of longitudinal profiles
- Interpretation of historical maps and photographs
- Interpretation of the ages of geomorphic surfaces
- Comparison of equilibrium and existing channel slopes

Field data were described in Chapters 2 and 3 of this report, and consisted of qualitative estimates of whether the channel had recently scoured or filled, and the depth of recent long-term scour. Longitudinal profiles were described in Chapters 4, and 5, and were used to estimate whether the bed elevation had moved up or down during the period of record. Geomorphic mapping of stream terraces was used to establish the net channel bed adjustments over the past 10,000 to 2,000,000 years. A summary of these data is shown in Table 6-30.

Predictions of the magnitude of long-term degradation or aggradation can also be made by comparing the predicted equilibrium slope with the existing channel slope. The slope difference multiplied by a stream reach length is the amount of adjustment in bed elevation at the upstream end of the reach. Reach lengths of 1,000 and 5,000 feet were used for the predictions shown in Table 6-30. Typically, long-term scour estimated using equilibrium slope is measured from the closest point of permanent grade control and would be applicable within Reaches 12 and 13 where grade control structures exist. However, elsewhere in the study area no permanent grade control is in place. Therefore, the estimates were based on reach lengths of 1,000 and 5,000 feet to illustrate the potential range of channel responses to long-term slope adjustment.

Table 6-30 Summary of Long-Term Degradation/Aggradation Data Sources

Reach	Field Assessment	Historic Profile Comparisons (ft/yr)	Geologic Mapping (ft/yr)	Equilibrium Slope Adjustment – Reach Length (ft)					
				Q100		Q10		Q2	
				1000 ft	5000 ft	1000 ft	5000 ft	1000 ft	5000 ft
1	Degradation	-0.71	-0.00001 to –0.0004	-1.7	-8.7	-0.4	-2.1	-0.4	-1.8
2	Degradation	-0.29		-3.1	-15.5	-2.9	-14.6	-2.4	-12.0
3	Degradation	-0.03		1.9	9.6	3.1	15.5	3.1	15.5
4	Degradation	-0.03		-0.6	-3.0	-0.5	-2.4	1.0	4.8
5	Degradation	-0.03		-1.0	-5.0	-0.8	-4.1	0.4	1.9
6	Degradation	-0.08		-0.6	-3.1	-0.5	-2.3	0.5	2.7
7	Degradation	-0.14		-0.9	-4.4	-0.7	-3.6	0.0	-0.1
8	Degradation	-0.11		-1.0	-4.8	-0.6	-3.0	0.2	1.1
9	Degradation	-0.08		-1.2	-5.9	-1.0	-5.2	0.1	0.4
10	Degradation	-0.12		-0.6	-3.1	-0.6	-2.8	0.3	1.4
11	Degradation	-0.09		-1.3	-6.7	-1.2	-6.0	-1.1	-5.7
12	Degradation	-0.09		-1.1	-5.6	-1.1	-5.3	-1.0	-4.9
13	Degradation	-0.09		-1.5	-7.5	-1.4	-7.0	-1.1	-5.6
14	Degradation	-0.07		-0.9	-4.6	-0.9	-4.5	-0.9	-4.4
15	Degradation	-0.01		-1.4	-6.8	-1.3	-6.3	-1.2	-5.9
Source of Data	Chapter 2 & 3	Chapter 4 & 5	Chapter 2 & 5	Values computed by the following equation: (equilibrium slope – existing channel slope) x reach length (ft.)					

Summary. General and long-term scour estimates for the streams in the study area indicate that long-term scour should be expected for the Agua Fria river, especially in the vicinity of gravel mines and bridge constrictions, while general scour will be limited. When scour occurs, it undermines the channel banks and increases the rate of lateral erosion. Therefore, the greatest amount of scour-induced bank erosion in the study area should be expected at channel bends, near obstructions, or where the channel has been excavated. Estimated bank erosion distances should be adjusted upward where bed scour is significant.

6.5.5 Comparison of Armoring, Scour, and Equilibrium Slope Predictions.
Channel degradation can be prevented by armoring of the channel bed, by achieving a non-scouring stable slope, or by physical barriers to scour such as bedrock or artificial grade control. A comparison of the armoring, scour and equilibrium slope estimates described in the previous sections of this chapter is provided in Table 6-31. The possible slope adjustment, or depth of long-term scour caused as the channel adjusts to stable slope, was estimated by multiplying the difference in the predicted (regime) and existing channel slopes by a specified reach length of 1,000 or 5,000 feet. The latter two distances were selected based on the reach lengths used for this study. The distances are intended to illustrate the order of magnitude of vertical change possible due to slope adjustments, rather than a specific prediction of long-term scour at any specific point in the study reach. Actually, long-term changes will depend on a variety of site-specific variables.

The "Armor v. Scour" and "Armor v. Slope" columns in Table 6-31 indicate whether total or long-term scour will be limited by armoring. That is, if the predicted depth of general scour (column 3 in Table 6-31) is less than the depth of scour required to form an armor layer, scour will not be limited by armoring at that flow rate. Similarly, if the difference between the predicted and existing channel slope is too small to cause long-term scour greater than the depth of scour required to form an armor layer, long-term scour will not be limited by armoring. A "no" code indicates that scour will not be limited by armoring. A "yes" code indicates that scour will be limited by an armor layer.

As shown in Table 6-31, armoring generally will not prevent long-term degradation (last column) on the Agua Fria River where it is predicted by the equilibrium slope analysis. Short-term or single event scour will be prevented by armoring in Reach 1, and upstream of Reach 3 during the 2- and 10-year events, and upstream of Reach 5 during the 100-year event. Bank stability will be most impacted by bed scour during the largest floods.

Table 6-31 Comparison of Armoring, Scour, and Equilibrium Slope Estimates

1	2	3	4		5		6	7
Reach	Depth to Armor (ft)	Scour Depth (ft)	Stable Slope		Slope Adjustments		Armor v. Scour	Armor v. Slope
			Regime	Actual	1000 ft.	5000 ft.		
Q100								
1	9.0	2.3	0.0002	0.0019	-1.7	-8.7	No	No
2	17.9	5.2	0.0002	0.0033	-3.1	-15.5	No	No
3	2.2	2.1	0.0025	0.0006	1.9	9.6	No	N/A
4	12.6	2.5	0.0024	0.0030	-0.6	-3.0	No	No
5	18.8	1.2	0.0023	0.0033	-1.0	-5.0	No	No
6	12.9	2.3	0.0024	0.0030	-0.6	-3.1	No	No
7	25.8	3.8	0.0021	0.0030	-0.9	-4.4	No	No
8	25.8	5.3	0.0018	0.0028	-1.0	-4.8	No	No
9	28.5	4.1	0.0017	0.0029	-1.2	-5.9	No	No
10	14.6	4.6	0.0016	0.0022	-0.6	-3.1	No	No
11	N/A	3.0	0.0009	0.0022	-1.3	-6.7	No	No
12	N/A	4.3	0.0008	0.0019	-1.1	-5.6	No	No
13	N/A	2.4	0.0008	0.0023	-1.5	-7.5	No	No
14	34.1	2.0	0.0009	0.0018	-0.9	-4.6	No	No
15	39.5	2.1	0.0011	0.0025	-1.4	-6.8	No	No
Q10								
1	1.9	0.9	0.0015	0.0019	-0.4	-2.1	No	Yes*
2	2.8	2.9	0.0004	0.0033	-2.9	-14.6	No	Yes
3	17.2	1.0	0.0037	0.0006	3.1	15.5	No	N/A
4	3.7	1.5	0.0025	0.0030	-0.5	-2.4	No	No
5	3.2	0.7	0.0025	0.0033	-0.8	-4.1	No	Yes*
6	6.0	1.4	0.0025	0.0030	-0.5	-2.3	No	No
7	3.3	2.4	0.0022	0.0030	-0.7	-3.6	No	Yes*
8	7.2	2.9	0.0022	0.0028	-0.6	-3.0	No	No
9	3.3	2.5	0.0019	0.0029	-1.0	-5.2	No	Yes*
10	6.0	2.9	0.0017	0.0022	-0.6	-2.8	No	No
11	14.3	1.6	0.0010	0.0022	-1.2	-6.0	No	No
12	19.4	1.8	0.0008	0.0019	-1.1	-5.3	No	No
13	16.1	1.0	0.0009	0.0023	-1.4	-7.0	No	No
14	13.0	0.9	0.0009	0.0018	-0.9	-4.5	No	No
15	16.0	1.4	0.0012	0.0025	-1.3	-6.3	No	No
Q2								
1	0.5	0.2	0.0015	0.0019	-0.4	-1.8	No	Yes
2	2.0	1.1	0.0009	0.0033	-2.4	-12.0	No	Yes
3	0.7	0.3	0.0037	0.0006	3.1	15.5	No	N/A
4	2.2	0.5	0.0039	0.0030	1.0	4.8	No	N/A
5	0.6	0.4	0.0037	0.0033	0.4	1.9	No	N/A
6	1.4	0.6	0.0035	0.0030	0.5	2.7	No	N/A
7	0.5	1.1	0.0029	0.0030	0.0	-0.1	Yes	Yes
8	1.8	1.0	0.0030	0.0028	0.2	1.1	No	N/A
9	2.0	1.0	0.0030	0.0029	0.1	0.4	No	N/A
10	2.0	0.8	0.0025	0.0022	0.3	1.4	No	N/A
11	8.0	1.1	0.0011	0.0022	-1.1	-5.7	No	No
12	7.9	1.0	0.0009	0.0019	-1.0	-4.9	No	No
13	4.5	0.4	0.0012	0.0023	-1.1	-5.6	No	Yes*
14	6.7	0.5	0.0010	0.0018	-0.9	-4.4	No	No
15	16.2	0.9	0.0013	0.0025	-1.2	-5.9	No	No

Notes: No = scour not limited by armoring
Yes = scour limited by formation of armor layer
Yes* = scour limited by formation of armor layer for long reaches but not shorter reaches
N/A = not applicable, aggradation is predicted (no long-term scour)
Armor v. Scour: compare column 3 to 1, i.e. will scour will be limited by armoring?
Armor v. Slope: compare column 5 to 1, i.e. will long-term scour be limited by armoring?

Conclusion. The engineering analyses described in the preceding sections predict mixed trends of aggradation and degradation for the Agua Fria River with degradation predominating for larger floods and aggradation or no change predicted in most reaches for the smaller floods. These mixed trends indicate that the streams are subject to erosive conditions during floods, and will experience scour and slope adjustments best depicted by the type of erosion and deposition documented in the recent historical record.

6.5.6 HEC-6 Modeling

HEC-6 models of the study area were prepared by Kimley-Horn & Associates (KHA) as part of the scope of services for the Agua Fria Watercourse Master Plan. The HEC-6 modeling effort is described in a separate report (KHA, 2001), but is summarized here.

Overview of HEC-6 Modeling. HEC-6 was designed to simulate long-term trends of scour and/or deposition in a stream channel that result from changing the natural hydrology, channel geometry, or sediment supply. The U.S. Army Corps of Engineers describes the HEC-6 computer program as follows:

> *HEC-6 is a one-dimensional movable boundary open channel flow numerical model designed to simulate and predict changes in river profiles resulting from scour and deposition over moderate time periods. Continuous flow records may be partitioned into a series of steady flows of variable discharge and duration. For each flow, a water surface profile is calculated providing hydraulic data at each cross section. These hydraulic data, combined with the discharge and flow duration information, allow volumetric accounting of sediment within stream reaches. The amount of scour or deposition at each section may then be computed and the cross section bed elevation adjusted accordingly. Hydraulic data associated with the next discharge are then computed using the updated geometry, and the channel geometry is again updated. This process is repeated through the entire duration of flows. (paraphrased, p. 1, USACOE, 1993)*

HEC-6 Model Assumptions and Limitations. The HEC-6 computer model is based on the following explicit or implied assumptions:

- One Dimensional. Flow in the stream is one dimensional, i.e., the model does not account for secondary currents from meandering, eddying, or turbulence that cannot be addressed through the use of energy loss coefficients. Gradually-varied flow conditions usually are modeled adequately using a one-dimensional model (p. 5, USACOE, 1993).
- Steady Discharge. The HEC-6 model simulates passage of a flood or annual hydrograph (unsteady flow) as a series of discrete steady flows of known duration. HEC-6 is best suited to simulating channel changes from hydrographs that rise and fall gradually over a relatively long duration (p. 7, USACOE, 1993).
- Uniform Scour or Deposition. Any change in bed elevation resulting from scour or deposition is applied uniformly across the entire moveable portion of channel. That is, a uniform depth of sediment is added to, or subtracted from, each station (GR) point used to describe the geometry of the active channel. The formation of point or lateral bars, bend scour holes, and local scour are not simulated (p. 17, USACOE, 1993).
- Sediment Continuity. HEC-6 computes changes in bed elevation based on the principal of conservation of sediment volume, which can be summarized in the following equations:

  $\text{Sediment}_{(in)} - \text{Sediment}_{(out)} = \text{Change in Sediment Volume}$

  $\text{Change in Bed Elevation} = \text{Change in Sediment Volume} \div \text{Reach Length}$
- Initial Conditions. The initial concentration of suspended bed material is assumed to be negligible. That is, all bed material is contained in the sediment reservoir at the start of the

computational interval and is returned to the sediment reservoir at the end of the interval (p. 16, USACOE, 1993)

- Time Scale. HEC-6 was developed "to predict changes in river profiles from scour and/or deposition over moderate time periods (typically years, although applications to single flood events are possible)." HEC-6 performs best for gradually changing hydraulic conditions, e.g. for large rivers with slow rising and falling hydrographs (p. 5, USACOE, 1993).
- Sediment Sources. The model assumes that there are only two sediment sources - inflowing water and the movable portion of the stream bed. HEC-6 does not consider lateral channel (bank) erosion - no sediment is supplied from the banks (p. 17, USACOE, 1993).
- Sediment Calculations. Several transport functions are coded into HEC-6, all of which apply the transport function by grain size (p. 41, USACOE, 1993).
- Equilibrium. The HEC-6 sediment transport function algorithms assume that sediment equilibrium conditions are reached during each time step of a single event, a condition which probably is not met for very short events. If equilibrium conditions are probably not established, then the modeling results should be interpreted in a qualitative manner (p. 5, USACOE, 1993).
- Time Step. Reach hydraulics and sediment transport potential are based on the channel geometry at the beginning of the time step. Therefore, the time step must be short enough that the computed change in bed elevation during a time step does not result in significant change in channel and reach geometry. Generally, a change in bed elevation of 1 foot, or 10 percent, of the flow depth is considered significant. In addition, the time step must be long enough that the flow would have sufficient time to travel through the longest stream segment[4] (p. 58, USACOE, 1993).

Table 6-32 lists these assumptions and indicates which assumptions may or may not be applicable to the study area. Given the assumptions and conditions that are not (or are marginally) valid for the study area, the HEC-6 modeling results are best suited to predicting relative trends of expected changes in the channel profiles, rather than calculating precise depths of channel scour and deposition at specific cross sections.

Table 6-32 HEC-6 Modeling Assumptions and Limitations

Assumption/Limitation	Assumption Valid for Study Reach?
One Dimensional	No. RAS results suggest not gradually varied
Uniform Scour or Deposition	No. Braided system with bars and swales
No Bank Erosion	No. Banks unstable in design flood
Steady Flow Condition Modeled	No. Flash flood hydrograph
Sediment Continuity	Yes.
Initial Conditions for Suspended Sediment	Yes. Ephemeral stream
Time Scale of Hydrograph	No. Flash flood conditions
Sediment Sources	Yes. Bed is primary source of sediment No. Banks supply significant sediment
Sediment Calculations	Yes.
Equilibrium Achieved in Time Step	No. Short duration hydrograph
Time Step Length Adequate	Yes. Adequate travel time No. Scour > 1 ft. indicated

[4] Stream segment as defined for HEC-6 is a reach with uniform discharge, no tributaries, or special conditions.

Given the conditions summarized in Table 6-32 above, the HEC-6 modeling results for the Agua Fria River are best interpreted in a qualitative manner. That is, the HEC-6 results may indicate broad trends that may occur in response to a design hydrograph, but probably do not represent accurate predictions of actual long-term or single-event channel change.

Application of HEC-6 Results to Lateral Stability. The HEC-6 model does not explicitly consider bank erosion. However, because HEC-6 is a sediment continuity model it computes a sediment deficit or surplus within each stream segment. The computed sediment deficit can be applied to the banks to estimate possible lateral erosion potential that might occur if the entire sediment deficit were satisfied solely by erosion of the channel bank.

Methodology. The sediment deficit predicted by the HEC-6 models was integrated over the reach lengths to estimate the amount of bank erosion required to satisfy the computed sediment deficit. The data required for this computation are shown in Table 6-33. Bank height was estimated from HEC-RAS bank stations, the minimum elevation in HEC-RAS cross sections, field data, and the data used in the bankfull discharge evaluation described elsewhere in this chapter. Because of the unrealistically high variability of net degradation and aggradation between adjacent cross sections predicted by the HEC-6 model, reach-averaged values for bank height, reach length, and sediment deficit were used. A value for the sediment deficit for each cross section was obtained by inserting a $VOL record[5] into the input code of the existing conditions HEC-6 model prepared by KHA. Where a sediment surplus was computed by the HEC-6 model for a given cross section, the data for that section were not used in computing the reach-average deficit. Note that this sediment deficit averaging procedure ignores the potential for lateral migration caused by braiding typically associated with long-term aggradation (sediment surplus). The resulting sediment deficit was applied to the left and right banks individually as if none of the deficit were satisfied from the opposite bank.

Because only a single hydrograph was evaluated in the KHA HEC-6 model, no long-term predictions of bank erosion could be made from the HEC-6 results similar to those made for other watercourse master plan lateral stability studies (JEF, 2000; JEF, 2001). However, the KHA model did include modeling of a 30-day constant discharge of 9,000 cfs that may provide some analogy to expected channel behavior and processes over a longer time frame than a single large event.

Results. The results of the HEC-6 based bank erosion estimates are shown in Table 6-33. In general, the HEC-6 results indicate that significant bank erosion can be expected throughout most of the study reach during a 100-year flood, although the results also depict some of the difficulties of applying the HEC-6 model to the Agua Fria River. Despite such difficulties, the HEC-6 results reasonably simulated the bank erosion distances observed in the study reach during the field visits and recorded by comparison of historical aerial photographs. Therefore, the HEC-6 results can be used as one method to estimate expected lateral erosion, but probably represent no better than order-of-magnitude estimates. HEC-6 modeling results are also discussed in technical report prepared by KHA for the Agua Fria River Watercourse Master Plan.

[5] See USACOE (1993) for complete explanation of the $VOL record. The $VOL record controls the level and type of output from the HEC-6 model.

Table 6-33 HEC-6 Sediment Deficit Translation to Bank Erosion Distance Estimates (ft)

HEC-6 Sediment Deficit Translation to Bank Erosion Distance Estimates (ft)						
	Average Bank Height		Average Channel Reach Length (ft)	Average HEC6 Deficit	Erosion Distance (ft) Deficit Applied to Bank (ft)	
					Left Bank	Right Bank
Reach	Left (ft)	Right (ft)		Q100 TOTAL yd^3	Q100 Total	Q100 Total
Upper	10	11	1699	-3,474	-57	-53
Middle	16	14	1620	-10,144	-30	-31
Lower	13	15	1066	-14,962	-91	-49
1	10	12	1253	-5,005	-67	-50
2	17	14	1810	-37,334	-44	-56
3	11	14	1324	-3,155	-39	-29
4	8	8	1821	-38,376	-88	-87
5	6	10	1766	23,449	-127	-113
6	9	9	1922	33,003	-6	-7
7	12	15	1833	-1,243	-11	-11
8	22	17	1709	-1,067	-29	-29
9	16	13	2069	-87,684	-82	-88
10	11	12	1337	17,962	-7	-6
11	13	12	1253	-2,763	-18	-22
12	15	16	851	1,978	-19	-18
13	17	18	691	17,587	-34	-32
14	8	14	1525	-34,191	-118	-67
15	4	10	1595	-123,241	-502	-192

Other conclusions drawn from the existing condition HEC-6 model included the following:

- Sediment concentration. The peak sediment concentration of 0.55 percent computed by the HEC-6 model occurs during the peak discharge of 54,000 cfs used in the discretized existing condition hydrograph. The average computed sediment concentration during the peak discharge was 0.2 percent. The average sediment concentration during the constant discharge of 9,000 cfs portion of the design hydrograph averaged about 0.1 percent. Assuming that bedload (computed by HEC-6) is approximately 10 percent of the total load, the total implied sediment concentrations that could be derived from the HEC-6 results range from about 2 to 6 percent at the peak flow rate. Measured sediment concentrations from arid region streams typically average between 5 and 20 percent. Therefore, bank erosion distances estimated from HEC-6 results may not be conservative if higher transport capacities than those computed by the HEC-6 models can be expected.
- Peak discharge – flow duration relationship. Bed elevation changes computed at each cross section for the time increments used in the HEC-6 model are shown in Figure 6-52. These data clearly show that sediment will be transported during the long-duration constant discharge (Day 1 to Day 30). Despite higher transport rates and sediment concentrations during the 24-hour, 100-year hydrograph, much larger sediment volumes are transported during the longer duration moderate discharge. Therefore, predictions of lateral erosion (or other channel changes) should account not only for maximum expected flow rates, but also should evaluate the effects of smaller, longer duration flows. During the largest discharges that inundate large portions of the floodplain, avulsive channel changes that are not associated with sediment continuity will cause the most channel movement. During long

duration flows that do not exceed bankfull conditions, bank erosion distances like those shown in Table 6-33 should be expected.

- Bed elevations changes. At most cross sections in the study reach, less than two feet of change in the bed elevation is predicted. Observed long-term bed elevation changes and computed scour depths exceed two feet, indicating that the HEC-6 results may not be conservative with respect to predictions of sediment movement.

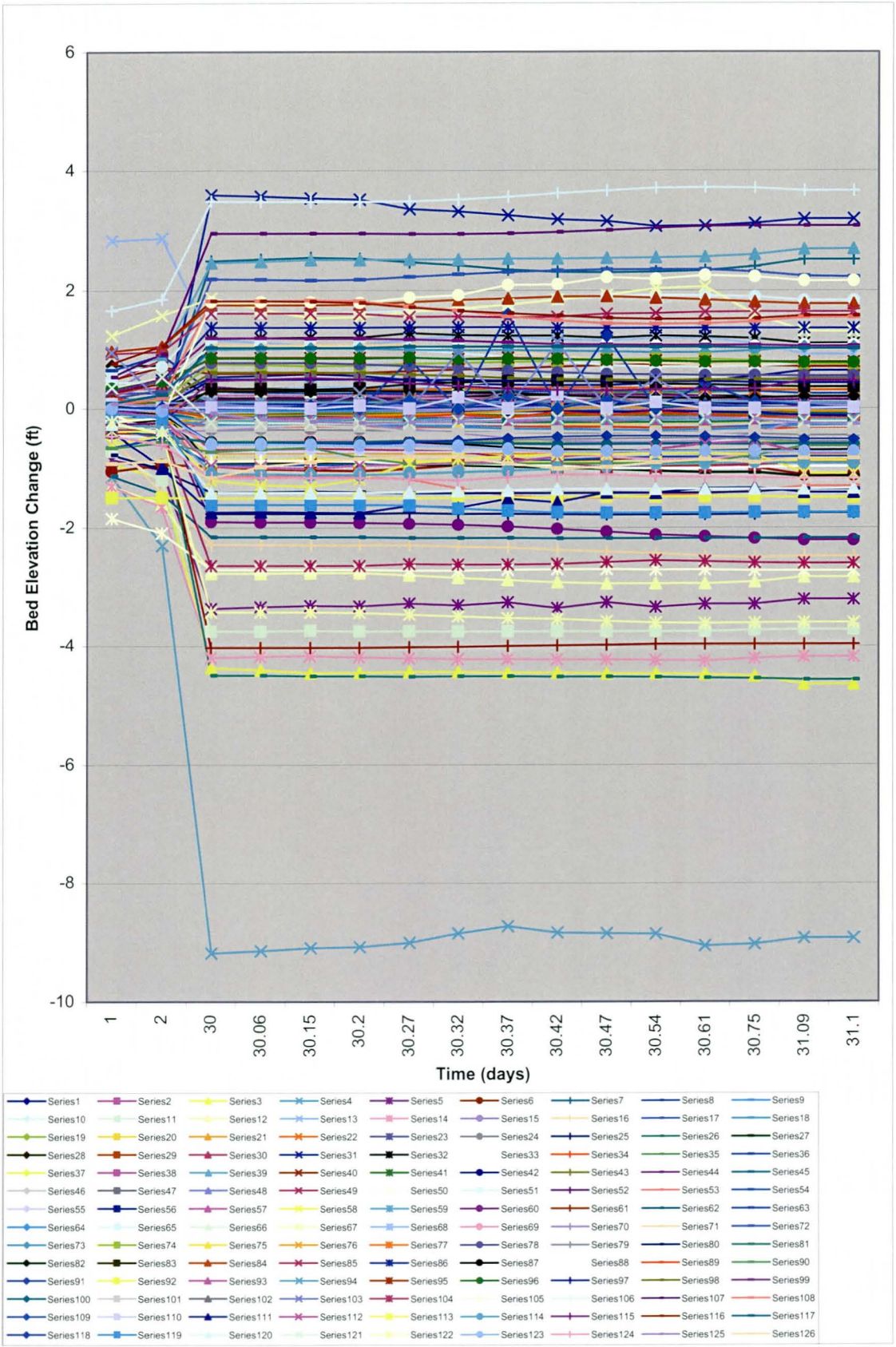

Figure 6-52 Cumulative Bed Elevation Change by Time Period in KHA Existing Conditions HEC6 Model

6.5.7 Lane relation

Lane (1955) developed the following equation that expresses the delicate balance and adjustment between several key geomorphic variables:

$$Q_s d \propto Q S;$$

Where Q_s = sediment discharge

d = sediment size

Q = water discharge

S = slope

Lane's equation implies that a change in one variable requires a change in one or more of the other variables to maintain stability, and provides a means to evaluate the effects of historical changes in watershed and channel conditions, and to estimate future river responses to change.

For the study area, watershed conditions have been significantly altered in the past 100 years, by the construction of first the Waddell Dam in 1927, and then the construction of New Waddell Dam in 1992. To balance the Lane equation, sediment quantities and size need to be balanced with the water discharge and channel slope. In the case of the Agua Fria River, both sediment and water discharges have been dramatically reduced by the construction of the Waddell and New Waddell Dams. Reduction of variables on both sides of the Lane relation suggest it might be possible for sediment size and channel slope to require little adjustment to maintain the balance of the system. However, some responses to slope downstream of the dam have been observed and are seen in the comparison of historical topography (Chapter 5).

Additionally, the dams are not the only things that have created changes in the variables in Lane's relation in the Agua Fria River watershed. Channelization of the river downstream of the New River confluence, diversion of additional drainage area into the Agua Fria River by the Arizona Canal Diversion Channel (ACDC), construction of dams on the New River, Skunk Creek, and Cave Creek, construction of McMicken Dam on Trilby Wash, urbanization throughout much of the watershed downstream of Reach 5, extensive sand and gravel mining, encroachment by numerous bridges, and encroachment by developments such as Coyote Lakes have caused additional alterations to the balance of variables in Lane's relation.

Channelization sets the river's width and lateral position within fixed limits. Also, in the case of the Agua Fria River, channelization in Reaches 12 and 13 have fixed the spatial extent of vertical adjustments in the channel slope by placement of grade control structures throughout the channelized reach.

Diversion of additional drainage area and the construction of dams in the New River watershed have brought more frequent and prolonged low discharges to the Lower Reach. Lane's relation suggests that the channel slope would need to decrease to adjust to the new condition or that sediment supply or sediment size would need to increase. Sediment supply has been generally reduced in the New River watershed by the combination of the construction of the dams and widespread urbanization. Field observations of the Agua Fria near its confluence with the New River show an area of channel bed armored by small cobbles. Therefore, the increase in flow was accommodated by an increase in sediment size which also fixed the channel slope (at least for lower discharges).

Urbanization reduces sediment supply and generally increases the frequency and magnitude of runoff in a watershed. However, in Maricopa County, development permitted since about 1986 should have had retention systems constructed to hold the 100-year, 2-hour storm runoff. In this area, that amounts to about 2.6 inches of rainfall. Therefore, runoff may actually decrease in frequency and magnitude with increasing urbanization. Such a reduction in sediment and

water discharges in the lower Agua Fria River watershed could lead to further reductions in sediment size and/or channel slope in the Agua Fria River.

Encroachments on the river channel tend to decrease widths and, therefore, increase flow depths and velocities. Increased velocity results in an increased energy slope. Lane's relation suggests increases in sediment supply and size to adjust to increases in slope. Again, simultaneous changes to sediment and water discharges complicate the anticipated adjustments expected in the Agua Fria River.

Finally, sand and gravel mining results in a decrease in sediment supply in the river. Lane's relation suggests a need for the channel to adjust its slope to a lower slope in response to removal of material from the river. While the long-term response may be a shallower gradient for the river bed, the short-term condition will be locally greater slopes upstream of the mines as the bed of the river is lowered as sediments are removed from the river.

Lane's relation highlights the complex nature and interconnected response of an alluvial system to changes in its sediment and water supplies. Many of the changes in the Agua Fria River watershed suggest that the future Agua Fria River will have smaller sediment sizes and/or a shallower channel slope than it had in the past. These adjustments should be anticipated in determination of flood control alternatives and flood and erosion hazards on the lower Agua Fria River.

6.6 Summary

The mathematical data examined for evaluation of erosion hazards on the Agua Fria River facilitate quantitative assessment of the lateral and vertical extents of erosion hazards in the study area. Horizontal limits of erosion hazards will remain within the historical limits of erosion expressed by the Pleistocene terraces along the study reach. Geologic limits to vertical erosion have been exceeded by changes to the system imposed by human activity. In particular, lowering of the channel bed elevation by sand and gravel mining along with reductions in upstream and watershed sediment supplies by dams and urbanization have caused the river to degrade its bed below levels experienced in thousands of years. The equilibrium approach analyses indicate that the study reach is not in equilibrium. The results suggest that the Agua Fria River is adjusting to a new equilibrium form and will continue to adjust to changes in the hydrologic and sedimentological inputs to its system. The future Agua Fria River channel is expected to be narrower, deeper, and have a lower elevation and shallower gradient than it has in the past. Finally, the analyses show that most of the future lateral and vertical erosion will occur during the largest floods, and that periods dominated by small floods may not experience any substantial changes in river morphology. These trends in adjustments are explored further in Chapter 7.

7. TREND ANALYSIS

The hydrology and sediment supply of the Agua Fria River have changed dramatically since completion of Waddell Dam in 1927. Closure of the much larger New Waddell Dam in 1992 further impacted the watershed hydrology and sediment supply of the river. This chapter compares predictions of the expected and observed channel response, hydrology and geomorphology of the Agua Fria River for the following conditions and time periods:

- Pre-Waddell Dam (before 1927)
- Post-Waddell Dam (1927-1992)
- Post-New Waddell Dam (1992- present).

The trends in channel response identified for each time period and watershed condition affect the delineation of the erosion hazard zones described in Chapter 8.

7.1 Pre-Waddell Dam (before 1927)

For the pre-Waddell Dam condition,[1] estimates of the 2- and 10-year hydrographs were interpreted from data presented in reports prepared by the Corps of Engineers (1982, 1988, 1995) as part of their analysis of the New Waddell Dam design. The Corps of Engineers' estimates of the 2- and 10-year peak discharges are unrealistically high, and are nearly equal in magnitude to comparable return period floods on the Salt River, a very different and larger river system. Therefore, for the pre-Waddell Dam condition, the 2- and 10-year peak discharges were adjusted by translating the discharge per unit area ratio computed for peaks at the Agua Fria near Rock Springs USGS stream gage[2] to the drainage area at the Waddell Dam site. Peak discharges from the Rock Springs gage were evaluated by JEF staff using WRC Bulletin 17B procedures[3] (USWRC, 1981) and annual flow data from 1970 to 2000 (N=31). For locations downstream of the dam site, the attenuation effect described in the Corps of Engineers' analyses was applied. The adjusted discharges for the pre-dam condition are presented in Table 7-1, and are contrasted with the discharge-frequency data presented in Chapter 2. The adjusted data were used for the trend analysis presented in this Chapter.

Mean annual discharge at Agua Fria River near Rock Springs USGS gage was also used to estimate the mean annual discharge for pre-Waddell Dam conditions in the study reach. While there may be some differences between average flow conditions at the Rock Springs gage and the watercourse master plan study reach, data from the Rock Springs gage are certainly more representative of the pre-Waddell Dam conditions than data from the gages within the study reach whose records are biased by the presence of the dam and post-1927 urbanization of the watershed (e.g. Agua Fria River at Avondale). The mean annual discharge for the Agua Fria River near Rock Springs for the period 1970-1999 is 91.2 cfs (Tadayon and others, 2000).

The pre-Waddell Dam discharges were entered in the modified HEC-RAS model described in Chapter 6 to generate hydraulic data for the study reach for comparison with the other two time periods and conditions.

---

[1] It is noted that other diversions existed in, or upstream of the study reach prior to 1927 that would have depleted low flows or at least modified the natural input of water and sediment. The conditions modeled attempt to simulate a no-diversion, natural condition in the study reach.

[2] The Rock Springs gage is located upstream of Lake Pleasant and the Watercourse Master Plan study reach.

[3] Computations made using the HECWRC.EXE software.

Table 7-1 Revised Pre-Waddell Discharges

	U.S. Army Corps of Engineers						Trend Analysis (JEF, 2001)						
RM (miles)	100-year (cfs)	50-year (cfs)	25-year (cfs)	10-year (cfs)	5-year (cfs)	2-year (cfs)	100-year (cfs)	50-year (cfs)	25-year (cfs)	10-year (cfs)	5-year (cfs)	2-year (cfs)	Drainage Area (sq. mi.)
33.82	135000	110000	90000	62000	43000	20000	135000	110000	90000	51900	27600	8640	1459
33.46	133160	109400	89300	61200	42400	19700	133160	109400	89300	51200	27200	8500	
31.39	131370	105700	85200	60300	41800	19500	131370	105700	85200	50500	26900	8400	
29.47	130000	102400	81400	59700	41400	19300	130000	102400	81400	50000	26600	8300	
27.86	128770	99600	78200	59100	41000	19100	128770	99600	78200	49500	26300	8200	
26.47	127440	97100	75500	58500	40600	18900	127440	97100	75500	49000	26100	8200	
25.192	124990	94900	72900	57400	39800	18500	124990	94900	72900	48100	25600	8000	
24.353	123000	93400	71300	56500	39200	18200	123000	93400	71300	47300	25100	7900	
23.504	121000	91900	69600	55600	38500	17900	121000	91900	69600	46500	24700	7700	
22.558	118940	90300	67700	54600	37900	17600	118940	90300	67700	45700	24300	7600	
20.675	115000	87000	64000	52800	36600	17000	115000	87000	64000	44200	23500	7400	1840
17.548	108120	81800	60200	49700	34400	16000	108120	81800	60200	41600	22100	6900	
16.385	109000	82000	59000	50100	34700	16100	109000	82000	59000	41900	22300	7000	
9.79	90000	66000	45000	41300	28700	13300	90000	66000	45000	34600	18400	5800	1900
9.696	95000	69700	47500	43600	30300	14100	95000	69700	47500	36500	19400	6100	2243
5.305	91000	66800	45500	41800	29000	13500	91000	66800	45500	35000	18600	5800	
3.77	90000	66000	45000	41300	28700	13300	90000	66000	45000	34600	18400	5800	2312
0.16	90000	66000	45000	41300	28700	13300	90000	66000	45000	34600	18400	5800	2388

	COE, 1995, Table 1.
	Jerry Jones, 1989, Agua Fria FIS.
	Ratio of QT/Q100 at RM 33.82 and at RM 20.675 for RM 17.548 50- and 25-yr
	Computed as proportional to increases and decreases for Q100 at same RM for 50-yr and 25-yr
	From COE, 1988, Plate 4
	Based on unit Q for Agua Fria Rock Springs frequency analysis by JEF for this study.

Ratios	1.00	0.81	0.67	0.46	0.32	0.15	1.00	0.81	0.67	0.38	0.20	0.06	@RM33.82
	1.00	0.76	0.56				1.00	0.76	0.56				@RM20.675

7.2 Post-Waddell Dam (1927-1992)

Discharge-frequency data for the post-Waddell Dam condition were taken directly from reports prepared by the Corps of Engineers (1995). The modified HEC-RAS model described in Chapter 6 was rerun using these discharges to generate hydraulic data used for comparison with the other two time periods and conditions.

7.3 Post-New Waddell Dam (1992-present)

Hydraulic data developed from the existing conditions HEC-RAS analysis presented in Chapters 2 to 6 of this report were used to represent channel conditions for the post-New Waddell time period. The results reported in previous chapters are included in this chapter for comparison with the pre-Waddell Dam and post-Waddell Dam conditions.

7.4 Results

Reach-average hydraulic data were obtained by entering the estimated peak discharges for the 2-, 10-, and 100-year events in the modified HEC-RAS model described in Chapter 6. The data shown in the figures in the following sections were averaged from all cross sections in each reach except those at bridges or in channelized areas. Therefore, no data are presented for Reaches 12 and 13, since those reaches are completely channelized. The pre-Waddell Dam and post-Waddell Dam conditions are identical for the 100-year flood because, according to the Corps of Engineers (1995), Waddell Dam did not affect the 100-year peak discharge. Similarly, the 2-year discharge results are identical for the post-Waddell and post-New Waddell Dam conditions, because the Corps of Engineers (1995) reports that the downstream watershed controls the peak flow rates for these more frequent recurrence intervals. The data for the 10-year flood is different for each time period and condition. The following types of hydraulic data are reported:

- Channel Velocity
- Right and Left Overbank Velocity
- Topwidth
- Maximum Flow Depth

In addition, the hydraulic data for each time period and condition were used to estimate the expected equilibrium slope, the expected channel pattern, and the regime width, depth, and velocity.

7.4.1 Comparison of Reach-Averaged Velocity

Figure 7-1 to Figure 7-9 show comparisons of reach-average velocity for the main channel, right overbank, and left overbank for the pre-Waddell, post-Old Waddell, and post-New Waddell Dam 100-year, 10-year, and 2-year flood conditions, respectively.

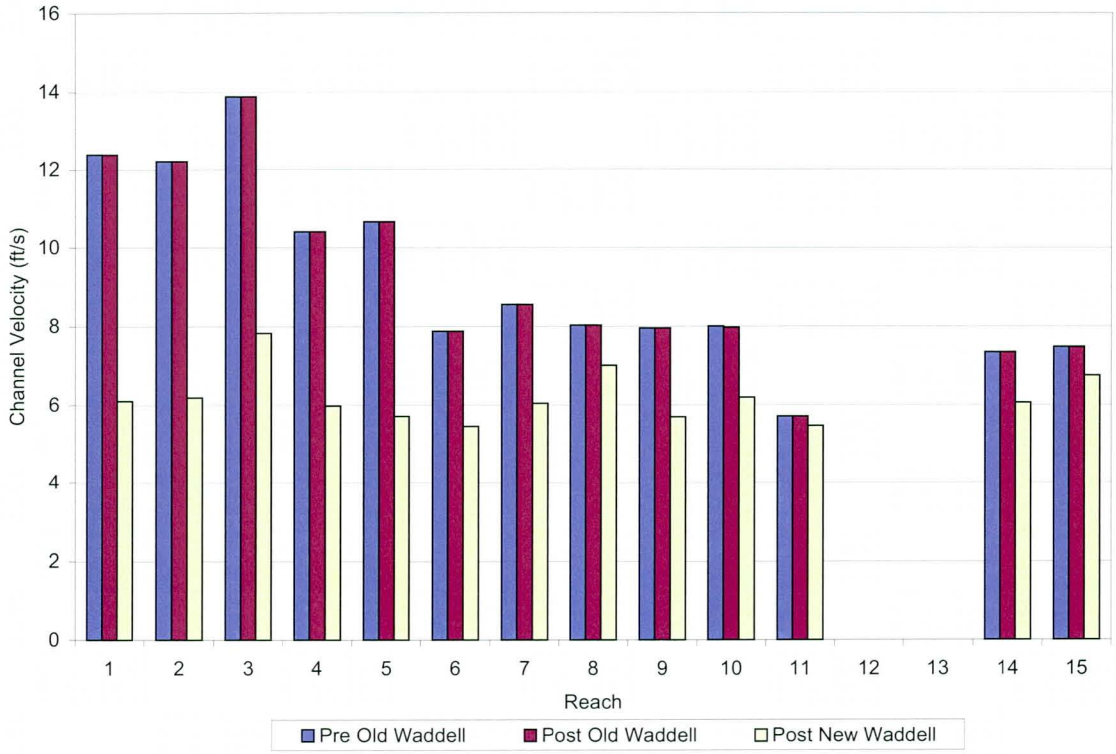

Figure 7-1 Comparison of reach-averaged channel velocities, 100-year flood

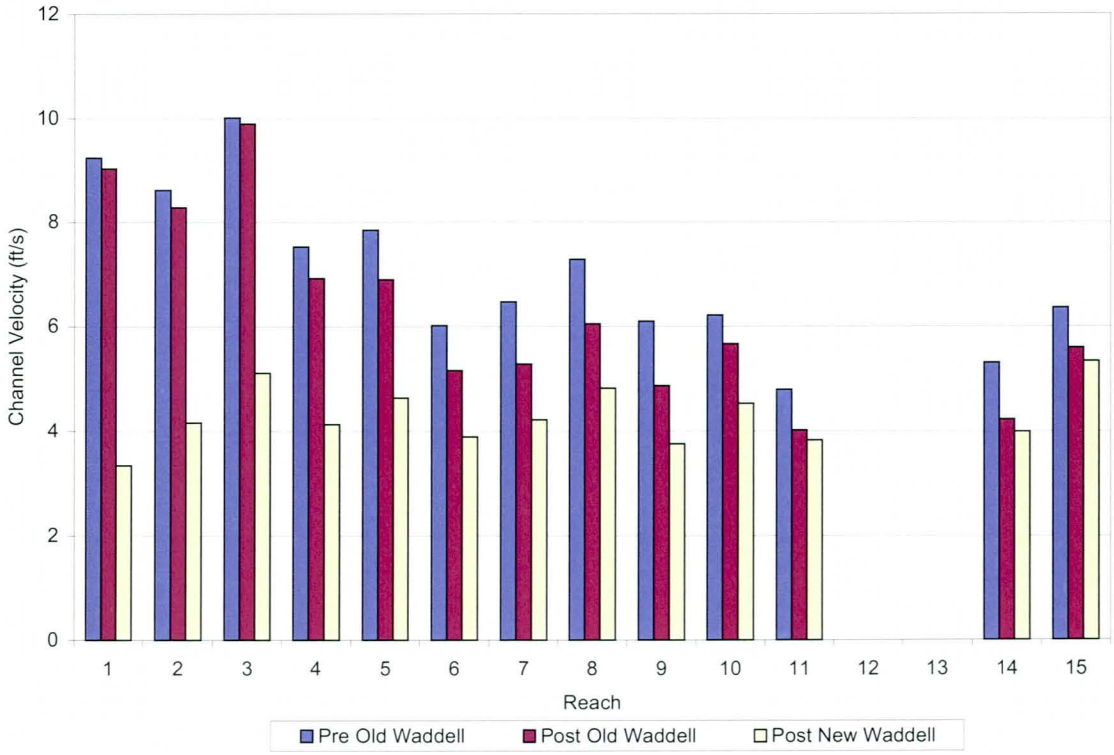

Figure 7-2 Comparison of reach-averaged channel velocities, 10-year flood

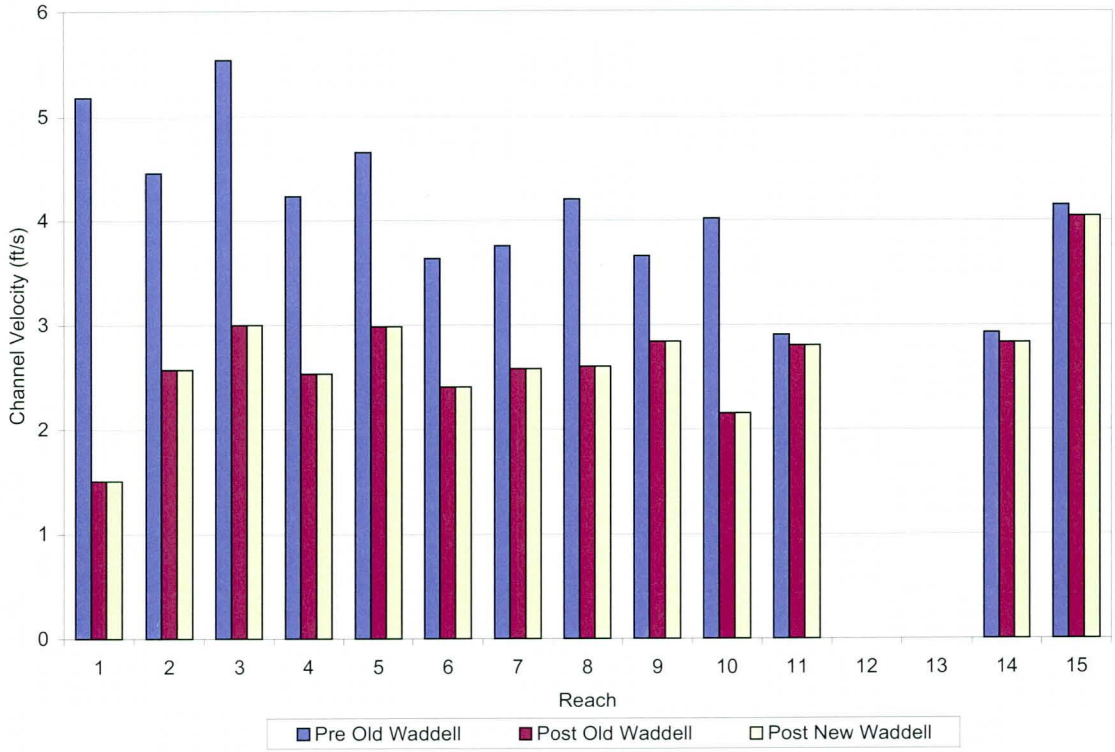

Figure 7-3 Comparison of reach-averaged channel velocities, 2-year flood

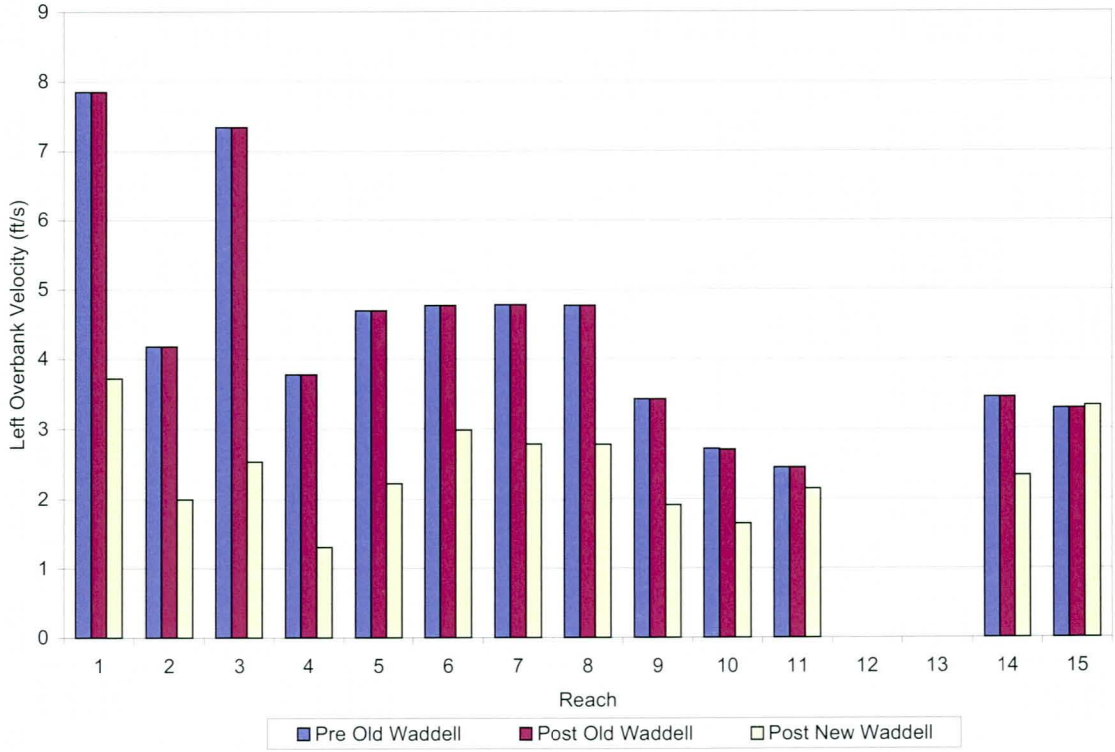

Figure 7-4 Comparison of reach-averaged left overbank velocities, 100-year flood

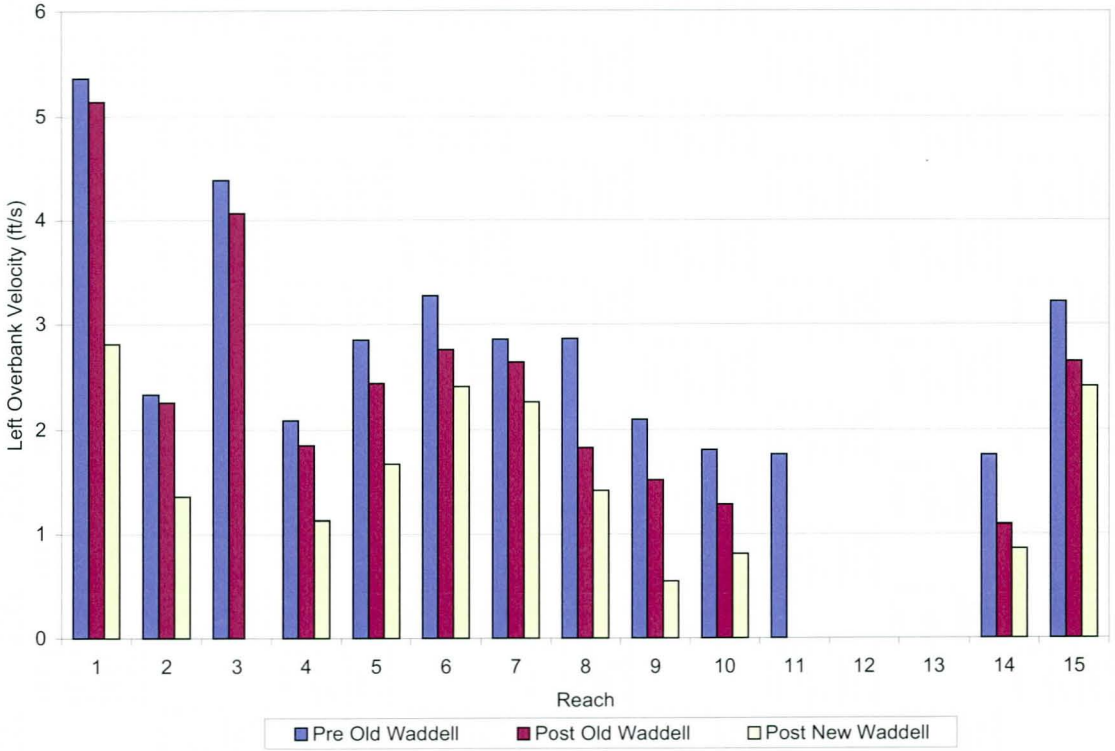

Figure 7-5 Comparison of reach-averaged left overbank velocities, 10-year flood

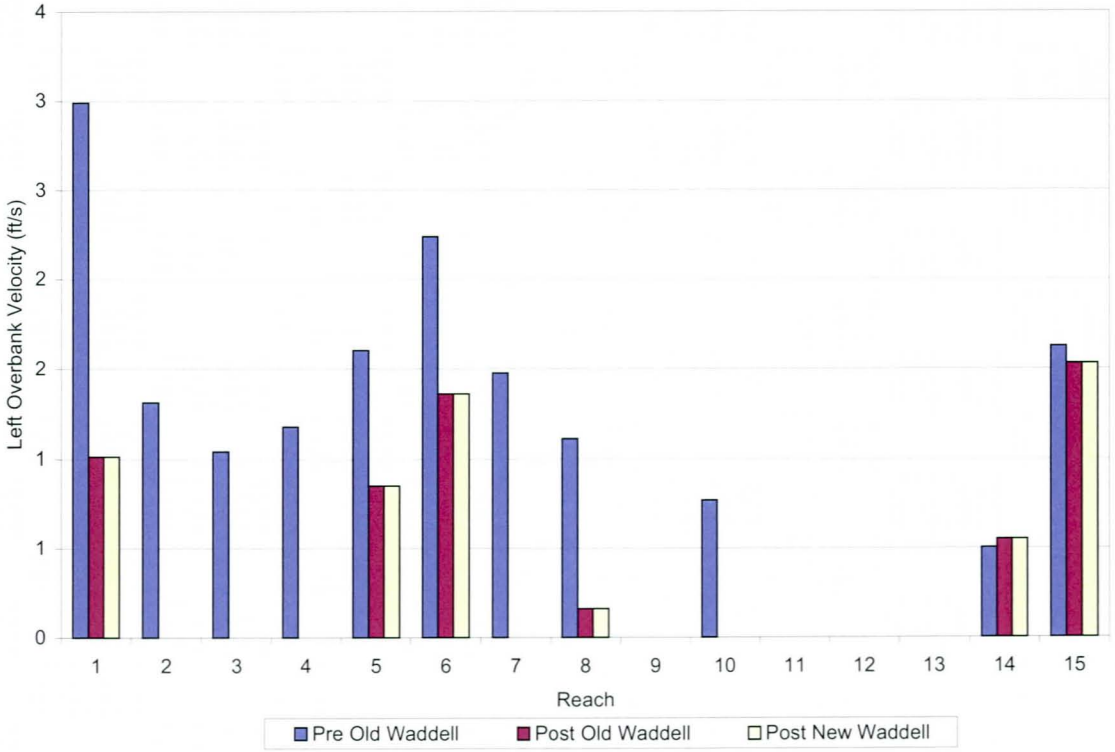

Figure 7-6 Comparison of reach-averaged left overbank velocities, 2-year flood

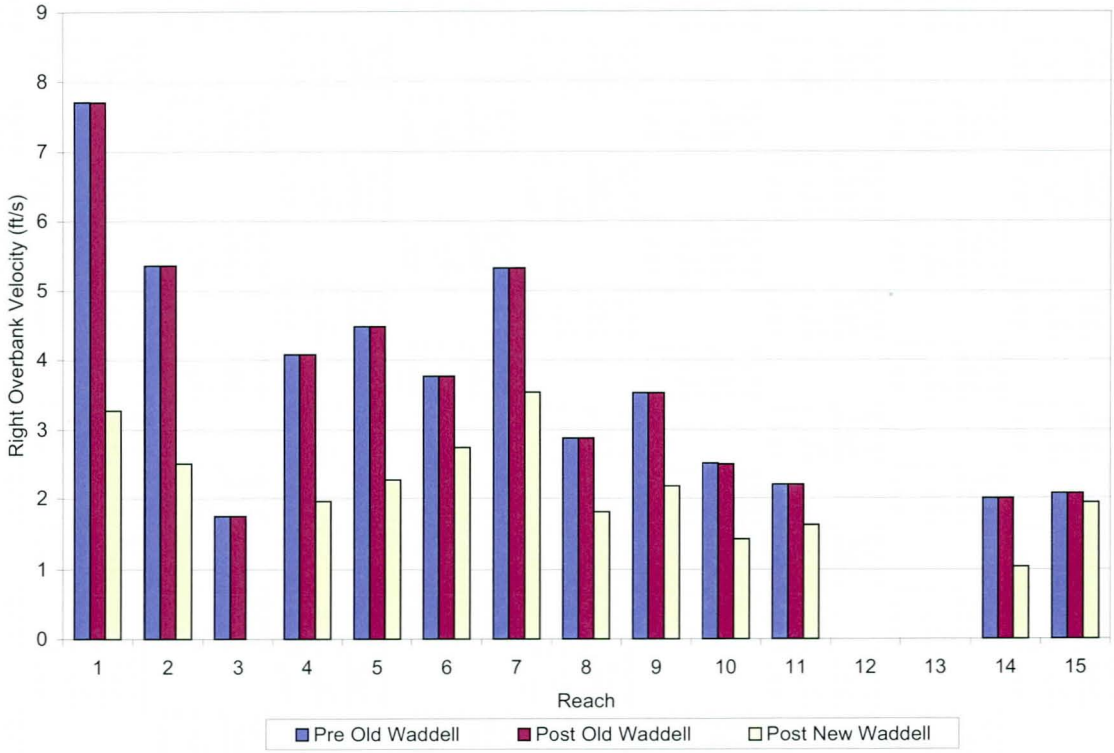

Figure 7-7 Comparison of reach-averaged right overbank velocities, 100-year flood

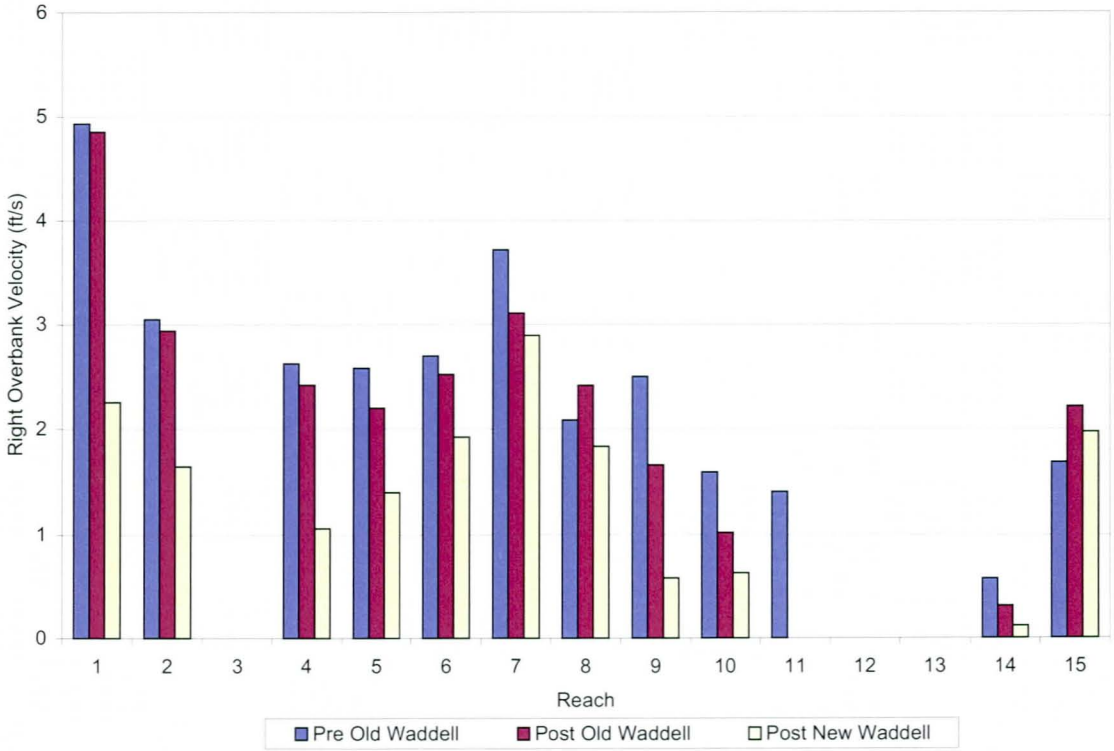

Figure 7-8 Comparison of reach-averaged right overbank velocities, 10-year flood

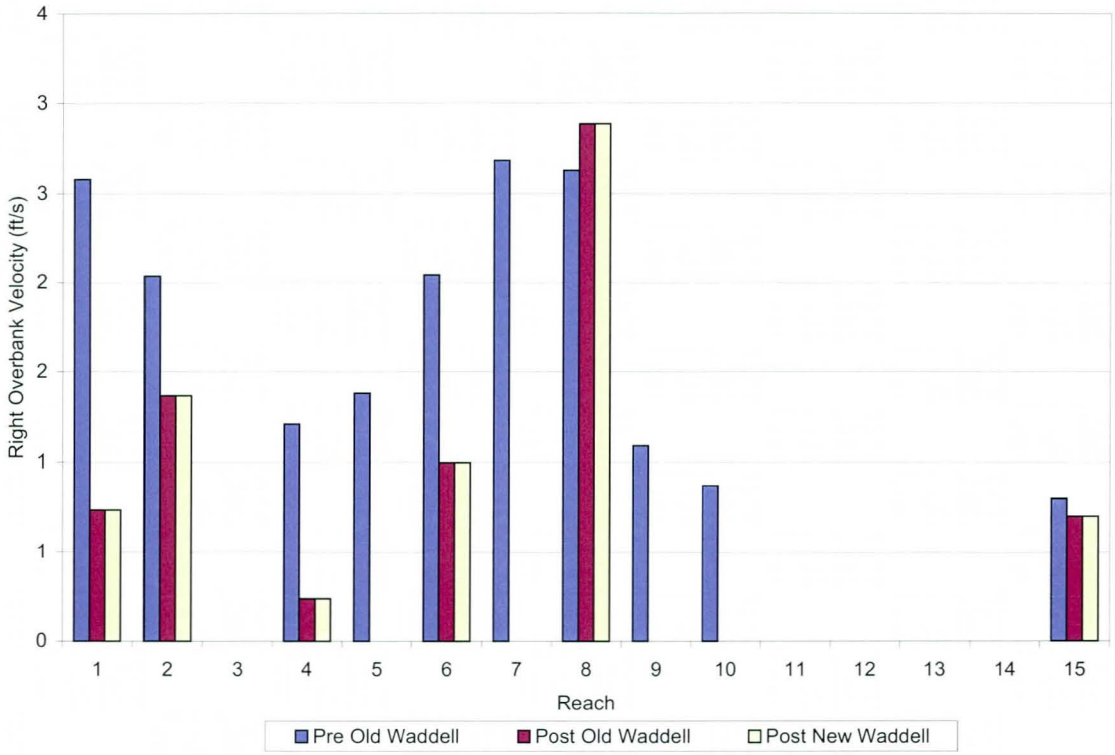

Figure 7-9 Comparison of reach-averaged right overbank velocities, 2-year flood

Figure 7-1 through Figure 7-9 show that the average velocities in the main channel and overbanks of the Agua Fria River declined due to construction of Waddell Dam and declined even more after construction of New Waddell Dam. The decrease in reach-averaged velocities is especially pronounced in the upstream end of the study reach (e.g., Reaches 1-5), particularly after Waddell Dam was built and before New Waddell was completed. Channel velocities decrease in the downstream direction prior to construction of New Waddell Dam in Reaches 1 to 5 and then remain relatively uniform downstream. After New Waddell was closed, the velocities are more uniform throughout the study reach. Reach-averaged 100-year channel velocities are generally erosive in the entire study reach for all the time periods analyzed, despite a 10 to 50 percent reduction in magnitude following dam construction. The 10-year pre-New Waddell channel velocities are erosive throughout the study area. However, for the post-New Waddell condition, the 10-year channel velocities are no longer erosive in the Upper Reach. The smaller bed material sizes in the Middle and Lower Reaches would be eroded by the 10-year post-New Waddell Dam velocities. For the 2-year flood, the Upper Reach has marginally erosive velocities prior to dam construction. After dam construction, only the finer sediments in the middle and lower reaches would be considered erodible. Overbank velocities largely "disappear" in the 2-year event after construction of the dams since the reduced discharge is mostly contained in the main channel.

7.4.2 Comparison of Reach-Averaged Top Width

Figure 7-10 to Figure 7-12 show comparisons of the reach-averaged top width for the pre-Waddell, post-Waddell, and post-New Waddell Dam 100-year, 10-year, and 2-year flood conditions.

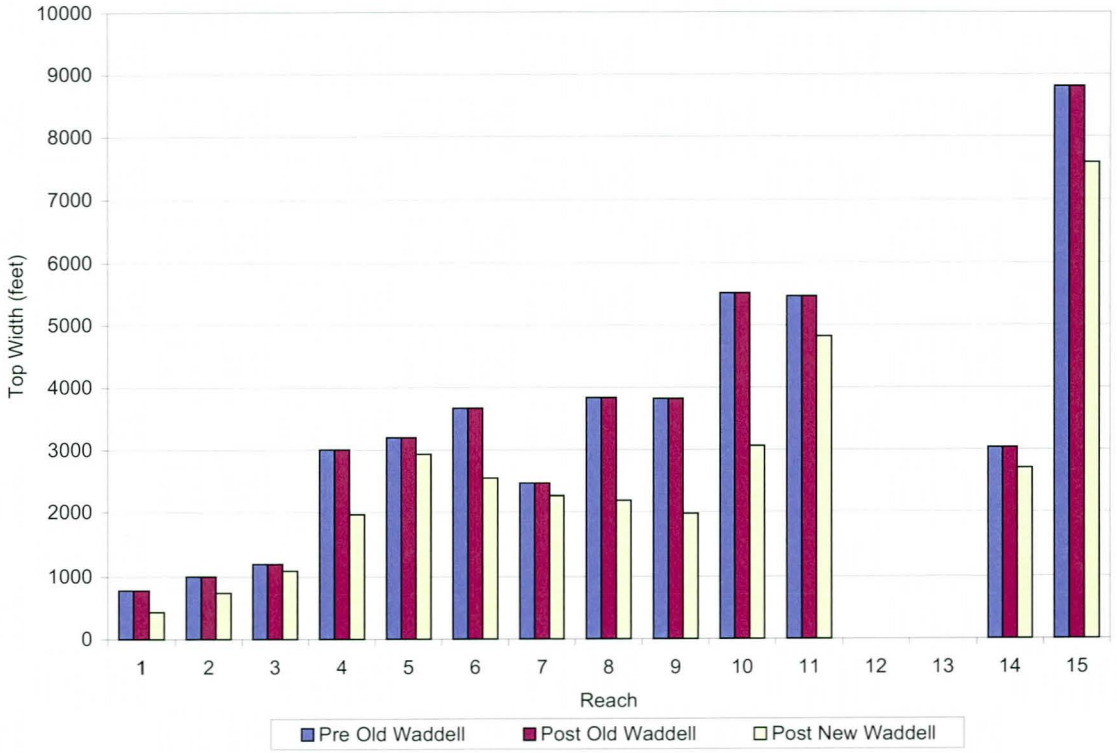

Figure 7-10 Comparison of reach-averaged top width for the 100-year flood

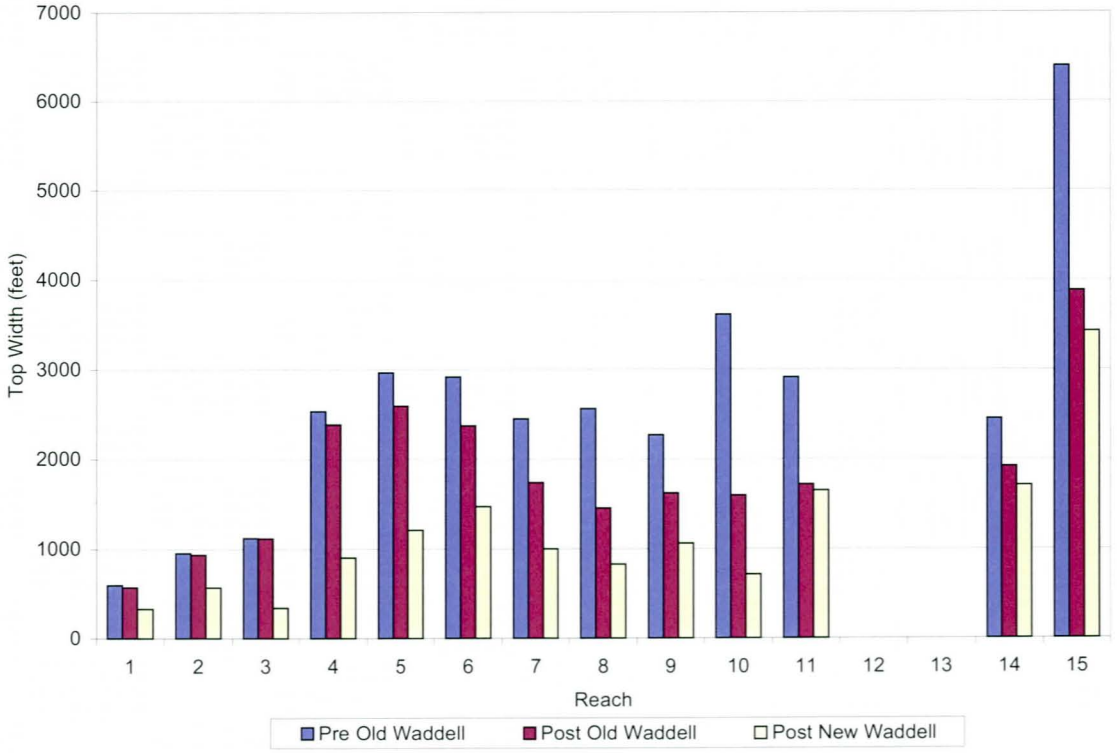

Figure 7-11 Comparison of reach-averaged top width for the 10-year flood

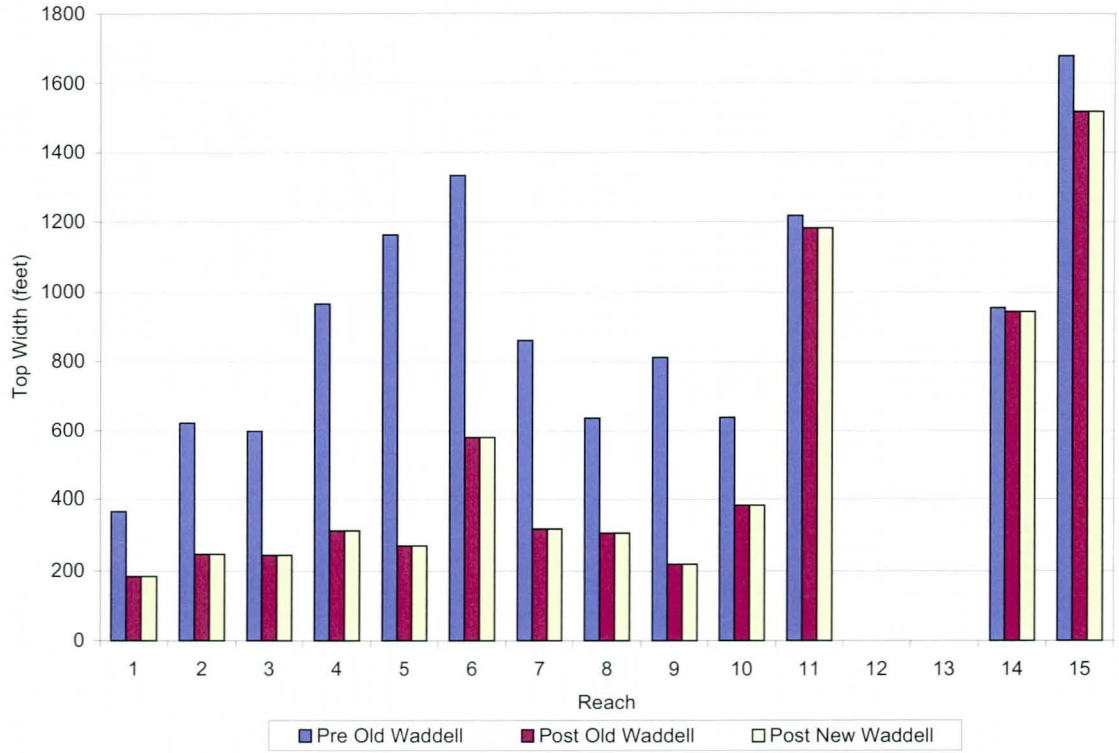

Figure 7-12 Comparison of reach-averaged top width for the 2-year flood

Figure 7-10 through Figure 7-12 show that the reach-averaged top width increases in the downstream direction within the Agua Fria River study reach. The decrease in top width in and around Reach 7 is due primarily to an increase in channel depth. After construction of Waddell Dam, reach-averaged top width decreased, especially at the 2- and 10-year recurrence interval. The reach-average top width decreased further after completion of New Waddell Dam. The reduction in top width is greatest in the Upper and Middle Reaches, and is minimal in Reaches 14 and 15 in the Lower Reach. The reduction of top width is primarily a function of the reduction in peak discharge.

7.4.3 Comparison of Reach-Averaged Maximum Channel Depth

Figure 7-13 to Figure 7-15 show comparisons of the reach-averaged maximum channel depth for the pre-Waddell, post- Waddell, and post-New Waddell Dam 100-year, 10-year, and 2-year flood conditions, respectively.

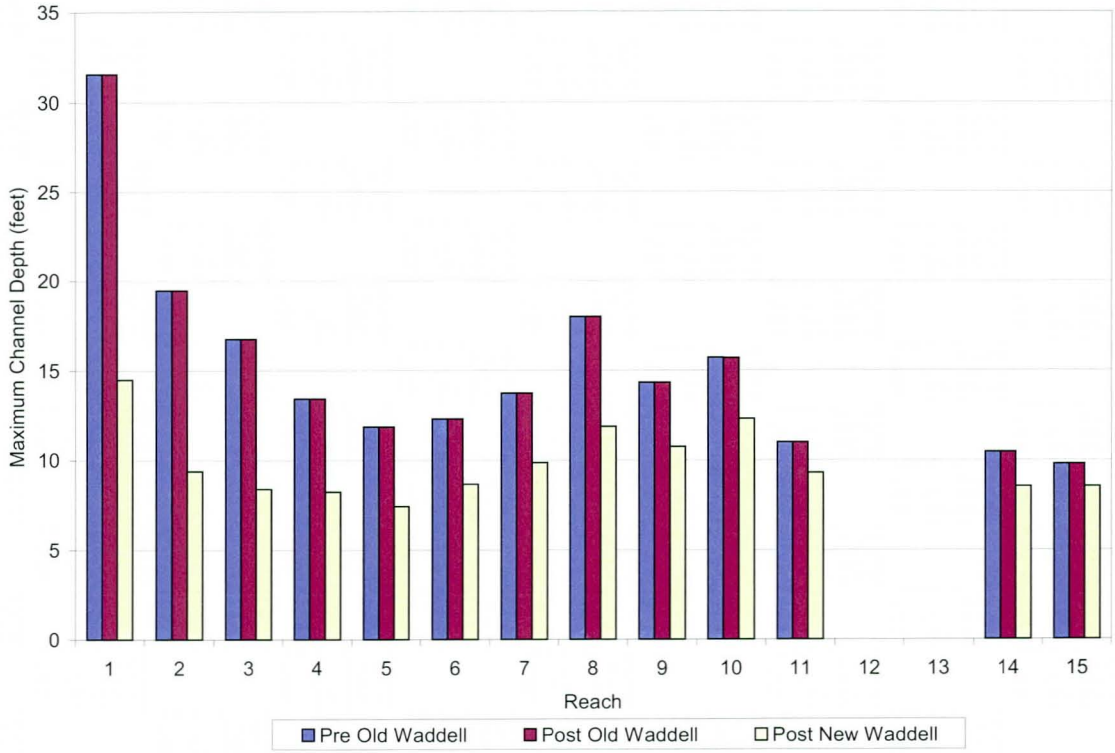

Figure 7-13 Comparison of reach-averaged maximum channel depth for the 100-year flood

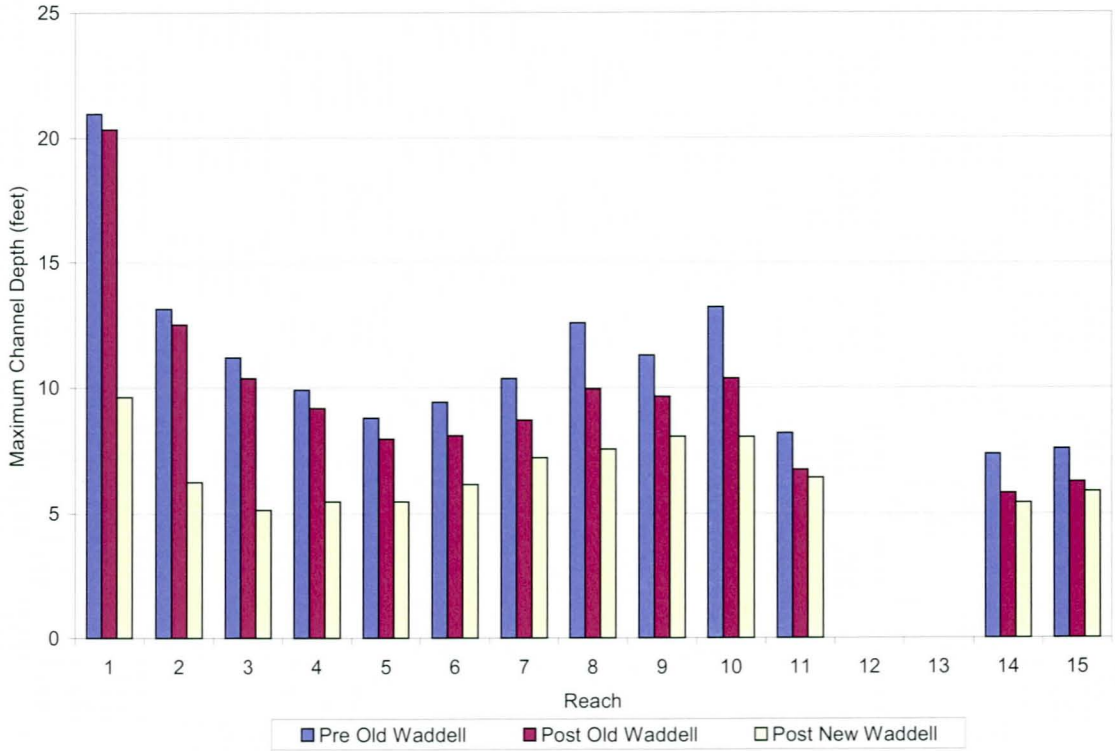

Figure 7-14 Comparison of reach-averaged maximum channel depth for the 10-year flood

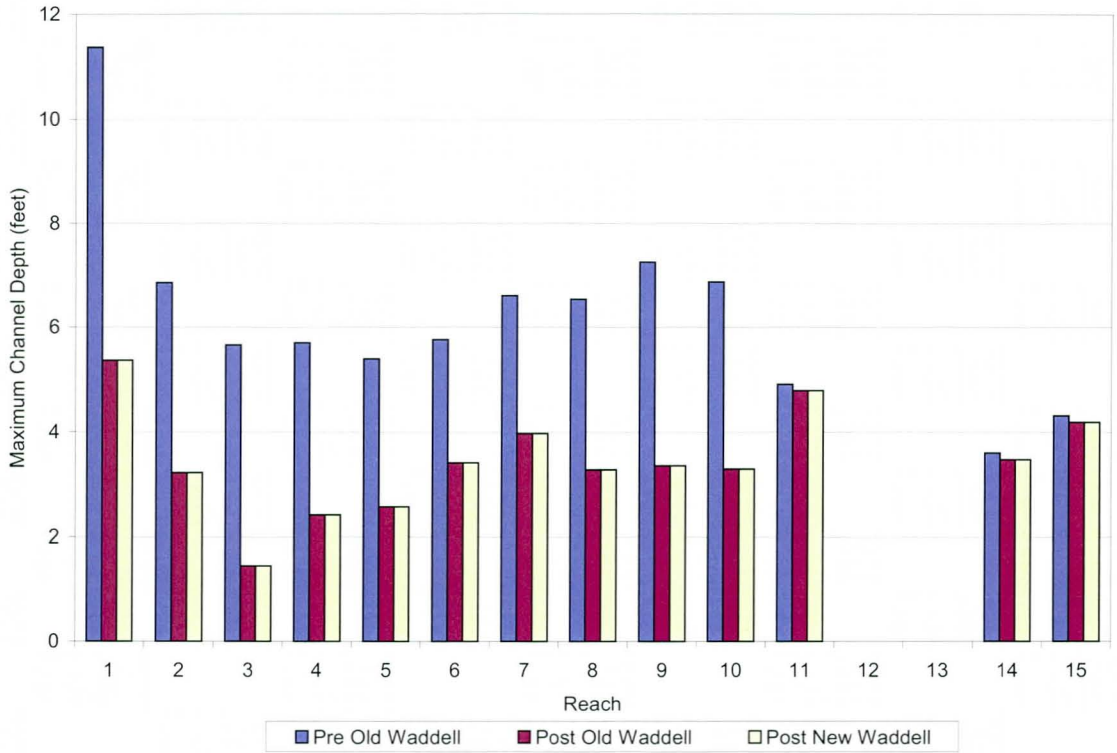

Figure 7-15 Comparison of reach-averaged maximum channel depth for the 2-year flood

Figure 7-13 through Figure 7-15 show that the reach-averaged maximum channel depth of the Agua Fria River generally decreases in the downstream direction, although not consistently. A slight increase in average maximum depth in the Middle Reach occurs due to the human-caused constrictions of the channel downstream of Beardsley Road. The narrower channel causes higher flood stages, with correspondingly greater flow depths. The construction of the Waddell Dam had little effect on the reach-averaged maximum channel depths for the 100-year and 10-year floods, but caused a reduction in the 2-year reach-averaged maximum channel depths. Conversely, the construction of the New Waddell Dam caused a decrease in the 100-year and 10-year maximum channel depths, but had little impact on the 2-year depths.

The Agua Fria River is very wide, and becomes significantly wider in the downstream direction. Therefore, small changes in depth correspond to large changes in discharge. Therefore, only when discharges have been reduced to the point where they are contained in the smaller inset low-flow channels do significant changes in depth occur. Such a change in discharge occurred for the 2-year event after construction of Waddell Dam, as shown in Figure 7-15.

7.4.4 Comparison of Equilibrium Slope Estimates

Figure 7-16 to Figure 7-18 show comparisons of the estimated equilibrium slope for the pre-Waddell, post-Waddell, and post-New Waddell Dam 100-year, 10-year, and 2-year flood conditions, respectively, relative to the existing channel slope. The equilibrium slope estimates were computed using the procedures and equations described in Chapter 6. The channel slope was measured from the modified HEC-RAS model input data.

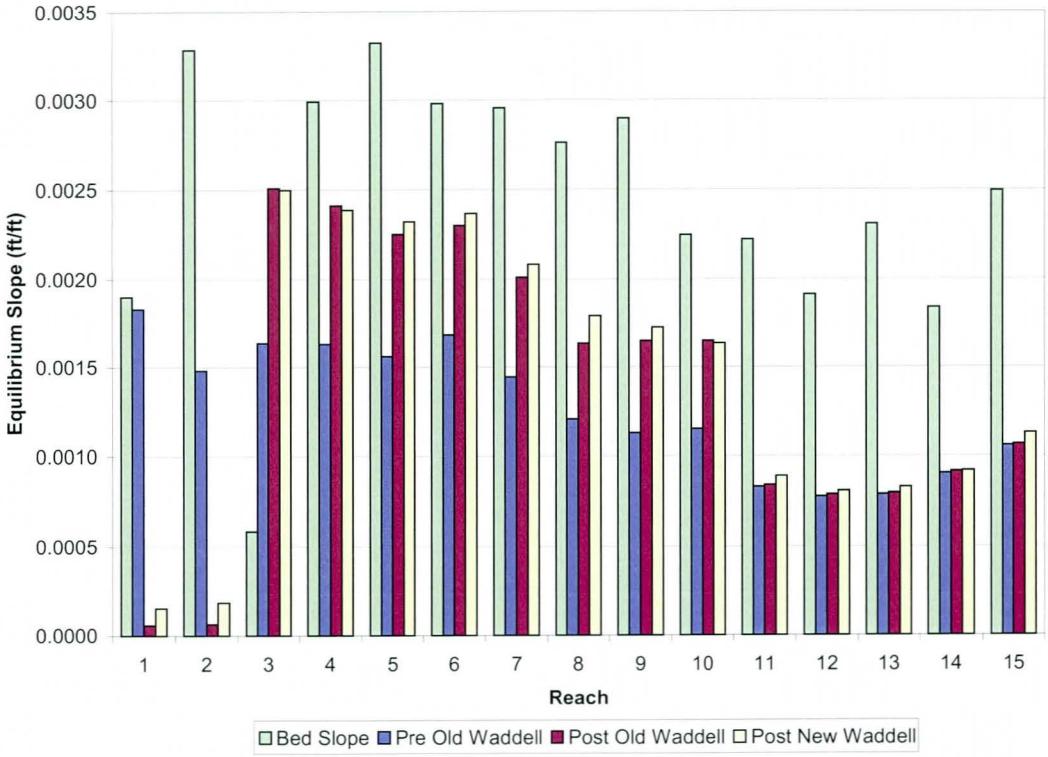

Figure 7-16 Comparison of equilibrium slope estimates and bed slope for the 100-year flood

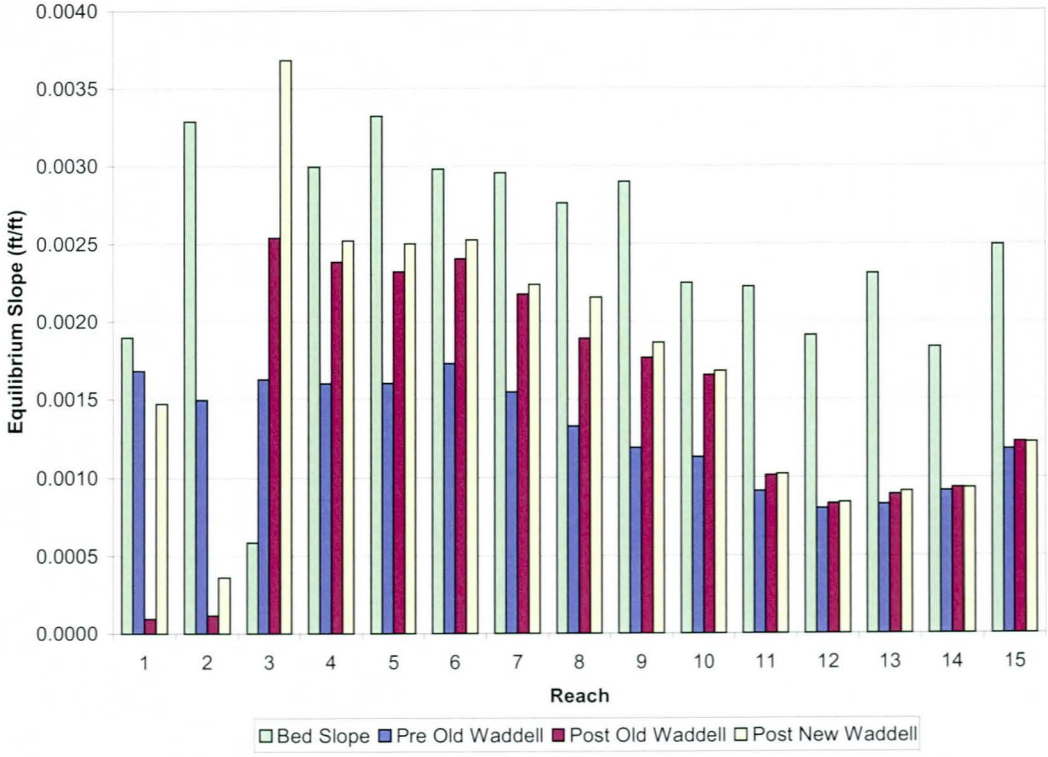

Figure 7-17 Comparison of equilibrium slope estimates and bed slope for the 10-year flood

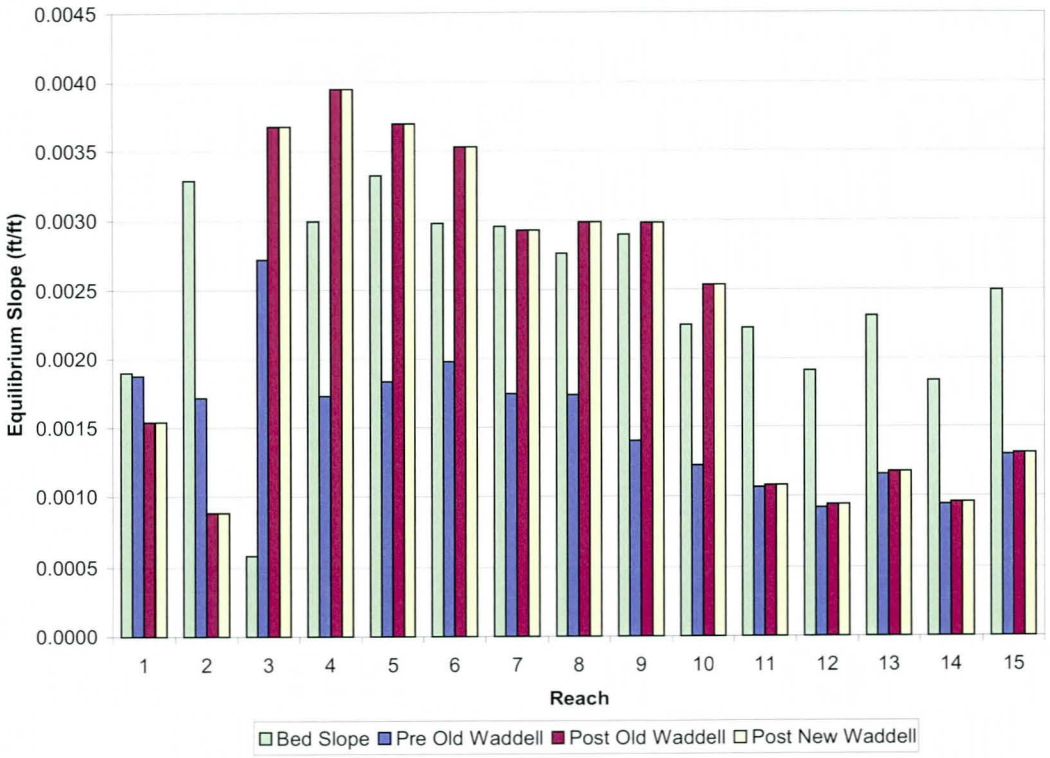

Figure 7-18 Comparison of equilibrium slope estimates and bed slope for the 2-year flood

Figure 7-16 through Figure 7-18 show a similar trend as indicated by the equilibrium slope analysis summarized in Chapter 6. That is, the Agua Fria River will tend to degrade in response to the largest floods, but is closer to an equilibrium condition during smaller flood discharges. A predicted equilibrium slope that is lower (shallower) than the existing channel slope suggests that the river will be prone to long-term degradation. The equilibrium slope results indicate that the river should be flatter (shallower slope) in the Lower Reach than in the Upper Reach, with a gradual decrease in slope in the downstream direction. The results shown in Figure 7-18 show that in Reaches 4 to 10, the reduction in the 2-year discharge after construction of Waddell Dam changed the natural tendency toward degradation to an equilibrium or aggrading condition. In general, for all three recurrence intervals, the reduction of discharge lessened the tendency for long-term degradation predicted by the equilibrium slopes.

7.4.5 Regime Channel Characteristics

The regime equations described in Chapter 6 were applied to the study reach to predict stable channel width, depth, and velocity using the modified discharges for each of the three time periods and conditions.

7.4.5.1 Width

Figure 7-19 to Figure 7-21 show comparisons of the average regime widths for the pre-Waddell, post-Waddell, and post-New Waddell Dam 100-year, 10-year, and 2-year flood conditions, respectively, to the value computed directly from the HEC-RAS model geometry.

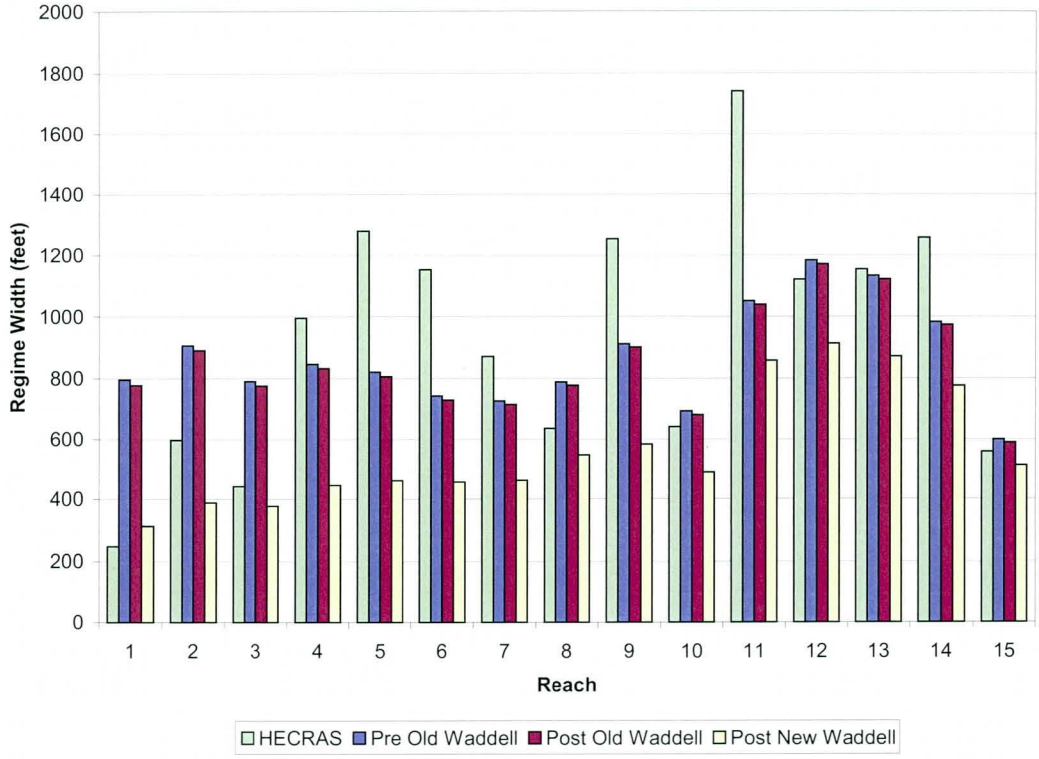

Figure 7-19 Average regime width for the 100-year flood

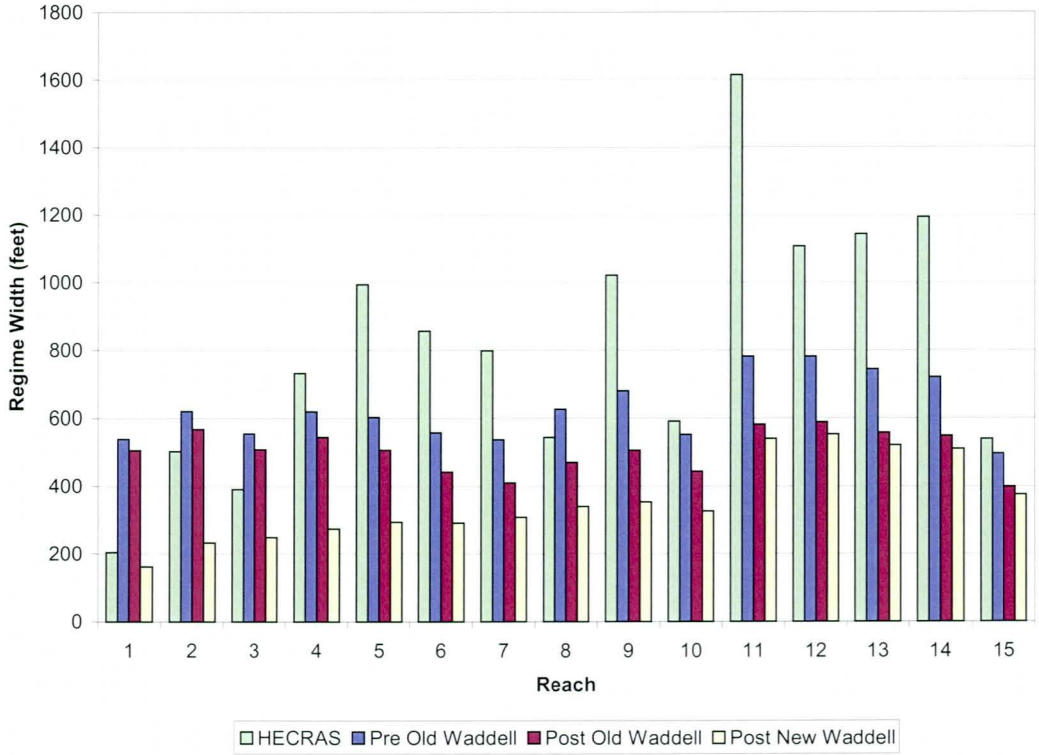

Figure 7-20 Average regime width for the 10-year flood

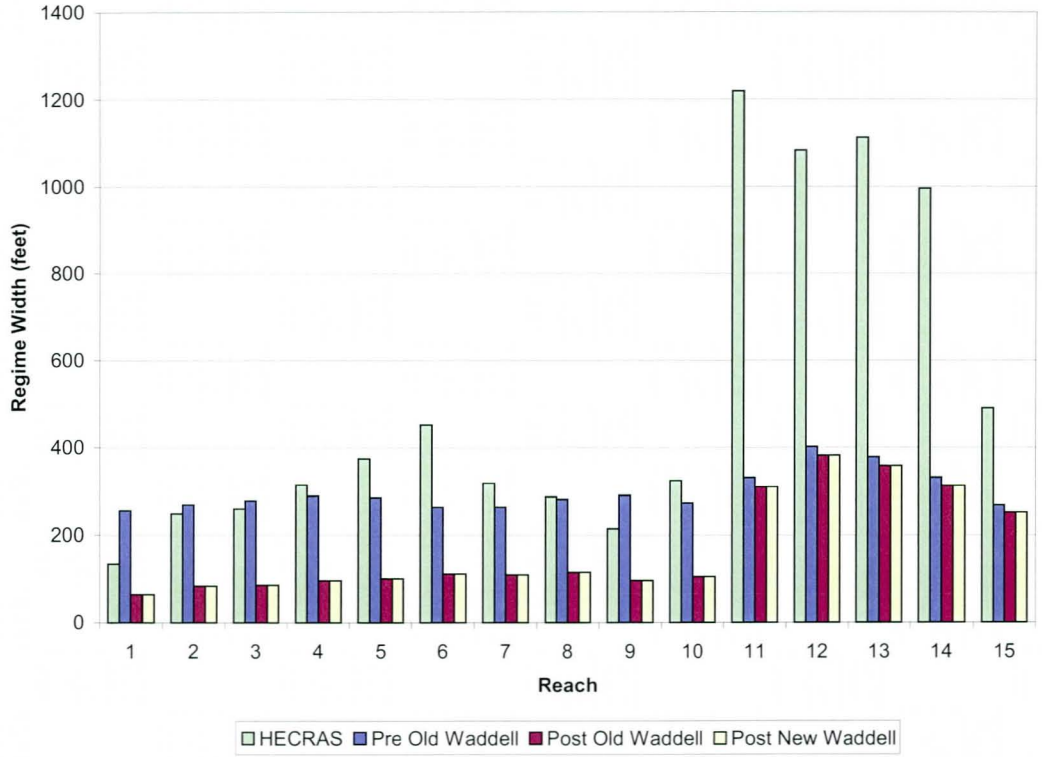

Figure 7-21 Average regime width for the 2-year flood

The regime widths shown in Figure 7-19 through Figure 7-21 generally decrease after construction of Waddell and New Waddell Dams. However, the comparison between the HEC-RAS and post-New Waddell values is of greatest prognostic value. In Figure 7-19, for example, Reaches 4, 5, 6, 9, and 11 have large differences in HEC-RAS and post-New Waddell Dam widths, indicating that they are probably out of equilibrium with the current hydrologic regime created by the New Waddell Dam. Therefore, stream narrowing is expected in these reaches. Furthermore, as demonstrated in Figure 7-21, almost every reach is significantly out of equilibrium for the 2-year flood. The very wide reaches downstream of Reach 10 are largely the result of the channel bank station definition used in the HEC-RAS model, in which the bank stations were defined at the levee margins of the channelized reaches. The levee channel is designed to convey very large floods, and was not sized for the 2-year flood. Therefore, the width trend analysis implies that at least a small amount of narrowing is expected along the entire length of the study reach.

7.4.5.2 Depth

Figure 7-22 to Figure 7-24 show comparisons of the average regime depths for the pre-Waddell, post-Waddell, and post-New Waddell Dam 100-year, 10-year, and 2-year flood conditions, respectively, to the value computed directly from the HEC-RAS model geometry.

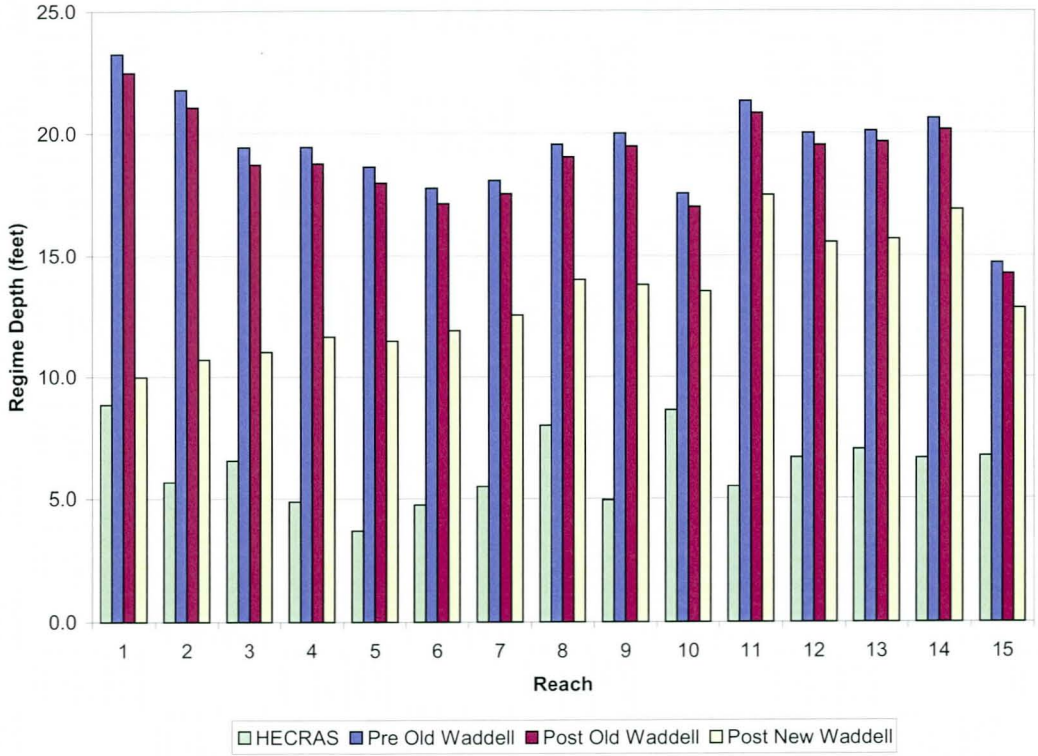

Figure 7-22 Average regime depth for the 100-year flood

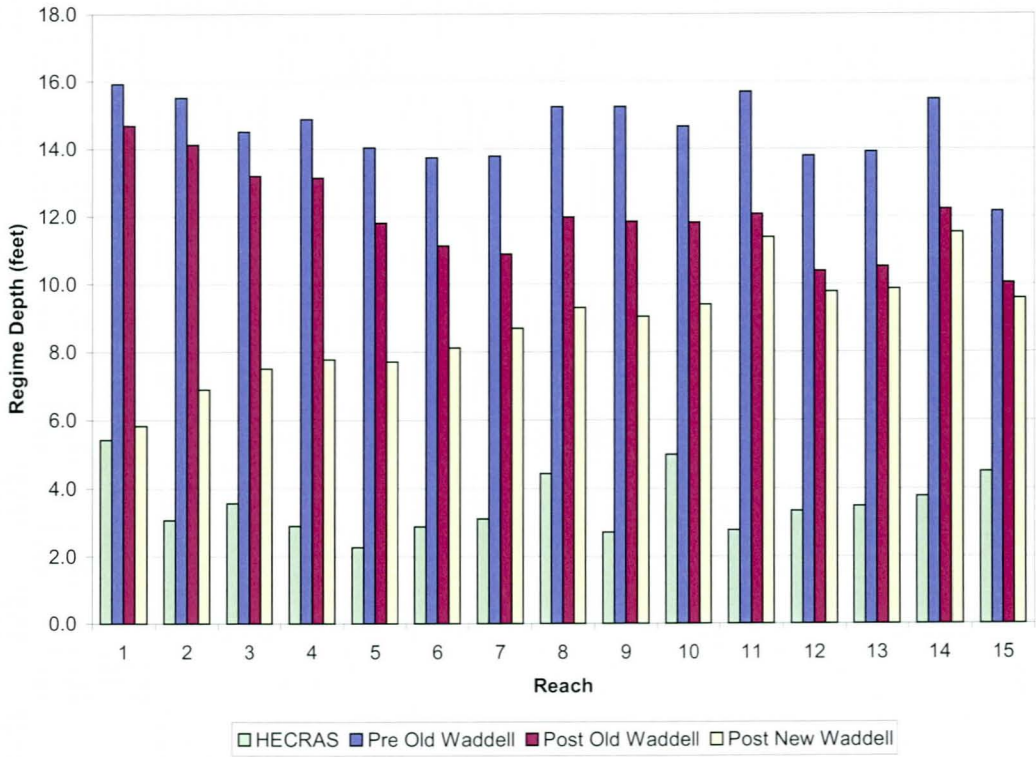

Figure 7-23 Average regime depth for the 10-year flood

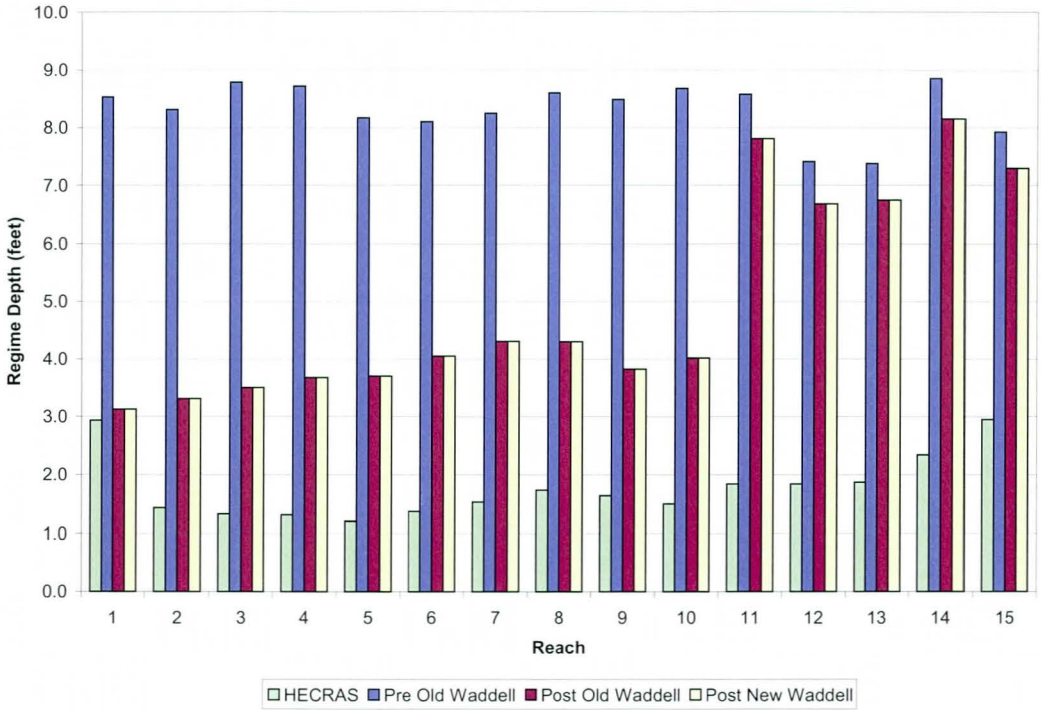

Figure 7-24 Average regime depth for the 2-year flood

Figure 7-22 through Figure 7-24 show that the predicted regime depth generally decreased after construction of Waddell Dam and New Waddell Dam, with several exceptions to this trend. For example, the 100-year flood displayed a decreasing trend in predicted regime depth from Reach 1 to Reach 6 for the pre-Waddell Dam and post-Waddell Dam conditions. After construction of the New Waddell Dam, the trend between those reaches became one of increasing predicted regime depth. The comparison between the calculated HEC-RAS depth values and the post-New Waddell Dam values have the greatest diagnostic value. For example, in Figure 7-22, Reaches 5, 6, 7, 9, 11, 12, 13, and 14, which have large differences between the HEC-RAS and post-New Waddell Dam predicted regime width, are probably out of equilibrium with the current hydrologic regime created by New Waddell Dam. Therefore, aside from the reaches with engineered grade control, long-term degradation is expected in these reaches. Note that many of the reaches that are out of equilibrium for depth are the same reaches for which narrowing was predicted. Stream narrowing and degradation often occur together. The results shown in Figure 7-24 indicate that almost every reach in the study area is significantly out of equilibrium for even the 2-year flood, implying that some degree of long-term degradation is expected along the entire length of the study reach.

7.4.5.3 Velocity

Figure 7-25 to Figure 7-27 show comparisons of the average regime velocities for the pre-Waddell, post-Waddell, and post-New Waddell Dam 100-year, 10-year, and 2-year flood conditions, respectively, to the value computed directly from the HEC-RAS model geometry.

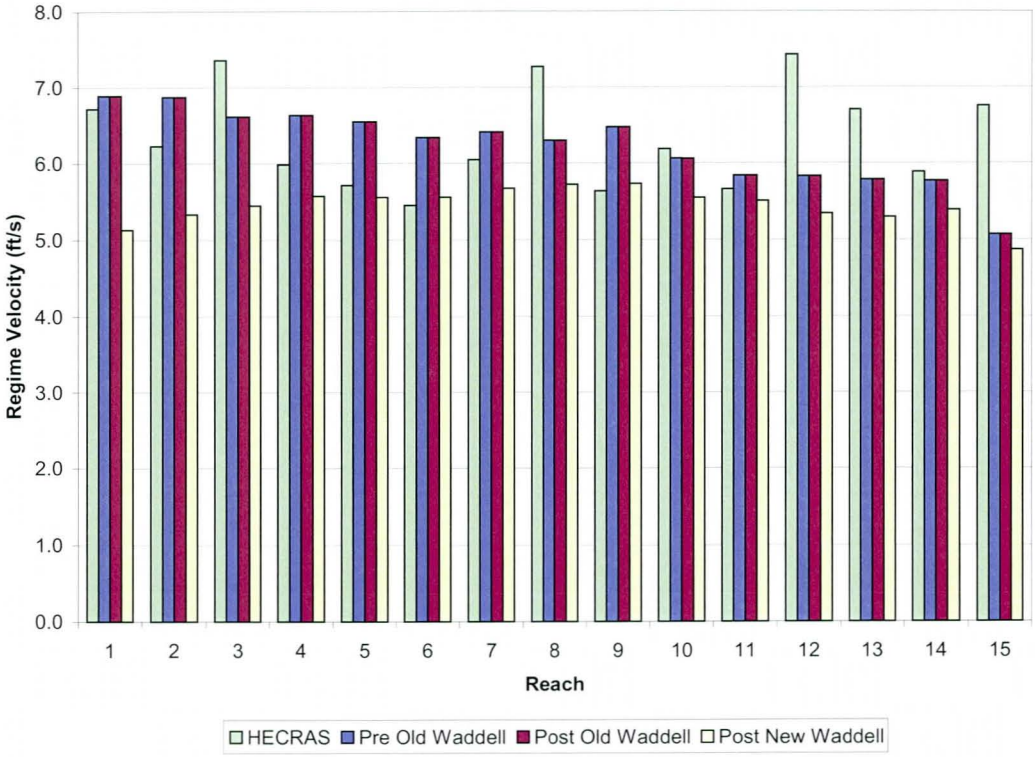

Figure 7-25 Average regime velocity for the 100-year flood

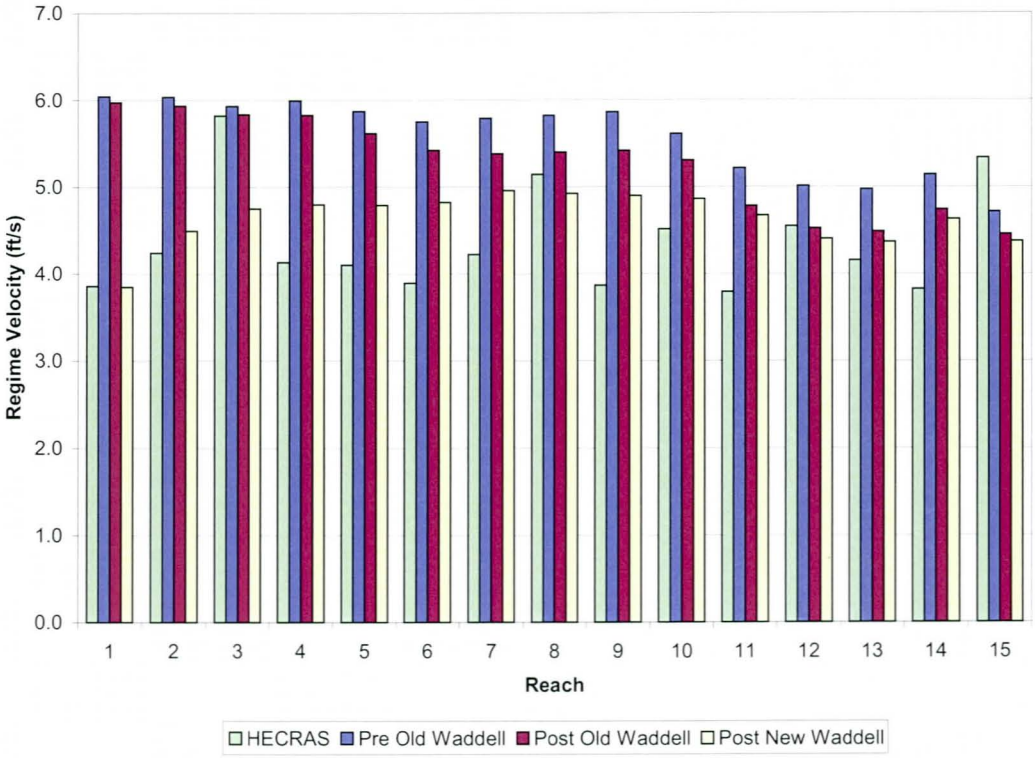

Figure 7-26 Average regime velocity for the 10-year flood

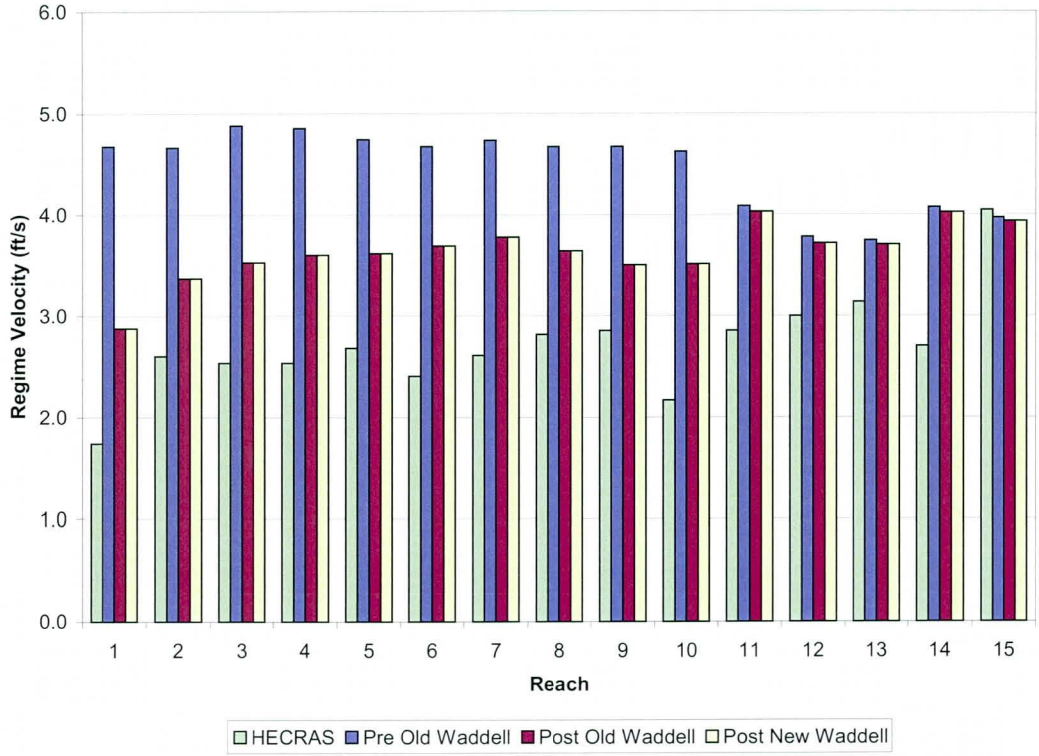

Figure 7-27 Average regime velocity for the 2-year flood

Figure 7-25 through Figure 7-27 show a general trend of slightly decreased regime velocity due to construction of the Waddell Dam and New Waddell Dam. The largest differences from the HEC-RAS values and predicted velocities occur for the pre-Waddell Dam condition at the 2-year recurrence interval in the Upper and Middle Reaches. The reductions in predicted regime velocities differ by an amount that represents a change between erosive and non-erosive velocities for many particle sizes. The reduction in velocity is expected given the reduction in 2-year peak discharge caused by the dams.

7.4.6 Channel Pattern

In Chapter 6, equations were presented which predict the type of planimetric channel pattern associated with a particular channel slope. These same equations were applied to the pre-Waddell Dam condition and the post-Waddell Dam conditions. The equations use the mean annual discharge, mean annual flood, and/or median particle size (see Chapter 6 for a description of the equations) to predict the expected channel pattern. The mean annual discharge and mean annual flood were interpreted to be similar, respectively, for both the post-Waddell Dam and post-New Waddell Dam conditions, based on the results presented by the Corps of Engineers (1995) and the gage data from the periods before and after 1992. The 2-year flood was used as a reasonable approximation of the mean annual flood. For the pre-Waddell Dam period, the mean annual discharge and mean annual flood were assumed to be similar to the gage data recorded at Agua Fria near Rock Springs USGS gage, as described above.

Table 7-2 presents the results of these calculations for the three time periods and conditions. The post-Waddell Dam and post-New Waddell Dam conditions use the same hydrologic data, and therefore, have the same results and are presented as a single column called "Post Dam."

Table 7-2 Comparison of slope for braided or meandering channel pattern

Reach	Lane				Leopold & Wolman		Henderson		Bed Slope
	Braided > shown		Meandering < shown		Braided > shown; Meandering < shown		Braided > shown		
	Post Dam	Pre Dam	Post Dam	Pre Dam	Post Dam	Pre Dam	Post Dam	Pre Dam	
1	0.00919	0.00324	0.00092	0.00032	0.00360	0.00111	0.00014	0.00004	0.00190
2	0.00919	0.00324	0.00092	0.00032	0.00336	0.00112	0.00013	0.00004	0.00329
3	0.00919	0.00324	0.00092	0.00032	0.00336	0.00113	0.00013	0.00004	0.00058
4	0.00919	0.00324	0.00092	0.00032	0.00301	0.00113	0.00012	0.00004	0.00299
5	0.00919	0.00324	0.00092	0.00032	0.00287	0.00114	0.00011	0.00004	0.00332
6	0.00919	0.00324	0.00092	0.00032	0.00275	0.00116	0.00011	0.00004	0.00298
7	0.00919	0.00324	0.00092	0.00032	0.00265	0.00118	0.00010	0.00005	0.00296
8	0.00919	0.00324	0.00092	0.00032	0.00265	0.00119	0.00005	0.00002	0.00276
9	0.00919	0.00324	0.00092	0.00032	0.00320	0.00122	0.00006	0.00002	0.00290
10	0.00919	0.00324	0.00092	0.00032	0.00313	0.00122	0.00005	0.00002	0.00225
11	0.00448	0.00324	0.00045	0.00032	0.00136	0.00130	0.00001	0.00001	0.00222
12	0.00448	0.00324	0.00045	0.00032	0.00136	0.00130	0.00001	0.00001	0.00191
13	0.00448	0.00324	0.00045	0.00032	0.00137	0.00133	0.00001	0.00001	0.00231
14	0.00448	0.00324	0.00045	0.00032	0.00138	0.00133	0.00001	0.00001	0.00184
15	0.00448	0.00324	0.00045	0.00032	0.00138	0.00133	0.00001	0.00001	0.00249

The following conclusions can be made from examination of Table 7-2:

- The Lane (1952) equation predicts an intermediate channel pattern for both the pre-dam and post-dam conditions. However, for the pre-dam condition, the predicted slopes begin to approach the threshold for a braided channel pattern. For the post-dam condition, the threshold slopes for braided channels are much higher than the observed bed slope, indicating the braided conditions will not occur.
- The Henderson (1961) equation predicts a strongly braided channel pattern for both the pre-dam and post-dam conditions.
- The Leopold & Wolman (1957) equation shows a mixed condition of meandering and braided channel pattern for the post-dam condition, with the upper reaches tending toward meandering and the lower reaches tending toward a braided pattern. However, for the pre-dam condition, their equation predicts a braided pattern throughout the study area. This result is consistent with the Lane equation results, and indicates that the channel is now less strongly braided than prior to construction of the dams.
- Changes imposed by the construction of the dams on the Agua Fria River may result in a change in channel pattern. Observations from historical aerial photographs suggest that the river is developing a straight to slightly sinuous single channel pattern in some reaches. In reality, these trends are strongly influenced by factors other than just the hydrologic changes imposed by construction of the dams, such as bridge construction, gravel mining, and channelization.

7.5 Summary

Significant changes in delivery of sediment and water to the Agua Fria River study reach have occurred over the past 70 years as a result of the construction of Waddell Dam in 1927 and New Waddell Dam in 1992. One result of dam construction has been to change the expected nature of flooding and erosion within the study area. Geomorphic changes in the Agua Fria River's behavior are expected as well. A trend toward a narrower and deeper channel, with shallower gradient (lower slope) is indicated. However, evolution of the river form will occur primarily in response to periods of significant flooding. Significant flooding on the river since completion of the New Waddell Dam has been limited. Therefore, some of the expected trends may not yet be fully expressed in the river. Other changes in the watershed and river environment are also capable of causing changes in river morphology. In particular, lowering of the channel bed by sand and gravel mining, and narrowing of the channel at bridge crossings and at mining operations also cause the river to have a lower, narrower, deeper channel with a shallower gradient, and a straight to slightly sinuous single channel. Despite these human induced changes in expected river morphology and behavior, infrequent very large discharges will still attempt to reestablish a wider, shallower, braided channel more similar to the historical river condition. The long-term result of these competing trends is likely to be a compound river which has a narrower, deeper, shallower gradient, slightly sinuous single channel inset into a larger, wider, shallower, braided high flow channel.

8. EROSION HAZARD ZONES

8.1 Introduction

Erosion hazard boundaries for the Agua Fria River were identified based on the results of the geomorphic, historical and engineering analyses of lateral stability. The geomorphic analysis included consideration of field data and analytical procedures. This chapter describes the methodology used to define the erosion hazard boundaries.

8.2 Methodology

The following types of information were considered in defining the erosion hazard zones:

- Field Data
- Historical Channel Changes
- Aerial Photographs
- Archaeological Data
- Mapping of Geomorphic Surfaces
- Longitudinal Profile Analysis
- Hydraulic Geometry/Regime Equations
- Expected Channel Pattern
- Allowable Velocity
- Equilibrium Channel Slope
- Armoring Potential
- Stable Bank Slope
- HEC-6 Modeling Results
- Expected Lateral Erosion Mechanism

A summary of the data types listed above was generated and plotted on a single work map so that the results of the various analyses could be collated and compared. The paragraphs below describe how those data were summarized into a single map element which was used to generate the erosion hazard zone maps.

8.2.1 Field Data

Collection of field data was described in Chapter 3. Detailed field inspections of the study reach were conducted at cross sections set about one mile intervals throughout the study reach. At each field section, and at significant points between sections, the relative bank stability was assessed, evidence of past erosion was documented, and the likelihood of future erosion was predicted. Field data were also used to identify reaches of historically recent scour and degradation, as well as to identify actively eroding areas outside the main channel. Based on the field observations, the right and left primary channel banks were classified as either stable or unstable, and mapped on a set of the semi-rectified aerial photographs of the study reach.

Map Elements for Field Data:

- Channel Bank Location – Right and Left
- Evidence of Active Degradation or Aggradation
- Evidence of Active or Historical Lateral Erosion
- Miscellaneous Notes
- Stable/Unstable Bank Designation

8.2.2 Historical Channel Movement

Mapping of historical channel movement was described in Chapters 4 and 5. The maximum measured channel movement within the 65 year period of record was used as a minimum predicted erosion distance. The thalweg position for the 65 years (1934 to 1999) of historical aerial coverage[1] is shown on the Historical Channel Position Map in the Exhibits Map Book. The maximum measured channel movement distance was plotted on the semi-rectified aerial photographs. Because the direction of future erosion cannot be predicted with 100 percent certainty, the maximum erosion distance was plotted as the lateral distance across the channel from each of the banks. That is, it was assumed future erosion could occur in either direction. In the reaches of the Agua Fria River which are subject to channel avulsions, the maximum channel movement distance during the period of record was about 2,200 feet, and was generally equal to the width of the geologic floodplain.

Map Element for Historical Channel Movement:

- Former Channel Positions

8.2.3 Historical Aerial Photographs

Information derived from historical aerial photographs was described in Chapters 2 and 5. This information includes changes in channel width, sinuosity, lateral erosion distances during single floods or over extended periods of record, former positions of channels and/or floodplains, and human disturbance of the river. During the 1980 flood, up to 1,100 feet of lateral movement was recorded in several locations within the study reach. Except where erosion is controlled by engineered bank protection or natural features, the maximum erosion distance recorded during the 1980 event was used as a guideline for depicted possible future erosion hazards.

Map Element for Historical Channel Movement:

- Maximum channel width changes
- Maximum single-event lateral movement
- Former channel positions

8.2.4 Historical Long-Term Scour

Historical long-term scour was described in Chapters 3 and 5. Historical long-term scour was identified using interpretation of channel thalweg profiles on topographic maps, historical stereo aerial photographs, field data, and archaeological evidence. Reaches that have experienced long-term scour are more vulnerable to bank erosion from undercutting, tensional failures, piping, and slumping. The reaches of greatest historical degradation were coincident with the reaches of historical in-stream mining. Channel segments that experienced recent, historical and pre-historic long-term degradation were identified, estimates for the magnitude of long-term scour were made, and the results were plotted on the semi-rectified aerial photographs.

---

[1] Length of record equals 130 years if the 1870 GLO survey channel positions are considered.

Map Element for Historical Long-Term Scour:

- Estimate of Historically Recent Degradation (<100 yrs)
- Estimate of Maximum Degradation in Recent Geologic Time (1,000-10,000 yrs)

8.2.5 Archaeological Data

Archaeological evidence of prehistorical channel change and scour was described in Chapter 5. Reaches of prehistoric irrigated agriculture sites and the implied depth of long-term scour were noted relative to the other information on the semi-rectified photographs of the study area.

Map Element for Archaeological Data:

- No map elements were plotted on Figures used in this report to remain in compliance with Arizona Antiquities Act that discourages publishing the location of known archaeological sites. However, these data were made available to JEF for the purposes of evaluating the erosion hazard zones for the Agua Fria River.

8.2.6 Mapping of Geomorphic Surfaces

The geomorphic mapping process was described in Chapters 2 and 4. Based on interpretation of stereo photographs, field investigations, surficial soil characteristics, channel and floodplain topography, published surficial mapping, and detailed soil profile descriptions contained in published report, detailed geomorphic mapping was prepared for the study reach. These data were used to estimate the age of the fluvial terraces in the study area, and to distinguish geologically recent geomorphic surfaces (0-1,000 years old) from older, more stable surfaces (1,000 – 700,000 years old.). Geomorphic age data were useful for distinguishing areas of active and inactive channel movement, and for constraining the maximum and minimum rates of channel evolution. The geomorphic surface map was overlaid on a set of the semi-rectified photographs of the study area.

Elements for Geomorphic Mapping:

- Geomorphic Surface Units and Relative Ages

8.2.7 Longitudinal Profile Analysis

The longitudinal profile analysis was presented in Chapters 4 and 5. Longitudinal profiles derived from recent and historical topographic maps were compared to identify reaches of historical degradation. The estimated long-term scour based on the comparison of profiles was plotted on the semi-rectified photographs of the study area.

Elements for Geomorphic Mapping:

- Long-term Scour Estimate

8.2.8 Hydraulic Geometry/Regime Equations

Regime equations and hydraulic geometry relationships were described in Chapters 6 and 7. Regime relationships for channel width were applied to the study reach using the 2-, 10-, and 100-year peak discharges, as well as the estimated bankfull discharge, to estimate the expected direction and possible magnitude of channel adjustment to flood flows. Bankfull discharge recurrence intervals averaged about 14 years for the study reach, except in the levee reaches where the channel has been too highly disturbed to yield meaningful results. A variety of equations based on empirical data were applied, and the average widths were plotted on the semi-rectified aerial photographs to indicate channel sections of expected widening (lateral erosion) or narrowing. The widths plotted on the aerial photographs were measured first from one bank, then the other bank, assuming that the adjustment occurred on each side of the channel independently. The existing channel widths appear to be adjusted to about the 2-year

width in the braided multiple channel reach, and the 10-year width for the single channel reaches.

Map Element for Hydraulic Geometry/Regime Equations:

- Average Expected Width Based on the 100-Year Peak Discharge
- Average Expected Width Based on the 10-Year Peak Discharge
- Average Expected Width Based on the 2-Year Peak Discharge

8.2.9 Expected Channel Pattern

Channel pattern analysis was described in Chapters 6 and 7. Published data relating expected channel pattern (braided, meandering, straight, intermediate) to channel slope, mean annual discharge, and/or the mean annual flood were used to predict the equilibrium channel pattern at each cross section in the study reach. The existing channel pattern was then compared to the predicted channel pattern and the anomalies were noted on the semi-rectified aerial photographs. In general, the expected channel pattern in the study area is a straight braided channel, with a greater tendency toward braiding at higher discharges.

Map Elements for Expected Channel Pattern:

- Predicted Equilibrium Channel Pattern

8.2.10 Allowable Velocity

Allowable velocity analyses were described in Chapters 6 and 7. Published values of non-erosive velocities were compared to existing channel velocities computed by HEC-RAS modeling. Each cross section where the 2-, 10- or 100-year channel velocity exceeded the allowable velocity was plotted on the semi-rectified aerial photographs of the study area.

Map Elements for Allowable Velocity

- Erosive Velocity by Recurrence Interval

8.2.11 Equilibrium Channel Slope

Equilibrium slope calculations were described in Chapters 6 and 7. The equilibrium channel slope was predicted based on channel hydraulics, bed sediment characteristics, empirical data, and flood discharges. Reaches expected to experience long-term degradation are more likely to experience lateral erosion due to undercutting. Aggrading reaches are more likely to experience avulsive channel changes. Reaches of expected long-term degradation or aggradation in response to expected slope adjustments were plotted on the semi-rectified aerial photographs of the study area.

Map Element for Equilibrium Slope:

- Expected Slope Adjustment (Degradation/Aggradation)

8.2.12 Armoring Potential

The channel bed armoring analysis was presented in Chapter 6. Bed armoring was computed using the sediment distribution of the bed material, HEC-RAS hydraulic data, and flood discharge estimates. Armoring can prevent general and long-term scour, and limit undercutting of the banks. However, armoring of the bed could lead to preferential erosion of the banks for reaches with a sediment deficit relative to the transport capacity. Cross sections likely to develop an armor layer were noted on the semi-rectified aerial photographs of the study area.

Map Element of Armoring

- Recurrence interval of flow likely to develop armor layer

8.2.13 Stable Bank Slope

Field observations in the study reach and elsewhere in central Arizona indicate that vertical banks are inherently unstable, although the time scale over which instability is expressed varies with the degree of erosivity and resistance of the local bank characteristics. Evidence of lateral instability observed on vertical or oversteepened banks in the study reach included the following:

- Lack of Bank Vegetation
- Piles of Collapsed Bank Materials at the Base of the Banks
- Tipped Vegetation
- Exposed Roots
- Age of Vegetation
- Overhanging Banks
- Tensional cracks

The angle of repose[2] of typical unconsolidated alluvial soil materials is about 20 °-40°, or about a 3:1 slope. Therefore, it was assumed that the minimum value for the magnitude of potential erosion would be estimated by measuring a 3:1 slope from the toe of the existing bank to the intercept of the existing ground. That is, if the toe of the bank were to experience no future erosion, what distance could the top of bank retreat before reaching a non-erosive (i.e., a 3:1) slope. The assumption that 3:1 bank slopes are stable along the Agua Fria River was verified using field data from the study reach, as presented in Chapters 3 and 4. The 3:1 intercept line was plotted on the semi-rectified aerial photographs as a minimum estimate of future bank erosion for the lateral migration erosion hazard zone. In some cases such as in Reach 6, naturally stable slopes of similar height are present. In these cases the observed stable slopes were used to define the limits of the lateral migration erosion hazard zone from the toe of the existing bank. Stable slope lengths in this area are about 300 feet.

Map Element for Stable Bank Slope:

- 3:1 Offset From Existing Bank Toe

8.2.14 HEC-6 Modeling Results

Sediment continuity routing was performed by Kimley-Horn & Associates for the 100-year existing condition hydrograph. The computed total[3] sediment deficit (scour) or surplus (deposition) was divided by the average bank height and the reach length to estimate the amount of lateral erosion, assuming all of the bank erosion occurred on only one side of the channel. For channel sections where aggradation or small amounts of degradation were predicted, the reach-averaged erosion distance was plotted.

Map Element for HEC-6 Results:

- 100-Year Erosion Line

8.2.15 Expected Lateral Erosion Mechanism

The expected mechanism of lateral erosion for the study reach was defined based on interpretation of historical aerial photographs, field data, the geologic history of the study area, the relative age of stream terraces adjacent to the active channel, and general geomorphic

---

[2] The angle of repose is the maximum angle of slope at which alluvium will remain in place without sliding.

[3] Total sediment deficit, not the cumulative sediment deficit reported in the HEC-6 output.

principles. The two primary mechanisms for lateral movement in the study reach are bank erosion and avulsions. Bank erosion occurs as the defined channel banks are eroded due to shear applied by flood waters, and typically results in moderate magnitudes of lateral movement. Avulsions are a sudden relocation of the main channel to another part of the floodplain due to concentration of overbank flows, interception of the main channel by an existing overbank channel, or formation of meander cutoffs during a large floods. Avulsive channel changes have been responsible for the largest channel movement recorded during the period of record.

Map Elements for Lateral Erosion Mechanism:

- Avulsion potential is reflected in the width of erosion hazard boundaries

8.2.16 Impacts of Mining-Induced Entrenchment

In-stream sand and gravel mining has lowered the bed elevations up to 40 feet within mined reaches along the Agua Fria River. In-stream mining is linked to accelerated rates of lateral erosion, undermining of flood control structures, and depletion of sediment supply. Where active or historical sand and gravel mines were identified, the erosion limits were generally wider than in reaches unaffected by mining. In general, pits located next to the main channel or within a distance that could be eroded or breached during a single event were considered to be in the severe erosion hazard zone.

Map Elements for Lateral Erosion Mechanism:

- Location of existing and historical sand and gravel excavations

8.2.17 Measurements

All measurements of expected or predicted erosion were taken from the top of bank. Top of bank was identified on the aerial photo-topographic maps using the criteria outlined in Chapter 6, which included the following:

- Change in contour density (bank slope to floodplain)
- Field notes (bank profile sketches, descriptions)
- Field photographs
- Change in vegetative characteristics (*riparian* zone)

All of the information described above, once it was plotted on the semi-rectified aerial photographs of the study area, was used to define the lateral migration hazard for the Agua Fria River.

8.3 Definition of Erosion Hazard Zones

Erosion hazard zones were defined adjacent to the main channel of the Agua Fria River. The erosion hazard zones were defined based on the channel stability assessment methodologies described in Chapters 2, 3, 4, 5, 6 and 7 of this report, as well as on the information plotted on the semi-rectified aerial photographs of the study area as summarized above. The following three erosion hazard zones were defined:

- Severe Erosion Hazard Zone
- High Erosion Hazard Zone
- Moderate Erosion Hazard Zone

8.3.1 Uncertainty

The use of erosion hazard zones rather than erosion hazard lines reflects the inherent uncertainty in predicting future channel changes such as lateral migration. Stream morphology and behavior are governed by a large number of variables, few of which can be predicted with certainty (Table 8-1). Therefore, prediction of future channel change and future lateral movement is subject to similar uncertainty. The uncertainty and/or measurement error associated with each of the specific methodologies used to assess channel stability was described in the previous chapters of this report. Even if the uncertainties associated with the methodologies used and the variables listed in Table 8-1 were eliminated, the sequence, timing, and magnitude of future floods cannot be predicted. Therefore, future erosion cannot be known with a high degree of certainty.

8.3.2 Floodplain Management

The erosion hazard zones are a distinct management tool for protecting the health, safety and welfare of landowners and users of the river corridors in the study area. Although they are based on the same hydraulic data, the erosion hazard zones are independent of the FEMA 100-year floodplain and floodway limits. That is, the severe erosion hazard zone is not coincident with the 100-year floodway, nor is the lateral migration erosion hazard zone coincident with the 100-year floodplain. The FEMA floodplain boundaries are primarily intended to prevent damage from flood inundation. The erosion hazard zones are intended to prevent damage from erosion during flooding, whether or not the property is located within the 100-year floodplain.

Table 8-1 Some Variables Affecting River Behavior and River Characteristics That Can Change With Time

Variable	Variable Subgroup	River Characteristics
Hydrology	Dominant Discharge Mean Annual Discharge Flow Duration Statistics Variation with Season Diversions and Storage Flow Source	Channel Width Channel Depth Bank Height Bank Slope Bank Materials Bank Stratification Stream Pattern Bed Forms Meander Amplitude Meander Wavelength Sinuosity Floodplain Width Depth of Floodplain Flow Stream Terraces Channel Slope Aggradation Degradation Local Scour Bed Sediment Bar Sediment Pool & Riffle Sequence Armoring Bedrock Outcrop & Control Human Modifications Bank Protection Grade Control Roadway Crossings Utility Crossings
Flow	Width Depth Hydraulic Radius Friction Factor Velocity Topwidth Turbulence Temperature Transmission Losses	
Flood Characteristics	Magnitude (peak) Duration (flashy?) Ratio of Peak to Base Flow Ratio of Rare to Frequent Floods Channel Capacity Losses Reservoirs/Flood Storage	
Streambed and Bank Sediment	Mean Diameter Size Distribution Armoring Potential Cohesion Stratigraphy	
Climate	Precipitation Type (snow?) Precipitation Intensity Precipitation Duration Seasonal Distribution Temperature/Evaporation	
Time Scale	Engineering (short-term) Geologic (long-term)	
Channel Vegetation	Vegetation Type Root Depth Root Density Branch/Foliage Density Trunk Pliability Growth Rate Germination Cycle Grazing Practices	
Watershed Characteristics	Vegetation Cover Slope Drainage Area Elevation Geology Valley Slope Sediment yield Human Impacts – Urbanization Grazing Practices	

The following three erosion hazard zones were defined for the Agua Fria River:

- **Severe Erosion Hazard Zone**. The Severe Erosion Hazard Zone encompasses the active channel, and the area next to the active channel that could reasonably be expected to erode during a large flood.
- **Lateral Migration Erosion Hazard Zone**. The Lateral Migration Erosion Hazard Zone includes the portion of the floodplain that could reasonably be expected to erode during a series of floods. This is the minimum area required to maintain the processes of natural channel movement. The Lateral Migration Erosion Hazard Zone is also the minimum area required for preservation of the natural form and function of the stream.
- **Long-Term Erosion Hazard Zone**. The Long-term Erosion Hazard Zone includes the area within and adjacent to the floodplain that could be subject to erosion and lateral migration as indicated by geologic and historic evidence. The Lateral Migration Erosion Hazard Zone is also the area necessary to implement nonstructural flood management.

The following types of data were considered in defining the erosion hazard boundaries:

- Field Observations
- Historical Channel Changes
- Archaeological Data
- Geomorphic and Soils Mapping
- Stream Classification Data
- Longitudinal Profiles
- Expected Channel Pattern Relationships
- Stable Bank Slope
- Expected Lateral Erosion Mechanism
- HEC-RAS Hydraulic Modeling Results
- Equilibrium Channel Slope Estimates
- Allowable Velocity Estimates
- Channel Morphology Relationships – Regime Equations & Hydraulic Geometry
- HEC-6 Sediment Transport Modeling Results

The following criteria were used to delineate the **long-term erosion hazard zones** for the Agua Fria River:

1. Surficial Geologic Mapping (Huckleberry, 1995 and Reynolds, 1997). The youngest geomorphic surfaces are generally located within the long-term erosion hazard zone. Surficial characteristics such as degree of soil development, vegetation (type, density, age), desert varnish, desert pavement, soil color, drainage texture, and topographic relief were used to distinguish surfaces of different age. Generally, map units described as Holocene in age (< 10,000 years) were considered within the long-term erosion hazard zone.
2. NRCS soil mapping. Detailed soils mapping by the NRCS were also considered when defining the long-term erosion hazard zones. Soil unit boundaries were used to distinguish areas of recent floodplain formation (deposition), active channel processes (erosion), and

recently abandoned channels and floodplains (avulsions) from alluvial fan and stream terraces.

3. 100-year floodplain. In general, areas mapped within the 100-year floodplain are within the long-term erosion hazard zone, except where geomorphic evidence strongly contradicts the floodplain limits or where flooding is the result of ponding, backwater, or other non-erosive low velocity flow.
4. Active channel position. The long-term erosion hazard zones are wider in areas where the active channel directly impinges on older geomorphic surfaces.
5. Avulsion potential. The long-term erosion hazard zone encompasses the areas subject to future avulsions. Avulsions form in response to processes of channel aggradation, capture of the main channel by overflow channels, excessive overbank flow, and capture of the main channel by tributaries.
6. Tributary position. The long-term erosion hazard zone is wider in reaches where tributaries are located close to the main channel and where significant overbank flooding occurs, where stream capture has the potential to occur.
7. Floodplain flow concentrations. The long-term erosion hazard zone is wider in reaches where visual characteristics or floodplain topography indicates that flow concentrates in (moderately) well defined alignments. Concentrated overbank flow is more erosive than unconcentrated overbank flow, and can lead to avulsions or braided/anastomosing channel patterns.
8. Channel pattern. The long-term erosion hazard zone is wider in reaches with braided, anastomosing, or distributary channel patterns than in straight, single channel reaches.
9. Channel pattern evolution. The long-term erosion hazard zone considers the expected direction of long-term movement of channel bends, meanders, and braids.
10. Floodplain width. The long-term erosion hazard zone considers the distribution of wider and narrower portions of the geologic floodplain, recognizing the potential for a more uniform width to develop with time.
11. Bedrock. The presence of bedrock in the banks was considered the outer boundary of the long-term erosion hazard zone, except where the 100-year floodplain elevation was significantly higher than the elevation of the bedrock outcrop.
12. Aggradation/degradation potential. Reaches of expected degradation are subject to erosion by undercutting. Reaches of expected aggradation are subject to erosion by braiding. Long-term erosion hazard zones are wider in reaches with expected future bed elevation changes than in more vertically stable reaches.
13. Field criteria. Evidence of on-going lateral erosion was considered in development of the long-term erosion hazard zones.
14. Topographic relief. Areas of very low relief were generally considered depositional, rather than erosional. Floodplain relief was considered evidence of overbank channelization processes.
15. Long-term channel stability. The long-term erosion hazard zone encompasses a belt width sufficient to allow expected channel processes to continue or occur over the long-term without impact by human activities along the stream corridor.

The following criteria were used to delineate the **lateral migration erosion hazard zones** for the Agua Fria River:

1. Relative hazard. The lateral migration erosion hazard zone is located within the moderate hazard zone boundaries, but outside the severe erosion hazard zone.
2. Geomorphic surfaces. Holocene-aged and recent geomorphic surfaces are generally located within the lateral migration erosion hazard zone. Surficial characteristics such as vegetation (type, density, age), desert varnish, desert pavement, soil color, drainage texture, and topographic relief were used to distinguish surfaces of different age. Soil descriptions from test pits were also collected to support estimates of age of the geomorphic surfaces.
3. 100-year floodplain. In general, the lateral migration erosion hazard zone is mapped within the 100-year floodplain, except where the 100-year flood limit is defined by a steep erosive cliff or bank, or where unique geologic conditions exist.
4. Active channel position. The lateral migration erosion hazard zones are wider in areas where the active channel directly impinges on older geomorphic surfaces.
5. Avulsion potential. The lateral migration erosion hazard zone encompasses the areas subject to future avulsions identified using topographic features within the floodplain, historical thalweg position, field interpretation, and active channel morphology. Avulsions form in response to processes of channel aggradation, capture of the main channel by overflow channels, excessive overbank flow, and capture of the main channel by tributaries.
6. Tributary position. The lateral migration erosion hazard zone is wider in reaches where tributaries are located close the main channel and where significant overbank flooding occurs, where stream capture has the potential to occur.
7. Floodplain flow concentrations. The lateral migration erosion hazard zone is wider in reaches where visual characteristics or floodplain topography indicates that flow concentrates in (moderately) well defined alignments. Concentrated overbank flow is more erosive than unconcentrated overbank flow, and can lead to avulsions or braided/anastomosing channel patterns.
8. Channel pattern. The lateral migration erosion hazard zone is wider in reaches with braided, anastomosing, or distributary channel patterns than in straight, single channel reaches.
9. Channel pattern evolution. The lateral migration erosion hazard zone considers the expected direction of long-term movement of channel bends, meanders, and braids.
10. Floodplain width. The lateral migration erosion hazard zone considers the distribution of wider and narrower portions of the geologic floodplain, recognizing the potential for a more uniform width to develop with time.
11. Bedrock. The presence of bedrock in the banks was considered the outer boundary of the lateral migration erosion hazard zone, except where the 100-year floodplain elevation was significantly higher than the elevation of the bedrock outcrop.
12. Aggradation/degradation potential. Reaches of expected degradation are subject to erosion by undercutting. Reaches of expected aggradation are subject to erosion by braiding. Lateral migration erosion hazard zones are wider in reaches with expected future bed elevation changes than in more vertically stable reaches.
13. Field criteria. Evidence of on-going lateral erosion was considered in development of the lateral migration erosion hazard zones.

14. Topographic relief. Areas of very low relief were generally considered depositional, rather than erosional. Floodplain relief was considered evidence of overbank channelization processes.

15. Historical channel change. The lateral migration erosion hazard zone encompasses the limits of past locations of channel thalwegs and banks, as digitized from historical aerial photographs and maps.

16. Floodway. The lateral migration erosion hazard zone is generally located outside the FEMA 100-year floodway delineated by others.

17. HEC-6 results. The lateral migration erosion hazard zone includes a setback from the existing channel bank a distance equal to the probability-weighted bank erosion estimate derived from the HEC-6 future conditions sediment deficit applied over a 60 year planning period, plus the 100-year HEC-6 future conditions sediment deficit.

18. Regime width. The lateral migration erosion hazard zone is at least as wide as the predicted 2-, 10-, or 100-year regime channel width, if wider than the existing active channel.

19. Stable slope. Where the floodplain abuts an oversteepened bank, a 3:1 stable slope was assumed to define the minimum limits of the lateral migration erosion hazard zone. In some cases such as in Reach 6, naturally stable slopes of similar height are present. In these cases the observed stable slopes were used to define the limits of the lateral migration erosion hazard zone from the toe of the existing bank. Stable slope lengths in this area are about 300 feet.

The following criteria were used to delineate the **severe erosion hazard zones** for the Agua Fria River:

1. Relative hazard. The severe erosion hazard zone is located within the moderate and lateral migration erosion hazard zones.

2. Geomorphic surfaces. The severe erosion hazard zone is coincident with the active channels, intermediate islands between active channels, incipient avulsion areas, areas immediately adjacent to active channels. These surfaces are generally of late Holocene or modern age. Surficial characteristics such as vegetation (type, density, age), desert varnish, desert pavement, soil color, drainage texture, and topographic relief were used to distinguish surfaces of different age. Soil characteristics from exposures observed in the field were also considered in support of estimates of age of the geomorphic surfaces.

3. 100-year floodplain. In general, the severe erosion hazard zone is mapped within the 100-year floodplain, except where the 100-year flood limit is defined by a steep erosive cliff or bank, or where unique geologic conditions exist.

4. Active channel position. The severe erosion hazard zones are wider in areas where the active channel directly impinges on older geomorphic surfaces.

5. Avulsion potential. The severe erosion hazard zone encompasses the areas subject to avulsions identified using topographic features within the floodplain, historical thalweg position, and active channel morphology. Avulsions form in response to processes of channel aggradation, capture of the main channel by overflow channels, excessive overbank flow, and capture of the main channel by tributaries.

6. Channel pattern. The severe erosion hazard zone is wider in reaches with braided, anastomosing, or distributary channel patterns than in straight, single channel reaches.

7. Bedrock. The presence of bedrock in the banks was considered the outer boundary of the severe erosion hazard zone, except where the 100-year floodplain elevation was significantly higher than the elevation of the bedrock outcrop.
8. Aggradation/degradation potential. Reaches of expected degradation are subject to erosion by undercutting. Reaches of expected aggradation are subject to erosion by braiding. Severe erosion hazard zones are wider in reaches with expected future bed elevation changes than in more vertically stable reaches.
9. Field criteria. Evidence of on-going lateral erosion was considered in development of the severe erosion hazard zones.
10. Historical channel change. The severe erosion hazard zone encompasses the limits of past locations of channel thalwegs and banks, as digitized from historical aerial photographs and maps.
11. HEC-6 results. The severe erosion hazard zone includes a setback from the existing channel bank a distance equal to the 100-year future conditions bank erosion estimate derived from the HEC-6 modeling.
12. Stable bank slope. The severe erosion hazard zone is set back from the existing channel bank a distance equal to three times the bank height, to allow erosion of the bank to a more stable 3:1 slope.
13. Regime width. The severe erosion hazard zone is at least a wide as the predicted 2- or 10-year regime channel width, if wider than the existing active channel.
14. Gravel pits. Gravel pits which cross or abut portions of the 100-year floodplain and are not protected by engineered measures from inundation during the 100-year flood were included in the severe erosion hazard zone.

8.4 Areas of Special Concern

Field observations and delineation of the erosion hazard zones revealed numerous areas of special concern. These areas of special concern are described in the following paragraphs. First, general comments are presented which address concerns observed throughout the study area or at multiple locations in the study area. The general comments are followed by a table of the specific areas of special concern. For each area listed, a potential solution(s) to the problem is provided. A map showing the locations of the areas of special concern is provided in the Exhibit Maps Book.

8.4.1 General Comments

1. The FEMA floodway is often incongruent with the geomorphic floodway. That is, the floodway is mapped as within active braided channel areas. This discrepancy is found in many areas throughout the study area, and suggests that a new floodway delineation is justified for the entire study reach.
2. Gravel pits in the study reach are often situated where they are at risk of intercepting or capturing the main channel, especially in the event of a breach of the levees or dikes that sometimes "protect" the mine from erosion and flooding. The propagation of severe headcuts upstream from the pits is a likely outcome of a breach and stream capture. The constantly changing nature of the pits also makes it difficult to predict the flow path and erosive potential of a given flood. Any number of eddies could result from a breach leading to accelerated erosion along steep unstable pit walls. Additionally, clearwater discharges

that would exit the pit into the river downstream create the potential for clearwater scour downstream.

3. Locations of significant cutbanks along the margin of the floodplain present a hazard outside the delineated flood limits. These cutbanks are often along Pleistocene-aged (< 10,000 years old) surfaces adjacent to the active channel of the Agua Fria River. The height of these cutbanks is in excess of 40 feet in some areas. Lateral migration erosion hazard limits have been identified along these cutbanks. These limits were set at a distance equivalent to the stable slope width observed at locations elsewhere along these terraces where the river is not actively eroding along the terrace. In general this distance is about 300 feet.
4. The bank protection and fill slopes along the terrace downstream of Grand Avenue is visually unappealing. Currently many of the fill slopes are covered by ugly piles of broken concrete, asphalt, and other assorted materials. Additionally, garbage is often dumped off of these terraces creating an environmental and health hazard. Adoption of a fill slope and/or bank protection treatment guideline should be considered for the watercourse master plan.
5. The downstream-most portion of the study area, south of the Broadway Road alignment, lies within the FEMA floodplain and geologic floodplain of the Gila River. Considerations of the flood and erosion hazards in this reach should include both the Agua Fria River and the Gila River.
6. The adequacy of existing bank protection measures in the study area needs to be evaluated. In particular, numerous reaches of privately developed land along the river has bank protection of various types for which no design plans appear to be available. A complete inventory of the existing bank protection measures and their design standards (e.g. toe down depth, D50, etc.) should be made as part of the watercourse master plan.
7. An inventory of bridges within the study area should also be conducted, including the information on the depth of the piers and abutments, design of scour protection, and channel stabilization, and any available information on bed elevation changes since construction. These data should be available through the data compiled for the bridge scour assessment program mandated by the federal government for completion in 1997. It is likely that many of the bridges in the study reach may be scour vulnerable, particularly if a reasonable estimate of long-term scour is included in the evaluation. Long-term channel degradation caused by gravel mining and the impacts of New Waddell Dam probably were not adequately recognized in the existing scour assessments.
8. An inventory and evaluation of protection of powerline facilities and other utility crossings within the river should also be conducted to determine the level of existing protection, the potential and risk of future failure, and alternatives for erosion protection. It is likely that some of these facilities are susceptible to erosion damage.
9. An inventory and evaluation of the adequacy of the existing grade control structures within the river should also be conducted to determine appropriate toe-down relative to local and long-term scour predictions, lateral tie-in and potential for flanking, and the need for additional structures. It is likely that some of these facilities are susceptible to erosion damage or do not provided the intended level of protection.

8.4.2 Location Specific Comments

Specific locations with erosion or stability concerns are identified in Table 8-2. These areas encompass over 11 square miles of land area located along the study reach. The specific locations of concern are listed in Table 8-2. An ArcView shapefile with a similar data table to that of Table 8-2 is provided on CD-ROM at the end of the Lateral Migration Report notebook.

Table 8-2 Locations and Nature of Areas of Concern

No.	Location	Nature of Problem	Possible Solution & EHZ
Reach 1			
1	T6N, R1E, Sec. 32. NE1/4	Stand of mesquite trees in right overbank, not currently in floodplain, part of old floodplain fringe. Habitat value.	Non-structural – LMEHZ or LTEHZ
2	T6N, R1E, Sec. 29, SE1/4 32, NE1/4	Intermittently very dense riparian vegetation. Standing water from Morgan City Wash inflow. Series of intermittently connected ponds. Habitat value.	Non-structural – mostly within floodway and LMEHZ or SEHZ
Reach 2			
3	T5N, R1E, Sec.5, NE1/4, T6N, R1E, Sec.32, SW1/4, SE1/4	Old gravel pit with headcutting progressing upstream. Depth of pit about 15 ft max. Current headcutting about 4 feet deep upstream to about 1400 feet from deepest part of pit	1) fill pit 2) grade control 3) do nothing – potential upstream limit of effects into intermittent riparian area upstream (to about 2nd downstream-most pool); SEHZ
4	T5N, R1E, Sec. 5, near center	Structures in right overbank area	Move, flood warning, leave there until damaged, then move activity elsewhere; SEHZ & LMEHZ
5	T5N, R1E, Section line between Sec. 5 and Sec. 8	At grade Cowtown Road crossing, potential for stranding people on west side, also hazard to life if crossed during flow	Build a bridge; Flood warning, Repair whenever damaged; SEHZ
6	T5N, R1E, Sec. 8, W1/2, NE1/4	8-16 ft high cutbank along left bank	Non-structural - LMEHZ & LTEHZ; Bank protection; Monitor
7	T5N, R1E, Section line between Sec. 8 and Sec. 17	CAP siphon, burial depth approx. 25 feet Potential long-term scour threat; Also, big scour hole at blowout structure	Grade control at some point in time; monitor Energy dissipater, additional scour protection measures; monitor; SEHZ
102	T5N, R1E, Sec. 8, NE1/4	Powerline tower near cutbank	Monitor, relocate when necessary; LTEHZ
Reach 3			
8	T5N, R1E, Sec. 17, N1/2	Active cutbank erosion of right bank adjacent to Beardsley Canal flume right abutment; metal jacks currently in place, but apparently not doing much	Monitor; structural bank protection measures; targeted protection for Beardsley Canal abutment; SEHZ
Reach 4			
9	T5N, R1E, Sec. 17, SE1/4, Sec. 20, NE1/4	1996 floodplain boundaries incongruent with surface characteristics and topography	Re-evaluate floodplain boundary; Non-structural - LMEHZ (see also Figure 2-43)
10	T5N, R1E, Section line between Sec. 20 and Sec. 21	Active cutbank erosion of left bank, 25-40 feet high cutbank	Monitor; Non-structural - LMEHZ

No.	Location	Nature of Problem	Possible Solution & EHZ
11	T5N, R1E, Section line between Sec. 20 and Sec. 21	Possible avulsion area in left overbank area outside of current floodplain. Location of old canal heading?	Non-structural – LMEHZ; Structural - levee and/or bank protection
12	T5N, R1E, portions of Sec. 17	FEMA floodway incongruent with geomorphic floodway in right portion of channel, i.e. floodway encroached into active braided channel areas	Non-structural – geomorphic definition of floodway or no rise floodplain; SEHZ
13	T5N, R1E, portions of Sec. 20, 28, & 29	Broad area of floodway fringe in lateral migration erosion hazard zone	Non-structural – SEHZ & LMEHZ
14	T5N, R1E, Sec. 29, E1/2 SW1/4, and Sec. 32 W1/2, NW1/4	FEMA floodway incongruent with geomorphic floodway along right edge of floodway, i.e. floodway encroached into active braided channel areas	Non-structural – geomorphic definition of floodway or no rise floodplain; SEHZ
Reach 5			
15	T5N, R1E, Sec. 32	FEMA floodway incongruent with geomorphic floodway along left edge of floodway, i.e. floodway encroached into active braided channel areas	Non-structural – geomorphic definition of floodway or no rise floodplain; SEHZ & LMEHZ
16	T5N, R1E, Sec. 32	Jomax Road crossing; at grade	Bridge; flood warning; repair as necessary; SEHZ
17	T5N, R1E, Sec. 32; T4N, R1E, Sec. 5	Broad area of floodway fringe in lateral migration erosion hazard zone	Non-structural – LMEHZ
18	T4N, R1E, Sec. 5 & Sec. 7	Broad area of floodway fringe in lateral migration erosion hazard zone	Non-structural – LMEHZ
19	T4N, R1E, Sec. 7, N1/2	Hatfield Road crossing, at grade	Bridge; flood warning; repair as necessary; SEHZ
20	T4N, R1E, Sec. 5, W1/2	107th Ave. runs parallel to river in left overbank of floodplain	Elevate; flood warning; Relocate divert east to Hatfield then out to Lake Pleasant Road; LMEHZ
21 & 22	T4N, R1E, Sec. 7	Powerline towers, in river and one is about 600 ft upstream of Cemex gravel pit – i.e. headcut and undermining powerline	Protect powerline foundation; install grade control; span powerline across river; SEHZ
Reach 6			
23	T4N, R1E, Sec. 7	Cemex gravel pit in historic main channel; diverts flow; headcut potential	Protect gravel levees with more hardened measures; Reclaim mine; SEHZ
24	T4N, R1E, Sec. 7, W1/2	FEMA floodway incongruent with geomorphic floodway along right edge of floodway, i.e. floodway encroached into area of outflow of Twin Buttes Wash and high flow channels of Agua Fria	Non-structural – geomorphic definition of floodway or no rise floodplain; SEHZ
25	T4N, R1E, Sec. 18, W1/2	Gravel pit in one of primary braids; headcut potential	Protect gravel levees with more hardened measures; Reclaim mine; SEHZ
26	T4N, R1E, Sec 18, NE1/4	FEMA floodway incongruent with geomorphic floodway along left edge of floodway, i.e. floodway encroached into historic main channel downstream of Cemex gravel pit	Non-structural – geomorphic definition of floodway or no rise floodplain; SEHZ
27	T4N, R1E, Sec 18, NW1/4	Structure (home) in LTEHZ	Monitor, address if problem arises; LTEHZ

No.	Location	Nature of Problem	Possible Solution & EHZ
28	T4N, R1E, Sec. 18, E1/2, and Sec. 19, N1/2	25-30 ft high cutbank; interesting visual feature	Monitor; Non-structural – LMEHZ; create stable slope (mimic old terrace profile); use material to reclaim inactive mines
29	T4N, R1E, Sec. 18, and Sec. 19, N1/2	Overhead powerline towers and poles in channel aligned roughly parallel to flow and upstream of gravel pit	Monitor, reinforce towers and poles; SEHZ
30	T4N, R1E, Sec 18, SW1/4, Sec 19, NW1/4, T4N, R1W, Sec. 13, SE1/4, Sec. 24, NE1/4	Gravel pit, possible breach from primary braid on upstream side leading to inundation outside of current floodplain; Possible breach from right bank of main channel over low 1 ft bank leading to possible eddying and erosion resulting in breach of access road to deeper active pits outside of current floodplain	Reclaim inactive areas; reinforce road to prevent further breaching; SEHZ
31	T4N, R1W, Sec. 24, E1/2	Housing development in historic floodplain situated precariously between two gravel pits	Buy out; flood warning; structural protection; SEHZ
32	T4N, R1E, Sec. 19, SW1/4, T4N R1W, Sec. 24, SE1/4	Gravel pit situated in main channel, very deep, active headcutting upstream	Reclaim inactive areas; reinforce levees and pit walls; SEHZ
33	T4N, R1E, Sec 19, and T4N, R1W, Sec 24 boundary	Rose Garden Lane at grade crossing, bank protection downstream is being undermined by active headcutting from downstream pit	Flood warning, repair as necessary; SEHZ
34	T4N, R1E, Sec 19 W1/2, Sec 30 W1/2, Sec 31 W1/2; T4N, R1W, Sec 25, E1/2, Sec 36, E1/2; T3N, R1E, Sec 6, W1/2; T3N, R1W, Sec 1, NE1/4	Geologically young surface; reduced discharges and probable degradation of channel make likelihood of future inundation slight; concern is with lateral erosion upstream of Beardsley flanking existing bank protection and between Paradise Lane and Greenway Road alignments	Monitor bank positions; bank protection tied into existing Coyote Lakes bank protection; LTEHZ
35	T4N, R1E, Sec. 19, W1/2	Location of waste water treatment facility on left overbank on geologically young surface	Monitor bank positions; bank protection tied into existing Coyote Lakes bank protection; LTEHZ
Reach 7			
36	T4N, R1W, Sec 25, W1/2	25-40 ft cutbank	Monitor, non-structural - LMEHZ & LTEHZ
37	T4N, R1W, Sec. 36, W1/2	10-20 ft cutbank	Monitor, non-structural – LMEHZ & LTEHZ
38	T4N, R1W, Sec 36 & T3N, R1W, Sec. 1 boundary	Bell Road Crossing, bridge and approach embankment, significant channel constriction; downstream gravel pit could possibly impact structure	Grade control; connect embankment dikes on left bank, upstream side; SEHZ
39	T4N, R1W, Sec. 25, E1/2, Sec. 36, E1/2	FEMA floodway incongruent with geomorphic floodway along left edge of floodway, i.e. floodway encroached into historic main channel adjacent to Coyote Lakes development	Non-structural – geomorphic definition of floodway or no rise floodplain; SEHZ

No.	Location	Nature of Problem	Possible Solution & EHZ
40	T4N, R1W, Sec. 36, SE1/4	Area outside of FEMA floodplain within EHZ	Non-structural – SEHZ
Reach 8			
41	T3N, R1W, Sec. 1 & 12, T3N, R1E, Sec. 7	Multiple gravel pits in channel and in overbank floodplain, headcutting in main channel; visually unappealing; channel over-constricted	Reclaim; widen channel; channelized along floodway; non-structural okay if mining ceased; SEHZ
42	T3N, R1W, Sec. 1, NW1/4	Cutbank along right bank at trailer park	Monitor; bank protection; LMEHZ & LTEHZ
43	T3N, R1E, Sec. 7, W1/2	Cutbank along left bank near Sun City upstream of Grand Ave.	Monitor; non-structural – LMEHZ
108	T3N, R1E, Sec. 18, W1/2	Cutbank along left bank at Youngtown residential structures downstream of Grand Avenue	Monitor; bank protection; LMEHZ
44	T3N, R1E, Sec. 7 & 18	Very narrow channel reach between terrace and gravel pit and landfill and terrace downstream of Grand Avenue	Formally channelized including grade control; SEHZ
45	T3N, R1W, Sec. 13	Culverts under US 60 / Grand Avenue and floodplain downstream west of landfill	Block off culverts and direct flow to Grand Ave. bridge; Channelize outflow downstream back to Agua Fria along west edge of landfill; LMEHZ & LTEHZ
46	T3N, R1E, Sec. 18, SW1/4	Fill along left bank terrace jutting out into channel being attacked by braid from main low flow channel	Improve bank protection; improve visual character of fill slope(s); SEHZ
47	T3N, R1E, Sec. 18, W1/2	Cholla Landfill is an island in the floodplain. The bank protection probably not adequate. There are long-term problems associated with a landfill at this location.	Protect adequately; Remove landfill; LMEHZ & LTEHZ
Reach 9			
48	T3N, R1E, Sec. 19, NW1/4	Cutbank along left bank terrace	Monitor; bank protect; Non-structural - LMEHZ
49	T3N, R1W, Sec. 24	Erosion hazard area outside current floodplain	Implement LMEHZ; structural solution to remove area from potential erosion
50	T3N, R1W, Sec. 24, SE1/4, Sec. 25, E1/2	Broad area of fringe in LMEHZ	Non-structural – LMEHZ
51	T3N, R1W, Sec. 25, Sec. 30	Lateral migration erosion hazard outside current FEMA floodplain	Non-structural – LMEHZ
52	T3N, R1W, Sec. 25, NW1/4	Erosion hazard outside current FEMA floodplain along right bank	Non-structural – SEHZ & LMEHZ; bank protection
53	T3N, R1W, Sec. 25, SW1/4	Cutbank along right bank	Non-structural – LMEHZ & LTEHZ; bank protection
104	T3N, R1E & R1W, Sec. 18, 24, & 30	Powerlines in floodplain	Monitor, investigate structural requirements; SEHZ & LMEHZ
105	T3N, R1E & R1W, Sec. 18, 24, & 30	Powerlines in floodplain	Monitor, investigate structural requirements; SEHZ & LMEHZ

No.	Location	Nature of Problem	Possible Solution & EHZ
106	T3N, R1E, Sec. 31	Overhead utilities in floodplain	Monitor, investigate structural requirements; LMEHZ
107	T3N, R1W, &1E, Sec. 13-24 line, Sec. 18-19 line	Overhead utilities in floodplain	Monitor, investigate structural requirements; SEHZ, LMEHZ, & LTEHZ
Reach 10			
54	T3N, R1W, boundary between Sec. 25 & 36	Olive Ave. bridge – deep gravel pit downstream about 700 feet (see also No. 55) – headcutting threat to bridge foundation	Grade control; SEHZ
55	T3N, R1W, Sec. 36, N1/2	Gravel pit, very deep (> 20 ft) in floodway downstream of Olive Ave.	Reclaim; grade control upstream; SEHZ
56 & 57	T3N, R1W, Sec. 36, E1/2	Two areas of piles of roadway debris	Clean up (fill in pit above?); SEHZ
58	T3N, R1W, Sec. 36, NE1/4	Old gravel pit in left overbank	Reclaim; SEHZ
59	T3N, R1W, Sec. 36, SE1/4	Cutbank along left bank	Non-structural – SEHZ; also in floodway; Bank protection
60	T3N, R1W, Sec. 36, E1/2, T3N, R1E, Sec. 31, NW1/4	Active gravel pits some expanded outside current floodplain	Redelineate floodplain; Non-structural – SEHZ; Reclaim
61	T3N, R1W, Sec. 36, SE1/4	FEMA floodway incongruent with geomorphic floodway along left edge of floodway, i.e. floodway encroached into area of historic high flow channels	Non-structural – geomorphic definition of floodway or no rise floodplain; SEHZ
62	Along section line between T3N, R1W, Sec. 36 and T2N,R1W, Sec. 1	At-grade Northern Avenue crossing	Flood warning; repair as necessary; Bridge; SEHZ
63	T2N,R1W, Sec. 1	Extremely narrow low flow channel around west edge of gravel pit	Widen to width of Glendale Ave. bridge; SEHZ
109	T2N, R1W, Sec. 1-12 line	Glendale Ave. bridge is extremely narrow relative to floodplain; significant contraction scour and long-term degradation	Widen bridge opening; SEHZ
110	T2N, R1W, Sec. 1, NE1/4	Glendale Recycling Facility levee within floodplain and below BFE along upstream portion of levee.	Raise levees; Widen conveyance in gravel pit to west and widen Glendale Ave. bridge; LMEHZ
64 & 65	T2N,R1W, Sec. 1, NW1/4	Two areas of active cutbanks along west terrace in narrow reach	Non-structural – LMEHZ & LTEHZ; Bank protect; Increase channel width (lessen flow against bank)
66	T2N,R1W, Sec. 1	Area of multiple large gravel pits and mining area	Reconfigure channel and mine activities; SEHZ
67	T2N,R1W, Sec. 1 & Sec. 12	Area of large vegetation largely within narrow channel downstream of Dysart Drain – high roughness in narrow channel	Cut trees; widen channel; make better use of water in watershed upstream; SEHZ
101	T2N, R1W, Sec. 12, NE1/4	Glendale Aquifer Recharge Facility partially in floodplain	Raise dikes if necessary; monitor and repair as required; SEHZ & LMEHZ

No.	Location	Nature of Problem	Possible Solution & EHZ
68	T2N,R1W, Sec. 12, SE1/4	Gravel pit in left overbank and jutting out into floodway; headcut potential; redirecting of floodwaters and erosion	Keep out of floodway; Reclaim; SEHZ
69	T2N,R1W, Sec. 12, S1/2	Area of new road and some kind of apparent drainage facilities under construction	Probably should not be constructed in floodplain. Check permitting; SEHZ
70	T2N,R1W, Sec. 12 & Sec. 13	Avulsion hazard in right overbank heading about 1400 feet downstream of Glendale Ave.	Non-structural – no rise floodplain; LMEHZ; levee and/or channelize
71	T2N,R1W, Sec. 12 & Sec. 13	Avulsion hazard in right overbank heading about 4500 feet downstream of Glendale Ave.	Non-structural – no rise floodplain; LMEHZ; levee and/or channelized
72	T2N,R1W, Sec. 13	Multiple gravel pits in right overbank; headcutting could cause possible capture of main channel via avulsion channels listed above	Reclaim; grade control upstream of pits; levee and/or channelize at avulsion locations upstream; SEHZ
73	T2N,R1E, Sec. 18, NW1/4	Erosion hazard potentially flanking soil cement levee around new Glendale water treatment facility	Monitor; Extend levee if required; LTEHZ
Reach 11			
111	T2N, R1E, Sec. 18 & 19	Soil cement levees north and south of Camelback Road are not connected. A 450 foot gap bridged only by the roadway embankment poses a potential opening to erosion east of the south levee	Connect the levees with soil cement or other engineered bank protection along the upstream side of Camelback Road; LMEHZ & LTEHZ
74	T2N,R1E, Sec. 18, & Sec. 19	Scour problem along east levee and at Camelback Road	Grade control; widen and/or reconfigure low flow channel from New River upstream; SEHZ
75	T2N, R1W, Sec. 13 & 24, T2N,R1E, Sec. 18, & 19	Camelback Road bridge – potential scour problems associated with headcutting from downstream gravel pit	Grade control; widen and/or reconfigure low flow channel from New River upstream; SEHZ
76	T2N, R1W, Sec. 24, T2N,R1E, Sec. 19	Gravel pits in main channel downstream of Camelback Road; headcutting and scour of levees and bridge	Grade control; widen and/or reconfigure low flow channel from New River upstream; reclaim; SEHZ
77	T2N, R1W, Sec. 24, SE1/4	Very deep gravel pits downstream of wing dikes – potential for gathering backwater flows and eddy currents enlarging pits	Connect wing dike to levee at Indian School Road; LMEHZ
Reach 12			
78	T2N, R1W, Sec. 25, NW1/4	Stand of large trees in channelized reach	Protect from cutting; SEHZ
80	T2N, R1W, Sec. 36	Grade control – some scour downstream	Monitor; SEHZ
81	T2N, R1W, Sec. 35	Grade control – some scour downstream	Monitor; SEHZ
82	T1N, R1W, Sec. 2	McDowell Road bridge – looks okay now	Monitor; SEHZ
Reach 13			
83	T1N, R1W, Sec. 2	Interstate 10 bridge – looks okay now	Monitor; SEHZ

No.	Location	Nature of Problem	Possible Solution & EHZ
84	T1N, R1W, Sec. 2	Grade control – some scour downstream	Monitor; SEHZ
85	T1N, R1W, between Sec. 2 & 11	Van Buren Street bridge – looks okay now	Monitor; SEHZ
86	T1N, R1W, Sec. 11	Grade control – some scour downstream	Monitor; SEHZ
87	T1N, R1W, between Sec. 11 & 14	Railroad and Buckeye Road bridge – large riprap under west two-thirds of bridge visible – unknown if protection exists for east third	Monitor; Extend riprap on east third if missing; SEHZ
Reach 14			
88	T1N, R1W, Sec. 14, S1/2	Area of headcutting upstream of Lower Buckeye Road	Non-structural – within floodway and SEHZ; Monitor
89	T1N, R1W, Sec. 14, SW1/4	Floodway fringe area mapped between levees	Redefine floodway boundary; SEHZ
90	T1N, R1W, between Sec. 14 & 23	Lower Buckeye Road at-grade crossing with two small elliptical culverts	Flood warning; repair as necessary; Span with a bridge; SEHZ
91	T1N, R1W, Sec. 14	Powerline tower with erosion hazard from scour and lateral erosion	Monitor; Research footing adequacy; replace if necessary; SEHZ
92	T1N, R1W, Sec. 22, SW1/4	Powerline tower with erosion hazard from lateral erosion	Monitor; Research footing adequacy; replace if necessary; SEHZ
94	T1N, R1W, Sec. 14, 22, 23, & 27	Powerline in river; specific towers of concern listed above, others may become problematic	Monitor; Research footing adequacy; replace if necessary; SEHZ
95	T1N, R1W, Sec. 22, NE1/4	Area of active cutbank about 3-4 feet near toe of soil cement levee	Monitor; SEHZ
96	T1N, R1W, Sec. 23, NW1/4, Sec. 22, E1/2, Sec. 27, N1/2	FEMA floodway incongruent with geomorphic floodway along left edge of floodway, i.e. floodway encroached into area of historic high flow channels	Non-structural – geomorphic definition of floodway or no rise floodplain; SEHZ
97	T1N, R1W, Sec. 22, SE1/4	Area of agricultural storage facilities behind earthen dike in floodplain	Move facilities; Reinforce dike; Repair and replace as necessary; SEHZ & LMEHZ
98	T1N, R1W, Sec. 22, SW1/4	Area of erosion hazard outside floodplain with existing homes and other structures	Extend west levee downstream; Monitor; LMEHZ & LTEHZ
103	T1N, R1W, Sec. 22, SW1/4	Powerline tower experiencing significant scour	Check toe down and structural safety; SEHZ
Reach 15			
93	T1N, R1W, Sec. 27, NW1/4	Powerline tower with erosion hazard from scour	Monitor; Research footing adequacy; replace if necessary; SEHZ
99	T1N, R1W, Sec. 27, NW1/4	Sand and gravel mine and processing area	Reclaim when mining ceases; SEHZ & LMEHZ
100	T1N, R1W, Sec. 27, 28, 33, and 34	Gila River floodplain and historical area of channel movement	Non-structural – SEHZ, LMEHZ, & LTEHZ

No.	Location	Nature of Problem	Possible Solution & EHZ
112	T1N, R1W, Sec. 27 & 28	Water supply line for the Palo Verde Nuclear Generating Station has a top of pipe elevation of about 900 feet which was about 20 feet below the river bed in 1988 (Jerry Jones topography)	Monitor degradation in this reach near the water line; protect if it becomes necessary; SEHZ, LMEHZ, & LTEHZ
Notes: EHZ = Erosion Hazard Zone; SEHZ = Severe EHZ; LMEHZ = Lateral Migration EHZ; LTEHZ = Long-Term EHZ			

Numerous areas along the Agua Fria River study reach are subject to various degrees of erosion hazards. Some areas may require immediate structural fixes. Others may be monitored until the point in time when imminent failure is likely. Many areas can be mitigated by adoption of the lateral migration hazard zone as the effective regulatory floodway (i.e. prevent further development within the lateral migration hazard zone). Gravel pits and long-term degradation of the Agua Fria River post the most significant erosion hazard in the study area. Erosion hazard zone limits should be updated on the regulatory maps in areas where erosion hazards are mitigated by engineered measures in the future.

8.5 Summary

The recommended erosion hazard zones for the Agua Fria River Watercourse Master Plan study area developed using the criteria outlined above are shown on the Erosion Hazard Zone Maps in the Exhibit Maps Book.

9. COMPARISON WITH OTHER STUDIES

This chapter summarizes the results of previously completed channel stability, floodplain, planning, or design studies of the Agua Fria River prepared by others. The studies summarized below include the following:

- Carriaga, C.C., Mays, L.W., and Ruff, P.F., 1994, Agua Fria River Sediment Transport Study, for FCDMC, Arizona State University, Tempe, AZ, February 28, 1994.
- Simons, Li & Associates (SLA), 1988, Scour Analysis of the Agua Fria River between Lower Buckeye Road and Broadway Boulevard, report prepared for Brown & Caldwell, Feb. 8, 1988. Simons, Li & Associates (SLA), 1984, Draft, Final Sediment Transport Report, submitted to Los Angeles District, US Army Corps of Engineers, Project No. PAZ-COE-03, RDN/R439, July 16, 1984. Simons, Li & Associates (SLA), 1983, Final Report, Hydraulic and Geomorphic Analysis of the Agua Fria River, submitted to FCDMC, SLA Project No. AZ-MC-05, Revised Sept. 13, 1983.

In addition, several bridge reports and miscellaneous studies of the Agua Fria River are noted. The results are discussed for their similarity to the findings of this study. It should be noted that none of these studies were performed for the explicit purpose of evaluating lateral erosion hazards on the Agua Fria River.

9.1 ASU sedimentation study (Carriaga, et al., 1994)

The objective of the ASU study was to "develop sediment transport models capable of simulating the long-term stream bed profile behavior of the Agua Fria using HEC-6" such that the "results [could be] used as a basis for development of regulatory management practices for the Agua Fria River floodplain under post-New Waddell scenarios."

- Three HEC-6 models were created. Of primary interest to the current study is Model I – existing conditions with ACDC and New Waddell, although Model II (Model I + permitted sand and gravel mines) is also of interest for the impacts of sand and gravel mining.
- The study used Jerry Jones (1989) HEC-2 model as basis for the HEC-6 modeling performed. The Jerry Jones HEC-2 model was also used in the current study for the portions of the study reach upstream of Jomax Road and downstream of Indian School Road.
- The authors note that sediments decrease in size in the downstream direction. The current study found the same pattern.
- The 100-year results, while supposedly based on post-New Waddell discharges, reports 100-year discharges that do not match the values listed in the Corps of Engineers report (1995), presumably because the ASU study predates the final Corps of Engineers report. The 100-year discharge used in the ASU report was 32,000 cfs to 14,500 cfs from dam to Gila River. Using these discharges, they show bed changes variable along the study reach with a range between +1.7 to –8.4 feet. Overall, their models express net degradation of the river over whole study reach. This agrees with the findings of the current study, and generally agrees with the results of the KHA HEC-6 modeling.
- The ASU report found that bridge reaches were generally degrading. The SR74 and the Grand Avenue/AT&SF railroad bridges were noted as especially subject to degradation and

scour. Field evidence at Grand Avenue described in the current study agrees with the conclusions of the ASU study.

- Serious headcutting was noted upstream and downstream of gravel pits in Model II along with significant aggradation at the mining sites themselves. The current study has similar findings. Headcuts and/or reaches of abrupt increased slope were identified in the field and in historical data upstream of gravel pits. Deltas were also observed deposited within gravel pits both in the field and in historical aerial photographs.

9.2 Simons, Li & Associates Work for COE and FCD

Simons, Li, and Associates (SLA) performed a number of studies in the Lower Reach in the early to mid 1980's in support of the flood control planning and design which eventually led to the channelization and grade control construction in the Lower Reach. Specific results from two of the studies are listed below.

9.2.1 SLA, 1983, Final Report, Hydraulic and Geomorphic Analysis of the Agua Fria River

The objective of the 1983 SLA report was to "conduct a system analysis" including "an assessment of existing conditions in the reach, and an assessment of proposed flood control projects between Camelback and Buckeye," to "provide design plans and specifications for a flood control project between Camelback and Thomas." "(The) primary objective of this report is to provide baseline information on hydraulic and sediment transport characteristics of the Agua Fria for future flood control projects."

The report covers primarily the reach from the New River to the Gila River but the report also comments on the entire reach from the Gila to Waddell Dam.

- The report notes a general trend of degradation in past 20 years (i.e. 1960's to 1980's), reportedly caused by extraction of large quantities of sand and gravel and by constriction of the channel by levees put up to protect mining operations. These findings are in agreement with the findings of the current study.
- The report suggests armoring in the Agua Fria is probable. Armoring depths for the large events like the 100-year flood are computed, but were considered too deep to be effective in the current study. As such, the current study disputes the SLA finding that a realistic armoring potential exists in the study area.
- The 10-year discharge in the SLA study is 31,000 cfs with velocities between 5 to 7 ft/s. The 100-year discharge is 90,000 to 95,000 cfs with velocities between 7 to 10 ft/s. The 25-year discharge is 50,000 cfs with velocities between 5 to 8 ft/s. The 100-year flood in the current study is approximately equivalent to the 25-30-year flood in the SLA study.
- Predictions of long-term response of channel in the SLA report are as follows:
    - stable between the New River and Indian School Road
    - slight degradation from Indian School Road to Buckeye Road
    - slight aggradation from Buckeye Road to Broadway Road
    - stable from Broadway Road to the Gila River
    - The current study concludes that degradation is expected during large floods, with little or no measurable channel change during small floods or periods without flow.
- Recommendations from the SLA report include:

- The bed and bank materials are erodible. Therefore, protection is needed. The current study makes the same conclusion, except where engineered bank protection or bedrock are present.
- There is a long-term trend for slight degradation. Therefore, some grade control is needed. The current study reaches the same conclusion.
- No in-stream gravel mining should be allowed in channelized section (except to remove any bars or islands that may form). The current study reaches a similar conclusion, although mining recommendations are part of the watercourse master report.
- Bridge piers need to be protected from scour. The current study did not compute bridge scour, but generally concurs with the need for scour protection at the bridges, particularly for long-term scour protection.

- Sediments in the river were noted as mainly sands with traces of gravels. Median sediment diameter (D_{50}) is between 0.7 to 1.3 mm. Maximum sediment diameter (D_{max}) is noted as about 4 inches.
- The SLA reports that "complete armoring" near NR confluence has not taken place. Field observations in summer of 2000 showed that this is one of the only places where some degree armoring is currently visible in the study area.
- Sediments are reported to fine in downstream direction. This trend is also noted in the current study.
- Surface armoring from Bethany Home Road to Waddell Dam was called "very significant". No significant armoring was observed in the summer of 2000. The armor layer reported by SLA has either been covered by finer sediments, disrupted by human activity, or removed by flows in the river since 1983.
- Elsewhere, armoring was noted "near McDowell Road, Thomas Road, Van Buren Street, and near and above Bethany Home Road." However, the armoring noted, as shown in photos in the SLA report, suggests the "armor" size is frequently less than 2 inches. The current study concludes that such material would be transported at velocities less than 5 ft/s at the current channel slope of 0.003 ft/ft. The Van Buren to Thomas Road reach has subsequently been channelized and as mentioned above, no significant armoring was noted other than near the New River confluence during the current study.
- Bed lowering between 1973 and 1981 was noted. The thalweg comparison plot shows 0 - 10 foot differences. Bed lowering during this period was also noted as occurring across the entire cross section. These results are consistent with the results of the current study.
- Sand and gravel mining were noted as having caused channel entrenchment and increased instability. Similar conclusions are drawn in the current study.
- The Agua Fria River was characterized as a braided, ephemeral stream. The current study agrees, however, notes that the river has been and will likely become less braided in the future.
- The report states that no geologic controls are present to control bed elevation in lower Agua Fria River. The current study is in agreement for the Lower Reach. In Reaches 1 and 2 of the current study, bedrock limits vertical erosion locally.
- The report states that the New Waddell Dam "will have the greatest impact on the future developments because of the increased flood control and reduction of downstream peak discharges. The reduction in flood peaks will also reduce downstream sediment

transportation capacities and slow the degradation response of the bed. ACDC will increase sediment and water inflows into the study reach. However, the New River Dam will more than offset the increased flows and sediment discharges into the Agua Fria"(p. 4.29).

- The report also states that "(g)ravel mining has significantly altered the shape of the Agua Fria and is one of the causes of degradation throughout the study reach" (pg. 4.29).
- Slight degradation throughout the study reach was reported based on equilibrium slope calculations (for which they considered a 10-year flood (31,000 cfs)) except downstream of Buckeye Road. Further increased degradational effects were reported when a 25% reduction in sediment supply was assumed. The current study has similar conclusions for similar discharges.
- Bankfull widths from 500 to 3500 feet were reported with variable widths between the Gila River and Glendale Avenue. These widths in this reach reflect conditions prior to channelization. The current study computed somewhat narrower bankfull widths. This is likely due to the lower bankfull discharges identified in the current study. In the SLA study the 10-year flood was used and was said to fill the main channel. The definition of the main channel in the SLA report is also not self evident as no cross sections and bank stations are presented.

9.2.2 SLA, 1984, Draft, Final Sediment Transport Report

This report is related to the 1983 report and contains many of the same analyses and conclusions.

- The study reach was from Glendale Avenue to the Gila River.
- The analysis was a three level approach consisting of the following with the bulleted items being the primary pertinent conclusions from each level of analysis:

1. Qualitative Geomorphic Analysis:
    - There has been a general tendency for the Agua Fria to degrade over past 20-years.
    - The bed and bank materials in study reach are very susceptible to erosion.
    - Armor layer formation is possible.
    - New Waddell Dam will have an great impact on future channel morphology response in the study area.
2. Quantitative Geomorphic Analysis:
    - Long-term trends showed most areas in equilibrium or having a slight degradation potential.
    - Slight long-term aggradation was predicted between the New River and Indian School Road and between Lower Buckeye and Broadway Roads.
    - (Further) reductions in sediment supply from the Agua Fria upstream of New River should cause degradation in the study reach. SLA states concerns about supply reductions due to armoring between Glendale Avenue and the New River.
    - The USACOE plan (i.e. channelization and grade control) "has not increased the degradation potential from the existing conditions" according to the SLA report.

3. Mathematical Model Analysis:

    - Aggradation/degradation responses were evaluated as "minor," that is, less than one foot in magnitude, except between Indian School Road and the RID flume where degradation ranged from 1.4 to 3.9 feet.
    - Average annual aggradation/degradation for all locations was less than 0.2 feet.
    - Minor maintenance was indicated for the channelized reach (i.e., occasional removal of bars/islands in the channel may be required periodically to maintain flood capacity of channel).

- The Agua Fria is a braided, ephemeral stream with a wide floodplain, multiple low-flow channels, and naturally unstable.
- Human activity can increase instability.
- A decrease in width and increase in velocity over long-term was predicted.
- The report states that there is an overall tendency to for the channel to degrade in the 100-year flood and degrade or be in near equilibrium in the 10-year flood (post-Old Waddell discharges).
- Hydraulic results for the 25-year flood (approximately equal to the current 100-year flood) showed channel velocities between 5 to 7 ft/s and overbank velocities from 1 to 2 ft/s. About 90% of the flow is within their main channel for the 25-year discharge.
- Historical profiles between 1972 and 1983 show degradation throughout the SLA study reach from the New River to the Gila River. Amounts range from 0 to 8 feet. The greatest degradation was shown near the New River confluence and from Broadway Road to the Gila River.
- "Gravel mining effects are not limited to the gravel pit area. Headcuts can intitiate at the upper boundary of the gravel pit and extend far upstream. A gravel pit can also act as a sink, trapping sediment, resulting in a sediment transport imbalance, an dcouasin possible downstream degradation. The overall effect from instream mining, if the pits are deep and extend significant distances along the river, is channel entrenchment and increased channel instability. If constriction of the river due to levees (constructed by mining operators) is excessive, channel degradation can be induced. Thus, main channel and flood plain gravel mining operations can have an impact on future channel stabilization."
- Sediment discharge capacity is limited primarily to the main channel (as defined by SLA).
- Bankfull discharge was interpreted to be about the 10-year discharge (31,000 cfs at Camelback).
- Dynamic equilibrium slope was computed as 0.0016 to 0.0029 for various subreaches from Glendale Avenue to the Gila River. Most subreaches were near equilibrium except for from Indian School Road to I-10 which was shown as a degradation reach. This reach is now channelized and slope controlled by soil cement grade control structures.
- Static equilibrium slope was computed as 0.0005 to 0.0026 for the different subreaches in the SLA study. Most subreaches have a static equilibrium slope of about 0.001 or about one-half to one-third the existing bed slope. These results are very similar to the current study results presented in Chapter 6.
- Sediment discharges for the 10-year flood yield about 1.5 – 2.0 % concentrations.

- QUASED modeling of sediment transport for 100-year flood (post-Old Waddell discharges) generally shows greater net degradation at the end of the simulation than at the peak. While not discussed in the SLA report, this is likely the result of the 1.25 days of relatively constant flow at about 20,000 cfs at the end of the simulation. This suggests that prolonged moderate discharges may have more effect on bed elevation than higher, but brief duration discharges. The HEC-6 modeling performed for the Watercourse Master Plan showed similar tendencies even at flow rates of 9,000 cfs (see Figure 6-51).

9.3 Various bridge reports

Bridge scour analyses normally estimate long-term degradation or scour in addition to other scour components in evaluating or designing bridges. Total scour estimates are used to set elevations for the bottoms of piers and/or abutments not founded on bedrock. Several bridge reports from the Agua Fria River study area are reported here.

- Camelback Rd. - PRC Toups (1983) using the post-Old Waddell peak discharges estimated general scour of 5 feet and long term scour of 7 feet.
- Buckeye Road – Inca (1997) using the post-New Waddell discharges reports an estimate of long term scour of 5 feet at Buckeye Road.
- Olive Avenue – Erikson & Salmon (1985) using post-Old Waddell discharges (102,000 cfs at Olive Avenue) interpreted the depth of long-term scour to be the level of gravel pit depths nearby at the time. The identified a downstream pit with an elevation of 1026 feet and assumed a natural river slope upstream from that point of 0.0023 to yield a long-term degradation elevation of 1040 feet. "Natural" ground elevation was about 1075 feet in 1965.
- Bell Road – Benson & Gerdin (1980) report that the old Bell Road bridge (designed in 1964) had spread footing piers at a depth of 15 feet. That bridge failed in the February 1980 flooding. Cross section comparisons show as much as 9 feet of net degradation in cross sections near the bridge between 1979 and 1980 following the flood. Local aggradation as much as 7 feet is also indicated. Evidence of 10 to 12 feet of general (contraction) scour is reported between piers during the Feb. 1980 flood. Total scour during the February 1980 flood was reported as greater than 30 feet.

9.4 Other Reports

SLA, 1988, Scour Analysis of the Agua Fria River between Lower Buckeye Road and Broadway Boulevard, report prepared for Brown & Caldwell, Feb. 8, 1988.

- This report describes an average widening of the river in their study reach of 720 feet between Dec. 1978 and Dec. 1980. This fits well with measurements made for this report that are presented in Chapter 5.
- The limits of the geologic floodplain shown on Figure 2 of the SLA report match well with the interpretations in the current report. These limits serve as a primary basis for definition of the long-term erosion hazard zone.
- Total single event scour (including safety factors) of 8.2 feet is reported for this reach for the 100-year discharge of 95,000 cfs.

Verville, H.J., 1985, Channel Change, Process, and Cross-sectional Flow Distributions in an Arid-Region Braided River, Agua Fria River, Arizona, M.A. Thesis, Arizona State University, Dept. of Geography, 128 p.

- Longitudinal variations in deposition and erosion are explained by geology and channel network structure which impose controls on fluvial processes during floods.
- Vegetation in the channel can cause lower discharges to result in larger inundation areas.
- Reports general aggradation for the period 1968 to 1979 for the study reach from just upstream of Calderwood Butte downstream 4.5 km (2.8 miles). For the period from 1979 to 1983 degradation is reported. Net degradation between 1968 and 1983 as reported for 24 of 28 cross sections. Quantities ranged from + 3 feet (aggradation) to –7 feet (degradation).

9.5 Summary

The studies presented above report that the Agua Fria is generally a degrading river. The reports also conclude that in-stream sand & gravel mining has negative effects on the river. Scour at bridges has been and can be significant. These conclusions are in agreement with the findings of the current study.

10. CONCLUSIONS

10.1 Summary

The Flood Control District of Maricopa County (FCDMC) prepared a watercourse master plan for the Agua Fria River. The watercourse master plan was prepared by a team of consultants led by Kimley-Horn & Associates, Inc. (KHA), who identified and evaluated structural and non-structural flood control alternatives to protect properties within and adjacent to the regulatory floodplain from flood damage. JE Fuller/ Hydrology & Geomorphology, Inc. (JEF) has prepared this lateral stability assessment to support the watercourse master planning process.

The interrelated watershed, geologic, and hydrologic characteristics of a stream combine to determine its unique geomorphology. These data for the study reach were presented in Chapter 2. The Agua Fria River is a wide, braided stream that has been heavily impacted by human activities. Sand and gravel mining, bridge constrictions, channelization and dam construction on the Agua Fria River and its primary tributaries have significantly impacted its form and behavior. Moreover, these impacts are likely to continue to influence its future as the river continues to respond to these impacts. Large floods in the past have caused significant movement of the stream channel both vertically and horizontally. Future large floods are expected to cause significant horizontal and vertical changes in the river channel and its floodplain. The existing characteristics of the river provide information on the nature and geographic location of erosion hazards along the river and its floodplain. An understanding of these characteristics along with the river's geologic and historical history facilitates definition of the extent and magnitude of erosion hazards.

The types of characteristics observed and recorded in the field and their relevance to the assessment of lateral and vertical erosion in the Agua Fria River were presented in Chapter 3. Field visits to the study area were conducted during the summer of 2000. Field visits consisted of walking the entire study reach, photographing and mapping key features, and recording descriptions of existing channel conditions. Detailed observations were recorded at typical cross sections every mile throughout the study area. Additionally, all road crossings and other structures in or adjacent to the river were visited, documented, and are described in the report.

The spatial extent and distribution of stream characteristics observed in the field, a discussion of the spatial distribution of these characteristics and how their distribution affects the distribution of lateral erosion hazards in the study area, geographic or spatial distribution of data relevant to vertical and horizontal erosion hazards in the Agua Fria River were presented in Chapter 4. The distribution of field characteristics varies spatially throughout the study area both longitudinally along the channel as well as horizontally across its valley. The distribution of these features helps explain the spatial distribution of erosion hazards in the study area. These patterns complement the historical information collected along with geomorphic and engineering computations to map the extent of erosion hazards defined and discussed in Chapter 8.

Historical and temporal data examined in Chapter 5 to support of the lateral migration assessment included geologic data, archeological data, and historical records including written records, aerial photographs, and topographic maps. The Quaternary geology investigations along the study reach indicate that the terraces are effective lateral limits to erosion. Subsidence near the study reach has had no impacts on the degradation of the river channel. Evidence of Hohokam settlement along the river corridor is limited to the stream terraces, and has not been found in the active floodplains. Anglo settlements and activity along the river had limited impact prior to World War II. The settlements along the river were established as either stage stops between Phoenix and Prescott, or as farming settlements. The major human

impacts on the river, namely sand and gravel mining, began with post-World War II population growth and the resulting need for building materials.

The Agua Fria River is highly variable in width along the study reach. Average channel widths have decreased over time. The width of the river is dependent on the local conditions such as bedrock outcrops and, in some instances, on the position of in-stream mining. However, recent net decreases in channel width does not preclude the chance of future widening or lateral movement. While smaller floods are not capable of causing the large lateral variations in channel position, larger floods have the capacity for massive lateral erosion. Although the magnitude and frequency of flood discharges has been greatly reduced by the New Waddell Dam, discharges larger than bankfull discharge are still possible on the Agua Fria River. These relatively infrequent, large floods are capable of causing the same types of significant changes in channel thalweg and bank locations as has been experienced in the past. The maximum single event change in width was approximately 1100 feet.

The examination of historical longitudinal profiles shows changes in bed elevation in the Agua Fria River from 1903 to 1995. The data generally show highly variable changes, ranging from no significant changes to significant degradation of the channel. The reaches that show degradation are primarily in areas impacted by the human activity. In particular, clear-water discharge from the dam, encroachments by bridges, channelization, and sand and gravel mining activity within the channel appear to be the primary causes of channel degradation. Historical channel bed lowering ranged from 0 to about 17 feet. No evidence of significant aggradation was found within the study reach.

Historical data show that channel sinuosity has not varied radically over time. This suggests that the Agua Fria River has not been changing the length of the low flow channel, and hence its slope, in response to changes in hydrologic or sediment inputs to the system. However, mathematical data presented in Chapter 6 suggest that adjustments in slope should be expected in the future.

Chapter 6 described various types of data examined using mathematical means (i.e. using equations or algorithms) to qualify or quantify the extent or degree of lateral and vertical erosion hazards on the Agua Fria River from New Waddell Dam to the Gila River confluence. The types of mathematical data presented include hydraulic data from HECRAS, sediment size data, geomorphic methods including bankfull discharge calculations and hydraulic geometry relationships, and engineering methods such as allowable velocity, equilibrium slope, armoring analysis, scour computations, Lane's relation, and HEC-6 modeling.

The mathematical analyses summarized in Chapter 6, in conjunction with the other analyses described in previous chapters, indicate that the horizontal limits of erosion hazards will remain within the historical limits of erosion expressed by the Pleistocene terraces along the study reach. Geologic limits to vertical erosion have been exceeded by changes to the system imposed by human activity. In particular, lowering of the channel bed elevation by sand and gravel mining along with reductions in upstream and watershed sediment supplies by dams and urbanization have caused the river to degrade its bed below levels experienced in thousands of years. The results also suggest that the Agua Fria River is adjusting and will continue to adjust to changes in the hydrologic and sedimentological inputs to its system. The future Agua Fria River channel is expected to be narrower, deeper, and have a lower elevation and shallower gradient than it has in the past.

In Chapter 7, trends in river behavior were examined in light of the mathematical, historical and field analyses of the study reach. Three conditions relating to the history of Waddell Dam were examined. Significant changes in deliveries of sediment and water discharges have occurred over the past 70 years in the study area as a result of the construction of first the (old) Waddell

Dam in 1927 and then the New Waddell Dam in 1992. The result has been to change the expected nature of flooding and erosion within the study area. Therefore, additional geomorphic changes in the Agua Fria River's behavior are expected, including a trend toward a narrower, deeper, shallower gradient river. However, evolution of the river form can only occur in response to flooding, especially in response to very large floods. Significant flooding on the river since completion of the New Waddell Dam has been limited. Therefore, some of the expected trends may not yet have fully expressed themselves in the river's form. Other changes in the watershed and river environment are capable of causing changes in the river's form. In particular, lowering of the channel bed by sand and gravel mining and significant narrowing of the channel at bridge crossings and around mining operations also push the river toward a lower, narrower, deeper, and shallower gradient channel with a straight to slightly sinuous single channel. However, infrequent very large discharges will attempt to reestablish a wider, shallower, braided channel. The long-term result is likely to be a compound river form with a narrower, deeper, shallower gradient slightly sinuous single channel inset into a larger, wider, shallower, braided high flow channel. Therefore, while severe erosion hazards will likely be confined to a smaller corridor than historically, the infrequent but probable larger flood will continue to pose erosion hazards throughout the areas historically subject to erosion except where protected by engineered structural measures.

Erosion hazard boundaries for the Agua Fria River were identified based on the results of the geomorphic, historical and engineering analyses of lateral stability, and were presented in Chapter 8. The geomorphic analysis included consideration of field data and analytical procedures. Erosion hazard boundaries are intended for use in floodplain management of the Agua Fria River, and for development of watercourse master plan alternatives. Three erosion hazard zones were defined. The three zones are the severe erosion hazard zone, the lateral migration erosion hazard zone, and the long-term erosion hazard zone. The lateral migration erosion hazard zone is recommended for adoption as the regulatory erosion zone for the watercourse master plan.

The results of previously completed studies, summarized in Chapter 9, indicate that the Agua Fria is generally a degrading river. The reports also conclude that in-stream sand & gravel mining has negative effects on the river. Scour at bridges has been and can be significant. Prolonged outflows from the New Waddell Dam may have more impact on vertical erosion than larger shorter duration floods. These conclusions are in agreement with the findings of the current study.

10.2 Recommendations

The following recommendations are made from the analyses conducted for this report:

1. New development should not occur within the lateral migration erosion hazard zone.
2. The District and other regulatory agencies should develop policies and sets of criteria for requirements related to variances and/or revisions to the lateral migration erosion hazard zone.
3. The District should monitor bank and bed erosion in susceptible areas near existing structures. Specific areas of concern include:
    a. Left bank of the river within the City of Youngtown
    b. Right bank of the river immediately downstream of Bell Road
    c. Channel bed and banks in all reaches upstream and downstream of gravel pits, particularly where public roads or utilities exist (e.g. power lines near Hatfield Road, Rose Garden Lane, Bell Road, Grand Avenue, Olive Ave., Glendale Avenue, Camelback Road, Indian School Road)

   d. Levee toe along the left bank of the river downstream of Camelback Road
   e. Power line towers downstream of Buckeye Road to the Gila River
4. The channel adjacent to the Cholla Landfill located downstream of Grand Avenue should be stabilized to prevent the landfill from being impacted by future lateral erosion.
5. Grade control protection should be constructed at bridges upstream of in-stream gravel mining where the potential for headcutting and long-term degradation has been identified.
6. The District should consider re-mapping the FEMA floodplain and floodway for the study reach, especially around gravel pits and areas of active braided channels. Effective regulation of in-stream sand and gravel mining requires a more accurate depiction of the floodway than currently exists.
7. The District should monitor the depth and extent of future activity of within existing gravel mining operations, with special attention paid to pit locations, pit depths, and levee construction. Also, the District should monitor progress of erosion or reaches of increased slope upstream from gravel pits.
8. The District should restrict the development of future gravel pits to areas outside the lateral migration erosion hazard zone, unless the pits are protected by engineered bank stabilization and measures are designed to prevent impacts to adjacent reaches. Evaluation of the future vertical and horizontal stability should be demonstrated before floodplain use permits are granted or extended for sand and gravel mines.

11. REFERENCES

Ackers, P. & Charlton, F.G., 1971, "The Slope and Resistance of Small Meandering Channels," Institute of Civil Engineers, Proceedings, Supplement 15, 1970, Paper 7362S.

Aerial Mapping Company, 1960, Aerial photographs. Flight date February 6, 1960.

Aerial Mapping Company, 1985, Aerial photographs. Flight date March 21, 1985.

Agricultural Stabilization and Conservation Service, 1949, Aerial photographs. Flight date February 14, 1949.

Agricultural Stabilization and Conservation Service, 1954, Aerial photographs. Flight date January 24, 1954.

Agricultural Stabilization and Conservation Service, 1964, Aerial photographs. Flight date January 23, 1964.

AMAFCA, 1994, See Resource Consultants and Engineers (RCE), 1984

Arizona Department of Transportation, 1989, Effects of in-stream mining on channel stability: FHWA-AZ89-250, prepared by Simons, Li and Associates, Inc.

Arizona Department of Water Resources (ADWR), 1985, Design Manual for Engineering Analysis of Fluvial Systems.

Arizona Department of Water Resources (ADWR), 1996, State Standard for Watercourse System Sediment Balance.

Arizona Navigable Stream Adjudication Commission, April 1997, Report, findings and recommendation regarding the navigability of the Agua Fria River and its tributaries, New River and Skunk Creek: reported to the Arizona Legislature, 14 p.

Arizona Salt River Project, 1934, Aerial photographs. Flight date 1934.

Benson & Gerdin, Inc., 1980, Design Report and Recommendations for the Replacement of the Bell Road Bridge Over the Agua Fria River, Maricopa County Highway Dept. Work Order No. 68067.

Birkeland, P. W., 1984, Soils and geomorphology: New York, Oxford University Press, 372 p.

Birkeland, P. W., Machette, M. N., and Haller, K. M., 1991, Soils as a tool for applied Quaternary geology: Utah Geological and Mineral Survey Miscellaneous Publication 91-3, 63 p.

Blench, T., 1951, "Regime Theory for Self-Formed Sediment-Bearing Channels," ASCE Proceedings, Vol. 77.

Blout, S.E. 1919, GLO Survey Notes on file at the U.S. Bureau of Land Management Office, Phoenix, Arizona.

Bowers, J. E., 1993, Shrubs and Trees of the Southwest Deserts, illustrations by B. Wignall, Southwest Parks and Monuments Association, Tucson, Arizona, 140 p.

Bray, D.I., 1979, "Estimating Average Velocity in Gravel Bed Rivers," ASCE Journal of the Hydraulics Division.

Brice, J.C., and Blodgett, J.C., 1978, Countermeasures for Hydraulic Problems at Bridges," Volumes 1 & 2, FHWA/RD-78-162,163. Federal Highway Administration, Washington, D.C.

Brown, D.E., 1982, Biotic Communities: Southwestern United States and Northwestern Mexico. University of Utah Press. Salt Lake City, Utah.

Camp, P.D., 1986, Soil Survey of the Aguila-Carefree Area, Parts of Maricopa and Pinal Counties, Arizona.

Carmody, T., 1980, General Report No. 1, A Critical Examination of the "Largest" Floods in Arizona, A Study to Advance the Methodology of Assessing the Vulnerability of Bridges to Floods for the Arizona Department of Transportation, Engineering Experiment Station, College of Engineering, University of Arizona, Feb. 1980, 55 p.

Carriaga, C.C., Mays, L.W., and Ruff, P.F., 1994, Agua Fria River Sediment Transport Study, for FCDMC, Arizona State University, Tempe, AZ, February 28, 1994.

Chang, H.H., 1988, Fluvial Processes in River Engineering, John Wiley & Sons, New York.

City of Tucson Engineering, 1989, *Standards Manual for Drainage Design and Floodplain Management.* Manual Prepared by Simons Li and Associates.

Chow, V.T., 1959, Open Channel Hydraulics, McGraw-Hill, New York.

Coe & Van Loo Consultants, Inc., 1996, Agua Fria River Floodplain Delineation Re-Study, FCD Contract No. 95-5.

Cooper Aerial Surveys Company, 1977, Aerial photographs. Flight date December 5, 1977.

Chronic, H., 1983, Roadside Geology of Arizona. Mountain Press Publishing Company, Missoula, Montana.

Dallett, 2000, The Agua Fria: a working river for the West Valley, themes and historic sites.

Dart, A., 1989, Prehistoric irrigation in Arizona: a context for canals and related cultural resources: Center for Desert Archaeology Technical Report 89-7, p. 13.

Dickinson, W. R., 1989, Tectonic setting of Arizona through geologic time, in Jenney, J. P. and Reynolds, S. J., 1989 Geologic evolution of Arizona: Tucson, Arizona Geological Society Digest 17 p. 1-16.

Dittert, A.E., Editor, 1974, An Archaeological Survey in the Gila River Basin, New River and Phoenix City Streams, Arizona Project Area. Report to the U.S. Army Corps of Engineers – L.A. District, Contract No. DAC W09-74-C-0016.

Dodge, C. N., 1973, Pebbles from the Chinle and Morrison Formations, in James, H. L., ed., Guidebook of Monument Valley and vicinity, Arizona and Utah: New Mexico Geological Society 24th Field Conference Guidebook, p. 114-121.

Dohrenwend, J. C., 1987, Basin and Range, *in* Graf, W. L., ed., Geomorphic systems of North America: Geological Society of America, Centennial Special Volume 2, p. 303-342.

Dorn, R. I., and Oberlander, T. M., 1982, Rock varnish: Progress in Physical Geography, v. 6, p. 317-367.

Dove, D.E., 1970, A site survey along the lower Agua Fria River, Arizona: The Arizona Archaeologist 5. Arizona Archaeological Society, Phoenix.

Durrenberger and Ingram, 1978, Major Storms and Flood in Arizona, 1862-1977. Cited in USACOE, 1982, Gila River New River and Phoenix City Streams, Arizona Design Memorandum No. 2, Part 2. L.A. District.

Erikson & Salmon, Inc., 1985, Olive Avenue Crossing of the Agua Fria River, Maricopa County, Arizona, Hydraulic Report, Volume I, report for Hoffman-Miller Engineers, Inc., who were working for the Maricopa County Highway Department.

FEMA, Federal Emergency Management Agency, 1999, Riverine Erosion Hazards Mapping Feasibility Study. Report by the FEMA Technical Services Division, Hazards Study Branch.

FHWA, Federal Highway Administration, 1991, Stream Stability at Highway Structures, Hydrologic Engineering Circular No. 20. FHWA Publication No. FHWA-IP-90-014. McLean, Virginia.

Flood Control District of Maricopa County, 1959, Digital aerial photographs. Flight date 1959.

Flood Control District of Maricopa County, 1999, Digital aerial photographs. Flight dates January 1999.

Fortier, S. and Scobey, F.C., 1926, "Permissible Canal Velocities," Transactions, ASCE, Vol. 89.

General Land Office, 1870, Township 1 North Range 1 West Survey Map.

General Land Office, 1870, Township 3 North Range 1 West Survey Map.

General Land Office, 1895a, Township 2 North Range 1 East Survey Map.

General Land Office, 1895b, Township 2 North Range 1 West Survey Map.

General Land Office, 1895c, Township 4 North Range 1 East Survey Map.

General Land Office, 1895d, Township 4 North Range 1 West Survey Map.

General Land Office, 1895e, Township 5 North Range 1 East Survey Map.

General Land Office, 1895f, Township 6 North Range 1 East Survey Map.

General Land Office, 1896, Township 3 North Range 1 East Survey Map.

Gindhart, M.A.M., 1987, Waddell Dam rose after years of woe for dedicated family, Arizona Republic, April 11, 1987.

Gladwin, H.S., 1937, Excavations at Snaketown, material culture: Medallion Papers 25, Globe, Arizona.

Garrett, J.M. and Gellenbeck, D.J.,1991, Basin Characteristics and Streamflow Statistics in Arizona as of 1989: U.S. Geological Survey, Water Resources Investigations Report 91-4041, 612 p.

Hartman, G.W., 1977, Soil Survey of Maricopa County, Central Part: Soil Conservation Service, USDA, 117 p., 128 maps, scale 1:20,000.

Haury, E.W., 1937, The Hohokam: desert farmers and craftsmen: excavations at Snaketown 1964-65: University of Arizona Press, Tucson.

Hedman, E.R., and Osterkamp, W.R., 1982, Streamflow Characteristics Related to Channel Geometry of Streams in Western United States. USGS Water-Supply Paper 2193.

Henderson, F.M., 1961, Stability of Alluvial Channels, ASCE Journal of Hydraulics.

Hereford, R., 1984, Climate and Ephemeral Stream Processes: Twentieth Century Geomorphology and Alluvial Stratigraphy of the Little Colorado River," Geological Society of America Bulletin, Volume 95, p. 654-668.

Huckleberry, G., 1995, Surficial Geology of the Lower Agua Fria River, Lake Pleasant to Sun City, Maricopa County, Arizona: Arizona Geological Survey Open-File Report 95-5, Tucson, AZ.

Inca Engineers, Inc, 1997, Bridge Scour Investigation and Design of Corrective Measures, Final Report, MC 85 Bridge over Agua Fria River, Contract No. CY 1997-26, Work Order NO. 80407, Maricopa County Dept. of Transportation, Aug. 28, 1997.

Introcaso, D.M., 1988, Waddell Dam, Maricopa County, Arizona: Photographs, written historical & descriptive data, reduced copies of drawings.

JE Fuller/ Hydrology & Geomorphology, Inc, 2001, Skunk Creek/Sonoran Wash Lateral Migration Report, Appendix to the Skunk Creek/Sonoran Wash Watercourse Master Plan. Report prepared for the Flood Control District of Maricopa County.

JE Fuller/ Hydrology & Geomorphology, Inc, 2000, Upper Cave Creek/Apache Wash Lateral Migration Report, Appendix to the Upper Cave Creek/Apache Wash Watercourse Master Plan. Report to the Flood Control District of Maricopa County.

Jerry R. Jones & Associates, Inc., 1988, Topographic Mapping for the Agua Fria River Flood Insurance Study, 1:4,800, 4 ft. contour interval.

Jerry R. Jones & Associates, Inc., 1989, Agua Fria River Flood Insurance Study, Report to the Flood Control District of Maricopa County, Arizona.

Jones, L.S., and Harper, J.T., 1998, Channel Avulsions and Related Processes, and Large-Scale Sedimentation Patterns Since 1875, Rio Grande, San Luis Valley, Colorado. GSA Bulletin, Vol. 110, No. 3, p. 411-421.

Jurnikis, A., 1971, Foundation Engineering. Intest Education Publishers, San Francisco, CA.

Kennedy, R.G., 1895, The Prevention of Silting in Irrigation Canals, Min. Proc., Inst. Civil Engineers, Vol. CXIX.

Kellerhals, R., 1967, "Stable Channels With Gravel-Paved Beds," Journal of the Waterways and Harbors Division, Proceedings of the American Society of Civil Engineers. February. Vol. 93, WW1, p. 63-83.

Kresan, P.L., 1988, "The Tucson, Arizona, Flood of October 1983 – Implications for Land Management Along Alluvial River Channels," in Baker, V.R., Kochel, R.C., and Patton, P.C., Editors, *Flood Geomorphology*, John Wiley & Sons, New York.

Lacey, E.C., Andersen, F., O'Brien, P., and Preisler, D., n.d., A historical analysis of the Agua Fria River and its tributaries, New River and Skunk Creek, Arizona: prepared by Research Management West for Larry J. Richmond, Ltd., Phoenix, Arizona, 40 p.

Lacey, G., 1929, Stable Channels in Alluvium, Min. Proc. Inst. Civil Engineers, Vol. 229.

Lagasse, P.F., and Schall, J.D., 1988, Delineation of a Flooding and Erosion Buffer for a Southwestern Arroyo, Proceedings of the Conference on Arid West Floodplain Management Issues, Association of State Flood Plain Managers Arid West Committee, Las Vegas, Nevada, October 19-21, 1988.

Landiscor Aerial Information, 1967, Aerial photographs. Flight date October 9, 1967.

Landiscor Aerial Information, 1980, Aerial photographs. Flight date December 30, 1980.

Lane, E.W., 1955, "Design of Stable Channels", Transactions, ASCE, v. 120, pp.1234-1260.

Lane, E.W., 1955, The Importance of Fluvial Morphology in Hydraulic Engineering, ASCE Proceedings, Volume 81, No. 745.

Lane, E.W., and Carlson, E.J., 1953, "Some Factors Affecting the Stability of Canals Constructed in Coarse Granular Materials." Proceedings Minnesota International Hydraulics Conference, Joint Meeting IAHR and ASCE Hydraulics Division.

Lane, E.W., 1952, Progress Report on Studies in the Design of Stable Channels of the Bureau of Reclamation, HYD-352, Vol. 79.

Lee, G. K., and Bell, J., 1975, Late Cenozoic geology along the Gila River near Gillespie Dam, central Arizona: [Abs] Geological Society of America Annual Meetings Abstracts with programs. v. 7, no. 3., p. 340.

Leopold, L.B., 1970, "An Improved Method for Size Distribution of Stream Bed Gravel," Water Resources Research. October. Vol. 6, No. 5, p. 1357-1366.

Leopold, L.B., and Maddock, T.M., 1953, The Hydraulic Geometry of Stream Channels and Some Physiographic Implications, USGS Professional Paper 252, Washington, D.C.

Leopold, L.B., Wolman, M.G., and Miller, 1964, Fluvial Processes in Geomorphology. Freeman Company. San Francisco.

Leopold, L.B., and Wolman, M.G., 1957, River Channel Patterns: Braided, Meandering, and Straight, USGS Professional Paper 282-B. Washington, D.C.

Livingston, D.E. and Damon, P.E., 1968, The ages of stratified Precambrian rock sequences in central Arizona and northern Sonora: Canadian Jour. Earth Sci., v. 5, p. 763-772.

MacBroom, J.G., 1981, Applied Fluvial Geomorphology. University of Connecticut – Storrs, Institute of Water Resources Report No. 31.

Machette, M. N., 1985, Calcic soils of the southwestern United States: Geological Society of America Special Paper 203, p. 1-21.

Marchand, D. E., 1971, Rates and models of denudation, White Mountains, eastern California: American Journal of Science, v. 270, p. 109-135.

Maricopa County Department of Transportation, 1998, Maricopa County Public Works 1998-1999 Regional Map.

Martineau, J.H., 1894, GLO Survey Notes on file at the U.S. Bureau of Land Management, Phoenix, Arizona.

Masse, W.B., 1981, Prehistoric irrigation systems in the Salt River Valley, Arizona: Science 214: 408-415.

Mavis, F.T., and Lushey, L.M., 1948, A Reappraisal of the Beginning of Bed-Movement-Competent Velocity, International Association for Hydraulic Research, Second Meeting, Stockholm.

Menges, C. M., and Pearthree, P. A., 1989, Late Cenezoic tectonism in Arizona and its impact on regional landscape evolution, *in* Jenney, J.P., and Reynolds, S.J., 1989, Geologic evolution of Arizona, Arizona Geological Society Digest 17, p. 649-680.

Meyer-Peter, E., and Muller, R., 1948, Formulas for Bed-Load Transport, International Association for Hydraulic Structures, Second Meeting, Stockholm.

Midvale, F.J., 1920-1971, Research notebooks, Department of Anthropology, Arizona State University, Tempe.

Mielke, J., 1993, Native Plants for Southwestern Landscapes, University of Texas Press, Austin, Texas, 310 p.

Morrison, R. B., 1985, Pliocene/Quaternary geology, geomorphology, and tectonics of Arizona, Geological Society of America, Special Paper 203, p. 123-146.

NRC, National Research Council, 1996, Alluvial Fan Flooding, Report by the Committee on Alluvial Fan Flooding, National Academy Press, Washington, D.C.

NRCS, USDA Soil Conservation Service, 1975, Soil Taxonomy. USDA Handbook No. 436.

Neill, C.R., 1975, Guide to Bridge Hydraulics. Roads and Transportation Association of Canada, University of Toronto Press, Toronto, Canada.

Hedman, E.R., and Osterkamp, W.R., 1982, Streamflow Characteristics Related to Channel Geometry of Streams in the Western United States. USGS Water Supply Paper 2193.

Parker, G., 1979, "Hydraulic Geometry of Active Gravel Bed Rivers," ASCE Journal of the Hydraulics Division.

Pemberton, E.L., and Lara, J.M., 1984, Computing Degradation and Local Scour, Technical Guideline for Bureau of Reclamation. Denver, Colorado. January.

Pewe, T.L., 1978, "Terraces of the Lower Salt River Valley in Relation to the Late Cenozoic History of the Phoenix Basin, Arizona," in Burt, D.M., and Pewe, T.L., eds., Guidebook to the Geology of Central Arizona: Arizona Bureau of Geology and Mineral Technology Special Paper 2, p. 1-45.

Pewe, T.L., 1976, Terraces of the lower Agua Fria River Valley, Maricopa County, Arizona (abst.): Jour. Arizona Acad. Sci., v. 11, proc. suppl., p. 93.

Phillips, J.V., and Ingersoll, T.L., 1998, Verification of Roughness Coefficients for Selected Natural and Constructed Stream Channels in Arizona. USGS Professional Paper 1584, Denver, Colorado.

Pierce, H. W., Shafiqullah, M., and Breed, W. J., 1985, Geochronology of some exotic cobbles, Chinle Formation, Arizona [abs]: Flagstaff, Museum of Northern Arizona Abstracts of the symposium on southwestern geology and paleontology 1985, p. 7.

Pope, G.L., Rigas, P.D., and Smith, C.F., 1998, Statistical Summaries of Streamflow Data and Characteristics of Drainage Basins for Selected Streamflow-Gaging Stations in Arizona Through Water Year 1996, USGS Water-Resources Investigations Report 98-4225.

PRC Toups, 1983, Design Report for the Camelback Road Bridge over the Agua Fria River, report prepared for the Maricopa County Highway Department, Feb. 28, 1983.

Rankin, A.G., and Katzer, K.L., 1989, Agricultural Systems in the ACS Waddell Project Area. In Settlement, Subsistence and Specialization in the Northern Periphery: The Waddell Project, Green, M. Editor, Cultural Resources Report No. 65. Archaeological Consulting Services, Ltd., Tempe.

Renard, K.G., and Stone, J.J., 1982, Sediment Yield from Small Semiarid Rangeland Watersheds, Proceedings of the Workshop of Estimating Erosion and Sediment Yield on Rangelands, Tucson, Arizona, March 7-9, 1981.

Reynolds, S.J., et al., 1997, Digital Representation of the Geological Map of the Phoenix North 30' x 60' Quadrangle, Central Arizona, Digital Information Series, DI-4, version 1.1: Arizona Geological Survey, Tucson, Arizona.

Reynolds, S.J., et al., 1997, Digital Representation of the Geological Map of the Phoenix South 30' x 60' Quadrangle, Central Arizona, Digital Information Series, DI-5, version 1.1: Arizona Geological Survey, Tucson, Arizona.

RCE, Resource Consultants & Engineers, Inc., 1994, Sediment and Erosion Design Guide, Manual prepared for the Albuquerque Metropolitan Arroyo Flood Control Authority (AMAFCA).

Rodgers, J.B., 1985, Prehistoric agriculture variability in the Hohokam Northern Periphery: Hohokam settlement and economic systems in the central New River Drainage, Arizona. David Doyel and Mark Elson, eds., Soil Systems Publications in Archaeology, No. 4, Phoenix.

Rodgers, J.B., 2000, The Agua Fria River watercourse master plan archeological assessment of northern Maricopa County, Arizona: prehistoric resources; prepared for Flood Control District of Maricopa County, Contract No. 97-41.

Rogge, A.E.; McWatters, D.L.; Keane, M.; and Emanuel, R.P.; 1995, Raising Arizona's dams: daily life, danger, and discrimination in the dam construction camps of Central Arizona, 1890's-1940's: University of Arizona Press, Tucson.

Rogge, A.E.; Myers, C.L.; McWatters, D.L.; 1987, Building dams on the Agua Fria: a historical archaeological perspective: paper prepared for the Arizona Historical Society 28th Annual Convention, Flagstaff, Arizona.

Rosgen, D., 1996, *Applied River Morphology*. Wildland Hydrology, Pagosa Springs, Colorado.

Rosgen, D., undated, Applied Fluvial Morphology – Short Course Notes.

Schumann, H.H., and O' Day, C.M., 1995, Investigation of Hydrogeology, Land Subsidence, and Earth Fissures, Luke Air Force Base, Arizona, USGS Administrative Report, 62 p.

Schumm, S.A., 1961, Effect of Sediment Characteristics on Erosion and Deposition in Ephemeral Stream Channels. USGS Professional Paper 352-C. Washington, D.C.

Schuyler, J.D., 1903, Report on the water supply of the Agua Fria River, and the storage reservoir project of the Agua Fria Water and Land Company for irrigation in the Gila River Valley, Arizona: manuscript on file at Arizona Historical Foundation, Tempe.

Sellers, W.D., Hill, R.H., and Sanderson-Rae, M., 1985, Arizona Climate – The First Hundred Years. University of Arizona Press, Tucson.

Shafiqullah, M., Damon, P.E., Lynch D.J., Reynolds, S.J., Rehrig, W.A., and Raymond, R.H., 1980, K-Ar geochronology and geologic history of southwestern Arizona and adjacent areas, *in* Jenney, J.P., and Stone, C., 1980, Studies in Western Arizona, Arizona Geological Society Digest Volume XII, p. 201-260.

Sheridan, T.E., 1995, Arizona, a history: University of Arizona Press, Tucson.

Shields, A., 1936, Anwendung der Aenlichkeitsmechanik und der Turbulenzforschung auf die Geschiebebewegung, Mitteil, PVWES, Berlin, No. 26.

Shulits, S., 1935, The Schoklitsch Bed-Load Formula, Engineering, London.

Silver, L.T., 1978, Precambrian formations and Precambrian history in Cochise County, southeastern Arizona, *in* Callender, J.F., Wilt, J.C., and Clemons, R.E., eds., Land of Cochise, New Mexico Geol. Soc. Guidebook, 29th Field Conference: Socorro, p. 157-163.

Silver, L.T., Bickford, M.E., and Van Schmus, W.R., 1977, The 1.4-1.5 b.y. transcontinental anorogenic plutonic perforation of North America [abs.]: Geol. Soc. America Abstracts with Programs, v. 9, p. 1176-1177,

Simons, Li & Associates (SLA), 1988, Scour Analysis of the Agua Fria River between Lower Buckeye Road and Broadway Boulevard, report prepared for Brown & Caldwell, Feb. 8, 1988.

Simons, Li & Associates (SLA), 1984, Draft, Final Sediment Transport Report, submitted to Los Angeles District, US Army Corps of Engineers, Project No. PAZ-COE-03, RDN/R439, July 16, 1984.

Simons, Li & Associates (SLA), 1983, Final Report, Hydraulic and Geomorphic Analysis of the Agua Fria River, submitted to FCDMC, SLA Project No. AZ-MC-05, Revised Sept. 13, 1983.

Soil Conservation Service (USDA-SCS), 1977, *Design of Open Channels – Technical Release 25.*

Spencer, J. E., Reynolds, S. J., 1989, Middle Tertiary tectonics of Arizona and adjacent areas, in Jenney, J. P. and Reynolds, S. J., 1989 Geologic evolution of Arizona: Tucson, Arizona Geological Society Digest 17 p. 539-574.

Tadayon, S. and others, 2000, Water Resources Data, Arizona, Water Year 1999, U.S.G.S. Water-Data Report AZ-99-01, 370 p.

Tellman, B., Yarde, R., Wallace, M.G., 1997, Arizona's changing rivers: how people have affected the rivers: Water Resources Research Center, University of Arizona, pp. 77-78.

Thomas, B.E., Hjalmarson, H.W., & Waltemeyer, S.D., 1994, Methods for Estimating Magnitude and Frequency of Floods in the Southwestern United States, USGS Open File Report 93-419.

Thomsen, B.W., and Hjalmarson, H.J., 1991, Estimated Manning's Roughness Coefficients for Stream Channels and Flood Plains in Maricopa County, Arizona. Report prepared by the US Geological Survey for the Flood Control District of Maricopa County.

Thomsen, B.W., 1980, Flood of February 1980 Along the Agua Fria River, Maricopa County, Arizona: USGS Water-Resources Investigations Open-File Report 80-767, Sheet 1 of 1.

Thorne, C.R., 1998, *Stream Reconnaissance Handbook – Geomorphological Investigation and Analysis of River Channels*. John Wiley & Sons, New York.

Topcon, 1999, Instruction Manual for Mirror Stereo Scope MS-3. Topcon Corporation, Tokyo, Japan.

U.S. Army Corps of Engineers, 1995, Hydrologic Evaluation of Impacts of New Waddell Dam on Downstream Peak Discharges in the Agua Fria River. July 1995, L.A. District.

U.S. Army Corps of Engineers, 1995, Hydraulic Design of Flood Control Channels, EM1110-2-1601. ASCE Republication

U.S. Army Corps of Engineers Hydrologic Engineering Center (USACOE HEC), 1993, HEC-6 Scour and Deposition in Rivers and Reservoirs, User's Manual.

U.S. Army Corps of Engineers, 1990, Stability of Flood Control Channels, Draft.

U.S. Army Corps of Engineers, 1989, Sedimentation Investigation of Rivers and Reservoirs, EM1110-2-4000.

U.S. Army Corps of Engineers, 1988, Hydrology for Evaluation of Flood Reduction by New Waddell Dam, Agua Fria River Below New Waddell Dam to the New River Confluence. September 1988, L.A. District.

U.S. Army Corps of Engineers, 1982, General Design Memorandum #2– Gila River Basin – Phoenix, Arizona and Vicinity – Hydrology Part 2. L.A. District

U.S. Army Corps of Engineers, 1970, Hydraulic Design of Flood Control Channels, EM1110-2-1601.

U.S. Army Corps of Engineers, 1968, Flood Plain Information, Agua Fria River, Maricopa County, Arizona, L.A. District, March 1968.

U.S. Bureau of Reclamation (BUREC), 1974, Design of Small Dams, U.S. Department of Interior, Washington, D.C.

http://dataweb.usbr.gov/dams/az00113.htm (Camp Dyer Diversion Dam), accessed May 18, 2001.

http://dataweb.usbr.gov/dams/az82929.htm (New Waddell Dam), accessed May 18, 2001.

U.S. Department of Agriculture, 1979, Aerial photographs. Flight date May 13, 1979.

U.S. Geological Survey, 1981, Baldy Mountain, Arizona, 7.5 Minute Topographic Quadrangle, Photorevised based on 1978 aerial photographs. Original publication 1964 based on 1962 aerial photographs.

U.S. Geological Survey, 1981, Calderwood Butte, Arizona, 7.5 Minute Topographic Quadrangle, Photorevised based on 1978 aerial photographs. Original publication 1957 based on 1954 aerial photographs.

U.S. Geological Survey, 1982, El Mirage, Arizona, 7.5 Minute Topographic Quadrangle, Photorevised based on 1978 aerial photographs. Original publication 1957 based on 1954 aerial photographs.

U.S. Geological Survey, 1982, Tolleson, Arizona, 7.5 Minute Topographic Quadrangle, Photorevised based on 1978 aerial photographs. Original publication 1957 based on 1954 aerial photographs.

U.S. Geological Survey, 1992, Aerial photographs. Flight date September 6, 1992.

U.S. Geological Survey, 1997, Aerial photographs. Flight date April 30, 1997.

U.S. Water Resources Council, 1981, Guidelines for Determining Flood Flow Frequency, Bulletin #17B of the Hydrology Committee; Washington, D.C.

Vanden Dolder, E. M., 1992, Rock varnish and desert pavement provide geological and archaeological records: Arizona Geology, v. 22, no. 1, p. 1, 4-7.

Verville, H.J., 1985, Channel change, process, and cross-sectional flow distribution in an arid-region braided river, Agua Fria River, Arizona: M.A. Thesis, Arizona State University, 128 p.

Weaver, D.E., 1974, Archaeological investigations at the Westwing site, Arizona, Agua Fria River valley, Arizona: Anthropological Research Paper 7, Arizona State University.

Weed, C.S., 1972, The Beardsley canal site: Kiva 38(2); p. 57-94.

Williams, G.P., 1978, Bankfull Discharge of Rivers. Water Resources Research, Volume 14, No. 6, p. 1141-1153.

Wolman, M.G., 1954, "A Method of Sampling Coarse River-Bed Material," Transactions American Geophysiscal Union. December. Vol. 35, No. 6, p. 951-956.

Wolman, M.G., and Miller, 1960, Magnitude and Frequency of Forces in Geomorphic Processes. Journal of Geology, Vol. 68, p. 54-74.

Wright, L. A., Troxel, B. W. Williams, E. E., Roberts, N. T., and Diehl, P. E., 1976, Precambrian sedimentary environments of the Death Valley Region, eastern California: California Division of Mines and Geology Special Report 106, p. 7-15.

Yang, C.T., 1973, Incipient Motion and Sediment Transport, Journal of the Hydraulics Division, ASCE, Vol. 99, No. HY10, Proceeding Paper 10067.

Yang, C.T., 1996, Sediment Transport Theory and Practice, McGraw Hill, New York.

Received from Ray Harris:

There are several studies that have reported subsidence over the years in the Luke basin/lower Agua Fria area:

Hammett, B.A., and Herther, R.L., 1995, Maps showing groundwater conditions in the Phoenix Active Management Area, Maricopa, Pinal and Yavapai Counties, Arizona - 1992: Arizona Department of Water Resources Hydrologic Map Series Report Number 27.

Kam, W., Schumann, H.H., Kister, L.R., and Artega, F.E., 1966, Basic ground-water data for western Salt River Valley, Maricopa County, Arizona: Arizona State Land Department Water-Resources Report 27, 72 p.

Koester, 1971, Salt domes in Arizona: Arizona Oil and Gas Conservation Commission Geologic Report 1, 23 p.

Laney, R.L., Raymond, R.H., and Winikka, C.C., 1978, Maps showing water-level declines, land subsidence, and earth fissures in south-central Arizona: U.S. Geological Survey Water-Resources Investigations Open-File Report WRI 78-0083, 2 sheets, scale 1:125,000.

Reeter, R.W., and Remick, W.H., 1986, Maps showing groundwater conditions in the West Salt River, East Salt River, Lake Pleasant, Carefree and Fountain Hills sub-basins of the Phoenix Active Management Area, Maricopa, Pinal and Yavapai Counties, Arizona - 1983: Arizona Department of Water Resources Hydrologic Map Series Report Number 12.

Schumann, H.H., and Genualdi, R.B., 1986, Land subsidence, earth fissures, and water-level change in southern Arizona: Arizona Bureau of Geology and Mineral Technology Map M-23, 1 sheet, scale 1:1,000,000.

Schumann, H.H., 1995, Land subsidence and earth-fissure hazards near Luke Air Force Base, Arizona, in Prince, K.R., Galloway, D.L., and Leake, S.A., editors, U.S. Geological Survey subsidence interest group conference, Edwards Air Force Base, Antelope Valley, California, November 18-19, 1992 - Abstracts and summary: US Geological Survey Open-File Report 94-532, p. 18-21.

12. GLOSSARY

Agglomerate – Sedimentary rock type formed of detrital volcanic material explosively ejected from a volcanic vent, with clasts larger than 32 millimeters.

Alluvial Fan – A fan-shaped deposit of sediment located where a stream issues from a narrow valley of high slope onto a plane or broad valley of low slope.

Alluvium – Deposits of clay, silt, sand, gravel, or other particulate material in a streambed , on a floodplain or delta, or at the base of a mountain.

Altithermal – A period of time within the Holocene epoch characterized by higher than average temperatures and/or decreased precipitation.

Anabranching – A river channel pattern in which the width of islands is more than three times the river width at average discharge.

Anastomosing – A stream pattern charcterized by a net-like or interwoven channel pattern, with individual flow paths better defined or permanent than braided channel flow paths.

Andesite – A volcanic rock type mostly composed of plagioclase and other mafic materials.

Angle of Repose – The maximum angle of a slope that can be maintained by an accumulation of material.

Argillic – Descriptive of a detrital sedimentary rock with particles less than 4 mm in diameter.

Arkosic – Rock type, generally sandstone, composed of more than 25 percent silica-feldspar minerals.

Armor – A natural layer of particles, usually gravel and cobble sizes, that may cover the surface of the streambed as a coarse residue after erosion of the finer bed materials. The layer, often just one to three particles thick, inhibits the erosion of underlying particles.

Avulsion – The sudden relocation of a stream away from its original flow path, usually due to catastrophic sediment deposition in the original flow path.

Bajada – A piedmont comprised of coalescing alluvial fans.

Bankfull Elevation – The elevation on the bank where flooding begins. Bankfull discharge is defined as the flow rate which fills the active channel just prior to inundating the floodplain.

Bed Load – The portion of sediment in a stream which is transported by rolling, bouncing, or sliding on the stream bed.

Bifurcation – The division of a stream into two or more channels in the downstream direction.

Bioturbation – The disruption of sediments mainly by the burrowing activities of organisms.

Boundary Shear Stress – A frictional resistance at the marginal area of a flow which results in a decrease in velocity at the boundary areas.

Breccia – A rock unit composed of coarse highly angular fragments.

Calcareous – Calcium-rich.

Caliche – Calcium Carbonate ($CaCO_3$) deposited and illuviated in arid region soils cemented into a petrocalcic horizon; often as Stage IV carbonate.

Carbonate Stage – Stage I carbonate is loose disseminated $CaCO_3$ in the soil matrix. State II carbonate is thin, discontinuous coatings of $CaCO_3$ on the bottoms of coarse clasts in the soil matrix. Stage III carbonate is continuous coatings of $CaCO_3$ on the majority of coarse clasts in the soil matrix. Stage IV carbonate is replacement of the original soil matrix by a thick, well-cemented layer of $CaCO_3$. Stage V carbonate has strongly expressed laminar and/or platey structure.

Clastic – Rock fragments or other material which has been transported.

Contraction Scour – A form of scour frequently occurring in rivers at bridge crossings where stream width rapidly contracts causing an increase in stream velocity and/or turbulence.

Crenulation Index – The ratio of the topographic contour length to the straight line distance along the arc of the contour. A low crenulation index indicates low relief and a uniform surface.

Critical Shear Stress – The component of shear stress parallel to a slip plane in a slip system which controls the activity along that plane.

Cut Bank – The outside bank of a channel bend, often eroding and on the opposite side of the stream from a point bar.

Dendritic Drainage Pattern – A drainage system with tributaries which join at all angles, similar to the branching pattern of a tree. The number of flow paths decrease in the downstream direction.

Desert Pavement – A layer of tightly packed coarse sediment found on the surface of desert soils formed by winnowing away finer sediment by wind, rainfall, or local runoff. Degree of pavement development is related to the intensity of the formative processes.

Desert Varnish – A dark stain substance with a glistening luster, composed of manganese or iron oxide, found on the exposed surfaces of coarse rock material in arid climates. Desert varnish is formed as microbiotic organisms fix eolian cations with oxygen during infrequent wetting by rain.

Discharge – The volume of water passing through a channel during a given time, usually measured in cubic feet per second.

Dynamic Equilibrium – A natural state of regular, expected channel change with time where stream characteristics naturally adjust to the physical conditions of the environment.

Embayment – Fault-bounded mountain ranges have highly linear mountain fronts upon formation. Headward erosion along stream forms canyons. With time, these canyons cause the mountain front to be increasingly non-linear or "embayed".

Entrenchment Ratio – A computed index value which is used to describe the degree of vertical containment of a river channel (width of the flood-prone area at an elevation twice the maximum bankfull depth/bankfull width).

Ephemeral Stream – A stream that only experiences flow in times of heavy runoff and precipitation. An ephemeral stream does not have a base flow, as the channel is always above groundwater.

Evaporites – Sedimentary rock types formed by evaporation of water; for example, halite and gypsum.

Facies – A grouping of sediments, rocks, or soils with a common or related origin.

Fanglomerate – Rock and soil material originally deposited as an alluvial fan which has since been transformed into bedrock. Fanglomerates are characterized by a wide range of grain sizes and bedding types.

Felsic – A term applied to K-feldspar and silica rich rock types.

Fluvial – Of or pertaining to rivers and stream flow.

Froude Number – A number describing the ratio of inertial to gravitational forces in flowing water. A Froude number greater than one indicates supercritical flow.

Geomorphology – The study of the shape and form of the Earth's surface.

Graywacke – A type of sandstone characterized by detrital sand grains in a clay matrix. A dirty hard sandstone.

Headcutting – Channel degradation associated with abrupt changes in the bed elevation (headcut) that migrate in an upstream direction.

Holocene – Recent; that period of geologic history (an epoch) since the last ice age in North America (the past 10,000 years); also the series of strata deposited during that epoch.

Hydraulic Geometry – The description of the graphical relations between plot points of the hydraulic characteristics of a stream, typically width, depth, velocity and discharge.

Illuviation – The downward transport of mineral or other material in a soil layer, usually the B or C soil horizon.

Imbrication – Overlapping alignment of pebbles and cobbles due to transport in water. The tail of one clast overlies the head of the next clast downstream.

Incised Channel – A channel that cuts vertically downward, below the level at which it originally formed.

Inselbergs – Isolated remnants of bedrock exposed as small hills or buttes in the alluvial plain or pediment.

Intermittent Streams – A stream or part of a stream that flows only in direct response to precipitation, receiving little or no water from springs, snowmelt or other sources. It may be dry for a large part of the year, generally more than three months. Its course may be marked by an eroded channel, sediment deposits, scour, or transport of leaf litter or soil.

Interrupted Stream – A stream which has short perennial segments with intervening ephemeral or intermittent segments.

Interfluves – The area between braided flow channels. The area is usually vegetated in contrast to the sandy channel beds.

Normal Fault – A fault in which the hanging-wall block moved down relative to the footwall block.

Paleoflood – any flood that occurred prior to, or without, human records.

Patina – a coating or layer of corrosion formed by oxidation. Desert varnish forms a patina on the surface of rocks.

Pediment – A gently sloped erosion surface composed of bedrock with a thin veneer of alluvium, often formed by mountain front planation.

Pedogenic Clay – Clay that forms as a result of in place weathering within a soil column.

Perennial Streams – A stream that normally has water in its channel at all times.

Petrocalcic – Calcium-rich rock material

Piedmont – A general term for the sloping land area adjacent to a mountain front.

Planform – The form or pattern contour of an object as viewed from above; map view.

Pool – A section of the river with relatively deep water and low flow velocities.

Riffle – A relatively shallow section of a river with high-velocity, turbulent flow.

Riparian – Pertaining to anything connected with or adjacent to the banks of a river or stream.

Riprap – Rock material placed on stream banks to protect a structure or embankment from erosion.

Runoff – That part of precipitation that appears in surface-water bodies. It is the same as streamflow unaffected by artificial diversions, storage or other human works in or on the stream channels.

Scour – Excessive erosion of a streambed or a bank.

Sediment Yield – The total sediment outflow from a watershed or a drainage area at a point of reference and in a specified period of time. This is equal to the sediment discharge from the drainage area.

Sherds – Broken pieces of pottery or ceramic ware.

Sinuous – The "curviness" of planform of a river channel, the degree of meandering.

Slackwater – A low-energy zone in a stream characterized by near-zero velocity and sediment deposition.

Strath Terrace – A stream terrace formed by erosion, rather than deposition.

Stratigraphy – The study of layered sedimentary or metamorphic rock, especially their relative ages and correlation between different areas.

Stream Order – A geomorphic parameter used to describe the complexity of a drainage system. A first order stream has no tributaries. A second order stream is formed by the confluence of two first order streams. A third order stream is formed by the confluence of two second order streams. No stream order system exists specifically for alluvial fans.

Stream Power – A technical term relating shear stress and velocity. The units signify power per unit area of stream bed.

Supply Reach – The reach located upstream of the reach studied in detail. Since water flows downstream, sediment and water are supplied from reaches upstream.

Suspended Load – The part of the total sediment load that moves above the bed load. The weight of the suspended sediment is totally supported by the fluid.

Swale – A small channel, ditch, or depression.

Tensional Cracks – Cracks that are elongate and that form as forces work to pull apart a soil or rock unit.

Thalweg – An imaginary line along the length of the river connecting the deepest points.

Torrifluvents – A type of soil characterized by stream deposits of gravelly, sandy material, and lack of significant soil horizon development.

Tuff – A rock type formed of compacted volcanic fragments and ash.

Watershed – An area confined by drainage divides, usually having only one streamflow outlet.